VOL.
11
1961

THE INTERNATIONAL JOURNAL OF

# Applied Radiation and Isotopes

Volume II 1961

*Editorial Board*

P. C. AEBERSOLD
Washington

A. H. W. ATEN, Jr.
Amsterdam

M. BRUCER
Oak Ridge

J. COURSAGET
Saclay

V. N. KONDRATIEV
Moscow

M. MAGAT
Paris

J. STERNBERG
Montreal

B. MANOWITZ
New York

J. L. PUTMAN
Wantage

H. SELIGMAN
Vienna

*Editorial Advisory Board*

*Austria*
B. Karlik, Vienna

*Argentina*
E. E. Galloni, Buenos Aires

*Belgium*
Z. M. Bacq, Liége
P. C. Capron, Louvain

*France*
P. Auger, Paris
L. Bugnard, Paris
C. H. Fischer, Saclay
B. Goldschmidt, Paris
M. Haissinsky, Paris

*Germany*
H. Langendorff, Freiburg
M. Maier-Leibnitz, Munich
F. Strassmann, Mainz
F. Weygand, Berlin

*Israel*
I. Dostrovsky, Rehovoth

*Italy*
E. B. Chain, Rome
A. Perussia, Milan
G. Trabacchi, Rome

*Portugal*
H. de Carvalho, Lisbon

*Scandinavia*
G. C. de Hevesy, Stockholm

*Switzerland*
H. H. Staub, Zürich

*U.N.E.S.C.O.*
P. Auger, Paris

*United Kingdom and Commonwealth*
J. S. Anderson, Victoria
R. H. Betts, Chalk River, Ontario
A. Charlesby, Shrivenham
Sir John Cockcroft, Cambridge
V. R. Khanolkar, Bombay
Sir Hans Krebs, Oxford
C. P. LeBlond, Montreal
D. R. Llewellyn, Auckland
A. S. McFarlane, London

*U.S.A.*
J. C. Bugher, New York
V. Conquest, Chicago
R. D. Evans, Cambridge, Mass.
M. Harris, Spokane, Wash.
W. F. Libby, Los Angeles
W. B. Mann, Washington
H. F. Mark, New York
S. Warren, Boston

*U.S.S.R.*
N. A. Bach, Moscow
G. M. Frank, Moscow
G. V. Kurdiumov, Moscow

Pergamon Press New York • London • Oxford • Paris

VOL.
11
1961

# CONTENTS OF VOLUME 11

## NUMBER 1

V. I. Goldanskii and Yu. M. Kagan: On the thermochemical action of ionizing radiation . . 1

D. C. Borg, R. E. Segel, P. Kienle and L. Campbell: Selective radioactivation and multiple coincidence spectrometry in the determination of trace elements in biological material. Measurement of manganese . . . . . 10

H. R. Lukens, Jr., J. W. Otvos and C. D. Wagner: Formation of metastable isomers by photoactivation with the Van de Graaff accelerator . . . . . 30

A. H. W. Aten, Jr. and M. G. J. Heijenbrok: Sources of quasi-monoenergetic gamma radiation . 38

Technical Notes

P. B. Mathur and N. F. Lewis: Storage behaviour of gamma-irradiated mangoes . . . . 43

M. R. Houlton and J. K. Thomas: The radiation-induced graft copolymerization of 4-vinyl pyridine to Terylene . . . . . 45

G. Moss: A simple device for the rapid routine liberation and trapping of $C^{14}O_2$ for scintillation counting . . . . . 47

Book Reviews . . . . . 49

International News . . . . . 53

## NUMBERS 2/3

W. B. Mann, W. F. Marlow and E. E. Hughes: The half-life of carbon-14 . . . . . 57

D. E. Watt, D. Ramsden and H. W. Wilson: The half-life of carbon-14 . . . . . 68

A. Gandy: Mesure absolue de l'activité des radionuclides par la méthode des coïncidences béta-gamma à l'aide de détecteurs de grande efficacité. Etude des coïncidences instrumentales . . . . 75

Y. Le Gallic, J. Legrand et B. Grinberg: Méthode rapide d'identification des émetteurs-$\beta$ et de dosage d'impuretés radioactives-$\beta$ . . . . . 92

J. D. Greig: The determination of low radon and radium concentrations in liquids and slurries . 101

A. C. Morris, Jr: Measurements in a total-body irradiation facility . . . . . 108

K. K. Harris and W. E. Price: A thin plastic radiation dosimeter . . . . . 114

A. J. Teller, F. L. Poska and H. A. Davies: Effect of gamma irradiation on the catalytic activity of zinc oxide and chromic oxide for the decomposition of methanol . . . . . 123

A. Catsch: Dekorporation von Radionukliden durch veresterte Polyaminopolycarbonsäuren . . 131

J. Kopoldová, J. Liebster and A. Babický: The mechanism of the radiation chemical degradation of amino acids—I. The degradation of α-aminobutyric acid . . . . . 139

P. Dupuy et O. Tremeau: Résistance aux radiations ionisantes de quelques souches de *Lactobacillus* . 145

Technical Notes

R. C. L. Bosworth, I. Ernst and J. L. Garnett: Cellulose as a radiation dosimeter . . . . 152

A. M. Downes and A. R. Till: On the assay of tritium as tritio-butane . . . . . 154

K. H. Kimbel and J. Willenbrink: An inexpensive disposable sample container for single phototube liquid scintillation counting . . . . . 157

Letters to the Editors

R. F. Glascock and R. W. Smith: Assay of tritium as tritio-butane . . . . . 158

A. M. Downes and A. R. Till: Reply to Glascock and Smith's letter . . . . . 158

International News . . . . . 159

NUMBER 4

W. SCHMIDT-LORENZ und A. BERGER: Untersuchungen zur Oberflächenpasteurisierung von verpackten, im Innern keimreichen Fisch- und Fleischproben mit weichen Röntgenstrahlen . . . . . 161

H. FAZAKERLEY, P. G. GARRATT, P. R. HILLS and R. ROBERTS: Olfactory and chemical changes in irradiated essential oils . . . . . 174

Technical Notes

R. L. BELL and G. J. HERTSCH: Radioisotope technique for determination of cerebral circulation time 184

I. D. CLARKE and S. J. G. FERNANDES: The effects of γ-radiation on the protein content of apples and pears . . . . . 186

D. SAMUEL and F. STECKEL: Research with the stable isotopes of oxygen ($O^{17}$ and $O^{18}$) during 1958–1960 . . . . . 190

Forthcoming Papers . . . . . 230

## AUTHOR INDEX

ATEN A. H. W., JR. 38
BABICKÝ, A. 139
BELL, R. L. 184
BERGER, A. 161
BORG, D. C. 10
BOSWORTH, R. C. L. 152
CAMPBELL, L. 10
CATSCH, A. 131
CLARKE, I. D. 186
DAVIES, H. A. 123
DOWNES, A. M. 154, 158
DUPUY, P. 145
ERNST, I. 152
FAZAKERLEY, H. 174
FERNANDES, S. J. G. 186
GANDY, A. 75
GARNETT, J. L. 152
GARRATT, P. G. 174
GLASCOCK, R. F. 158
GOLDANSKII, V. I. 1
GREIG, J. D. 101
GRINBERG, B. 92
HARRIS, K. K. 114
HEIJENBROK, M. G. J. 38
HERTSCH, G. J. 184
HILLS, P. R. 174
HOULTON, M. R. 45
HUGHES, E. E. 57
KAGAN, YU. M. 1
KIENLE, P. 10
KIMBEL, K. H. 157
KOPOLDOVÁ, J. 139
LE GALLIC, Y. 92
LEGRAND, J. 92
LEWIS, N. F. 43
LIEBSTER, J. 139
LUKENS, H. R., JR. 30
MANN, W. B. 57
MARLOW, W. F. 57
MATHUR, P. B. 43
MORRIS, A. C., JR. 108
MOSS, G. 47
OTVOS, J. W. 30
POSKA, F. L. 123
PRICE, W. E. 114
RAMSDEN, D. 68
ROBERTS, R. 174
SAMUEL, D. 190
SCHMIDT-LORENZ, W. 161
SEGEL, R. E. 10
SMITH, R. W. 158
STECKEL, F. 190
TELLER, A. J. 123
THOMAS, J. K. 45
TILL, A. R. 154, 158
TREMEAU, O. 145
WAGNER, C. D. 30
WATT, D. E. 68
WILLENBRINK, J. 157
WILSON, H. W. 68

VOL.
11
1961

## SUBJECT INDEX


### A

**Abundance** M30; R1; T6
in air V15
in air dissolved in ocean water V15
in carbon dioxide in air K8
in meteorites V9; V10; V11; V13; V14
in minerals C12; C13; C18; D28; E3; E7; E8; E9; H25; H26; H32; K11; L10; L19; L20; P6; R1; T5; T6; V8; V9; V10; V11; V12; V13; V14
in photosynthetic oxygen V15; V16
in stellar atmospheres M11
in sulphur deposits D19
**Abundance in water** C22; D11; R1; Y1; Y2
from arctic regions A20; D8
from atmosphere D5
in $D_2O$ B2
from glaciers D7; E10; S16
from rain D7
from seas C23
from snow G10; P8
**Acetal**
chemical shift of C7
**Acetaldehyde**
auto-oxidation of B45
chemical shift of C7
**Acetals**
hydrolysis of C4
**Acetate**
analysis of B69; G2
**Acetate, 3-chloropropyl**
analysis of D25
formation of oxide from D25
**Acetate, 3-chloropropyl-O$^{18}$**
preparation of D25
**Acetate, ethyl**
chemical shift of C7; D22
**Acetate, 9-fluorenyl**
hydrolysis of B59
**Acetate, glycol**
chemical shift of C7
**Acetate, hexyl-O$^{18}$**
preparation of B30
**Acetate, methyl**
analysis of W4
chemical shift of C7
**Acetate, potassium-O$^{18}$**
preparation of G2
**Acetate, trifluoro, methyl**
hydrolysis of B56
**Acetic acid**
analysis of (see **Acetate**)
azeotropic distillation of H3
chemical shift of C7; D22
**Acetic acid-O$^{18}$**
preparation of B30
**Acetic acid, triphenyl**
decarbonylation of R7; R8
**Acetic anhydride**
chemical shift of C7
hydrolysis of B67
**Acetic benzoic anhydride**
hydrolysis of B67
**Acetic mesitoic anhydride**
hydrolysis of B67
**Acetoacetate**
analysis of F1
decarboxylation of H11
exchange with water H11
formation of F1
**Acetoacetate—*carbonyl*-O$^{18}$**
preparation of H11
**Acetoacetate, ethyl**
chemical shift of C7; D22
**Acetoacetate, maleyl**
analysis of C24
exchange with water C24
formation of C24
**Acetoin, methyl**
reaction of, with periodate B69
**Acetone**
analysis of B69; H11; S39
chemical shift of C7
exchange with oxygen S39
exchange with water H11; R13
formation of R13
photoxidation of D34
**Acetylacetone** (see **2;4-Pentadione**)
**Acetyl cyanide**
microwave spectrum of K24
**Acetyl cyanide-O$^{18}$**
preparation of K24
**Acetyl fluoride**
microwave spectrum of P9
**Acetyl fluoride-O$^{18}$**
preparation of P9
**Acidity**
of cobalt complexes H39
**Acids** (see parent anions)
**Actomyosin**
action of L12; L13

**Adenosine monophosphate (AMP)**
formation of L14
**Adenosine triphosphate (ATP)**
analysis of L13
formation of A22
hydrolysis of C2; C17; D33; H24; L12; L13
turnover of F7; F8
**Adenosine triphosphate—*terminal phosphate*-O$^{18}$**
preparation of M24
**Alanine**
exchange with water K18
oxygen transfer to phosphate of B18
**Alanine-O$^{18}$**
preparation of B18
**Alanine, phenyl, benzoyl**
analysis of B17
exchange with water, B17
**Alanine, phenyl, benzoyl-*carbonyl*-O$^{18}$**
preparation of B17
**Alcohols**
dehydration of B33; B34; M12
(see also individual alcohols)
**Aldolase**
terminal amino acid in K18
**Allyl alcohol**
oxidation of B46
**Allyl alcohol, α-phenyl**
analysis of G5
exchange with water B68; D24; G5
rearrangement of B68; D24; G5
**Allyl alcohol, α-phenyl-O$^{18}$**
preparation of G5
**Allyl alcohol, γ-phenyl (Cinnamyl alcohol)**
exchange with water B68; G5
formation of G5
**Allyl alcohol, γ-phenyl-O$^{18}$**
preparation of G5
**Allylic rearrangement**
study of B68; D24; G5; G6; G7; P12
**Alumina**
cleavage of benzoyloxycholestene by D2
exchange with oxygen R14
exchange with water vapour R14; W6
reaction of, with benzamide D2
self-diffusion in O2
(see also **Boehmite** and **Oxides, mixed**)
**Aluminium**
corrosion of B45; F9
**Aluminium ion**
hydration of B5; J1
**Alumino silicates**
exchange with water S8
**Amines**
reaction of, with benzoic anhydride D16
reaction of, with benzoyl peroxide D12; D18
**Amino acids**
activation of B18
terminal acid determination K18
***tert.*-Amyl alcohol**
analysis of B33; B34
exchange with water B33; B34
**Amylases**
hydrolysis of glycogen by M19; M20; M21
**Analysis, elemental (using oxygen-18)** P5; R11
**Analysis, isotopic**
calculations H1; M26
general methods of A7; D3; D4; G13; L8; L9; M3; M26
inorganic compounds A7; A8; A12; A16; A17; B50; B61; B62; B63; B65; B66; B67; B69; B71; C9; C13; C16; C17; C18; C19; F5; F7; F8; H4; H21; H24; H25; H26; H27; H36; H38; J8; J9; K10; L6; M1; M3; R3; R12; S23; S24; S25; S30; S31; S35; S41; T2; T15; V8; V14; W2; W11; Y3; Z1.
organic compounds B13; B14; B16; B17; B25; B30; B33; B34; B38; B40; B42; B54; B55; B56; B57; B59; B60; B62; B64; B66; B67; B69; C24; D2; D12; D14; D15; D17; D25; D26; D31; D33; F1; F2; F5; F6; G2; G5; G7; G8; G11; G13; G16; H5; H6; H7; H8; H9; H10; H11; H22; H24; H37; J9; K26; K32; L1; L13; M19; M21; M24; M31; N1; P12; S1; S3; S6; S9; S24; S39; S40; S44; T11; V5; V17; W4; W8; W9.
of water A5; K23; S16; S17
**Analytical methods**
activation analysis F7; F8
density of water B50; B51; K4; K6; K23; L4; L5; L8; T13
infra-red spectrometry S30; S31
mass spectrometry B28; C9; D6; D27; F13; H1; H4; H9; H11; L6; L9; M1; M3; M22; P1; R3; S40
purification of compounds E2; L7; M1
**Anhydrides**
formation of W3; W4
**Aniline**
oxidation of B46
**Anions** (see parent acids)
***p*-Anisidine**
oxidation of B46
**Anisole, *o*-nitro**
oxidation of B46
**Anodes**
processes at F14; G3
**Anthranil**
formation of B46
**Anthranilic acid**
formation of K31

**Anthraquinone, 2-ethyl**
auto-oxidation of B45
**Arsenate**
analysis of A7; S24
exchange with water K17; S24
**Arsenate-O$^{18}$**
preparation of A7; S24; V1
**Arsenolysis**
study of S24; V1
**Ascorbic acid**
oxidation of H2
reaction of, with $HNO_2$ B53
**Aspartic acid, formyl**
formation of H20
**Auto-oxidation** (see **Oxidation and oxygen transfer**)
**Azeotropes**
vapour pressure of H30; H31
**Azide**
reaction of, with nitrite B71

**B**

**Bacteria** (see **Micro-organisms**)
**Benzal, di-*tert*-butyl**
hydrolysis of C4
**Benzaldehyde**
auto-oxidation of B45
**Benzaldehyde-O$^{18}$**
preparation of G5
**Benzaldehyde, *o*-chloro**
autoxidation of B45
**Benzamide**
analysis of B16; D2; L1
diazotization of L1
exchange with water B16; L1
hydrolysis of B16
reaction of, with $Al_2O_3$ D2
**Benzamide, *p*-chloro-O$^{18}$**
preparation of D4
**Benzanilide-O$^{18}$**
preparation of D12
**Benzene**
oxidation of B46; S44
**Benzene, 1-bromo, 4-nitro**
analysis of S3
exchange with water S3
von Richter reaction of S3
**Benzene, 1-chloro, 4-nitro**
analysis of S3
exchange with water S3
von Richter reaction of S3
**Benzene, nitro**
formation of B46
**Benzene sulphonate**
exchange with water V17
**Benzene sulphonate, 3-butenyl**
analysis of D17; K32
formation of D17
**Benzene sulphonate, *cyclo*butyl**
analysis of D17; K32
formation of D17
**Benzene sulphonate, *o*-nitro, 2,4-dinitrophenyl**
hydrolysis of V17
**Benzene sulphonate, *p*-nitrophenyl**
hydrolysis of V17
**Benzene sulphonate, phenyl**
exchange with water C8
**Benzene sulphonate, *cyclo*propylcarbinyl**
analysis of D17; K32
rearrangement of D17; K32
**Benzene sulphonate, *cyclo*propylcarbinyl-*alkoxy*-O$^{18}$**
preparation of D17; K32
**Benzoate**
analysis of B60; P12
reaction of, with phenylallyl benzoate P12
**Benzoate, *o*-acetoxy (Acetyl salicylate)**
hydrolysis of B13
**Benzoate, *p*-chloro, methyl-O$^{18}$**
preparation of D4
**Benzoate, *p*-chloro, methyl-*carbonyl*-O$^{18}$**
preparation of D4
**Benzoate, dimethylaminoethyl, N-oxide**
analysis of S9
hydrolysis of S9
**Benzoate, α-ethoxy**
analysis of D14; D26; D31; F2
formation of D14; D26; D31; F2
**Benzoate, ethyl**
analysis of B16
exchange with water B16
**Benzoate, *cyclo*hexenyl**
analysis of D26
formation of D26
**Benzoate, *cyclo*hexyl**
analysis of D26
formation of D26
**Benzoate, 2-hydroxy, 4-methoxyphenyl**
analysis of D12
hydrolysis of D12
**Benzoate, 1-methoxyvinyl**
reaction of, with benzoic acid W3; W4
**Benzoate, *p*-nitro, *trans*-dimethylallyl**
analysis of G7
rearrangement of G7
**Benzoate, *p*-nitro, *trans*-dimethylallyl-*carbonyl*-O$^{18}$**
preparation of G7
**Benzoate, *p*-nitro, *trans*-methyl, 2-*cyclo*hexyl**
analysis of G7
rearrangement of G7



VOL. 11 1961

**Benzoate, *p*-nitro, *trans*-methyl, 2-*cyclo*hexyl-*carbonyl*-O$^{18}$**
preparation of G7
**Benzoate, *p*-nitro, γ-phenylallyl**
analysis of B40
infra-red spectrum of B40
rearrangement of B40
**Benzoate, *p*-nitro, γ-phenylallyl-*carbonyl*-O$^{18}$**
preparation of B40
**Benzoate, phenyl**
reaction of, with benzoate V6
**Benzoate, α-phenylallyl**
analysis of P12
reaction of, with benzoate P12
rearrangement of P12
**Benzoate, γ-phenylallyl**
analysis of P12
infra-red spectrum B40
reaction of, with benzoate P12
rearrangement of P12
**Benzoate, γ-phenylallyl-*carbonyl*-O$^{18}$**
preparation of B40
**Benzoate, silver**
reaction of, with *p*-nitrobenzoyl chloride K32
**Benzoate, silver-O$^{18}$**
preparation of D4
**Benzoate, triphenylmethyl**
analysis of D26
formation of D26
**Benzoate, triphenylmethyl-*alkoxy*-O$^{18}$**
preparation of D26
**Benzoate, triphenylmethyl-*carbonyl*-O$^{18}$**
preparation of D26
**Benzoic acid**
analysis of B60; B67 (see also **Benzoate**)
exchange with water B43; B60; G14
formation of B67
reaction of, with 1-methoxyvinyl benzoate W3; W4
reaction of, with phenylallyl benzoate P12
reaction of, with phenyl benzoate V6
**Benzoic acid-O$^{18}$**
preparation of D4; V6
**Benzoic acid, *m*-amino**
exchange with water G14
**Benzoic acid, *o*-amino (Anthranilic acid)**
exchange with water G14
**Benzoic acid, *p*-amino**
exchange with water G14
**Benzoic acid, *m*-bromo**
analysis of S3
formation of S3
**Benzoic acid, *m*-chloro**
analysis of S3
exchange with water G14
formation of S3
**Benzoic acid *p*-chloro**
exchange with water G14
**Benzoic acid, 2;3-dihydroxy**
formation of M16
**Benzoic acid, *m*-hydroxy**
exchange with water G14
**Benzoic acid, *o*-hydroxy (Salicyclic acid)**
analysis of B13
exchange with water G14
hydroxylation of M16
**Benzoic acid, *p*-hydroxy**
exchange with water G14
**Benzoic acid, *m*-nitro**
exchange with water G14
**Benzoic acid, *o*-nitro**
exchange with water G14
**Benzoic acid, *p*-nitro**
exchange with water G14
**Benzoic acid, *o*-thiol (o-Mercaptobenzoic acid**
exchange with water G14
**Benzoic acid, 2;4;6-trimethyl (Mesitoic acid)**
analysis of B60; B67
exchange B60
formation of B67
**Benzoic anhydride**
formation of G15
hydrolysis of B67
reaction of, with amines D16
**Benzophenone**
analysis of H7
infra-red spectrum of H7
**Benzophenone-O$^{18}$**
preparation of H7
**Benzoyl chloride-O$^{18}$**
preparation of D26
**Benzoyl chloride, *p*-nitro**
analysis of K32
reaction of, with silver benzoate K32
**Benzoyl chloride, *p*-nitro-*carbonyl*-O$^{18}$**
preparation of G7; K32
**Benzoyl peroxide**
analysis of D12
decomposition of D14; D26; D31
reaction of, with amines D12; D18
reaction of, with ether D14; F2
reaction of, with phenols D12; D18
reaction of, with phosphines G15
**Benzoyl peroxide-*carbonyl*-O$^{18}$**
preparation of D12; D26; F2; G15
**Beryllium ion**
hydration of J1
**Biacetyl** (see **2;3-Butandione**)
**Bicarbonate** (see **Carbonate**)
**Biochemistry** (see **Enzymes**)
**Bisulphate** (see **Sulphate**)

**Blood**
clinical treatment of G12
**Boehmite**
exchange with water B19; W6
**Borates**
exchange reaction of, with silicates K27
exchange with water B43
**Borate, trimethyl-O$^{18}$**
preparation of K27
**Bromate**
exchange with water B43
**2;3-Butandione (Diacetyl)**
chemical shift of C7
reaction of, with periodate B69
**Butane 1;2;3-triol**
analysis of S1
formation of S1
**Butanone-2(Methyl ethyl ketone)**
chemical shift of C7; D22
***n*-Butyl alcohol**
reaction of, with ethyl propionate K26
***sec*.-Butyl alcohol**
exchange with water M12
***sec*.-Butyl alcohol-O$^{18}$**
preparation of M12
***tert*.-Butyl alcohol**
analysis of B33; B34
exchange with water B33; B34
**Butyraldehyde**
auto-oxidation of B45
chemical shift of C7

**C**

**Cadmium**
corrosion of B45; F10
**Cadmium oxide**
diffusion and exchange of oxygen in H15
**Carbon**
combustion of W2
**Carbonate**
abundance in C18; D28; E3; E7; V8 (see also **Paleotemperatures**)
analysis of C18; V8
exchange with water C11; C12; C13
(see also individual carbonates)
**Carbonate, calcium**
exchange with water J10
**Carbonate, 2;2-dimethyl propane, 1;3-diol**
analysis of S6
exchange with water S6
hydrolysis of S6
**Carbonate, potassium**
analysis of J9
**Carbonate, potassium-O$^{18}$**
preparation of F11, J9
**Carbonate, sodium**
exchange with water S35
**Carbon dioxide**
abundance in K8
analysis of H21; H36; L6; M1; M3; R3; R12; Y3; Z1 (see also carbonates)
exchange with carbonate S13
exchange with CO B39
exchange with $H_2SO_4$ H40
exchange with oxygen B6; H22; W2
exchange with $UO_2$ A21; B12
exchange with water K5; M25; R12; S20
infra-red spectrum of C21
isotope effect, in reduction by zinc S14
purification of B33; B34; E2
in respiration of animals M4; M5; M6; M7; M8
thermal diffusion of B11
**Carbon monoxide**
analysis of C9; L6; Y3
distillation of liquid D21; E1; J7; L16; T9
exchange with $CO_2$ B39
exchange with $H_2SO_4$ R8
exchange with oxygen M15; W2
mass ratio of R10
thermal diffusion of H12; T16; V20; V21
vapour pressure of J5; J6
**Carboxypeptidase**
action of K18
**Casein**
dephosphorylation of A17; K1
**Catalase**
decomposition of $H_2O_2$ by J3
**Catalysis**
diffusion in W1
(see also **Exchange** and individual reactions)
**Catechol**
analysis of V5
exchange with water V5
hydroxylation of V5
**Cathodes**
reduction of oxygen at A1; B45
**Cations**
hydration of B5; C20; J1; S42
(see also individual metals)
**Cell membranes**
permeability of A13; U2
**Cellulose**
exchange with water L3
**Chemical shift**
of oxygen-17 compounds C7; D22
(see also **Nuclear magnetic resonance**)
**Chlorate**
analysis of H27
exchange with water B43; H27
**Chlorate, potassium-O$^{18}$**
preparation of H27
**Chloride, manganous**
oxidation to $MnO_2$ B46

**Chlorite**
analysis of H27
exchange with water H27
**Chloroformate** (see **Formate, chloro**)
**Chloroplasts**
oxidation of ascorbic acid by H2
**3β-Cholestene-(1)-benzoyloxy**
analysis of D2
reaction of, with $Al_2O_3$ D2
**3β-Cholestene-(1)-benzoyloxy-O$^{18}$**
preparation of D2
**3β-Cholestene-(1)-ol-O$^{18}$**
preparation of D2
**3β-Cholestene-(1)-one-O$^{18}$**
preparation of D2
**Cholinesterase**
action of S9
**Chromic complexes**
exchange with water L15
**Chromic ion**
hydration of B5; C20; L15
**Chromic oxide ($Cr_2O_3$)**
exchange with CO W13
exchange with oxygen W13
(see also **Oxides, mixed**)
**Chromyl chloride**
oxidation of hydrocarbons by B46; S44
**Chromyl chloride-O$^{18}$**
preparation of S44
**Chymotrypsin**
action of B17
**Cinnamyl alcohol** (see **Allyl alcohol, γ-phenyl**)
**Citrulline**
arsenolysis of S24
**Cobaltic complexes**
absorption of oxygen by P2
acidity of H39
exchange of water of H38
hydrolysis of F12
oxygen transfer in K25
**Cobaltic ion**
hydration of J1
**Cobaltic oxide**
analysis of A7
**Cobaltous ion**
hydration of C20; S42
**Combustion** (see **Oxidation and oxygen transfer**)
**Copper oxides** (see **Cupric oxides** and **Cuprous oxides**)
**Corrosion**
of metals B45; F9; F10
***p*-Cresol**
reaction of, with benzoyl peroxide D12
**Crotyl alcohol**
hydroxylation of S1
**Cumene**
analysis of T11
auto-oxidation of T11
**Cumene peroxide**
analysis of D15; T11
formation of T11
reaction of, with phosphine D15
**Cumyl alcohol**
analysis of D15
formation of D15
**Cupric ion**
hydration of C20; S42
**Cupric oxide**
analysis of A7
exchange with oxygen M14; R14
exchange with water vapour R14
**Cuprous oxide**
exchange and diffusion in M28
**Cyanate**
analysis of S41
exchange with water S41
formation of S41
**Cyanide**
reaction of, with permanganate S41

**D**

***trans*-9-Decalol**
analysis of D15
formation of D15
***trans*-9-Decalyl hydroperoxide**
reaction of, with phosphines D15
**Decarbonylation**
of carboxylic acids R7; R8
**Decarboxylation**
of acetoacetate H11; R12
**Dehydrogenase**
action of P4
**Diacetyl** (see **2;3-Butandione**)
**Dichromate, nickel**
exchange with oxygen K13
**Diethyl ether (Ethyl ether)**
chemical shift of C7; D22
reaction of, with benzoyl peroxide D14; F2
**Diethyl ketone** (see **3-Pentanone**)
**Diffusion**
in catalysts W1
in ice K29
in living cells A13; U2
in oxide lattices H15; K14; M28; M29; O2; W10
in polyethylene S11
(see also **Separation by thermal diffusion**)
**Diffusion, thermal**
of CO H12; T16; V20; V21
of $CO_2$ B11
of oxygen D23
of water vapour D10

**Dioxan**
chemical shift of C7
**Di*iso*propyl ketone** (see **3-Pentanone, 2;4-dimethyl**)
**Disilyl ether**
Raman spectrum of M10
**Disilyl ether-O$^{18}$**
preparation of M10
**Distillation, fractional** (see **Separation by fractional distillation**)
**Distribution (partition)**
of water in cells A13; U2
**"Dole" effect** L2

E

**Electrodes**
oxygen D9
(see also **Anodes** and **Cathodes**)
**Electrolysis**
formation of peroxyacids by B45 F11; G3
microapparatus for H37
**Enzymes (reactions catalysed by enzymes)**
action of B37
activation of methionine C2
arsenolysis with S24; V1
decarboxylation of acids by H11; R12
decomposition of $H_2O_2$ J3
dephosphorylation of casein K1
determination of protein terminal acids K18
enolization of pyruvate R9
exchange reactions B17; B36; C16
formation of acetoacetate F1
acetylglutamic acid M24
AMP L14
ATP A22
carbamyl phosphate J9
formyl aspartic acid H20
maleyl acetoacetate C24
orsellinic acid C2
threonine F5; F6
tryptophan hydroxamate H24
hydrolysis of acetyl phosphate P4
ATP C17; H24; L12; L13
glycogen M19; M20; M21
phosphates F5; F6
starch H10
sulphates S28; S29; S31
hydroxylation of catechol V5
kynurenine S2
nicotinic acid H37
pyrocatechol H19
salicylic acid M16
steroids H21
incorporation of oxygen by H16
isotope fractionation by F3
oxidation of ascorbic acid H2

**Enzymes** (*continued*)
oxidative phosphorylation B35; D33
oxygen transfer 2S3
phosphate transfer A23
**Esters** (see parent anions and **Transesterification**)
**Ethanol**
analysis of B55
auto-oxidation of R13
chemical shift of C7; D22
exchange with water R13
**Ethanol, 2-chloro**
chemical shift of C7
**Ethylene**
oxidation of H22
**Ethylene, chlorohydrin** (see **Ethanol, 2-chloro**)
**Ethylene oxide**
analysis of H22
formation of H22
**Ethyl ether** (see **Diethyl ether**)
**Exchange**
inorganic compounds with water A6; A8; A9; A14; A16; A22; B19; B43; B44; B47; B48; B49; B52; B63; B65; B69; B70; B71; C11; C12; C13; C16; F11; G4; H25; H26; H27; H38; H41; J8; J10; K5; K7; K10; K14; K17; L15; M9; M25; R9; R12; R13; R14; S7; S8; S24; S33; S34; S35; S36; S37; S38; S41; S45; T3; T5; T15; T17; W6; W11; W15.
miscellaneous A16; B1; G4; H40; K7; S12; S13; S32; S39; W2; Y4.
organic compounds with water B14; B15; B16; B17; B33; B34; B43; B44; B54; B57; B60; B62; B64; B66; B68; C8; C24; C25; D24; G5; G14; H5; H8; H10; H11; K18; L1; L3; M12; M21; M25; M32; R4; R13; S3; S6; V5; V17.
theoretical B21; V18; V19
**Exchange, enzyme catalysed** B17; B36; C16
**Exchange (isotopic) on surfaces**
CO with $CO_2$ B39
CO with oxides W12; W13; Y7
CO with oxygen M15; W2
$CO_2$ with oxides W12; W13; Y7
$CO_2$ with $UO_2$ A21; B12
glass with water M2
$N_2O$ with NiO W14
oxides with oxygen B7; H15; H22; K9; K13; K14; M14; M28; M29; R14; S36; W10; W12; W13
oxides with water R14; W6; Y5; Y6
oxygen with oxygen M13; M14; M23; W2
oxygen with salts K13; S35; S36; S37; S38; W15
oxygen with silica H41; S36
oxygen with water G4; H22
silica with water H41

VOL. 11 1961

**Extraction, liquid**
exchange in H14

**F**

**Ferric ion**
decomposition of $H_2O_2$ by J3
hydration of B5; C20; S42
**Ferric oxide**
analysis of A7
exchange with CO W12; W13
exchange with $CO_2$ W12; W13
exchange with oxygen K13; W12
(see also **Oxides, mixed**)
**9-Fluorenyl alcohol**
analysis of B59
**Formal, diethyl**
chemical shift of C7
**Formamide**
chemical shift of C7
**Formate, chloro, ethyl**
chemical shift of C7
**Formate, chloro, hexyl**
analysis of B30
reaction of, with $AgNO_3$ B30
**Formate, chloro hexyl-*alkoxy*-O$^{18}$**
preparation of B30
**Formate, methyl**
chemical shift of C7
exchange with water C25
microwave spectrum of C25
**Formate, methyl-*alkoxy*-O$^{18}$**
preparation of C25
**Formate, methyl-*carbonyl*-O$^{18}$**
preparation of C25
**Formic acid**
chemical shift of C7; D22
decarbonylation of R7; R8
microwave spectrum of C26
**Formic acid-O$^{18}$**
preparation of C26
**Formic acid, benzoyl**
decarbonylation of R7; R8
**Fractional distillation** (see **Separation by fractional distillation**)
**Fumarate, methyl**
hydrolysis of cobalt complex F12
**Fungi** (see **Micro-organisms**)
**Furan**
chemical shift of C7
**Furfural**
chemical shift of C7

**G**

**Gallic ion**
hydration of J1
**Gentisic acid**
formation of M16
**Glass**
exchange with water M2
(see also **Silicon dioxide**)
**Glucose**
analysis H10; S24
exchange with water R4
formation of H10
mutarotation of R4
**Glucose-1-O$^{18}$**
preparation of R4
**Glutamic acid, acetyl**
analysis of J9; M24
formation M24
**Glutamic acid, acetyl-*carbonyl*-O$^{18}$**
preparation of J9; M24
**Glutamine**
arsenolysis of V1
**Glycerol**
formation of B46
**Glycogen**
arsenolysis of S24
hydrolysis of M19; M20; M21
**Glycols**
analysis of B41; B54; S6
chemical shift of C7
hydrolysis of cyclic esters of B41; B42; B54; S6
oxidation of B69
**Glycosides**
hydrolysis of H10
**Granite**
exchange with water W15
**Grignard reaction**
study of M31

**H**

**Hexadecane**
bacterial oxidation of S40
***cyclo*Hexanone**
chemical shift of C7
***cyclo*Hexene**
oxidation of B46; S44
reaction of, with perbenzoate D13; D18; F2
***cyclo*Hexene-2-one, 5;5-dimethyl, 3-methoxy**
analysis of W9
formation of W9
***cyclo*Hexene oxide**
hydrolysis of B41; B42
**Hexyl alcohol-O$^{18}$**
preparation of B30
**Homomolecular reactions**
of nitric oxide S32
of oxygen B7; D23; H40; M13; M14; M23; W2

**Hydration**
of ions, in flow systems B5
(see also individual metal ions)
**Hydrazoic acid**
reaction of, with nitrite B71
reaction of, with oxygen B4
**Hydrocarbons**
bacterial oxidation of L11
catalytic oxidation of M15
hydroxylation of unsaturated S1; W8
reaction of, with $CrO_2Cl_2$ B46; S44
reaction of, with peroxides D13; D18; F2; G16
**Hydrogen peroxide**
decomposition of A10; B46; J3; M18; W1
exchange with water S45
formation of A1; B1; B45; D9
reaction of, with halides S45
reaction of, with olefines S1
reaction of, with permanganate L18
**Hydrogen peroxide-$O^{18}$**
preparation of J3
**Hydrolysis**
using oxygen-18 to indicate point of bond fission B10; B13; B14; B16; B41; B42; B45; B54; B55; B56; B58; B59; B60; B61; B62; B66; B67; B73; C2; C4; C17; D12; D33; F5; F6; F11; F12; H6; H10; H21; H24; L12; L13; M16; M19; M20; M21; P4; S6; S9; S23; S28; S29; S31; T10; V17.
**Hydroperoxides, organic**
formation of S45
reaction of, with phosphines and phosphites D15; G11
**Hydroxylamine**
oxidation of A4
**Hydroxylamine, N;N-dibenzyl, O-benzoyl**
analysis of D12
formation of D12
reaction of, with ethanol D12
rearrangement of D12
**Hydroxylamine, N;N-dibenzyl, O-*benzoyl*-$O^{18}$**
preparation of D12
**Hydroxylation**
of kynurenine S2
of nicotinic acid H37
of olefines S1; W8
of phenols H19; M16
of steroids H21
**Hydroxyl radical**
exchange with water G4; K7
**Hypobromite**
exchange with water A14; A16
reaction of, with nitrite A16
**Hypochlorite**
exchange with water A9; A16
reaction of, with nitrite A16
**Hypophosphorous acid**
exchange with water B43

**I**

**Ice**
diffusion in K29
fractional crystallization in K29
(see also **Abundance in water**)
**Infra-red spectrum** (see **Spectra, infra-red**)
**Inorganic compounds**
analysis of A7
exchange with water, reviews of B44; B47; B48; B49
(see also **Analysis**, **Exchange** and individual compounds)
**Iodate**
analysis of B69
exchange with water B43; B69
**Ion pairs**
study of D15; D16; D17; D25; G5; G6; G7; G8; G11; G15; G16; K32; P12; W7
**Iron**
analysis of oxygen in P5
corrosion of F9
(see also **Ferric ion**)
**Iron oxides**
abundance in C13
***iso*propyl alcohol** (see ***iso*Propyl alcohol**)
**Isotope effects**
in biology, review of B31
in decomposition of $H_2O_2$ M18; W1
in decomposition of $N_2O$ H28
in enzyme reactions F3
in exchange reactions B21; J10
in growth of micro-organisms B29
in polymerization of oxazolidinediones H23
in reduction of $CO_2$ by zinc S14
in respiration L2
(see also **Separation**, **Spectra** and **Vapour pressure**)

**K**

**Kinases**
action of R9
**Kynurenine**
hydroxylation S2

**L**

**Lead oxide** (see **Plumbic oxide**)

**M**

**Magnesium**
corrosion of B45, F9

VOL. 11 1961

**Magnesium ion**
hydration of J1
**Magnesium oxide**
band spectra of P7
exchange with CO W12; W13
exchange with $CO_2$ W12; W13
exchange with oxygen W12; W13
(see also **Oxides, mixed**)
**Malonate, diethyl**
chemical shift of C7; D22
**Maltose**
exchange with water H10; M21
**Manganate**
exchange with water B43; M9
**Manganese dioxide**
analysis of A7
effect on decomposition of $H_2O_2$ W1
effect on decomposition of perchlorate G1
exchange with oxygen R14
exchange with water vapour R14
formation of B46
**Manganese dioxide-O$^{18}$**
preparation of A7
**Manganous ion**
hydration of C20; S42
**Mass, isotopic**
of CO R10
of light nucleons F13
by mass spectrometer S26
(see also **Analysis** and **Analytical Methods**)
**o-Mercaptobenzoic acid** (see **Benzoic acid o-thiol**)
**Mercuric oxide**
analysis of A7
**Mercuric sulphide**
combustion of W2
**Mesitoic acid** (see **Benzoic acid, 2;4;6-trimethyl**)
**Mesityl oxide**
chemical shift of C7
**Metabolism**
intermediary, review of A18
oxygen, review of M17
of respiration in mice M4; M5; M6; M7; M8
of water in plants V4
**Metals**
analysis of oxygen in P5
(see also **Corrosion** and individual elements)
**Meteorites**
abundance in V9; V10; V11; V13; V14
**Methane, triphenyl**
oxidation of B46; S44
**Methanol**
analysis of B55; B56; B62; B66
chemical shift of C7; D22
exchange with water B66
formation of L11
**Methanol** (*continued*)
formation of enol ethers with W9
separation by fractional distillation of Z2
**Methanol-O$^{18}$**
preparation of K27
**Methanol, *p*-methoxydiphenyl**
analysis of B64
exchange with water B64
racemization of B64
**Methanol, *p*-methoxydiphenyl-O$^{18}$**
preparation of B64
**Methanol, *cyclo*propyl**
analysis of D17
**Methanol, *cyclo*propyl-O$^{18}$**
preparation of D17
**Methanol, triphenyl**
analysis of D26; M31; S44
Grignard synthesis of M31
oxidation of S44
**Methanol, triphenyl-O$^{18}$**
preparation of D26
**Methionine**
activation of C2
**Methoxy derivatives** (see parent compounds)
**Methyl derivatives** (see parent compounds)
**Micro-organisms**
formation of orsellinic acid by G2
isotope effect in growth of B29
oxidation in presence of L11; S40
oxidation of thiosulphate by S5
(see also **Bacteria**)
**Minerals** (see **Abundance**—in minerals)
**Molybdate**
exchange with oxygen S35
exchange with water B43

**N**

**Naphthalene, 2-methoxy**
analysis of W9
formation of W9
**Naphthamide, *cyclo*hexyl, N-nitroso**
rearrangement of W7
**Naphthamide, *cyclo*hexyl, N-nitroso-O$^{18}$**
preparation of W7
**Naphthamide, 1-phenylethyl, N-nitroso**
rearrangement of W7
**Naphthamide, 1-phenylethyl, N-nitroso-O$^{18}$**
preparation of W7
**β-Naphthol**
reaction of, with methanol W9
**β-Naphthol, *p*-nitroso**
oxidation of B46
**Nef reaction**
study of A15

**Nickel oxide**
exchange with CO W12; W13
exchange with $CO_2$ W12; W13
exchange with $N_2O$ W14
exchange with oxygen K9; W12; W13
**Nickelous ion**
hydration of B5; C20; S42
**Nicotinic acid**
analysis of H37
hydroxylation of H37
**Niobates**
exchange with water S34; S38
**Niobium**
recovery of oxygen from H13
**Nitrate**
exchange with water B43; B70
infra-red spectrum of A11; P13
**Nitrate, potassium-O$^{18}$**
preparation of A11
**Nitrate silver**
oxidation to silver peroxide B46
reaction of, with hexyl chloroformate B30
**Nitric acid**
chemical shift of C7; D22
(see also **Nitrate**)
**Nitric oxide**
analysis of T2
exchange with NO S32
exchange with NOCl Y4
exchange with water S7; T3
vapour pressure of B22; C14; C15; K28
**Nitric oxide-O$^{18}$**
preparation of C14; C15
**Nitrite**
analysis of A16; B63; B65; B71
exchange with water B63; B71
infra-red spectrum of A11
reaction of, with azide B71
reaction of, with hypohalites A16
**Nitrite, silver-O$^{18}$**
preparation of A11
**Nitrite, sodium-O$^{18}$**
preparation of B63
**Nitrobenzene** (see **Benzene, nitro**)
**Nitrogen dioxide**
exchange with $N_2O_4$ M27; S20
**Nitromethane**
analysis of (by mass spectrometer) H9
infra-red spectrum of H9
**Nitromethane-O$^{18}$**
preparation of H9
**Nitroparaffins**
exchange with water A15
**Nitrosation**
study of T17
**Nitrosyl chloride**
exchange with NO Y4
**Nitrous acid**
analysis of (see **Nitrite**)
exchange with water, B63; B65; T17
formation of B4
infra-red spectrum of B4
reaction of, with ascorbic acid B53
**Nitrous oxide**
decomposition of H28
exchange with NiO W14
**Normalization of water (removal of excess deuterium)**
methods of K4; K6; T13; Y1; Y2
**Nuclear magnetic resonance**
of oxygen-17 compounds C7; C20; D1; D22; J1; O3; S19; S42
**Nuclear reactions**
of oxygen-17 and oxygen-18 A2; A3; B23; B24; B25; B26; B74; C3; C10; F7; F8; H3; I1; J2; K12; S10; S15; T14

**O**

**Olefines** (see **Hydrocarbons**)
**Oleic acid**
oxidation by permanganate W8
**Organic compounds**
analysis of D3; D4; G13; L8; L9
methods of synthesis of M32; T7
(see also **Analysis**, **Exchange** and individual compounds)
**Orsellinic acid**
analysis of G2
formation of G2
**Oxalate, diethyl**
chemical shift of C7
**Oxalic acid**
exchange with water M25
oxidation of M25
**2;5-Oxazolidinediones**
isotopic effect in polymerization of H23
**Oxidases**
action of C24; H17
isotope fractionation by F3
(see also **Oxygenases**)
**Oxidation and oxygen transfer**
of carbon W2
of fatty acids H35
of inorganic compounds in solution A4; A9; B10; B46; G3; K25; S41
of mercuric sulphide W2
of metals F9; F10
of organic compounds on catalysts M15
of organic compounds in solution B45; B46; B69; L11; M25; R13; S44; T11; W5; W8
photochemical D34

VOL. 11 1961

**Oxidation and oxygen transfer** (*continued*)
review of R5; R6
of sulphur W2
of thiosulphate S5
**Oxidative phosphorylation**
study of B35; D33
**Oxides, mixed**
exchange with CO Y7
exchange with $CO_2$ Y7
exchange with water vapour Y5; Y6
(see also individual metal oxides)
**Oxygen, molecular**
absorption of P2
analysis of H36
cathode reduction of A1
concentration in blood of G12
diffusion in oxides H15; K14; M28; M29; W10
enzymatic fixation of C24; H16; H17; H18; H19; H20; H21; K19; S40; V5
(see also **Photosynthesis**)
exchange with acetone S39
exchange with CO M15; W2
exchange with $CO_2$ H20
exchange with oxides B7; H15; H22; H41; K13; K14; M28; M29; R14; S36; W10; W12; W13
exchange with oxygen (homolecular reactions) H40; M13; M14; M23; W2
exchange with salts K13; S35; S36; S37; S38
exchange with $SO_2$ W2
exchange with water G4; H22
formation of G1
fractional distillation of D21
fractionation of, in mass spectrometer leak B28
as intensity standard in election spin resonance F4
reaction of, with aldehydes B45
reaction of, with azide B4
reaction of, with cumene T11
reaction of, with ethylene H22
reaction of, with hydrocarbons M15
reaction of, with ketones D34
reaction of, with mercuric sulphide W2
reaction of, with sulphur W2
recovery of, from niobium H13
thermal diffusion of D23
vapour pressure of B27; J5
**Oxygen, molecular, $O_2^{18}$**
preparation of H37; W2
**Oxygen-17**
chemical shift of (see **Nuclear magnetic resonance**)
effect on decomposition of $H_2O_2$ M18
effect on Pu analysis H4
hyperfine structure of B20
quadrupole moment of B9; K2
**Oxygenases**
action of H16; H17; H18; H19; H20; H21; L11; S2; V5
**Ozone**
exchange with oxygen P1; S12

**P**

**Paleotemperatures** (temperatures of geological formation of carbonates from oxygen isotope ratio)
study of C11; C12; C18; D28; E4; E5; E6; L19; R1; T4; T15
**Palmitate, cetyl**
analysis (by mass spectrometer) S40
formation of S40
**Paraldehyde**
chemical shift of C7
**Pelargonic acid**
oxidation of H35
**Pelargonic acid-$O^{18}$**
preparation of H35
**2;4-Pentadione (Acetylacetone)**
chemical shift of C7; D22
***cyclo*Pentanone**
chemical shift of C7
**3-Pentanone (Diethylketone)**
oxidation of D34
**3-Pentanone, 2;4-dimethyl (Di*iso*propyl ketone)**
infra-red spectrum of K3
**3-Pentanone, 2;4-dimethyl-$O^{18}$**
preparation of K3
**Peracids** (see **Peroxyacids**)
**Perbenzoate, *tert.*-butyl**
reaction of, with *cyclo*hexene D13; D18; F2
reaction of, with phosphines G8; G11
**Perbenzoate, *tert.*-butyl-*carbonyl*-$O^{18}$**
preparation of F2; G11
**Perchlorate**
analysis of A8; H27
effect on iodine uptake in thyroid A8
exchange with water A8; B43; H27
**Perchlorate, ammonium**
decomposition of G1
**Perchlorate, potassium-$O^{18}$**
preparation of A8
**Perchloric acid**
analysis of (see **Perchlorate**)
chemical shift of C7
electrolysis of G3
exchange with water B43
**Periodate**
exchange with water B43
oxidation of glycols and diketones B69

**Permanganate**
exchange with water M9
oxidation of oleic acid W8
reaction of, with cyanide S41
reaction of, with $H_2O_2$ L18
**Permeability**
of cells A13; U2
**Peroxidase**
action of M16
**Peroxide, silver**
formation of B46
**Peroxides, organic**
reaction of, with amines D18
reaction of, with olefines D13; D18; G16
reaction of, with phenols D18
reaction of, with phosphines G15
**Peroxyacids**
exchange with water, F11
formation of B45; F11
hydrolysis of B45; F11
**Perrhenyl fluoride**
microwave spectrum of L17
**Perrhenyl fluoride-O$^{18}$**
preparation of L17
**Persulphate**
decomposition of B45; G4
formation of B45; G3
**Phenol**
analysis of V17
(see also individual phenols)
**Phenol, 2;4-dinitro**
analysis of D33; V17
exchange with water V17
effect on oxidative phosphorylation D33
**Phenol, 2;4-dinitro-*hydroxyl*-O$^{18}$**
preparation of D33
**Phenol, *p*-nitro**
analysis of V17
exchange with water V17
**Phenol, *p*-nitroso**
oxidation of B46
**Phosphatases**
action of K1
**Phosphate**
abundance in T5
analysis of A7; A12; A17; B61; B62; B66; C16; F5; F7; F8; H24; J9; K10; S24; T15, W11
exchange with water A22; B43; C16; R9; S24; T5; T15; W11
metabolism of F7; F8
from ribonucleic acids K15
in thiosulphate oxidation S5
**Phosphate-O$^{18}$**
preparation of A7; S24; V1
**Phosphate, acetyl**
arsenolysis of P4
hydrolysis of P4
**Phosphate, adenosine** (see **Adenosine phosphates**)
**Phosphate, carbamyl**
formation of J9; M24
**Phosphate, carbamyl-phosphate-O$^{18}$**
preparation of M24
**Phosphate, creatine**
turnover of F7; F8
**Phosphate dimethyl**
hydrolysis of B66
**Phosphate, D-glucose-1**
hydrolysis of B61
**Phosphate, 5-ionisine-6-O$^{18}$**
preparation of L14
**Phosphate, methyl**
exchange with water B62
hydrolysis of B62
**Phosphate, pyruvyl**
role of R9
**Phosphate, O-seryl**
hydrolysis of F5; F6
**Phosphate, transfer**
enzymic A23; S23
**Phosphate, urethane**
hydrolysis of H6
**Phosphine oxide, tributyl**
analysis of D15
formation of D15
**Phosphine oxide, triphenyl**
analysis of D15; G11; H8
exchange with water H8
formation of D15; G11
infra-red spectrum of H8
**Phosphine oxide, triphenyl-O$^{18}$**
preparation of H8
**Phosphine, tributyl**
reaction of, with peroxides D15; G11
**Phosphine, triphenyl**
reaction of, with peroxides D15; G8; G11; G15
**Phosphinic chloride, diethyl**
exchange with water H5
**Phosphinic fluoride, dimethyl**
exchange with water H5
**Phosphofluoridate, di*iso*propyl**
exchange with water H5
**Phosphonates**
analysis of H5
**Phosphoric acid**
analysis (see **Phosphate**)
exchange with water B43; K10
**Phosphoric acid-O$^{18}$**
preparation of A7

VOL. 11 1961

**Phosphorous acid**
exchange with water B43
**Phosphorylation, oxidative** (see **Oxidative phosphorylation**)
**Phosphourethane** (see **Phosphate, urethane**)
**Photochemistry**
decomposition of $N_2O$ H28
decomposition of persulphate T12
exchange between acetone and oxygen S39
oxidation of ketones D34
**Photophosphorylation**
study of A22
**Photosynthesis**
study of C1; H2; K19; U1; V15; V16
**Phthalamic acid**
hydrolysis of B14
**Phthalic acid**
analysis of B14
exchange with water B14
**Phthaloyl peroxide**
analysis of G16
reaction of, with *trans*-stilbene G16
**Phthaloyl peroxide-*carbonyl*-O$^{18}$**
preparation of G16
**Pinacol**
analysis of B57
exchange with water B57
reaction of, with periodate B69
rearrangement of B57
**Plumbic dioxide**
analysis of A7
**Plutonium**
effect of oxygen isotopes in analysis of H4
**Polyethylene**
diffusion of water in S11
**Polyorganoborosiloxanes**
formation of K27
**1;2-Propanediol, 2-methyl (*iso*Butylene glycol)**
reaction of, with periodate B69
**Propanol**
chemical shift of C7
**1-Propanone, 2-anilino, 1-phenyl**
analysis of N1
rearrangement of N1
**2-Propanone, 1-anilino, 2-phenyl**
analysis of N1
rearrangement of N1
**Propionaldehyde**
chemical shift of C7
**Propionate, ethyl**
analysis of K26
chemical shift of C7
reaction of, with butyl alcohol K26
**Propionate, ethyl-*alkoxy*-O$^{18}$**
preparation of K26
**Propionic acid**
chemical shift of C7
**Propionic acid, β-phenyl**
analysis of B17
exchange with water B17
**Propionic anhydride**
chemical shift of C7; D22
***iso*-Propyl alcohol**
auto-oxidation of B45; R13
chemical shift of C7
exchange with water R13
***cyclo*Propyl carboxylic acid**
analysis of D17
***cyclo*Propyl carboxylic acid-O$^{18}$**
preparation of D17
**Proteins**
determination of terminal acids in K18
**Pyrimidine**
biosynthesis, review of R2
**Pyrocatechase**
action of H19
**Pyrocatechol**
hydroxylation of H19
**Pyrophosphatase**
action of C16
**Pyrophosphate**
analysis of C17
**Pyruvate, ethyl**
chemical shift of C7

**Q**

**Quadrupole moment**
of oxygen-17 B9; K2
**Quartz**
abundance in C13; E8; K11
(see also **Silicon dioxide**)

**R**

**Radicals** (see **Hydroxyl radical, Triphenylmethyl radical**)
**Radiolysis**
of $H_2O_2$ A10
of water B1
**Rearrangements**
allylic B68; D24; G5; G6; G7; P12
of 2-anilino-1-phenylpropanone N1
anthranilic K31
of carbinamine nitrosoamides W7
pinacol B57
*cyclo*propylcarbinyl D17
**Resorcinol, dimethyl dihydro**
reaction of, with methanol W9
**Respiration**
animal C6; M4; M5; M6; M7; M8
isotope effect in L2
plant V2; V3

**Reviews** M30; R15; S4
analysis D3; D4; P1; S17; S18
biochemistry A18; A23; B35; B37; B38; C1; H17; H18; M17; R2
biology B31; H34; O1
chemistry B72; D1; M32; S27; S43; Z3
exchange B15; B43; B44; B47; B48; B49; M32
geochemistry E4; E9; J4; M22; M30; R1; T6; V7
inorganic chemistry B10; K20; R5; R6
nuclear magnetic resonance C7; D1
preparation of compounds M32; T7
separation A19; K21; P1; T1; Z3
**Rhenate**
exchange with water B43
**Ribonucleic acids**
ester linkages in tobacco mosaic virus of K15
**Rocks** (see **Abundance**—in minerals)
**Rusting** (see **Corrosion**)

VOL. 11 1961

S

**Salicylate, acetyl** (see **Benzoate, *o*-acetoxy**)
**Salicyclic acid** (see **Benzoic acid, *o*-hydroxy**)
**Selenate**
exchange with water B43
**Selenite**
exchange with water B43
**Separation by absorption**
of oxygen P2; S8
**Separation by chemical exchange**
A19; B21; B52; P1; S7; S8; S12; S13; S21; T1; T3; Y4
**Separation by diffusion**
of water vapour G17
(see also **Separation by thermal diffusion**)
**Separation by fractional crystallization**
of water K29
**Separation by fractional distillation**
of azeotropes H29; H30; H31
of CO D21; E1; J7; L16; T9
of methanol Z2
of oxides of nitrogen K28
of oxygen D21
of water B3; B8; D29; D30; D32; K21; K22; S22; T8; Z4
**Separation by thermal diffusion**
of CO H12; T16; V20; V21
of $CO_2$ B11
of oxygen D23; P1
of water P3
of water vapour D10
**Shift, chemical** (see **Nuclear magnetic resonance**)
**Shift, isotope** (see **Spectra**)
**Silica** (see **Silicon dioxide**)
**Silicates**
exchange with water S8; S36; S37; W15
reaction of, with borates K27
**Silicon dioxide**
abundance in C13; E8; K11
exchange with oxygen H41; S36
exchange with water H41
**Silicon, tetramethoxy**
chemical shift of C7
**Silicon, tetramethoxy-O$^{18}$**
preparation of K27
**Silver, oxide**
analysis of A7
**Silver, oxide-O$^{18}$**
preparation of W2
**Silver, peroxide**
formation of B46
solubility of water and tri-ethylamine K16
**Spectra, infra-red** (of oxygen-18 labelled compounds)
of alkali nitrates P13
of barium sulphate S30; S31
of benzophenone H7
of cinnamyl *p*-nitrobenzoate B40
of $CO_2$ C21
of 2;4-dimethyl-3-pentanone K3
of nitromethane H9
of nitrous acid B4
of 1-phenylallyl *p*-nitrobenzoate B40
of potassium nitrate A11
of silicon suboxide H33
of silver nitrite A11
of triphenylphosphine oxide H8
of water G9; P10; P11
**Spectra, microwave**
of acetyl cyanide K24
of acetyl fluoride P9
of formic acid C26
of methyl formate C25
of trimethylene oxide C5
**Spectra, nuclear magnetic resonance** (see **Nuclear magnetic resonance**)
**Spectra, Raman**
of disilyl ether M10
**Spectra, ultra-violet**
of MgO P7
**Starch**
hydrolysis of H10
**Stearic acid**
oxidation of H35
**Stearic acid, 9;10-dihydroxy**
analysis of W8
formation of W8
**Steel**
analysis of oxygen in P5

**Steroids**
analysis of B73
hydrolysis of sulphates of B73
hydroxylation of H21
reaction of, with $Al_2O_3$ D2
**Stilbene**
reaction of, with phthaloyl peroxide G16
**Stilbene, diol** (**1;2-Diphenylethane diol**)
analysis of G16
formation of G16
**Succinate**
analysis of F1
conversion to acetoacetate F1
**Succinate, dimethyl**
chemical shift of C7
**Succinic acid-O$^{18}$**
preparation of F1
**Sulphatases**
action of S28; S29; S30; S31
**Sulphate**
analysis of A7; S25; S30; S31
exchange with oxygen S35; S37
exchange with water B43
**Sulphate, *p*-acetylphenyl**
hydrolysis of S28; S29
**Sulphate, barium**
infra-red spectrum of S30; S31
**Sulphate, barium-O$^{18}$**
preparation of S30; S31
**Sulphate, *cyclo*hexane-1;2-diol**
hydrolysis of B41; B42
**Sulphate, 2-hydroxy-5-nitrophenyl**
hydrolysis of S28; S29
**Sulphate, lead**
formation of B46
**Sulphate, *p*-nitrophenyl**
hydrolysis of S28; S29; S31
**Sulphates, steroid**
hydrolysis of B73
**Sulphide, lead**
oxidation of B46
**Sulphinate** (see parent hydrocarbon)
**Sulphite**
exchange with water B43
**Sulphite, diethyl**
hydrolysis of B55
**Sulphite, dimethyl**
hydrolysis of B55
**Sulphite, ethylene**
exchange with water B54
hydrolysis of B54
**Sulphite, ethylene-*sulphoxy*-O$^{18}$**
preparation of B54
**Sulphite, propylene**
exchange with water B54
hydrolysis of B54
**Sulphonates** (see parent hydrocarbon)
**Sulphone, diphenyl**
exchange with water C8
**Sulphoxide, dimethyl**
chemical shift of C7
**Sulphur**
combustion of W2
**Sulphur dioxide**
exchange with $H_2SO_4$ H40
exchange with oxygen W2
exchange with $SO_3$ H40
reactions in liquid N2
separation of isotopes, by exchange B52
**Sulphur dioxide-O$^{18}$**
preparation of B54; H40
**Sulphuric acid**
analysis of (see **Sulphate**)
chemical shift of C7
exchange with CO R8
exchange with $CO_2$ H40
exchange with $SO_2$ H40
**Sulphuric acid-O$^{18}$**
preparation of A7
**Sulphur trioxide**
exchange with $SO_2$ H40

**T**

**Tantalates**
exchange with water, S34; S38
**Targets** (see **Nuclear reactions**)
**Tellurate**
exchange with water B43
**Tetrahydrofuran**
chemical shift of C7
**Tetramethoxy silicon** (see **Silicon, tetramethoxy**)
**Thionates**
exchange with water B43
**Thiosulphate**
exchange with water B43
oxidation of S5
**Threonine**
analysis of F5; F6
formation of F5; F6
**Threonine synthetase**
action of F5; F6
**Thyroid gland**
uptake of perchlorate in A8
**Tin**
corrosion of B45
**Tobacco mosaic virus**
ester linkages in K15
**Toluene**
oxidation of S44

**Toluene, *o*-nitro**
oxidation of S44
reaction of, with KOH B46
rearrangement of K31
**Toluene, 2-nitro, 4-sulphonic acid**
reaction of, with KOH B46
***p*-Toluene sulphinate, methyl**
hydrolysis of B58
***p*-Toluene sulphonate, 2;4-dinitrophenyl**
hydrolysis of V17
***p*-Toluene sulphonate, 1-*p*-methoxyphenyl-2-propyl**
analysis of G8
formation of G8
***p*-Toluene sulphonate, 2-methoxyphenyl-1-propyl**
analysis of G8
rearrangement of G8
**Transesterification**
study of K26
**Tributylphosphine** (see **Phosphine, tributyl**)
**Trimethylene, oxide**
analysis of (by mass spectrometer) D25
formation of D25
microwave spectrum of C5
**Trimethylene, oxide-O$^{18}$**
preparation of C5; D25
**Triphenylmethyl radical**
reaction of, with peroxides D26
**Triphenylphosphine** (see **Phosphine, triphenyl**)
**Tryptophan**
analysis of H24
oxygen transfer to phosphate B18; H24
**Tryptophan-O$^{18}$**
preparation of B18; H24
**Tryptophan, acetyl**
analysis of B17
exchange with water B17
**Tryptophan, acetyl-*carboxyl*-O$^{18}$**
preparation of B17
**Tungstates**
exchange with water B43; S33; S34
**Tungstic acid**
in hydroxylation of olefines S1
**Tyrosine**
exchange with water K18
**Tyrosine-*carboxyl*-O$^{18}$**
preparation of K18

U

**Uranium dioxide-O$^{18}$**
preparation of A21; B12
**Uranium oxides**
abundance in H25; H26
analysis of H25; H26; J8
diffusion of oxygen in A21; B12
exchange with $CO_2$ A21; B12
exchange with water H25; H26; J8
**Uranyl ferrocyanide-O$^{18}$**
preparation of A7
**Uranyl ion**
analysis of A7
exchange with water A6
**Urea**
chemical shift of C7
hydrolysis of S23
**Urease**
action of S23
**Urethane phosphate** (see **Phosphate, urethane**)

V

**Vanadium pentoxide**
exchange with oxygen R14
exchange with water R14
**Vapour pressure**
of azeotropes H30; H31
calculations of D20
of CO J5; J6
of NO B22; C14; C15; K28
of oxygen B27; J5; J6
of water K30
**Von Richter reaction**
study of S3

W

**Water** (see **Abundance, Analysis, Exchange, Hydrolysis, Radiolysis, Separation** and **Spectra**)

Z

**Zinc**
corrosion of B45, F9
isotope effect in reduction of CO S14
**Zinc oxide**
diffusion and exchange in M29; W10; W12; W13
exchange with CO W12; W13
exchange with $CO_2$ W12; W13
(see also **Oxides, mixed**)

VOL. 11 1961

# AUTHOR INDEX

## A


A-1 Abramova, T. M., Gankina, I. L. and Fomenko, A. S. The cathode reduction of oxygen to hydrogen peroxide on a carbon–nickel electrode. *Dopovidi Akad. Nauk Ukr. R.S.R.* 974–6 (1958). *C.A.* **53,** 6837i.

A-2 Amiel, S. and Segel, R. E. Search for oxygen-20. *J. Inorg. & Nuclear Chem.* **10,** 4–7 (1959). *C.A.* **53,** 15802i.

A-3 Amsel, G. and Smulkowski, O. High resolution spectroscopy using p-n junctions, applied to the study of nuclear reactions: $O^{18}$(d, α) $N^{16}$ reaction. *Compt. rend.* **251,** 950–2 (1960).

A-4 Anbar, M. Reactions of hydroxylamine with various oxidising agents. *Bull. Research Council Israel* **7A,** 206–7 (1958).

A-5 Anbar, M. Isotope analysis of oxygen in water. *Intern. J. Appl. Radiation and Isotopes* **3,** 131–4 (1958). *C.A.* **52,** 12661i.

A-6 Anbar, M. and Guttmann, S. The isotopic exchange of oxygen between uranyl ions and water. *Bull. Research Council Israel* **8A,** 146 (1959).

A-7 Anbar, M. and Guttmann, S. Isotope analysis of oxygen in inorganic compounds. *Intern. J. Appl. Radiation and Isotopes* **3,** 233–5 (1959). *C.A.* **53,** 18671d.

A-8 Anbar, M., Guttmann, S. and Lewitus, Z. The mode of action of perchlorate ions on the iodine uptake of the thyroid gland. *Intern. J. Appl. Radiation and Isotopes* **7,** 87–96 (1959).

A-9 Anbar, M., Guttmann, S. and Rein, R. The isotopic exchange between hypohalites and halide ions—II. The exchange between hypochlorous acid and chloride ions. *J. Am. Chem. Soc.* **81,** 1816–21 (1959). *C.A.* **53,** 14656a.

A-10 Anbar, M., Guttmann, S. and Stein, G. Radiolysis of highly enriched oxygen-18 water solutions containing hydrogen peroxide-$O_2^{16}$. *Nature* **187,** 57 (1960).

A-11 Anbar, M., Halmann, M. and Pinchas, S. The infra-red spectrum of oxygen-18 labelled salts—I. Silver nitrite and potassium nitrate. *J. Chem. Soc.* **1960,** 1242–5. *C.A.* **54,** 12777a.

A-12 Anbar, M., Halmann, M. and Silver, B. Determination of oxygen-18 in phosphate ion. *Anal. Chem.* **32,** 841 (1960).

A-13 Anbar, M. and Lewitus, Z. Rate of body water distribution studied with triple-labelled water. *Nature* **181,** 344 (1958). *C.A.* **52,** 13915g.

A-14 Anbar, M. and Rein, R. The isotopic exchange between hypohalites and halide ions—I. The exchange between hypobromous acid and bromide ions. *J. Am. Chem. Soc.* **81,** 1813–5 (1959). *C.A.* **53,** 14655f.

A-15 Anbar, M. and Samuel, D. The elucidation of the mechanism of acid hydrolysis of nitroparaffins using tracers. *Bull. Research Council Israel* **8A,** 139–40 (1959).

A-16 Anbar, M. and Taube, H. The exchange of hypochlorite and of hypobromite ions with water. *J. Am. Chem. Soc.* **80,** 1073–7 (1958). *C.A.* **52,** 12525b.

A-17 Anderson, L. and Kelley, J. J. The dephosphorylation of casein by alkalies. *J. Amer. Chem. Soc.* **81,** 2275–6 (1959). *C.A.* **53,** 20182d. *Federation Proc.* **18,** 182 (1959).

A-18 Arnstein, H. R. V. and Grant, P. T. The use of isotopes in the study of intermediary metabolism. *Progress in Biophysics and Biophysical Chemistry.* Vol. 7, pp. 167–224. Pergamon Press, London (1957). *C.A.* **52,** 17352e.

A-19 Augood, D. R. Chemical exchange. *Ind. Chemist* **34,** 16–26 (1958). *C.A.* **53,** 36c.

A-20 Ault, W. U. Oxygen isotope measurements on arctic cores. *USAF Cambridge Research Center Geophys. Res. Papers No. 63 Scientific studies at Fletchers Ice Island, T-3 (1952–1955)* **1,** 159–68. *Geophys. Abst.* **181,** 223 (1959).

A-21 Auskern, A. B. and Belle, J. Self diffusion of oxygen in uranium dioxide. *J. Chem. Phys.* **28,** 171–2 (1958). *C.A.* **52,** 7802h.

A-22 Avron, M. and Sharon, N. A study of photophosphorylation with oxygen-18. *Biochem. Biophys. Research Commun.* **2,** 336–9 (1960).

A-23 Axelrod, B. Enzymatic phosphate transfer. *Advances in Enzymology* Vol. 17, pp. 159–88. Interscience, New York (1956).

VOL. 11 1961

## B


B-1 BACKHURST, I. D., JOHNSON, G. R. A., SCHOLES, G. and WEISS, J. Determination of the yields of molecular hydrogen peroxide in the radiolysis of water labelled with oxygen-18. *Nature* **183,** 176–7 (1959). *C.A.* **54,** 6392f.

B-2 BAERTSCHI, P. and THÜRKAUF, M. A simplified float method for the $D_2O$ analysis of water. *Helv. Chim. Acta* **42,** 282–92 (1959). *C.A.* **53,** 13459i.

B-3 BAERTSCHI, P. and THÜRKAUF, M. The isotope effect in the separation of the isotopes of oxygen oxygen-16 and oxygen-18 by the rectification of light and heavy water. *Helv. Chim. Acta* **43,** 80–9 (1960). *C.A.* **54,** 12818c.

B-4 BALDESCHWIELER, J. D. and PIMENTEL, G. C. Light induced *cis-trans* isomerization of nitrous acid formed by photolysis of hydrazoic acid and oxygen in solid nitrogen. *J. Chem. Phys.* **33,** 1008–15 (1960).

B-5 BALDWIN, H. W. and TAUBE, H. Flow adaptation of the isotopic dilution method for the study of ionic hydration. *J. Chem. Phys.* **33,** 206–10 (1960).

B-6 BANK, C. A. Kinetics of the isotopic exchange in the system $CO_2$–$O_2$ with oxygen-18 as tracer in a transparent quartz vessel. *J. Inorg. & Nuclear Chem.* **7,** 145–6 (1958). *C.A.* **52,** 19360e.

B-7 BARRY, T. I. and STONE, F. S. The reactions of oxygen at dark and irradiated zinc oxide surfaces. *Proc. Roy. Soc. London* **A255,** 124–44 (1960). *C.A.* **54,** 14902d.

B-8 BARTKY, W. and DEMPSTER, A. J. The approach to equilibrium in fractionation. *Rev. Modern Phys.* **20,** 123–7 (1948). *C.A.* **42,** 4428i.

B-9 BARTON, G., BRINK, D. M. and DELVES, L. M. Quadruple enhancement in $O^{17}$ and $F^{17}$. *Nuclear Phys.* **14,** 256–62 (1959). *C.A.* **54,** 22073a.

B-10 BASOLO, F. and PEARSON, R. G. *Mechanisms of Inorganic Reactions* pp. 157–63. John Wiley, N.Y. (1958). *C.A.* **52,** 12648h.

B-11 BECKER, E. W. and DÖRNENBURG, E. Relation between reversal temperature of thermal diffusion of isotopes and mean molecular mass. *Naturwissenschaften* **37,** 165–6 (1950). *C.A.* **45,** 45g.

B-12 BELLE, J. and AUSKERN, A. B. Oxygen ion self-diffusion in uranium dioxide. *Kinetics of High-temperature Processes* (Edited by KINTER, W. D.) pp. 44–9. M.I.T. and John Wiley, N.Y. (1959). *C.A.* **54,** 6241a.

B-13 BENDER, M. L., CHLOUPEK, F. and NEVEU, M. C. Intramolecular catalysis of hydrolytic reactions—III. Intramolecular catalysis by carboxylate ion in the hydrolysis of methyl hydrogen phthalate. *J. Am. Chem. Soc.* **80,** 5384–7 (1958).

B-14 BENDER, M. L., CHOW, Y-L and CHLOUPEK, F. Intramolecular catalysis of hydrolytic reactions—II. The hydrolysis of phthalamic acid. *J. Am. Chem. Soc.* **80,** 5380–4 (1958).

B-15 BENDER, H. L. and GINGER, R. D. Solvent effects in the hydrolysis of an ester, an amide, and an acid chloride involving carbonyl oxygen exchange. *Suomen Kemistilehti* **B33,** 25–30 (1960).

B-16 BENDER, M. L., GINGER, R. D. and UNIK, J. P. Activation energies of the hydrolysis of esters and amides involving carbonyl oxygen exchange. *J. Am. Chem. Soc.* **80,** 1044–8 (1958). *C.A.* **52,** 115 38f.

B-17 BENDER, M. L. and KEMP, K. C. The kinetics of the α-chymotrypsin catalysed oxygen exchange of carboxylic acids. *J. Am. Chem. Soc.* **79,** 116–20 (1957).

B-18 BERNLOHR, R. W. and WEBSTER, G. C. Transfer of oxygen-18 during amino-acid activation. *Arch. Biochem. Biophys.* **73,** 276–8 (1958). *C.A.* **52,** 9254i.

B-19 BERNSTEIN, R. B. Hydrogen and oxygen isotopes applied to the study of water metal reactions. Exchange of $D_2O^{18}$ with α-alumina monohydrate. *U.S. Atomic Energy Commission ANL-5889* pp. 1–15 (1958). *C.A.* **53,** 2756c.

B-20 BESIS-MAZLOUM, N. and LEFEBVRE-BRION, H. Calculation of the hyperfine structure constants of the atoms $N^{14}$ and $O^{17}$ by the method of configuration interaction. *Compt. rend.* **251,** 648–50 (1960).

B-21 BIGELEISEN, J. Temperature independent isotope effects in chemical exchange equilibria involving linear molecules. *Proc. U.N. Intern. Conf. Peaceful Uses Atomic Energy, 2nd Geneva 1958* **4,** 480–4 (1958).

B-22 Bigeleisen, J. Vapour presures and related thermodynamic properties of the isotopic nitric oxide molecular. *J. Chem. Phys.* **33,** 1775–7 (1960).

B-23 Bilaniuk, O. M. Structure of oxygen-18. *Dissertation Abstr.* **18,** 2183–4 (1958).

B-24 Bilaniuk, O. M. and Hough, P. V. C. Spin, parity, and *j–j* expansion coefficients for states of low excitation in oxygen-18. *Phys. Rev.* **108,** 305–10 (1957). *C.A.* **52,** 4344i.

B-25 Blair, J. M. and Leigh, J. J. Total cross sections of the $O^{18}$ (p, α)$N^{15}$ and $O^{18}$ (p, n)$F^{18}$ reactions. *Phys. Rev.* **118,** 495–8 (1960). *C.A.* **54,** 23893i.

B-26 Blaser, J. P., Boehm, F., Marmier, P. and Scherrer, P. Excitation function of (p, n) reactions—III. Light elements. *Helv. Phys. Acta* **24,** 465–82 (1951). *C.A.* **46,** 2417d.

B-27 Boato, G., Scoles, G. and Valiauri, M. E. Vapour pressure of isotopic liquids—I. A, $N_2$, $O_2$ below boiling point. *Nuovo cimento* **14,** 735–47 (1959).

B-28 Boerboom, A. J. H. and Tasman, H. A. Fractionation of gaseous samples in a mass-spectrometer viscous leak. *Physica* **24,** 683–91 (1958). *C.A.* **53,** 2819f.

B-29 Borek, E. and Rittenberg, D. Anomalous growth of micro-organisms produced by changes in isotopes in their environment. *Proc. Natl. Acad. Sci. U.S.* **46,** 777–82 (1960).

B-30 Boschan, R. The reaction of alkylchloroformates with silver nitrate. Evidence for the stereoselective intramolecular formation of nitrate esters. *J. Am. Chem. Soc.* **81,** 3341–6 (1959).

B-31 Bowen, H. J. M. Biological fractionation of isotopes. *Intern. J. Appl. Radiation and Isotopes,* **7,** 261–72 (1960).

B-32 Bowers, K. D., Kamper, B. A. and Knight, R. B. D. A precision paramagnetic resonance spectrometer. *J. Sci. Instr.* **34,** 49–53 (1957). *C.A.* **51,** 8534f.

B-33 Boyd, R. H. Rate of isotopic oxygen exchange between water and aliphatic alcohols and its relation to the mechanism of alcohol olefin interconversion. *Dissertation Abstr.* **20,** 516–7 (1959).

B-34 Boyd, R. H., Taft, R. W., Jr., Wolf, A. P. and Christman, D. R. Studies on the mechanism of olefin–alcohol interconversion. The effect of acidity on the oxygen-18 exchange and dehydration rates of *tert.*-alcohols. *J. Am. Chem. Soc.* **82,** 4729–36 (1960).

B-35 Boyer, P. D. On the nature of the oxidative phosphorylation process. *Proc. Intern., Symposium Enzyme Chem. Tokyo and Kyoto* **2,** 301–7 (1957). *C.A.* **53,** 15145i.

B-36 Boyer, P. D. Uses and limitations of measurements of rates of isotopic exchange and incorporation in catalysed reactions. *Arch. Biochem. Biophys.* **82,** 387–410 (1959).

B-37 Boyer, P. D. and Harrison, W. H., *The Mechanism of Enzyme Action* Ed. W. D. McElroy and B. Glass pp. 658–70. Johns Hopkins, Baltimore (1954).

B-38 Boyer, P. D. and Stulberg, M. P. Tracing of the *in vivo* path from amino and to protein. *Proc. Natl. Acad. Sci. U.S.* **44,** 92–7 (1958). *C.A.* **52,** 12027g.

B-39 Brandner, J. D. and Urey, H. C. Kinetics of the isotopic exchange reaction between carbon monoxide and carbon dioxide. *J. Chem. Phys.* **13,** 351–62 (1945). *C.A.* **39,** 5159.

B-40 Braude, E. A. and Turner, D. W. Anionotropic systems—VI. The rearrangement of 1-phenylallyl *p*-nitrobenzoate in chlorobenzene. Tracer studies. *J. Chem. Soc.* **1958,** 2404–11. *C.A.* **52,** 17081g.

B-41 Brimacombe, J. S., Foster, A. B., Hancock, E. B., Overend, W. G. and Stacey, M. Aspects of stereochemistry—III. Acidic and basic hydrolysis of some diol cyclic sulfates and related compounds. *J. Chem. Soc.* **1960,** 201–11. *C.A.* **54,** 9787e.

B-42 Brimacombe, J. S., Foster, A. B. and Stacey, M. Hydrolysis of the cyclic sulphates of *cyclo*hexane-*cis*- and *trans*-1,2-diol and related compounds. *Chem. and Ind. (Rev.)* **1959,** 262–3. *C.A.* **53,** 14967i.

B-43 Brodskii, A. I. Mechanism of chemical exchange reactions by the use of isotopes—II. Exchange and mobility of oxygen, sulphur and nitrogen. *J. chim. phys.* **55,** 40–52 (1958). *C.A.* **52,** 11537b.

B-44 Brodskii, A. I. Isotope exchange. *Khim. Nauka i Prom.* **4,** 423–34, (1959). *C.A.* **54,** 7260h.

VOL. 11 1961

B-45 Brodskii, A. I. Study of reaction mechanisms producing hydrogen peroxide and peroxy acids by isotope methods. *Kernenergie* **3,** 822–7 (1960).

B-46 Brodskii, A. I. Study of mechanisms of certain oxidation–reduction reactions by isotope methods. *Kernenergie* **3,** 827–33 (1960).

B-47 Brodskii, A. I. and Vysotskaya, N. A. An exchange of oxygen in inorganic acids. *Problemy Kinetikii Kataliza, Akad. Nauk S.S.S.R.* 1956 **9,** 245–50 (1957). *C.A.* **53,** 8783d.

B-48 Brodskii, A. I. and Vysotskaya, N. A. Oxygen isotope exchange in solutions of salts and acids and its mechanism *Zhur. Fiz. Khim.* **32,** 1521–31 (1958). *C.A.* **53,** 1901d.

B-49 Brodskii, A. I., Vysotskaya, N. A., Kukhtenko I. I., Miklukhin, G. P., Strizhak, L. L. and Sulima, L. V. Isotope exchange mechanism of oxygen, nitrogen and sulphur in solutions. *Trudy Vsesoyuz. Nauch.-Tekh. Konf. po Primenen. Radioakiv. i Stabil. Izotopov i Izluchenii v Narod. Khoz. i Nauke, Moscow 1957, Izotopy i Izlucheniya v Khim.* 20–9 (1958). *C.A.* **53,** 19537e.

B-50 Brown, J. B. Determination of oxygen isotope ratios by density measurements. *J. Sci. Labs. Denison Univ.* **44,** Article 6, 96–105 (1957). *C.A.* **52,** 4260i.

B-51 Brown J. B. Coefficient of expansion of Pyrex glass floats used in density determinations. *J. Sci. Labs. Denison. Univ.* **44,** Article 7, 106–15 (1957). *C.A.* **52,** 3413f.

B-52 Brown, L. L. and Drury, J. S. The fractionation of oxygen isotopes between water and sulphur dioxide. *J. Phys. Chem.* **63,** 1885–6 (1959). *C.A.* **54,** 5283c.

B-53 Bunton, C. A., Dahn, H. and Loewe, L. Oxidation of ascorbic acid and similar reductions by nitrous acid. *Nature* **183,** 163–5 (1959). *C.A.* **53,** 16980b.

B-54 Bunton, C. A., De La Mare, P. B. D., Greaseley, P. M., Llewellyn, D. R., Pratt, N. H. and Tillett, J. D. Nucleophilic displacement in organic sulphites—I. The position of bond fission in the hydrolysis of some 1,2- and 1,3-cyclic sulphites. *J. Chem. Soc.* **1958,** 4751–4. *C.A.* **53,** 7978d.

B-55 Bunton, C. A., De La Mare, P. B. D. and Tillett, J. G. Nucleophilic displacement in organic sulphites—V. The acid-catalysed hydrolysis of diethyl sulphite and of dimethyl sulphite. *J. Chem. Soc.* **1959,** 1766–74.

B-56 Bunton, C. A. and Hadwick, T. Tracer studies in ester hydrolysis—VI. The hydrolysis of methyl trifluoracetate. *J. Chem. Soc.* **1958,** 3248–56. *C.A.* **53,** 5188d.

B-57 Bunton, C. A., Hadwick, T., Llewellyn, D. R. and Pocker, Y. Tracer studies in alcohols—III. Intermediates in the pinacol–pinacolone rearrangement. *J. Chem. Soc.* **1958,** 403–8. *C.A.* **52,** 10874g.

B-58 Bunton, C. A. and Hendy, B. N. Hydrolysis of methyl toluene-*p*-sulphinate. *Chem. and Ind. (Rev.)* **1960,** 466.

B-59 Bunton, C. A., Israel, G., Mhala, M. M. and Williams, D. L. H. Tracer studies in ester hydrolysis—VII. The hydrolysis of 9-fluorenyl acetate. *J. Chem. Soc.* **1958,** 3718–20. *C.A.* **53,** 5189g.

B-60 Bunton, C. A., James, D. H. and Senior, J. B. Tracer studies in ester hydrolysis—VIII. The oxygen exchange between water and carboxylic acids. *J. Chem. Soc.* **1960,** 3364–7.

B-61 Bunton, C. A., Llewellyn, D. R., Oldham, K. G. and Vernon, C. A. Reactions of organic phosphates—II. The hydrolysis of α-D-glucose-1-(dihydrogen phosphate). *J. Chem. Soc.* **1958,** 3588–94. *C.A.* **53,** 10050c.

B-62 Bunton, C. A., Llewellyn, D. R., Oldham, K. G. and Vernon, C. A. Reactions of organic phosphates—I. The hydrolysis of methyl dihydrogen phosphate. *J. Chem. Soc.* **1958,** 3574–87. *C.A.* **53,** 10050b.

B-63 Bunton, C. A., Llewellyn, D. R. and Stedman, G. Oxygen exchange between nitrous acid and water. *J. Chem. Soc.* **1959,** 568–73. *Chemistry Society Special Publication* No. 10, pp. 113–22 (1959). *C.A.* **53,** 8780b.

B-64 Bunton, C. A., Llewellyn, D. R. and Wilson, I. Tracer studies on alcohols—IV. The oxygen exchange and racemisation of 4-methoxydiphenyl methanol. *J. Chem. Soc.* **1958,** 4747–51. *C.A.* **53,** 5836f.

B-65 Bunton, C. A. and Masui, M. Oxygen exchange between nitrous acid and water—II. Exchange in acetate buffer. *J. Chem. Soc.* **1960,** 304–8. *C.A.* **54,** 9455a.

B-66 Bunton, C. A., Mhala, M. M., Oldham, K. G. and Vernon, C. A. The reactions of organic phosphates—III. The hydrolysis of dimethyl phosphate. *J. Chem. Soc.* **1960,** 3293–301.

B-67 Bunton, C. A. and Perry, S. G. The acid-catalysed hydrolysis of carboxylic anhydrides. *J. Chem. Soc.* **1960,** 3070–9.

B-68 Bunton, C. A., Pocker, Y. and Dahn, H. A carbonium ion intermediate in the rearrangement of 1- to 3-phenylallyl alcohol. *Chem. and Ind. (Rev.)* **1958,** 1516. *C.A.* **53,** 12228e.

B-69 Bunton, C. A. and Shiner, V. J., Jr. Periodate oxidation of 1,2-diols, diketones and hydroxyketones; the use of oxygen-18 as tracer. *J. Chem. Soc.* **1960,** 1593–8. *C.A.* **54,** 15236d.

B-70 Bunton, C. A. and Stedman, G. Oxygen exchange between nitric acid and water—IV. The nitration of 2-mesitylethanesulphonic acid. *J. Chem. Soc.* **1958,** 2420–1. *C.A.* **52,** 14295h.

B-71 Bunton, C. A. and Stedman, G. Mechanism of azide-nitrite reaction—III. Reaction in oxygen-18 water. *J. Chem. Soc.* **1959,** 3466–74. *C.A.* **54,** 6272c.

B-72 Burr, J. G., Jr. *Tracer Applications for the Study of Organic Reactions.* Interscience, New York, London (1957).

B-73 Burstein, S. and Lieberman, S. Kinetics and mechanism of solvolysis of steroid hydrogen sulphates. *J. Am. Chem. Soc.* **80,** 5235–9 (1958). *C.A.* **53,** 9288e.

B-74 Butler, J. W. and Holmgren, H. D. Radiative proton capture by oxygen-18. *Phys. Rev.* **116,** 1485–9 (1959). *C.A.* **54,** 238931g.

## C

C-1 Calvin, M., Anderson, J. M., Bassham, J. A., Blass, U., Holm-Hansen, O., Moses, V., Pon, N. G., Sogo, P. B. and Tollin, G. Photosynthesis. *Proc. U.N. Intern. Conf. Peaceful Uses Atomic Energy, 2nd Geneva 1958* **24,** 24–32 (1958).

C-2 Cantoni, G. L. and Durell, J. Activation of methionine for transmethylation—II. The methionine-activating enzyme: studies on the mechanism of the reaction. *J. Biol. Chem.* **225,** 1033–48 (1957).

C-3 Carlson, C. H., Singer, L., Service, D. H. and Armstrong, W. D. Preparation of carrier-free radiofluoride with a new estimate of the half-life of fluorine-18. *Intern. J. Appl. Radiation and Isotopes* **4,** 210–2 (1959). *C.A.* **53,** 8859d.

C-4 Cawley, J. J. and Westheimer, F. H. Mechanism of the hydrolysis of di-*t*-butyl benzal. *Chem. and Ind. (Rev.)* **1960,** 656.

C-5 Chan, S. I., Zinn, J., Fernandez, J. and Gwinn, W. D. Trimethylene oxide—I. Microwave spectrum dipole moment and double minimum vibration. *J. Chem. Phys.* **33,** 1643–55 (1960).

C-6 Chinard, F. P., Enns, T. and Nolan, M. F. Contribution of bicarbonate ion and of dissolved carbon dioxide to expired carbon dioxide in dogs. *Am. J. Physiol.* **198,** 78–88 (1960). *C.A.* **54,** 10095e.

C-7 Christ, H. A. The measurement of the chemical shift of oxygen-17 nuclear resonance lines. *Helv. Phys. Acta* **33,** 572–576 (1960).

C-8 Christman, D. R. and Shigeru, O. Non-oxygen exchange in sulphone group in alkaline decomposition of diphenyl sulphone and in alkaline hydrolysis of phenylbenzene sulphonate. *Chem. and Ind. (Rev.)* **1959,** 1251–2. *C.A.* **54,** 4451e.

C-9 Chupakhin, M. S. Recording of the oxygen isotope ratio in carbon monoxide. *Zhur. Anal. Khim.* **14,** 331–5 (1959). *C.A.* **54,** 8170d.

C-10 Clarke, R. L., Almqvist, E. and Paul, E. B. Properties of levels excited in (p, α) reactions on $O^{18}$, $P^{31}$, $Cl^{35}$ $Cl^{37}$, $K^{39}$ and $K^{41}$. *Nuclear Phys.* **14,** 472–97 (1959). *C.A.* **54,** 23894a.

C-11 Clayton, R. N. Oxygen isotope fractionation in the system calcium carbonate–water. *J. Chem. Phys.* **30,** 1246–50 (1959). *C.A.* **53,** 17646e.

C-12 Clayton, R. N. and Degens, E. T. Use of carbon isotope analyses of carbonates for differentiating fresh water and marine sediments. *Bull. Am. Assoc. Petrol. Geologists* **43,** 890–7 (1959). *C.A.* **53,** 14863c.

C-13 Clayton, R. N. and Epstein, S. The relationship between $O^{18}/O^{16}$ ratios in coexisting quartz carbonate and iron oxides from various geological deposits. *J. Geol.* **66,** 352–71 (1958). *C.A.* **52,** 19770f.

VOL. 11 1961

C-14 Clusius, K. and Schleich, K. Low temperature research—XX. Direct comparison of vapour pressures of $N_2^{14}$, $N^{14}N^{15}$, $N_2^{15}$, $N^{14}O^{16}$, $N^{15}O^{16}$ and $N^{14}O^{18}$ between their melting and boiling points. *Helv. Chim. Acta* **41,** 1342–58 (1958). *Proc. U.N. Intern. Conf. Peaceful Uses Atomic Energy, 2nd Geneva 1958* **4,** 485–90 (1958). *C.A.* **53,** 3813d.

C-15 Clusius, K., Schleich, K. and Vecchi, M. Low temperature research—XXIX. The abnormally large difference in vapour pressure between $N^{14}O^{16}$ and $N^{15}O^{16}$. *Helv. Chim. Acta* **42,** 2654–66 (1959). *C.A.* **54,** 11618c.

C-16 Cohn, M. Phosphate-water exchange reaction catalysed by inorganic pyrophosphatase of yeast. *J. Biol. Chem.* **230,** 369–79 (1958). *C.A.* **52,** 9312d.

C-17 Cohn, M. Enzymic hydrolysis of nucleoside triphosphate to nucleoside monophosphate and inorganic pyrophosphate. *Biochim. et Biophys. Acta* **37,** 344–6 (1960). *C.A.* **54,** 11110b.

C-18 Compston, W. Carbon isotopic compositions of certain marine invertebrates and coals from the Australian Permian. *Geochim. et Cosmochim. Acta* **18,** 1–22 (1960). *C.A.* **54,** 15138f.

C-19 Compston, W. and Epstein, S. A method for the preparation of carbon dioxide from water vapour for oxygen isotope analysis. *Trans. Am. Geophys. Union, 39th Meeting, May 1958* **39,** (1958).

C-20 Connick, R. B. and Poulson, R. E. Effect of paramagnetic ions on the nuclear magnetic resonance of oxygen-17 in water and the rate of elimination of water molecules from the first coordination sphere of cations. *J. Cheml. Phys.* **30,** 759–61 (1959). *C.A.* **53,** 14695d.

C-21 Courtoy, C. P. Infrared spectra of carbon dioxide at high dispersion and constant molecular concentration. *Ann. soc. sci. Bruxelles, Ser. I* **73,** 5–230 (1959). *C.A.* **53,** 15763a.

C-22 Craig, H. Deuterium-oxygen-18 tritium relationships in natural waters. *Proc. Conf. New Research Methods Hydrology, Scripps Inst.* Feb. 2–3 1957 14–21 (1957).

C-23 Craig, H., Mayeda, T. and Suess, H. E. Isotope composition of water from Neusiedler Lake near Vienna. *Monatsh. Chem.* **89,** 173–4 (1958). *C.A.* **52,** 16815g.

C-24 Crandall, D. I., Krueger, R. C., Anan, F., Yasunobu, K. and Mason, H. S. Oxygen transfer by the homogentisate oxidase of rat liver. *J. Biol. Chem.* **235,** 3011–5 (1960).

C-25 Curl, R. J. Jr. Microwave spectrum, barrier to internal rotation and structure of methyl formate. *J. Chem. Phys.* **30,** 1529–36 (1959). *C.A.* **53,** 18631b.

C-26 Curl, R. F., Jr. and Kwei, G. H. Microwave spectra of formic acid-$O^{18}$ and structure of formic acid. *J. Chem. Phys.* **32,** 1592–4 (1960).

**D**

D-1 Dahn, H. Isotopes of oxygen in organic chemistry. *Bull. Soc. Chim. France* **1960,** 1875–80.

D-2 Dahn, H., Menasse, R. and Tamm, C. A substitution reaction of 3-benzoyloxy-cholestene-1 by aluminium oxide. Investigation with the aid of isotopic oxygen. *Helv. Chim. Acta* **42,** 2189–98 (1959).

D-3 Dahn, H. and Moll, H. A new method for the determination of oxygen-18 in organic compounds. *Chem. and Ind. (Rev.)* **1959,** 399–400. *C.A.* **53,** 17754d.

D-4 Dahn, H. Moll, H. and Menasse, R. A new method for the determination of the isotopes of oxygen in organic compounds. *Helv. Chim. Acta* **42,** 1225–36 (1959). *C.A.* **53,** 21375j.

D-5 Dansgaard, W. The abundance of oxygen-18 in atmospheric water and water vapour. *Tellus* **5,** 461–9 (1953).

D-6 Dansgaard, W. Comparative measurements of standards for carbon isotopes. *Geochim. et Cosmochim. Acta* **3,** 253–6 (1953). *C.A.* **47,** 10367d.

D-7 Dansgaard, W. Some meteorological and glaciological problems shown by measurements of the stable isotopes of oxygen in water. *Fysisk Tidsskr.* Nr. 2–3, 49–65 (1958).

D-8 Dansgaard, W., Nief, G. and Roth, E. Isotopic distribution in a Greenland iceberg. *Nature* **185,** 232 (1960). *C.A.* **54,** 13776c.

D-9 Davies, M. O., Clark, M., Yaeger, E. and Hovorka, F. The oxygen electrode—I. Isotopic investigation of electrode mechanism. *J. Electrochem. Soc.* **106,** 56–61 (1959). *C.A.* 53, 3934h.

D-10 Davies, R. H. and Kendall, J. T. Thermal diffusion of water vapour. *Nature* **165,** 487 (1950).

D-11 Degens, E. T. The $O^{18}/O^{16}$ ratio in the primordial ocean and the geochemical exchange of matter. *Neues Jahrb. Geol. u. Palaontol. Monatsh.* No. 4, 1806 (1959). *C. A.* **53,** 14863e.

D-12 Denney, D. B. and Denney, D. Z. Studies of the mechanisms of the reactions of benzoyl peroxide with secondary amines and phenols. *J. Am. Chem. Soc.* **82,** 1389–93 (1960).

D-13 Denney, D. B., Denney, D. Z. and Feig, G. Some observations concerning the copper-salt catalysed reactions of *tert.*-butyl perbenzoate with olefins. *Tetrahedron Letters* No. 15, 19–23 (1959).

D-14 Denney, D. R. and Feig, G. A study of the induced decomposition of benzoyl peroxide in diethyl ether. *J. Am. Chem. Soc.* **81,** 5322–4 (1959).

D-15 Denney, D. B., Goodyear, W. F. and Goldstein, B. Concerning the mechanism of the reduction of hydroperoxides by trisubstituted phosphines and trisubstituted phosphites. *J. Am. Chem. Soc.* **82,** 1393–5 (1960). *C.A.* **54,** 15287d.

D-16 Denney, D. B. and Greenbaum, M. A. Concerning the mechanism of the reaction of anhydrides with amines. *J. Am. Chem. Soc.* **78,** 877–8 (1956). *C.A.* **50,** 13805h.

D-17 Denney, D. B. and Kupchik, E. J. An oxygen-18 tracer study of the isomerisation of *cyclo*propylcarbinyl benzenesulphonate. *J. Am. Chem. Soc.* **82,** 859–62. (1960).

D-18 Denney, D. Z. Studies of some peroxide reactions. *Dissertation Abstr.* **20,** 4274–5 (1960).

D-19 Dessau, G., Gionfantini, R. and Tongiorgi, E. The origin of Italian sulphur deposits. *Lo Zolto* No. *15–16,* 9–27 (1959).

D-20 Devyatykh, G. G. The application of a statistical method for calculating the effect of isotopes on vapour pressure. *Trudy Khim. i Khim. Tekhnol.* **1,** 239–49 (1958). *C.A.* **54,** 5197h.

D-21 Devyatykh, G. G., Zorin, A. D. and Nikolaev, N. I. Separation of carbon and oxygen isotopes by fractional distillation of carbon monoxide, methane and oxygen. *Zhur. Priklad. Khim.* **31,** 368–75 (1958). *C.A.* **52,** 12607e.

D-22 Dharmatti, S. S., Sundara Rao, K. J. and Vijayaraghavan, R. The construction and working of a wide line n-m-r spectrometer and the measurement of some chemical shifts. *Nuovo cimento* **11,** 656–69 (1959).

D-23 Dickel, G. Does catalysis displace the equilibrium in the separation tube? *Z. Electrochem.* **63,** 14–7 (1959). *C.A.* **53,** 7740a.

D-24 Dilgren, R. E. The rearrangement of α-phenylallyl alcohol in aqueous dioxan—I. Acid-catalysed rearrangement and loss of optical activity of α-phenylallyl alcohol in aqueous dioxan—II. Oxygen-18 exchange during the acid catalysed rearrangement of α-phenylallyl alcohol in aqueous dioxan. *Dissertation abstr.* **20,** 2012 (1959).

D-25 Dittmer, D. C., Hertler, W. R. and Winicov, H. Mechanism of trimethylene oxide formation from 3-chloropropyl acetate. *J. Am. Chem. Soc.* **79,** 4431–5 (1957). *C.A.* **52,** 344e.

D-26 Doering, W. V. E., Okamoto, K. and Krauch, H. On the distribution of oxygen-18 in triphenyl benzoate from the reaction of triphenylmethyl and benzoyl peroxide *carbonyl*-$O^{18}$. *J. Am. Chem. Soc.* **82,** 3579–82 (1960).

D-27 Dontsova, E. I. Method of determining isotope ratios for oxygen. *Geokhimia* **1959,** 669–78.

D-28 Dorman, F. H. and Gill, E. D. Oxygen isotope paleotemperature determinations of Australian cainozoic fossils. *Science* **130,** 1576 (1959). *Proc. Roy. Soc. Victoria* **71,** No. 1, 73.

D-29 Dostrovsky, I. The production and distribution of isotopes of oxygen. *Proc. U.N. Intern. Conf. Peaceful Uses Atomic Energy, 2nd Geneva, 1958* **4,** 605–7 (1958).

D-30 Dostrovsky, I. and Raviv, A. Separation of the heavy isotopes of oxygen by distillation. *Proc. Intern. Symposium Isotope Separation Amsterdam 1957* 336–49 (1958). *C.A.* **52,** 11597d.

D-31 Drew, E. H. and Martin, J. C. Induced decomposition of benzoyl peroxide. *Chem. and Ind. (Rev.)* 925–6 (1959). *C.A.* **54,** 1402c.

D-32 Drury, J. S. and Klima, P. B. Preliminary estimate of cost of producing enriched oxygen-18 water by distillation. CF-58-10-5 ORNL (1958). *Nuclear Sci. Abstr.* **13,** 1602g.

D-33 Drysdale, G. R. and Cohn, M. Mode of action of 2,4-dinitrophenol in uncoupling oxidative phosphorylation. *J. Biol. Chem.* **233,** 1574–7 (1958). *C.A.* **53,** 8241i.

VOL
11
196

D-34 Dunn, J. R. and Kutsche, K. O. Photo-oxidation of ketones in an oxygen-18 enriched environment. *Can. J. Chem.* **36,** 421–4 (1958). *C.A.* **52,** 11738b.

**E**

E-1 Edmunds, A. O. and Loveless, F. C. Production of boron-10 and other stable isotopes. *Proc. U.N. Intern. Conf. Peaceful Uses Atomic Energy, 2nd Geneva, 1958* **4,** 576–84 (1958). *C.A.* **54,** 23911f.

E-2 Ehrensvärd, G. Octadecylamine as absorption medium for $CO_2$[18]. *Z. Naturforsch.* **14b,** 607 (1959). *C.A.* **54,** 5344g.

E-3 Emiliani, C. Oxygen isotope measurements of deep-sea sediments. *Natl. Acad. Sci. Natl. Research Council Publ. No.* **473,** 67–78 (1956). *C.A.* **52,** 8872a.

E-4 Emiliani, C. Ancient temperatures. *Sci. American* **198,** No. 2, 54–63 (1958).

E-5 Emiliani, C. Paleotemperature analysis of core 280 and Pleistocene correlations. *J. Geol.* **66,** 264–75 (1958).

E-6 Emiliani, C. and Edwards, G. Tertiary ocean bottom temperatures. *Nature* **171,** 887–8 (1953).

E-7 Engel, A. E. J., Clayton, R. N. and Epstein, S. Variations in isotopic composition of oxygen and carbon in Leadville limestone, (Mississippian, Colorado), and its hydrothermal metamorphic phases. *J. Geol.* **66,** 374–93 (1958). *C.A.* **52,** 19770i.

E-8 Engel, A. E. J. and Engel, C. G. Progressive metamorphism and granitization of the major paragneiss Northwest Adirondack Mountains, New York—I. Total rock. *Bull. Geol. Soc. Am.* **69,** 1369–414 (1958). *C.A.* **53,** 4042a.

E-9 Epstein, S. The variations of the $O^{18}/O^{16}$ ratio in nature and some geological implications. *Researches in Geochem.* **1959,** 217–40. *C.A.* **53,** 12110c.

E-10 Epstein, S. and Sharp, R. P. Oxygen isotope variations in the Malaspina and Saskatchewan Glaciers. *J. Geol.* **67,** 88–102 (1958). *C.A.* **53,** 9933f.

**F**

F-1 Falcone, A. B. and Boyer, P. D. Studies concerning the mechanism of action of acetoacetyl succinic thiophorase by use of oxygen-18. *Arch. Biochem. Biophys.* **83,** 337–44 (1959). *C.A.* **53,** 20182a.

F-2 Feig, G. A study of some reactions of benzoyl peroxides and tert-butyl perbenzoate. *Dissertation Abstr.* **20,** 1166–7 (1959).

F-3 Feldman, D. E., Yost, H. T. and Benson, B. B. Oxygen isotope fractionation in reactions catalysed by enzymes. *Science* **129,** 146–7 (1959). *C.A.* **53,** 10927c.

F-4 Filipovich, G. and Sanders, T. M. Jr. $O^{16}O^{18}$ molecules as intensity standards in electron spin resonance spectroscopy. *Rev. Sci. Instr.* **30,** 293–4 (1959). *C.A.* **54,** 14961e.

F-5 Flavin, M. and Kono, T. Threonine synthetase mechanism: Studies with isotopic oxygen. *J. Biol. Chem.* **235,** 1109–11 (1960).

F-6 Flavin, M. and Slaughter, C. Mechanism of enzymic formation of threonine from o-phosphorohomoserine. *Biochem. et Biophys. Acta* **36,** 554–6 (1959). *C.A.* **54,** 5779c.

F-7 Fleckenstein, A., Gerlach, E. Janke, J. and Marmier, P. The determination of the turnover of ATP, creatine phosphate and orthophosphate in living muscle with $H_2O^{18}$ and subsequent activation by proton bombardment. *Naturwissenschaften* **46,** 365–7 (1959) *C.A.* **53,** 20416b.

F-8 Fleckenstein, A., Gerlach, E., Janke, J. and Marmier, P. The incorporation of labelled oxygen from water in the ATP, creatine phosphate and orthophosphate fractions of intact muscle at rest. *Arch. ges. Physiol., Pflügers* **271,** 75–104 (1960).

F-9 Fomenko, A. S., Abramova, T. M. and Gankina, I. L. Study of the mechanisms of corrosion of iron, magnesium, zinc and aluminium, using heavy oxygen. *Trudy Chetvertogo Soveshchaniya Elektrokhim., Moscow 1956* 299–302 (1959). *C.A.* **54,** 7501a.

F-10 Fomenko, A. S., Abramova, T. M. and Gankina, I. L. Studies on metallic corrosion with the aid of the heavy oxygen isotope—II. Moist atmospheric corrosion of cadmium. *Zhur. Fiz. Khim.* **33,** 2249–52 (1959). *C.A.* **54,** 11943b.

F-11 Franchuk, I. F. and Brodskii, A. I. The isotope exchange method of investigation of the electrolytic formation and decomposition of peroxycarbonates, perborates and peroxyphosphates. *Doklady Akad. Nauk S.S.S.R.* **118,** 128–31 (1958). *C.A.* **52,** 19353a.

VOL. 11 1961

F-12 Fraser, R. T. M. and Taube, H. Activation of bridging groups in electron transfer—II. The position of bond breaking in ester hydrolysis. *J. Am. Chem. Soc.* **81,** 5000–1 (1959). *C.A.* **54,** 7555b.

F-13 Friedman, L., Henkes, W. and Christman, D. Carbon-14 nitrogen-14 mass difference and mass excess of some light nuclides. *Phys. Rev.* **115,** 166–9 (1959). *C.A.* **54,** 7367d.

F-14 Frumkin, A. N. The use of oxygen-18 in the investigation of the mechanism of anodic processes. *Proc. Intern. Comm. Electrochem. Thermodynam. Kinet.* 396–403 (1959). *C.A.* **54,** 8351d.

G

G-1 Galwey, A. K. and Jacobs, P. W. M. The thermal decomposition of ammonium perchlorate in the presence of manganese dioxide. *Trans. Faraday Soc.* **55,** 1165–72 (1959).

G-2 Gatenbeck, S. and Mosbach, K. Acetate carboxyl oxygen (oxygen-18) as donor for phenolic hydroxy groups of orsellinic acid produced by fungi. *Acta Chem. Scand.* **13,** 1561–4 (1959).

G-3 Gerovich, M. A. and Kaganovich, R. I. The study of the mechanisms of some anodic processes by combining electrochemical with tracer methods. *Trudy Chetvertogo Soveshchaniya Elektrokhim., Moscow 1956* 277–81 (1959). *C.A.* **54,** 8351h.

G-4 Giuliano, C. R., Schwartz, N. and Wilmarth, W. K. The aqueous chemistry of inorganic free radicals—II. The peroxydisulphate induced exchange of oxygen atoms between water and molecular oxygen and evidence regarding the acidity constant of the hydroxyl radical. *J. Phys. Chem.* **63,** 353–8 (1959). *C.A.* **53,** 13752b.

G-5 Goering, H. L. and Dilgren, R. E. Oxygen exchange associated with the acid catalysed rearrangement of α-phenylallyl alcohol in aqueous dioxan. *J. Am. Chem. Soc.* **82,** 5744–9 (1960).

G-6 Goering, H. L. and Doi, J. T. Stereochemistry of allylic rearrangements—XI. The isomeric rearrangement of *trans*-5-methyl-2-*cyclo*hexenyl-*p*-nitrobenzoate-*carbonyl*-$O^{18}$ in aqueous acetone. *J. Am. Chem. Soc.* **82,** 5850–4 (1960).

G-7 Goering, H. L. and Pombo, M. M. Stereochemistry of allylic rearrangements—X. The isomeric rearrangement and solvolysis of *trans*-α,γ-dimethylallyl-p-nitrobenzoate in aqueous acetone. *J. Am. Chem. Soc.* **82,** 2515–21 (1960).

G-8 Goldstein, B. An oxygen-18 tracer study of external ion pair formation and a study of the mechanism of the reaction of peresters with trisubstituted phosphines. *Dissertation Abstr.* **19,** 228–229 (1958).

G-9 Gompertz, G. and Orville-Thomas W. J. Calculated vibrational frequencies of $H_2O^{18}$ and $D_2O^{18}$. *J. Phys. Chem.* **63,** 1331–2 (1959).

G-10 Gionfiantini, R. and Picciotto, E. Oxygen isotope variations in antarctic snow samples. *Nature* **184,** 1557–8 (1959). *C.A.* **54,** 9397d.

G-11 Goodyear, W. F. Jr. Studies of the reactions of peresters and hydroperoxides with trisubstituted phosphines. *Dissertation Abstr.* **20,** 4276 (1960).

G-12 Görisch, V., Ludewig, R. and Hübner, G. Evaluation of a clinical treatment method using the stable isotope oxygen-18. *Kernenergie* **3,** 853–4 (1960).

G-13 Gragerov, I. F. A rapid mass-spectrometric method of analysis of oxygen isotope in organic compounds. *Problemy Kinetiki i Kataliza, Akad. Nauk S.S.S.R. 1956* **9,** 373–7 (1957). *C.A.* **53,** 6786i.

G-14 Gragerov, I. P. and Ponomarchuk, M. P. Isotope exchange of oxygen of substituted benzoic acids with $H_2O^{18}$. *Zhur. Obshchei Khim.* **29,** 3895–7 (1959).

G-15 Greenbaum, M. A., Denney, D. B. and Hoffmann, A. K. A study of the mechanism of the conversion of benzoyl peroxide to benzoic anhydride by triphenyl-phosphine. *J. Am. Chem. Soc.* **78,** 2563–5 (1956). *C.A.* **51,** 1086d.

G-16 Greene, F. H. Cyclic diacyl peroxides—IV. Phthaloyl peroxide-*carbonyl*-$O^{18}$. *J. Am. Chem. Soc.* **81,** 1503–6 (1959). *C.A.* **53,** 17959f.

G-17 Gverdtsiteli, L. G., Kucherov, R. Y. and Tskhakaya, V. K. Isotope separation by diffusion in a current of steam. *Proc. U.N. Intern. Conf. Peaceful Uses Atomic Energy, 2nd Geneva 1958* **4,** 608–18 (1958).

VOL. 11 1961

## H


H-1 Haase, G. Mathematical evaluations for mass-spectrometry. *Kernenergie* **3,** 915–7 (1960).

H-2 Habermann, H. M. and Vernon, L. P. Isotope experiments on the 2,6-dichlorophenol-indophenol-mediated oxidation of ascorbic acid by illuminated chloroplasts. *Arch. Biochem. Biophys.* **76,** 424–9 (1958). *C.A.* **53,** 3394a.

H-3 Hänni, H. P. Methods of target preparation. *Helv. Phys. Acta* **33,** 987–91 (1960).

H-4 Hall, G. R. and Palmer, G. H. Effect of oxygen isotopes in the analysis of plutonium isotopes by using plutonium oxide ion beams in the solid source spectrometer. *Atomic Energy Research Establ.* (*Gt. Brit.*) C/R-1150 5 pp (1957). *C.A.* **52,** 968d.

H-5 Halmann, M. Hydrolysis of dialkylphosphinic fluorides and dialkyl phosphorofluoridates. Kinetic and tracer studies. *J. Chem. Soc.* **1959,** 305–10. *C.A.* **53,** 7971b.

H-6 Halmann, M. and Lapidot, A. Kinetic and tracer studies of the hydrolysis of phosphourethan. *J. Chem. Soc.* **1960,** 419–24. *C.A.* **54,** 12992g.

H-7 Halmann, M. and Pinchas, S. The isotope effect of oxygen-18 on the infra-red spectrum of benzophenone. *J. Chem. Soc.* **1958,** 1703–5. *C.A.* **52,** 14331c.

H-8 Halmann, M. and Pinchas, S. The oxygen-18 effect on the infra-red absorption of triphenylphosphine oxide, and the structure of the triphenylphosphine oxide hydrate. *J. Chem. Soc.* **1958,** 3264–7. *C.A.* **53,** 1919a.

H-9 Halmann, M. and Pinchas, S. The infrared absorption of oxygen-18 labelled nitromethane. *J. Chem. Soc.* **1960,** 1246–9.

H-10 Halpern, M. and Leibowitz, J. On the mechanism of the glucosidic bond cleavage in the enzymic hydrolysis of starch. *Biochim. et Biophys. Acta* **36,** 29–34 (1959). *C.A.* **54,** 4705f.

H-11 Hamilton, G. A. and Westheimer, F. H. On the mechanism of the enzymatic decarboxylation of acetoacetate. *J. Am. Chem. Soc.* **81,** 6332–3 (1959).

H-12 Haring, A., Vries, A. E. de, and Vries, H. de Radiocarbon dating up to 70,000 years by isotopic enrichment. *Science* **128,** 472–3 (1958). *C.A.* **53,** 2976e.

H-13 Harris, W. F., Hickman, W. M., Loefller, M. H. and Shaffer, D. H. Quantitative addition and recovery of oxygen isotopes in niobium. *Trans. Am. Inst. Mining, Met. Petrol. Engrs.* **218,** 625–8 (1960). *C.A.* **54,** 19387h.

H-14 Haul, R., Blennemann, D., Ginsberg, A., Ihle, H. and Rose, E. Exchange of deuterium in liquid extraction columns. *Z. Elektrochemie* **63,** 1014 (1959).

H-15 Haul, R. and Just, D. Measurement of diffusion in oxide crystals by isotopic exchange with gaseous oxygen. *Naturwissenschaften* **45,** 435–6 (1958). *C.A.* **53,** 5803h.

H-16 Hayaishi, O. Incorporation of atmospheric oxygen into the cell constituents of a growing culture of *Pseudomonas*. *J. Am. Chem. Soc.* **79,** 5576–7 (1957). *C.A.* **52,** 2169g.

H-17 Hayaishi, O. Studies on oxygenases. *Proc. Intern. Symposium Enzyme Chem. Tokyo and Kyoto* **2,** 207–11 (1957). *C.A.* **54,** 4724f.

H-18 Hayaishi, O. The distribution and significance of oxygenases in nature. *Proc. Fourth International Congress of Biochemistry* Vienna Vol. 13, pp. 137–41 Pergamon Press (1958).

H-19 Hayaishi, O., Patchett, A. A. and Witkop, B. Mechanism of the pyrocatechol oxidase (pyrocatechase) reaction. *Annalen.* **608,** 158–67 (1957). *C.A.* **52,** 9248c.

H-20 Hayaishi, O., Tabor, H. and Hayaishi, T. N-formimino-L-aspartic acid as an intermediate in the enzymatic conversion of imidazoleacetic acid to formyl-aspartic acid. *J. Biol. Chem.* **227,** 161–80 (1957). *C.A.* **51,** 15665e.

H-21 Hayano, M., Saito, A. and Dorfman, R. On the enzymatic mechanism of the hydroxylation of steroid hormones. *Proc. Intern. Symposium Enzyme Chem. Tokyo and Kyoto, 1957* **2,** 204–6 (1957). *C.A.* **54,** 4724e.

H-22 Hayes, K. E. The role of reaction products in the silver catalysed oxidation of ethylene. *Can. J. Chem.* **38,** 2256–68 (1960).

H-23 Heyns, K. and Schultze, H. Isotope effect in the polymerization of 2,5-oxozolidinediones. *Annalen* **611,** 40–57 (1958). *C.A.* **52,** 12764c.

H-24 Hoagland, M. B., Zamecnik, P. C., Sharon, N., Lipman, F., Stulberg, M., and Boyer, P. D. Oxygen transfer to AMP in the enzymic synthesis of the hydroxamate of trypophan. *Biochim. et Biophys. Acta* **26,** 215–7 (1957). *C.A.* **52,** 2130a.

H-25 Hoekstra, H. R. Oxygen isotope variations in some uranium minerals. *Natl. Acad. Sci. Natl. Research Council Publ.* No. 400 *Nuclear Soc. Sci.* Reprint No. 19, 160–5 (1956). *C.A.* **52,** 998b.

H-26 Hoekstra, H. R. and Katz, J. J. The isotope geology of some uranium minerals. *Proc. U. N. Intern. Conf. Peaceful Uses of Atomic Energy 1st Geneva 1956* **6,** 547–60 (1956). *C.A.* **50,** 15357f.

H-27 Hoering, T. C., Ishimori, F. T. and McDonald, H. O. The oxygen exchange between oxy-anions and water—II. Chlorite, chlorate and perchlorate. *J. Am. Chem. Soc.* **80,** 3876–9 (1958). *C.A.* **53,** 3851e.

H-28 Hoffman, M. Z. and Bernstein, R. B. Relative quenching cross sections in the reaction of $Hg(6^3P_1)$ atoms with isotopic $N_2O$ molecules. *J. Chem. Phys.* **33,** 526–9 (1960).

H-29 Holmberg, K. E. Exchange distillation for separation of isotopes particularly production of $B^{10}$. *Proc. Intern. Symposium Isotope Separation, Amsterdam* 201–3 (1958).

H-30 Holmberg, K. E. Physical properties of isotopic forms of azeotropic systems formed from acetic acid and some tertiary amines. *Acta Chem. Scand.* **13,** 717–21 (1959).

H-31 Holmberg, K. E. Physical properties of isotopic forms of some inorganic acid-water azeotropics. *Acta Chem. Scand.* **14,** 1660–6 (1960).

H-32 Holmes, A. Spitskop carbonatite, Eastern Transvaal. *Bull. Geol. Soc. Am.* **69,** 1525–6 (1958). *C.A.* **53,** 4040c.

H-33 Hrostowski, H. J. and Alder, B. J. Evidence for the internal rotation in the fine structure of the infra-red absorption of oxygen in silicon. *J. Chem. Phys.* **33,** 980–90 (1960).

H-34 Hübner, G. Separation and use of stable isotopes—III. The use of stable isotopes in biology—I. The exchange of material in plants. *Chem. Tech.* **12,** 699–705 (1958). *C.A.* **53,** 14721b.

H-35 Hübner, G. Explanation of the mechanism of fatty acid oxidation using oxygen-18. *Kernenergie* **3,** 839–43 (1960).

H-36 Hübner, G., Ludewig, R. Görisch, V. and Birkenfeld, H. Oxygen isotope analysis of the respiratory air in animal research with application of the mass-spectrometer. *Z. Naturforsch.* **15b,** 128–31 (1960).

H-37 Hunt, A. L., Hughes, D. E. and Lowenstein, J. M. The hydroxylation of nicotinic acid by *Pseudomonas fluorescents*. *Biochem. J.* **69,** 170–3 (1958). *C.A.* **52,** 16468e.

H-38 Hunt, H. R. and Taube, H. Effect of temperature, pressure, acidity and solvent on an aquo–ion exchange reaction. *J. Am. Chem. Soc.* **80,** 2642–6 (1958). *C.A.* **52,** 16017a.

H-39 Hunt, H. R. and Taube, H. Relative acidity of $H_2O^{18}$ and $H_2O^{16}$ co-ordinated to a tripositive ion. *J. Phys. Chem.* **63,** 124–5 (1959). *C.A.* **53,** 9792h.

H-40 Huston, J. L. Exchange reactions in certain acidic solvents. *J. Phys. Chem.* **63,** 389–92 (1959). *C.A.* **53,** 14655d.

H-41 Hutchison, D. A. Isotopic exchange of oxygen in the systems water–silica and oxygen–silica. *J. Chem. Phys.* **22,** 758–9 (1954). *C.A.* **48,** 10414e.

**I**

I-1 Ivanova, V. V., Nazarov, A. I., Polunskaya, E. V., Khabakhpashev, A. G. and Tsenter, E. M. Use of the $O^{18}$ (α, n) $Ne^{21}$ reaction to measure α-activities of aqueous solutions. *Atomnaya Energ.* **7,** 166–8 (1959). *Nuclear Sci. Abstr.* **13,** 20105.

**J**

J-1 Jackson, J. A., Lemons, J. F. and Taube, H. Nuclear magnetic resonance studies on hydration of cations. *J. Chem. Phys.* **32,** 553–5 (1960). *C.A.* **54,** 13864d.

J-2 Jarmie, N. and Silbert, M. G. Oxygen-20. *Phys. Rev. Letters* **3,** 50 (1959). *C.A.* **54,** 2978i.

J-3 Jarnagin, R. C. and Wang, J. H. Investigation of the catalytic mechanism of catalase and other ferric compounds with doubly oxygen-18 labelled hydrogen peroxide. *J. Am. Chem. Soc.* **80,** 786–7 (1958). *C.A.* **52,** 9237e.

J-4 Jensen, M. L. Geologic importance of variations in stable isotopic abundances. *Econ. Geol.* **48,** 161–76 (1953). *C.A.* **48,** 11997f.

J-5 Johns, T. F. Vapour-pressure differences between some of the isotopic species of CO, $CH_4$ and $O_2$—I. Experimental. *Atomic Energy Research Establ. (Gt. Brit.)* GP/R2166, 53 pp (1957). *C.A.* **52,** 5914b.

J-6 Johns, T. F. Vapour pressure of some isotopic substances. *Proc. Intern. Symposium Isotope Separation* Amsterdam 74–102 (1958). *C.A.* **52,** 11596g.

VOL. 11 1961

J-7 JOHNS, T. F. and LONDON, H. Enrichment of the carbon-13 and oxygen-18 isotopes by fractional distillation of carbon monoxide. *Atomic Energy Research Establ.* (*Gt. Brit.*) G/R661 pp. 131 (1951).

J-8 JOHNSTON, F. J., HUTCHISON, D. A. and KATZ, J. J. Oxygen exchange between uranium oxides and water. *J. Inorg. Nuclear Chem.* **7,** 392–6 (1958). *C.A.* **53,** 5836g.

J-9 JONES, M. E. and SPECTOR, L. The pathway of carbonate in the biosynthesis of carbamyl phosphate. *J. Biol. Chem.* **235,** 2897–901 (1960).

J-10 JOY, H. W. and LIBBY, W. F. Size effects among isotopic molecules. *J. Chem. Phys.* **33,** 1276 (1960).

## K

K-1 KALAN, E. B. and TELKA, M. The enzymatic dephosphorylation of casein fractions in the presence of $H_2O^{18}$. *Arch. Biochem. Biophys.* **85,** 273–5 (1959). *C.A.* **54,** 8943d.

K-2 KAMPER, R. A., LEA, K. R. and LUSTIG, C. D. Hyperfine structure and nuclear electric quadrupole moment of $O^{17}$. *Proc. Phys. Soc.* **70B,** 897–8 (1957). *C.A.* **52,** 15237f.

K-3 KARABATSOS, G. J. Infrared spectra of isotopically labelled compounds—I. Diisopropylketones. *J. Org. Chem.* **25,** 315–8 (1960).

K-4 KARPACHEVA, S. M. and ROZEN, A. M. Method for complete isotope analysis of water. *Problemy Kinetiki i Kataliza, Akad. Nauk S.S.S.R., 1956* **9,** 386–90 (1957). *C.A.* **53,** 7859f.

K-5 KATS, M. YA. and LAPTEVA, F. S. The oxygen isotope exchange between water and carbon dioxide. *Zhur. Fiz. Khim.* **32,** 864–8 (1958). *C.A.* **52,** 19361i.

K-6 KATS, M. YA. and LAPTEVA, F. S. Isotopic water analysis. *Zhur. Anal. Khim.* **14,** 227–33 (1959). *C.A.* **53,** 12923c.

K-7 KAZARNOVSKII, I. A., LIPIKHIN, N. P. and TIKHOMIROV, M. V. Isotopic exchange of oxygen between free hydroxyl radicals and water. *Doklady Akad. Nauk S.S.S.R.* **120,** 1038–41 (1958). *C.A.* **53,** 11960f.

K-8 KEELING, CH. D. The concentration and isotopic abundances of atmospheric carbon dioxide in rural areas. *Geochim. et Cosmochim. Acta* **13,** 322–34 (1958). *C.A.* **52,** 12476i.

K-9 KEIER, N. P. Active surface of catalysts from study of isotope exchange. *Problemy Kinetiki i Kataliza, Akad. Nauk S.S.S.R., 1956* **9,** 283–93 (1957). *C.A.* **53,** 7742i.

K-10 KEISCH, B., KENNEDY, J. W. and WAHL, A. C. The exchange of oxygen between phosphoric acid and water. *J. Am. Chem. Soc.* **80,** 4778–82 (1958). *C.A.* **53,** 2753e.

K-11 KEITH, M. L., TUVE, M. A., DAVIS, G. L. and DOAK, J. B. Ratio of oxygen isotopes in quartz of contrasted origin. *Bull. Geol. Soc. Am.* **63,** 1270 (1952).

K-12 KHABAKHPASHEV, A. G. and TSENTER, E. M. Measurement of the lifetime of the first excited level of $Ne^{21}$. *Zhur. Eksptl. i Teoret. Fiz.* **37,** 991–3 (1959). *C.A.* **54,** 8329f.

K-13 KINGERY, W. D., HILL, D. C. and NELSON, R. P. Oxygen mobility in polycrystalline $NiCr_2O_4$ and $\alpha$-$Fe_2O_3$. *J. Am. Ceram. Soc.* **43,** 473–6 (1960). *C.A.* **54,** 23565g.

K-14 KINGERY, W. D., PAPPIS, J., DOTY, M. E. and HILL, D. C. Oxygen mobility in cubic $Zr_{0.85}$, $Ca_{0.15}$, $O_{1.85}$. *J. Am. Ceram. Soc.* **42,** 393–8 (1959). *C.A.* **53,** 20735c.

K-15 KOSHLAND, D. E. JR., SIMMONS, N. S. and WATSON, J. D. Absence of phosphotriester linkages in tobacco mosaic virus. *J. Am. Chem. Soc.* **80,** 105–7 (1958). *C.A.* **52,** 7449e.

K-16 KOTEL'NIKOV, V. V. and SKRIPOV, V. P. Isotope effect in the mutual solubility of water and triethylamine. *Doklady Vysshei Shkoly Khim. i Khim Teknol.* No. 2 248–9 (1959). *C.A.* **53,** 19525f.

K-17 KOUBA, R. F. and VARNER, J. E. Properties of the arsenate–water oxygen-18 exchange reaction. *Biochem. Biophys. Research Communs.* **1,** 129–32 (1959). *C.A.* **54,** 5222f.

K-18 KOWALSKY, A. and BOYER, P. D. A carboxy peptidase–$H_2O^{18}$ procedure for determination of COOH— terminal residues and its application to aldolase. *J. Biol. Chem.* **235,** 604–8 (1960).

K-19 KRALL, A. R., AVRON, M. and JAGENDORF, A. T. Non-participation of oxygen in photosynthetic phosphorylation by spinach chloroplasts. *Biochim. et Biophys. Acta* **26,** 431–2 (1957). *C.A.* **52,** 3048b.

K-20 KRAUSE, A. Exchange of oxygen-18 in metal oxides. *Bull. acad. polon. sci., Classe III chim.* **8,** 277–9 (1960).

K-21 KRELL, E. Separation and use of stable isotopes—I. Production of stable isotopes as a distillation problem. *Chem. Tech.* Berlin **9,** 333–40 (1957). *C.A.* **51,** 17301g.

K-22 KRELL, E. Preparation of the stable isotope $O^{18}$ by countercurrent distillation of water. *Chem. Ingr. Tech.* **32,** 233–40 (1960). *C.A.* **54,** 13887c.

K-23 KRELL, E. Densimetric determination of deuterium and oxygen-18 concentration in water by the falling drop method. *Kernenergie* **3,** 897–902 (1960).

K-24 KRISHER, L. C. and WILSON, E. B., JR. Microwave spectrum of acetyl cyanide. *J. Chem. Phys.* **31,** 882–9 (1959). *C.A.* **54,** 6310b.

K-25 KRUSE, W. and TAUBE, H. The transfer of oxygen in some oxidation–reduction reactions of aquo-complexes. *J. Am. Chem. Soc.* **82,** 526–8 (1960).

K-26 KUDRYAVTSEV, R. V. and KURSANOV, D. N. Use of oxygen-18 in the study of the mechanism of alkaline transesterification of esters. *Zhur. Obshchei Khim.* **27,** 1686–7 (1957). *C.A.* **52,** 3676g.

K-27 KUDRYAVTSEV, R. V., KURSANOV, D. N. and ANDRIANOV, K. A. A study of the mechanism of formation of polyorganoborosiloxanes with oxygen-18. *Zhur. Obshchei Khim.* **29,** 1497–9 (1959). *C.A.* **54,** 8595a.

K-28 KUHN, W., NARTEN, A. and THÜRKAUF, M. Separation parameters of isotopically labelled nitrogen oxides $N^{15}N^{14}O/N_2{}^{14}O$, $N_2O^{18}/N_2O^{16}$, $N^{15}O/NO$, $N^{15}O_2/N^{14}O_2$. *Helv. Chim. Acta* **42,** 1433–6 (1959). *C.A.* **53,** 17e.

K-29 KUHN, W. and THÜRKAUF, M. Separation of isotopes by freezing of water and the diffusion constants of deuterium and oxygen-18 in ice. Possibility of the multiplication of separation on freezing in a hairpin countercurrent apparatus. *Helv. Chim. Acta* **41,** 938–71 (1958). *C.A.* **52,** 16825b.

K-30 KUHN, W., THÜRKAUF, M. and NARTEN, A. Exact determination of small differences in the volatility of isotopes. *Proc. U. N. Intern. Conf. Peaceful Uses Atomic Energy, 2nd Geneva 1958* **4,** 371–4 (1958). *C.A.* **54,** 23909f.

K-31 KUKHTENKO, I. I. Study of the mechanism of anthranilic rearrangement with oxygen-18. *Doklady Akad. Nauk S.S.S.R.* **132,** 609–11 (1960).

K-32 KUPCHIK, E. J. I. An oxygen-18 tracer study of the isomerisation of cyclopropylcarbinyl benzene-sulphonate. III. Attempted syntheses of unsymmetrically substituted benzoic anhydrides. *Dissertation Abstr.* **20,** 4278 (1960).

## L

L-1 LADENHEIM, H. and BENDER, M. L. Acylium ion formation and the reactions of carboxylic acid derivatives—I. Application of the $H_R$ acidity function to the diazotisation of benzamide in sulphuric acid. *J. Am. Chem. Soc.* **82,** 1895–900 (1960).

L-2 LANE, G. A. and DOLE, M. Fractionation of oxygen isotopes during respiration. *Science* **123,** 574–6 (1956).

L-3 LANG, A. R. G. and MASON, S. G. The exchange of oxygen-18 between cellulose absorbed water and water vapour. *Canad. J. Chem.* **37,** 1829–33 (1959).

L-4 LAUDER, I. Theory and application of the Gilfillan–Polanyi micropyknometer technique. *Australian J. Chem.* **12,** 32–9 (1959). *C.A.* **53,** 10855a.

L-5 LAUDER, I. The partial molal volumes of gases in water at 0°C. *Australian J. Chem.* **12,** 40–6 (1959). *C.A.* **53,** 10907g.

L-6 LAUDER, I. The mass-spectrometric analysis of oxygen in carbon monoxide and carbon dioxide. *Australian J. Chem.* **12,** 630–6 (1959). *C.A.* **54,** 5335e.

L-7 LAUDER, I. and WILSON, I. R. The purification of oxygen-18 water. *Australian J. Chem.* **12,** 29–31 (1959). *C.A.* **53,** 10880h.

L-8 LAUDER, I. and WILSON, I. R. The conversion of oxygen in compounds to water for isotopic analysis by a density technique. *Australian J. Chem.* **12,** 613–20 (1959). *C.A.* **54,** 5177f.

L-9 LAUDER, I. and ZERNER, B. Conversion of oxygenic compounds to carbon monoxide for mass-spectrometric analysis. *Australian J. Chem.* **12,** 621–9 (1959). *C.A.* **54,** 5326a.

L-10 LAZAREV, A. Z., AREFEVA, M. G., BOBYREV, N. A., CHAPUKHIN, M. S. and KHAIDAROV, A. A. Isotope composition of some elements of gold-bearing ore deposits. Development of the method of analysis of the isotope composition of the oxygen of carbonates. *Trudy Tsentral, Nauch. Issledovatel. Gornorazvedoch Inst.* No. 27, 12–14 (1958). *C.A.* **54,** 23978a.

VOL. 11 1961

L-11 LEADBETTER, E. R. and FOSTER, J. W. Incorporation of molecular oxygen in bacterial cells utilizing hydrocarbons for growths. *Nature* **184,** 1428–9 (1959). *C.A.* **54,** 10047b.

L-12 LEVY, H. M. and KOSHLAND, D. E., JR. Evidence for an intermediate in the hydrolysis of adenosine triphosphate (ATP) by muscle proteins. *J. Am. Chem. Soc.* **80,** 3164–5 (1958). *C.A.* **53,** 3336c.

L-13 LEVY, H. M. and KOSHLAND, D. E. JR. Mechanism of hydrolysis of adenosine triphosphate by muscle proteins and its relationship to muscular contraction. *J. Biol. Chem.* **234,** 1102–7 (1959). *C.A.* **53,** 15281g.

L-14 LIEBERMAN, I. and ETO, W. H. Enzymatic synthesis of adenosine-5′-phosphate from inosine-5′-phosphate. *J. Biol. Chem.* **223,** 327–39 (1956). *C.A.* **51,** 3708f.

L-15 LLEWELLYN, D. R. and ODELL, L. The use of the isotopes oxygen-18, carbon-13 and carbon-14 in the study of exchange reactions of tris oxalato-chromium(III) anion. *Proc. Aust. Atomic Energy Symposium* **1958,** 623–7. *C.A.* **53,** 17744.

L-16 LONDON, H. Isotope separation by fractional distillation. *Proc. Intern. Symposium Isotope Separation, Amsterdam* 319–35 (1958). *C.A.* **52,** 11597d.

L-17 LOTSPEICH, J. F., JAVAN, A. and ENGELBRECHT, A. Microwave spectrum and structure of perrhenyl fluoride. *J. Chem. Phys.* **31,** 633–43 (1959). *C.A.* **54,** 2942i.

L-18 LOTT, K. A. K., SYMONS, M. C. R. and TREVALION, P. A. The mechanism of reaction between permanganate and hydroperoxide in alkaline solution. *Proc. Chem. Soc.* (*London*) **1960,** 357.

L-19 LOWENSTAM, H. A. and EPSTEIN, S. Paleotemperatures of the Post-Aptian Cretaceous as determined by the oxygen-isotope method. *J. Geol.* **62,** 207–48 (1954). *C.A.* **48,** 8140h.

L-20 LOWENSTAM, H. A. and EPSTEIN, S. The origin of sedimentary aragonite needles of the Great Bahama Bank. *J. Geol.* **65,** 364–75 (1957). *C.A.* **52,** 194c.

**M**

M-1 MAAS, I. Separation and use of stable isotopes—II. Preparation of gas samples for mass-spectrometric determination of isotopic abundance. *Chem. Tech.* Berlin **10,** 17–22 (1958). *C.A.* **52,** 14409h.

M-2 MAASS, I. Oxygen-18 exchange between water and instrument glass. *Kernenergie* **3,** 843–6 (1960).

M-3 MAASS, I. Preparation of mass-spectrometer samples. *Kernenergie* **3,** 883–7 (1960).

M-4 MCCLINTOCK, R. and LIFSON, N. Use of deuterium and oxygen-18 to measure total carbon dioxide output of obese-hyperglycemic mice. *Federation Proc.* **15,** 127 (1956).

M-5 MCCLINTOCK, R. and LIFSON, N. Applicability of the $D_2O^{18}$ method to the measurement of the total carbon dioxide output of obese mice. *J. Biol. Chem.* **226,** 153–6 (1957). *C.A.* **51,** 12307h.

M-6 MCCLINTOCK, R. and LIFSON, N. $CO_2$ output and energy balance of hereditary obese mice. *Am. J. Physiol.* **189,** 463–9 (1957). *C.A.* **51,** 16816b.

M-7 MCCLINTOCK, R. and LIFSON, N. Determination of the total carbon dioxide output of rats by the $D_2O^{18}$ method. *Am. J. Physiol.* **192,** 76–8 (1958). *C.A.* **52,** 6479h.

M-8 MCCLINTOCK, R. and LIFSON, N. Carbon dioxide output of mice measured by $D_2O^{18}$ under conditions of isotope re-entry into the body. *Am. J. Physiol.* **195,** 721–5 (1958). *C.A.* **53,** 5457d.

M-9 MCDONALD, H. O. The oxygen exchange between oxyanions and water-manganate and permanganate. *Dissertation Abstr.* **21,** 454–5 (1960).

M-10 MCKEAN, D. C., TAYLOR, R. and WOODWARD, L. A. Raman spectra and structure of disilyl ether-$O^{18}$. *Proc. Chem. Soc.* **1959,** 321–2. *C.A.* **54,** 8283i.

M-11 MCKELLAR, A. Isotopes in stellar atmospheres. *Publ. Astron. Soc. Pacific* **61,** 199–209 (1949). *C.A.* **44,** 32a.

M-12 MANASSEN, J. and KLEIN, F. S. Reactions of *n*-butene and butan-2-ol in dilute acid. The elucidation of the mechanism and the intermediate in elimination of secondary alcohols and in hydration of olefins. *J. Chem. Soc.* **1960,** 4203–13.

M-13 MARGOLIS, L. YA. Fundamental principles for the catalytic oxidation of hydrocarbons—II. Adsorption of oxygen on oxidation catalysts. *Izvest. Akad. Nauk S.S.S.R., Otdel. Khim. Nauk* 225–31 (1959). *C.A.* **53,** 21104f.

M-14 MARGOLIS, L. YA. and KISELEV, V. A. Isotope exchange of oxygen on oxidation catalysts. *Doklady Akad. Nauk S.S.S.R.* **130,** 1071–3 (1960).

M-15 MARGOLIS, I. YA. and ROGINSKI, S. Z. A mechanism of catalytic oxidation of simplest unsaturated hydrocarbons on metals and semiconductors. *Problemy Kinetiki i Kataliza, Akad. Nauk S.S.S.R.* **9,** 107–16 (1957). *C.A.* **53,** 7742b.

M-16 MASON, H. S. The transfer of oxygen by peroxidase. *Proc. Intern. Symposium Enzyme Chem. Tokyo and Kyoto* **2,** 220–4 (1957). *C.A.* **54,** 4725b.

M-17 MASON, H. S. Mechanisms of oxygen metabolism. *Advances in Enzymology* Vol. 19, pp. 79–233. Interscience, New York (1957). *C.A.* **52,** 6512g.

M-18 MATTERN, J. A. Comparison of $O^{18}/O^{16}$ and $O^{17}/O^{16}$ isotope effects in some reactions of hydrogen peroxide. *J. Inorg. & Nuclear Chem.* **15,** 388–9 (1960).

M-19 MAYER, F. C., JR. Substrate cleavage points of carbohydrases as determined by oxygen-18 studies. *Dissertation Abstr.* **18,** 380 (1958).

M-20 MAYER, F. C. JR. and LARNER, J. Substrate cleavage points of α- and β-amylases. *Biochim. et Biophys. Acta* **29,** 465 (1958). *C.A.* **52,** 20313d.

M-21 MAYER, F. C., JR. and LARNER, J. Substrate cleavage point of the α- and β-amylases. *J. Am. Chem. Soc.* **81,** 188–93 (1959). *C.A.* **53,** 10319c.

M-22 MAYNE, K. I. Stable isotope geochemistry and mass-spectrometric analysis. *Methods in Geochimistry* (Edited by SMALES, A. A. and WAGER, L. R.) pp. 148–99. Interscience, New York (1960).

M-23 MEISENHEIMER, R. G., RITCHIE, A. W., SCHISSLER, D. O., STEVENSON, D. P., VOGE, H. H. and WILSON, J. N. Oxygen adsorption and exchange on silver catalysts. *Proc. Intern. Congr. Surface Activity, 2nd London 1957* **2,** 299–308 (1957). *C.A.* **52,** 17890h.

M-24 METZENBERG, R. L., MARSHALL, M., COHEN, P. P. and MILLER, W. G. Further studies on the mechanism of action of carbamyl phosphate synthetase. *J. Biol. Chem.* **234,** 1534–7 (1959). *C.A.* **53,** 16255a.

M-25 MILBURN, R. L. and TAUBE, H. Tracer experiments on the oxidation of oxalic acid. *J. Am. Chem. Soc.* **81,** 3515–7 (1959). *C.A.* **54,** 2161i.

M-26 MILLER, W. G. and ANDERSON, L. Isotope distribution in the Unterzaucher analysis of labelled oxygen compounds. *Anal. Chem.* **31,** 1668–9 (1959). *C.A.* **54,** 4245i.

M-27 MONSE, E. U. Calculation of equilibrium constants for several isotope exchange reactions involving $N_2O_4$. *J. Chem. Phys.* **33,** 312–4 (1960).

M-28 MOORE, W. J., EBISUZAKI, Y. and SLUSS, J. A. Exchange and diffusion of oxygen in crystalline cuprous oxide. *J. Phys. Chem.* **62,** 1438–41 (1958). *C.A.* **53,** 5804a.

M-29 MOORE, W. J. and WILLIAMS, E. L. Diffusion of zinc and oxygen in zinc oxide. *Discussions Faraday Soc.* **28,** 86–93 (1960). *C.A.* **54,** 13794f.

M-30 MÜHLENPFORDT, J. The importance of stable isotopes. *Kernenergie* **3,** 816–22 (1960).

M-31 MURASHOV, G. M., NEFEDOV, V. D., SKOROBOGATOV, G. A. and SMIRNOV, V. M. Study of the mechanism of the Grignard synthesis of alcohols by oxygen labelling. *Zhur. Obshchei Khim.* **29,** 2864–8 (1959).

M-32 MURRAY, A. and WILLIAMS, D. L. Organic compounds labelled with isotopes of the halogens, hydrogen, nitrogen, oxygen, phosphorus and sulphur. *Organic Synthesis with Isotopes* Vol. 2. pp. 1865–97. Interscience, New York (1958). *C.A.* **53,** 2068i.

**N**

N-1 NELSON, K. L. and SEEFELD, R. L. The mechanistic fate of carbonyl oxygen in the rearrangement of 2-anilino-1-phenyl-1-propanone. *J. Am. Chem. Soc.* **80,** 5957–9 (1958). *C.A.* **53,** 11289c.

N-2 NORRIS, T. H. Isotopic exchange reaction in liquid sulphur dioxide and related non-aqueous systems. *J. Phys. Chem.* **63,** 383–9 (1959). *C.A.* **53,** 14654g.

**O**

O-1 OEHME, I. Isotope effects in biological reactions. *Kernenergie* **3,** 854–8 (1960).

O-2 Oishi, Y. and Kingery, W. D. Self diffusion of oxygen in single crystal and polycrystalline aluminium oxide. *J. Chem. Phys.* **33,** 480–6 (1960).

O-3 Orgel, L. E. Comment on effects of dissolved $Gd^{3+}$ on the $H_2O^{17}$ nuclear resonance. *J. Chem. Phys.* **30,** 1617–8 (1959). *C.A.* **53,** 19573h.

**P**

P-1 Panchenkov, G. M., Semiokhin, I. A. and Akishin, P. A. Chemistry and separation of isotopes. *Vestnik Moskov. Univ., Ser. Mat. Mekh. Astron., Fiz. Khim.* **12,** 199–214 (1957). *C.A.* **53,** 3924f.

P-2 Panchenkov, G. M., Tolmachev, A. M. and Kondratova, V. B. A new method for separating isotopes. *Zhur. Fiz. Khim.* **33,** 734–5 (1959). *C.A.* **53,** 21246a.

P-3 Panson, G. S. and Sullivan, P. The enrichment of water in $H_2O^{18}$ by liquid thermal diffusion. *J. Phys. Chem.* **64,** 825–6 (1960). *C.A.* **54,** 23937i.

P-4 Park, J. H. and Koshland, D. E. Jr. The hydrolytic activity of glyceraldehyde 3-phosphate dehydrogenase. *J. Biol. Chem.* **233,** 986–90. (1958). *C.A.* **53,** 2316d.

P-5 Pearce, M. L. and Masson, C. R. Determination of oxygen in iron and steel. *Nature* **185,** 373–4 (1960).

P-6 Perederev, V. A. The isotope composition of oxygen of pyrolusites, manganites and psilimelanes of Nikopol region. *Mineral. Sbornik Lovov Geol. Obshchesto* **9,** 221–5 (1955). *C.A.* **52,** 14463d.

P-7 Pešić, D. S. Isotope effect in band spectra of magnesium oxide. *Proc. Phys. Soc.* **76,** 844–8 (1959).

P-8 Picciotto, E., De Maere, X. and Friedman, I. Isotopic composition and temperature of formation of antarctic snows. *Nature* **187,** 857–9 (1960).

P-9 Pierce, L. and Krisher, L. C. Microwave spectrum, internal barrier, structure, conformation and dipole moment of acetyl fluoride. *J. Chem. Phys.* **31,** 875–82 (1959). *C.A.* **54,** 6309i.

P-10 Pinchas, S. and Halmann, M. The infra-red absorption of $D_2O^{18}$. *Bull. Research Council Israel* **7A,** 101 (1958).

P-11 Pinchas, S., Halmann, M. and Stoicheff, B. P. Fundamental vibration frequencies of $D_2O^{18}$ vapour. *J. Chem. Phys.* **31,** 1692–3 (1959).

P-12 Pocker, Y. Intermediates in allylic rearrangements—II. Rates and mechanism of exchange and rearrangements in 1- and 3-phenylallyl benzoate. *J. Chem. Soc.* **1958,** 4323–9. *C.A.* **53,** 10105g.

P-13 Price, W. C., Sherman, W. F. and Wilkinson, G. R. Infrared studies on polyatomic ions isolated in alkali halide lattices. *Spectrochim. Acta* **16,** 663–76 (1960). *C.A.* **54,** 23732a.

**R**

R-1 Rankama, K. *Isotope Geology* pp. 238–70. McGraw-Hill, N.Y.; Pergamon Press, London (1954).

R-2 Reichard, P. Some aspects of pyrimidine biosynthesis. *Proc. Intern. Congr. Biochem. 4th Congr. Vienna* **13,** 119–33 (1958).

R-3 Riesz, P. and Biegeleisen, I. Solvent effect on a primary carbon isotope effect. Decarboxylation of trinitrobenzoate ion in water and ethanol–water mixture. *J. Am. Chem. Soc.* **81,** 6187–9 (1959).

R-4 Rittenberg, D. and Graff, C. A comparison of the rate of mutarotation and oxygen-18 exchange of glucose. *J. Am. Chem. Soc.* **80,** 3370–2 (1958). *C.A.* **52,** 19362a.

R-5 Roginskii, S. Z. The mechanism of catalysis on the basis of isotopic data. *Geterogennyi Kataliz v Khim. Prom. Sbornik* **1955,** 72–85. *C.A.* **53,** 3857f.

R-6 Roginskii, S. Z. Investigations of the mechanism of catalysis based on isotopic data. *Radioisotopes Sci. Research Proc. Intern. Conf. Paris 1957* **2,** 1–20 (1958). *C.A.* **54,** 56e.

R-7 Ropp, G. A. Isotopic evidence for the mechanisms of decarbonylation of three carboxylic acids in sulphuric acid. *J. Am. Chem. Soc.* **80,** 6691 (1958). *C.A.* **53,** 8064e.

R-8 Ropp, G. A. Studies involving isotopically labelled formic acid and its derivatives—V. Studies of the decarbonylation of formic, benzoylformic and triphenylactic acids in sulphuric acid. *J. Am. Chem. Soc.* **82,** 842–52 (1960).

VOL. 11 1961

R-9 Rose, I. A. Studies on the enolisation of pyruvate by pyruvate kinase. *J. Biol. Chem.* **235,** 1170–7 (1960).

R-10 Rosenblum, B., Nethercot, A. H. Jr. and Townes, C. H. Isotopic mass ratios, magnetic moments and the sign of the electric dipole moment in carbon monoxide. *Phys. Rev.* **109,** 400–12 (1958). *C.A.* **52,** 9758a.

R-11 Rosenblum, C. Principles of isotope dilution assays. *Anal. Chem.* **29,** 1740–4 (1957). *C.A.* **52,** 4388e.

R-12 Rothberg, S. and Steinberg, D. Studies on the mechanism of enzymatic decarboxylation. *J. Am. Chem. Soc.* **79,** 3274–8 (1957). *C.A.* **51,** 14860b.

R-13 Rottenberg, M. and Thürkauf, M. On the oxidation of alcohols with platinum and oxygen—II. Investigation of the primary step with oxygen-18. *Helv. Chim. Acta* **42,** 226–31 (1959). *C.A.* **53,** 14918f.

R-14 Rozen, A. M., Karpacheva, S. M. and Shavelev, Ya. V. Mobility of oxygen in oxides and kinetics of oxygen exchange. *Problemy Kinetiki i Kataliza, Akad. Nauk S.S.S.R 1956* **9,** 251–63 (1957). *C.A.* **53,** 7732i.

R-15 Ruderman, I. New horizons for stable isotopes. *Proc. U.N. Intern. Conf. Peaceful Uses Atomic Energy, 2nd Geneva 1958* **20,** 257–60 (1958).

## S

S-1 Saegebarth, K. A. Mechanism of the tungstic acid catalysed hydroxylation of olefines. *J. Org. Chem.* **24,** 1212–4 (1959).

S-2 Saito, Y., Hayaishi, O., Ayengar, P. K. and Rothberg, S. Enzymic hydroxylation of kynurenine. *Med. J. Osaka Univ.* Suppl. **8,** 37–9 (1958). *C.A.* **53,** 14169f.

S-3 Samuel, D. The elucidation of the mechanism of the von Richter reaction by use of oxygen-18 as tracer. *J. Chem. Soc.* **1960,** 1318–20. *C.A.* **54,** 14174g.

S-4 Samuel, D. and Steckel, F. *Bibliography of Stable Isotopes of Oxygen* ($O^{17}$ *and* $O^{18}$) pp. 224. Pergamon Press, London (1959).

S-5 Santer, M. The role of oxygen-18 phosphate in thiosulphate oxidation by *Thiobacillus thioparus*. *Biochem. Biophys. Research Commun.* **1,** 9–12 (1959). *C.A.* **54,** 4750h.

S-6 Sarel, S., Levin, I. and Pohoryles, L. A. Organic carbonates—V. The mechanism of hydrolysis of organic carbonates. Tracer studies. *J. Chem. Soc.* **1960,** 3079–82.

S-7 Saxena, S. C. and Taylor, T. I. Enrichment of oxygen-18 by chemical exchange of nitric oxide with nitric acid solutions. *NYO-7763* (Part III), 57 pp (1959). *Nuclear Sci. Abstr.* **14,** 6576.

S-8 Saxena, S. C. and Taylor, T. I. Water and alumino-silicate (molecular sieve) absorbents using carbon dioxide as monitor. *NYO-7763* (Part IV) 25 pp (1959). *Nuclear Sci. Abstr.* **14,** 6577.

S-9 Schätzle, E., Rottenberg, M. and Thürkauf, M. Cholinesterase models. *Helv. Chim. Acta* **42,** 1708–25 (1959). *C.A.* **54,** 3565g.

S-10 Schellenberg, L., Baumgartner, E., Huber, P. and Seiler, F. Total effective cross section of $N^{15}$ and $O^{18}$ for neutrons in the MeV energy region. *Helv. Phys. Acta* **32,** 357–76 (1959). *C.A.* **54,** 5278e.

S-11 Schumacher, E. Storage of reagents and isotopic water in polythene flasks. *Chimia* **12,** 215 (1958). *C.A.* **53,** 6705a.

S-12 Semiokhin, I. A., Panchenkov, G. M., Korovkin, V. K. and Borisov, A. V. The separation of oxygen isotopes by electrical synthesis of ozone. *Zhur. Fiz. Khim.* **33,** 1933–8 (1959). *C.A.* **54,** 12833c.

S-13 Semiokhin, I. A., Panchenkov, G. M. and Zhurov, Yu. A. Use of isotope exchange between carbon dioxide and the carbonate ion to separate the isotopes of carbon and oxygen. *Zhur. Fiz. Khim.* **33,** 2633–5 (1959). *C.A.* **54,** 22081e.

S-14 Senegačnik, M. Isotopes effects in the reduction of carbon dioxide by zinc. *Comm. énergie atomique* (*France*) *Rappt. No 726* 82 (1957). *C.A.* **52,** 19368g.

S-15 Serdyukova, I. A., Khabakhpashev, A. G. and Tsenter, E. M. Investigation of the (α, n) reaction in oxygen. *Izvest. Akad. Nauk S.S.S.R., Ser. Fiz.* **21,** 1017–9 (1957). *C.A.* **52,** 2588d.

S-16 Sharp, R. P. and Epstein, S. Oxygen-isotope ratios and glacier movement. *Calif. Inst. Tech., Div. Geol. Sci. Contr. No. 875,* 359–69. *Geophys. Abs.* 179–281 (1959).

S-17 SHATENSTEIN, A. I. *Isotopic Analysis of Water* pp. 235. *Izd. Akad. Nauk S.S.S.R.*, Moscow (1957). *C.A.* **52,** 19582a.

S-18 SHATENSTEIN, A. I. Isotopic Analysis of Water *Physicochemical Methods of Separation and Measurement.* Vol. 4. Deutscher Verlag der Wissenschaften, Berlin (1960).

S-19 SHULMAN, R. G. and WYLUDA, B. J. Effects of gadolinium upon $H_2O^{17}$ nuclear resonance. *J. Chem. Phys.* **30,** 335–6 (1959). *C.A.* **53,** 10971h.

S-20 SHUPACK, J., SAXENA, S. C. and TAYLOR, T. I. Measurement of isotopic exchange equilibria—A. Exchange of oxygen-18 between NO and $H_2O$ ($HNO_3$). *NYO-7763* (Part VI) 6 pp. (1959). *Nuclear. Sci. Abstr.* **14,** 6579.

S-21 SHUPAK, J. and TAYLOR, T. I. Reflux system for the NO–$H_2O$($HNO_3$) exchange experiments on the decomposition of nitric oxide by catalysis and electric discharge. *NYO-7763* (Part V) 13 pp (1959). *Nuclear Sci. Abstr.* **14,** 6578.

S-22 SILVESTRI, M., VILLANI, S., ADORNI, N. and ANGELINO, G. C. Diffusional distillation in a gas stream. *Proc. U.N. Intern. Conf. Peaceful Uses Atomic Energy, 2nd Geneva 1958* **4,** 619–25 (1958).

S-23 SLOCUM, D. H., KOUBA, R. and VARNER, J. E. Some oxygen-transfer reactions catalysed by urease. *Arch. Biochem. Biophys.* **80,** 217–8 (1959). *C.A.* **53,** 10339i.

S-24 SLOCUM, D. H. and VARNER, J. E. Transfer of oxygen-18 in arsenolysis reactions. *J. Biol. Chem.* **235,** 492–5 (1960). *C.A.* **54,** 13213i.

S-25 SMIRNOV, V. M. and KARPUNIN, V. I. Mass spectrographic determination of the isotopic composition of oxygen in sulphuric acid. *Zavodskaya Lab.* **26,** 831 (1960). *Nuclear Sci. Abstr.* **14,** 25527.

S-26 SMITH, L. G. Measurements of light masses with the mass spectrometer. *Phys. Rev.* **111,** 1606–19 (1958). *C.A.* **53,** 3925d.

S-27 SOMMERVILLE, J. *The Isotope Index. The Complete Purchasing Guide to the Isotopes, Stable, Radioactive, Compounds* Vol. 4, No. 1. Scientific Equipment, Indianapolis (1959).

S-28 SPENCER, B. The mechanism of arylsulphatase action. *Proc. Intern. Symposium Enzyme Chem. Tokyo and Kyoto,* **2,** 96–9. (1957). *C.A.* **53,** 18129i.

S-29 SPENCER, B. Studies on sulphatases—XX. Enzymic cleavage of aryl hydrogen sulphates in the presence of $H_2O^{18}$. *Biochem. J.* **69,** 155–9 (1958). *C.A.* **52,** 14725h.

S-30 SPENCER, B. Detection of $BaSO_3{}^{16}O^{18}$ by infra-red spectroscopy. *Biochem. J.* **71,** 19 (1959). *C.A.* **53,** 6880h.

S-31 SPENCER, B. Sulfatases—XXV. The determination of $BaSO_3{}^{16}O_2{}^{18}$ by infra-red spectroscopy. *Biochem. J.* **73,** 442–7 (1959). *C.A.* **54,** 11119d.

S-32 SPINDEL, W. and STERN, M. J. Atomic exchange in NO. *J. Chem. Phys.* **32,** 1579–81 (1960). *C.A.* **54,** 23637d.

S-33 SPITSYN, V. I. Some applications of tracer isotopes to the study of the chemistry of complex compounds. *Acta Chim. Acad. Sci. Hung.* **12,** 119–40 (1957). *C.A.* **52,** 18057f.

S-34 SPITSYN, V. I. The use of isotope methods in investigating the structure and properties of heteropoly compounds. *Radioisotopic in Scientific Research Vol. III. Proceedings of the UNESCO International Conference* pp. 361–78. Pergamon Press, London (1958).

S-35 SPITSYN, V. I. and FINIKOV, V. G. Study of the isotope exchange between gaseous oxygen and salts of some oxygen-containing acids at high temperature. *Problemy Kinetiki i Kataliza, Akad. Nauk S.S.S.R. 1956* **9,** 264–6 (1957). *C.A.* **53,** 8784d.

S-36 SPITSYN, V. I. and FINIKOV, V. G. Isotopic exchange between free oxygen and some silicon compounds. *Izvest. Akad. Nauk S.S.S.R., Otdel Khim. Nauk* **1959,** 1351–2. *C.A.* **53,** 21078b.

S-37 SPITSYN, V. I. and FINIKOV, V. G. Use of oxygen-18 for determination of bond strength of oxygen in the crystal lattices of solids. *Kernenergie* **3,** 834–6 (1960).

S-38 SPITSYN, V. I., LAPITSKII, A. V., AISTOVA, R. I., NISHANOV, D. and PCHELKIN, V. A. Oxygen isotope exchange between heavy oxygen water and some niobates and tantalates. *Doklady Akad. Nauk S.S.S.R.* **118,** 107–9 (1958). *C.A.* **52,** 19358a.

S-39 SRINIVASAN, R. and NOYES, W. A. JR. Photochemical production of acetone-$O^{18}$ in the system acetone–$O_2{}^{18}$ at 3130 Å. *J. Am. Chem. Soc.* **82,** 5591–3 (1960).

S-40 Stewart, J. E., Kallio, R. E., Stevenson, D. P., Jones, A. C. and Schissler, D. O. Bacterial hydrocarbon oxidation—I. Oxidation of hexadecane by a Gram-negative coccus. *J. Bacteriol.* **78,** 441–8 (1959). *C.A.* **53,** 22238e.

S-41 Stewart, R. and Van der Linden, R. The mechanisms of permanganate oxidation—VI. The oxidation of cyanide ion. *Can. J. Chem.* **38,** 2237–55 (1960).

S-42 Stover, E. D. Rate of elimination of water molecules from the first coordination sphere of paramagnetic cations as determined by n-m-r measurements of oxygen-17. *UCRL-9265*, UC-4 Chemistry General. TID 4500.

S-43 Stranks, D. R. Isotopes in fundamental chemical research. *J. Roy. Inst. Chem.* **83,** 678–92 (1959). *C.A.* **54,** 2963a.

S-44 Sulima, L. V. and Gragerov, I. P. Mechanism of oxidation of hydrocarbons with chromyl chloride. *Zhur. Obshchei Khim.* **29,** 3825–31 (1959). *C.A.* **54,** 19450e.

S-45 Symons, M. C. R. Interaction between hydrogen peroxide and nucleophiles. *Chem. and Ind. (Rev.)* **1960,** 1480–1.

## T

T-1 Taylor, T. I. Separation of isotopes. *NYO-7763*, 179 pp (1959); *Nuclear Sci. Abstr.* **14,** 6574.

T-2 Taylor, T. I. An electrical discharge method of preparing samples for mass-spectrometric analyses of nitrogen-15 and oxygen-18. *NYO-7763* (Part VIII), 10 pp (1959). *Nuclear Sci. Abstr.* **14,** 6580.

T-3 Taylor, T. I. and Clarke, J. C. Exchange of nitric oxide with water in nitric acid solutions as a means of concentrating oxygen-18. *J. Chem. Phys.* **31,** 277–8 (1959). *C.A.* **54,** 1992c.

T-4 Teis, R. V., Chupakhin, M. S. and Naidin, D. P. Determination of paleotemperatures according to isotopic composition of oxygen in calcite of shells of some Cretaceous fossils from Crimea. *Geokhimiya* **4,** 271–7 (1957). *C.A.* **52,** 12701e.

T-5 Teis, R. V., Gromova, T. S., and Kochetkova, S. N. The isotopic composition of natural phosphates. *Doklady Akad. Nauk. S.S.S.R.* **122,** 1057–60 (1958). *C.A.* **54,** 18230e.

T-6 Thode, H. G. Variations in abundance of isotopes in nature. *Research* **2,** 154–61 (1949).

T-7 Thomas, S. L. and Turner, H. S. The synthesis of isotopically labelled organic compounds. *Quart. Revs. (London)* **7,** 407–43 (1953). *C.A.* **48,** 3239b.

T-8 Thürkauf, M., Narten, A. and Kuhn, W. Separation and concentration of isotopes of oxygen, oxygen-16, oxygen-17 and oxygen-18 by distillation of water in a precision distillation plant. *Helv. Chim. Acta* **43,** 989–1004 (1960).

T-9 Tikhomirov, M. V. and Tunitski, N. N. Separation of carbon and oxygen isotopes by rectification of CO in a 12 m column. *Zhur. Priklad. Khim.* **32,** 531–6 (1959). *C.A.* **53,** 12048i.

T-10 Tillett, J. G. Nucleophilic displacements in organic sulphites—VI. Comparison of the alkaline hydrolysis of cyclic and open-chain sulphites. *J. Chem. Soc.* **1960,** 37–40.

T-11 Trayler, T. G. and Bartlett, P. D. Oxygen-18 tracer evidence of the termination mechanism in the autoxidation of cumene. *Tetrahedron Letters* No. 24, 30–6 (1960).

T-12 Tsao, M-S. and Wilmarth, W. K. The aqueous chemistry of inorganic free radicals—I. The mechanism of the photolytic decomposition of aqueous persulphate ion and evidence regarding the sulphate-hyrodxyl radical interconversion equilibrium. *J. Phys. Chem.* **63,** 346–53 (1959). *C.A.* **53,** 13751g.

T-13 Tschang, T-L. Analysis of heavy water by densitometric methods. *Kernenergie* **3,** 892–7 (1960).

T-14 Tsenter, E. M., Khakhpashev, A. G. and Pirkin, I. A. $\gamma$-rays from $PoO^{18}$ neutron source. *Zhur. Eksptl. i Teoret. Fiz.* **37,** 1133–4 (1959).

T-15 Tudge, A. P. A method of analysis of oxygen isotopes in orthophosphates—its use in measurement of Paleotemperatures. *Geochim. et Cosmochim. Acta* **18,** 81–93 (1960).

T-16 Tunitskii, N. N., Devyatykh, G. G., Petrov, P. S. and Torlin, B. Z. Separation of carbon isotopes by thermal diffusion of carbon monoxide. *Soviet Phys. Tech. Phys.* **3,** 822–6 (1958). *Zhur. Tekh. Fiz.* **28,** 881–5 (1958). *C.A.* **53,** 17705h.

T-17 Turney, T. A. and Wright, G. A. Nitrous acid and nitrosation. *Chem. Rev.* **59,** 497–513 (1959). *C.A.* **53,** 16663b.

VOL. 11 1961


## U

U-1 Ulubekova, M. V. Isotopic composition of oxygen of cells of algae in photosynthesis. *Doklady Akad. Nauk S.S.S.R.* **112,** 772–3 (1957). *C.A.* **51,** 12238g.

U-2 Ussing, H. H. Some aspects of the application of tracers in permeability studies. *Advances in Enzymology* Vol. 13, pp. 21–65. Interscience, New York (1952).

## V

V-1 Varner, J. E., Slocum, D. H. and Webster, G. C. Transfer of oxygen in the arsenolysis of glutamine. *Arch. Biochem. Biophys.* **73,** 508–10 (1958). *C.A.* **52,** 10252e.

V-2 Vartapetyan, B. B. Study of chemistry of biological oxidation in plants with application of oxygen-18. *Problemy Kinetiki i Kataliza, Akad. Nauk S.S.S.R. 1956* **9,** 124–8 (1957). *C.A.* **53,** 8328e.

V-3 Vartapetyan, B. B. and Kursanov, A. L. Participation of oxygen of water and atmospheric oxygen on plant respiration. *Doklady Akad. Nauk S.S.S.R.* **104,** 272–5 (1955). *C.A.* **50,** 5850e.

V-4 Vartapetyan, B. B. and Kursanov, A. L. Water metabolism investigated by use of water-$O^{18}$. *Fiziol. Rastenii, Akad. Nauk S.S.S.R.* **6,** 144–9 (1959). *C.A.* **53,** 19053i.

V-5 Vartapetyan, B. B. and Kursanov, A. L. A study of oxidative condensation of catechols with the aid of $O^{18}$ and $H_2O^{18}$. *Doklady Akad. Nauk S.S.S.R.* **129,** 447–50 (1959). *C.A.* **54,** 13199b.

V-6 Vasilev, V. G. and Kharlamova, E. N. The study of the strength of the C—O bond by isotopic exchange. *Doklady Akad. Nauk S.S.S.R.* **133,** 152–4 (1960).

V-7 Vedder, R. The role of stable isotopes in geology. *Chem. Tech. Berlin* **11,** 173–80 (1959).

V-8 Vedder, R. Methodics of isotope analysis in geological samples for oxygen-18 and carbon-13. *Kernenergie* **3,** 890–2 (1960).

V-9 Vinogradov, A. P. Meteorites and the earth's crust (geochemistry of isotopes). *Proc. U. N. Intern. Conf. Peaceful Uses Atomic Energy, 2nd Geneva 1958* **2,** 255–69 (1958). *C.A.* **53,** 2976h.

V-10 Vinogradov, A. P. Isotopic composition of rocks of the earth and of meteorites. *Geochim. et Cosmochim. Acta* **15,** 80–90 (1958). *C.A.* **53,** 6000i.

V-11 Vinogradov, A. P. The isotopic composition of terrestrial rocks and meteorites. *Atomnaya Energ.* **4,** 409–16 (1958). *C.A.* **54,** 1194d.

V-12 Vinogradov, A. P. Isotope relations in magmatic rocks as applied to the problem of the genesis of rocks of the earth crust. *Geokhim. Redkikh Elementov v Svyazi s Problemoi Petrogenezisa, Trudy Geokhim. 1957* pp. 120–30. Simpoziuma, Moscow (1959). *C.A.* **54,** 5368a.

V-13 Vinogradov, A. P., Dontsova, E. I. and Chupakhin, M. S. Isotopic composition of oxygen in igneous rocks and meteorites. *Geokimiya* **1958,** 187–90. *C.A.* **52,** 16997g.

V-14 Vinogradov, A. P., Dontsova, E. I. and Chupakhin, M. S. Isotopic ratios of oxygen in meteorites and igneous rocks. *Geochim. et Cosmochim. Acta* **18,** 278–93 (1960). *C.A.* **54,** 15138i.

V-15 Vinogradov, A. P., Kutyurin, V. M. and Zadorozhnyi, I. K. Fractionation of isotopes of oxygen in the atmosphere. *Geokhimiya* **1959,** 195–205. *C.A.* **53,** 16744f.

V-16 Vinogradov, A. P., Kutyurin, V. M., Ulubekova, M. V. and Zadorozhnyi, I. K. Isotopic composition of photosynthetic oxygen. *Doklady Akad. Nauk S.S.S.R.* **125,** 1151–3 (1959). *C.A.* **53,** 20302g.

V-17 Vizgert, R. V., Savchuk, E. K. and Ponomarchuk, M. P. Study of the mechanism of hydrolysis of nitrosubstituted arylsulphonates with oxygen-18 tracing. *Doklady Akad. Nauk S.S.S.R.* **125,** 1257–9 (1959). *C.A.* **53,** 21765g.

V-18 Vojta, G. Statistical thermodynamic basis of isotope systems in chemical reactions. *Kernenergie* **3,** 917–27 (1960).

V-19 Vojta, G. Approximation formulas for quantum statistical calculations of chemical isotope exchange equilibria and application to molecules with oxygen-18. *Kernenergie* **3,** 927–30 (1960).

V-20 Vries, A. E. de and Haring, A. An improvement on age determination by the carbon-14 method. *Proc. U.N. Intern. Conf. Peaceful Uses Atomic Energy, 2nd Geneva 1958* **2,** 249–50 (1958). *C.A.* **53,** 2976f.

V-21 Vries, A. E. de, Haring, A. and Slots, W. Separation of $C^{14}O^{16}$ and $C^{12}O^{18}$ by thermal diffusion. *Proc. Intern. Symposium Isotope Separation Amsterdam* 478–82 (1958).

## W

W-1 Wang, J. H. Role of diffusion in catalysis. *J. Phys. Chem.* **59,** 1115–6 (1955). *C.A.* **50,** 659c.

W-2 Wang, J. H. and Fleischer, E. B. Tracer studies on the mechanism of combustion of carbon, sulphur and mercuric sulphide. *J. Am. Chem. Soc.* **80,** 3874–5 (1958). *C.A.* **52,** 19648d.

W-3 Wasserman, H. H. and Wharton, P. S. 1-Methoxyvinyl esters. *Tetrahedron* **3,** 321–2 (1958). *C.A.* **53,** 4187c.

W-4 Wasserman, H. H. and Wharton, P. S. 1-Methoxyvinyl esters—II. An oxygen-18 study of anhydride formation. *J. Am. Chem. Soc.* **82,** 1411–3 (1960). *C.A.* **54,** 15296d.

W-5 Waters, W. A. Mechanisms of oxidation by compounds of chromium and manganese. *Quart. Revs. (London)* **12,** 277–300 (1958). *C.A.* **53,** 7965d.

W-6 Wei, Y-K. and Bernstein, R. B. Deuterium exchange between water and boehmite (α-alumina monohydrate). Activation energy for proton diffusion in boehmite. *J. Phys. Chem.* **63,** 738–41 (1959). *C.A.* **53,** 19538e.

W-7 White E. H. and Aufdermarsh, C. A. Jr. Intramolecular reactions of secondary carbinamine nitrosoamides. *J. Am. Chem. Soc.* **80,** 2597–8 (1958). *C.A.* **52,** 19998e.

W-8 Wiberg, K. B. and Saegebarth, K. A. The mechanisms of permanganate oxidation—IV. Hydroxylation of olefins and related reactions. *J. Am. Chem. Soc.* **79,** 2822–4 (1957). *C.A.* **51,** 14570a.

W-9 Wiberg, K. B. and Saegebarth, K. A. An oxygen-18 tracer study of the acid-catalysed formation of enol ethers. *J. Org. Chem.* **25,** 832–3 (1960).

W-10 Williams, E. L. Diffusion of zinc and oxygen in single crystals of zinc oxide. *Dissertation Abstr.* **20,** 1200 (1959).

W-11 Williams, F. R. and Hager, L. P. Determination of oxygen-18 content of inorganic phosphate. *Science* **128,** 1434 (1958). *C.A.* **53,** 6887g.

W-12 Winter, E. R. S. Studies of chemisorption on oxides using oxygen-18. *Chemisorption, Proc. Symposium, Keele 1956* 189–204 (1957). *C.A.* **52,** 8677g.

W-13 Winter, E. R. S. Reactivity of oxide surfaces. *Advances in Catalysis and related Subjects* Vol. 10, pp. 196–241. Academic Press, New York (1958).

W-14 Winter, E. R. S. Decomposition of nitrous oxide upon doped nickel oxides. *Discussions Faraday Soc.* **28,** 183–191 (1960).

W-15 Wyart, J., Sabatier, G., Curien, H., Duchylard, G. and Severin, A. Isotope exchange of oxygen atoms in silicates. *Bull. Soc. France Minerall. Cristall.* **82,** 387 (1959).

## Y

Y-1 Yakimenko, L. M., Kuznets, E. D., Rabinovich, M. A. and Vitashkina, M. A. Determination of the isotope composition of some natural sources of water. *Zhur. Priklad. Khim.* **32,** 1244–50 (1959). *C.A.* **53,** 19231c.

Y-2 Yakimenko, L. M., Rabinovich, M. A., Vitashkina M. A. and Kuznets, E. D. Determination of the isotope composition of water from the Moscow water system. *Zhur. Priklad. Khim* **32,** 1251–4 (1959). *C.A.* **53,** 19231e.

Y-3 Yankwich, P. E. and Copeland, J. L. The pyrolysis of lead oxalate; isotope effects and product composition. *J. Am. Chem. Soc.* **79,** 2081–6 (1957). *C.A.* **51,** 12616i.

Y-4 Yeatts, L. B., Jr. Fractionation of nitrogen and oxygen isotopes between gaseous NO and liquid NOCl. *J. Chem. Phys.* **28,** 1255 (1958). *C.A.* **52,** 18006c.

Y-5 Yoneda, Y., Fujimotoa, F. and Makishima, S. Exchange of deuterium and heavy oxygen among hydrogen, water vapour and oxide catalysts of the spinal type. *J. Chem. Soc. Japan* **80,** 693–7 (1959). *C.A.* **54,** 57g.

Y-6 Yoneda, Y., Fujimoto, A. and Makishima, S. Exchange of deuterium and heavy oxygen among hydrogen, water vapour and oxide catalysts of spinel type. *J. Phys. Chem.* **63,** 1987–90 (1959).

Y-7 Yoneda, Y., Makishima, S. and Hirasa, K. Exchange of oxygen atoms among carbon dioxide, carbon monoxide and oxide catalysts of spinel type. *J. Am. Chem. Soc.* **80,** 4503–7 (1958). *C.A.* **53,** 2759b.

## Z

Z-1 ZAVITSANOS, P. D. Kinetics and isotope effects of the thermal decomposition of some solid metal oxalates. *Dissertation Abstr.* **20,** 4547 (1960).

Z-2 ZELVENSKII, YA. D., SOKOLOV, V. E. and SHALYGIN, V. A. Separation of isotopes by rectification. Rectification of methanol. *Nauk. Doklady Vysshei Shkoly, Khim. i Khim. Tekhnol.* No. 2, 388–90 (1958). *C.A.* **52,** 16933c.

Z-3 ZHAVORONKOV, N. M., BABKOV, S. I., ORLOV, V. YU., SAKODYNSKII, K. I., SEVRYUGOVA, N. N., SOKOLSKII, V. A. and CHERNYKH, G. N. Preparation and utilisation of stable isotopes. *Khim. Nauka i Prom.* **4,** 487–98. (1959). *C.A.* **54,** 6335g.

Z-4 ZHAVORONKOV, N. M., BABKOV, S. I. and UVAROV, O. V. Concentration of stable isotopes by a method of fractional distillation and isotopic exchange. *Collection Czechoslov. Chem. Communications* **23,** 1727–34 (1958). *C.A.* **53,** 18671f.

VOL. 11 1961

# forthcoming papers

F. A. Loewus: **The use of bis-(2-alkoxyethyl)-ethers as antifreeze in naphthalene-1,4-dioxane scintillation mixtures**

J. Myhill: **Theory of multichannel collimated scintillation detectors**

C. A. Ziegler and J. C. McCue: **Alloy composition analysis using radio-isotope excited X-rays**

T. J. Hardwick and W. S. Guentner: **Design and performance characteristics of an X-ray target for electron accelerators**

M. C. Kordecki and M. B. Gandy: **Surface area measurement by the sorption of stearic acid-1-carbon-14**

M. S. Foster, D. L. Weaver and A. F. Voigt: **Photoproduction of calcium-47** (Technical Note)

G. Leliaert and D. Decat: **The determination of copper by radioactivation** (Technical Note)

R. Stiennon-Bovy and G. Geladi: **Nomogramme pour l'utilisation des radioisotopes** (Technical Note)

L. Ekman, E. Valmet and B. Åberg: **Behaviour of yttrium-91 and some lanthanons towards serum proteins in paper electrophoresis, density gradient electrophoresis and gel filtration**

P. F. Berry and J. F. Cameron: **Leak detection using $Kr^{85}$** (Letter)

S. J. Leach and G. L. Walker: **Measurement of longitudinal dispersion of an airborne dust cloud in a tunnel**

M. W. Greene and W. D. Tucker: **An improved gallium-68 cow** (Technical Note)

VOL
11
196

International Journal of Applied Radiation and Isotopes, 1961, Vol. 11, pp. 1–9. Pergamon Press Ltd. Printed in Northern Ireland

# On the Thermochemical Action of Ionizing Radiation

V. I. GOLDANSKII and Yu. M. KAGAN
Academy of Sciences of the U.S.S.R., Moscow, U.S.S.R.

(*Received* 10 *October* 1960)

VOL. 11 1961

General characteristics of the thermochemical action of ionizing radiation are considered, namely the initiation of endothermic reactions by local heating up of microvolumes along nuclear particle tracks, and also by the overall heating up of the system irradiated.

The following problems are treated: (1) determination of the maximum (quasi-equilibrium) thermochemical action of radiation; (2) determination of the amount of heat spent in an endothermic reaction within a microvolume along the ionizing particle track; (3) determination of the total efficiency for a quasi-stationary case of averaged heating up of a mixture; (4) determination of the energy imparted to the reaction by a narrow beam of charged particles coaxial to a cylindrical volume. The results obtained (especially in Part 2) may also be of some interest for discussing the problems of annealing and retention effects upon nuclear transformations in solids.

## SUR L'ACTION THERMOCHIMIQUE DU RAYONNEMENT IONIZANT

On considère les caractéristiques générales de l'action thermochimique du rayonnement ionizant, soit l'initiation des réactions endothermiques par le chauffage local des micro-volumes le long du chemin des particules nucléaires, ainsi que par le chauffage général du système irradié.

On traite des problèmes suivants: (1) la mesure du maximum (en quasi-équilibre) de l'action thermochimique du rayonnement; (2) la mesure de la quantité de chaleur prise par une réaction endothermique dans un micro-volume le long du chemin d'une particule ionizante; (3) la mesure de l'efficacité totale pour un cas quasistationnaire du chauffage moyenné d'un mélange; (4) la mesure de l'énergie rendue à une réaction par un faisceau mince de particules chargées co-axial à un volume cylindrique.

## О ТЕПЛОХИМИЧЕСКОМ ДЕЙСТВИИ ИОНИЗИРУЮЩИХ ИЗЛУЧЕНИЙ

Рассматриваются общие характеристики теплохимического действия ионизирующих излучений, т.е. инициирования эндотермических химических реакций вследствие локального разогрева микрообъемов вдоль траекторий ядерных частиц, а также общего разогрева облучаемой системы.

Решаются следующие конкретные задачи: (1) определение максимального (квазиравновесного) КПД теплохимического действия излучений (2) определение количества тепла, расходуемого на эндотермическую реакцию в микрообъеме вдоль траектории ионизирующей частицы (3) определение суммарного КПД для квазистационарного случая усредненного общего разогрева смеси (4) определение энергии, передаваемой на химическую реакцию узким пучком заряженных частиц, проходящим по оси цилиндрического сосуда. Полученные результаты (особенно в задаче 2) могут представить определенный интерес и для обсуждения эффектов отжига и удержания после ядерных превращений в твердых телах.

## UBER DIE THERMOCHEMISCHE WIRKUNG IONISIERENDER STRAHLUNG

Die allgemeine Charakteristik der thermochemischen Wirkung von ionisierender Strahlung wird untersucht, im Hinblick auf die Auslösung endothermer Reaktionen durch lokale

Erwärmung von Mikrovolumen entlang der Bahnen nuklearer Teilchen, sowie durch die allgemeine Erwärmung des bestrahlten Systems.

Die folgenden Probleme werden behandelt: (1) Bestimmung der maximalen thermochemischen Wirkung der Strahlung (quasi Gleichgewicht); (2) Bestimmung der für endotherme Reaktionen innerhalb des Mikrovolumens entlang der Bahn des ionisierenden Teilchens verbrauchten Wärmeenergie; (3) Bestimmung der gesamten Ausbeute im quasi-stationären Fall der mittleren Erwärmung eines Gemisches; (4) Bestimmung der durch einen ausgeblendeten Strahl geladener Teilchen entlang der Achse eines zylindrischen Volumens abgegebenen Reaktionsenergie.

## INTRODUCTION

THE initiation of chemical reactions by ionizing radiation is a problem obtaining an ever-increasing importance both in theory and practice. Of especial interest from the standpoint of nuclear energy applied to chemistry would be the possibility of conducting energy-consuming syntheses i.e. of accomplishing radiation-induced initiation of endothermic chemical reactions. Such an application of the nuclear energy may in principle be directed along two paths. The first would involve individual hot atoms formed in the interaction between radiation and the substance at the primary or some other reaction stage. These atoms have an energy above the threshold energy of endothermic reactions and readily participate in the latter. The second path would be connected with a local heating up of microvolumes along nuclear particle tracks, as well as with the heating up of the overall system. A corresponding rise in temperature markedly increases the rates of endothermic reactions, especially in microvolumes along tracks of ionizing particles.

Despite the amount of energy spent in chemical conversions, the temperature of heated microvolumes appears to be above that of the environment. Of great importance is the fact that, in the subsequent levelling out of temperature by diffusion and heat conduction, the rate of inverse decomposition of reaction products may already be neglected (especially if the amount of these products is far from equilibrium even at a maximum initial heating up). Thus the products of conversion in heated up microvolumes are so-to-say "quenched" and their yield may appear to be appreciably higher than that at equilibrium with uniform heating up of the overall system by ionizing radiation.

However, the times of reactions within a a macrosystem are considerably longer than the cooling time of microvolumes along particle tracks, and the overall volume of the system considerably exceeds the sum of these microvolumes. Consequently, for a general case, the contribution of reactions in a system with averaged heating up may appear to be comparable to that of reactions in microvolumes.

The action of ionized radiation, defined here as "thermochemical", is obviously non-equilibrium, i.e. of kinetic origin, and it will correspondingly depend on the reaction rates, diffusion and heat conduction, both in microvolumes along particle tracks and in the overall system. Unlike the mechanism of hot atom reactions, the thermochemical action of ionizing radiation is subject to ready investigation. The given paper will in fact be concerned with a mostly qualitative investigation of this kind.

## CHARGED PARTICLE TRACKS IN A CONDENSED MEDIUM

Charged particle tracks may fall into three classes depending upon the localization of energy losses:

(1) *Tracks of the fragmentary type.* These involve the liberation of very high energies within small track lengths (ionization density of the order of 40,000 MeV/g.cm$^2$, i.e. exceeding that of the relativistic ionization by a factor of almost 20,000). The zone of effective "thermal damage" of the substance will in this case be much larger than the volume of the primary ionization core along

the track. The primary core may thus be considered as a thread-like source of energy located along the axis of a heated cylinder.[1]

(2) *Tracks of fast but essentially non-relativistic heavy particles.* In this case the ionization zone may be modelled by a cylinder with a certain radial distribution of the ionization density, for instance of the type described in[2].

The effective diameter of the ionization zone decreases with increase in the particle velocity. Processes characterized by a certain energy threshold will ultimately occur, not throughout the "averaged" volume but along the primary particle track and the tracks of individual $\delta$-electrons. At the limit the increase in velocities will obviously lead to a third type of track.

(3) *Tracks of relativistic particles.* Processes involving an energy threshold are concentrated in preference along discrete tracks of $\delta$-electrons and, to a certain extent, in regions of elevated ionization density (of a fluctuation origin) along the primary particle track.

The models used in discussing tracks of the first and second type can naturally be applied to conversions along tracks of individual $\delta$-electrons as well.

The given classification of tracks is of course largely conditional, any intermediate case may virtually take place. This paper will be concerned only with the thermochemical action of heavy ionizing particles corresponding to the first and second track models.

## DETERMINATION OF THE MAXIMUM (QUASI-EQUILIBRIUM) THERMOCHEMICAL ACTION OF RADIATION

Let us begin with a most simple case—the determination of the thermochemical action of radiation under conditions when all the energy input is spent in the heating up of the mixture and in the endothermic reaction, while heat release is vanishingly low. Analysis of a quasi-stationary case of this kind is a strictly thermodynamic problem and no kinetic characteristics need be introduced. However, as criterions should be established for the applicability of the discussed variants, let us mention three time characteristics, taken as a basis for these criterions, namely:

$\tau_r$, the proper time of a reaction, i.e. the time necessary for attaining equilibrium (inversely proportional to the rate constant and consequently directly proportional to $e^{E/kT}$, $E$ being the activation energy);

$\tau_l$, the time of effective levelling out of the temperature microdistribution, accounted for by the heat release from track microvolumes;

$\tau$, time of the mixture exposure to radiation.

In the quasi-stationary case under discussion, $\tau_r \ll \tau_l$. i.e. the reaction is completed long before the termination of heat release.

The heated-up microvolumes along tracks of heavy charged particles will be considered as the reaction zone, since at normal flow densities these tracks do not overlap. The value of $\tau$ will then be determined by the rate of diffusion and will obviously be close to $\tau_l$. Thus, as $\tau_r \ll \tau$, it may be disregarded. It will be assumed in qualitative terms that chemical equilibrium corresponding to the new temperature will be established within a time, $t$, much shorter than that necessary for heat release ($\tau_l$) and diffusion ($\tau$). Cooling is accounted for solely by the endothermic reaction, and consequently the final temperature, $T_f$, will fail to attain its maximum possible value, $T_m$ (in the absence of endothermic processes). It will also be assumed that the initial system was also at equilibrium, as consistent with its initial temperature, $T_0$. The microvolumes will be considered as axially symmetrical. Temperature changes along their axes will be neglected. Then, after heating, the temperature becomes $T_m = T_m(r)$, where $r$ is the distance from the track axis. This results in an endothermic reaction, the temperature falling off in every point. A new equilibrium depending upon $r$ will be attained. The condition $T_0 < T_f(r) < T_m(r)$ for the final temperature $T_f(r)$ will be valid at every point.

Let us estimate the amount of substance

having reacted within a microvolume before the new equilibrium set in or, in other words, the amount of energy spent in the chemical reaction.

For the sake of definiteness the reaction will be considered as occurring in a condensed phase, and possible phase transitions will be neglected.

The chemical equilibrium before heating is

$$\prod_i C_{i0}^{\nu_i} = K(T_0) \tag{1}$$

and the final stage

$$\prod_i C_{if}^{\nu_i}(r) = K[T_f(r)] \tag{2}$$

where $C_i = \frac{n_i}{n}$ and is the concentration of reagents and reaction products; $n = \Sigma n_i$ the mixture density, and $\nu_i$ are the corresponding stoichiometric coefficients (positive for reaction products and negative for initial substances).

The amount of heat absorbed per unit volume at the expense of the reaction is

$$q(r) = \frac{n_{ik}(r) - n_{i0}}{\nu_i} q_0 = N(r) q_0 \tag{3}$$

where $n_{ik}$ and $n_{i0}$ correspond to final and initial conditions respectively, $q_0$ is the heat of reaction, and $N(r)$ is the number of elementary reactions per unit volume.

Let us express $C_{if}(r)$ through $C_{i0}$:

$$C_{ik} = \frac{n_{i0} + N\nu_i}{n_0 + N\sum_i \nu_i} = C_{i0} \frac{1 + \dfrac{N\nu_i}{n_{i0}}}{1 + \dfrac{N\sum \nu_i}{n_0}}. \tag{4}$$

Substituting (4) into (2) we obtain after transformation

$$\prod_i \left( \frac{1 + \dfrac{N\nu_i}{n_{i0}}}{1 + \dfrac{N\sum \nu_i}{n_0}} \right)^{\nu_i} = \frac{K[T_f(r)]}{K(T_0)}. \tag{5}$$

The final temperature distribution after completion of the reaction in the given case ($\tau_r \ll \tau_1$), at a moment $t$ for which $\tau_r \ll t \ll \tau_1$, is accounted for by

$$T_f(r) = T_m(r) - \frac{N(r) q_0}{C\rho} \tag{6}$$

where $C$ is the specific heat and $\rho$ the density.

In a general case the product $C\rho$, equal to the specific heat per unit volume, will be related to temperature, first of all due to the temperature dependence of the density. However, it may be assumed here that no essential change in the substance density succeeds in taking place within a microvolume during $t$. On the other hand, if one allows for the fact that the heat capacity increases with temperature, it would be possible to assume, disregarding the slight decrease in density, that $C\rho = \text{const}$.

Once the $T_m(r)$ function is known, equations (5) and (6) provide an unambiguous description for $N(r)$ and $T_f(r)$.

The amount of product $i$ formed per unit path length will, obviously, be

$$W_i = \int_{r_{\min.}}^{r_{\max.}} N(r) \nu_i \, 2\pi r \, dr \tag{7}$$

where the limits $r_{\min.}$ and $r_{\max.}$ will be selected according to the given mode of $T_m(r)$ determination.

The amount of heat absorbed in the chemical reaction is

$$Q = \int_{r_{\min.}}^{r_{\max.}} N(r) q_0 \, 2\pi r \, dr. \tag{8}$$

Since we wish to establish what amount of the nuclear radiation energy is imparted to the chemical reaction, of main interest would be the efficiency value

$$\eta = \frac{q_0 \int_{r_{\min.}}^{r_{\max.}} N(r) \, 2\pi r \, dr}{\int_{r_{\min.}}^{r_{\max.}} [T_m(r) - T_0] C\rho \, 2\pi r \, dr} \tag{9}$$

Reaction $A + B \rightarrow D + F$ (where $\sum_i \nu_i = 0$) will be discussed for the sake of simplicity, assuming that $n_{A0} = n_{B0}$ and $n_{D0} = n_{F0}$. The equation

$$\frac{N(r)}{n_{A0}} = \frac{\exp\left[\dfrac{q_0}{2k}\left(\dfrac{1}{T_0} - \dfrac{1}{T_f(r)}\right)\right] - 1}{\dfrac{1}{\sqrt{k(T_0)}} + \exp\left[\dfrac{q_0}{2k}\left(\dfrac{1}{T_0} - \dfrac{1}{T_f(r)}\right)\right]} \tag{10}$$

will be readily obtainable.

Substituting then into (10) the expression (6) for $T_r(r)$, and assuming a definite form of $T_m(r)$, we obtain a simple transcendental equation for $N(r)$ and consequently for the values $W_i$, $Q$ and $\eta$ under question (see equations 7–9).

If the distribution of $T_m(r)$ may be approximated over a Π-shaped function, a quite obvious relation for $\eta$ will be obtained:

$$\eta = \frac{q_0 N}{C\rho(T_m - T_0)}. \tag{11}$$

## THE KINETIC PROBLEM OF REACTIONS IN MICROVOLUMES ALONG TRACKS OF IONIZING PARTICLES

Let a large volume be exposed to radiation. An endothermic reaction will consequently take place within this volume. Heat excess will be withdrawn via the system surface. Due to the continuous removal of reaction products their concentration remains unchanged. An averaged steady-state picture with a temperature distribution of $T_s(r)$ will thus be attained. However, an investigation of this picture will be insufficient for our purpose, since a large amount of energy spent in chemical reactions is due to non-stationary processes connected with individual particle tracks. Assuming that there is no overlapping of tracks, we may estimate the total contribution of these local non-stationary processes for one track.

When the time of the mixture exposure is sufficiently short, conditions may be obtained under which the inverse reaction in the averaged steady state will be negligible. These would apparently be (a) $\tau \ll \tau_r(T_s, C_i^s)$ and (b) $\tau_1 \ll \tau_r$ $(T_{\text{track}}, C_i^s)$. The first condition corresponds to a short time of exposure as compared with the time required for the attainment of equilibrium at a constant temperature, $T_s$, and steady-state concentrations $C_i^s$. The second corresponds to conditions under which the heat release and diffusion from microvolumes is sufficiently fast and consequently the chemical equilibrium, similar to that described in the preceding section of this paper and corresponding to elevated temperatures, does not succeed in becoming established. Thus the concentration of end-products is supposed to be always considerably below that at equilibrium.

Let us now consider tracks of the fragmentary type. As stated before, they may be considered as thread-like heat sources.

In the absence of heat release, the rise in temperature $\Delta T$ within the volume at a moment, $t$, upon passage of a particle, may be approximately written as

$$\begin{aligned} \Delta T &= \frac{Q_0}{4\pi C\rho\chi t} \quad (r^2 < 4\chi t) \\ \Delta T &= 0 \qquad\qquad (r^2 > 4\chi t) \end{aligned} \tag{12}$$

where $\chi$ is the thermal diffusivity coefficient (cm²/sec), $\lambda = C\rho\chi$ and is the heat conduction coefficient (cal/cm sec grad), $Q_0$ is the amount of heat liberated per unit track length (cal/cm), $C$ is the specific heat, and $\rho$ is the density.

When the reaction is endothermic, a part of the energy will be absorbed, the rate of absorption per unit volume being $Ae^{-E/kT}$ (cal/cm³ sec) (where $E$ is the activation energy, and $A$ is the product of the reaction heat by the reaction rate pre-exponential).

On the assumption that the heat propagation rate remains unchanged in the course of the reaction, the latter's progress may be considered as an effective decrease in $Q_0$. Then, instead of equation (12) we obtain

$$\Delta T(t) = \frac{Q(t)}{4\pi C\rho\chi t} \quad (r^2 < 4\chi t). \tag{13}$$

The overall integral relation for $Q(t)$ will be

$$Q(t) = Q_0 - \Delta Q(t) = Q_0 - 4\pi A \times \int_0^t \chi t'\,dt' \exp\left\{-\frac{E}{k}\frac{1}{T_s + \dfrac{Q(t')}{4\pi C\rho\chi t'}}\right\}. \tag{14}$$

For a general case, equation (14) may be solved only by the method of successive approximations. In practice, however, the first approximation, with replacing of $Q(t')$

by $Q_0$ in the exponent of the integral, already appears to be adequate. Strictly speaking, this corresponds to absorption of a small part only of the liberated energy. The main contribution to the integral of equation (14) is made by temperatures above $T_s$ $\left(\text{of the order } \frac{E}{k}\right)$. Assuming a power dependence of $\chi$ on $T$ and taking into account that within the temperature range under question $\Delta T \gg T_s$, we may write $\chi \simeq \beta(\Delta T)^s$.

We obtain, then, from equation (13)

$$\Delta T = \left(\frac{Q_0}{4\pi C\rho\beta t}\right)^{1/1+s}. \qquad (15)$$

The heat absorbed by the chemical reaction will be accounted for by the approximate expression

$$\Delta Q(t) \approx 4\pi A\beta \left(\frac{Q_0}{4\pi C\rho\beta}\right)^{s/1+s} \times \int_0^t t^{1/1+s}dt \exp\left\{-\frac{E}{k}\frac{t^{1/1+s}}{\left(\frac{Q_0}{4\pi C\rho\beta}\right)^{1/1+s}}\right\}. \qquad (16)$$

Of interest is the overall value of heat absorbed during the time taken by the track to become diffuse. Since with the rise in $t$ the integral in equation (16) rapidly converges, it may be assumed that at the upper limit $t = \infty$ and then, as $s$ is nearly always positive,

$$\Delta Q_\infty \approx \frac{1}{4\pi}\frac{A}{\chi\left(T = \frac{E}{k}\right)}\left(\frac{Q_0\kappa}{\rho CE}\right)^2 \times (1+s)\Gamma(2+s). \qquad (17)$$

where $\Gamma$ is the gamma-function.

By allowing for the path length of the fragments and their total number per unit volume in unit time, it is possible to determine from equation (17) the specific absorption of their energy in an energy-consuming chemical synthesis. It will be noted that the conversion on nuclear into chemical energy is more effective with processes of a lower activation energy ($\Delta Q_\infty \sim E^{-(2+s)}$) (assuming, however, as before that $E > kT_s$).

Since the above considerations seem to be of fairly wide practical importance, it would be feasible to make the most general qualitative estimates pertinent to equations (12) and (17).

| Condensed phase | Gases |
|---|---|
| $\rho C \sim 1$ cal/cm³ grad | $\rho C \sim 10^{-4}$ cal/cm³ grad |
| $\chi \sim 10^{-3}$ cm²/sec | $\chi \sim 1$ cm²/sec |
| $Q_0 \sim 10^{-9}$ cal/cm (for fission fragments) | $Q_0 \sim 10^{-13}$ cal/cm (for fission fragments) |
| If $r^2 < 5 \times 10^{-3}\, t$ cm², $\Delta T \approx \frac{6 \times 10^{-6}}{t}$ grad | If $r^2 < t$ cm², $\Delta T \approx \frac{2 \times 10^{-9}}{t}$ grad |

It will be assumed that the effective course of endothermic reactions would require a heating up of no less than $\Delta T \approx 1000$°C. As may be seen from the above figures such a heating up will occur both in the condensed and in the gas phase within a cylinder along a fission fragment track of the radius $r \approx 10^{-6}$ cm. However, in the condensed phase the heating up time for such a cylinder will be $t \sim 10^{-10}$ sec which is about three orders higher than the characteristic time interval, $\tau$, between molecular collisions in a liquid ($\tau \sim \frac{1}{\pi d^2 n}\sqrt{\frac{\overline{6M}}{kT}} \sim 10^{-13}$ sec), whereas in the gas phase $t \sim 10^{-12}$ sec which is two orders lower than the characteristic $\tau$ value for gases. Thus the reaction in microvolumes along fission fragment tracks may be considered as taking place effectively in the condensed phase, while the very use of equation (12) for the gas phase is possible only under definite restrictions.

It will be seen in passing to equation (17) that the fundamental factor $\frac{AQ_0}{\chi}\left(\frac{k}{\rho CE}\right)^2$, characteristic of the efficiency given by the thermochemical utilization of the particle energy $\frac{\Delta Q_\infty}{Q_0}$, is also different for the condensed and the gas phase (the numerical factor

$$\frac{(1+s)\Gamma(2+s)}{4}$$

changes from 0·32 to 7·6 with changing of $s$ from 1 to 3, i.e. tends to unity). Under the assumption that $E = 2q$ and $q \approx 2{\cdot}5$ eV, the

value of $\frac{\Delta Q_\infty}{Q_0}$ will be about unity for fission fragments in the condensed phase and about $10^{-3}$ in the gas phase. This provides another confirmation for the efficiency of thermochemical utilization of fission fragment energies in the condensed phase. It will be noted, moreover, that the additional thermochemical effect connected with molecular thermal dissociation and the consequent reactions between free atoms and radicals was not accounted for in any section of this paper.

## THE QUASI-STATIONARY PROBLEM OF AVERAGED HEATING UP

Let us now consider the chemical reaction yield in terms of an averaged stationary problem, i.e. the yield of a macrosystem heated up uniformly under the action of ionizing radiation. A problem of this kind may be encountered, for instance, in a case when a mixture of substances capable of undergoing an endothermic reaction is utilized for the removal of energy in various reactors. The efficiency of utilizing the energy liberated in the averaged heating up of a system is, as a rule, considerably lower than that of the local heating up of microvolumes along tracks of heavy ionizing particles with subsequent "quenching". However, the energy concentrated in microvolumes may be a very insignificant part only of the total energy of nuclear particles emitted by a radiation source. Besides, practical accomplishment of the removal of "averaged" heat is often obtained by more simple means than the utilization of heat from the microvolumes. Consequently the averaged stationary problem would also be of interest. The part played by the time criterions cited above should then also be taken into account, assuming again that the time of reaction, $\tau_r$, in an "averaged" system considerably exceeds that of the removal of reagents ($\tau$).

If the heat sources are distributed uniformly throughout the volume, the equation for heat conduction in the given case will be

$$\operatorname{div}(\lambda \operatorname{grad} T_s(\mathbf{r})) + W - A \exp\left[\frac{E}{kT_s(\mathbf{r})}\right] = 0 \tag{18}$$

where $W$(cal/cm³ sec) is the amount of heat liberated per unit volume in unit time (subtracting the energy spent for chemical reactions in regions adjacent to tracks).

Obviously

$$W = nl\,(Q_0 - \Delta Q_\infty) \tag{19}$$

where n($\mathrm{cm^{-3}\,sec^{-1}}$) is the density of appearing tracks, and $l$ their track length. For certainty, let us consider a reaction proceeding in a parallel plate vessel at a fixed wall temperature $T_0$.

Assuming that $T_s(\mathbf{r}) - T_0 = \Delta T$ is relatively low compared with $T_0$, we may use the approximate transformation of the exponential term in equation (18). Then neglecting the temperature dependence of $\lambda$, we get, instead of equation (18),

$$\lambda \frac{d^2(\Delta T)}{dZ^2} + W - A^* \exp\left(\frac{E}{kT_0^2}\Delta T\right) = 0 \tag{20}$$

where $A^* = A \exp\left(-\frac{E}{kT_0}\right)$, the boundary conditions being

$$\left(\frac{d\Delta T}{dZ}\right)_{Z=0} = 0 \quad \text{and} \quad (\Delta T)_{Z=Z_0} = 0. \tag{21}$$

Integrating equation (20) and allowing for (21,) we get a solution in an implicit form

$$\int_0^{(\Delta T)_Z} \frac{dy\sqrt{\lambda}}{\sqrt{2\frac{A^*kT_0^2}{E}\exp\left(\frac{E}{kT_0^2}y\right) - 2Wy + F}} = Z_0 - Z \tag{22}$$

where

$$F = 2W(\Delta T)_{Z=0} - \frac{2A^*kT_0^2}{E} \times \exp\left(\frac{E}{kT_0^2}(\Delta T)_{Z=0}\right). \tag{23}$$

The value of $(\Delta T)_{Z=0}$ is obtained by solving equation (22) at $Z = 0$.

The energy absorbed by a chemical reaction per unit time inside a column $2Z_0$ long with a unit base area ($s = 1$ cm$^2$) will be determined by the relation

$$U = 2Z_0W - 2\lambda\left(\frac{d\Delta T}{dZ}\right)_{Z=Z_0}. \quad (24)$$

As follows from equation (20)

$$\left(\frac{d\Delta T}{dZ}\right)_{Z=Z} = -\sqrt{\frac{1}{\lambda}\left(\frac{2A^*kT_0^2}{E}+F\right)} \quad (25)$$

so that

$$U = 2\left\{Z_0W - \sqrt{\lambda\left(\frac{2A^*kT_0^2}{E}+F\right)}\right\}. \quad (24')$$

The total amount of nuclear energy absorbed by a chemical reaction inside the column under question ($2Z_0 \times 1$ cm$^3$) per unit time will be

$$U_{\text{tot.}} = U + nl2Z_0\Delta Q_\infty = 2\left\{Z_0nlQ_0 - \sqrt{\lambda\left(\frac{2A^*kT_0^2}{E}+F\right)}\right\} \quad (26)$$

$nlQ_0$ being the overall nuclear radiation energy liberated per unit time in unit volume.

Thus the total part of the utilized nuclear energy will be

$$\eta = 1 - \frac{\sqrt{\lambda}}{Z_0nlQ_0}\sqrt{2\frac{A^*kT_0^2}{E}+F}. \quad (27)$$

It will again be emphasized that the efficiency of the utilization of energy liberated in the averaged heating up of the system is, as a rule, less with the heating up of microvolumes along particle tracks.

## THE THERMOCHEMICAL EFFECT OF A NARROW BEAM OF CHARGED PARTICLES

Narrow beams of accelerated charged particles are often used in practice. Analysis of reactions along individual tracks of the beam reveals no specific characteristics provided the tracks do not overlap. In order to describe stationary conditions outside the beam, it would be feasible to consider the geometry of a cylinder coaxial with the beam and having a radius $R_0$.

Making use of equation (18) and assuming that $\lambda = \text{const}$, we have

$$\lambda\left\{\frac{d^2(\Delta T)}{dr^2}+\frac{1}{r}\frac{d\Delta T}{dr}\right\} - A^*\exp\left(\frac{E}{kT_0^2}\Delta T\right) = 0. \quad (28)$$

Let us introduce an effective beam radius, $r_0$. Neglecting the energy absorption within a range $r < r_0$ and assuming that the energy liberated per unit beam length considerably exceeds that absorbed in a similar volume at a wall temperature, $T_0$, we obtain for boundary conditions

$$-\lambda\frac{d\Delta T}{dr}2\pi r\Big|_{r=r_0} = \varepsilon \qquad (\Delta T)_{r=R_0} = 0 \quad (29)$$

where $\varepsilon$ (cal/cm sec) is the energy lost every second per unit path length.

A transformation of the exponent similar to transition from equation (18) to (20) is assumed to hold within the range $r > r_0$.

Substituting the variables we get

$$\exp\left(\frac{E}{kT_0^2}\Delta T\right) = \frac{1}{Z^2}. \quad (30)$$

Equation (28) may then be rewritten as

$$Z\frac{d^2Z}{dr^2} - \left(\frac{dZ}{dr}\right)^2 + \frac{1}{r}Z\frac{dZ}{dr} + B = 0 \quad (31)$$

where

$$B = \frac{A^*E}{2\lambda kT_0^2}. \quad (32)$$

Equation (31) will be solved as

$$Z = \alpha_1 r^a + \alpha_2 r^b. \quad (33)$$

Direct substitution readily shows that the solution of equation (33) satisfies (31) if

$$a + b = 2 \quad \alpha_1\alpha_2 = -\frac{B}{(b-a)^2}. \quad (34)$$

VOL 11 196

Making use of the first boundary condition of equation (29), we obtain

$$\frac{a + \frac{\alpha_2}{\alpha_1}(2-a)\, r_0^{2(1-a)}}{1 + \frac{\alpha_2}{\alpha_1} r_0^{2(1-a)}} = \gamma_0 = \frac{E\varepsilon}{4\pi\lambda k T_0^2}. \tag{35}$$

The second boundary condition of equation (29) will be, allowing for equation (30).

$$\alpha_1 R_0^a + \alpha_2 R_0^{2-a} = 1. \tag{36}$$

Multiplying both parts of equation (36) by $\alpha_1$ and making use of equation (34) we get

$$\alpha_1 = \frac{1}{2R_0^a}\left\{1 + \sqrt{1 + \frac{BR_0^2}{(1-a)^2}}\right\}. \tag{37}$$

Determining $\alpha_2$ from equations (37) and (34), we readily obtain the ratio of $\alpha_2/\alpha_1$. The value of $a$ may then be obtained from equation (35).

If $\gamma_0 < 1$, the limit $r_0 \to 0$ can be used in equation (35). The first boundary condition of equation (29) will then be represented by a conventional condition for a threadlike source. The value of $a$ (lower index) will then be readily obtained:

$$a = \frac{E\varepsilon}{4\pi\lambda k T^2} = \gamma_0 \quad . \tag{38}$$

Besides, the coefficient of the term with a lower index will be positive in this case, and consequently at $r_0 \to 0$ the root of $\alpha_1$ in equation (37) will also be positive. The energy imparted by the beam to the chemical reaction per unit path length may now be determined:

$$W = \varepsilon - \lambda 2\pi R_0 \left(\frac{d\Delta T}{dr}\right)_{r=R_0}$$

$$= \varepsilon - \frac{\varepsilon}{a}(\alpha_1 a R_0^a + \alpha_2 b R_0^b) \quad . \tag{39}$$

Making use of equation (36) we obtain the following expression for the efficiency of the thermochemical utilization of the beam energy.

$$\eta = \frac{W}{\varepsilon} = 1 - \frac{1}{a}\left\{(2-a) - 2\alpha_1 R_0^a (1-a)\right\} \tag{40}$$

## CONCLUSIONS

The given work is concerned with general characteristics of the thermochemical effect of ionizing radiation, no quantitative illustrations being given.

It will be emphasized that a more explicit discussion of the problems treated above would involve data on radial temperature distribution along tracks of ionizing particles, as well as allowance for the fact that many parameters obtained for macroscopic systems under ordinary conditions may be essentially different under irradiation, especially at a high density of ionization. Indetermined phase transitions in the zone affected by radiation may also be of importance. All this makes the given work essentially qualitative. Nevertheless it may be anticipated that comparison with more definite results would permit more precise definition and development of the given calculations. The latter would also be of assistance in finding out whether the main part in the chemical action of radiation is played by the thermochemical action of ionizing radiation (either localized in microvolumes or averaged) or by the effects due to hot atoms and radicals. In addition, the given calculations may be of use in discussing the possible application of energy-consuming chemical systems for the utilization of heat energy emitted by various radiation sources.

## REFERENCES

1. Lifshitz I. M., Kaganov M. I. and Tanatarov L. V. *Atomnaya Energiya* **6,** 391 (1959).

2. Kagan Yu. M. *Dokl. Akad. Nauk SSSR* **119,** 247 (1958).

VOL. 11 1961

International Journal of Applied Radiation and Isotopes, 1961, Vol. 11, pp. 10–29. Pergamon Press Ltd. Printed in Northern Ireland

# Selective Radioactivation and Multiple Coincidence Spectrometry in the Determination of Trace Elements in Biological Material

## MEASUREMENT OF MANGANESE*

D. C. BORG, R. E. SEGEL,† P. KIENLE‡ and L. CAMPBELL§
Medical, Reactor, and Instrumentation and Health Physics Departments
Brookhaven National Laboratory, Upton, New York, U.S.A.

(*Received* 10 *October* 1960)

The capacity of activation analysis to detect trace constituents in samples solely by radioanalytical means can be advanced dramatically by enhancing the specificity of both the activation and the detection methods.

Coincidence spectrometric techniques frequently can resolve the radiations from complicated mixtures of radioisotopes by capitalizing on differentiating characteristics of the pertinent decay schemes. When isotopes with distinctive $\beta$–$\gamma$-decay chains are selected for detection, scintillation spectrometry may be employed. Then the $\gamma$-spectrum from a NaI(Tl) crystal can be recorded by a multichannel pulse-height analyzer that is gated by a coincidence circuit when it simultaneously receives signals from the $\gamma$-counter and from a $\beta$-scintillation spectrometer. When used in this way, the power of a two-crystal $\beta$–$\gamma$-detector to resolve a single $\beta$–$\gamma$-decay branch is limited by the $\gamma$-response of the $\beta$-sensing element, which thus records interfering $\gamma$–$\gamma$-cascades. A marked improvement in selective $\beta$–$\gamma$-discrimination is provided by a three-crystal coincidence geometry, where an additional plastic or anthracene crystal (which is so thin as to have negligible $\gamma$-sensitivity) is placed in front of the thicker crystal of the $\beta$-spectrometer to distinguish $\beta$- from $\gamma$-rays.

When radiometric analysis is applied to neutron-activated sources, detection of certain nuclides with low-energy (n, $\gamma$) resonances (e.g. $Mn^{55}$, $Co^{59}$) may be further enhanced relative to other isotopes without such resonances (e.g. $Na^{23}$, $Cl^{37}$) by irradiating with resonance neutrons.

In an example of neutron activation analysis of manganese, selective activation with a filtered reactor neutron spectrum and triple coincidence spectrometry were combined. The former enhanced the ratios of $Mn^{56}/Na^{24}$ and $Mn^{56}/Cl^{38}$ activation to about seven times and fifteen times, respectively, the values produced by thermal neutrons; while the latter suppressed by a factor of about 100 the interference due to $Na^{24}$ in the detection of $Mn^{56}$ by $\gamma$-spectrometry. In this way, manganese in blood plasma may be measured without recourse to radiochemical separations.

### LA RADIO-ACTIVATION SELECTIVE ET LA SPECTROMETRIE A COINCIDENCE MULTIPLE DANS LE DOSAGE DES ELEMENTS-TRACES DANS LES MATIERES BIOLOGIQUES

On peut élever dramatiquement la capabilité de l'analyse à l'activation de découvrir les composants-traces dans les échantillons seulement par les moyens radio-analytiques, en augmentant la spécificité et de la méthode d'activation et de la méthode de détection.

* This work was supported by the U.S. Atomic Energy Commission.
† Guest scientist from The Aeronautical Research Laboratory, Dayton, Ohio.
‡ Present address: Technische Hochschule, München, Germany.
§ Present address: Massachusetts Institute of Technology, Cambridge, Mass.

Les techniques spectrométriques à coïncidence peuvent souvent résoudre les rayonnements des mélanges compliqués de radio-isotopes en prenant avantage des différents caractères particuliers des systèmes pertinents de décadence. Lorsqu'on a choisi des isotopes ayant des chaines distinctives de décadence $\beta$–$\gamma$ pour la détection, on peut employer la spectrométrie à scintillement. Alors on peut enregistrer le spectre $\gamma$ d'un cristal NaI(Tl) avec un analyzateur de hauteur de pulsation à cannelation multiple, lequel est barré par un circuit à coïncidence lorsqu'il reçoit simultanément des signaux du compteur $\gamma$ et du spectromètre à scintillement $\beta$. Lorsqu'il s'emploie en cette façon, la capabilité d'un détecteur $\beta$–$\gamma$ à deux cristaux de résoudre une seule branche de décadence $\beta$–$\gamma$ se limite par la réponse aux $\gamma$ de l'élément répondant aux $\beta$, qui enregistre ainsi les cascades gênantes $\gamma$–$\gamma$. Une amélioration considérable de la discrimination sélective $\beta$–$\gamma$ provient d'une géométrie de coïncidence à trois cristaux, où un cristal supplémentaire de plastique ou d'anthracène (lequel est mince de sorte à avoir une sensibilité négligeable aux $\gamma$) est situé devant le cristal plus épais du spectromètre $\beta$ afin de reconnaître les rayons $\beta$ des rayons $\gamma$.

Lorsque le dosage radiométrique s'applique aux sources activées aux neutrons, la détection de certains nucléides ayant des résonances (n,$\gamma$) de faible énergie (e.g. $Mn^{55}$, $Co^{59}$) peut être améliorée encore plus enrapport avec d'autres isotopes sans telles résonances (e.g. $Na^{23}$, $Cl^{37}$) en faisant l'irradiation avec des neutrons à résonance.

Dans un example du dosage de manganèse par activation aux neutrons, on combina l'activation sélective avec un spectre filtré de neutrons d'un réacteur et la spectrométrie à triple coïncidence. Le premier augmenta la proportion d'activation $Mn^{56}/Na^{24}$ jusqu'à environ sept fois, et celle $Mn^{56}/Cl^{38}$ à environ quinze fois, les valeurs données par les neutrons thermiques; tandis que le dernier supprima par un facteur d'environ 100 l'intervention produite par le $Na^{24}$ dans la détection du $Mn^{56}$ par la spectroscopie $\gamma$. De cette façon, on peut doser le manganèse dans le plasma de sang, sans avoir recours aux séparations radiochimiques.

## ИЗБИРАТЕЛЬНАЯ РАДИАЦИОННАЯ АКТИВАЦИЯ И СПЕКТРОМЕТРИЯ ПО СХЕМЕ МНОГИХ СОВПАДЕНИЙ ПРИ ОПРЕДЕЛЕНИИ НИЧТОЖНО МАЛЫХ КОЛИЧЕСТВ ЭЛЕМЕНТОВ В БИОЛОГИЧЕСКОМ МАТЕРИАЛЕ

### Измерения марганца

Возможность определения активационным анализом ничтожно малых примесей может быть очень сильно увеличена путем использования специфики методов активации и обнаружения.

При применении спектрометрического метода совпадений часто удается разделить радиоактивное излучение сложных смесей радиоизотопов, учитывая особенности соответствующих схем распада. Когда требуется определять изотопы с отчетливо выраженными цепями $\beta$–$\gamma$-распада можно применять сцинтилляционную спектрометрию. Далее гамма-спектр NaI(Tl) можно зарегистрировать путем применения многоканального амплитудного анализатора импульсов, причем в тех случаях, когда импульсы поступают одновременно от $\gamma$-счетчика и сцинтилляционного $\beta$-спектрометра, его снабжают селекторной схемой совпадений. В этом случае способность $\beta$–$\gamma$-детектора с двумя кристаллами разрешать простую ветвь $\beta$–$\gamma$-распада лимитируется $\gamma$-чувствительностью $\beta$-спектрометра, обуславливающей регистрацию помех от $\gamma$–$\gamma$-каскадов. Избирательное $\beta$–$\gamma$-разделение можно значительно улучшить применением геометрии с тремя кристаллами, при которой дополнительный пластмассовый или антрацитовый кристалл (настолько тонкий, что его $\gamma$-чувствительность ничтожно мала) помещают впереди более толстого кристалла $\beta$-спектрометра, что обеспечивает возможность разделения $\beta$ и $\gamma$ лучей.

При радиометрическом анализе с применением источников, активируемых нейтронами, облучение некоторых изотопов (например $Mn^{55}$, $Co^{59}$) с низкой энергией (n, $\gamma$) резонанса позволяет выделить их из числа других изотопов, не обладающих таким резонансом (например $Na^{23}$, $Cl^{37}$).

В случае нейтронного активационного анализа марганца избирательная активация получаемыми от реактора нейтронами с фильтруемым спектром комбинировалась со спектрометрией тройных совпадений. В результате активации значения отношений активностей $Mn^{56}/Na^{24}$ и $Mn^{56}/Cl^{38}$ возрастают, соответственно, в семь и пятнадцать раз по сравнению со значениями, полученными при активации тепловыми нейтронами.

Применение спектрометрии тройных совпадений позволяет уменьшить по-мехи от $Na^{24}$ при определении $Mn^{56}$ примерно в 100 раз. Такая методика дает возможность измерять содержание марганца в кровяной сыворотке, не прибегая к радиационно-химическому разделению.

## SELEKTIVE RADIOAKTIVIERUNG UND MULTIPLE KOINZIDENZSPEKTROSKOPIE BEI DER BESTIMMUNG VON SPURENELEMENTEN AN BIOLOGISCHEM MATERIAL

Die Empfindlichkeit der Aktivierungsanalyse zur Auffindung von Spurenelementen in Proben allein durch radioanalytische Methoden kann ausserordentlich erhöht werden durch Spezifizierung von sowohl Aktivierung, wie auch der Nachweismethode.

Die Methode der Koinzidenzspektroskopie ist häufig imstande die Strahlung komplizierter Isotopengemische zu unterscheiden, dadurch, dass die verschiedenen Charakteristiken der vorkommenden Zerfallsschemata herangezogen werden. Werden $\beta$-$\gamma$-strahlende Isotopen zum Nachweis herangezogen, so empfiehlt sich die Szintillationsspektrometrie. Das mit Hilfe eines NaI (Tl)-Kristalles aufgenommene $\gamma$-Spektrum kann dann mit einem Vielkanal-Impulshöhen-Analysator registriert werden, welcher zufolge eines Koinzidenzkreises nur dann anspricht, wenn er gleichzeitig Signale vom $\gamma$- und vom $\beta$-Detektor erhält. Die Genauigkeit dieses Verfahrens wird durch die $\gamma$-Empfindlichkeit des $\beta$-Detektors begrenzt, welcher imstande ist, auch $\gamma$-$\gamma$-Kaskaden zu registrieren. Eine deutliche Verbesserung der selektiven $\beta$-$\gamma$-Diskriminierung wird durch die 3-Kristall-Koinzidenz-Geometrie erreicht, bei welcher ein zusätzlicher Plastik oder Anthrazenkristall (welcher so dick ist, dass seine $\gamma$-Empfindlichkeit vernachlässigbar ist) vor den dicken Kristall des $\beta$-Spektrometers gesetzt wird, zur Unterscheidung der $\beta$- und der $\gamma$-Strahlen.

Wird die radiometrische Methode auf Neutronen-aktivierte Quellen angewendet, kann die Nachweisgenauigkeit gewisser Nuklide mit niederenergetischer (n,$\gamma$)-Resonanz (z.B. $Mn^{55}$, $Co^{59}$) weiter verstärkt werden, relativ zu anderen Isotopen, welche diese Resonanz nicht besitzen (z.B. $Na^{23}$, $Cl^{37}$), indem die Bestrahlung mit Resonanzneutronen durchgeführt wird.

Bei einem Beispiel der Neutronenaktivierungsanalyse des Mangan wurde die selektive Aktivierung mittels eines gefilterten Reaktorneutronenspektrums mit der 3-fach-Koinzidenzspektroskopie kombiniert. Dadurch wurde das Verhältnis der Aktivierungen $Mn^{56}/Na^{24}$ und $Mn^{56}/Cl^{38}$ auf das 7- bzw. 15-fache des Wertes bei aktivierung mit thermischen Neutronen erhöht. Die Bestimmung des $Mn^{56}$ mit Hilfe der $\gamma$-Spektrometrie setzte den durch $Na^{24}$ verursachten störenden Effekt um einen weiteren Faktor 100 herab. Auf diese Weise ist es möglich, Mangan im Blutplasma nachzuweisen ohne eine radiochemische Trennung vornehmen zu müssen.

THE value of radioactivation analysis for the determination of trace elements has been generally recognized.[1] However, in biological materials the many macroconstituents characteristically present complicate the procedure. Usually radioisotopes produced from the relatively large concentrations of these other elements that also become activated vastly overshadow the radioactivities induced in trace materials. Thus gamma-ray spectrometry of tissues following thermal neutron bombardment reveals predominantly sodium and chlorine, and at times potassium.[1,2,3]

For trace element analysis in such cases, instrumental techniques have been advocated that resolve spectroscopically the many radio-emanations induced by activation. The alternative of removing interfering radioelements with chemical separations has been more widely practiced but lacks the flexibility, ease of sample processing and other advantages recognized for the purely radioanalytical procedures.[1,4,5,6] Application of gamma-ray scintillation spectrometry and differential absorption beta measurements has markedly facilitated discrimination of mixed radioactivities.[1,4,5,7] Yet the contemporary utilization of these methods has lacked the resolution to measure, by means of their neutron-induced radioactivities, the small traces of some metals endogenous to certain biological substances; and radiochemical isolation has been required.[1,3,8]

We have sought to improve the specificity of the instrumental approach to activation analysis through the use of coincidence spectrometry and selective methods of sample activation.[1] This paper will discuss sequentially the effects upon detection sensitivity of several aspects of sample irradiation (isotopic abundance, irradiation time, isotopic half-life, activitation cross section) and of radioactivity measurement (radioactive decay, branching ratios, properties of $\beta$- and $\gamma$-counters). With this basis, some further advanced coincidence techniques and a more rigorous exposition of the special activation principle will be presented. Their application may be generalized to many radioactivation problems, and the spectrometry described here can be useful in analyzing other mixtures of radioisotopes and in working out isotopic decay schemes.[9]

However, for clarity the present concepts will be developed as they pertain to the solution of a specific problem. Extrapolation to other circumstances then will be readily apparent.

VOL. 11 1961

## A REPRESENTATIVE RADIO-ACTIVATION PROBLEM: Mn IN BLOOD PLASMA

Frequently we have had occasion to determine the manganese content of human plasma or blood. Favorable nuclear characteristics have suggested the suitability of neutron activation analysis, and in many instances tissue manganese has been measured thereby.[1] However, in plasma there are higher concentrations of sodium and chlorine than in other tissues, and whole blood also contains considerable potassium; whereas body manganese concentrations are *lower* in plasma than elsewhere. The extensive radioactivity induced in these other elements upon neutron irradiation[2,3,8] has heretofore precluded identification and quantitation of the relatively much less frequent radiodisintegrations produced from manganese, except following chemical separations.[8,10]

Successful measurement of the very small concentration of manganese in plasma[8] requires an analytical method that is extremely selective, and hence the bulk of this paper considers in detail those factors which determine the selectivity of a system we have developed, which can detect manganese in human plasma. The discussion is generalized to facilitate application of the underlying principles to other cases, although, for the most part, each step has been examined experimentally only in the context of the particular manganese detection problem.

## SELECTIVITY OF MEASUREMENT

A detection ratio, $D_j^i$, is defined as the promotion of element $i$ relative to that of element $j$, such that $D_j^i = x$ signifies that an atom of $i$ has $x$ times the likelihood of being identified by the system under consideration as does one of element $j$. With several competing radioactivities, each step in the analytical procedure, $m$, introduces a series of $D_j^i$'s, denoted $D_j^i(m)$, such that changes in the experimental parameters of each step will generally vary the relative value of the respective $D_j^i(m)$'s.

It is emphasized that the value of $D_j^i(m)$ connotes selectivity as a *ratio* of measurement sensitivities without stipulation as to *absolute* sensitivity. Hence, optimization of an overall system depends on a series of compromises between the sensitivity for detection of $i$ and the selectivities, $D^i_{j,k,\text{etc.}}(m)$, for each step, such that the final product retains both sufficient sensitivity *and* selectivity to analyze quantitatively for $i$ in the environment in question. Thus the optimum parameters for measurement of manganese in plasma could differ from those for its detection in other situations or for the analysis of trace amounts of other elements.

As indicated above, certain nuclear properties of manganese imply a high sensitivity to neutron-activation analysis, notably the large cross section for low-energy neutron capture by $Mn^{55}$ and the energetic radiations

emitted in the subsequent decay of $Mn^{56}$.[11] Accordingly, in this work the moderated neutron spectrum of the BNL graphite research reactor has been used as a neutron source. The resultant selectivity of the analytical procedure subsequently applied has been determined by the amounts of competing radioactivities simultaneously produced and the ability of the detecting system to discriminate against them.

In blood plasma, neutron irradiation induces gamma-ray activity predominantly in sodium, chlorine and potassium.[2,8] From published data on manganese concentrations in plasma,[8] there are for each atom of manganese approximately $4 \times 10^5$ atoms of sodium, $3 \times 10^5$ of chlorine and $10^4$ of potassium. Hence the present problem requires a system with $D_{Na}^{Mn} \simeq 4 \times 10^5$, $D_{Cl}^{Mn} \simeq 3 \times 10^5$ and $D_{K}^{Mn} \simeq 10^4$.

## RADIOACTIVITIES PRODUCED BY REACTOR NEUTRONS

Competing activities from neutron capture on the above elements are[11,12]:

*Sodium.* $Na^{23}$ (100 per cent isotopic abundance) + n → $Na^{24}$. $\sigma = 0{\cdot}525$; decay = $\beta^-$; $T_{\frac{1}{2}} = 15{\cdot}0$ hr. ($\sigma$ represents the thermal activation cross section for the reaction in barns, $10^{-24}$ cm².)

*Chlorine.* $Cl^{35}$ (75·5 per cent) + n → $Cl^{36}$. $\sigma = 30$; decay = $\beta^-$, EC; $T_{\frac{1}{2}} = 3{\cdot}1 \times 10^5$ years. With so long a half-life ($T_{\frac{1}{2}}$), an irradiation of a few hours will produce little $Cl^{36}$ activity.

$Cl^{37}$(24·5 per cent) + n → $Cl^{38}$. $\sigma = 0{\cdot}56$ decay = $\beta^-$; $T_{\frac{1}{2}} = 37$ min.

*Potassium.* $K^{39}$(93·1 per cent) + n → $K^{40}$. $\sigma = 3$; decay = $\beta^-$, EC; $T_{\frac{1}{2}} = 1{\cdot}3 \times 10^9$ years Again the isotope is too long-lived to be of present concern.

$K^{41}$ (6·9 per cent) + n → $K^{42}$. $\sigma = 1{\cdot}3$; decay = $\beta^-$; $T_{\frac{1}{2}} = 12{\cdot}5$ hr.

In contrast, results for manganese are[9]:

*Manganese.* $Mn^{55}$(100 per cent) + n → $Mn^{56}$. $\sigma = 13{\cdot}3$; decay = $\beta^-$; $T_{\frac{1}{2}} = 2{\cdot}58$ hr.

### (1) *Effect of isotopic abundance*

The detection ratios due to isotopic abundance, $N$, then become: $D_{Na}^{Mn}(N) = 1$; $D_{Cl}^{Mn}(N) = 4{\cdot}1$; $D_{K}^{Mn}(N) = 14{\cdot}5$.

### (2) *Effect of irradiation time and isotopic half-life*

After irradiation in a constant neutron flux for a time $t$, a sample will have a radioactivity $A$, such that

$$A_i = A_{0i}(1 - e^{-\lambda_i t}) \qquad (1)$$

where $A_0$ = radioactivity produced at saturation = decay rate following infinitely long irradiation, and $\lambda$ = decay constant = $\frac{0{\cdot}693}{T_{\frac{1}{2}}}$. The effect of varying irradiation time on the detection ratios can be taken from equation (1) as

$$D_j^i(T_p) = \frac{(1 - e^{-\lambda_i t})}{(1 - e^{-\lambda_j t})}. \qquad (2)$$

Thus if $\lambda_i > \lambda_j$, $D_j^i(T_p)$ will be a monotonically decreasing function of time; while for $\lambda_i < \lambda_j$, $D_j^i(T_p)$ will increase monotonically with time. The limiting values in both cases will be:

$$\begin{aligned} D_j^i(T_p) &\to 1 \text{ as } t \to \infty \\ D_j^i(T_p) &\to \frac{\lambda_i}{\lambda_j} \text{ as } t \to 0. \end{aligned} \qquad (3)$$

When, as in the present work, there are both shorter ($Cl^{38}$) and longer-lived ($Na^{24}$, $K^{42}$) competing radioactivities, an irradiation time of $\sim \frac{1}{\lambda_{Mn}}$ probably will be optimal; although the actual optimum also will depend on the values of $D_j^{Mn}$ achievable in the other steps of the analytical procedure. However, for $t \ll \frac{1}{\lambda_{Mn}}$ the $Mn^{56}$ activity produced will vary directly with $t$, and thus in certain cases, counting statistics also *can* set a lower limit on irradiation time.

For the data reported here most samples were irradiated for about 2 hr $\left(\frac{1}{\lambda_{Mn}} = 3{\cdot}72 \text{ hr}\right)$.

VOL 11 196

The reflection of this irradiation time and of the pertinent half-lives on the detection ratios is thus: $D^{Mn}_{Na}(T_p) = 4{\cdot}7$; $D^{Mn}_{Cl}(T_p) = 0{\cdot}47$; $D^{Mn}_{K}(T_p) = 4{\cdot}0$.

(3) *Effect of activation cross section*

For moderated reactor ("pile") neutron spectra most of the total neutron flux is in the "thermal" region. For example, at the sample-activating positions in the Brookhaven graphite research reactor, ~97 per cent of the neutrons are thermalized. In such a case a good approximation is

$$D_j'(\sigma_{pile}) \simeq \frac{\sigma_{ti}}{\sigma_{tj}} \qquad (4)$$

where $\sigma_t$ is the activation cross section for thermal neutrons. Hence $D^{Mn}_{Na}(\sigma_{pile}) = 25{\cdot}3$; $D^{Mn}_{Cl}(\sigma_{pile}) = 23{\cdot}8$; $D^{M}_{K}(\sigma_{pile}) = 10{\cdot}2$.

Since $D_j'(N,T,\sigma_{pile})$ is simply the product of $(D_j'(N))(D_j'(T_p))(D_j'(\sigma_{pile}))$, the overall effect on the detection ratios that results from the radioactivities produced by reactor neutrons can be summarized: $D(^{Mn}_{Na}N,T_p,\sigma_{pile}) = 119$; $D^{Mn}_{Cl}(N,T_p,\sigma_{pile}) = 46$; $D^{Mn}_{K}(N,T_p,\sigma_{pile}) = 592$.

With this high $D^{Mn}_{K}$ combined with the relatively lower concentration of potassium in plasma, potassium clearly will interfere with $Mn^{56}$ detection to a much smaller extent than will either sodium or chlorine. Hence the subsequent discussion will be confined to detecting traces of manganese in the presence of far larger quantities of sodium and chlorine.

## SELECTIVE ACTIVATION WITH RESONANCE NEUTRONS

A further increment toward $D^{Mn}_j$ often can be realized by activating the sample with resonance ("$1/E$") neutrons[13] rather than with thermal or "pile" neutrons.

The amount of radioactivity produced at saturation, $A_0$, from isotope $i$ varies with $\sigma_i(E)$—the isotopic neutron-capture cross section at energy $E$ for producing radioactivity in $i$—and with the neutron spectrum:

$$A_{0i} = \lambda_i \int \sigma_i(E) \,.\, n(E) \,.\, dE, \qquad (5)$$

where $n(E)$ is the number of neutrons in the energy interval between $E$ and $E + dE$. In general, the activation cross section, $\sigma_i(E)$, is a sharply varying function of energy, exhibiting discrete resonances.[12,13,14] Manganese has resonances low in the resonance-neutron region, whilst sodium's lowest lying resonance is at a higher energy,[12] where the reactor neutron flux is much less intense[13]; also chlorine has only a negative-energy resonance (Appendix I) in the low-energy region. Hence, very high $D^{Mn}_j$'s could be achieved by activating with neutrons of energy corresponding to the sharp capture resonance in manganese, ideally reaching a $D^{Mn}_{Na}(\sigma_f)$ of perhaps $\sim 10^4$ with truly monoenergetic neutrons.

Unfortunately, a monoenergetic source of "resonance" neutrons[13] ($1 < E_n < \sim 10^3$ eV) of sufficient intensity for sample activation is extremely difficult to produce. However, the moderated neutron flux of a reactor consists of a sharp thermal-energy spike and a "$1/E$" spectrum in the resonance region.[13] In certain cases, such as the present problem, considerable advantage can be taken of the resonance behavior of $\sigma(E)$ by suitably filtering the reactor neutron spectrum. It is shown in Appendix I that, by introducing a low-pass neutron filter between the sample and the reactor flux that is virtually opaque in the thermal–epithermal region, manganese can be "selectively activated" with respect to sodium and chlorine.

This selective activation with resonance neutrons has been achieved by irradiating samples in an aluminum capsule, the hollow walls of which are filled with metallic $B^{10}$ powder (enriched to ~93 per cent $B^{10}$). The capsule usually is enclosed in an outer can of cadmium which shields the $B^{10}$ from thermal neutrons and thus markedly diminishes heating from the $B^{10}(n, \alpha)Li^7$ reaction. In practice, this heating presents a major problem and has required either irradiation in a cooled reactor facility to prevent thermal destruction of biological samples or the use of previously ashed biological materials.

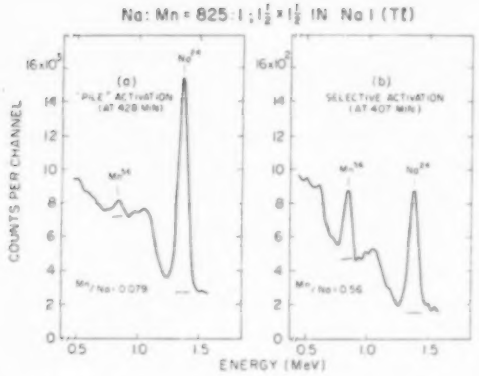


FIG. 1. Gamma-ray singles spectra of two samples containing identical ratios of $Na^{23}$ : $Mn^{55}$. These spectra illustrate the selective activation of manganese by reactor resonance neutrons as opposed to an unfiltered reactor spectrum of "pile" neutrons. After correction for $Mn^{56}$ decay, the Mn/Na detection ratio of (b) is 6·5 times that of (a).

However, with ashed or other thermoresistant materials the cadmium outer can may be omitted, thus simplifying the handling of the sample container by avoiding the intense cadmium radioactivity otherwise induced in it.

The calculations of Appendix I show that filtered neutron activation can be expected to produce the following approximate detection ratios: $D_{Na}^{Mn}(\sigma_f) \simeq 175$; $D_{Cl}^{Mn}(\sigma_f) \geqslant 340$. The $D_{Na}^{Mn}(\sigma_f)$ calculated for selective activation is about seven times the $D_{Na}^{Mn}(\sigma_{pile})$ provided by an unfiltered reactor flux. The validity of this estimate is confirmed by Fig. 1, where scintillation counter spectra (discussed in more detail below) are shown of samples irradiated with both pile and filtered neutrons. It is seen that $D_{Na}^{Mn}$ is enhanced by about 6·5 times, using the selective activation procedure with filtered neutrons, and this is in good agreement with the calculated improvement factor.

Summarizing the $D_j^{Mn}(m)$'s ascribable to the radioactivities produced by *selective* activation then gives: $D_{Na}^{Mn}(N, T_p, \sigma_f) \simeq 825$; $D_{Cl}^{Mn}(N, T_p, \sigma_f) \geqslant 655$.

## DETECTION OF RADIOACTIVITY

The enhanced production of $Mn^{56}$ indicated by the $D_j^{Mn}(N, T_p, \sigma_f)$'s above, is still insufficient to make this isotope the dominant radioactivity following activation of plasma or most other tissue samples. To measure successfully the $Mn^{56}$ activity induced in human plasma, a highly selective detection system is required as well. This is achieved largely by exploiting differences in the decay schemes of the prominent radioisotopes present, as will be discussed; however, in many cases, relatively enhanced detection of a desired radioactivity also can be gained by selecting an appropriate time interval between activation and sample counting.

### (1) *Effect of radioactive decay and isotopic half-life*

In analogy to optimizing the duration of irradiation to enhance relatively the production of $Mn^{56}$, selection of a best time after activation for the sample to be counted similarly takes advantage of differences in the half-lives for radioactive decay of the competing radioactivities. In the general case, the effect on detection ratios is:

$$D_j^i(T_D) = \frac{e^{-\lambda_i t}}{e^{-\lambda_j t}} = e^{(\lambda_j - \lambda_i)t}. \qquad (6)$$

Of course, from equation (6) it is clear that $D_j^i(T_D) \to 1$ as $t \to 0$. But if $\lambda_i < \lambda_j$, $D_j^i(T_D)$ will be a monotonically increasing function of time, with $D_j^i(T_D) \to \infty$ as $t \to \infty$. However, with $\lambda_i > \lambda_j$, $D_j^i(T_D)$ will decrease monotonically with time, and $D_j^i(T_D) \to 0$ as $t \to \infty$.

In the present example, there is both a shorter-lived and a longer-lived contaminating activity, so a reasonable compromise is to count the samples about one $Mn^{56}$ half-life (2·58 hr) following radioactivation. The resultant detection ratios are: $D_{Na}^{Mn}(T_D) = 0{\cdot}56$; $D_{Cl}^{Mn}(T_D) = 9$.

### (2) *Effect of branching ratios*

Frequently it is possible to pick out a salient feature of a particular decay scheme and to detect this decay mode with a minimum

VOL. 11 1961

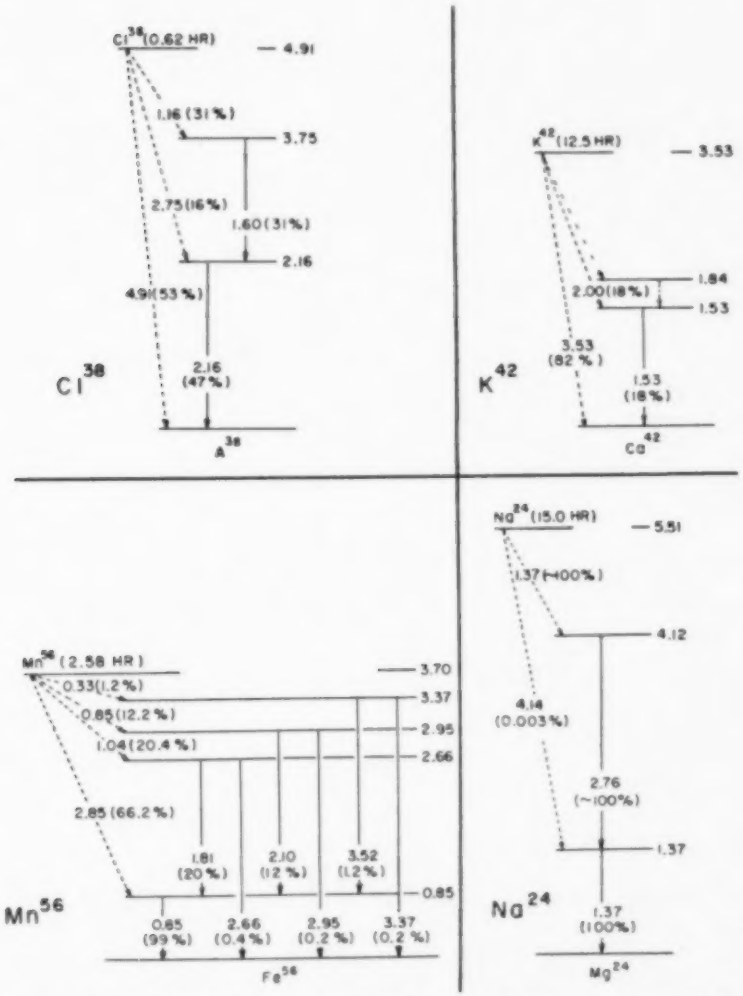


FIG. 2. Decay schemes of $Mn^{56}$ and competing activities. Dashed arrows indicate $\beta$-decay, and solid ones represent $\gamma$-ray emission. Data are from the recent compilation of STROMINGER *et al.*[11] and from a later investigation of $Mn^{56}$ decay.[9]

of interference from decay branches of competing radioisotopes. The fact that the 2·85 MeV $\beta$–0·85 MeV $\gamma$-decay chain is the predominant mode of radioactive disintegration of $Mn^{56}$ provides an opportunity to isolate this branch from contaminating activities (Fig. 2). The technique involves viewing the sample simultaneously with both a $\gamma$- and a $\beta$-counter and to require a (time) coincidence between the two counters.[1] The electronics of the coincidence spectrometers used in the present experiments are standard and are amply described elsewhere.[15]

It will be seen in later discussion, and it can be inferred from inspection of Fig. 2, that the primary background for the selected $Mn^{56}$ decay chain is the 1·37 MeV $\beta$–2·76 MeV $\gamma$–1·37 MeV $\gamma$-cascade from $Na^{24}$ and the 2·75 MeV $\beta$–2·16 MeV $\gamma$-branch from $Cl^{38}$. The effect of the respective $\beta$-decay branching ratios on $D_\gamma^{Mn}$ are: $D_{Na}^{Mn}(B.R.) = 0{\cdot}66$; $D_{Cl}^{Mn}(B.R.) = 4{\cdot}1$.

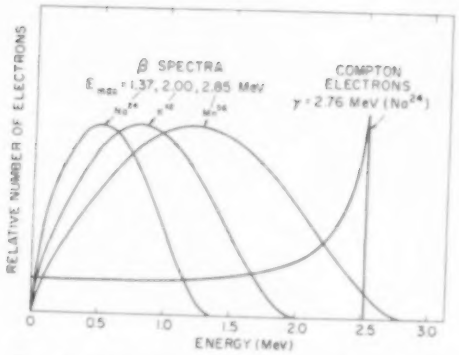


FIG. 3. Calculated electron spectra from $\beta$-decay and Compton scattering. These theoretical spectra are smeared experimentally by the finite resolution of the crystals. The value of a variable energy bias, $E_\beta$, in discriminating $\beta$-decays with different cut-off energies is apparent. When Compton electrons from the 2·76 MeV $\gamma$-ray of $Na^{24}$ interfere seriously with $\beta$-ray detection, the ratio of desired $\beta$ responses to the unwanted $\gamma$-responses can be increased if the upper discriminator of the $\beta$-counter's energy channel is kept below the Compton cut-off.

(3a) *Effect of beta-ray counter*

One advantage in the analysis of the coincidence method of detecting radioactively emitted particles (counting photons as particles) is that the overall detection ratio of the system is equal to the product of the detection ratios of the two counters. Therefore the two counters are discussed separately.

In order for counting rates to be sufficient for coincidence measurement, it is almost always necessary to use scintillation crystals for both the $\beta$- and $\gamma$-counters. Although other types of spectrometers theoretically might provide a higher $D_j^i$ for either particle alone, a higher *overall* detection ratio results from using two high efficiency detectors in coincidence. An effective $\beta$-counter for this purpose is a plastic scintillator of sufficient thickness so that the most energetic electrons to be discriminated against will lose all of their energy in the crystal. In this work, a $\frac{1}{4}$ in. thick crystal has been sufficient, although occasionally a $\frac{1}{2}$ in. crystal has been used.

Since $\beta$-decay is in reality a three-body break-up,[16] the energy spectrum, and therefore the pulse-height spectrum, from any single $\beta$-branch is a continuum, with electrons being present at all energies up to the maximum $\beta$-ray energy. For example, the "2·85 MeV $\beta$" from $Mn^{56}$ is actually a continuum of electron energies up to 2·85 MeV (Fig. 3). However, the energy spectra ("shape") of electrons from $\beta$-decay (Fig. 3) are sufficiently well known[14,16] so as to introduce negligible error in virtually all radioanalysis problems involving $\beta$-counting.

It follows that pulses from $\beta$-scintillation detectors above a certain energy of pulse height discrimination, $E_\beta$, will contain contributions from *all* $\beta$-branches of maximum energy greater than $E_\beta$. Hence, if background from $\gamma$-radiation is neglected for the moment, the detection ratios that can be achieved in a $\beta$-counter with regard to $\beta$-radiation *alone* are: $D_j^i(\beta) \sim 1$ if $E_{\beta i} \leqslant E_{\beta j}$, and $D_j^i(\beta) \rightarrow$ "$\infty$" if $E_{\beta i} \geqslant E_{\beta j}$. (The symbol "$\infty$" is used loosely: it signifies that a sufficiently high detection ratio can be attained for most practical problems.)

Unfortunately, however, a $\beta$-scintillation spectrometer also is sensitive to $\gamma$-rays. It is true that $\beta$-ray stopping power depends essentially only on the total number of target electrons, whereas the likelihood of $\gamma$-ray photoelectric capture varies approximately as the fifth power of the atomic number of the target material[15]; and hence light-element plastic scintillators make effective $\beta$-counters with minimal $\gamma$-sensitivity. Nonetheless, $\gamma$-rays will lose energy to electrons in a plastic crystal chiefly through Compton scattering, which will again produce a continuum of electron energies (Fig. 3), this time with a maximum energy just below that of the incident $\gamma$-ray energy.[15]

In the present instance, the $\gamma$-induced electron background in the $\beta$-detector is due predominantly to the 2·76 MeV $\gamma$ in $Na^{24}$ (Fig. 3). However, this $\gamma$-ray is in coincidence with a 1·37 MeV $\gamma$ (Fig. 2), and as a result, unwanted $\gamma$–$\gamma$ coincidences from $Na^{24}$ can interfere with the desired $\beta$–$\gamma$ coincidences from $Mn^{56}$. A crystal, thick enough to discriminate the higher-energy electrons from $Mn^{56}$ decay from the lower energy $\beta$-rays from $Na^{24}$ (and $K^{42}$), was found to be ~10 per cent as sensitive to the 2·76 MeV $\gamma$

VOL. 11 1961

from $Na^{24}$ as it was to $Mn^{56}$ electrons. This detection ratio in the $\beta$-counter of $D^{Mn}_{Na}(\beta) \simeq 10$ has facilitated radioactivation analysis for manganese in solid body tissues, employing a two-crystal $\beta$–$\gamma$ coincidence spectrometer[1]; but it is not sufficiently high to detect manganese in plasma.

A preliminary investigation showed that another type of $\beta$-ray spectrometer, the magnetic spectrometer,[15] was not satisfactory. Undoubtedly magnetic spectrometers can have lower relative $\gamma$-ray sensitivities than do single-crystal $\beta$-spectrometers, but only a few of the magnetic geometries provide sufficient electron transmission or "counting efficiency" to permit coincidence measurements. One of the latter which *was* investigated for $\beta$–$\gamma$ coincidence counting, namely the intermediate image magnetic $\beta$-spectrometer of ALBURGER,[17] proved unsuitable because of the poor resolution of the $\gamma$-ray crystal-spectrometer component which resulted from the requirement of a long light-pipe between the crystal and photomultiplier due to the strong magnetic field all around the sample.[17] A modified magnetic spectrometer on the style of SLÄTIS and HERRLANDER[18] might obviate this requirement, but investigations have not been pursued along these lines.

In addition to the Compton electron background from 2·76 MeV $\gamma$-rays of $Na^{24}$, a more direct electron background is present in the $\beta$-counter due to the 2·75 MeV $\beta$–2·16 MeV $\gamma$-branch from $Cl^{38}$ decay (Fig. 2). The 2·75 MeV $\beta$ is too close in energy to the 2·85 MeV $\beta$ from $Mn^{56}$ to be separated on the basis of pulse-height discrimination, $E_\beta$. However, this decay chain from chlorine does not become a limiting factor in the problem at hand, because considerations already discussed lead to an aggregate $D^{Mn}_{Cl}$ ($N$, $T_v$, $\sigma_f$, $T_D$, B. R.) $\geq 2{\cdot}4 \times 10^4$; and when multiplied by the detection ratio in the $\gamma$-counter (see below), this provides sufficient suppression of $Cl^{38}$ detection. Moreover, $D^{Mn}_{Cl}$ can be greatly amplified even further, at the price of a modest reduction in $D^{Mn}_{Na}$, simply by increasing the period of radioactive decay between the end of irradiation and the time of counting. Hence the subsequent discussion will be illustrated primarily as it affects $D^{Mn}_{Na}$, because $Na^{24}$ activity has presented the greatest difficulty in plasma and tissue manganese determination.

(3b) *Effect of beta-ray counter-telescope*

The $\gamma$-sensitivity of the $\beta$-counter can be reduced by introducing between the source and the thick plastic scintillator of the $\beta$-spectrometer another crystal, so thin ($\sim 15 \times 10^{-3}$ in.) as to have negligible $\gamma$-ray sensitivity while still eliciting a small light pulse from *all* electrons passing through it. The arrangement of counters, including the $\gamma$-counter, is shown in Figs. 4 and 5. A coincidence pulse is then required from the thin "guard" crystal as well as from the other two crystals. In this way the relative $\gamma$-sensitivity of the two-crystal "counter-telescope" $\beta$-spectrometer system is reduced to the $\gamma$-sensitivity of the thin crystal alone, which has been estimated to be $\sim 10^{-3}$. In practice, the triple-coincidence system has not achieved this great a suppression of $Na^{24}$ detection. Events caused by electrons energized in the vicinity of the source by the 2·76 MeV $\gamma$-ray from $Na^{24}$ are recorded by the $\beta$-counter-telescope. Care has been taken to minimize the amount of extraneous material in the vicinity of the source, but with the two-crystal $\beta$-counter it has been possible to attain only $D^{Mn}_{Na}(\beta) \simeq 150$.

Possibly this detection ratio could be improved by a meticulous inquiry into the source of the extraneous high-energy electrons. Such an investigation has not been attempted in the present work.

However, another source of background exists from events wherein the $Na^{24}$ $\beta$-ray enters the thin "guard" crystal in coincidence with an interaction in the thick crystal with the 2·76 MeV $\gamma$-ray from the same $Na^{24}$ disintegration, such that a Compton electron is formed there with an energy above the discrimination level, $E_\beta$. This combination of a $\beta$–$\gamma$ coincidence in the $\beta$-counter telescope simultaneously with the entry of the accompanying 1·37 MeV $Na^{24}$ $\gamma$-ray into the $\gamma$-counter can satisfy all the restrictions of the triple-coincidence detection system, and thus produce a recorded background from

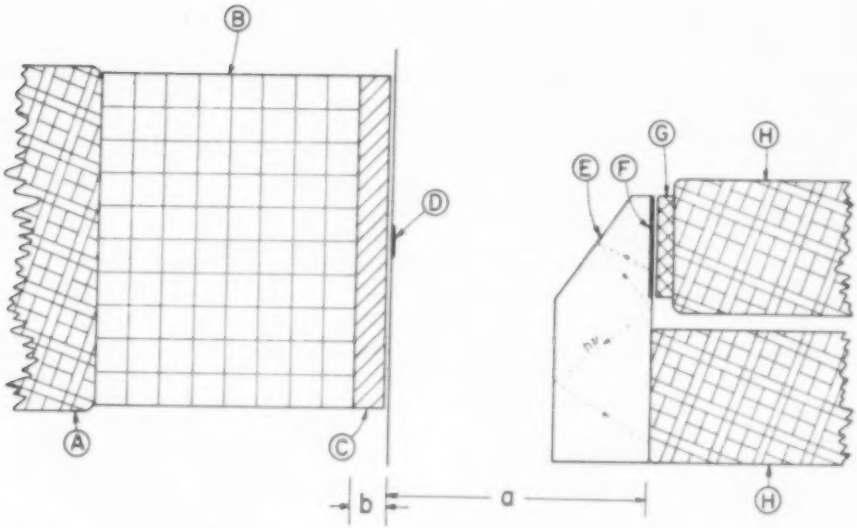


FIG. 4. Schema of coincidence counting geometry.

A = 5 in. (diam.) photomultiplier tube
B = 4 × 5 in. NaI(Tl) crystal } light shield omitted
C = plastic Bremsstrahlung shield
D = source mounted on thin foil
E = reflecting chamber of aluminized Mylar® on thin frame
F = 0·015 in. (thick) pilot B® crystal; note reflected path of an emitted photon, $h\nu$
G = 0·25 (or 0·50) in. (thick) pilot B® crystal
H = 2 in. (diam.) photomultiplier tube } light shield omitted
b = usually 0·5 in.
a = variable, but for Mn: Na resolution 4 in. so that (F) subtends solid angle of $\sim 0{\cdot}2\pi$ at source.

This diagram represents the counting geometry used to record most of the coincidence spectrometric data cited in this report. Subsequently the "guard" crystal, F, was remounted in a thin lucite light pipe or "paddle". This reduced the bulk of the light path from crystal to photomultiplier and allowed measurements to be made in appropriate cases with distance, a, being very small. However, the light-piping efficiency of the thin lucite was less than that of the Mylar®-enclosed reflecting chamber, E.

$Na^{24}$. The contribution from such events can be made negligible, at the expense of overall counting efficiency, by moving the $\beta$-telescope back so as to subtend a small solid angle at the source ($\sim 0{\cdot}2\,\pi$ in these investigations) (Fig. 4). The small solid angle suppresses detection of the contaminating *triple*-event coincidences from $Na^{24}$ more strongly than it does the desired $\beta$-$\gamma$ *double*-event coincidence from $Mn^{56}$.

The total detection ratio dependent upon $\beta$-counting is the product of the component due to branching ratio and that due to the $\beta$-counter telescope itself. Therefore, due to $\beta$-counting there is $D^{Mn}_{Na}(e) = D^{Mn}_{Na}(\text{B.R.},\beta) = 0{\cdot}66 \times 150 \simeq 100$.

Experimental confirmation of this result is given by Fig. 6, where pulse-height spectra from a NaI(Tl) crystal and a mixed Mn–Na source are shown. It is seen that the 0·85 MeV $\gamma$-peak of $Mn^{56}$ is indeed enhanced relative to the $Na^{24}$ 1·37 MeV $\gamma$ (which is the $\gamma$-ray in coincidence with the 2·76 MeV $\gamma$ —Fig. 2) by a factor of about 100, when triple coincidence with the $\beta$-counting system is required.

### (4) *Effect of gamma-ray counter*

With regard to $\gamma$-counting, the situation differs somewhat from $\beta$-counting in that the *source* spectrum is monoenergetic, but the *detector* response is a continuum. In a NaI(Tl) scintillating crystal, the pulse spectrum from

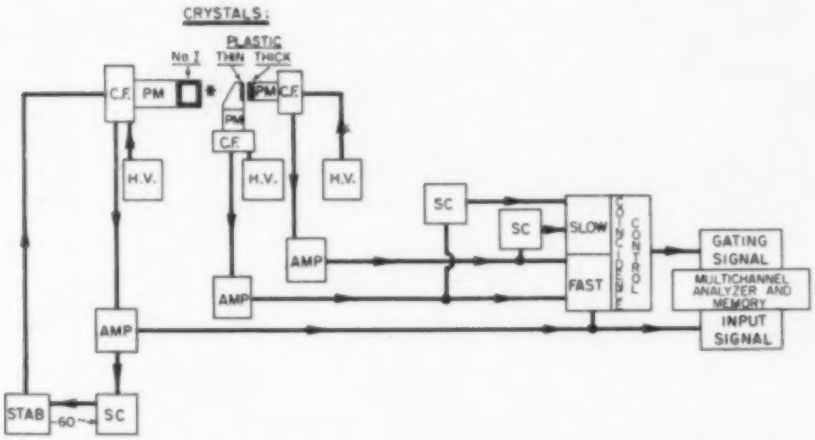


FIG. 5. Block diagram of the coincidence circuitry employed in these investigations.

* = source
PM = photomultiplier tube
C.F. = cathode follower
H.V. = high voltage supply
AMP = linear amplifier
SC = single channel analyzer
STAB = stabilizing circuit.

"FAST" coincidence resolving time was $10^{-7}$ sec, with the coincidence output signal then combined with the "SLOW" discriminator channels, with a resolving time of $2 \times 10^{-6}$ sec. A stabilizing circuit of the type of DE WAARD[22] reduced the drift of the amplified $\gamma$-ray signal.

a monoenergetic source consists of a "full-energy" peak, corresponding to events where the incident radiation dissipates all of its energy in the crystal, and a low energy tail, corresponding to events where some $\gamma$-radiation energy leaves the crystal, largely due to escaping secondary photons following Compton scatters.[6,15] The full-energy peak may have some structure for higher energy $\gamma$-rays ($\geq 2$ MeV) where pair production is important. The parameter of greatest present relevance in the response function of the $\gamma$-crystal spectrometer is the height (number of pulses per unit energy interval) of the full-energy peak relative to the height of the tail. This aspect of the response function in the case of a given energy $\gamma$-ray depends primarily on crystal dimensions, namely, the larger the crystal, the greater the "peak-to-total" ratio.[6,15] For the studies reported here, the $\gamma$-detector has been a 5 in. diameter by 4 in. thick NaI(Tl) crystal. With this crystal, the height of the low-energy tail is ~15 per cent of the height of the full-energy peak, as depicted by the $\gamma$-singles spectrum of Fig. 6. Neglecting the variation with energy of both the efficiency and response function, which is a small variation when a large crystal is used over a limited $\gamma$-ray

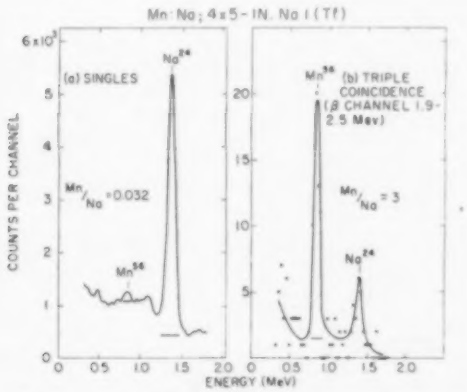


FIG. 6. Two $\gamma$-ray spectra of the same mixture of $Mn^{56}$ and $Na^{24}$. When corrected for the decay of $Mn^{56}$ occurring between the recording of these two spectra, the Mn/Na ratio of (b) is ~ 100 times that of (a).

energy,[15] there is, due to $\gamma$-counting: $D_j^i(\gamma) \sim 6$ if $E_{\gamma i} < E_{\gamma j}$, and $D_j^i(\gamma) =$ "$\infty$" (again using "$\infty$" loosely) if $E_{\gamma i} > E_{\gamma j}$, and $D_j^i(\gamma) \approx 1$ if $E_{\gamma i} \approx E_{\gamma j}$ ($\pm 10$ per cent).
It is estimated that $D_j^i(\gamma)$ for $E_{\gamma i} < E_{\gamma j}$ could be improved by a factor of two if a larger NaI(Tl) crystal (of the order of 12 in. linear dimensions) were to be used.

In analogy with the case of $\beta$-counting, there are known $\gamma$-spectrometers with a response function (resolution) superior to that of the single-crystal spectrometer,[15] but in the $\gamma$-energy range of current interest, these have too low a yield (counting efficiency) to permit useful coincidence measurements.

## TRIPLE COINCIDENCE SPECTROMETRY

The final data in the present type of experiment are the coincident spectra from the NaI(Tl) crystal, as recorded by a multichannel pulse-height analyzer (Fig. 5). In determining the maximum sensitivity of such a system it is not the detection ratio of the $\gamma$-counter that is really of interest, but rather the related figure of merit which defines how weak a $\gamma$-ray line can be detected in the presence of a more intense line, this problem being especially critical when the stronger line is of higher energy.

Designating the relative peak heights or, more accurately, the relative areas under the peaks, by $S$, one has

$$S_j^i = C_j^i \times D_j^i(p), \qquad (7)$$

where $C_j^i$ represents the relative concentrations of $i$ and $j$ in the original sample, and $D_j^i(p)$ is the product of all component detection ratios *except* that of the $\gamma$-counter, i.e. $D_j^i(p) = \Pi_x D_j^i(m)_x$.

The aggregate $D_{Na}^{Mn}$, resulting from factors related to the *detection* of radioactivity, excluding the $\gamma$-counter, is the product of the ratio due to radioactive decay and half-life and that due to $\beta$-counting, giving $D_{Na}^{Mn}(T_D, e) = 56$. $D_{Na}^{Mn}(p)$ is then the product of this and the previously cited $D_{Na}^{Mn}(N, T_g, \sigma_f)$ of 825 for the *production* of radioactivity, i.e. $D_{Na}^{Mn}(p) = 4{\cdot}6 \times 10^4$, calculated.

A direct measure of the total detection ratio attained is exemplified by Fig. 7, where a triple coincidence spectrum from a prepared source with a Mn:Na atomic ratio of $1:10^5$ is shown. The peak at 2·76 MeV from $Na^{24}$ is caused by accidental coincidences[15]; although in this work sample radioactivities have been low enough to maintain accidental coincidences in the region of 0·85 MeV at a negligibly low background. (However, should accidental coincidences prove to be limiting in other investigations, the coincidence resolving time of the electronics could be reduced easily to $\sim 10^{-8}$ sec, in comparison with the $10^{-7}$ sec used in the present instance.) After correcting for decay time, Fig. 7 implies the detection ratio $D_{Na}^{Mn}(p) = 5{\cdot}6 \times 10^4$, experimental. This is in satisfactory agreement with the calculated value.

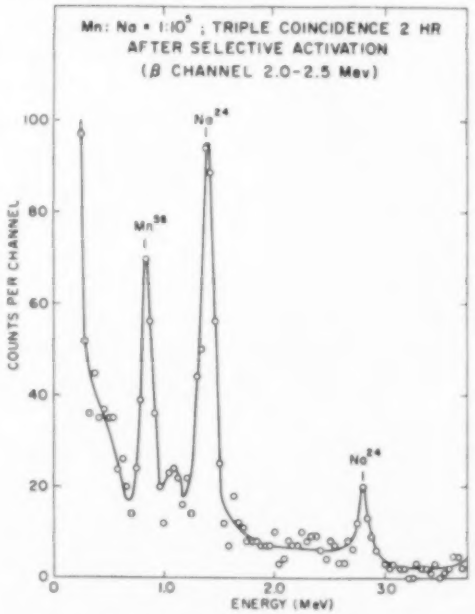


FIG. 7. Gamma-ray coincidence spectrum. The Mn : Na ratio of this sample approaches that of plasma, although the absolute concentrations of the elements and the absence of other radioisotopes are different. When corrected for radioactivity decay over the 2 hr interval following irradiation, the areas of the main $Mn^{56}$ and $Na^{24}$ peaks become about equal.

VOL 11 196

From the singles spectrum of Fig. 6 it can be seen that in order to detect the 0·85 MeV $Mn^{56}$ $\gamma$-peak in the presence of the 1·37 MeV $Na^{24}$ line, it is necessary to have $S_{Na}^{Mn} \geq 1/30$, with $S_j^i$ defined as in equation (7). Therefore, in order to measure manganese with the entire radioactivation system described in this article, there must be

$$C_{Na}^{Mn} = \frac{S_{Na}^{Mn}}{D_{Na}^{Mn}(p)} \geq \frac{1/30}{4 \times 10^4} = \frac{1}{1{\cdot}5 \times 10^6} \simeq 10^{-6}.$$

This estimate of manganese detection sensitivity is about three times greater than was indicated as necessary by the previously stated estimates of manganese concentration in plasma, although some very recent radioactivation data using chemical techniques imply an even lower level of plasma manganese[10]. Thus the system should prove applicable to radioactivation analysis for manganese in human plasma without recourse to radiochemical processing.[1,3,8,10]

## REPRESENTATIVE RESULTS

An illustrative example of the application of the selective activation–triple coincidence counting method is given by Fig. 8. In these particular experiments, the limited volume of the Cd–$B^{10}$ capsule used to filter the reactor neutron spectrum required ashing of the plasma and blood samples.

The samples were drawn and handled by instruments and containers previously cleansed with mineral acid, a metal-sequestering agent (Na-K-EDTA), and demineralized water. After ashing by gradual heating to 600°C in a muffle furnace, samples and standards were wrapped in similarly cleansed high-purity aluminum foil and irradiated for 1 hr in a Cd–$B^{10}$ can in an external flux of $1{\cdot}4 \times 10^{13}$ neutrons $cm^{-2}$ $sec^{-1}$ from the Brookhaven graphite research reactor. Standards, containing sodium, chlorine and potassium, in approximately the concentration ratios found in human plasma, plus about the amount of manganese expected, were included, plus another similar standard containing no manganese.

The coincidence spectra observed for these samples are those depicted in Fig. 8. The 0·85 MeV $Mn^{56}$ $\gamma$-ray peak is clearly discernable in all of the spectra except that of the "blank" standard lacking added manganese. The results are summarized in Table 1. However, the incidental practical considerations that restricted sample size and irradiation time in this example produced a lower statistical accuracy of counting and hence of manganese determination than is intrinsically implied by this analytical method.

The spectral peak at ~1·53 MeV from the blood sample derives from $K^{42}$. Blood contains a much higher concentration of potassium than does plasma, and the $\beta$-counter was channeled to accept electrons between 1·7 and 2·2 MeV in this example, thus allowing some $\gamma$-rays to be recorded from the 2·0 MeV $\beta$–1·53 MeV $\gamma$-decay mode of $K^{42}$ (Fig. 2).

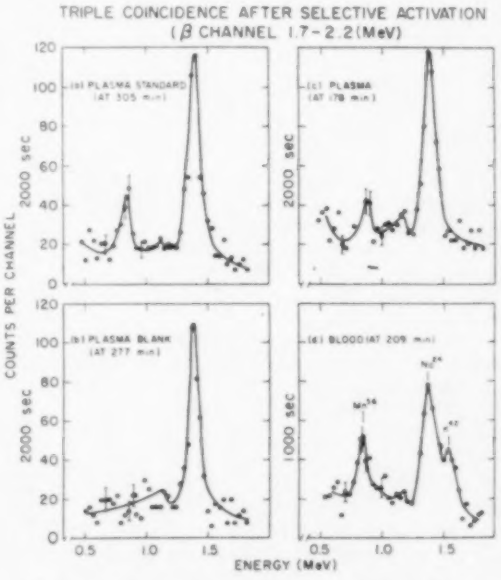


FIG. 8. Gamma-ray coincidence spectra: (a) a known mixture of reagents, the content of Na, K and Cl of which approximates that in 7 g of plasma. 0·14 mcg of Mn also are present (Na : Mn = $4 \times 10^4$); (b) same as (a), but without added Mn; (c) ash from 6·12 g of plasma; (d) ash from 6·06 g of whole blood.

From Fig. 8 the $Mn^{56}$ activity induced in

TABLE 1

| | Wet weight before ashing | Coincidences per unit time in full absorption peak (Fig. 8) | | | Correction factor for radioactive decay prior to counting | Corrected coincidences per unit time | Mn in sample (mcg) | Mn (mcg/g) |
|---|---|---|---|---|---|---|---|---|
| | | $Mn^{56}$-channel (0·76–0·92 MeV) | | | | | | |
| | | Total | Interpolated Compton bkg. | Net | | | | |
| Standard | —* | 185 | 98·6 | 86·4 | 3·908 | 338 | 0·140† | — |
| Plasma | 6·12 g | 195 | 134·0 | 61·0 | 2·215 | 135 | 0·056‡ | 0·009 |
| Blood | 6·06 g | 228 | 138·0 | 180·0 | 2·543 | 458 | 0·190‡ | 0·031 |
| | | $Na^{24}$-channel (1·27–1·50 MeV) | | | | | Na in sample (mg) | Na (mequiv./l) |
| Standard | | 468 | 96·5 | 371·5 | 1·265 | 470 | 23·0* | — |
| Plasma | | 542 | 184·0 | 358·0 | 1·147 | 411 | 20·1‡ | 143§ |

* Na, 23·0 mg, with K and Cl in the same proportions as in plasma (i.e. 77·74 mg NaCl, 28·01 mg NaF, 3·97 mg KCl), plus 0·140 mcg of Mn(see†) added by microburet from a 0·001 % (wt/wt) solution of Mn, made up from $MnSO_4 \cdot H_2O$ and deionized water.

† Comparison of Fig. 8 with data gathered subsequently under related—but not identical—conditions implies that there may have been a dilution error in the preparation of the standards referred to in this Table, such that their Mn contents may have been different from the intended value listed. Accordingly, the plasma and blood Mn concentrations calculated by comparison with these standards cannot be taken as accurate; although they are consistent with reported values.[10] Nonetheless, this Table serves to illustrate the *method* of analysis to be followed in carrying out procedures such as those discussed in the text.

‡ Calculated by comparison with standard.

§ Normal range: 135–147 mequiv./l.

blood appears to be more than three times as great as that in plasma. However, at least a major portion of this difference can be attributed to transmutation from the $Fe^{56}(n,p)Mn^{56}$ reaction[19] on the large quantity of iron present in whole blood.[8] Contamination of this sort, involving high-energy neutrons[14] from the fission neutron portion of the reactor flux spectrum,[12] becomes relatively more prominent with more energetic ("harder") neutron fluxes, such as the filtered spectrum employed here in selective activation; and the interference from energetic neutron reactions is estimated in Appendix II.

It is emphasized that the purpose of this paper is to demonstrate the feasibility of detecting trace constituents in biological samples by instrumental means of radioactivation analysis, with particular emphasis on the important case of manganese in human plasma. Although the plasma concentration indicated by Table 1 is within the range of reported values,[8] no biological or medical significance is attached to the findings on the single samples reported here (see footnote†, Table 1). Further data of biological interest will be presented elsewhere.

## CONCLUSIONS

Coincidence spectroscopy and selective activation can impart very high resolution to radioactivation analysis, usually with some concomitant loss in absolute sensitivity. Many of the steps of the analytical procedure outlined in this article can be altered in straightforward fashion to enhance the sensitivity to other trace constituents than manganese. For example, $Br^{81}$ has low-lying neutron resonances[12] and a half-life more

than twice that of $Na^{24}$, so the "singles" spectrum of a blood sample recorded a few days after selective activation reflects the high resultant $D^{Br}_{Na}$ by revealing characteristic $Br^{82}$ $\gamma$-peaks (Fig. 9). At the same time, the 1·53 MeV peak of $K^{42}$, that is undetectable in the singles spectrum, becomes readily apparent in the coincidence spectrum when the $\beta$-channel is optimized for $D^{K}_{Na}$ (Fig. 9).

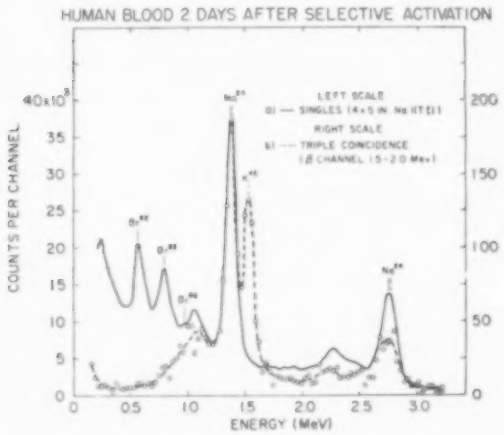


FIG. 9. Gamma-ray spectra. In (a) the prominent peaks at 0·55 and 0·77 MeV correspond to the most intense $\gamma$-emissions in the $Br^{82}$ decay scheme[11] and give evidence for its enhanced activation ($T_{\frac{1}{2}} = 36$ hr) by resonance neutrons. The $\beta$-channel used for (b) optimizes $D^{K}_{Na}$ and incidentally provides a very large $D^{K}_{Br}$, because $Br^{82}$ has no $\beta$-energy $> 0{\cdot}44$ MeV in its $\beta$-decay[11], and hence $Br^{82}$ is not seen in the coincidence spectrum.

In addition to varying the obvious parameters of irradiation time, energy channels on the counters, crystal thicknesses, sample decay before counting, etc., many more subtle and radical changes can be made when detection of other elements is being sought. Thus the principles expounded in the present work can be extended, where appropriate, to utilize some of the following: resonance absorption of neutrons which induce competing activities; activation with charged particles or fast neutrons produced by accelerators; $\gamma$–$\gamma$ coincidence measurements; $e^+$–$\gamma$ coincidence measurements with positrons selectively detected with a three-crystal pair spectrometer,[16] and so on.

It is felt that the work reported herein demonstrates that highly selective radioanalyses can be achieved with the aid of nuclear techniques.

*Acknowledgments*—LEE GRODZINS, now of the Massachusetts Institute of Technology, gave valuable assistance in the early development of this work. JOHN V. KANE suggested the utilization of a $\beta$-counter telescope, and there were illuminating discussions with ROBERT B. SCHWARTZ pertaining to the calculations of Appendix I. JOHN J. FLOYD provided invaluable aid in securing facilities for resonance activation, and GEORGE C. COTZIAS consistently encouraged this work.

## REFERENCES

1. BORG D. C. *Proceedings of the Second International Conference on the Peaceful Uses of Atomic Energy, Geneva*, 1958, P/841, Vol. 24, p. 283. United Nations, New York (1959).
2. SPENCER R. P., MITCHELL T. G. and KING E. R. *Amer. J. Roentgenol.* **74,** 1053 (1958).
3. SPENCER R. P., MITCHELL T. G. and KING E. R. *Int. J. appl. Rad. Isotopes* **3,** 104 (1958).
4. Öbrink K. J. and ULFENDAHL H. R. *Int. J. appl. Rad. Isotopes* **5,** 99 (1959).
5. GUINN V. P. and WAGNER C. D. *Analyt. Chem.* **32,** 317 (1960).
6. CROUTHAMEL C. E. *Applied Gamma-Ray Spectrometry*, Pergamon Press, New York (1960).
7. LEE W. *Analyt. Chem.* **31,** 800 (1959).
8. BOWEN H. J. M. *J. Nucl. Energy* **3,** 18 (1956).
9. KIENLE P. and SEGEL R. E. *Phys. Rev.* **114,** 1554 (1959).
10. PAPAVASILIOU P. S. and COTZIAS G. C. *Fed. Proc.* **19,** 250 (1960).
11. STROMINGER D., HOLLANDER J. M. and SEABORG G. T. *Rev. mod. Phys.* **30,** 585 (1958).
12. HUGHES D. J. and SCHWARTZ R. B. *Neutron Cross-Sections*. BNL-325 (1958); Suppl. No. 1 (1960).
13. HUGHES D. J. *Pile Neutron Research*, Addison–Wesley, Cambridge, Mass. (1953).
14. BLATT J. M. and WEISSKOPF V. F. *Theoretical Nuclear Physics*, Wiley, New York (1952).
15. SIEGBAHN K. (Ed.) *Beta- and Gamma-Ray Spectroscopy*, Interscience, New York (1955).
16. FERMI E. *Phys.* **88,** 161 (1934).
17. ALBURGER D. E. *Rev. sci. Instrum.* **27,** (1956).

18. Slätis H. and Herrlander C. J. *Rev. sci. Instrum.* **26,** 613 (1955).
19. Rochlin R. S. *Nucleonics* **17,** 54 (1959).
20. Endt P. M. and Demeur M. (Ed.) *Nuclear Reactions*, North Holland, Amsterdam (1959).
21. Borg D. C. and Cotzias G. C. *Nature, Lond.* **182,** 1677 (1958).
22. Waard H. de *Nucleonics* **13**(7), 36 (1955).

## APPENDIX I

## CALCULATION OF SELECTIVE MANGANESE ACTIVATION BY RESONANCE NEUTRONS

The following conventional symbols are used (viz. Chap. VIII[14]):

$\lambda$ de Broglie wavelength of relative motion, divided by $2\pi$
$g$ a statistical weighting factor
$\Gamma$ total width of a resonance state of a compound nucleus
$\Gamma_n$ partial width of a resonance level for emission of a neutron
$\Gamma_\gamma$ partial width of a resonance level for emission of a $\gamma$-ray
$\sigma_{n,\gamma}$ cross section for radiative capture, $(n,\gamma)$, i.e. . . . for "activation"

The activation cross section at an energy, $E$, due to a resonance at an energy, $E_0$, is given by Blatt and Weisskopf[14]:

$$\sigma_{n,\gamma}(E) = \pi\lambda\lambda_0\, g\, \frac{\Gamma_n\,\Gamma_\gamma}{\frac{\Gamma^2}{4} + (E - E_0)^2}. \quad (1)$$

Consider only the common case, which holds true for both $Mn^{55}$ and $Na^{23}$, wherein both the thermal neutron cross section and the resonance integral[13] are dominated by one single resonance. Then, if the nuclei are irradiated by a continuous spectrum of neutrons, the number of captures per unit time will be

$$N_{\text{cap}} = \int_0^\infty \sigma_{n,\gamma} N(E)\, dE \quad (2)$$

$$= Kg\Gamma_n\Gamma_\gamma \frac{1}{\sqrt{E_0}} \int_0^\infty \frac{1}{\sqrt{E}} \frac{N(E)\, dE}{[\Gamma^2 + (E - E_0)^2]},$$

where $K$ is a numerical factor, and $N(E)\, dE$ is the number of neutrons of energy between $E$ and $E + dE$. For the case of "resonance neutrons" in a reactor, $N(E) = 1/E$.[13]

In the present example of selective activation, a "1/v" absorber has been introduced in the form of $B^{10}$. This absorbs all neutrons up to energies $E_1$, well above thermal, but is effectively "transparent" at the resonance energies. Hence $N(E)$ can be approximated by $N(E) = 0$ at $E < E_1$, where $E_0 - \Gamma \gg E_1 \gg 1/40$ eV (i.e. "thermal") but with $E_1$ otherwise variable. Then

$$N_{\text{cap.}} = Kg\Gamma_n\Gamma_\gamma \frac{1}{\sqrt{E_0}} \times \int_{E_1}^\infty \frac{1}{E^{3/2}} \frac{dE}{[\Gamma^2 + 4(E - E_0)^2]}. \quad (3)$$

If the simplified notation $G(E)dE$ represents the integrand in equation (3), one can write

$$N_{\text{cap.}} = Kg\Gamma_n\Gamma_\gamma \frac{1}{\sqrt{E_0}} \left[ \int_{E_1}^{E2 \ll \text{res.}} G(E)\, dE + \left(\int_{\text{res}}\right) G(E)\, dE + \int_{E3 \gg \text{res.}}^\infty G(E)\, dE \right]. \quad (3a)$$

Since it has been assumed that only one resonance contributes to the resonance integral:

$$\int_{E3 \gg \text{res.}}^\infty G(E)\, dE = 0. \quad (4)$$

$\left(\int_{\text{res}}\right) G(E)\, dE$ can also be integrated by making the usually physically correct approximation that $\Gamma \ll E_0$, to obtain

$$\left(\int_{\text{res}}\right) G(E)\, dE = \frac{1}{E_0^{3/2}} \frac{\pi}{2\Gamma}. \quad (5)$$

There then remains for evaluation

$$\int_{E_1}^{E_2} G(E)\, dE = \int_{E_1}^{E_2} \frac{1}{E^{3/2}} \frac{dE}{[\Gamma^2 + 4(E - E_0)^2]} \simeq \frac{1}{4} \int_{E_1}^{E_2} \frac{dE}{E^{3/2}(E - E_0)^2}, \quad (6)$$

with the approximate form of the equation deriving from the fact that $\Gamma \ll |E - E_0|$ over the energy region $E < E_2$.

Because integration is being carried out only up to the vicinity of the resonance, the major contribution to equation (6) will be from the energy region just $>E_1$. Hence

$$\int_{E_1}^{E_2} G(E)\,dE \simeq \frac{1}{4E_0^2}\int_{E_1}^{E_2}\frac{dE}{E^{3/2}} = \frac{-1}{2E_0^2}\frac{1}{\sqrt{E}}\Bigg|_{E_1}^{E_2} \simeq \frac{1}{2E_0^2}\frac{1}{\sqrt{E_1}}. \quad (7)$$

If, as is again implied by $E_1 \ll \Gamma$, $E_2 \gg E_1$, then combining equations (3), (4), (5) and (7) gives

$$N_{\text{cap.}} = Kg\Gamma_n\Gamma_\gamma\frac{1}{\sqrt{E_0}}\left[\frac{1}{2E_0^2\sqrt{E_1}} + \frac{\pi}{E_0^{3/2}\,2\Gamma}\right] = Kg\Gamma_n\Gamma_\gamma\frac{1}{2E_0^2}\left[\frac{1}{\sqrt{E_0E_1}} + \frac{\pi}{\Gamma}\right]. \quad (8)$$

Thus there are two contributions to the resonance capture from a single resonance: (1) the "normal" integral over the resonance, $N(E_0)\frac{\pi}{2}\sigma_0\Gamma$, where $\sigma_0$ is the peak cross section, and (2) an additional contribution from the low-energy wing of the resonance, because the number of captures is weighted by the neutron spectrum of $1/E$. This second contribution is significant only if $E_0E_1 \lesssim \Gamma^2$, that is to say, only if $E_1 \lesssim \frac{\Gamma^2}{E_0}$.

(A) *Sodium*

For the case of $Mn^{55}$ and $Na^{23}$, the resonance parameters are[12]:

| | $Mn^{55}$ | $Na^{23}$ |
|---|---|---|
| $E_0$ | 337 eV | 2850 eV |
| $\Gamma$ | 21 eV | 410 eV |
| $\Gamma^2/E_0$ | 1·3 eV | 5·9 eV |

Thus it can be seen that the contribution to capture from low-energy neutrons is relatively greater for sodium than for manganese. Therefore in attempting to suppress activation of sodium relative to capture in $Mn^{55}$, it pays to thicken the neutron absorber until $E_1 \simeq 6$ eV. Further increases in $E_1$ will not affect substantially the production of either $Mn^{56}$ or $Na^{24}$ until, of course, $E_1$ approaches 337 eV. The ultimate ratio of capture in $Mn^{55}$ to that in $Na^{23}$ is thus

$$\frac{N_{\text{cap, Mn}}}{N_{\text{cap, Na}}} = \frac{E_{0,\text{Na}}^2}{E_{0,\text{Mn}}^2}\frac{\left(g\frac{\Gamma_n}{\Gamma}\Gamma_\gamma\right)_{\text{Mn}}}{\left(g\frac{\Gamma_n}{\Gamma}\Gamma_\gamma\right)_{\text{Na}}} \simeq \frac{E_{0,\text{Na}}^2(g\Gamma_\gamma)_{\text{Mn}}}{E_{0,\text{Mn}}^2(g\Gamma_\gamma)_{\text{Na}}}, \quad (9)$$

because for both nuclei $\Gamma_\gamma \ll \Gamma_n \simeq \Gamma$.

From the de Broglie wave equation, $\lambda = \frac{h}{2\pi mv} = \frac{h}{\pi\sqrt{m}\sqrt{E}}$, the approximation $E_0 \gg E_{\text{Th}}$, and the known thermal cross sections, $\sigma_{\text{Th}}$, equation (1) may be used to find

$$\frac{(g\Gamma_\gamma)_{\text{Mn}}}{(g\Gamma_\gamma)_{\text{Na}}} \simeq \frac{\sigma_{\text{Th,Mn}}\sqrt{E_{0,\text{Mn}}}\,\Gamma_{\text{Na}}\left(\frac{\Gamma_{\text{Mn}}^2}{4} + E_{0,\text{Mn}}^2\right)}{\sigma_{\text{Th,Na}}\sqrt{E_{0,\text{Na}}}\,\Gamma_{\text{Mn}}\left(\frac{\Gamma_{\text{Na}}^2}{4} + E_{0,\text{Na}}^2\right)} = 2{\cdot}46. \quad (10)$$

Substituting the numerical value of equation (10) and the known resonance energies into (9) yields

$$\frac{N_{\text{cap, Mn}}}{N_{\text{cap, Na}}} = 176$$

for resonance neutron activation. This compares with the ratio of $D_{\text{Na}}^{\text{Mn}}(\sigma_{\text{pile}}) = 25{\cdot}3$ for the thermal activation cross sections, so that selective activation (resonance activation) contributes to $D_{\text{Na}}^{\text{Mn}}$ by a factor of $\sim$7.

(B) *Chlorine*

The situation with regard to chlorine is somewhat more complicated, because more than one resonance contributes significantly to $Cl^{38}$ production. This is deduced from the fact that the known $Cl^{37}$ resonances[12] are not sufficient to account for the $Cl^{37}$ thermal capture cross section, and therefore this capture must be due to one or several negative energy resonances. In order to handle this situation, equation (8) must be generalized to include more than one resonance, in which case there is, after a slight rearrangement

$$N_{\text{cap.}} = \frac{K}{2}\sum_i g_i\,\Gamma_{n,i}\,\Gamma_{\gamma,i}\,|E_{0,i}|^{-5/2} \times\left(\frac{1}{\sqrt{E_1}} + \delta(E_{0,i})\frac{\pi\sqrt{|E_{0,i}|}}{\Gamma_i}\right) \quad (8a)$$

where

$$\delta(E_{0,i}) = 1 \qquad \text{if } E_{0,i} > E_1$$
$$\delta(E_{0,i}) = 0 \qquad \text{if } E_{0,i} < E_1;$$

and the summation is taken over all resonances which contribute significantly.

The negative energy resonances do not contribute a $\frac{\pi}{\Gamma}$ term in equations (8) or (8a) (i.e. one does not integrate over the resonance). The neutron capture cross section due to negative energy resonances will fall off at least as fast as 1/v, faster if there is a resonance close to zero energy. In the case of $Cl^{37}$, the small thermal cross section renders it likely that the negative energy resonance is well below zero energy. One can therefore evaluate the contribution from the negative energy resonances if the known thermal capture cross section is used, and then, *considering only the negative energy* $Cl^{37}$ *resonances*, equation (8a) implies

$$\frac{N_{\text{cap,Mn}}}{N_{\text{cap,Cl}}} = D_{\text{Cl}}^{\text{Mn}}(\sigma_{\text{pile}}) \left( \frac{\dfrac{1}{\sqrt{E_1}} + \pi \left( \dfrac{\sqrt{E_0}}{\Gamma} \right)_{\text{Mn}}}{\dfrac{1}{\sqrt{E_1}}} \right). \tag{11}$$

If $E_1$ is just $< E_{0,\text{Mn}} (= 337$ eV), there is a maximum suppression of the $Cl^{37}$ capture component due to negative energy resonances. The $B^{10}$ neutron filter actually used had a cut-off at about $E_1 = 100$ eV; and with $D_{\text{Cl}}^{\text{Mn}}(\sigma_{\text{pile}}) = 23{\cdot}8$, this gives

$$\frac{N_{\text{cap,Mn}}}{N_{\text{cap,Cl}}} \approx 678.$$

However, it is emphasized that if the cross section decreases faster than 1/v, then chlorine activation would be even further suppressed, relative to that of manganese.

The only positive energy resonance which contributes significantly to $Cl^{38}$ is the resonance at 8·7 keV.[12] Since for this resonance $\frac{\Gamma^2}{E_0} = 0{\cdot}29$ eV, only the $\frac{\pi}{\Gamma}$ term in equation (8) is important. However, this term cannot be evaluated in the manner used for manganese and sodium in equation (10). In the case of chlorine, $g\Gamma_\gamma$ cannot be deduced from the thermal cross section which is dominated by another resonance. Nonetheless, $\Gamma_\gamma$ does not vary greatly from resonance to resonance or from element to element,[20] so one can make the estimate

$$(g\Gamma_\gamma)_{\text{Cl}} \simeq (g\Gamma_\gamma)_{\text{Mn}}$$

in which case, from the *positive* energy $Cl^{37}$ resonances, there is

$$\frac{N_{\text{cap,Mn}}}{N_{\text{cap,Cl}}} \simeq \left( \frac{8{\cdot}7}{0{\cdot}337} \right)^2 = 670.$$

Thus, due to selective activation with filtered neutrons,

$$D_{\text{Cl}}^{\text{Mn}}(\sigma_f) \geq \frac{1}{\dfrac{1}{670} + \dfrac{1}{678}} \geq 338.$$

This detection ratio is some 14 times that achievable with thermal neutrons and is consistent with our experimental results.

## APPENDIX II

## ESTIMATION OF BACKGROUND DUE TO $Fe^{56}(n, p)Mn^{56}$ IN SAMPLES

$Mn^{56}$ can be produced adventitiously in iron and cobalt from the reactions $Fe^{56}(n,p)Mn^{56}$ and $Co^{59}(n, \alpha)Mn^{56}$, respectively, but the yields are very small because these reactions have significant energy thresholds and small reaction cross sections.[19] The cobalt reaction may be ignored in the light of cobalt's trace concentration in blood, but the large amount of iron in the hemoglobin of blood forces further consideration of $Mn^{56}$ arising from that source, especially with the use of selective activation, wherein the irradiating flux becomes relatively enriched in more energetic neutrons (see text).

### (A) *Calculation from physical parameters*

The 6 ml aliquot of blood whose spectrum is depicted in Fig. 8(d) contained 14·5 g of

hemoglobin per 100 ml by direct measurement. This corresponds to a number of iron atoms, $S$, in the sample $= 3{\cdot}11 \times 10^{19}$.

With an energy threshold of 2·94 MeV,[19] the (n,p) reaction on iron will reflect only the high-energy or "fission neutron"[13] portion of the total neutron flux, $n_T$. But the reactor fission neutron flux, $n_F$, can be taken as about equal to the resonance neutron flux, $n_R$.[13] Then, according to HUGHES[13]:

$$n_F \simeq n_R = \frac{n_T}{R_{Cd}}, \qquad (1)$$

where $R_{Cd}$ is the measured cadmium ratio of the activating spectrum, here determined as 34 with $n_T = 1{\cdot}43 \times 10^{13}$. With an isotopic abundance, $\theta$, of 0·917 for $Fe^{56}$,[11] the number of $Mn^{56}$ atoms, $N$, produced over time $t$, becomes

$$N = \int_0^t (n_F \sigma_F \theta S - \lambda N)dt = \frac{n_F \sigma_F \theta S}{\lambda}(1 - e^{-\lambda t}), \qquad (2)$$

where $\sigma_F = 0{\cdot}44 \times 10^{-27}$ cm², the effective reaction cross section for the (n,p) reaction averaged over the entire spectrum of *fission* neutrons.[19] The corresponding radioactivity, $A$, is:

$$A = \lambda N = \frac{0{\cdot}693\ N}{T_{\frac{1}{2}}}, \qquad (3)$$

where $\lambda$ is the decay constant and $T_{\frac{1}{2}}$ the half-life of $Mn^{56}$. The actual counting rate due to $Mn^{56}$ produced from iron will be

$$C = E_p B_c A = E_p E_c n_F \sigma_F \theta S(1 - e^{-\lambda t}), \qquad (4)$$

where $E_p$ is the overall efficiency for detecting $Mn^{56}$ by means of its 0·85 MeV total absorption peak in the NaI(Tl) crystal of Fig. 4, and $E_c$ is the relative efficiency of counting $Mn^{56}$ for the triple coincidence system compared with $\gamma$-singles counting.

Experimentally, $E_p$ was found to be about 14 per cent, using the isolated 0·845 MeV $\gamma$-ray accompanying decay by orbital electron capture in a calibrated standard of $Mn^{54}$.[11] Comparing coincidence and singles count rates for a $Mn^{56}$ source gave an apparent $E_c$ of $5{\cdot}8 \times 10^{-4}$. Substituting these, and the other numerical values given before, into equation 4 yields a count rate of 201 coincidences per unit time, due to $Fe^{56}(n,p)Mn^{56}$.

(B) *Comparison with experimental data*

The data of Table 1 indicate that 201 coincidences per unit time represent $\frac{201}{338} \times 0{\cdot}140 = 0{\cdot}083$ mcg of "manganese equivalent", or 0·014 mcg in each gram of blood. Hence the 0·031 mcg/g manganese concentration determined for whole blood would be corrected to 0·018 mcg/g, which is about twice the 0·009 mcg/g in plasma, considering the roughness of some of the assumptions implicit in the correction.

Upon neutron activation, iron reference standards always are seen to be contaminated with small quantities of manganese; although biological substances rich in iron, such as hemin, may contain only traces of manganese.[21] Yet aliquots of iron and manganese could be activated in a fully thermalized neutron beam (free of fission neutrons) while other aliquots were irradiated with the filtered neutron spectrum described in these experiments. The amount of manganese contaminating the iron sample could be determined from the "thermal" activation run, and the $Mn^{56}$ radioactivity to be expected from this impurity after "selective activation" could be calculated from the similar irradiations of the manganese standards. Any further increment in $Mn^{56}$ activity found in the iron, when compared with the amount calculated for contaminating manganese, would permit experimental evaluation of the transmutations induced in iron specifically by fast neutrons as a check on the calculations of this Appendix. This has been done in a preliminary fashion, with tentative results that support the conclusion that much of the difference between blood and plasma $Mn^{56}$ values derives from $Fe^{56}(n,p)Mn^{56}$.

In plasma, iron is but 1/400 as concentrated as in whole blood. Therefore the (n,p) reaction on iron presents a negligible correction to the plasma manganese determination.

International Journal of Applied Radiation and Isotopes, 1961, Vol. 11, pp. 30–37. Pergamon Press Ltd. Printed in Northern Ireland

# Formation of Metastable Isomers by Photoactivation with the Van de Graaff Accelerator

H. R. LUKENS, JR., J. W. OTVOS and C. D. WAGNER
Shell Development Company, Emeryville, California, U.S.A.

(*Received* 30 *October* 1960)

VOL.
11
196

Bremsstrahlung from a 3 MeV 1 mA electron beam was used to form nuclear isomers $Se^{77m}$, $Sr^{87m}$, $Rh^{103m}$, $Ag^{107m}$, $Cd^{111m}$, $In^{115m}$, $Lu^{176m}$, $Au^{197m}$, $Hg^{199m}$, $Y^{89m}$, $Sn^{117m}$, $Ba^{137m}$, $Hf^{179m}$, $Ir^{191m}$ and $Pt^{195m}$ by photoactivation. The latter six isomers were prepared in this manner for the first time. In addition, the very short half-life activity generated in erbium can with little doubt be ascribed to $Er^{167m}$.

Photoactivation appears to be a useful supplement to neutron activation as an alternate means of purely instrumental elemental analysis for most of the above elements in the 10–10,000 p.p.m. range. It also has possible applications in determination of electron beam energy and in radiation dosimetry.

## LA FORMATION DES ISOMERES METASTABLES PAR LA PHOTO-ACTIVATION AU MOYEN DE L'ACCELERATEUR VAN DE GRAAFF

On employa les Bremsstrahlung d'un faisceau d'électrons de 3 MeV, 1 mA pour former par la photo-activation les isomères nucléaires $Se^{77m}$, $Sr^{87m}$, $Rh^{103m}$, $Ag^{107m}$, $Cd^{111m}$, $In^{115m}$, $Lu^{176m}$, $Au^{197m}$, $Hg^{199m}$, $Y^{89m}$, $Sn^{117m}$, $Ba^{137m}$, $Hf^{179m}$, $Ir^{191m}$ et $Pt^{195m}$. Les six derniers isomères furent préparés ainsi pour la première fois. En outre, on peut attribuer avec peu de doute à $Er^{167m}$ l'activité de très courte période de demi-valeur générée dans l'erbium.

La photo-activation semble être un supplément à l'activation neutronique utile comme moyen alternatif pour le dosage élémental simplement instrumental pour la plupart des éléments cités ci-dessus dans la gamme 10–10.000 p.p.m. Il serait possible aussi de l'appuyer à la mesure de l'énergie du faisceau d'électrons et dans la dosimétrie du rayonnement.

## ОБРАЗОВАНИЕ МЕТАСТАБИЛЬНЫХ ИЗОМЕРОВ ПУТЕМ ФОТОАКТИВАЦИИ С ПРИМЕНЕНИЕМ УСКОРИТЕЛЯ ВАН-ДЕ-ГРААФА

Тормозное излучение от пучка электронов в 3 мэв 1 мА было использовано для получения ядерных изомеров $Se^{77m}$, $Sr^{87m}$, $Rh^{103m}$, $Ag^{107m}$, $Cd^{111m}$, $In^{155m}$, $Lu^{176m}$, $Au^{197m}$, $Hg^{199m}$, $Y^{89m}$, $Sn^{117m}$, $Ba^{137m}$, $Hf^{179m}$, $Ir^{191m}$ и $Pt^{195m}$ посредством фотоактивации. Последние шесть изомеров были получены таким путем впервые. Найденную в эрбии радиоактивность с очень коротким периодом полураспада можно с уверенностью приписать $Er^{167m}$.

Фотоактивация может с успехом заменить активацию нейтронами в тех случаях, когда требуется чисто механический анализ на большинство из вышеупомянутых элементов при концентрации от 10 до 10.000 частей на миллион. Фотоактивация пригодна также для измерения энергии электронов и при дозиметрии излучения.

## BILDUNG METASTABILER ISOMERE DURCH PHOTOAKTIVIERUNG MIT VAN DE GRAAFF BESCHLEUNIGER

Bremsstrahlung von einem 3 MeV, 1 mA Elektronenstrom wurde benützt zur Herstellung der Isomere Se-77$^m$, Sr-87$^m$, Rh-103$^m$, Ag-107$^m$, Cd-111$^m$, In-115$^m$, Lu-176$^m$, Au-197$^m$, Hg-199$^m$, Y-89$^m$, Ba-137$^m$, Hf-179$^m$, Ir-191$^m$ und Pt-195$^m$ durch Photoaktivierung. Die letztgenannten

6 Isomeren wurde auf diesem Wege erstmalig hergestellt. Überdies kann eine sehr kurzlebige in Erbium erzeugte Aktivität mit geringem Zweifel dem Er-167$^{m}$ zugeschrieben werden.

Photoaktivierung erscheint als nützliche Ergänzung zur Neutronenaktivierung auf anderem experimentellem Wege für die Analyse der meisten der oben genannten Elemente im 10–10·000 p.p.m. Gebiet. Sie kann ausserdem zur Bestimmung der Energie des Elektronenstromes und in der Strahlungsdosimetrie angewendet werden.

BREMSSTRAHLUNG from absorption of a 3 MeV 1 m/Ampere electron beam in a gold target[1] is estimated to amount to $4 \times 10^{15}$ photons/sec, and in the forward direction the photon flux 1 cm from the target is estimated to be $3 \times 10^{14}$ photons/cm$^2$ sec. With such an intense photon source, it was of interest to look for photoactivation of nuclei to metastable states, and to determine whether analytical or other use could be made of such nuclear reactions.

## EXPERIMENTAL

### *Irradiations*

Elements were used in chemical forms that were easily available in a state of high purity. (Reagent Grade was used in most cases.) All of the stable elements were included in the study, except $Z = 1, 2, 3$ and 4 and the inert gases. The compounds were irradiated in 30 ml or 6 ml polyethylene vials, depending on the volume of the compound at hand. Amounts of the elements used varied from 1 to 250 g. For the sake of brevity, the approximate amounts of the elements used are shown by the following groupings:

| Elements | Weight range (g) |
|---|---|
| F, Sc, Ru, In, Tb, Tm, Lu, Os | 1–3 |
| B, C, N, Al, Si, Ti, Ge, Rb, Sr, Y, Rh, Cd, Ba, La, Ce, Nd, Sm, Eu, Gd, Dy, Ho, Er, Yb, Hf, W, Ir, Pt | 4–10 |
| O, Na, P, Mg, S, Cl, K, Ca, Cr, Ga, Zr, Pd, Ag, Cs, Pr, Ta, Re, Au | 11–30 |
| V, Mn, Fe, Co, As, Se, Br, Mo, Sb, Te, I, Hg, Tl | 31–100 |
| Ni, Cu, Zn, Sn, Pb, Bi | 101–250 |

Samples were irradiated for 3–30 min (20–30 min periods were used for those elements giving slight or no activity). As the program developed, new and improved irradiation techniques were used. Thus, the techniques varied from irradiation of the sample in a horizontal position beneath a linear 3 in. X-ray target to that of a sample in a 6 ml polyethylene vial placed directly below a point X-ray source. Estimated average photon fluxes range from $1 \times 10^{13}$/cm$^2$ sec to $10 \times 10^{13}$/cm$^2$ sec in these arrangements. The flux was constant within $\pm$ 3 per cent during each irradiation.

The Bremsstrahlung spectrum from the 3 mm thick gold target used for the photoexcitations is shown in Fig. 1. The dotted line shows the calculated distribution of emitted photons, and the solid line shows that emitted in the forward direction after photoelectric absorption of the lower energy photons. The total photon production in all directions is approximately $4 \times 10^{15}$ photons/sec, or about $\frac{1}{3}$ photon for every electron absorbed. However, a large fraction of the Bremsstrahlung is absorbed in the target. The spectrum in the forward direction is such that the average energy is nearly exactly 1·0 MeV, with upper and lower limits 0·3 and 3·0 MeV.

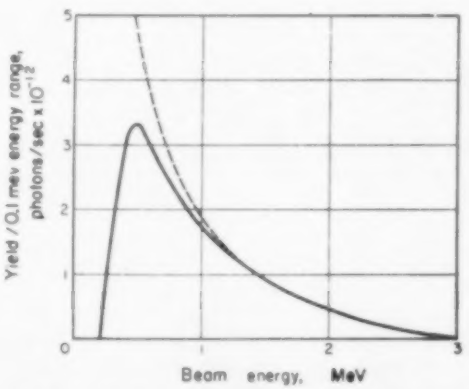


FIG. 1. Energy distribution and yield of Bremsstrahlung photons (within 10° of beam axis).

*Counting techniques*

When the irradiation was finished the bottle was removed, placed in a 3 in. well-type scintillation crystal and counted. The time interval between irradiation and counting was 0·75–1·5 min.

Pulses from the counter were fed through a linear amplifier and to both a scaler, for periodic readings of count for decay time determinations, and to a 100 channel analyzer for recording of the gamma-ray spectrum. Background was approximately 270 c.p.m., in a distribution almost monotonically decreasing with increasing pulse height (Fig. 2). Gain of the amplifier ordinarily was such as to record pulses corresponding to photons of from 0·04 to 1·0 MeV; if previously reported findings or the appearance of the spectrum suggested it, the setting was changed to a more appropriate one.

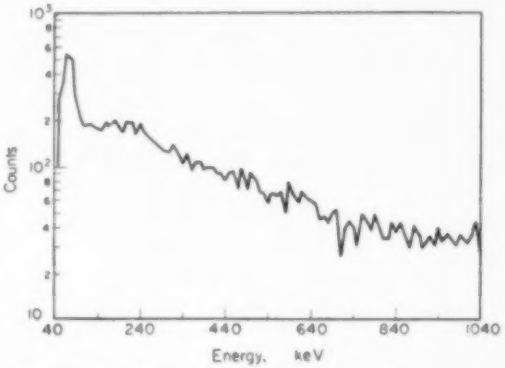


FIG. 2. Background spectrum for counting equipment (3 in. well-type crystal counter, 38 min background).

## RESULTS

Activation of the samples was considered detectable if the net counting rate of the sample was at least 1·5 times the standard deviation for the counting period used. Data for those elements giving detectable activity are shown in Table 1.

Where the activity was sufficient, it was characterized by half-life and/or energy of electromagnetic radiation, as shown in Table 1. The Table includes also the induced counting rate extrapolated back to the end of the irradiation, and the estimated specific activity for a 1 hr irradiation (considered to be the practical maximum for analytical use).

## DISCUSSION

The only probable mechanisms that can account for generated activity are (1) photoexcitation to metastable states, and (2) neutron activation, by means of neutrons generated from the deuterium of the cooling water of the target or from a beryllium impurity. Thresholds for other photon-excited nuclear reactions are too high to permit them to be induced by 3 MeV photons.

*Photoexcitation*

Direct photoexcitation by photons less than 3 MeV has previously been observed for Se, Kr, Sr, Nb, Rh, Ag, Cd, In, Lu, Au and Hg to give nuclear isomers of half-lives of seconds to days. It is pertinent to compare the results with data for known isomers of stable nuclides, including not only those above, but also those isomers generated by radioactive decay or by charged particle excitation. This has been done in Table 2 for all of the known nuclear isomers with half-lives greater than 1 sec. It is interesting that, of the known isomers, the ones that could not be detected in this study have very short half-lives, of less than 6 sec, or long half-lives, of hours to days. The former would not be observed because more than ten half-lives elapse between irradiation and counting; the latter may be formed with the same probability, or cross section, but possess activities that are too low because of their long half-life.

From Table 2 it is concluded that photoactivations previously observed with Se, Sr, Rh, Ag, Cd, In, Lu, Au and Hg have been

TABLE 1. Irradiation results

| Element | Weight (g) | Irradiation time (min) | Activity observed in first counting period (c.p.m. ± st'd deviation) | Activity extrapolated back to end of irradiation (c.p.m.) | Calculated specific activity after irradiation for 1 hr (c.p.m./g) | Half-lives observed | Photon energies observed (keV) |
|---|---|---|---|---|---|---|---|
| Fe | 82 | 30 | 69 ± 42 | Activity too small | | | |
| Cu | 103 | 30 | 109 ± 44 | Activity too small | | | |
| As | 63 | 30 | 70 ± 6 | 70 | 2·7 | 30 ± 15 hr | 550 ± 10 |
| Se | 73 | 30 | 500,000 ± 1000 | 10,000,000 | 140,000 | 18 ± 1 sec | 160 ± 10 |
| Br | 46 | 30 | 667 ± 32 | 716 | 20 | 18 ± 4 min (small) hours or days | 530 ± 30<br>630 ± 30 |
| Sr | 1·0* | 10 | 3,150 ± 20 | 3150 | 20,000 | | 380 ± 20 |
| Y | 7·4 | 3 | 3,600 ± 60 | 50,000 | 6000 | 16 ± 1 sec | 890 ± 20 |
| Mo | 88 | 15 | 200 ± 11 | 200 | 5 | 22 ± 2 min | 200 ± 30, 310 ± 30 |
| Rh | 10·4 | 20 | 8000 ± 100 | 8000 | 800 | 57 min | 21 ± 5 |
| Ag | 1·4* | 10 | 23,800 ± 300 | 300,000 | 200,000 | 40 ± 2 sec | 90 ± 30 |
| Cd | 1·28† | 10 | 40,750 ± 350 | 40,750 | 130,000 | 50 ± 1 min | 140, 230 |
| In | 0·265† | 5 | 6216 ± 35 | 6220 | 300,000 | 4·2 ± 0·2 hr | 150 ± 10, 330 ± 10 |
| Sn | 138 | 20 | 440 ± 8 | 440 | 10 | 14·0 ± 0·2 days | 150 ± 10 |
| I | 66 | 30 | 1100 ± 18 | 1100 | 25 | 26 ± 2 min | 450 ± 10 |
| Ba | 1·7* | 10 | 1350 ± 40 | 2700 | 1600 | 2·7 ± 0·1 min | 660 ± 20 |
| Gd | 8·2 | 10 | 130 ± 20 | 17[illegible] | 40 | Activity too small | |
| Er | 9·0 | 1 | 10,000 ± 4000 | 2,500,000‡ | 300,000 | <3 sec | |
| Lu | 0·88 | 10 | 1400 ± 40 | 1400 | 10,000 | 3·8 ± 0·1 hr | 86 ± 5 |
| Hf | 8·2 | 5 | 4,740,000 ± 5000 | 30,000,000 | 4,000,000 | 20 ± 2 sec | 65, 220 ± 10 |
| Ir | 6·36 | 3 | 970 ± 110 | 6,000,000§ | 1,000,000 | 6 ± 1 sec | 130 ± 20 |
| Pt | 4·5 | 20 | 1540 ± 14 | 1540 | 1000 | 4·1 ± 0·1 days | 69 ± 3 |
| Au | 26·7 | 3 | 15,730 ± 400 | 10,000,000§ | 400,000 | 7·4 ± 0·2 sec | 70 ± 10, 270 ± 10 |
| Hg | 16·5 | 30 | 23,200 ± 80 | 23,500 | 2000 | | 74 ± 10, 155 ± 10, 390 ± 10 |

* Dissolved in 30 ml $H_2O$.
† Dissolved in 5 ml $H_2O$.
‡ Semiquantitative only, with extrapolation using literature value for the half-life.
§ Extrapolation using literature value for the half-life.

duplicated. Several apparent discrepancies are worth noting. (1) The rhodium photon energy does not agree with the literature value. This is thought to be due to the X-ray emission subsequent to the highly probable internal conversion of the 40 keV gamma ray of the Rh isomer. (2) The gamma-ray spectrum of the activity generated in indium has a shoulder on the high side of the 335 keV photo peak and the activity has a shorter half-life. This suggests that some $In^{113m}$ is present as well as $In^{115m}$. The significance of the rather weak peak at 150 keV is not known. (3) There are indications that the 130 keV photon from gold may be present, but if so, it is very weak. K X-rays in gold and mercury were observed from internal conversion of some of the photons.

From Table 2 it is also concluded that $Y^{89m}$, $Sn^{117m}$, $Ba^{137m}$, $Hf^{179m}$, $Ir^{191m}$ and $Pt^{195m}$ have been prepared for the first time by direct photoexcitation. The short half-life activity (1–5 sec) observed with erbium is believed to be due to $Er^{167m}$. Agreement with literature data is good with the following exceptions: (1) the 160 keV photon from $Hf^{179m}$ and the $Pt^{197m}$ gamma rays were absent because of internal conversion, and the K X-rays were observed instead, and (2) the 42 keV photon from iridium was

TABLE 2. Comparison with known nuclear isomers*

| Isomer | Ref. | Literature half-life | Observed half-life | Literature γ-energy (keV) | Observed γ-energy (keV) |
|---|---|---|---|---|---|
| $Se^{77m}$ | 2 | 17·5 sec | 18 ± 1 sec | 160 | 160 ± 10 |
| $Kr^{85m}$ | 3 | 1·9 hr | | 32 | |
| $Sr^{87m}$ | 4 | 2·8 hr | | 390 | 380 ± 20 |
| $Y^{89m}$ | | 16 sec | 16 ± 1 sec | 910 | 890 ± 20 |
| $Nb^{93m}$ | 4 | 12 years | | 30 | |
| $Rh^{103m}$ | 5 | 57 min | 57 min | 40 | 21 ± 10 |
| $Ag^{107m}$ | 6 | 44 sec | | 93 | |
| $Ag^{109m}$ | 6 | 39 sec | 40 ± 2 sec | 88 | 90 ± 30 |
| $Cd^{111m}$ | 6 | 49 min | 50 ± 1 min | 149,247 | 140 ± 10, 230 ± 20 |
| $Cd^{113m}$ | | 5·1 years | | 265 | |
| $In^{113m}$ | 7 | 1·9 hr | | 390 | |
| $In^{115m}$ | 8 | 4·5 hr | 4·2 ± 0·2 hr | 335 | 150 ± 10, 330 ± 10 |
| $Sn^{117m}$ | | 14 days | 14·0 ± 0·2 days | 159 | 150 ± 10 |
| $Sn^{119m}$ | | 250 days | | 65 | |
| $Te^{123m}$ | | 110 days | | 89,159 | |
| $Te^{125m}$ | | 58 days | | 110 | |
| $Xe^{129m}$ | | 8 days | | 40 | |
| $Xe^{131m}$ | | 12 days | | 165 | |
| $Ba^{135m}$ | | 29 hr | | 268 | |
| $Ba^{137m}$ | | 2·6 min | 2·7 ± 0·1 min | 662 | 660 ± 20 |
| $Er^{167m}$ | | 2·5 sec | <3 sec | 210 | |
| $Lu^{176m}$ | 9 | 3·7 hr | 3·8 ± 0·1 hr | 89 | 86 ± 5 |
| $Hf^{178m}$ | | 4·8 sec | | 88 | |
| $Hf^{179m}$ | | 19 sec | 20 ± 2 sec | 160,215 | 65 ± 10, 220 ± 10 |
| $Ta^{180m}$ | | 8·2 hr | | 93,100 | |
| $W^{183m}$ | | 5·5 sec | | 100,155 | |
| $Os^{187m}$ | | 39 hr | | (K X-ray) | |
| $Os^{189m}$ | | 5·7 hr | | 30 | |
| $Os^{190m}$ | | 9·5 min | | 186,356,510,620 | |
| $Ir^{191m}$ | | 4·9 sec | 6 ± 1 sec | 130,42 | 130 ± 20 |
| $Ir^{193m}$ | | 11·9 days | | 80 | |
| $Pt^{195m}$ | | 3·5 days | 4·1 ± 0·1 days | 31,100,130 | 69 ± 10 |
| $Au^{197m}$ | 4 | 7·2 sec | 7·4 ± 0·2 sec | 130,280 | 70 ± 10, 270 ± 10 |
| $Hg^{199m}$ | 4 | 42 min | | 160,370 | 74 ± 10, 155 ± 10, 390 ± 10 |
| $Pb^{204m}$ | | 67 min | | 290,375,622,899, 912 | |

* Isomers of stable nuclides only, with half-lives greater than 1 sec.
† Includes photons with high internal conversion coefficients.[1–9]

missed, probably because of insufficient sensitivity of recording in that energy region with the spectrometer setting used.

It is possible to calculate approximate cross sections for reaction of this Bremsstrahlung with the element of interest. With $3 \times 10^{13}$ assumed as the flux, of photons of all energies, the calculated cross sections range from $4 \times 10^{-10}$ mB for molybdenum to $2 \times 10^{-5}$ mB for indium. It should be noted that these calculated values would be considerably larger if one included the factor of inefficiency of counting due to internal conversion and self-absorption, and the fact that the flux includes many photons below the photoactivation threshold.

*Neutron activation*

Activities generated from four of the elements, arsenic, bromine, iodine, and molybdenum, resemble those ordinarily produced by neutron addition, as shown in Table 3. The experimentally obtained activity from molybdenum has a longer half-life than that

TABLE 3. Comparison with nuclides from neutron addition

| Element | Neutron addition species | $t_{\frac{1}{2}}$ | $\gamma$-energy (keV) | $t_{\frac{1}{2}}$ found | $\gamma$-energy found |
|---|---|---|---|---|---|
| As | $As^{76}$ | 16 hr | 560 | 30 ± 15 hr | 550 |
| Br | $Br^{80m}$ | 4·5 hr | 37, 48 | | |
| | $Br^{80}$ | 17·6 min | 510*, 620 | 18 ± 4 min | 530,630 |
| | $Br^{82}$ | 36 hr | Several | | |
| I | $I^{127}$ | 25 min | 450 | 26 ± 2 min | 450 |
| Mo | $Mo^{101}$ | 14 min | 150, 190, 960 | 22 ± 2 min | 210,310 |

* Annihilation radiation.

of $Mo^{101}$ because of the generated activity of the 15 min $Tc^{101}$ daughter.

The only ways by which neutrons can be formed from 3 MeV electrons or photons are the following:

$$_5Be^9 + \gamma \rightarrow 2\,_2He^4 + {}_0n^1$$

$$_1H^2 + \gamma \rightarrow {}_1H^1 + {}_0n^1.$$

The reactions are endothermic by 1·67 and 2·23 MeV respectively, so photons of at least these energies are required. The most obvious source of neutrons in these experiments is the natural deuterium in the thin sheet of cooling water that flows past the target. The neutrons from this thin source must be essentially unmoderated, so they are in an energy distribution from thermal energies up to 0·4 MeV, skewed strongly in favor of the lower energies. Therefore activation can occur by means of epithermal and faster neutrons as well as slow neutrons. It is then pertinent to inquire how neutron activation can occur with these elements and not detectably with any others under these conditions.

To do this, it was first determined whether the amounts of activity generated in arsenic, bromine, iodine and molybdenum were consistent with their cross sections for neutron capture. This in turn required a determination of the neutron flux. Examination of thermal neutron capture cross sections and half-lives disclosed that under practical conditions manganese and vanadium would provide the highest sensitivity; their use gave observed thermal neutron fluxes of 3·4 and 4·6 neutrons/cm² sec, respectively. Use of similar data plus the observed activities with arsenic, bromine, molybdenum and iodine gave apparent neutron fluxes of 106, 68, 75, and 98, respectively. Obviously, these are far too high, and the explanation lies in the contribution of epithermal or fast neutron capture processes.[10] That no other activities resulting from this type of reaction were detected merely means that the combination of product half-life and cross section for this neutron-energy spectrum was adequate for only these elements.

## APPLICATIONS OF PHOTOACTIVATION

*Analytical*

The most obvious application is in elemental analysis, as a supplement to instrumental neutron activation analysis.[11] Thus, direct irradiation followed by gamma-ray spectrometry can be used for quantitative estimation of several of the elements, with rather good sensitivity. Data from Table 1 are re-cast in Table 4 in terms of sensitivity. It is assumed that a 30 ml organic or aqueous sample is irradiated for 1 hr (less if saturation is reached more quickly), and counted at irradiation end for counting periods of optimum length up to 1 hr. Sensitivity values are then the concentration of the element determinable to ± 10 per cent standard deviation. It is assumed that background counting rate is 300 c.p.m. determined accurately in a long count.

It is clear that the method is potentially useful for Se, Sr, Y, Rh, Ag, Cd, In, Ba, Lu, Hf, Ir, Pt, Au and Hg. While the method is

TABLE 4. Sensitivity of photoactivation analysis

| Element | Required* activity at irradiation end (c.p.m.) | Specific† activity in 1 hr irradiation (c.p.m./g) | Minimum‡ weight determinable (mg) | Minimum concentration determinable (p.p.m.) |
|---|---|---|---|---|
| Se‡ | 460 | 140,000 | 3·3 | 110 |
| Sr | 32 | 10,000 | 3·2 | 110 |
| Y | 460 | 6000 | 77 | 2600 |
| Rh | 50 | 800 | 62 | 2100 |
| Ag | 300 | 100,000 | 3·0 | 100 |
| Cd | 64 | 65,000 | 1·0 | 33 |
| In | 32 | 150,000 | 0·21 | 7·0 |
| Sn | 32 | 10 | 3200 | 110,000 |
| Ba | 160 | 800 | 200 | 6700 |
| Er | 3000 | 300,000 | 10 | 330 |
| Lu | 32 | 5000 | 6·4 | 210 |
| Hf | 440 | 4,000,000 | 0·11 | 3·7 |
| Ir | 1300 | 1,000,000 | 1·3 | 43 |
| Pt | 32 | 500 | 64 | 2100 |
| Au | 1000 | 400,000 | 2·5 | 83 |
| Hg | 74 | 2000 | 37 | 1200 |

* For 10 per cent standard deviation in sample count.
† From Table 1. Data for 1–5 g samples divided by two to approximate activity from 30 ml sample.
‡ These numbers may be cut by 50–70 per cent if a smaller sample is used.

less sensitive than neutron activation analysis with the same accelerator by factors from 1 to 1000 for all of these elements[11] except platinum for which it appears to be slightly more sensitive, it has potential usefulness in being more specific, so that interferences causing difficulty in neutron activation analysis may often be eliminated.

It may be noticed that none of the elements between $Z = 5$ and $Z = 32$ can interfere, since they neither form isomers with suitably long half-life nor do they have sufficient fast neutron cross section to undergo the n, $\gamma$ reaction detectably. It is pertinent to point out, however, that for Se, Y, Er, Hf, Ir and Au, for which the method is quite sensitive, fast transfer methods are required to move the sample into the counter after irradiation.

The sensitivity is affected considerably by the sample size. For example, barium in a 5 ml vial gave a specific activity three times that in a 30 ml vial. For silver the ratio was slightly less than two. Obviously, the ratio is affected greatly by photon energy because of sample self-absorption and counter efficiency. For concentration sensitivity a 30 ml sample size is considered about optimum, but even this would have to be modified for those elements giving isomers with low photon energies.

It is conceivable that interferences might occur with aqueous or organic samples by moderation of the fast neutrons to give a higher thermal flux than the 4–5 neutrons/cm$^2$ sec observed. This was tested by irradiation of a 30 ml sample of 50% manganous nitrate solution. Activity produced corresponded to that expected from a flux of 56 neutrons/cm$^2$ sec, a ten-fold increase due to the presence of the water.

*Checking of beam energy*

For a given position of an indium foil, the specific activity induced is a sensitive function of electron beam energy. Thus, for a given experimental arrangement in equal irradiation time, it was found that the specific activity at 3 MeV is 2·2 times that at 2·5 MeV. This corresponds to a change at 3 MeV of 11 per cent per 0·1 MeV. The actual increment is probably greater since

the curve of specific activity vs. beam energy is concave upward.

The fact that counting rate is a sensitive function of beam energy suggests the use of photoactivation as a method for determining beam energy. Where the electron beam itself cannot be utilized with the more accurate partial absorption method[12], photoactivation might have particular usefulness. The method would consist in obtaining the curve of counting rate vs. beam energy, and determinations could then be made subsequently by merely observing counting rate for an identical irradiation arrangement. Irradiation to about 1 Mrad should provide sufficient accuracy to determine beam energy to $\pm$20,000 V with little difficulty. It is more useful than the deuterium threshold method in that (1) the determination is made at 3·0 MeV, and no extrapolations from 2·23 MeV is required, (2) extreme voltage stability is not required, since one is dealing with an average value and not a threshold, and (3) a single determination is sufficient once the standard curve is established.

*Dosimetry*

The simplicity of measurement of indium activity suggests its use as a dosimeter for Bremsstrahlung radiation. To test its relative response to Bremsstrahlung of different energy distribution, indium foils were wrapped around small vials of ceric solution and irradiated with doses of several megarads, as measured by loss in ceric ion. Specific activity of the foil vs. electron-beam energy is plotted in Fig. 3 for doses of 1 Mrad (corrected for zero decay during irradiation). It is evident that the specific activity for a given dose is rather sensitive to Bremsstrahlung energy. Thus, its use would have to be restricted to dosimetry with Bremsstrahlung produced in standard fashion at an accurately known beam energy with little energy degradation by intervening materials.

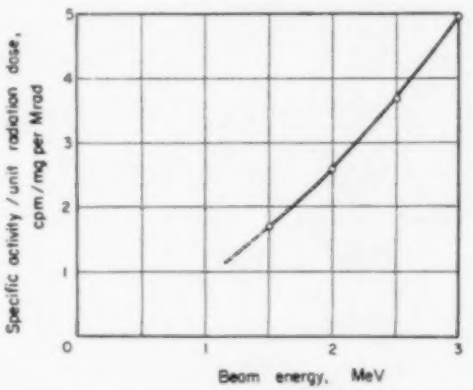


FIG. 3. Dependence of indium dosimeter for Bremsstrahlung on energy of bombarding beam.

*Acknowledgment*—The authors are grateful to DR. VINCENT P. GUINN for the calculations on Bremsstrahlung flux and energy distribution.

## REFERENCES

1. WAGNER C. D. and CAMPANILE V. A. *Nucleonics* **17** (7), 99 (1959).
2. GIDEON D. N., MILLER W. C. and WALDMAN B. *Phys. Rev.* **75,** 329 (1949).
3. WIEDENBECK M. L. *Phys. Rev.* **68,** 237 (1945).
4. WIEDENBECK M. L. *Phys. Rev.* **68,** 1 (1945).
5. WIEDENBECK M. L. *Phys. Rev.* **67,** 267 (1945).
6. FELDMEIER J. R. and COLLINS G. B. *Phys. Rev.* **59,** 937 (1941).
7. DUNWORTH J. V. and PONTECORVO B. *Proc. Camb. phil. Soc.* **43,** 123 (1947).
8. PONTECORVO B. and LAZARD A. *C.R. Acad. Sci., Paris* **208,** 99 (1938).
9. DUNWORTH J. V. and PONTECORVO B. *Proc. Camb. phil. Soc.* **43,** 429 (1947).
10. HUGHES D. J. and SCHWARTZ R. B. *Neutron Cross-Sections,* BNL-325, 2nd Ed. Brookhaven National Laboratory, New York, 1958.
11. GUINN V. P. and WAGNER C. D. *Analyt. Chem.* **32,** 317 (1960).
12. CAMPANILE V. A. and WAGNER C. D. *Nucleonics* **17** (7), 74 (1959).

International Journal of Applied Radiation and Isotopes, 1961, Vol. 11, pp. 38–42. Pergamon Press Ltd. Printed in Northern Ireland

# Sources of Quasi-Monoenergetic Gamma Radiation

A. H. W. ATEN, Jr. and M. G. J. HEIJENBROK
Institute for Nuclear Physics Research, Amsterdam, Netherlands

(*Received* 22 *December* 1960)

A series of approximately monoenergetic $\gamma$-ray sources is discussed. $Co^{60}$ is satisfactory as such, but $Cs^{137}$, $Se^{75}$ and $Eu^{155}$ can be made more nearly monoenergetic if the material is surrounded by suitable filters.

DES SOURCES DE RAYONNEMENT GAMMA QUASI-MONOENERGETIQUE

On discute une série de sources de rayons $\gamma$ à peu près monoénergétiques. Le $Co^{60}$ suffit tel qu'il est, mais on peut rendre le $Cs^{137}$, le $Se^{75}$ et l'$Eu^{155}$ plus prochement mono-énergétiques en entourant le matériel de filtres convenables.

ИСТОЧНИКИ КВАЗИ-МОНОЭНЕРГЕТИЧЕСКОГО ГАММА-ИЗЛУЧЕНИЯ

Рассматривается ряд приблизительно монознергетических источников $\gamma$-лучей. $Co^{60}$ является в этом отношении удовлетворительным сам по себе, но $Cs^{137}$, $Se^{75}$ и $Eu^{155}$ можно сделать более монознергетическими, окружив их соответствующими фильтрами.

GAMMA-QUELLEN MIT QUASI-MONOENERGETISCHER STRAHLUNG

Eine Reihe von annähernd monoenergetischen $\gamma$-Strahlenquellen wird besprochen. Co-60 ist diesem Sinne zufriedenstellend, jedoch Cs-137, Si-75 und Eu-155 können noch besser fast monoenergetisch gemacht werden, indem das Material mit geeigneten Filtern versehen wird.

## INTRODUCTION

For different purposes, both connected with thickness measurements by means of absorption and with the calibration of radiation measuring instruments, it is of importance to have available $\gamma$-ray sources emitting approximately monoenergetic radiations of various energies, without requiring the energy of all the photons of one source to be exactly the same. There are, however, two points which are quite essential: (1) the energies available should cover as large a range as possible, and (2) the half-lives of the nuclides used should be as long as possible.

In the range of X-ray energies, sources of this kind can be constructed from $\beta$-emitters with suitable absorbers.[1,2] These combinations, however, have a very low X-ray quantum-yield per $\beta$-particle. As in most countries, special permits are required for the use of radioactive sources outside research laboratories, a high quantum-yield per millicurie resulting in a small total activity and correspondingly small danger of radioactive contamination is likely to facilitate in obtaining the required permits. From $\beta$-sources electromagnetic radiation with energies above 0·1 MeV can be obtained only as Bremsstrahlung which is far from monoenergetic.

It is therefore proposed to base a series of quasi-monoenergetic standard gamma-sources on the following nuclides, all of which are already being used widely as radiation sources at present: (1) $Co^{60}$, (2) $Cs^{137}$, (3) $Se^{75}$, and (4) $Eu^{155}$.

In the cases of $Co^{60}$ and $Cs^{137}$, half-lives are so long and known with such a high

VOL. 11 1961

accuracy that these nuclides, once calibrated, can be used as such a source for periods of the order of 1 year for most purposes. The half-life of $Eu^{155}$ (1·7 years) is long enough to make the nuclide useful as a $\gamma$-radiation source for at least a few years, but the published values[3] indicate that the accuracy of the half-life is not at present sufficiently good to allow an absolute calibration to be used for more than a few months at the utmost if really accurate knowledge of the strength of the radiation field is desired. The half-life of $Se^{75}$ is the least favourable of the whole series (120 days). Here again the disagreement between observed values of the half-life[3] is such that a single calibration of the specific $\gamma$-ray emission can be used for a few months only if an accuracy of a few per cent is required. This means that although $Se^{75}$ and $Eu^{155}$ $\gamma$-sources have a much longer useful life than sources of $Hg^{203}$—which nuclide is now in frequent use as a source of low-energy $\gamma$-rays—calibrations of the three nuclides at present retain their validity for periods of roughly equal lengths. It should not, however, be very difficult to obtain values for the half-lives of $Se^{75}$ and $Eu^{155}$ of much greater accuracy than those at present available.

## DISCUSSION OF INDIVIDUAL SOURCES

(1) $Co^{60}$. The two $\gamma$-rays of 1·17 MeV and 1·33 MeV are so nearly equal, that for most purposes the radiation may be considered to be monochromatic with an energy of 1·25 MeV.

(2) $Cs^{137}$. Most measuring devices register mainly the 0·661 $\gamma$-radiation. However, the K-radiation of 33 keV, which furnishes 8·5 photons per 100 $\gamma$-photons[4,5], may contribute quite appreciably to the response of an instrument the sensitivity of which decreases sharply with increasing energy. If, however, the $Cs^{137}$ sample is surrounded by a cylinder of about 200 mg Sn/cm² thickness the $Cs^{137}$ K-radiation is absorbed to such a degree as to become negligible as shown in Fig. 1. That this must be the case is easily seen from the graph published by WAPSTRA *et al*[5]. It is by no means essential to use tin for the filter, although this metal is specially suitable as it has an exceptionally low value for the half-thickness at 33 keV. Almost any material may be used which does not have too low a value of Z. However, if one uses a lead filter, or a filter made of an element with a similar value of Z, some K-X-rays of the filter material appear in the radiation emitted.

Most samples of $Cs^{137}$ contain $Cs^{134}$ as an impurity. This contamination does not constitute an objection against the use of such material as a quasi-monoenergetic $\gamma$-source, as the main $\gamma$-lines of $Cs^{134}$ have energies of 0·605 and 0·796 MeV quite near to the $\gamma$-line of $Cs^{137}$. The half-life of $Cs^{134}$ is, however, much shorter (2 years) than that of $Cs^{137}$ which complicates decay corrections for preparations containing too much of the former nuclide. The Radiochemical Centre, Amersham offers material containing less than 2 per cent of $Cs^{134}$ for which decay

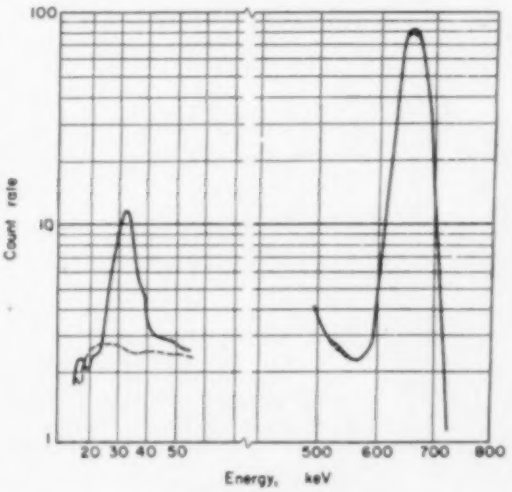


FIG. 1. X-rays and $\gamma$-rays of $Cs^{137}$ measured in a scintillation spectrometer. Full line spectrum measured through aluminium only, dotted line measured through aluminium surrounded by 212 mg Sn/cm². (Note different energy scales for low-energy and high-energy range!)

corrections do not offer any difficulty. It may be mentioned that the presence of more than about 1 per cent of $Cs^{134}$ in $Cs^{137}$ can be recognized in the scintillation spectrum as a shoulder on the high-energy slope of the 0·661 peak.

(3) $Se^{75}$. This nuclide has the advantage of being a reactor product and as such being easily available with a reasonably high specific activity. Although the $\gamma$-spectrum is extremely complicated, it consists essentially of three groups of $\gamma$-rays, one group around 135 keV, one around 270 keV and one $\gamma$-line of lower intensity at 402 keV. This is shown in Fig. 2. From the graph in the book by WAPSTRA *et al.*[5] it is evident, that the 135 keV group can be almost entirely eliminated by a suitable choice of absorber without much effect on the intensity of the other groups. This is easily done by means of an absorber consisting of about 7 g Sn/cm². Such a cylinder has, however, the disadvantage of being fairly bulky. For this reason it

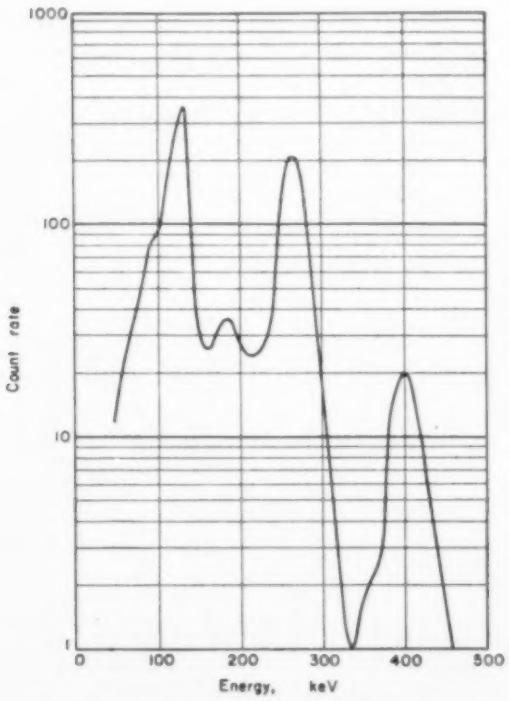


FIG. 2. Scintillation spectrum of $Se^{75}$ filtered through aluminium only.

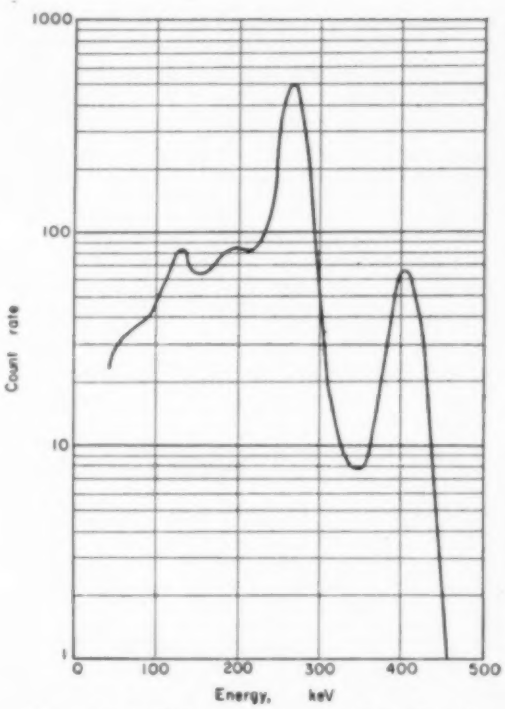


FIG. 3. Scintillation spectrum of $Se^{75}$ filtered through aluminium surrounded by a double filter consisting of 1·6 g Pb/cm² (inside) and 1·5g Sn/cm² (outside).

is preferable to absorb most of the photons of the 135 keV group in lead. On the other hand this brings in the complication of the production of Pb X-rays. Under these conditions the outer part of the absorber must consist of a lighter element, and for this tin is again a suitable choice, as its half thickness for the Pb X-rays is quite small. Thus $Se^{75}$ surrounded by two cylinders, an inner one made of lead and an outer one made of tin, provides a $\gamma$-source emitting two groups of $\gamma$-rays, one group around 270 keV and one group at 402 keV. For many purposes such a source will be very useful. The thickness of the two cylinders will be determined by the fraction of the 135 keV group which may be allowed to leave the source. Figure 3 shows the scintillation spectrum through 1·6 g Pb/cm² surrounded by 1·5 g Sn/cm². The intensity of 135 keV group has been very much reduced.

(4) $Eu^{155}$. This nuclide has the advantage of a fairly long half-life, and it is easily obtained in great strength. Again the $\gamma$-ray spectrum is very complicated but it consists mainly of an 87 keV and a 105 keV line, the latter having a somewhat lower intensity than the former (intensity ratio = 0·62).

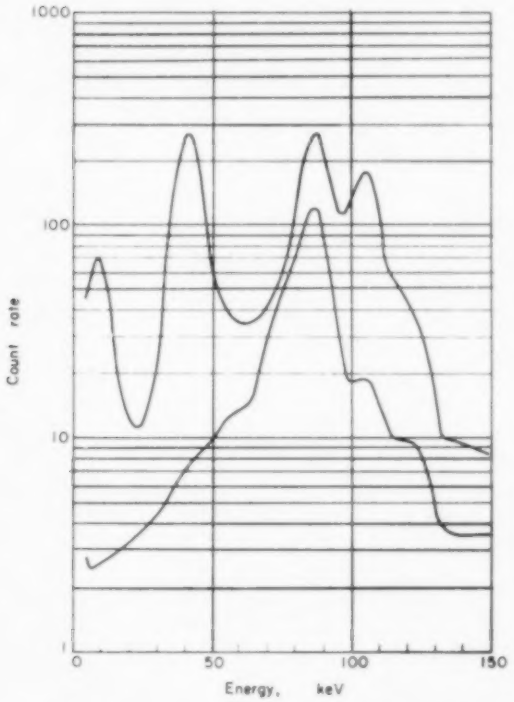


FIG. 4. Scintillation spectrum of $Eu^{155}$ filtered through aluminium only (upper graph) and through aluminium surrounded by 0·49 g Pb/cm² (lower graph). (The counts registered at the high-energy edge of the Figure are due to a contamination with $Eu^{152}$.)

In combination with these lines we find a strong K-line around 42 keV (Fig. 4). This complicated spectrum can be greatly simplified by the application of a lead filter of about 500 mg Pb/cm². This thickness provides a practically complete absorption of the 42 keV group. Of the 87 keV radiation about one half passes through the filter, as 87 keV is just below the absorption edge in lead (88 keV). Of the 105 keV line, by far the larger part is absorbed, although a faint trace of this line can still be recognized in the filtered radiation. The absorption of the 105 keV radiation results, however, in the formation of a fairly strong K-radiation of lead. The energy of this radiation (about 74 keV) is so near to that of the 87 keV line that on the whole the filtered spectrum is nearly monoenergetic, with an energy around 83 keV.

In the use of $Eu^{155}$, a special complication can arise from the presence of the 12·5 year $Eu^{152}$. $Eu^{155}$ is prepared by irradiation of samariumoxide in a reactor, and $Eu^{155}$, arising from the $\beta$-decay of $Sm^{155}$ formed by the $Sm^{154}$ (n,$\gamma$) process, is the only long-lived activity present, apart from the 80 years $Sm^{151}$. $Sm^{151}$ hardly contributes to the $\gamma$-radiation, due to its long half-life and to the low energy and low intensity of its $\gamma$-rays. However, if during the neutron irradiation the samarium contains traces of europium, an appreciable activity of $Eu^{152}$ is formed due to the fact that $Eu^{151}$ has a much higher cross section for neutron capture than $Sm^{154}$. ($\sigma$ $Eu^{151}$ for total production of 12·5 year $Eu^{152}$ = 7550b, $\sigma$ $Sm^{154}$ = 5·5b). This complication is rendered specially serious by the fact that the purification method normally used for samarium, i.e. reduction to amalgam, does not separate this element from europium. Nor is it easy to separate the two elements by means of ion-exchange methods because of their neighbouring positions in the periodic system, although elution with a solution of α-hydroxybutyric acid at a carefully adjusted pH is quite satisfactory for this purpose. An efficient method to eliminate traces of europium from samarium samples is of great importance if it is desired to use $Eu^{155}$ as a quasi-monoenergetic $\gamma$-source.

*Acknowledgments*—This investigation was performed as part of the programme of the Foundation for Fundamental Research of Matter (F.O.M.) with financial support of the Organization for Pure Research (Z.W.O.). Thanks are also due to MISS H. J. KAPTEIJN and to MR. P. J. WEIJERS for help with the measurements.

## REFERENCES

1. Cameron J. F. and Rhodes J. R. *Conference on the Use of Radioisotopes in the Physical Sciences and Industry* RICC/14. Copenhagen (1960).
2. Filosofo I., Reiffel L., Stone C. A. and Voyvodic L. *Conference on the Use of Radioisotopes in the Physical Sciences and Industry* RICC/200. Copenhagen (1960).
3. *Nuclear Data Sheets.* National Academy of Sciences, National Research Council, Washington.
4. Block S. *Health Phys.* **1,** 357 (1958).
5. Wapstra A. H., Hijgh G. J. and Van Lieshout R. *Nuclear Spectroscopy Tables,* pp. 67, 133. North Holland Publishing Co,, Amsterdam (1959).

VOL
11
196

VOL.
11
1961

# technical notes

## Storage Behaviour of Gamma-Irradiated Mangoes

(*First received* 7 *October* 1960 *and in revised form* 14 *November* 1960)

BROWNELL *et al.*[1] irradiated bananas with 10,000 r of X-rays and found that the rate of softening was decreased. According to HANNAN[2] a dose of 10,000 r of X-rays is sufficient to delay appreciably the ripening of hard green bananas and under-ripe tomatoes. Data obtained in an investigation where Alphonso mangoes were treated with 12,000 rad of gamma rays are presented in this note.

### Material and methods

Fully grown and green Alphonso mangoes were picked from an orchard in the suburbs of Bombay and were packaged in polyethylene (200 gauge) bags (6 × 8 in.) individually, each bag having twelve respiration vents. The diameter of each respiration vent was $\frac{1}{8}$ in. Half of the packaged fruits were irradiated with 12,000 rad of $Co^{60}$ gamma rays on the day of picking. The dose rate was 120 rad/min.

Reducing and non-reducing sugars were estimated by the Lane Eynon method.[3] For the estimation of ascorbic acid, mango pulp was macerated in an extraction mixture containing 1 per cent $HPO_3$, 1 per cent $(NH_4)_2SO_4$ and 4 per cent $(COOH)_2$. Subsequently the filtered solution was titrated against a standard solution of 2:6-dichlorophenol indophenol. Percentage moisture was determined by drying the mango pulp at 80°C for 5 hr.

### Data and discussion

The physiological losses in weight (i.e. losses in weight due to respiration and transpiration) were lower in irradiated mangoes as compared to the controls (Table 1). The data with regard to percentage of waste are presented in Table 2. Irradiation appeared to reduce the percentage of waste. HANNAN[2] found a reduction in wastage in under-ripe tomatoes irradiated with 10,000 r of X-rays. On 10 per cent wastage basis, the storage life of irradiated mangoes was about 24 days as compared to approximately 16 days for the controls when stored at room temperature (23–39°C; R.H., 60–75 per cent).

TABLE 1. Physiological losses in weight* in control and irradiated mangoes stored at 23–39°C (R.H., 60–75 per cent)

| Treatment | Percentage losses after | | | | | |
|---|---|---|---|---|---|---|
| | 4 days | 8 days | 12 days | 16 days | 20 days | 24 days |
| | Set No. 1 | | | | | |
| Control | 1·4 | 2·8 | 4·2 | 5·2 | 5·9 | 7·2 |
| Irradiated | 1·0 | 1·9 | 2·8 | 3·3 | 3·9 | 5·0 |
| | Set No. 2 | | | | | |
| Control | 1·6 | 3·0 | 4·4 | 5·3 | 6·2 | 7·7 |
| Irradiated | 1·1 | 1·4 | 2·6 | 3·1 | 3·6 | 4·8 |

* Means of two determinations.

The retention of moisture appeared to be greater in the treated fruits (Table 3, Fig. 1). As a result of irradiation, part of the ascorbic acid content of mangoes was destroyed (Table 3, Fig. 1). CLARKE[4] observed a reduction in the ascorbic acid content of $\gamma$-irradiated strawberries.

TABLE 2. Wastage in control and irradiated mangoes stored at 23–39°C (R.H., 60–75 per cent)

| Treatment | No. of mangoes | Percentage wastage after | | | | | | |
|---|---|---|---|---|---|---|---|---|
| | | 4 days | 8 days | 12 days | 16 days | 20 days | 24 days | 28 days |
| | Set No. 1 | | | | | | | |
| Control | 20 | 0·0 | 0·0 | 5·0 | 10·0 | 15·0 | 20·0 | 35·0 |
| Irradiated | 20 | 0·0 | 0·0 | 0·0 | 0·0 | 5·0 | 10·0 | 20·0 |
| | Set No. 2 | | | | | | | |
| Control | 20 | 0·0 | 0·0 | 0·0 | 5·0 | 15·0 | 25·0 | 40·0 |
| Irradiated | 20 | 0·0 | 0·0 | 0·0 | 0·0 | 0·0 | 5·0 | 15·0 |

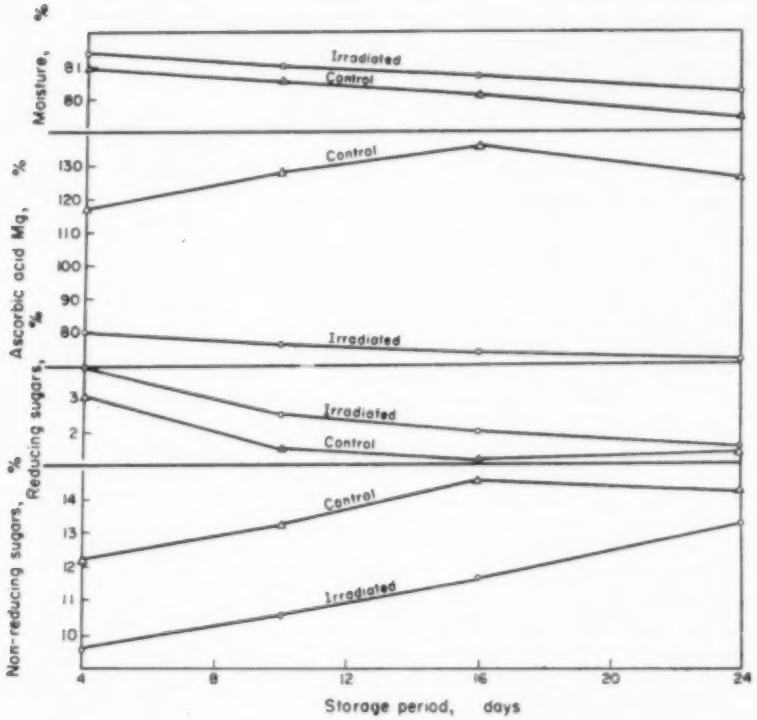


FIG. 1. Chemical changes in control and irradiated mangoes stored at 23–39°C (R.H., 60–75 per cent). Data regarding ascorbic acid, reducing sugars and non-reducing sugars have been calculated on initial moisture content basis.

TABLE 3. Chemical changes* in control and irradiated mangoes stored at 23–39°C (R.H., 60–75 per cent)

| Storage period (days) | Control | | | | Irradiated | | | |
|---|---|---|---|---|---|---|---|---|
| | Moisture (%) | Ascorbic acid (mg. %) | Reducing sugars (%) | Non-reducing sugars (%) | Moisture (%) | Ascorbic acid (mg. %) | Reducing sugars (%) | Non-reducing sugars (%) |
| 4 | 80·9 | 117 | 3·1 | 12·2 | 81·4 | 80 | 3·9 | 9·6 |
| 10 | 80·5 | 128 | 1·5 | 13·2 | 81·0 | 76 | 2·5 | 10·5 |
| 16 | 80·1 | 136 | 1·1 | 14·5 | 80·7 | 73 | 2·0 | 11·6 |
| 24 | 79·4 | 126 | 1·3 | 14·2 | 80·2 | 71 | 1·4 | 13·2 |

* Estimations were made on composite samples of two fruits.

Contrary to reducing sugars, the content of non-reducing sugars was higher in the controls (Table 3, Fig. 1). This shows that the controls ripened at a faster rate as compared to the irradiated mangoes. This was confirmed also by the visual examination of the change in skin colour of the fruits, from green through greenish-red to yellow, which took place faster in controls.

A panel of judges did not find any adverse effect on the colour, taste, flavour and texture of irradiated fruits.

P. B. MATHUR
N. F. LEWIS

*Biology Division*
*A.E.E., Trombay*
*Byculla, Bombay 8, India*

**References**

1. BROWNELL L. E. *et al. Utilization of the Gross Fission Products.* Engineering Research Institute, University of Michigan Progress Report Nos. 1 and 2. (1951 and 1952).
2. HANNAN R. S. *Food Investigation Special Report No.* 61. D.S.I.R., H. M. Stationery Office, London (1955).
3. LEPPER H. A. *Official Methods of Analysis* p. 506. Assoc. Official. Agri. Chem., Washington, D.C. (1950).
4. CLARKE I. D. *Int. J. appl. Rad. Isotopes* **6**, 175 (1959).

VOL. 11 1961

## The Radiation-Induced Graft Copolymerization of 4-Vinyl Pyridine to Terylene

(*Received* 16 *November* 1960)

THIS work was carried out to investigate the mechanism of radiation-induced grafting to Terylene and the properties of the copolymer so produced.

Of the various methods[1,2] of grafting tried, it was found that that of irradiation of dry fabric in air, followed by reaction with the monomer in aqueous solution in the absence of oxygen, gave the best results.

### Experimental

*Materials*

Terylene filament yarn fabric (100 per cent), finish-free, was supplied by I.C.I. All Terylene used was Soxhlet extracted with methanol for 24 hr to remove any material adhering to the surface. 4-Vinyl pyridine (ex Aldrich Chemical Co.) was distilled under vacuum and kept under nitrogen at −5°C until required for use. A fresh quantity was distilled every few days.

*Irradiation technique and grafting procedure*

The Terylene fabric was irradiated in air by $\gamma$-rays from a 120 curie $Co^{60}$ source at a dose rate of $10^5$ rad/hr. Approximately 0·2 g of fabric was weighed accurately after irradiation, introduced into a 25 ml flask and covered with freshly prepared 2% aqueous 4-vinyl pyridine such that the liquor:fabric ratio was 100:0 by weight. The clear space above the solution was evacuated with the solution deaerated by a standard procedure on a vacuum line. The flask was then sealed and placed in an oil bath, thermostatically controlled at an appropriate temperature, for a specified time. Concurrently, the same procedure was followed using unirradiated fabric in order to determine the extent of reaction taking place in the absence of radiation effects.

At the end of the reaction time the flask was cooled rapidly in cold water and broken open. Two millilitres of the solution were diluted to a predetermined extent in 0·01 N $H_2SO_4$ and the optical density measured on a Hilger u.v. spectrophotometer at 265 m$\mu$. Previous calibration with 4-vinyl pyridine gave an extinction coefficient of $1{\cdot}636 \times 10^4$ thus permitting calculation of the molarity of the solution with respect to 4-vinyl pyridine.

At the time of introduction of the 2 % solution into the flask containing the fabric, a sample of the solution was diluted and its optical density measured.

These two measurements enabled the decrease of 4-vinyl pyridine in the reactant solution to be calculated. This figure should be a measure of the graft copolymer plus the homopolymer formed in the solution.

The fabric was removed from the solution, washed in cold running water for 15 min, digested with 1 % acetic acid, which was heated from room temperature to about 85°C over 1 hr to remove any non-grafted adhering homopolymer and finally washed in cold running water. The fabric was then dried in a vacuum oven at 50°C for 1 hr and weighed. The increase in weight was corrected to give the increase per 0·20 g of fabric.

The results indicated that the homopolymer formed in the solution over the irradiated terylene was of the same order as that formed in the solution over the unirradiated Terylene.

### Results

Graphs were plotted of grammes of polymer grafted per 0·20 g of fabric against time of reaction in hours, for the total graft obtained from the irradiated Terylene experiments and for the graft obtained on unirradiated Terylene. Subtraction of the latter ordinates from the former gave a graph of the actual graft polymer due to the effect of radiation.

Figure 1 shows the effect of temperature variation on the rate of grafting at a dose of 1·5 Mrad. It is seen that, as the temperature of polymerization increases, the graft due to irradiation decreases. This can be explained as being the resultant of two processes. As

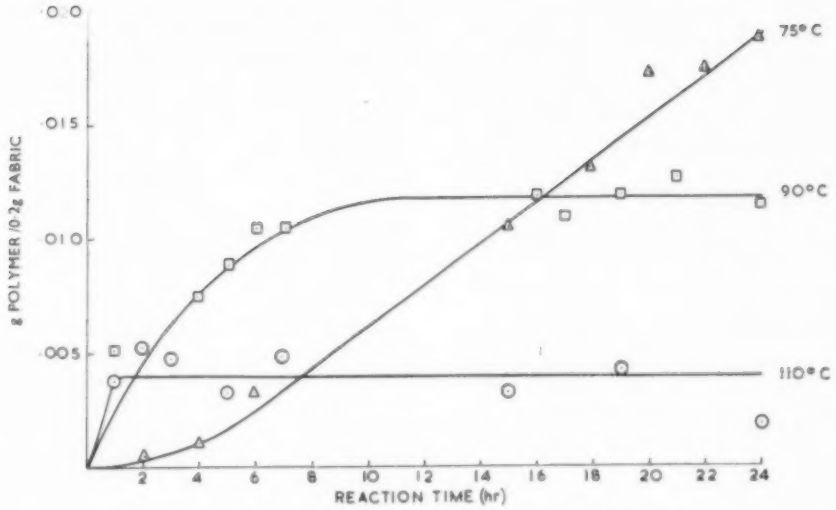


FIG. 1. Effect of temperature on the rate of grafting of 4-vinyl pyridine to Terylene. (Dose 1·5 Mrad.)

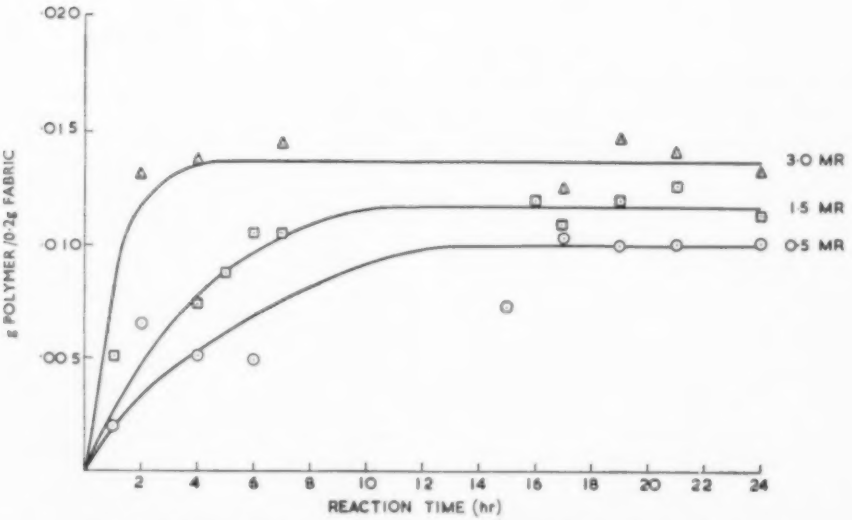


FIG. 2. Effect of dose on the rate of grafting of 4-vinyl pyridine to Terylene. (Temperature 90°C).

the temperature is increased, the rate of decomposition of peroxidic material to radicals increases. On the other hand, unless the monomer can diffuse rapidly to these radical sites, they will react possibly as shown:

$$ROOR \rightarrow R\dot{O} + \dot{O}R \rightarrow RC = O + ROH.$$

Thus, if the radical sites are lost due to "lack" of monomer in their vicinity, decreased grafting will result.

Figure 2 shows the effect of variation of total dose given to the fibre on the amount grafted. This latter increases with the total dose due to the increase in the concentration of peroxidic and free-radical groups formed by increasing doses of radiation.

### Subsequent experiments

Several experiments were carried out on the grafted Terylene, (a) to determine dyeability and (b) to produce an antistatic finish.

Dyeing was carried out using acid wool dyes at a concentration of 0·05 g/l containing 0·1 % acetic acid. It was found that Terylene, having grafted onto it at least 10 per cent wt/wt of 4-vinyl pyridine, had a fair acceptability for these dyes giving pale shades which were fast to hot soap and water scrubbing. At a graft of about 17 per cent, the depth of colour was very much greater.

An antistatic finish was obtained by quaternizing the nitrogen atom in the grafted poly(4-vinyl pyridine) by treatment with a 5 % methanolic solution of dimethyl sulphate. By this method, up to 30 per cent of the graft could be quaternized[3] to form an antistatic surface coating, fast to hot, soapy water scrubbing, which reduced the surface resistance from $10^{13}\ \Omega$ to $10^{9}\ \Omega/cm^2$, which latter figure is adequate for removal of static.

### Polyacrilonatile and polypropylene

4-Vinyl pyridine was grafted onto these two polymers using similar conditions to the Terylene grafting. With doses of 1 Mrad, 20 per cent graft was obtained on polyacrylonitrile, and greater than 100 per cent graft on polypropylene. Needless to say, the dyeability of these grafted materials was greatly increased with respect to acid dyes. Examination of the dyed grafted fibres under a microscope revealed that the dyeing was actually ring dyeing.

M. R. Houlton
J. K. Thomas

*Isotope Research Division (A.E.R.E.) Wantage Research Laboratory Wantage, Berks.*

### References

1. Thomas J. K. and Roberts R. *I.A.E.A.* Warsaw, CW/IIB/86 (Sept. 1959).
2. Thomas J. K. and Roberts R. *J. Soc. Dy. Col.* **76,** 342 (1960).
3. Richards L. M. U.S. Pat. 2487829.

## A Simple Device for the Rapid Routine Liberation and Trapping of $C^{14}O_2$ for Scintillation Counting*

(*Received* 20 *November* 1960)

When $C^{14}$ labeled compounds are utilized in metabolic studies, it is frequently desirable to examine the $C^{14}O_2$ which is often one of the end products. Since it exists chiefly as bicarbonate or carbonate in tissues and fluids, it must be liberated by acidification, and trapped. Furthermore, other biological compounds are often degraded to $CO_2$ in the process of ascertaining the position or intensity of labeling.

When liquid scintillation counting is employed, the production, trapping and counting of this gas is often a slow cumbersome process requiring elaborate and expensive equipment. The gas is usually extracted and collected by means of a van Slyke apparatus, and then transferred to an alkaline trapping medium which must be compatible with the relatively non-polar solvent of the scintillation solution. These procedures require extreme care and experience, and are not practical for the routine examination of large numbers of samples.

The simple device (see Fig. 1) was designed to allow quantitative production of $CO_2$, and its simultaneous entrapment within the vial used for scintillation counting, in one rapid step. It was constructed in minutes of inexpensive commonly available laboratory materials.

### Materials

"Pyrex" glass "Y": 12 mm o.d.; #2 one-hole rubber stopper; #4 one-hole rubber stopper; self-sealing puncturable rubber stopper; 40 ml sample bottle; 5 dram scintillation vial.

### Procedure

The stem of the "Y" was cut to a length of $\frac{1}{2}$ in. by means of a glass cutting disc, and the self-sealing puncturable rubber stopper was inserted. The limbs of the "Y" were inserted into the one-hole rubber stoppers.

The #4 stopper was inserted into the 40 ml sample bottle containing the $C^{14}$ specimen. The #2 stopper was inserted into the scintillation vial which contained the alkaline trapping medium. A non-volatile acid was introduced into the sample bottle via hypodermic syringe and needle, inserted through the puncturable stopper and angled into the appropriate limb of the "Y".

The entire unit was then placed in an agitator, straddling a supporting bar, to achieve equilibration. This operation was carried out in a "cold room", as too much $H_2O$ is also absorbed at higher temperatures. Scintillation fluid was then added to the vial, and the sample counted.

### Experimental

Twenty-five milliliters of $H_2O$ or plasma, containing 40,000 d.p.m. and 0·5 mequiv. of $C^{14}O_3^{2-}$ was placed in the sample bottle, 0·5 ml of undiluted Primene 81–R (8N) (Rohm and Haas[1]) was placed

* Financial support was obtained through the kind cooperation of Dr. Frank Ferguson, Jr., Professor and Chairman of the Department of Pharmacology, Albany Medical College.

in the scintillation vial. One milliliter of 85% lactic acid (approximately 10 mequiv.) was introduced into the sample bottle via a syringe and hypodermic needle. The apparatus was agitated at 2°C for 24 hr. Fifteen milliliters scintillation fluid* was added to the vial which was then placed in a scintillation counter.†

**Results**

| Sample No. | Fluid | $C^{14}$ (d.p.m.) | $CO_3^{2-}$ (mequiv.) | c.p.m. | % of predicted |
|---|---|---|---|---|---|
| 1 | $H_2O$ | 40,000 | 0·5 | 26,152 | 99·0 |
| 2 | $H_2O$ | 40,000 | 0·5 | 26,747 | 101·4 |
| 3 | $H_2O$ | 40,000 | 0·5 | 25,877 | 97·9 |
| 4 | Plasma | 40,000 | 0·5 | 25,830 | 97·8 |
| 5 | Plasma | 40,000 | 0·5 | 26,460 | 100·2 |

Note: Counting efficiency—66 per cent.

**Discussion**

The simple and inexpensive device described has been successfully utilized for the routine (lots of 40–50) analyses of $C^{14}$ in the form of $C^{14}O_3^{2-}$. Results are accurate and reproduceable. The units are completely interchangeable, and there is no need for individual calibration. There was no demonstrable difference in the results obtained with aqueous solutions of $C^{14}O_3^{2-}$ when protein was present (plasma).

Five samples of $C^{14}O_3^{2-}$ solutions, 3 aqueous and 2 plasma, containing 40,000 d.p.m. of $C^{14}$, showed quantitative recovery with an average deviation of 1·2 per cent.

If quantitation of the $CO_2$ is desired, the $C^{14}O_2$ can be trapped as $C^{14}O_3^{2-}$ in an aqueous solution containing a known quantity of NaOH. Counting can be done by the methods of STEINBERG,[2,3] by adding the scintillator as an insoluble solid phase, as filaments, beads or crystals. After counting, the aqueous solution can be quantitatively recovered and analyzed.[3]

G. Moss

*Department of Biochemistry*
*Albany Medical College*
*Albany, New York, U.S.A.*

* 1,540 cm³ Toluene (Scintillation grade, Matheson, Coleman and Bell), 54 mg 1,4-bis-2 (5-Phenyloxazolyl)-benzene (POPOP) (Pilot Chemicals, Inc.), 4 gm 2,5-Diphenyloxazole (PPO) (Pilot Chemicals, Inc.).

† Packard "Tricarb" liquid scintillation counter, made available through the cooperation of Mr. Irving Sax, head of Radiological Sciences Group, New York State Department of Health, Division of Laboratories and Research.

**References**

1. OPPERMANN R. A., NYSTROM R. F., NELSON W. O. and BROWN R. E. *Int. J. appl. Rad. Isotopes* **7,** 38 (1959).
2. STEINBERG D. *Nature, Lond.* **182,** 740 (1958).
3. STEINBERG D. *Analyt. Biochem.* **1,** 23 (1960).

VOL
11
196

VOL.
11
1961

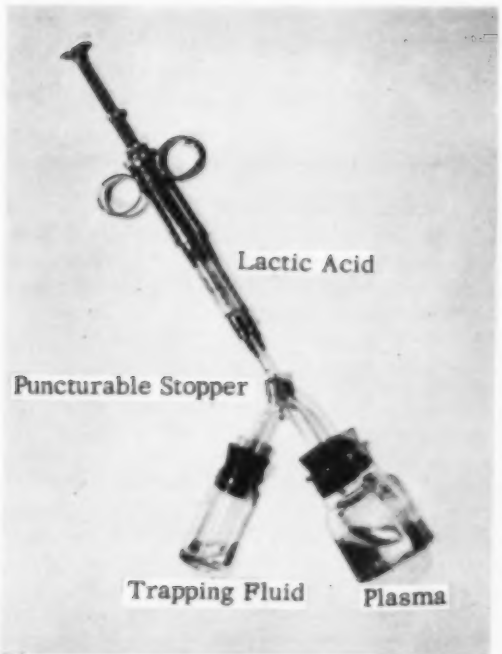


FIG. 1.

# book reviews

**Radioactive Wastes—Their Treatment and Disposal.** J. C. Collins (General Ed.), 1960. E. and F. N. Spon Ltd., 55*s*.

This book is a most interesting and valuable introduction to the study of radioactive waste disposal. It aims to fulfil a long felt need for a compilation of technical and scientific knowledge covering this field and undertakes the formidable task of compressing the information into one small volume.

The book is extremely well produced and contains a wealth of information. There is no doubt that a study of the work described would be of great value to anyone contemplating the use of radioactive isotopes. The first half of the book is devoted to the fundamental approach whilst the latter deals specifically with waste disposal in practice. Each chapter is well written, the authors all being experts actively concerned with the subject upon which they write.

The first two chapters, on the 'Nature of Radioactivity' and the 'Sources of Radioactive Waste', serve as a good introduction. These are followed by an excellent account of the 'Hazards of Radiation'. In this the biological effects of radiation are described in detail, followed by a comprehensive account of occupational exposure and control limits which must be applied. A clear and concise account of the 'Measurement of Radioactivity' follows, the summary of the various types of counter and their uses given on page 105 being particularly useful.

The short chapter dealing with the 'Law on Radioactive Wastes in Great Britain' is undoubtedly one of the most valuable. With the passing of the Radioactive Substances Bill it is now essential for all users of radioactive isotopes to understand fully the legal position.

The treatment and disposal of liquid, solid and gaseous wastes are fully described in further chapters. Details of current practices used in this country are given and also references made to those in use in other parts of the world. A most interesting account of the treatment of radioactive liquors by biological methods is included.

The book is at times highly technical but the inclusion of 7 pages of explanatory notes on symbols used in the text and a ten-page glossary of terms make it suitable for the newcomer to this field as well as to the specialist. The Editor is to be congratulated on having produced what is probably the most comprehensive and authoritative work on the subject yet published. The book should be a welcome addition to the libraries of all who are connected with the subject.

J. H. Clarke

---

**Atomic Energy Waste: Its Nature, Use and Disposal.** Edited by E. Glueckauf. Interscience (New York): Butterworths (London), 1961. xi + 420 pp., 95*s*.

The book consists of sixteen articles. Its first quarter is taken up by the first article, which describes in some detail the fission process and the physical properties of the fission products. The chemical properties are described in less detail as necessary in subsequent articles.

In the second article, the hazard of alpha-emitters in reactor wastes is assessed comparatively in terms of the ratio of their concentration to their permissible levels in air and water. Such an assessment is necessarily incomplete and may be misleading.

The third article is devoted to the physical and chemical effects of radiation. It goes into the mechanisms of the latter in some detail, but does not review the effects on biologically important compounds.

The next three articles ('Effects of Radiation on Living Cells', 'Movement of Radioactive Substances in Food Chains' and 'Radiation Protection—A Problem in Occupational and Public Health') contain good discussions of fundamentals but are not nearly so detailed: there are only two pages on aquatic food chains, for example.

There is a short, careful article on legal requirements for waste disposal and transport of radioactive materials.

A good balance between theory and practice is achieved in the five articles on the treatment of liquid wastes, which provide a firm basis for further study of the literature. One noted a misprint of "2" for "20" in the last entry on page 251 and a confusion between the slow sand filtration process for water treatment and the trickling filter process for sewage treatment.

One would have liked to see a similarly full treatment of gaseous, particulate and solid waste arisings, but there is only one article, a good, clear discussion of dispersion from chimney stacks. The treatment of these wastes is not discussed.

The last four articles are sober appreciations of the

uses of radiation in agricultural research, food preservation and induction of chemical reactions, but strangely not in teletherapy.

The small-scale use of radionuclides is deliberately excluded.

It is hoped that the definition of the "rad" as a unit of amount of radiation will be corrected in future definitions.

The editor's intention is that the book will illuminate the background from which future developments in use of waste radiation can emerge. In this, despite the omissions noted, it is successful and is recommended.

A. W. KENNY

---

R. C. KOCH: **Activation Analysis Handbook.** Academic Press, 1960, 64*s*.

THIS tabulation of data has appeared at a time when more and more analysts are exploiting the very high sensitivity of the radioactivation technique. In a brief introduction in somewhat stilted language, Dr. KOCH gives a useful summary of the underlying theory. Practical points are only dealt with in the most general terms, and few uninitiated readers could attempt an experimental assay on the basis of this work alone.

The bulk of the book consists of tables of nuclear data for all activation reactions investigated to date. The bibliography, which extends to September 1959, appears to be tolerably complete. Slow neutron reactions are given most prominence, but an important feature of the tables is the collection of data concerning activation reactions which have not yet been used much for analysis, for example (n, 2n), (p, pn) and (d, p) reactions. Other useful items are the lists of interfering nuclear reactions (though these are seldom important in practice) and the sensitivities of detection calculated from a standard set of assumptions. It is not a simple matter to use the tables without auxiliary data (e.g. a wall chart of the nuclides); in particular, it is difficult to find the half-lives of the products of reactions other than (n, $\gamma$) processes. The index and glossary are incomplete. The former would have benefited by giving fuller details of matrices in which different elements have been determined by activation, and the latter omits several important definitions e.g. barn, curie, and rad. There is no table of abbreviations.

The introductory type is good, but I would have preferred the tables in larger print. The introductory layout, with two columns per page, seems an unnecessary waste of space. However, this is nothing to the tabulation in which no less than 20 pages, or 10 per cent of the book, are like the Bellman's map, a perfect and absolute blank! This raises the question of binding of a work of this kind. Since the tables will need considerable revision in five years time, a loose leaf system might have saved expense. The cost of this work is depressingly high, and in view of this I find it difficult to recommend its purchase by practising analysts, though it should find a place in most reference libraries.

H. J. M. BOWEN

---

E. BRODA: **Radioactive Isotopes in Biochemistry** Translated by P. OESPER. Elsevier, 1960. x + 376 pp., 57*s*. 6*d*

THIS is a translation from the German of Dr. BRODA's important work. The references are no longer given as footnotes, but are collected at the end of each chapter: the text has not been much altered since the German edition, which was reviewed earlier in this journal. There is little to add to the comments I made there. The treatment is wide ranging but concise, and the literature has been thoroughly abstracted. The book will be indispensable to libraries and to all serious students of the subject.

Two minor criticisms involve the sections on radiation chemistry and on metabolism of inorganic elements. Chapter VI, on radiation chemistry, is much too short and the account of the radiation chemistry of water is misleading. The treatment of inorganic elements might also be expanded with advantage. For example, the table of sensitivity of activation analysis includes aluminium, strontium, silver, antimony and gold, as elements of biochemical importance, but omits cobalt, molybdenum and manganese. Neither of these points detracts much from the main purpose of this book, which is to review the impact of tracer techniques on the whole field of biochemistry. This purpose has been admirably achieved.

H. J. M. BOWEN

---

H. LINSER and K. KAINDL: **Isotope in der Landwirtschaft.** Verlag Paul Parey, Hamburg, 1960. 442 pp., 86 D.M.

MOST of this book does not deal with agricultural research or problems particularly concerned with agriculture but with straight tracer technique and

application of ionizing radiation, subjects which are dealt with in other books also in the German language. The portion which is concerned with agriculture is of a very variable quality. Take for example the first chapters dealing with problems related to agriculture: Chapter 13, p. 171—'Preparation of Labelled Compounds, Mainly Fertilizers'. Accent is here placed on labelling commercial products, but surely a student wanting to use radiochemical methods will not start with commercial products. If he wants to use, for instance, labelled mono- or di-calcium phosphate he will, if he is a sound experimenter, go to the standard method books for inorganic syntheses, where he will find methods which with little modification can be used for preparation of labelled compounds. When it comes to basic slag and mineral phosphate no laboratory method exists for the preparation of these. However, the authors mention a laboratory procedure for preparation of basic slag labelled with $P^{32}$ suggested by Professor TRÖMEL who is an authority on basic slag. This method seems worthwhile trying but is by no means a ready-to-use method. The same is true, only more so, for labelling mineral phosphate by neutron irradiation. Very significant quantities of non-orthophosphate containing $P^{32}$ is formed during this treatment and it is not at all likely that this phosphate is reverted to its original form by heat treatment.

It is a pity that such scanty information is given on preparation of labelled standard compounds because such information is always useful, much more so than results of other people's work which one will have to look up in any case. The authors have attempted to compile the relevant literature and at the end of the book one finds a very long list (45 pages, nearly 1,400 references) of the literature up to 1959. However, this list suffers from a serious drawback, namely that the numbers of the pages on which the content of the papers is mentioned in the book are not given. Surely it would have been a great help to the users if those numbers were given, and perhaps the literature references could have been grouped according to the type of publication (periodicals and books), and subject.

A more serious defect of this list is the omission of important papers like S. L. JANSSON (1958): 'Tracer Studies on Nitrogen Transformations in Soil with Special Attention to Mineralization-Immobilization Relationships', *Ann. Roy. agric. Sweden* **24,** 101-361. Such an omission is hard to forgive.

Considering the length of the book there are few misprints and only one worth mentioning, which was found on page 418 (Mettingly should read *Mattingly*, as is spelt on page 242, the last line; incidently, Mattingly has produced several more papers on the subject than the review mentioned).

In a second edition of this book much valuable space could be saved by omitting many technical details which the reader should be expected to find in the appropriate handbooks.

S. LARSEN

---

L. G. LAJTHA: **The Use of Isotopes in Haematology.** Blackwell Scientific Publications, Oxford, 1961. 83 + x pp., 21*s*.

THIS small monograph is intended primarily for haematologists and reviews the more important and well-established isotope techniques used in this branch of clinical pathology. Some sections, such as that on the measurement of blood volume, will be of wider interest to surgeons and others concerned with clinical physiology generally.

The first three chapters are concerned with the measurement of red cell and plasma volumes, the survival of transfused labelled red cells and the metabolism of radiocobalt-labelled vitamin $B_{12}$. All the procedures described are well established, widely used in diagnostic work and here is now a good foundation of clinical experience on which to base the evaluation and interpretation of the data. Although the literature on the use of radio-iron in haematological studies is very extensive and numerous diagnostic procedures using this isotope have been proposed, the subject is one which is by no means completely explored and the value of radio-iron as a diagnostic tool remains uncertain. Dr. LAJTHA has succeeded in presenting an excellent survey of the work which has been done with radio-iron indicating both the possibilities and the aspects which require further elucidation. There are brief chapters on the labelling of white cells and platelets and on autoradiography of bone marrow cells. The author has modestly given comparatively little space to the latter subject although it is one with which his name is closely associated. It might have been better had he treated this subject more extensively, since it has not been well covered in other reviews and monographs; and the techniques can be used in most haematology laboratories without capital outlay on equipment or the collaboration of physicists and electronic experts.

The reader is expected to look elsewhere for information of radioisotope measurement techniques and instrumentation. In a book of this nature this policy is probably reasonable, since in this country at least it is usually possible for a haematologist to seek practical advice from a hospital physics department, but in view of the fact that the prospective user may have to spend a considerable time and effort getting budgetary allocations for equipment it is felt that a small

appendix giving brief specifications of the apparatus which would be regarded as essential together with a rough indication of the overall cost would enormously add to the practical value of the book. The stated aim of the book is to consolidate present-day knowledge of the subject for the benefit of haematologists and the excellent bibliography at the end of each chapter helps to realize this objective. However, hospital physicists and other collaborating workers can also derive a great deal of benefit from reading this book.

N. VEALL

---

LEWIS E. ETTER: **Glossary of Words and Phrases used in Radiology and Nuclear Medicine.** Chas. C. Thomas, Illinois.

THE idea of a glossary of words and phrases used in an individual branch of Medicine as opposed to a general medical dictionary is a new one.

This particular work covering Radiology and Nuclear Medicine which is intended primarily for medical secretaries, could well have a wider appeal but it loses much in value in this country by using American idiom and spelling which has not yet become standard on this side of the Atlantic.

The sections on suggested terminology for reports and on writing reports have much to commend them, and would repay study by those beginning their careers in radiology, but the sample reports are rather too wordy for use in general hospital practice. The glossary itself is very full and the definitions clear and precise.

Many of the definitions in connexion with radiotherapy and physics are poor as compared, for instance, with the British Standards Institution Glossary.

In general the idea and execution are excellent, but use and value of the glossary in this country will be limited.

F. ELLIS

VOL. 11 1961

# international news

## Second Accelerator Conference Amsterdam, 4-6 October 1960

The full proceedings of this conference on low energy accelerators are published in *Nucl. Instrum. Meth.* **11**, No. 1 (Jan. 1961).*

The following papers were presented:

**Nuclear Physics**

P. M. ENDT: Resonance reactions

L. KATZ and K. H. LOKAN: The generation of positrons in a thick target bombarded by fast electrons

L. KATZ: Desirable linear electron accelerator characteristics for nuclear research

T. HUUS: Coulomb excitation

G. GOLDRING: Experiments using ultra-fast pulse techniques

E. COTTON: Durées de vie nucléaires

A. SCHOCH: A discussion of colliding beam techniques

**Particle Research**

P. H. ROSE: The three-stage tandem accelerator

H. E. GOVE: Current experimentation with the tandem accelerator at the Chalk River laboratories

K. W. ALLEN: Recent research in nuclear reactions using the Aldermaston Tandem Generator

R. FLEISCHMANN: Sources of polarized ions (for protons and similar particles)

R. J. CONNOR: Millimicrosecond pulsing

J. C. NYGARD and R. F. POST: Recent advances in high power microwave electron accelerators for physics research

**Physics and Radiation Research (I)**

PHYSICS

U. GONSER and K. LÜCKE: The use of Van de Graaff accelerators for high intensity neutron irradiation of metals

K. H. BECKURTS: Reactor physics research with pulsed neutron sources

F. AMMAN: The KS-3 MeV Van de Graaff injector of the Frascati Electron Synchrotron

J. KISTEMAKER: On ion sources with high efficiency and intensity

**Physics and Radiation Research (II)**

RADIATION RESEARCH AND INDUSTRIAL APPLICATION

J. W. OTVOS, V. P. GUINN, H. R. LUKENS, JR. and C. D. WAGNER: Photoactivation and photoneutron activation analysis

P. BARUCH: The use of the electron accelerator in solid state physics

W. HUBER: High energy radiation for research in biochemistry and microbiology

S. H. PINNER and W. T. H. DAVISON: The development of radiation process applications

D. MOORE: Neutrons, electrons and X-ray beams used for radiation research from a Van de Graaff generator

D. A. TRAGESER: Future accelerators: Intense sources for processing

* Published by North Holland Publishing Co.

## ABSTRACTS OF PAPERS PRESENTED IN PART (IV)

### Physics and Radiation Research (II)

**Photoactivation and photoneutron activation analysis.** JOHN W. OTVOS, V. P. GUINN, H. R. LUKENS, JR. and C. D. WAGNER

For the last two years the 3 MeV Van de Graaff electron accelerator at Shell Development Company, Emeryville, California, has been in routine use in neutron activation analysis. Over 30 elements can be analyzed for, some in the parts per million range and some in macro concentrations. The 3 kW electron beam produces Bremsstrahlung in a gold target and the photons, in turn, liberate neutrons from a large (15 cm cube) beryllium block immersed in a moderator. The thermal neutron flux available in a volume of over 3 l. is more than $5 \times 10^7/cm^2$ sec. Twenty-four samples of 25 ml each can be irradiated simultaneously. The activities produced are measured instrumentally in a scintillation counter using gamma ray spectroscopy. Several activities in the same sample may be distinguished by taking advantage of differences in half-life and gamma energy.

Recently it has been found possible to extend the scope of activation analysis by activating directly with photons. Eighteen metastable isomers of the stable nuclides have been produced, 7 for the first time by direct photoactivation. Bremsstrahlung from the gold target is allowed to act directly on the samples. Although sensitivities are lower, the method is more specific than neutron activation, and in many cases interferences in neutron activation can be eliminated by activating a sample with photons alone. Applications of photoactivation other than chemical analysis are (1) beam energy measurement and (2) dosimetry.

**The use of the electron accelerator in solid state physics.** P. BARUCH

Among the many processes by which electrons in the energy range 300 keV to 3 MeV interact with matter,

two are important for the physics of crystalline solids: ionization and nuclear recoils.

These processes and their secondary effects are reviewed. Examples are given of their importance:

1. The ionization creates in semiconductors electron-hole pairs in large excess; these extra carriers relax, their recombination laws are studied by various means, such as "electron-voltaic" effect, excess conductivity decay, emission and decay of fluorescent light.

2. The nuclear recoils are the cause of radiation damage in most materials. The energy transfer in an electron collision is small, and the incident electron energy has to be greater than a certain threshold to produce permanent displacements, thus creating lattice defects. In electron irradiation these defects are simple point defects (vacancies and interstitials at low temperature, which can combine into simple associations by warming). Electron irradiation can then be used to obtain knowledge of interatomic forces to test the laws of displacement of atoms by radiation, or to introduce in a crystal point defects in a controllable way.

Examples are given such as measurement of threshold in metals, and study of lifetime in semiconductors. A curious phenomenon is the failure of the reciprocity law: the magnitude of damage in germanium is dependent not only on the total dose, but also on the dose rate.

Some emphasis is put on the experimental requirements for electron irradiation of solids: energy and intensity stability, beam steering and controlling, large range of beam currents, including pulsed operation. The design and mounting of samples are also discussed, specially for low temperature irradiation.

**High energy radiation for research in biochemistry.** WOLFGANG HUBER

The applications of accelerators to biological problems were initiated some thirty years ago and have since been increasing at an ever-growing rate. Today they are useful for applications requiring anywhere from a few electron volts to a few billion volts. In fact, intense beams of particles of homogeneous composition and uniform LET are available only from accelerators and these are becoming more and more standard tools for chemists and biologists alike.

Work during recent years has shown that an understanding of the enormously involved pattern of biochemical radiation effects may be obtained by approaching the subject indirectly through the study of the factors which modify radiation injury. It is this subject of parameters that is discussed to demonstrate the usefulness of high energy radiation as a research tool in biochemistry and microbiology.

Linear energy transfer (LET)
dose rate
composition of surrounding medium
atmosphere (oxygen effect)
temperature
chemical modifiers.

These parameters can be classified roughly into two general groups; that is, those which are inherent to the radiation itself and those that are extraneous to the radiation but influence the radiation effect. All these parameters are discussed in detail.

**The development of radiation process applications.** S. H. PINNER and W. H. T. DAVISON

The patent literature provides a measure of applications for radiation processes. At present, there are well over 200 U.K. and U.S. patents, which can be classified into (a) polymerisation, (b) crosslinking of polymers, (c) degradation of polymers, (d) multicomponent polymers (graft and block copolymers), (e) general chemical reactions and petroleum products, (f) sterilisation, (g) specific articles and shapes, (h) uses for irradiated polymers, (i) inorganic compounds, (j) machines for generating radiation (including isotopes). Processes involving polymers account for more than 75% of these patents, so it can be fairly claimed that the major application of radiation will lie in the polymer field. The first polymerisation patent was granted in 1927 and the first crosslinking patent in 1933 but the first patent on multicomponent polymers was only granted in 1958 and this is the topic selected for detailed consideration in this paper.

The development of multicomponent polymers can be classified into (i) direct grafting, (ii) indirect grafting, (iii) peroxidation grafting, (iv) block copolymers and (v) attenuated network polymers. These methods are outlined and exemplified, by reference to continuous process techniques.

More recently, the application of radiation processes to polyvinyl chloride has attracted interest. This can be converted into infusible and insoluble rigid sheet with potential use as a solvent-resistant and corrosion-resistant structural material, by incorporating a plasticiser containing two or more olefinic double bonds and subjecting to radiation. The plasticiser is caused to polymerise and form a net-work which is attentuated by the polyvinyl chloride molecular chains.

The drawback to this material is its brittleness but recent work has shown this can be overcome by incorporating a small amount of a saturated elastomer. By inference, well-crosslinked materials are not necessarily brittle and this widens the scope for attenuated network copolymers in industrial applications.

VOL. 11 1961

The factors that have been recognized to influence the radiation response of biochemical systems include:

**Neutron, electron and X-ray beams used for radiation research from a Van De Graaff Generator.** D. MOORE

The Van de Graaff generator of the Medical Research Council at Hammersmith Hospital, has been used for radiation research for the past ten years. Details of its special design are given. The accelerator provides neutron, electron and X-radiations up to energies of 2 MeV. High intensity outputs are possible with beam currents of several hundred microamperes. The conversion from an output of neutrons to an output of X-rays is accomplished within a few minutes.

Methods of dosimetry are discussed for the delivery of defined doses of either of these radiations for studies in chemical, biological and pathological research. Examples of the versatility of the accelerator output, together with some of the published work are included.

**Future accelerators: intense sources for processing.** D. A. TRAGESER

Developments are described which will lower the unit cost of radiation power below $1 (U.S.) per kilowatt-hour under a wide variety of design criteria. These criteria are analyzed so that the breadth of design approach can be appreciated.

Potential industrial applications indicate the need for electron accelerators in the energy range from below 0·5 MeV to 12 MeV and with beam currents of 1–20 mA.

Progress on the development of direct accelerators below 3 MeV is noted. An insulating Core Transformer has produced a sustained d.c. beam current of 20 mA at 1 MeV. Its adaption at 0·3 MeV or 0·6 MeV would produce power for less than $10000 (U.S.) per kilowatt. All the components of the direct accelerator are analyzed in the light of large beam currents. Separation of the accelerator tube from the generator is discussed, and the advantages are cited.

The progress in r.f. power tubes of linear accelerators is outlined. Tubes for industrial purposes at 15 kW average r.f. are now available, while future tubes at ten times the power level are in prospect.

Unit capital and operating costs are summarized as a function of power.

VOL.
11
196

International Journal of Applied Radiation and Isotopes, 1961, Vol. 11, pp. 57–67. Pergamon Press Ltd. Printed in Northern Ireland

# The Half-Life of Carbon-14

W. B. MANN, W. F. MARLOW* and E. E. HUGHES
National Bureau of Standards, Washington 25, D.C.

(*Received* 27 *February* 1961)

The half-life of carbon-14 has been determined with an accuracy believed to be higher than that of previously reported values. Carbon dioxide was liberated by the action of perchloric acid on barium carbonate which contained $C^{14}$ in approximately 44 per cent isotopic abundance. Samples of this $C^{14}$ dioxide were analyzed mass spectrometrically, and other portions were diluted quantitatively with inert carbon dioxide and counted in the NBS length-compensated internal gas counters. Technical difficulties encountered in this work, which are characteristic of this type of experiment, particularly problems of adsorption and the methods used to overcome them, are discussed in detail. On the basis of a thorough analysis of all results obtained, the half-life of $C^{14}$ is believed to be 5760 $\pm$ 50 years, where the indicated uncertainty denotes an estimated overall probable error of the result.

LA PERIODE DE DEMI-VALEUR DU CARBONE-14

On a déterminé la période de demi-valeur du carbone-14 avec une précision que l'on croit supérieure à celle rapportée préalablement. Du bi-oxyde de carbone fut libéré par l'action de l'acide perchlorique sur du carbonate de baryum contenant du $C^{14}$ en une abondance isotopique d'environ 44 pour cent. Des échantillons de ce bi-oxyde de $C^{14}$ furent dosés au spectromètre de masses, et d'autres portions furent diluées quantitativement avec du bi-oxyde de carbone inerte, puis comptées dans les compteurs à gaz intérieur du NBS, compensés pour longueur. On discute en détail les difficultés techniques que l'on rencontre dans ce travail, et qui sont typiques de ce genre d'expériences, surtout les problèmes d'absorption et les méthodes servant à les surmonter. Sur la base d'une analyse complète de tous les résultats obtenus, on croit la période de demi-valeur du $C^{14}$ être 5.760 $\pm$ 50 années, où l'incertitude indiquée montre une estimation de l'erreur probable effective du résultat.

ПЕРИОД ПОЛУРАСПАДА $C^{14}$

Период полураспада $C^{14}$ был определен с точностью, повидимому, превосходящей полученные ранее значения. Выделение $CO_2$ производилось воздействием хлорной кислоты на карбонат бария, углерод которого примерно на 44% состоял из изотопов $C^{14}$. Образцы $C^{14}O_2$ были подвергнуты масс-спектрометрическому анализу, другая часть $C^{14}O_2$ была смешана количественно с инертным $CO_2$ и измерялась газовым счетчиком НБС внутреннего наполнения, компенсированным по длине. Подробно рассмотрены встретившиеся в этой работе технические трудности, связанные с адсорбцией, и методы их преодоления. На основе тщательного анализа всех полученных результатов было выведено значение периода полураспада $C^{14}$, равное 5760 $\pm$ 50 лет указанная погрешность учитывает все вероятные ошибки.

DIE HALBWERTSZEIT VON KOHLENSTOFF-14

Die Halbwertszeit von C-14 wurde mit einer Genauigkeit bestimmt, die vermutlich grösser ist als bei den früher angegebenen Werten. Kohlendioxyd wurde durch Einwirkung von Perchlorsäure auf Bariumkarbonat gebildet, welches etwa 44%C-14 enthält. Proben dieses Kohlendioxyds wurden massenspacktroskopisch analysiert, während andere Teile davon quantitativ mit inaktiver Kohlensäure verdünnt und in NBS längenkompensierten internen Gaszählern gemessen wurden. Technische Schwierigkeiten dieser Bestimmung, welche für

* Present address: Division of Biology and Medicine, U.S. Atomic Energy Commission, Washington 25, D.C.

diese Art der experimentellen Methode charakteristisch sind, besonders Adsorptionsprobleme, und die Methoden mit welchen diese Schwierigkeiten überwunden wurden, werden im Detail besprochen. Als Ergebnis einer gründlichen Analyse aller erhaltenen Resultate wird eine Halbwertszeit von 5760 ± 50 Jahren angenommen, wobei die angegebene Ungenauigkeit aus dem wahrscheinlichen Fehler aller Resultate abgeschätzt wurde.

## I. INTRODUCTION

It has been stated that much could be learned if only good experimenters would write about their failures! While we can lay no claim to belonging to such an elite company we can, however, confess to many failures in the course of the work described in this paper. These failures may in fact be the chief justification for writing this paper, except that the wisdom that we have had forced upon us and the ability that we have now acquired of producing, on request, any half-life for $C^{14}$ between 4600 and 6200 years may also have endowed us with a peculiar authority in this field. This then is the chapter of our failures that has been so eagerly awaited by our friends, coupled, however, with a value of the half-life of $C^{14}$ which intuitively, or otherwise, we believe to be more accurate than that which is currently in use.

A few years ago one of us was asked by W. F. Libby to consider re-measuring the half-life of $C^{14}$ in view both of the wide divergences of the reported experimental results (4700–7200 years[1]) and also of the fact that the presently used value of 5568 years is somewhat arbitrary as it is a weighted average of three values in which the activities of the samples had been determined by gas counting.[1] After having considered these divergences for a great many years, and having initially contributed to them, the author in question assumed, wrongly as it now transpires, that the cause of such wide discrepancies should be sought chiefly in the measurements of isotopic abundance. Accordingly the United States Atomic Energy Commission was approached with a view to obtaining a sample in which the carbon contained $C^{14}$ in about 50 per cent isotopic abundance, so that in the mass-spectrometric measurements two peaks of about equal magnitude would be compared. The Atomic Energy Commission kindly made available on loan such a sample of barium carbonate containing about 44 atoms per cent $C^{14}$ relative to $C^{12}$ plus $C^{13}$. The isotopic-abundance measurements on this sample have been consistent to within about $1\frac{1}{2}$ per cent, and the chief difficulty has been in quantitatively diluting the samples in order to obtain counting rates that could be accommodated by the National Bureau of Standards internal, compensated, gas counters.[2] For this purpose it was necessary to make quantitative dilutions of the order of $10^8$, but in so doing it became necessary to guard against spurious results arising from adsorption of gas of high specific activity on to the walls of the volumetric glass vessels. The activities of different samples have been determined by counting both in the proportional and Geiger regions.

## II. GAS PREPARATION

The procedure described by Mann *et al.*[2] was used for the generation of carbon dioxide from the 44 atoms per cent $C^{14}$ barium carbonate, with the exception that 70 per cent perchloric acid was used instead of sulphuric acid. A further dry-ice-alcohol trap was also added to ensure the complete removal of water vapor. It was, however, not necessary that the generation of carbon dioxide from the barium carbonate should in this case be quantitative, as was required in the calibration of the National Bureau of Standards Carbon-14 Standards. In determining the half-life it is not necessary to link the carbon dioxide quantitatively with the barium carbonate but merely to determine

the isotopic abundance of a given number of gram molecules of carbon dioxide (determined by measurements of pressure, temperature and volume) which is then quantitatively diluted for gas counting. For this purpose the initial specimen of carbon dioxide (usually about 15 ml of gas at a pressure of about 90 cm Hg) was generally expanded into a 13.4548 ml flask to a pressure of from 9 to 10 cm Hg. The 13.4548 ml flask was then sealed and the rest of the carbon dioxide, in some 100 ml of connecting tubes, was completely frozen back into the 15 ml flask and sent for mass-spectrometric analysis.

## III. GAS DILUTION

In the early experiments the 13.4548 ml flask, which had been filled with the high-specific-activity carbon dioxide, was attached to the counting system together with a 5290 ml flask*, containing a known quantity of inert carbon dioxide, and the "mass-spectrometer" flask of about 15 ml. The gas in the 13.4548 ml flask was expanded into the barometer system of the counters and the 15 ml flask, and its pressure carefully measured. The 13.4548 ml flask was sealed, its temperature being noted, and the rest of the gas frozen into the 15 ml flask which was then detached for mass-spectrometric measurement. The known quantity of gas in the 13.4548 ml flask was then completely mixed with that in the 5290 ml flask to achieve the first dilution, and then a quantity of this diluted mixture was sealed at a pressure of about 15 cm Hg (which was accurately measured and the temperature of the flask noted) in the 13.4548 ml flask. This gas, amounting to the order of $10^{-4}$ gram molecule, was then mixed with about 0.4 gram molecule of methane (contained in the "counting-gas" plus barometer system) to give the final dilution for counting. An automatic Toepler pump was used for this mixing.

In two experiments using this procedure and counting in the proportional region, values of 4745 and 4595 years were obtained for the half-life of $C^{14}$.

With such low results it was suspected that adsorption of the high-specific-activity carbon dioxide was occurring in the 13.4548 ml flask prior to the first dilution and that this was then exchanging with the carbon dioxide during the mixing with the counting gas in the final dilution to give too high a disintegration rate. It has already been observed that, in the approximately 10 l. volume of the "counting-gas" system, as much as 10 ml of methane at NTP could be adsorbed.

To test this hypothesis the 13.4548 ml flask was again filled with high-specific-activity carbon dioxide which was then *entirely* frozen back into the 15 ml flask. A "blank" mixing procedure was carried out with the inert carbon dioxide in the 5290 ml flask. The 13.4548 ml flask was then filled with inert carbon dioxide at a pressure of 14.5 cm Hg and sealed. The rest of the system was then quickly and thoroughly evacuated to about $10^{-4}$ mm Hg, and the dilution of the sample in the 13.4548 ml flask with the counting gas was carried out by means of the automatic Toepler pump as before; the 13.4548 ml flask contained, however, only the nominally inert carbon-dioxide sample instead of being filled with diluted active carbon dioxide at a pressure of about 15 cm Hg.

On counting this sample in the proportional region, the "background" counting rate in this "blank" experiment was found to be about 30 per cent of that of the previously observed counting rates with the active samples and some 20 times that of the normal background!

From the counting rate and the dilution constants it would thus appear that something like 0.02 per cent of the sample of high-specific-activity carbon dioxide had been retained by adsorption in the 13.4548 ml flask and connecting tubing of the counter barometer system. While a loss of 0.02 per cent in dilution would represent a negligible error in itself, this amount of activity, picked

* Calibrated by the Capacity, Density and Fluid Meters Section to be 5289.625 ml.

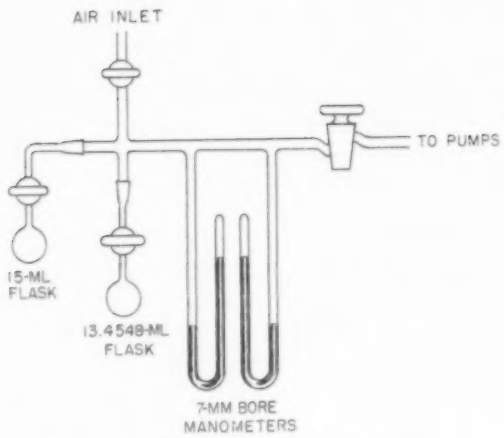


FIG. 1. Schematic drawing of the high-specific-activity manifold.

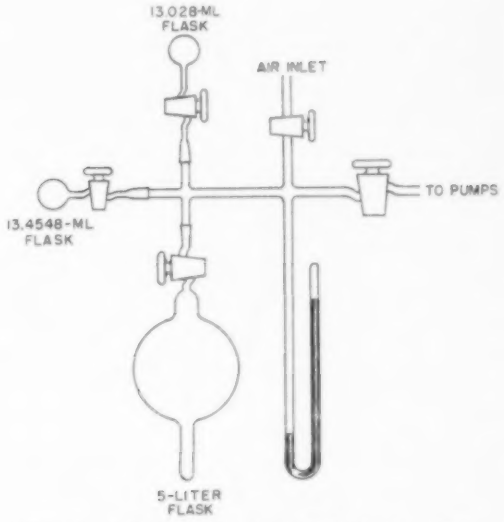


FIG. 2. Schematic drawing of the low-specific-activity manifold.

up at a later stage in the dilution process, is intolerable. A rough correction, for the 30 per cent increase in counting rate, raises the 4600 year half-life to about 6570 years!

The later contamination caused by the 0.02 per cent of activity lost in the first dilution could, however, be easily avoided by substituting a second and clean 13 ml flask and manifold for the second dilution. Such a flask was obtained with a volume of 13.028 ml and high-level and low-level dilution manifolds were constructed. These are shown schematically in Figs. 1 and 2, while Fig. 3 shows a photograph of the two manifolds assembled for operation. Both manifolds were thoroughly evacuated for about 1 week before any dilutions were carried out.

The dilution procedure now consisted of taking the freshly prepared carbon dioxide at a pressure of about 90 cm Hg in the 13.4548 ml flask and attaching it to the high-specific-activity manifold (Fig. 1) which was then thoroughly evacuated with the 13.4548 ml flask sealed. After evacuation for at least 1 hour the stopcock to the pumps was closed and the gas in the 13.4548 ml flask expanded to a pressure of between 9 and 10 cm Hg which was read with a precision of about 2 parts in 9000 on the sealed pair of mercury manometers. The temperature of the 13.4548 ml flask, which was surrounded with aluminum foil, was noted and this flask was sealed. The remainder of the high-specific-activity carbon dioxide was now frozen back into the 15 ml flask, using liquid nitrogen, and then this flask was sealed and sent for mass-spectrometric analysis.

The 13.4548 ml flask was now detached from the system and the grease from the conical joint carefully removed with ether. The conical joint and the glass tubing, up to within 2 or 3 mm of the stopcock, were now very carefully cleaned with chromic acid cleaning solution, sodium hydroxide solution and distilled water, using absorbent cotton wrapped on the end of a wooden applicator.

The 13.4548 ml flask was now attached to the low-specific-activity manifold (Fig. 2) which was thoroughly evacuated for 1 hour or more; the 5 l. flask, in which inert carbon dioxide had been sealed at a known temperature and pressure, had already been attached to this manifold. The cleaned 13.028 ml flask, which was also attached to this manifold, was evacuated at this time and also sparked with a Tessla coil in the process.

After evacuation, the stopcocks to the pumps and the 13.028 ml flask were closed and the stopcock of the 5 l. flask opened so as to flush the manifold with inert carbon

VOL.
11
1961

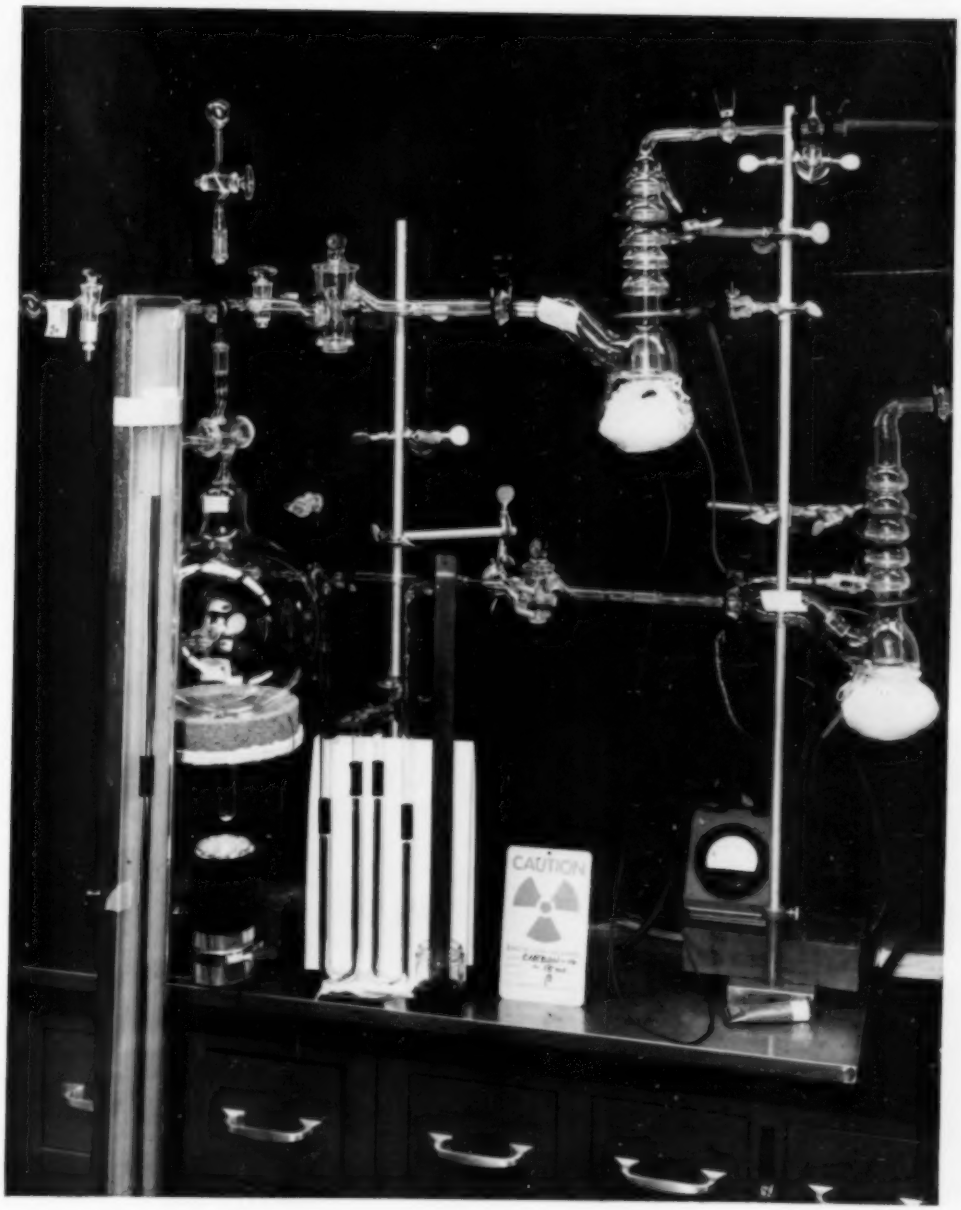


FIG. 3. Photograph of high- and low-specific-activity manifolds. The vertical steel rule is for checking the accuracy of the cathetometer readings on the two "high-level" barometers.

VOL
11
196

VOL. 11 1961

dioxide at a pressure of about 65 cm Hg. The inert carbon dioxide was now also admitted to the 13.4548 ml flask by opening its stopcock and then all the carbon dioxide was frozen back into the finger on the 5 l. flask until the pressure was less than 1 mm Hg. The stopcock of the 5 l. flask was closed and the carbon dioxide allowed to sublime, assisted by an infra-red lamp which was left to shine on the flask so as to induce good mixing by convection. The carbon dioxide was now allowed to expand again into the manifold and 13.4548 ml flask, and the freezing and mixing cycle repeated some four or five times, in order thoroughly to "scour" out the 13.4548 ml flask.

During the few minutes that the inert carbon dioxide was left in the 13.4548 ml flask in this "scouring", it is possible that some of the high-specific-activity gas adsorbed to the walls of the flask may have been desorbed and therefore have eventually erroneously given rise to too high a counting rate, with too low a half-life. It is believed, from the results of the blank experiment described earlier, that the error introduced by such an effect is unlikely to exceed 0.06 per cent. Toward the end of the mixing procedure in this manifold, the mixed carbon dioxide was allowed to enter the 13.028 ml flask which was finally sealed and transferred to the counting system, where the pressure of gas in it, at a known temperature, could be accurately measured. All dilution factors were calculated using the van der Waals' equation of state.

The mixed gas in the 5 l. flask could be stored for future counting in either the proportional or Geiger regions. For such purposes samples could readily be taken by replacing the cleaned 13.028 ml flask and 5 l. flask on to the low-specific-activity manifold (with a blank cover in place of the 13.4548 ml flask), evacuating the manifold and 13.028 ml flask and then sharing between the 13.028 ml and 5 l. flasks. After such a sampling, however, the gas was always checked for leakage by freezing back into the 5 l. flask and testing with a Tessla coil.

Having developed these procedures, a series of measurements carried out in May and June 1960 led to a value of the half-life of around 6200 years. However, a series of new peaks appeared in the mass-spectrometric analyses which were eventually identified as being due to ethyl ether and a very close examination revealed the presence of an almost invisible grey film of small area on the tubing inside the stopcock of the 15 ml flask. This flask had undergone vigorous chemical cleaning which had, however, been insufficient therefor, so that cleaning of all glass-ware was henceforth stringently controlled with careful inspection under a lens for possible grease contamination. The cleaning of grease from ground-glass joints by means of ethyl ether was also replaced wherever possible by wiping with lintless tissue only.

Two main dilutions were subsequently, and finally, carried out starting with two freshly prepared high-specific-activity samples of carbon dioxide in the 13.4548 ml flask and in each of these two main dilutions (on 15 August and 22 August 1960) a sample in the 15 ml flask was sent for mass-spectrometric analysis. The 13.4548 ml flask, after filling with low-specific-activity carbon dioxide on the low-specific activity manifold, was also sent for mass-spectrometric analysis of its contents for the presence of ethyl ether. This contaminant was never again, however, found to be present. The diluted samples of carbon dioxide from each of these two main dilutions were stored in two similar 5 l. flasks having accurately measured volumes of 5289.625 ml (15 August 1960 dilution) and 5306.39 ml (22 August 1960 dilution). For convenience the two main samples will therefore be identified by the numbers 5290 and 5306.

Results were obtained by counting samples from both the 5290 and 5306 dilutions in both the proportional and Geiger regions using respectively methane and a mixture of argon and ethyl alcohol as the counting gas. In each case a little inert carbon dioxide was added to the counting gas and care was taken in the final mixing of active sample with inert counting gas, with the automatic Toepler pump, to admit a quantity of the

inert counting gas, with its added small amount of inert carbon dioxide, to both the copper and stainless-steel counters *before* mixing with any of the active sample. In this way any adsorption taking place in the counters themselves would be of inert gases.

## IV. DISINTEGRATION-RATE MEASUREMENTS

Measurements of the activities of the samples were made both by proportional and Geiger-Müller counting using the electronic equipment which has already been described.[2] However, uncomfortably long plateaux of nearly 1000 V were obtained in the proportional region and one could not but suspect that the continuation of these plateaux to such high voltages might possibly be due to an increase in dead-time in the counting mechanism. After a most helpful discussion with L. Costrell, it was accordingly decided to adjust the voltage applied to the counters so as to limit the pulses from the cathode follower to about 0.5 V, in order to avoid excessive pile-up in the non-overloading amplifier, and then to obtain the true counting rate by careful extrapolation of the discrimination curves to zero pulse height. Actually no significant difference has been noted between these results and those obtained by measuring on the plateaux. Discrimination curves for both the copper and stainless-steel counters are shown in Fig. 4.

Activity measurements were made on samples from both the 5290 and 5306 dilutions. Initially the 13.028 ml flask was used to take samples from both dilutions for proportional counting and then a further sample was taken from the 5306 dilution using a 112.48 ml flask in order to give high

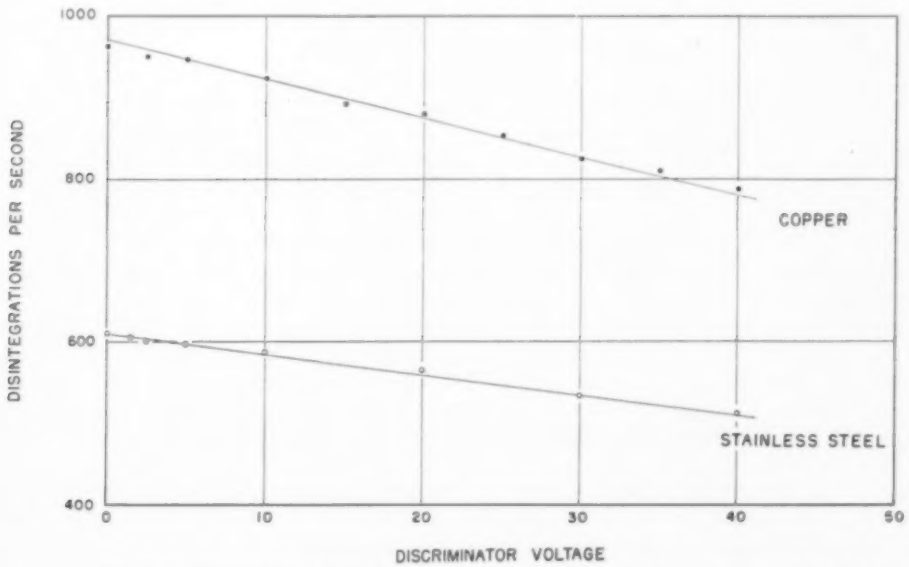


FIG. 4. Discrimination curves for the copper and stainless-steel counters operating in the proportional region with methane plus sample at a pressure of 66.926 cm Hg. The calibration of the discriminator showed its zero to be at about −0.5 V but, because of uncertainty as to the shape of the discrimination curve, it is accurate enough to extrapolate to zero. Linear extrapolation of the stainless-steel-counter results to −0.5 V gives 613 instead of 610 d.p.s. but the curve should probably also fall away from linearity towards zero. The points at zero discriminator voltage should be disregarded as they are almost certainly affected oppositely by spectral shape and noise.

counting rates, and good statistics, to determine more exactly the shapes of the discrimination curves. Subsequently a 27.350 ml flask was used to obtain one more sample from both the 5290 and the 5306 dilution for Geiger–Müller counting. Thus three sets of results were obtained on both the copper and stainless-steel counters in the proportional region and two sets on each of the counters in the Geiger region.

The proportional counting was carried out at pressures of counting gas (methane) and sample of approximately 65, 45 and 35 cm Hg, while the Geiger-Müller counting was carried out at pressures of counting gas (argon plus ethyl alcohol) and sample of approximately 40, 20 and 15 cm Hg. An electronic gate was set to 50 and 400 $\mu$sec for counting respectively in the proportional and Geiger regions.

In the course of performing the second set of measurements in the Geiger region, it was noticed that at the pressure of 40 cm Hg a decrease in counting rate occurred on increasing the discriminator voltage. This was very puzzling at first. However, oscilloscope photographs of the pulses from the cathode follower showed that the dead times of the long counters were exceeding 400 $\mu$sec at a pressure of 40 cm Hg. The effect of discrimination was therefore to remove Stever pulses which were occurring in the recovery times of the counters. Extrapolation to zero discrimination was therefore completely justifiable to obtain the true counting rate but, as the effect of changing the discrimination level was not investigated in the first set of Geiger–Müller measurements at a pressure of 40 cm Hg, the results obtained at this pressure in the first set were eventually discarded (points *C* and *D* in Fig. 5, to be discussed later).

## V. WALL EFFECT

A 1 or 2 per cent wall effect had previously been observed, relative to the activity measurements in the proportional region at about atmospheric pressure, for the stainless-steel counters but practically none with the copper counters.[3] The range of pressures over which such measurements can be made in the proportional region is, however, quite limited, extending, in actual practice, from about 25–65 cm Hg.

In the present experiments, however, where the method of extrapolation to zero discrimination voltage has been used it is extremely probable that the extrapolated value of the activity corresponds to the detection of primary ionizing events comprised of as low as one ion pair. The results of measuring activity as a function of pressure in the proportional region can therefore be directly related to similar measurements in the Geiger region, thereby extending the lower limit of pressure to about 15 cm Hg. On plotting results for the copper and stainless-steel counters, obtained in both the proportional and Geiger regions, as a function of reciprocal pressure, a small wall effect became immediately apparent for both sets of counters. The magnitude of this effect, again in terms of the difference between infinite pressure and a pressure of about 1 atm., was only of the order of 0.3 per cent for both the copper and the stainless-steel counters. This is less than was previously reported in the case of the stainless-steel counters, but this may be due either to slight changes in the cathode surfaces or possibly to the fact that extrapolation to zero discrimination voltage achieves nearer to the 100 per cent efficiency, previously given wholly by the wall-effect extrapolation.

In order to carry out the wall-effect extrapolation with all the data possible, it is necessary either to normalize for changes in isotopic abundance from sample to sample or to carry out the extrapolation using the final half-life figures themselves (i.e. essentially by plotting $N/(dN/dt)$ as a function of reciprocal pressure). It was considered to be more convenient and more instructive, in the present instance, to adopt the latter procedure and accordingly the implementation of this correction will be referred to again (Fig. 5).

## VI. MASS-SPECTROMETRIC ANALYSES

Samples of carbon-14-enriched carbon dioxide were analyzed at the National Bureau of Standards by both the Mass Spectrometry and the Molecular Structure and Properties of Gases Sections, the latter analyzing the master samples for dilutions 5290 and 5306 which were the ones ultimately used for the determination of the half-life of $C^{14}$. In both sections the analyses were carried out using modified Consolidated Model 21–101 mass spectrometers. Comparative measurements were also carried out between the two spectrometers and also with that of the United Kingdom Atomic Energy Authority's laboratories at Aldermaston.

The two main dilutions, 5290 and 5306, were carried out on 15 and 22 August 1960, and in each case the 15 ml flask containing the master sample of gas was submitted for mass-spectrometric analysis. One week thus elapsed between the analysis of each sample and, as other analyses were performed in the intervening period, the possibility of cross contamination between the samples is negligible. Exchange on the walls of the system between adsorbed atmospheric carbon dioxide and the carbon dioxide in the samples was found to be significant. For this reason, at least four separate portions of each sample were analyzed over a period of 2 days. Several spectra of each portion were obtained while the sample remained in the gas-handling system of the spectrometer. The reported results are the last obtained after the ratio of the concentration of the two forms of carbon dioxide had reached a constant value.

The results were calculated from the ratio of the ion currents at the parent peaks assuming that the various ions contributing to the different peaks were as follows.

| Mass number | Ion |
|---|---|
| 44 | $C^{12}O_2^{16+}$ |
| 45 | $C^{12}O^{16}O^{17+}$, $C^{13}O_2^{16+}$ |
| 46 | $C^{14}O_2^{16+}$, $C^{12}O^{16}O^{18+}$ |
| 47 | $C^{14}O^{16}O^{17+}$ |
| 48 | $C^{14}O^{16}O^{18+}$ |

Other isotopic combinations would not contribute significant ion currents at any of the masses under consideration. It was further necessary to assume that the response of the instrument in terms of the ion current relative to the partial pressure of a species was the same for all species.

The concentration of $C^{14}$ is proportional to

$$\frac{C^{14}O_2^{16} + C^{14}O^{16}O^{17} + C^{14}O^{16}O^{18}}{C^{12}O_2^{16} + C^{12}O^{16}O^{17} + C^{13}O_2^{16} + C^{14}O_2^{16} + C^{12}O^{16}O^{18} + C^{14}O^{16}O^{17} + C^{14}O^{16}O^{18}}$$

$C^{14}O_2^{16}$ is proportional to the total ion current at mass 46 less the contribution from $C^{12}O^{16}O^{18}$. This latter quantity is equal to the ion current at mass 48 multiplied by the ratio $C^{12}/C^{14}$. The total ion current at 48 is only a fraction of the total and an approximate value for $C^{12}O^{16}O^{18}$ is (44/46)48. With this simplification, the expression for the concentration of $C^{14}$ in percentage of total carbon is

$$\frac{(46) + (47) + (48)\left(1 - \frac{(44)}{(46)}\right)}{(44) + (45) + (46) + (47) + (48)} \times 100$$

where the bracketed numbers represent the ion current at the indicated mass number.

The results shown in Table 1 are a series of values obtained on analysis of each of the two samples after the relative concentration of the isotopic forms had reached an apparently stable value.

TABLE 1. Percentage concentration of $C^{14}$ relative to total carbon

| 5290 dilution | 5306 dilution |
|---|---|
| $43.78_5$ | $43.42_8$ |
| $43.79_4$ | $43.38_0$ |
| $43.86_3$ | $43.40_9$ |
| $43.89_4$ | $43.37_1$ |
| $43.82_0$ | $43.38_1$ |
| $43.80_2$ | $43.44_3$ |
| $43.77_7$ | |
| $43.83_2$ | |
| Average 43.82 ± 0.03* atoms per cent $C^{14}$ | Average 43.40 ± 0.03* atoms per cent $C^{14}$ |

* Average deviation.

## VII. INTERCOMPARISON OF ISOTOPIC-ABUNDANCE MEASUREMENTS

At the time that low results for the half-life of $C^{14}$ were being obtained, due to adsorption, it was felt that it would be useful to obtain a check on the isotopic-abundance ratios. Henry W. Wilson, of the Atomic Weapons Research Establishment, Aldermaston, England, kindly agreed to participate in such an intercomparison and accordingly six samples of gas, in break-seal ampoules, were prepared in February 1960 by expanding a single sample of high-specific-activity carbon dioxide into a highly evacuated glass manifold to which the six break-seal ampoules were attached Two of these ampoules were then given to V. H. Dibeler (NBS) for mass-spectrometric analysis and the remaining four were sent to H. W. Wilson (AWRE). The results obtained for the $C^{14}/(C^{12} + C^{13} + C^{14})$ ratio were in good agreement, being equal to 44.7 atoms per cent (AWRE) and 45.3 atoms per cent (NBS). The average deviations of both these measurements were 0.25 per cent and 0.1 per cent, respectively. The estimated uncertainty in the NBS value was, however, $\pm 1$ per cent, due to the fact that the mass spectrometer had not been calibrated for such an isotopic abundance.

Subsequently the residue from one of the samples sent to AWRE was returned to the National Bureau of Standards for analysis in the same mass spectrometer in which the master samples for the 5290 and 5306 dilutions had been analyzed.

The result obtained was 44.59 atoms per cent for the $C^{14}/(C^{12} + C^{13} + C^{14})$ ratio using this second NBS mass spectrometer. The average deviation of this result was 0.1 per cent.

Each of the NBS results was based on a very large number of individually measured spectra so that it is evident that there is a systematic difference of about 1.6 per cent between the two NBS mass spectrometers. Accordingly the results of the analyses of the master samples for the 5290 and 5306 dilutions, which were carried out on the "low-reading" mass spectrometer only, have been increased by approximately 0.8 per cent in order that they should represent an average value for the two NBS mass spectrometers.

## VIII. THE HALF-LIFE OF CARBON-14

The high-specific-activity sample of carbon dioxide that was used to give the 5290 dilution was found to contain $43.82 \pm 0.03$ atoms per cent of $C^{14}$, while that which gave the 5306 dilution was found to contain $43.40 \pm 0.03$ atoms per cent of $C^{14}$. Each of these values was then multiplied by the factor 1.008 to give an average NBS value.

In Fig. 5 all the values of the half-life of $C^{14}$ which have been obtained with the copper or stainless-steel counters, from both the 5290 and 5306 dilutions, are shown plotted as a function of reciprocal pressure. It will be seen that considering the proportional and Geiger-Müller results as a whole a small wall effect is apparent.

In Fig. 5 are shown the linear functions of half-life vs. reciprocal pressure derived by least-squares analysis for both the copper and the stainless-steel counters. The intercepts at zero reciprocal pressure give half-life values of $5772 \pm 26$ and $5748 \pm 34$ years for the copper and stainless-steel counters, respectively. This agreement is very satisfactory and the average of these two values is $5760 \pm 20$ years. (Twenty years is the standard deviation.)

In carrying out this least-squares analysis the lowest value, shown in Fig. 5, of 5547 years (obtained by proportional counting in the copper counters) and the two values of 5900 and 5908 years (obtained by Geiger-Müller counting respectively with the copper and stainless-steel counters at a pressure of 40 cm Hg using a sample from the 5306 dilution) have been rejected. The former value (point *A* in Fig. 5) is in complete disagreement with the value obtained by measuring the activity of the same sample in the stainless-steel counters (point *B* in Fig. 5). The other two rejected values, obtained by Geiger-Müller counting (points

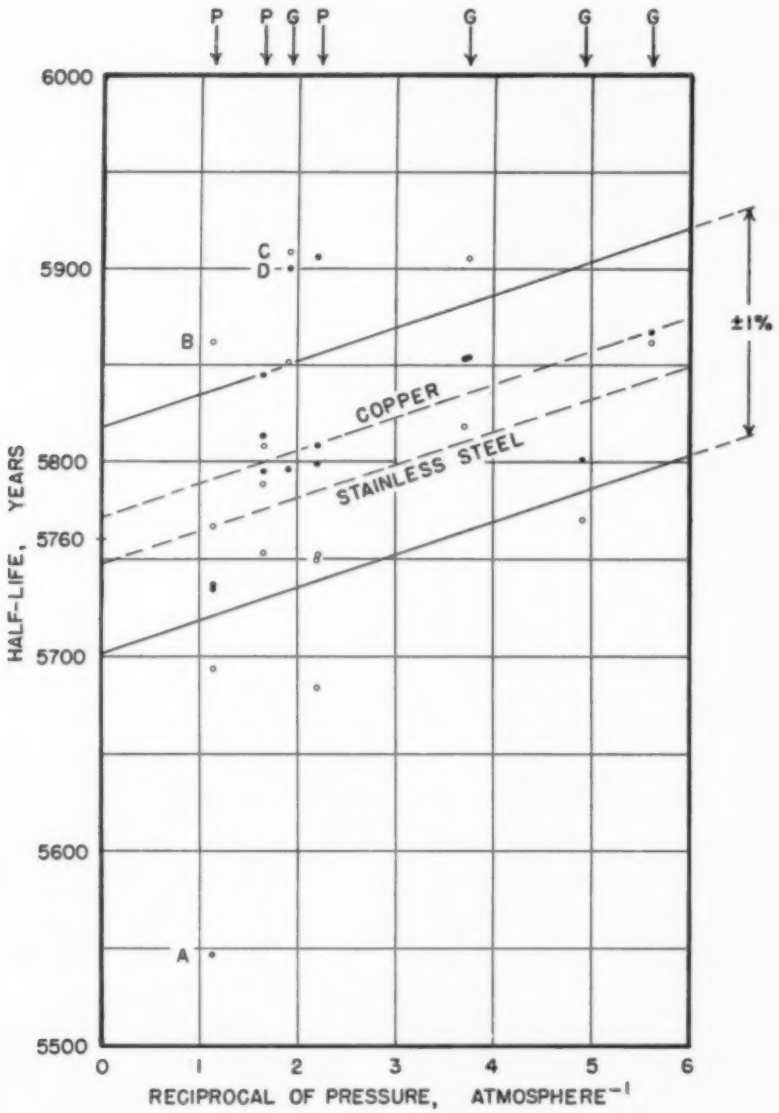


FIG. 5. Half-life vs. reciprocal pressure. Results for the copper counters are shown as filled points while those for the stainless-steel counters are represented by open circles. The measurements taken respectively in the proportional and Geiger regions are indicated by the letters *P* and *G* along the upper border of the graph. The two dashed lines indicate the least-squares slopes for the two sets of counters, as labelled, while the continuous lines indicate the ±1 per cent spread from the average of the two least-squares slopes.

VOL
11
196

*C* and *D* in Fig. 5), are certainly in error because of the discrimination effect, found at pressures of about 40 cm Hg, which has been discussed in Section IV of this paper. Actually, if one were to correct these points, using the discrimination curves obtained with the 5290 dilution in the Geiger region at a pressure of about 40 cm Hg (Fig. 4), values are obtained for the half-life of 5706 years (for point *C* in Fig. 5; copper counters, correction 3.4 per cent) and 5826 years (for point *D* in Fig. 5; stainless-steel counters, correction 1.4 per cent). These values are quite consistent but the correction for the copper counters is a little uncertain as, for these counters, the correction naturally depended on the degree of amplification and varied from 3.1 per cent for 100 V pulses from the amplifier to 4.8 per cent for 60 V pulses. The discrimination curve for the stainless-steel counters was much flatter and no difference could be distinguished between the 60 V and 100 V pulses.

The precision (standard deviation) of 20 years of the final value of the half-life does not represent the *accuracy* with which this quantity has been determined. It merely reflects the consistency of the counting results and the analyses of isotopic abundance using *one* of the NBS mass spectrometers. The counting results are believed to be devoid of any appreciable systematic error but there is, however, inherent in the isotopic-abundance measurements an uncertainty of $\pm 0.8$ per cent, or $\pm 45$ years, because of the very reproducible difference of 1.6 per cent between the two NBS mass spectrometers. The probable error is, therefore, estimated to be 0.9 per cent and the half-life of $C^{14}$ is believed to be equal to $5760 \pm 50$ years.

*Acknowledgments*—We wish to make very grateful acknowledgments of help to the following colleagues: V. H. Dibeler and R. M. Reese for a number of mass-spectrometric analyses; J. C. Hughes and B. C. Keyser for several volumetric calibrations; L. Costrell and S. B. Garfinkel for helpful discussion, construction and calibration of a suitable electronic gate; W. J. Youden for helpful discussion and analysis of the accuracy of the results; R. W. Medlock, for assistance in preparing the carbon dioxide samples; A. S. Friedman and W. F. Libby of the United States Atomic Energy Commission for their assistance in making a high-specific-activity sample of $C^{14}$ available, and H. W. Wilson of the United Kingdom Atomic Energy Authority for his intercomparison measurements of the isotopic abundance.

## REFERENCES

1. Libby W. F. *Radiocarbon Dating* (2nd Ed.). University of Chicago Press (1955).
2. Mann W. B., Seliger H. H., Marlow W. F. and Medlock R. W. *Rev. sci. Instrum.* **31,** 690 (1960).
3. Mann W. B. and Seliger H. H. Radioactivity Standardization in the United States. *Proceedings of the Second International Conference on the Peaceful Uses of Atomic Energy, Geneva,* Vol. 21, p. 90. United Nations, New York (1958).

International Journal of Applied Radiation and Isotopes, 1961, Vol. 11, pp. 68–74. Pergamon Press Ltd. Printed in Northern Ireland

# The Half-Life of Carbon-14

D. E. WATT, D. RAMSDEN and H. W. WILSON
Atomic Weapons Research Establishment, Aldermaston, Berks.

(*Received* 27 *February* 1961)

Specific activity measurements on pure samples of carbon dioxide containing respectively 45 and 2 per cent $C^{14}$ by atoms, using mass spectrometry and proportional counting, have resulted in a new value of 5780 ± 65 years for the $C^{14}$ half-life.

Gas adsorption difficulties have been surmounted by careful gas handling and the introduction of an adsorption test. Counting rate corrections for dead-time losses, end effect, wall effect and discriminator bias have been determined.

LA PERIODE DE DEMI-VALEUR DU CARBONE-14

Des mesures de l'activité spécifique faites sur des échantillons purs de bi-oxyde de carbone contenant 45 pour cent et 2 pour cent par atomes de $C^{14}$, avec l'emploi de la spectrométrie de masses et le comptage proportionnel, ont donné une nouvelle valeur, 5780 ± 65 ans pour la période de demi-valeur du $C^{14}$.

On a surmonté des difficultés d'adsorption gazeuse par la manipulation soigneuse du gaz et par l'introduction d'une épreuve d'adsorption. On a trouvé les ajustements nécessaires aux taux de compte à cause des pertes en temps-mort, de l'effet du bout (effet géométrique), de l'effet des parois et du biais du discriminateur.

ПЕРИОД ПОЛУРАСПАДА $C^{14}$

При помощи масс-спектрометрического метода и метода пропорциональных счетчиков была измерена удельная активность образцов чистого $CO_2$, содержащих, соответственно, 45 и 2% атомов $C^{14}$. Было получено новое значение периода полураспада $C^{14}$, равное 5780 ± 65 лет.

Затруднения, связанные с адсорбцией газа, были устранены путем тщательного обращения с газом и испытаниями на адсорбцию. При определении скорости счета были сделаны поправки на мертвое время, краевой эффект, эффект стенки и смещение дискриминации.

DIE HALBWERTSZEIT VON KOHLENSTOFF-14

Messungen der spezifischen Aktivität an reinen Kohlendioxyd-Proben, welche 45 % bzw. 2% C-14 Atome enthalten und mit Hilfe von Messungen am Massenspektrographen und im Proportionalzähler durchgeführt wurden, ergaben einen neuen Wert von 5780 ± 65 Jahren für die Halbwertszeit von C-14.

Schwierigkeiten infolge von Gasadsorption wurden durch sorgfältige Behandlung des Gases vermieden und durch Einführung eines Adsorptionstests. Korrekturen für Totzeitverluste, Endeffekt, Wandeffekt und Diskriminator Einstellung wurden berücksichtigt.

## I. INTRODUCTION

Carbon-14, the naturally occurring isotope of carbon, is of well-known importance in the field of archaeological dating. The precision of dating a specimen is fundamentally dependent on the accuracy with which the $C^{14}$ half-life is known. As shown in Table 1, considerable uncertainty in this half-life still exists.

Our interest arose initially from discussions with Dr. W.B. Mann of the National Bureau of Standards whence came an agreement to carry out confirmatory mass spectrometer

TABLE 1. $C^{14}$ half-lives to date

| Authors | Date | Method | Half-life |
|---|---|---|---|
| REID *et al.*[1] | 1946 | End-window Geiger counting of solid source | 4700 ± 235–470 years |
| NORRIS and INGHRAM[2] | 1946 | End-window Geiger. Plateau slope 4 per cent/100 V | 5300 ± 800 years |
| YAFFE and GREENLAND[3] | 1948 | End-window Geiger | 7200 ± 500 years |
| HAWKINGS *et al.*[4] | 1949 | Geiger compensated counters with $CO_2 + CS_2$ | 6360 ± 200 years |
| JONES[5] | 1949 | Geiger counter with measured end effects | 5589 ± 75 years |
| MILLER *et al.*[6] | 1950 | Geiger counter with $CO_2 + CS_2$<br>Proportional counter with $CH_4 + CO_2$ | 6360 ± 190 years<br>5513 ± 165 years |
| ENGELKEMEIR and LIBBY[7] | 1950 | Geiger counter—wall effect and end corrections applied | 5580 ± 45 years |
| MANOV and CURTISS[8] | 1951 | Pairs of Geiger counters with $CO_2 + CS_2$ | 5370 ± 200 years |
| CASWELL *et al.*[9] | 1954 | From energy emission rates in extrapolation chamber. Involves average energy of $\beta$ for $C^{14}$ | 5900 ± 250 years |
| JENKS and SWEETON[10] | 1952 | Calorimetry method—assumes average energy of $\beta$ for $C^{14}$ | 6030 ± — years for 49·5 keV average energy |

analyses of the samples used in the National Bureau of Standards determination. The existence of suitable counting techniques encouraged us to undertake an independent measurement of the half-life.

A list of previous work is summarized in Table 1. The specific activity is obtained by measuring the isotopic ratio of very pure samples of carbon dioxide, highly enriched in $C^{14}$, by mass spectrometer techniques, and the disintegration rate by various counting methods or energy measurements. In the cases where end-window Geiger counters have been used, uncertainties due to self-absorption, scattering and counter sensitivity are inevitable, and it would appear that the errors on these results are somewhat optimistic with the possible exception of the values of NORRIS and INGHRAM[2].

Disadvantages in the use of $CO_2 + CS_2$ gas-filled Geiger counters used in some of the determinations include the probability of after-pulsing, adsorption on the counter walls with a consequent reduction in counter efficiency, end effects and wall effects. The use of counters of different lengths with identical cross sections have been sucessfully used to eliminate end effects. HAWKINGS *et al.*[4] have deduced that the wall effect is very small by using Geiger counters of different cross sections but equal lengths. More recently MANN *et al.*[11] have estimated the wall effect for proportional counters by varying the pressure of the gas filling. A small wall effect of $\sim$ 1 per cent was obtained for stainless-steel counters. Copper counters constructed identically had a negligible wall effect, this being attributed to the lower work function for copper. Experiments to be described later on the counters used in this work demonstrate that the effect is $\sim$ 0·2 per cent.

MILLER *et al.*[6] concluded from their measurements and an analysis of previous

work that $CO_2 + CS_2$ filled Geiger counters were 15 per cent less efficient than proportional counters. This discrepancy is not supported by the recent work of MANN *et al.*[11], where excellent agreement is obtained between Geiger and proportional counting assays.

The most recent measurements of the disintegration rate by CASWELL *et al.* and JENKS and SWEETON, using rate of energy emission in an extrapolation ion chamber and using calorimetry respectively, involve only a knowledge of the average energy of the $C^{14}$ spectrum and are independent of most of the aforementioned uncertainties.

In this work the half-life is calculated from measurements of the specific activity of active $CO_2$ using the standard techniques of mass spectrometry and proportional counting. Since the major uncertainty in gas counting is adsorption of the source on the walls of the counters, an adsorption check has been introduced to show conclusively whether or not adsorption has occurred, and only runs which pass this test have been accepted. The value of the half-life obtained from the experiments to be described is 5780 $\pm$ 65 years.

## II. GAS HANDLING PROCEDURE

Two completely independent samples of carbon dioxide gas were analysed.

The first sample was kindly supplied by DR. W. B. Mann of the National Bureau of Standards, Washington. This sample was contained in four glass ampoules of about 20 ml volume, each phial containing 1 mc activity, and nominally 45 per cent $C^{14}$ by atoms. The preparation of this sample is fully described in the preceding report by MANN, MARLOW and HUGHES. Two of the ampoules were used for the mass spectrometric determination of the isotopic ratio of carbon and the remainder for counting.

The second sample of carbon dioxide was prepared from barium carbonate at the Radiochemical Centre, Amersham, England. Two ampoules of this gas were obtained and specimens from these taken for mass spectrometric analyses, the remainder of the gas being used for disintegration rate measurements. This sample contained $\sim$2 per cent $C^{14}$ by atoms.

### (1) *Gas handling system*

A dilution factor of approximately $10^8$ is involved to produce a sample of activity suitable for counting. The gas dilution and transfer to the counters were carried out in the apparatus shown in Fig. 1. Narrow bore connexions and stopcocks were kept to a minimum reducing the possibility of adsorption. The manometer was of $\frac{1}{2}$ in. bore, this being sufficient to prevent any serious error caused by the possibility of the mercury sticking to the glass. An auxiliary manometer, fitted to the counting gas cylinder side of the glass manifold, ensured sufficient pressure to prevent possible back-diffusion of the sample gas.

To ensure sufficient accuracy in the dilution, all the volumes in the manifold were determined to better than 0·2 per cent by filling with distilled mercury and weighing. Distilled water was used to determine the volume of the 4 l. flask used as the reservoir for the diluted sample. These volumes were checked by observing the change in pressure on sharing a known volume of argon gas with the various parts of the system. Pressure readings were observed with a cathetometer with scale divisions at 0·0005 cm intervals.

The volumes of the counters and associated filling tubes were deduced by sharing with argon gas at a known pressure and volume. These agreed well with the geometrically measured volumes.

### (2) *Gas dilution*

The gas dilution was made by filling the known sample volume from the initial ampoule to a pressure of about 10 cm Hg. This was then shared with the reservoir flask which had previously been filled to 1·0 cm Hg with natural $CO_2$. The natural gas makes any possible adsorption of the active gas quite negligible. The flask was then topped up to atmospheric pressure with

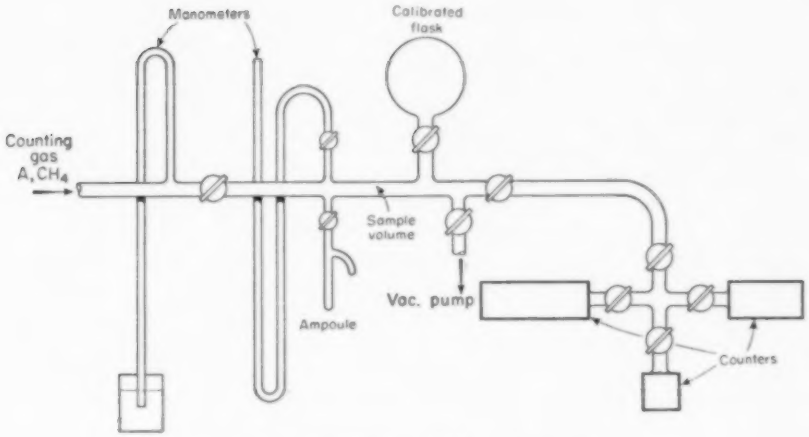


FIG. 1. Gas dilution and filling system.

TABLE 2. Measured volumes of relevant parts of apparatus at normal temperature

| | |
|---|---|
| Sample volume | 25·31 ± 0·01 ml |
| Stopcock bores | 0·620 ± 0·005 ml |
| Calibrated flask | 5195·1 ± 0·5 ml |
| Manometer to predetermined level | 34·76 ± 0·03 ml |
| Manometer volume per centimeter length | 0·515 ml |
| Large counter | 4814 ± 2 ml |
| Medium counter | 3204 ± 2 ml |
| Small counter | 1577 ± 2 ml |

$CO_2$ plus argon and methane, and allowed to mix thoroughly before closing the tap and evacuating the remainder of the system. The barometric pressure was constant throughout and the temperature noted from the thermometer scaled at 0·1°C intervals. Aliquots of the diluted sample for counting were then measured at known barometric pressure and temperatures into the sample volume as desired. Pressures in the region of 10 cm Hg were chosen to ensure sufficient accuracy in reading the height of the mercury column. This gas was then shared with the evacuated counters and the residual gas in the system carefully washed through with argon plus 10 per cent methane to atmospheric pressure. The process was carried out in many stages to avoid trapping any of the original sample in the stopcock recesses. Inconsistent counting results on preliminary runs using this filling method indicated adsorption was occurring. Consistency was attained by adding about 1 cm pressure of natural $CO_2$ to the counters before filling with the sample and counting gas. Variations of the filling procedure were tried: (i) freezing the sample and allowing it to mix slowly with the counting gas, (ii) adding natural $CO_2$ after the sample gas had been admitted to the counters. Consistent results were obtained by each method indicating negligible gas adsorption.

## III. COUNTING PROCEDURE

The main experimental corrections to counting are the accurate determination of counter and wall effects, electronic paralysis time and possible gas adsorption. The counting system was designed with these points in mind.

(1) *Counter construction*

Three proportional counters of length 22·9, 45·6 and 65·8 cm were constructed from 8·9 cm diameter brass tubing. Identical electrode assemblies with brass guard and field tubes and employing ebonite insulation

were fitted to each counter, care being taken to ensure closely similar dead volumes thus permitting measurement of the end-effect by the method of differences. Tungsten wire (0·001 in.) was used as the anode.

In the early experiments it was found that the field distortion along the length of the smaller counter was greater than in the larger counters causing unsatisfactory plateau characteristics and reduced sensitivity. Field correction tubes were fitted to remove these defects. MANOV and CURTISS[8] have shown that, if guard tube assemblies only are used, the length to diameter ratio must be greater than 6:1 to prevent field distortion along the total length of the counter.

(2) *Counting and dead time*

Two types of counter were used.

(a) A Dynatron type 1430 main and head amplifier with a Dynatron type 1009 scaler. This is a linear amplifier with conventional valves, in which the paralysis time is dependent on the number of pulses from the counter which overload the amplifier. The paralysis time was measured to be about 20 $\mu$s at the time constants and highest count rates used. Consequently a constant dead time of 25 $\mu$s was included in the circuit.

(b) A transistorized charge amplifier with an EKCO type N530 scaler. This type of amplifier is much less subject to overload troubles. The dead time of the equipment is accurately known at 60 $\mu$s and is defined solely by the scaler so that $\tau$ is independent of counting rate. Results from both methods are in good agreement. Dead-time corrections to the count rate are in the region of 5 per cent at most. Since this correction is known to an accuracy of 5 per cent the error introduced is only 0·25 per cent.

(3) *End effects*

The end effects were determined by plotting the count rate against the total counter length for each of the three counters used. The resultant plot should yield a straight line, the intercept of which gives the equivalent length of the dead volume thus permitting calculation of the end corrections. The mean of twenty results indicated an end effect of 11·5 $\pm$ 0·2 cm length at atmospheric pressure.

(4) *Wall effect and discriminator bias correction*

The wall effect can be most accurately deduced for any suitable gas pressure by using counters constructed with identical end-assemblies but with different bore tubing. However, the counters available for this experiment were constructed from the same size of tubing. The wall effect was therefore deduced by introducing the active sample into the counters and varying the added counting gas pressure

At any particular gas pressure there may exist low energy particles which, although spending all their energy in the counting gas, may not produce sufficient ion pairs to count above the discriminator bias levels. This is different from wall effect which is caused by failure of a particle to produce any ionization before colliding with the cathode walls. Since both these effects are pressure-dependent, their respective magnitudes can be resolved by obtaining discriminator bias curves for a range of gas pressures and by correcting the count rates to zero discriminator bias voltage. The half-life is then calculated and plotted against reciprocal counting gas pressure. Extrapolation to infinite pressure yields the magnitude of the wall effect.

At 1 atm gas pressure, the discriminator bias corrections were found to be 0·43, 0·61 and 1·2 per cent for the large, medium and small counters respectively, and the wall-effect correction was 0·2 $\pm$ 0·1 per cent

As any gas adsorption on the counter walls would produce an erroneous result, only runs which passed the adsorption test described in the next section were accepted for these measurements.

(5) *Counter backgrounds*

Each counter was operated inside the low-background cell[13] to keep the correction for

background to a minimum. The backgrounds on the normal discriminator bias level and operating voltage were respectively 750, 420 and 220 counts/min for the large, medium and small counters. This correction introduces a possible error of 0·02 per cent in the final result.

## IV. ADSORPTION TEST

Since the fraction of adsorped gas is proportional to the surface area of the counters, it can be shown that, for a set of counters which are in every way identical with the exception of length, the observed difference in counts between any two counters will be given by an equation of the form

$$\sigma_0 = c_t(\sigma_v - K\sigma A)$$

where $\sigma_0$ = difference in count rates; $\sigma_v$ = difference in volume; $\sigma A$ = difference in surface area; $c_t$ = disintegration rate per unit volume, and $K$ is a constant involving the fraction of gas adsorbed and the efficiency of detection of the adsorbed layer.

When $\sigma_0$ is plotted against $\sigma_v$, then the straight line of gradient $c_t$ should intercept the origin if there is no adsorption.

All runs used for calculation of the half-life were required to pass this test. After each run a blank experiment was carried out with inactive $CO_2$ and a count taken to ensure that no contamination of the system had occurred.

## V. RESULTS

Half-life determinations were made on four separate dilutions, each providing sufficient sample for several runs. Two of the dilutions were made on the National Bureau of Standards samples, and two dilutions of the Amersham sample.

## VI. MASS SPECTROMETRY

(1) Mass spectrometric analyses of the carbon dioxide samples were carried out on the Aldermaston Metropolitan-Vickers type M.S.2 spectrometer. The National Bureau of Standards samples were found to contain $44{\cdot}7 \pm 0{\cdot}1$ per cent of $C^{14}$ by atoms, whilst in the Amersham sample the percentage was $2{\cdot}20 \pm 0{\cdot}01$ per cent.

These figures are in fact the values of $\frac{C^{14} \times 100}{C^{12} + C^{13} + C^{14}}$. The samples were also examined for contamination gases which might have reduced the percentage of $C^{14}$ present but the quantities detected had no appreciable effect.

*Counting*

Typical counter plateaux are shown in Fig. 2. Also on the same Figure are the difference plateaux for the counters taken in pairs. It is from these difference plateaux that the half-life is calculated. For

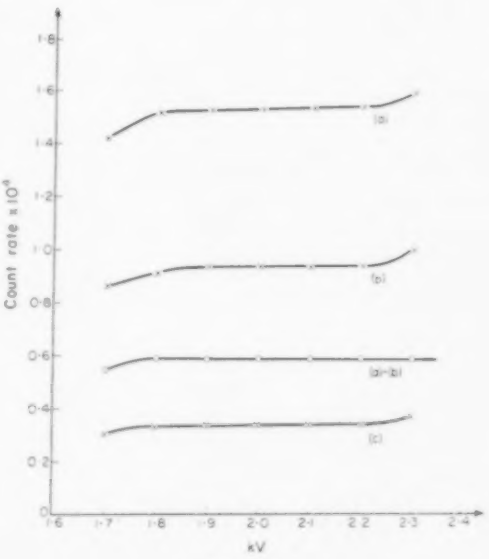


FIG. 2.

the disintegration-rate measurements, the counters were operated in the middle of the plateaux (2100 V) at 5 V discriminator bias.

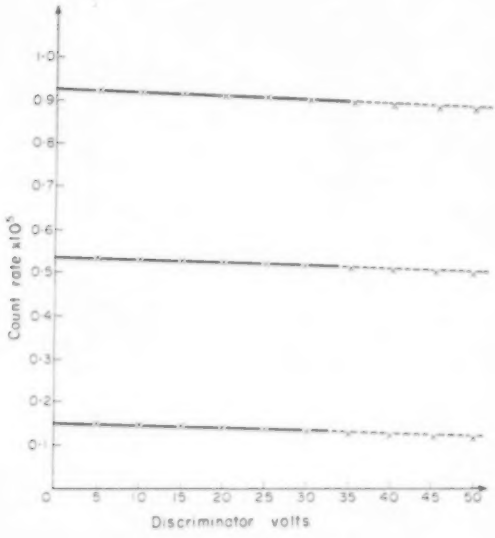


FIG. 3.

Typical discriminator bias curves are shown in Fig. 3.

The half-life obtained from six runs on the National Bureau of Standards sample which passed the adsorption test mentioned earlier is 5775 ± 36 years. This error is the standard deviation of the mean. In the case of the Amersham sample, four runs passing the adsorption test gave 5804 ± 70 years. The weighted mean of these two determinations is 5779 ± 32 years.

The results are fully corrected for dead-time, counter background, discriminator bias, wall effect and end effect. The error involved in making these corrections plus the error in the dilution factors amount to an overall uncertainty of less than 1 per cent. Taking this additional possible error into account, we conclude that the half-life is 5780 ± 65 years.

*Acknowledgments*—We wish to record our indebtedness to MISS N. C. CAMPBELL who carried out the mass spectrometric analysis. We also wish to thank the Director of the Establishment for permission to publish this paper.

## REFERENCES

1. REID A. F., DUNNING J. R., WEINHOUSE S. and GROSSE A. V. *Phys. Rev.* **70,** 431 (1946).
2. NORRIS L. D. and INGHRAM M. G. *Phys. Rev.* **70,** 772 (1946); **73,** 350 (1948).
3. YAFFE L. and GREENLAND J. M. *Phys. Rev.* **74,** 696 (1948).
4. HAWKINGS R. C., HUNTER R. F. and MANN W. B. *Canad. J. Res.* **27B,** 545, 555 (1949).
5. JONES W. M. *Phys. Rev.* **76,** 885 (1949).
6. MILLER W. W., BALLENTINE R., BENSTEIN W., FRIEDMAN L., NIER A. O. and EVANS R. D. *Phys. Rev.* **77,** 714 (1950).
7. ENGELKEMEIR A. G. and LIBBY W. F. *Rev. sci. Instrum.* **21,** 550 (1950).
8. MANOV G. G. and CURTISS L. F. *J. Res. Nat. bur. Stand.* **46,** 328 (1951).
9. CASWELL R. S., BRABANT J. M. and SCHWEBEL A. *J. Res. Nat. bur. Stand.* **53,** 27 (1954).
10. JENKS G. H. and SWEETON F. H. *Phys. Rev.* **86,** 803 (1952).
11. MANN W. B., SELIGER H. H., MARLOW W. F. and MEDLOCK R. W. *Rev. sci. Instrum.* **31,** 69 (1959).
12. WILSON H. W., RAMSDEN D. and WATT D. E. *Int. J. appl. Rad. Isotopes* **10,** 158 (1961).

International Journal of Applied Radiation and Isotopes, 1961, Vol. 11, pp. 75–91. Pergamon Press Ltd. Printed in Northern Ireland

# Mesure Absolue de l'Activité des Radionuclides par la méthode des Coïncidences Béta–Gamma à l'Aide de Détecteurs de Grande Efficacité. Etude des Coïncidences Instrumentales*

A. GANDY
Fondation Curie, Paris

(*First received* 31 *October* 1960 *and in final form* 15 *February* 1961)

Après avoir rappelé les données du problème, on étudie en détail, et d'une façon générale, la création des coïncidences instrumentales. On est ainsi amené à en distinguer deux espèces: les coïncidences "fortuites" et les coïncidences "virtuelles".

Les calculs, effectués en suivant deux méthodes distinctes, montrent que la fréquence moyenne d'apparition des coïncidences instrumentales dépend du retard que peuvent avoir les impulsions de l'une des voies par rapport à celles de l'autre voie. Les formules auxquelles on arrive tiennent compte de cet effet.

Les conclusions précédentes sont ensuite vérifiées expérimentalement.

On déduit enfin les conséquences pratiques de cette étude.

## ABSOLUTE MEASUREMENT OF THE ACTIVITY OF RADIONUCLIDES BY THE BETA-GAMMA COINCIDENCE METHOD WITH HIGH EFFICIENCY DETECTORS. STUDY OF INSTRUMENTAL COINCIDENCES

After assembling the data of the problem, an examination is made, both detailed and general, of the production of instrumental coincidences. This leads us to recognize two kinds, "chance" and "virtual" coincidences.

Calculations made according to two different methods show that the mean frequency of occurrence of instrumental coincidences depends on the delay which may be imposed on the pulses from one channel compared with those from the other channel. The formulae which are deduced allow for this effect.

The conclusions are then verified by experiment.

Finally, the practical consequences of this examination are deduced.

## ИЗМЕРЕНИЯ АБСОЛЮТНОЙ АКТИВНОСТИ РАДИОИЗОТОПОВ МЕТОДОМ БЕТА-ГАММА СОВПАДЕНИЙ ПРИ ПОМОЩИ ДЕТЕКТОРОВ ВЫСОКОЙ ЭФФЕКТИВНОСТИ. ИЗУЧЕНИЕ СЛУЧАЙНЫХ СОВПАДЕНИЙ

Приводится краткое описание основных данных по рассматриваемому вопросу. Затем дается общее и подробное обсуждение возникновения случайных совпадений. Последние можно разделить на два вида—совпадения ''ложные'' и ''истинные''.

Расчеты, сделанные двумя независимыми методами, показывают, что средняя частота случайных совпадений зависит от задержки импульсов в одном из каналов по сравнению с другим. Выведенные формулы учитывают этот эффект.

Указанные выводы проверены экспериментально.

Рассмотрены возможности практического применения полученных результатов.

* Nous avons employé le terme "instrumentales" là où il est usuel d'employer "fortuites" ou "accidentelles" car la suite de ce travail montre que les coïncidences "instrumentales" doivent être considérées comme formées de deux types distincts de coïncidences.

## ABSOLUTE AKTIVITÄTSBESTIMMUNG MIT HILFE DER $\beta$-$\gamma$- KOINZIDENZMETHODE UND ZÄHLERN MIT GROSSER AUSBEUTE. UNTERSUCHUNG DES KOINZIDENZGERÄTES

Nach einem Überblick über den Charakter des Problems wird die Entstehung von Koinzidenzen in der Apparatur im einzelnen und in allgemeiner Weise untersucht. Auf diese Weise gelangt man dazu 2 Arten von Koinzidenzen zu unterscheiden, die "zufälligen" und die "virtuellen".

Die Berechnungen, welche hierauf nach 2 verschiedenen Methoden durchgeführt wurden, zeigen, dass die Häufigkeit des Auftretens von Koinzidenzen in der Apparatur von der Verzögerung abhängen, welche die Impulse auf dem einen Wege in Bezug auf den anderen Weg besitzen.

Die Formeln zu denen man gelangt, tragen diesem Effekt Rechnung. Diese Ergebnisse werden hierauf experimentell verifiziert. Die praktischen Konsequenzen dieser Studie werden hierauf abgeleitet.

## I. INTRODUCTION

Dans un mémoire publié sous le même titre général que le présent article[1], Campion a montré l'intérêt que présente l'emploi de détecteurs de grande efficacité pour la mesure absolue de l'activité des radionuclides par la méthode des coïncidences-$\beta$–$\gamma$. Il est possible, en effet, lorsqu'on utilise un compteur $4\pi$ dans la voie-$\beta$, de mesurer l'activité de nuclides dont la désintégration s'effectue selon un schéma compliqué, sans que le résultat de la mesure soit affecté d'une façon sensible par les incertitudes que laisse subsister la connaissance imprécise des rapports d'embranchements ou des coefficents de conversion.

Il ne reste alors, comme corrections importantes, que celles qui proviennent des pertes de comptage dues aux temps morts de l'ensemble électronique et des coïncidences instrumentales provoquées par le temps de résolution nécessairement fini du sélecteur de coïncidences.

La méthode est donc susceptible de fournir des résultats très précis, si l'on sait effectuer ces corrections avec rigueur. Or les formules, qui lient les taux de comptages observés $N'$ aux taux de comptages réels $N$, dans les voies-$\gamma$ et -$\beta$, sont connues[2]:

$$N_\gamma' = \frac{N_\gamma}{1 + \theta_\gamma N_\gamma}$$

$$N_\beta' = \frac{N_\beta}{1 + \theta_\beta N_\beta}$$

$\theta_\gamma$ et $\theta_\beta$ étant les temps morts (non cumulatifs) des deux voies.

Nous avons pu établir d'autre part[3], en collaboration avec Barra*, la relation entre le nombre de coïncidences "vraies"† enregistrées $C_v$ et le nombre de coïncidences réelles† $C$, dans le cas où les deux voies ont le même temps mort (non cumulatif) $\theta$.

$$C_v = \frac{C}{1 + (N_\beta + N_\gamma - C)\theta + \mathrm{O}(N_\beta, N_\gamma, C, \theta)} \tag{1}$$

$\mathrm{O}(N_\beta, N_\gamma, C, \theta)$ étant une fonction développable en série et de l'ordre de $\theta^2/2\ N_\beta N_\gamma$. Comme $N_\gamma$ est très petit devant $N_\beta$, lorsqu'on emploie un compteur $4\pi$ dans la voie-$\beta$, $\mathrm{O}(N_\beta, N_\gamma, C, \theta)$ est le plus souvent négligeable et nous omettrons ce terme dans la suite de notre étude.

Le problème de la correction des pertes de comptage est donc résolu d'une façon satisfaisante.

Par contre, nous voulons reprendre ici le problème des coïncidences instrumentales afin de montrer l'existence d'un phénomène qui, à notre connaissance, n'a pas encore été signalé et qui risque d'introduire une erreur systématique non négligeable aux taux de comptages élevés: il s'agit de la variation du nombre de ces coïncidences en fonction du retard que l'inégalité des temps de transit des chaînes électroniques $\gamma$ et $\beta$ fait subir aux impulsions d'une voie par rapport à celles de l'autre voie.

* Institut Henri Poincaré, Paris.

† Voir la terminologie au Paragraphe II.

## II. DONNEES DU PROBLEME—DEFINITIONS DES TERMES

Considérons les deux séries d'impulsions délivrées respectivement par le compteur-$\gamma$ et le compteur-$\beta$.

Chacune de ces séries est formée de deux types d'impulsions:

(1) Les coïncidences "réelles" c'est à dire les impulsions qui correspondent à la détection simultanée du même évènement* dans les deux compteurs et que l'on retrouve dans chaque série. Nous les appellerons les impulsions $\mathscr{C}$. Il en apparaît en moyenne $C$ par seconde;

(2) Les impulsions qui correspondent à la détection dans un compteur seulement. Nous les appellerons $\nu_\gamma$ ou $\nu_\beta$ selon le cas. Leurs fréquences moyennes d'apparition sont $n_\gamma$ et $n_\beta$.

Ces deux séries sont réparties dans le temps suivant la loi de Poisson avec des paramètres ayant respectivement les valeurs:

$$N_\gamma = n_\gamma + C \tag{2}$$

$$N_\beta = n_\beta + C. \tag{3}$$

Elles passent ensuite par deux chaînes électroniques qui imposent des temps morts.

Nous considérons le cas où ces temps morts sont "non-cumulatifs", égaux dans les deux voies et ont la valeur $\theta$.

Les impulsions qui sortent de ces deux chaînes—nous les appellerons $\mathscr{N}_\beta'$ et $\mathscr{N}_\gamma'$—sont alors dirigées vers le sélecteur de coïncidences et vers deux échelles de comptage. Elles ne sont plus distribuées selon la loi de Poisson et leurs fréquences moyennes valent:

$$N_\gamma' = \frac{n_\gamma + C}{1 + N_\gamma\theta} \tag{4}$$

$$N_\beta' = \frac{n_\beta + C}{1 + N_\beta\theta}. \tag{5}$$

Ce sont les taux de comptages observés expérimentalement dans chaque voie.

En entrant dans le sélecteur de coïncidences, les impulsions sont mises sous forme d'impulsions rectangulaires de durées $\tau_\gamma$ pour celles de la voie-$\gamma$ et de durée $\tau_\beta$ pour celles de la voie-$\beta$. Les durées $\tau_\gamma$ et $\tau_\beta$ sont généralement inférieures à $\theta$. Nous supposerons de plus, pour simplifier les calculs ultérieurs, que $\tau_\gamma$ et $\tau_\beta$ sont très petits par rapport à $\theta$.

Le sélecteur enregistre une coïncidence chaque fois qu'une impulsion-$\gamma$ et une impulsion-$\beta$, mises en forme, se chevauchent dans le temps.

Le temps de résolution du sélecteur,—que nous noterons $2\tau$, pour nous conformer à l'usage établi—vaut donc

$$2\tau = \tau_\gamma + \tau_\beta.$$

Les temps de transit des électroniques $\gamma$ et $\beta$ étant strictement égaux, nous appellerons coïncidences "vraies" les coïncidences enregistrées lorsque les deux impulsions débutent au même instant et coïncidences "instrumentales" celles qui correspondant aux autres cas.

Le nombre de coïncidences "vraies", enregistrées par unité de temps, est donné par

$$C_v = \frac{C}{1 + (N_\beta + N_\gamma - C)\theta} \tag{6}$$

et le taux comptage de l'échelle des coïncidences est

$$N_e' = C_v + C_i \tag{7}$$

$C_i$ étant la fréquence moyenne des coïncidences instrumentales que nous nous proposons maintenant de déterminer.

## III. CALCUL DE LA FREQUENCE MOYENNE DES COINCIDENCES INSTRUMENTALES

Nous allons successivement effectuer ce calcul en suivant deux méthodes très différentes. Comme ces deux méthodes ne font pas appel aux mêmes hypothsèses simplificatrices, les expressions que nous obtiendrons ne seront pas strictement identiques mais les résultats numériques seront pratiquement indiscernables.

* En employant le mot évènement au lieu de désintégration, nous incluons le "mouvement propre" des compteurs dans les séries d'impulsions des voies $\gamma$ et $\beta$.

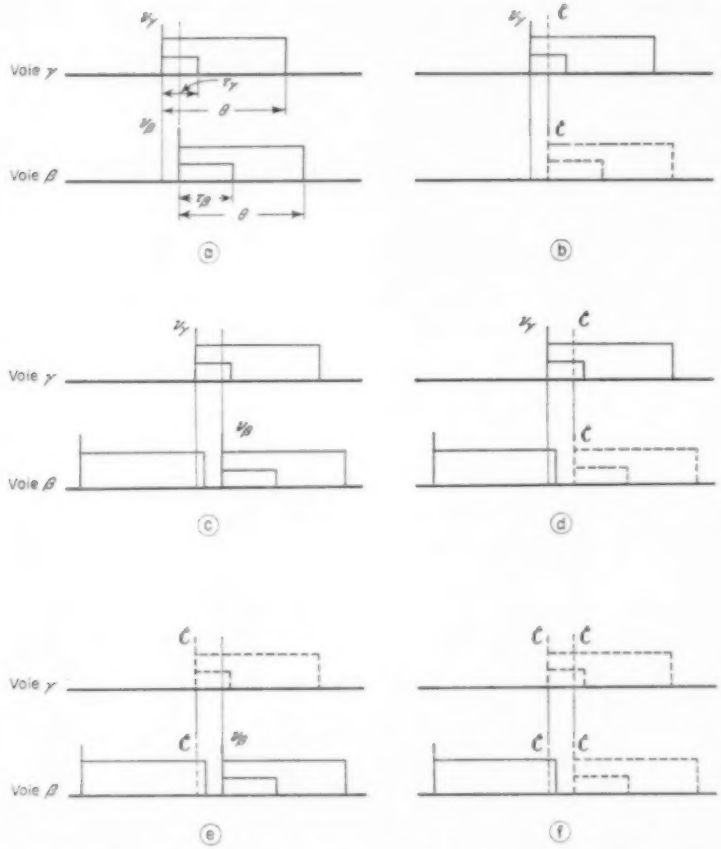


FIG. 1. Différentes configurations permettant l'enregistrement de coincidences instrumentales, la première impulsion étant comptée dans la voie $\gamma$.

Le première méthode conduit à une formule d'application commode mais certains aspects du problème lui échappent. Ces aspects seront mis en évidence par la seconde qui fait une analyse plus détaillée des phénomènes.

(A) *Première méthode de calcul*

(1) *Nous aborderons d'abord le cas où aucun décalage ne s'introduit entre les trains d'impulsions* $\mathcal{N}_\gamma'$ *et* $\mathcal{N}_\beta'$ (les temps de transit des deux chaînes électroniques étant égaux ou leur différence ayant été compensée exactement).

Considérons en premier lieu les coïncidences instrumentales qui se produisent lorsqu'une impulsion-$\beta$ est comptée pendant l'intervalle de temps $\tau_\gamma$ qui suit l'enregistrement d'une impulsion-$\gamma$. Les seuls cas possibles sont illustrés par la Fig. 1.

(a) Les dessins 1-(a) et 1-(b) correspondant aux cas où l'impulsion-$\gamma$ se produit alors que le canal $\beta$ est libre. Il est évident que cette impulsion ne peut alors être que du type $\nu_\gamma$ car si elle était du type $\mathscr{C}$ elle serait accompagnée d'une impulsion jumelle sur le canal $\beta$ et l'on enregistrerait alors une coïncidence vraie.

Par contre, l'impulsion-$\beta$ qui produira une coïncidence instrumentale peut indifféremment être du type $\nu_\beta$ (Fig. 1a) ou $\mathscr{C}$ (Fig. 1b).

Nous admettrons (voir §III C) que la

probabilité pour que le canal $\beta$ soit libre à l'instant où se produit l'impulsion-$\gamma$ vaut

$$P_1 = \frac{1}{1 + N_\beta\theta}.$$

Puisque nous nous sommes limités aux cas où $\tau_\gamma$ est très petit, la probabilité pour qu'il se produise une impulsion-$\beta$ pendant l'intervalle de temps $\tau_\gamma$ vaut

$$P_2 = N_\beta\tau_\gamma.$$

Comme le canal $\beta$ est libre au moment où cette impulsion apparaît, elle sera comptée et provoquera une coïncidence instrumentale. La probabilité d'observer cette dernière est donc $P_1 . P_2$ et, puisque le sélecteur de coïncidences reçoit en moyenne $(n_\gamma/1 + N_\gamma\theta)$ impulsions $\nu_\gamma$ pendant l'unité de temps, la fréquence moyenne probable des coïncidences instrumentales du type envisagé est égale à

$$C_{i\gamma} = \frac{n_\gamma N_\beta \tau_\gamma}{(1 + N_\gamma\theta)(1 + N_\beta\theta)}. \qquad (8)$$

(b) Les Fig. 1(c, d et f) montrent qu'il est également possible d'observer des coïncidences instrumentales lorsque l'impulsion-$\gamma$ (qui peut alors être $\nu_\gamma$ ou $\mathscr{C}$), se produit avant la fin d'un temps mort de la voie $\beta$; mais le calcul montre que la probabilité de telles configurations est extrêmement faible et que l'on peut négliger les coïncidences instrumentales de cette expèce, leur fréquence moyenne s'exprimant à l'aide d'une formule du second degré en $\tau_\gamma$.

(c) Le calcul du nombre des coïncidences instrumentales, qui se produisent lorsque la première impulsion comptée est une impulsion de la voie-$\beta$, est symétrique de celui que nous venons d'effectuer et conduit à l'expression suivante:

$$C_{i\beta} = \frac{n_\beta N_\gamma \tau_\beta}{(1 + N_\beta\theta)(1 + N_\gamma\theta)}. \qquad (9)$$

Les expressions (8) et (9) épuisant tous les cas (au second ordre près), nous obtenons, pour le nombre total de coïncidences instrumentales,

$$C_i = \frac{n_\beta N_\gamma \tau_\beta + n_\gamma N_\beta \tau_\gamma}{(1 + N_\beta\theta)(1 + N_\gamma\theta)}. \qquad (10)$$

(2) *Influence d'un délai introduit dans la voie-$\beta$.* Nous avons supposé, en A (1), que les temps de transit des deux électroniques étaient égaux ou que leur différence avait été compensée exactement. En pratique il est difficile d'effectuer cette compensation d'une façon absolue et il est important de savoir comment se modifie l'expression (10) lorsque les impulsions d'une voie sont décalées dans le temps par rapport à celles de l'autre voie.

Si nous introduisons un retard algébrique $\delta$ dans la voie-$\beta$, deux impulsions $\mathscr{C}$ jumelles (c'est à dire provenant de la détection du même évènement) seront décalées de $\delta$. Si aucune des jumelles n'a été effacée par un temps mort, on observera une coïncidence vraie lorsque $\delta$ est compris entre $-\tau_\beta$ et $+\tau_\gamma$. On n'en observera plus si $\delta$ est extérieur à cet intervalle.

Le sélecteur de coïncidences enregistrera toujours une coïncidence instrumentale si le temps, $t'$, qui sépare les instants de comptage dans les voies $\gamma$ et $\beta$ est compris entre $-\tau_\beta$ et $+\tau_\gamma$, mais cela signifie maintenant que l'instant réel d'apparition de l'impulsion-$\beta$, qui est

$$t = t' - \delta$$

doit se situer entre $(-\tau_\beta - \delta)$ et $(\tau_\gamma - \delta)$.

Tout se passe donc comme si, sans avoir introduit de délai dans la voie $\beta$, on avait modifié les durées des impulsions

$$\tau_\beta' = \tau_\beta + \delta$$
$$\tau_\gamma' = \tau_\gamma - \delta$$

tout en conservant constant le temps de résolution

$$2\tau = \tau_\beta + \tau_\gamma = \tau_\beta' + \tau_\gamma'.$$

Le nombre de coïncidences instrumentales doit donc s'écrire

$$C_i(\delta) = \frac{n_\beta N_\gamma(\tau_\beta + \delta) + n_\gamma N_\beta(\tau_\gamma - \delta)}{(1 + N_\beta\theta)(1 + N_\gamma\theta)}$$

soit encore, en tenant compte des équations (2) et (3)

$$C_i(\delta) = \frac{n_\beta n_\gamma(\tau_\beta + \tau_\gamma)}{(1 + N_\beta\theta)(1 + N_\gamma\theta)} + C\frac{n_\beta\tau_\beta + n_\gamma\tau_\gamma}{(1 + N_\beta\theta)(1 + N_\gamma\theta)} + C\frac{\delta(n_\beta - n_\gamma)}{(1 + N_\beta\theta)(1 + N_\gamma\theta)} \qquad (11)$$

Nous voyons que, lorsque $(n_\beta - n_\gamma)$, qui est égal à $(N_\beta - N_\gamma)$, est différent de zéro, il apparait un terme qui dépend linéairement de $\delta$. Or nous avons rappelé plus haut que lorsqu'on utilise un compteur $4\pi - \beta$, $N_\gamma \ll N_\beta$, de telle sorte que le nombre de coïncïdences instrumentales—donc le nombre de coincidences enregistrées—augmente lorsque le délai introduit dans la voie-$\beta$ varie de $-\tau_\beta$ à $+\tau_\gamma$.

Pour comprendre la raison de cette dépendance nous allons faire une analyse plus détaillée des phénomènes qui conduisent à l'enregistrement des coïncidences instrumentales. Cette analyse nous fournira la seconde méthode de calcul.

(B) *Seconde méthode de calcul*

Considérons à nouveau les séries d'impulsions $\mathcal{N}_\gamma$ et $\mathcal{N}_\beta'$. Jusqu'ici nous avons admis que chacune d'entre elles était formée de deux types d'impulsions mais une analyse plus fine nous conduit à en distinguer trois, les impulsions du type $\mathscr{C}$ pouvant être classées en deux espèces.

(a) Les impulsions qui correspondent à la détection du même évènement par les deux compteurs et qui cheminent par paires; une jumelle dans chaque voie. Ce sont les impulsions $\mathscr{C}_v$. Nous avons vu que leur fréquence moyenne est donnée par l'équation (6).

(b) Les impulsions qui correspondent à la détection du même évènement par les deux compteurs, mais qui ne cheminent plus par paires; l'une des jumelles ayant été éliminée par un temps mort. Nous les appellerons selon le cas $\mathscr{C}_\beta$ ou $\mathscr{C}_\gamma$. Leurs fréquences moyennes sont respectivement

$$C_\beta = \frac{C}{1 + N_\beta\theta} - C_v = \frac{Cn_\gamma\theta}{(1 + N_\beta\theta)[1 + (N_\beta + N_\gamma - C)\theta]} \quad (12)$$

$$C_\gamma = \frac{C}{1 + N_\gamma\theta} - C_v = \frac{Cn_\beta\theta}{(1 + N_\gamma\theta)[1 + (N_\beta + N_\gamma - C)\theta]}. \quad (13)$$

Nous avons bien trois espèces d'impulsions: les $\mathscr{C}_v$, les $\mathscr{C}_\beta$ ou $\mathscr{C}_\gamma$ et les $\nu_\beta$ ou $\nu_\gamma$. Nous allons successivement étudier les coïncidences qui peuvent être associées à chacune d'entre elles.

(1) *Impulsions du type $\mathscr{C}_v$—coïncidences vraies.* Tant que le délai $\delta$ est compris entre $-\tau_\beta$ et $+\tau_\gamma$, nous l'avons vu plus haut, chaque paire d'impulsions du type $\mathscr{C}_v$ donne lieu à l'enregistrement d'une coïncidence "vraie". Dès que $\delta$ excède ces valeurs, tout en restant compris entre $-(\theta - \tau_\gamma)$ et $(\theta - \tau_\beta)$, on n'enregistre plus aucune coïncidence (vraie ou instrumentale) car chaque impulsion $\mathscr{C}_v$ est nécessairement précédée et suivie d'un intervalle de temps supérieur ou égal à $\theta$ sur lequel on ne peut rencontrer aucune impulsion.

Ce n'est que lorsque $\delta$ est extérieur à l'intervalle $[-(\theta - \tau_\gamma),(\theta - \tau_\beta)]$ que les impulsions $\mathscr{C}_v$ peuvent donner lieu à des coïncidences instrumentales avec d'autres impulsions. Ces coïncidences sont alors des coïncidences "fortuites".

(2) *Impulsions $\mathscr{C}_\beta$ ou $\mathscr{C}_\gamma$—coïncidences virtuelles.*

(a) Envisageons d'abord le cas $\delta = 0$.

Les impulsions $\mathscr{C}_\beta$ et $\mathscr{C}_\gamma$ sont caractérisées par le fait qu'elles apparaissent obligatoirement pendant un temps mort de l'autre voie. Elles sont donc associées à une impulsion de l'autre voie, impulsion qui ne peut être que du type $\nu_\gamma$ ou $\nu_\beta$ selon le cas.

Considérons, à titre d'exemple, une impulsion $\mathscr{C}_\beta$. Elle apparait pendant l'intervalle de temps $\theta$ qui suit une impulsion $\nu_\gamma$ (Fig. 2a). Nous admettrons qu'elle a une probabilité égale d'apparaître à n'importe quel instant de l'intervalle $\theta$ (§IIIC). La condition pour qu'une coïncidence instrumentale soit enregistrée est que cet instant d'apparition soit compris entre 0 et $\tau_\gamma$. La probabilité d'une telle configuration est alors $\tau_\gamma/\theta$ et le nombre de coïncidences enregistrées par unité de temps est $C_\beta(\tau_\gamma/\theta)$.

Le même raisonnement s'applique aux impulsions $\mathscr{C}_\gamma$ et l'on obtient alors, pour la fréquence moyenne de ce type de coïncidences instrumentales

$$C_{iv} = C_\beta\frac{\tau_\gamma}{\theta} + C_\gamma\frac{\tau_\beta}{\theta}.$$

VOL 11 196

VOL. 11 1961

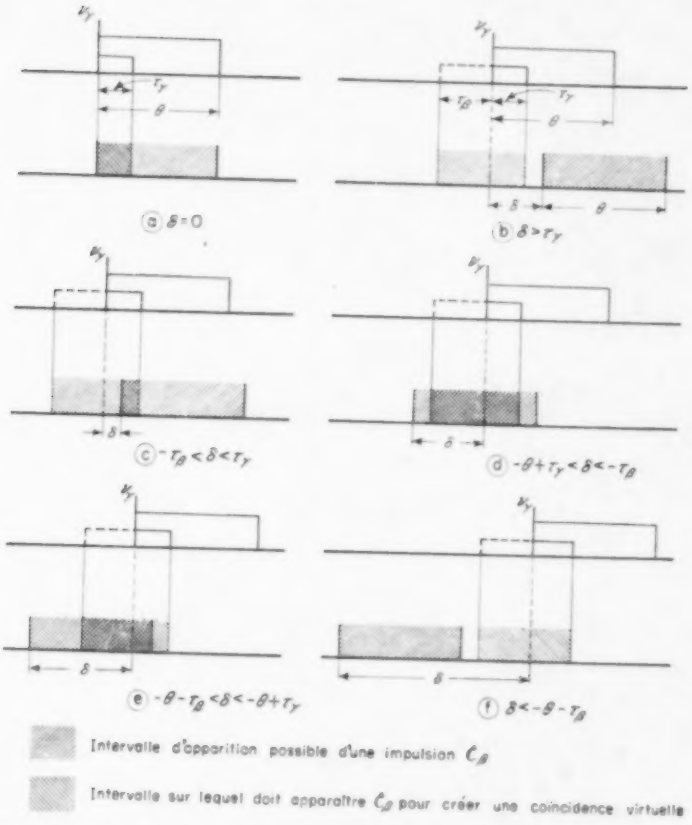


FIG. 2. Etude, selon les valeurs de $\delta$, de la probabilité d'enregistrement d'une coincidence virtuelle due à une impulsion $\mathscr{C}_\beta$.

Nous appellerons de telles coïncidences des coïncidences "virtuelles"* car elles sont produites par des impulsions qui, s'il n'y avait ni temps-morts ni temps de résolution, auraient donné lieu à l'enregistrement de coïncidences vraies.

(b) Considérons maintenant le cas général, c'est à dire $\delta \neq 0$ et examinons d'abord ce qui se passe pour les impulsions $\mathscr{C}_\beta$.

L'impulsion $\mathscr{C}_\beta$ apparaît à un instant de l'intervalle de temps $\theta$ dont le début est décalé de $\delta$ par rapport à l'impulsion $\nu_\gamma$. Une coïncidence "virtuelle" sera enregistrée, si l'instant d'apparition de $\mathscr{C}_\beta$ est situé sur l'intervalle de temps $\tau_\gamma$ qui suit l'impulsion $\nu_\gamma$ ou sur l'intervalle de temps $\tau_\beta$ qui la précède.

Différents cas sont à envisager selon les valeurs de $\delta$. Ils sont représentés schématiquement sur la Fig. 2 (b—f).

Le calcul de la fréquence moyenne des coïncidences "virtuelles" s'effectue dans chaque cas de la même façon qu'en (a) et les résultats sont rassemblés dans le Tableau 1—première ligne.

La seconde ligne du même Tableau donne les résultats concernant les impulsions $\mathscr{C}_\gamma$.

(c) Nous négligerons, car leur probabilité d'enregistrement est du second ordre en $\tau$,

* W. B. Mann, du National Bureau of Standards, nous a signalé que R. W. Haywards (N.B.S.) avait déjà reconnu la nature particulière de ces coïncidences et les rangeait parmi les coïncidences vraies. Nous sommes tombés d'accord pour les désigner par le qualificatif "virtuelles".

TABLEAU 1

| $\delta$ | | $-\theta-\tau_\beta$ | $-\theta+\tau_\gamma$ | $-\tau_\beta$ | 0 | $\tau_\gamma$ | $\theta-\tau_\beta$ | $\theta+\tau_\gamma$ |
|---|---|---|---|---|---|---|---|---|
| Fréquence moyenne des coïncidences virtuelles | Dues aux $\mathscr{C}_\beta$ | 0 | $C_\beta\dfrac{\theta+\tau_\beta+\delta}{\theta}$ | $C_\beta\dfrac{\tau_\gamma+\tau_\beta}{\theta}$ | $C_\beta\dfrac{\tau_\gamma-\delta}{\theta}$ | 0 | | |
| | Dues aux $\mathscr{C}_\gamma$ | 0 | | | $C_\gamma\dfrac{\tau_\beta+\delta}{\theta}$ | $C_\gamma\dfrac{\tau_\beta+\tau_\gamma}{\theta}$ | $C_\gamma\dfrac{\theta+\tau_\gamma-\delta}{\theta}$ | 0 |
| Fréquence moyenne des coïncidences fortuites | | ? | $\left(\dfrac{n_\gamma}{1+N_\gamma\theta}-C_\beta\right)\left(\dfrac{n_\beta}{1+N_\beta\theta}-C_\gamma\right)(\tau_\beta+\tau_\gamma)$ | | | | ? | |
| Fréquence moyenne des coïncidences instrumentales | | ? | $C_\beta\dfrac{\tau_\gamma+\tau_\beta}{\theta}+\left(\dfrac{n_\gamma}{1+N_\gamma\theta}-C_\beta\right)\times\left(\dfrac{n_\beta}{1+N_\beta\theta}-C_\gamma\right)\times(\tau_\beta+\tau_\gamma)$ | $\dfrac{C_\beta(\tau_\gamma-\delta)+C_\gamma(\tau_\beta+\delta)}{\theta}+\left(\dfrac{n_\gamma}{1+N_\gamma\theta}-C_\beta\right)\times\left(\dfrac{n_\beta}{1+N_\beta\theta}-C_\gamma\right)\times(\tau_\beta+\tau_\gamma)$ | $C_\gamma\dfrac{\tau_\gamma+\tau_\beta}{\theta}+\left(\dfrac{n_\gamma}{1+N_\gamma\theta}-C_\beta\right)\times\left(\dfrac{n_\beta}{1+N_\beta\theta}-C_\gamma\right)\times(\tau_\beta+\tau_\gamma)$ | ? | |

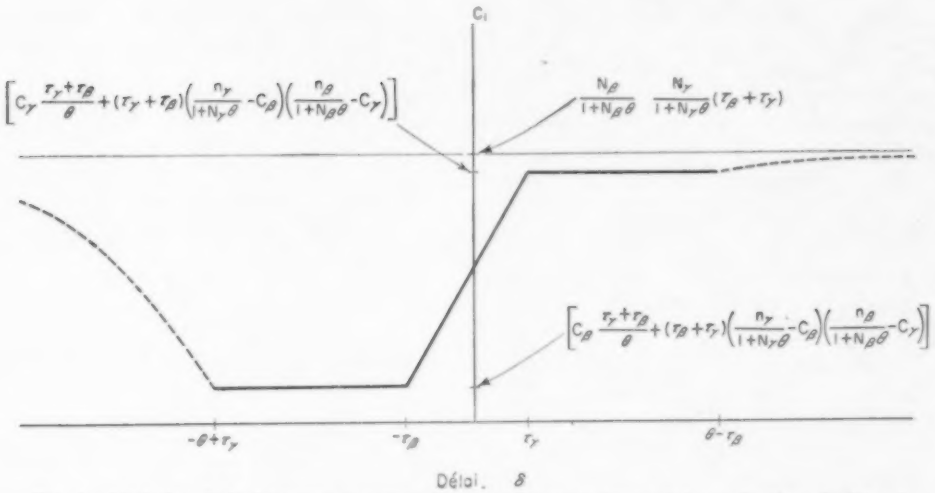


FIG. 3. Variation de la fréquence moyenne des coïncidences instrumentales en fonction du délai $\delta$ (seconde méthode de calcul). Les parties en tirets ne représentent pas le résultat d'un calcul mais indiquent l'allure probable de la courbe en dehors de l'intervalle étudié.

les coïncidences "fortuites" qui peuvent se produire entre une impulsion $\mathscr{C}_\beta$ ou $\mathscr{C}_\gamma$ et une impulsion d'un autre type qui ne lui est pas associée.

(3) *Impulsions $v_\beta$ et $v_\gamma$—coïncidences fortuites proprement dites.* Parmi les impulsions $v_\beta$, il y en a $C_\gamma$ qui sont associées aux impulsions $\mathscr{C}_\gamma$ et qui, par suite, ont une probabilité négligeable de donner lieu à des coïncidences "virtuelles".

Le même raisonnement s'applique aux impulsions $v_\gamma$ et, en définitive, il reste $\left(\frac{n_\beta}{1+N_\beta\theta}-C_\gamma\right)$ impulsions $v_\beta$ qui peuvent donner lieu à des coïncidences instrumentales avec $\left(\frac{n_\gamma}{1+N_\gamma\theta}-C_\beta\right)$ impulsions $v_\gamma$. Comme ces impulsions sont absolument indépendantes les unes des autres, les coïncidences ainsi produites seront des coïncidences "fortuites" au sens habituel de ce terme et leur fréquence moyenne d'apparition est

$$C_{if}=\left(\frac{n_\beta}{1+N_\beta\theta}-C_\gamma\right)\left(\frac{n_\gamma}{1+N_\gamma\theta}-C_\beta\right)\times(\tau_\beta+\tau_\gamma)$$

Cette dernière est indépendante de $\delta$ tant que d'autres types d'impulsions ne participent pas à la création de coïncidences "fortuites", c'est à dire tant que l'on a

$$-\theta+\tau_\gamma<\delta<\theta-\tau_\beta.$$

En dehors de ces limites, les trois espèces d'impulsions participent à la création de coïncidences "fortuites" et le calcul de la fréquence moyenne de ces dernières devient inextricable.

Cependant, lorsque $\delta$ augmente en valeur absolue, la corrélation entre les impulsions $\mathscr{N}_\beta'$ et $\mathscr{N}_\gamma'$ s'efface progressivement et on n'observe plus que des coïncidences "fortuites" dont la fréquence moyenne tend vers

$$\frac{N_\beta N_\gamma}{(1+N_\beta\theta)(1+N_\gamma\theta)}(\tau_\beta+\tau_\gamma).$$

Pour chaque valeur de $\delta$, la fréquence moyenne des coïncidences enregistrées est la somme des différents termes que nous venons d'étudier en (1), (2) et (3).

La dernière ligne du Tableau 1 rassemble tous les résultats concernant les coïncidences instrumentales.

Compte tenu du fait que $C_\gamma$ est supérieur à $C_\beta$ lorsqu'on utilise un compteur $4\pi$ dans la voie-$\beta$, la Fig. 3 représente qualitativement les variations de la fréquence des coïnci-

dences instrumentales lorsque $\delta$ passe de $(-\theta + \tau_\gamma)$ à $(\theta - \tau_\beta)$.

On retrouve, sur l'intervalle $(-\tau_\beta + \tau_\gamma)$, l'augmentation linéaire prévue par la première méthode de calcul. On constate également que, de part et d'autre de cet intervalle, la fréquence reste constante mais présente des valeurs différentes selon le signe de $\delta$.

(C) *Comparaison des résultats fournis par les deux méthodes*

Dans l'intervalle $(-\tau_\beta + \tau_\gamma)$, les deux méthodes de calcul que nous avons employées mettent en évidence le même phénomène. Il est intéressant de comparer les résultats quantitatifs auxquels on arrive dans les deux cas.

La première méthode conduit à l'équation (11). La seconde conduit à la formule qui figure en bas du Tableau 1. En tenant compte des équations (2), (3), (12) et (13), cette formule peut s'écrire

$$C_i'(\delta) = \frac{n_\beta n_\gamma(\tau_\beta + \tau_\gamma)}{(1 + N_\beta\theta)(1 + N_\gamma\theta)} - \left[\frac{C_\gamma n_\gamma}{1 + N_\gamma\theta} + \frac{C_\beta n_\beta}{1 + N_\beta\theta} - C_\beta C_\gamma\right](\tau_\beta + \tau_\gamma) + \frac{C_\beta\tau_\gamma + C_\gamma\tau_\beta}{\theta} + \delta C\frac{n_\beta - n_\gamma}{(1 + N_\beta\theta)(1 + N_\gamma\theta)}. \quad (14)$$

Le premier et le dernier terme sont respectivement identiques au premier et au dernier terme de la formule (11). La pente de la droite qui représente la variation de $C_i$ est donc la même dans les deux cas. Par contre on observe une différence entre les termes centraux. Ceci est dû à ce que les approximations faites au cours des deux méthodes de calcul ne sont pas les mêmes ainsi que nous allons le montrer maintenant.

(1) *Première méthode de calcul.* La formule (8) peut s'interpréter de la façon suivante.

Pour qu'une impulsion $N_\beta$ produise une coïncidence instrumentale du type considéré, il faut:

(a) qu'elle soit comptée dans sa propre voie. La probabilité de cette éventualité est

$$P_a = \frac{1}{1 + N_\beta\theta}$$

(b) qu'elle se produise pendant l'un des intervalles de temps $\tau_\gamma$ qui suivent une impulsion $\nu_\gamma$.

Puisqu'on néglige $\tau_\gamma^2$ devant $\tau_\gamma$, la probabilité de cette situation est

$$P_b = n_\gamma\tau_\gamma$$

(c) que l'impulsion $\nu_\gamma$ dont il vient d'être question soit comptée dans sa propre voie.

Probabilité:

$$P_c = \frac{1}{1 + N_\gamma\theta}$$

La formule (8) revient donc à écrire

$$C_i = N_\beta P_a P_b P_c.$$

Or le théorème des probabilités composées n'est applicable sous cette forme que si les évènements $a$, $b$ et $c$ sont indépendants en probabilité. Ce n'est pas le cas ici puisque les deux séries d'impulsions $\mathcal{N}_\beta$ et $\mathcal{N}_\gamma$ ont entre elles une corrélation qui est exprimée par la présence d'impulsions du type $\mathcal{C}$ dans chacune d'elles.

En particulier, l'application sous cette forme erronée du théorème des probabilités composées conduirait, pour la fréquence moyenne des coïncidences "vraies", à l'expression

$$C_v = \frac{C}{(1 + N_\beta\theta)(1 + N_\gamma\theta)}$$

alors que la valeur correcte est donnée par l'équation (1).

L'équation (11) contient donc deux approximations: d'une part tous les termes du deuxième degré en $\tau$ ont été négligés; d'autre part, le dénominateur est inexact. Ces approximations sont cependant justifiées par le fait que $C_i$ n'est qu'un terme correctif dont l'importance est relativement faible dans le cas qui nous préoccupe.

(2) *Seconde méthode de calcul.* Pour obtenir la formule (14) nous avons également effectué deux approximations.

(a) Nous avons négligé les coïncidences *fortuites* produites entre $\mathcal{C}_\beta$ ou $\mathcal{C}_\gamma$ d'une part et $\nu_\gamma'$ ou $\nu_\beta$ d'autre part, ce qui revenait à négliger *certains* termes du second degré en $\tau$.

(b) Nous avons admis que la probabilité de trouver une impulsion du type $\mathcal{C}$ sur le

VOL 11 196

temps mort qui suit une impulsion $r$ était uniforme sur l'intervalle $\theta$, c'est à dire que la probabilité d'observer une impulsion pendant un intervalle $dt$ était indépendante de la situation de cet intervalle sur le temps mort $\theta$.

Or, s'il est vrai que la probabilité d'observer une impulsion $\mathscr{C}$ sur un intervalle $dt$, choisi au hasard, s'exprime par $Cdt$, et est indépendante de l'instant $t$ où est situé $dt$ il n'en est plus de même si l'on sait que cette impulsion doit être la première à se produire après l'instant 0. La probabilité vaut alors

$$dp = e^{-Ct} Cdt.$$

La probabilité d'observer une coïncidence virtuelle avec une impulsion $\mathscr{C}_\beta$ vaut donc, si $\delta = 0$

$$P = \frac{1 - e^{-C\tau_\gamma}}{1 - e^{-C\theta}}$$

et ne devient égale à $\tau_\gamma/\theta$ que si l'on peut négliger $(C\theta)^2$ devant $C\theta$. C'est donc l'hypothèse que nous avons faite implicitement pour calculer $C_i$ par la seconde méthode. Cette hypothèse est d'ailleurs compatible avec celle qui nous avait déjà permis de négliger le terme $O(N_\beta, N_\gamma, C, \theta)$ de la formule (1).

(3) *Formule de correction complète.* Il résulte de l'analyse que nous venons de faire que ni l'une ni l'autre des expressions (11) et (14) n'est perfaitement correcte, chacune étant une approximation différente de la fréquence moyenne des coïncidences instrumentales. L'une et l'autre approximations sont toutefois justifiées pour le calcul du terme correctif que constitue $C_i$ et les résultats numériques fournis par les deux expressions sont pratiquement identiques. Or l'expression (11) se prête mieux au calcul que la formule (14). C'est donc elle que nous utiliserons pour établir une formule permettant de déterminer $C$ à partir des données expérimentales.

Pour cela, il convient d'abord de modifier la formule (11) en tenant compte des équations (2) et (3), afin de n'y laisser figurer que $N_\beta$, $N_\gamma$ et $C$. L'expression ainsi trouvée est portée dans l'équation (7) et, en considérant que, dans la plupart des sélecteurs de coïncidences, $\tau_\beta$ et $\tau_\gamma$ sont égaux (donc égaux à $\tau$), on obtient

$$N_e'(\delta, \tau) = \frac{C}{1 + (N_\beta + N_\gamma - C)\theta} + \frac{2\tau N_\beta N_\gamma - \tau C(N_\beta + N_\gamma) + \delta C(N_\beta - N_\gamma)}{(1 + N_\beta\theta)(1 + N_\gamma\theta)}. \tag{15}$$

L'équation (15) est du second degré en $C$ et l'expression que l'on obtient pour $C$ se prête mal au calcul. Or nous venons de voir que le dénominateur $(1 + N_\beta\theta)(1 + N_\gamma\theta)$ n'est qu'une approximation, il n'y a donc aucun inconvénient à le changer par l'expression peu différente $[1 + (N_\beta + N_\gamma - C)\theta]$ qui a une signification physique analogue. On obtient alors une équation du premier degré en $C$, équation dont la solution est

$$C = \frac{N_e'(\delta, \tau)[1 + \theta(N_\beta + N_\gamma)] - 2\tau N_\beta N_\gamma}{1 + \theta N_e'(\delta, \tau) - \tau(N_\beta + N_\gamma) + \delta(N_\beta - N_\gamma)}. \tag{16}$$

Cette formule est valable pour $\delta$ compris entre $-\tau$ et $+\tau$.

## IV. VERIFICATION EXPERIMENTALE

Afin de vérifier expérimentalement les conclusions précédentes, nous nous sommes proposés: (1) de montrer que l'équation (15) représente bien les variations de $N_e'$ en fonction de $\delta$ et $\tau$;

(2) de mettre en évidence la différence entre la fréquence moyenne des coïncidences instrumentales pour $\delta < -\tau$ et $\delta > +\tau$.

(A) *Appareillage*

Nous nous sommes servis, pour cette étude expérimentale, d'une installation à coïncidences $\beta$–$\gamma$ couramment utilisée pour effectuer des mesures absolues d'activité.

Cette installation est conçue selon le schéma de la Fig. 4.

Le compteur $\gamma$ utilisé est un compteur à

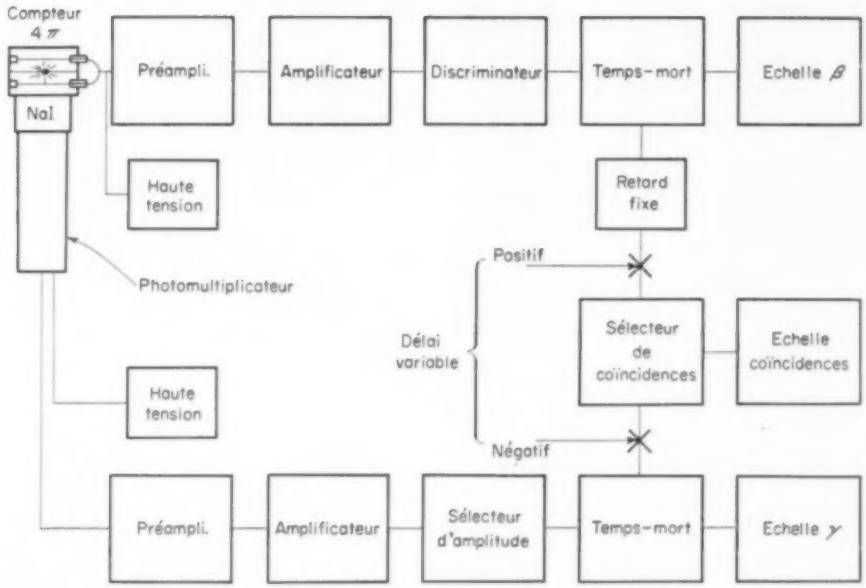


FIG. 4. Schéma de l'installation $4\pi\beta - \gamma$ utilisée au cours de cette étude.

scintillations équipé d'un cristal d'iodure de sodium, de 5 cm de diamètre et 5 cm d'épaisseur.

Le compteur $\beta$ est un compteur $4\pi$ proportionnel qui fonctionne avec une circulation de propane à la pression atmosphérique.

L'amplificateur de la voie $\beta$ n'ayant qu'une bande passante de 2M·Hz, il n'est pas possible, si l'on veut avoir un bon rapport signal-bruit, d'effectuer la mise en forme des impulsions avec une constante de temps inférieure à 1 $\mu s$. Cette mise en forme relativement longue se traduit par l'apparition de temps morts aléatoires qui peuvent atteindre 10 $\mu$s lorsque les impulsions passent par le discriminateur. Il est donc nécessaire que le temps mort imposé $\theta$ ait une valeur minima de 20$\mu$s environ pour qu'il reste bien défini jusqu'à des taux de comptage atteignant 10.000 impulsions/sec.

Le sélecteur de coïncidences permet de choisir un nombre discret de valeurs de $\tau_\beta = \tau_\gamma = \tau$ comprises entre 0,1 et 2$\mu$s.

Un retard fixe, introduit entre la voie $\beta$ et le sélecteur de coïncidences, compense la différence entre les temps de transit des deux électroniques.

Le délai variable est introduit dans le circuit en l'un des points indiqués sur la Fig. 4, selon le signe de $\delta$.

(B) *Détermination des conditions expérimentales*

Afin d'éviter toute correction de décroissance, nous avons opéré avec des sources de $Co^{60}$. Pour diminuer l'importance relative du mouvement propre du compteur $\gamma$, le sélecteur d'amplitude était réglé pour n'admettre que les pics photoélectriques. L'efficacité absolue $\varepsilon_\gamma$ du compteur $\gamma$ était ainsi égale à environ 0,03.

L'équation (15) montre que, dans ces conditions, lorsque l'activité de la source est $10^4$ d.p.s. (désintégrations par seconde), $N_e'$ varie d'environ 1% quand $\delta$ ou $\tau$ varient de 1$\mu$s.

Pour obtenir un résultat probant dans les deux cas, il serait nécessaire de mesurer $N'_e$ à 0,1% près, or une source de $10^4$ d.p.s. donne un taux de comptage de l'ordre de 300 impulsions/sec. Il faudrait donc environ 1 hr de mesure par point. Il n'est pas certain que l'électronique de la voie $\gamma$ serait suffisamment stable pour que l'ensemble des résultats ait la précision désirée.

On peut éviter cet écueil en étudiant les variations du quotient $N'_c/N'_\gamma$ qui est connu avec beaucoup plus de précision que $N_c'$ ou $N'_\gamma$ pris individuellement. Ce quotient est en effet pratiquement indépendant des fluctuations de l'électronique de la voie $\gamma$ et sa variance est beaucoup plus faible que celle de l'un ou l'autre terme. On peut le montrer de la façon suivante.

Chaque évènement compté dans la voie $\gamma$ a une probabilité $\varepsilon_\beta$ (efficacité du compteur $\beta$) d'être détecté par le compteur $\beta$ et, ensuite, une probabilité

$$[1/\{1 + (N_\beta + N_\gamma - C)\theta\}]$$

d'être enregistré par le sélecteur de coïncidences (on ne tient compte ici ni des coïncidences instrumentales ni des mouvements propres des compteurs).

On peut donc dire qu'à chaque impulsion enregistrée par la voie $\gamma$, la voie de coïncidences totalise une variable aléatoire $x$ dont la loi de probabilité est la suivante.

| $x$ | $p\ (x)$ |
|---|---|
| 1 | $\dfrac{\varepsilon_\beta}{1 + (N_\beta + N_\gamma - C)\theta}$ |
| 0 | $1 - \dfrac{\varepsilon_\beta}{1 + (N_\beta + N_\gamma - C)\theta}$ |

Lorsqu'au bout du temps $T$ la voie $\gamma$ a enregistré $N_\gamma' T$ impulsions, la voie de coïncidences en a totalisé en moyenne

$$\overline{N_c' T} = N_\gamma' T \frac{\varepsilon_\beta}{1 + (N_\beta + N_\gamma - C)\theta}$$

l'écart type sur cette moyenne étant

$$\sigma = \sqrt{N_\gamma' T \frac{\varepsilon_\beta}{1 + (N_\beta + N_\gamma - C)\theta}\left\{1 - \frac{\varepsilon_\beta}{1 + (N_\beta + N_\gamma - C)\theta}\right\}}.$$

Cela signifie que si l'on effectue une série de mesures pour lesquelles on prédétermine le nombre d'impulsions $N_\gamma' T$, on observera une série de valeurs de $N_c' T$, qui se distribueront autour de $\overline{N_c' T}$ avec l'écart type $\sigma$.

Les quotients $N_c'/N_\gamma'$ se distribueront donc autour de la valeur

$$\frac{\varepsilon_\beta}{1 + (N_\beta + N_\gamma - C)\theta}$$

avec l'écart type

$$\sigma' = \frac{\sigma}{N_\gamma' T}\ .$$

En d'autres termes, une mesure isolée donnera une valeur du quotient $N_c'/N_\gamma'$ dont la précision statistique sera

$$\frac{\sigma'(1 + (N_\beta + N_\gamma - C)\theta)}{\varepsilon_\beta} = \sqrt{\frac{1 - \dfrac{\varepsilon_\beta}{1 + (N_\beta + N_\gamma - C)\theta}}{N_c' T}}$$

On voit donc que, pour obtenir une précision de 0,1%, il suffira d'avoir

$$N_c' T = 10^6\left[1 - \frac{\varepsilon_\beta}{1 + (N_\beta + N_\gamma - C)\theta}\right]$$

c'est à dire qu'une mesure d'environ 10 min suffira pour une source de $10^4$ d.p.s., alors qu'il aurait fallu une heure pour obtenir $N_c'$ avec cette précision.

L'indépendance du résultat en fonction des instabilités de l'électronique de la voie $\gamma$ découle du fait que c'est en réalité une mesure de $\varepsilon_\beta$ (aux effets de temps-morts près) que nous effectuons; or cette grandeur est extrêmement stable.

(C) *Résultats*

(1) *Vérification de l'équation* (15). Nous avons étudié $N_c'/N_\gamma = f\ (\delta)$ pour deux valeurs de $\tau$: 1$\mu$s et 2$\mu$s. Cette étude a été faite à l'aide de deux sources dont les activités, déduites des mesures, ont été trouvées respectivement égales à 4410 et 9090 d.p.s. à 0,1% près.

Les résultats sont représentés sur les Fig. 5 et 6. Afin de les comparer à la théorie, nous avons, dans chaque cas, appliqué la méthode

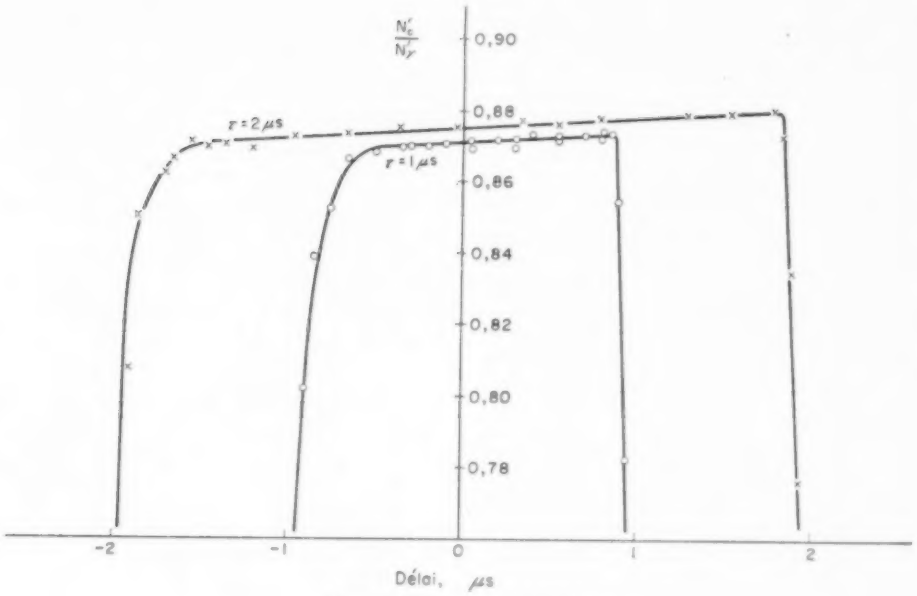


FIG. 5. Valeurs expérimentales de $N_c'/N_\gamma'$ en fonction de $\delta;(-\tau < \delta < \tau)$.

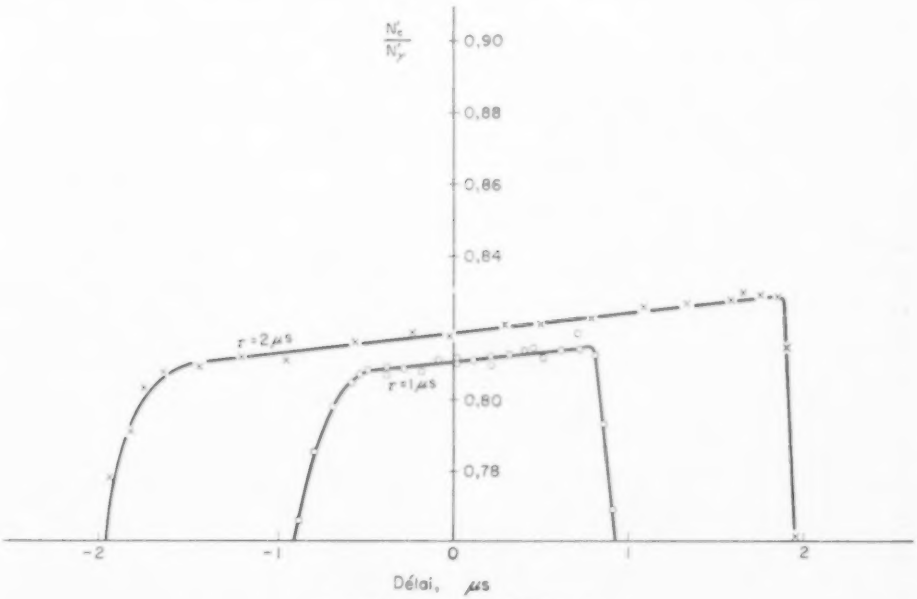


FIG. 6. Valeurs expérimentales de $N_c'/N_\gamma'$ en fonction de $\delta;(-\tau < \delta < \tau)$.

des moindres carrés pour déterminer les paramètres $a$ et $b$ de la droite

$$\frac{N_e'}{N_\gamma'} = a + b\delta.$$

On a d'autre part calculé le paramètre $b$ à partir de l'équation (15). Les valeurs ainsi trouvées sont rassemblées dans le Tableau 2

TABLEAU 2

| Activité de la source (d.p.s.) | $\tau$ ($\mu$s) | $a$ | $b$ (sec$^{-1}$) | |
|---|---|---|---|---|
| | | | Mesuré | Calculé |
| 4410 | 1 | 0,8709 ± 0,0002 | 3200 ± 320 | 3480 |
| 4410 | 2 | 0,8752 ± 0,0006 | 3200 ± 520 | 3480 |
| 9090 | 1 | 0,8102 ± 0,0004 | 6300 ± 860 | 6570 |
| 9090 | 2 | 0,8183 ± 0,0003 | 6400 ± 240 | 6570 |

Pour une même source la différence

$$a(\tau = 2) - a(\tau = 1)$$

est égale à

$$\frac{N_e'}{N_\gamma'}(\delta = 0, \tau = 2) - \frac{N_e'}{N_\gamma'}(\delta = 0, \tau = 1).$$

Elle peut être calculée théoriquement ou déduite des résultats du Tableau 2. La comparaison des valeurs ainsi obtenues est faite sur le Tableau 3.

TABLEAU 3

| Activité de la source (d.p.s.) | $a(\tau = 2) - a(\tau = 1)$ | |
|---|---|---|
| | Mesuré | Calculé |
| 4410 | 0,0043 ± 0,0006 | 0,0040 |
| 9090 | 0,0081 ± 0,0005 | 0,0076 |

(2) *Etude des coïncidences instrumentales en dehors de l'intervalle* $(-\tau, +\tau)$. Pour des raisons pratiques (délai variable disponible atteignant au maximum 3,5 $\mu$s, mesures très longues) cette étude n'a été faite que dans le cas ou $\tau = 1$ $\mu$s et pour la source la plus active.

L'ensemble des résultats expérimentaux est représenté en coordonnées logarithmiques sur la Fig. 7.

On constate que, comme le prévoit la théorie, le nombre des coïncidences instrumentales est indépendant de $\delta$, de part et d'autre de l'intervalle $(-\tau, +\tau)$, mais a une valeur différente selon le signe de $\delta$.

La comparaison quantitative entre la théorie et l'expérience est faite sur la Tableau 4 où les valeurs théoriques ont été calculées en utilisant les formules de la dernière ligne du Tableau 1.

L'examen des Tableaux 2, 3 et 4 montre que l'expérience confirme en tous points les calculs effectués au Paragraphe III.

On observe toutefois sur le Tableau 4 que les valeurs théoriques sont en dehors des limites d'erreurs des valeurs expérimentales. Cette divergence est atténuée, mais ne disparait pas complètement, si l'on tient compte des coïncidences *fortuites* que nous avons négligées et qui peuvent se produire entre impulsions des types $\mathscr{C}_\beta$ ou $\mathscr{C}_\gamma$ et $\nu_\gamma$ ou $\nu_\beta$, lorsque $\delta$ est extérieur à l'intervalle $(-\tau, +\tau)$.

Cette divergence est néanmoins très faible en valeur absolue et ne risque pas de causer une erreur appréciable lorsqu'on utilise la formule (16) pour corriger les résultats enregistrés dans la voie de coïncidences.

Avant de'n terminer les résultats enre- expérimentaux, nous voudroins faire une remarque au sujet de la courboure observée sur les Fig. 5 et 6 pour

$$-\tau < \delta < -\tau + 0{,}3\ \mu\text{s}$$

et sur la Fig. 7 pour

$$\tau < \delta < \tau + 0{,}3\ \mu\text{s}.$$

TABLEAU 4

| $\delta$ | $N_e'/N_\gamma'$ | |
|---|---|---|
| | Mesuré | Calculé |
| $< -\tau$ | $(1{,}38 \pm 0{,}15)\ 10^{-3}$ | $1{,}04\ 10^{-3}$ |
| $> +\tau$ | $(14{,}9 \pm 0{,}15)\ 10^{-3}$ | $14{,}1\ 10^{-3}$ |

Activité de la source 9090 d.p.s., $\tau = 1$ $\mu$s

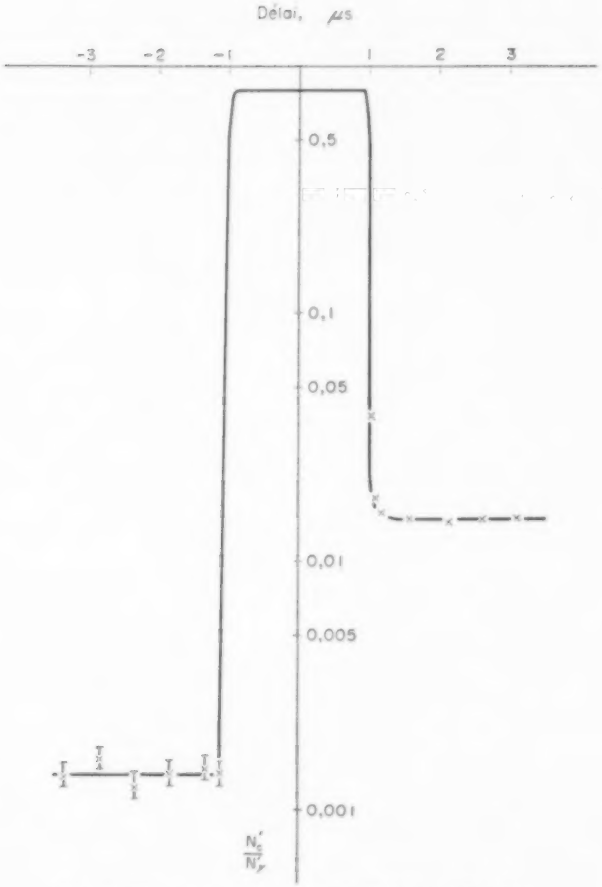


FIG. 7. Valeurs expérimentales de $N_c'/N_\gamma'$ en fonction de $\delta$. Entre $-1$ $\mu$s et $+1$ $\mu$s les valeurs sont celles de la Fig. 6 pour $\tau = 1$ $\mu$s.

Cette courbure provient du temps de montée des impulsions-$\gamma$. Celui-ci étant precisément de l'ordre de 0,3 $\mu$s, l'instant où l'impulsion-$\gamma$ arrive au sélecteur de coïncidences n'est défini qu'à 0,3 $\mu$s près. Il en résulte une perte de coïncidences lorsque $\delta$ est très peu supérieur à $-\tau$ et, au contraire, une possibilité de compter des coïncidences même lorsque $\delta$ est supérieur à $\tau$ mais plus petit que $\tau + 0{,}3$ $\mu$s.

## V. CONCLUSION

L'étude des coïncidences instrumentales que nous venons de faire nous a permis de mettre en évidence la variation de la fréquence moyenne de ces dernières en fonction du délai introduit dans la voie $\beta$. Cette variation présente deux aspects pratiques qu'il nous semble important de souligner.

(a) La formule de correction (16) à laquelle nous sommes arrivés nécessite la connaissance du délai $\delta$ avec une précision d'autant plus grande que l'activité de la source mesurée est plus élevée.

En effet, si pour une source de 2000 d.p.s., une erreur de 0,5 $\mu$s sur $\delta$ n'introduit qu'une

erreur de 0,1% sur le résultat, il suffit d'une incertitude de 0,1 $\mu$s sur $\delta$ pour que la mesure d'une source de 20,000 d.p.s.— réalisable à l'aide d'une électronique rapide[4]— soit entachée d'une incertitude de 0,2%. On voit que ce phénomène impose une limite à la précision de la mesure car il est difficile de compenser la différence des temps de transit à mieux que 0,1 $\mu$s près.

(b) L'équation (11) qui donne la fréquence moyenne des coïncidences instrumentales lorsque $\delta$ est compris entre $-\tau_\beta$ et $+\tau_\gamma$ peut être modifiée de façon à faire intervenir les efficacités $\varepsilon_\beta$ et $\varepsilon_\gamma$ des deux compteurs*. On obtient, dans le cas où $\tau_\beta = \tau_\gamma = \tau$, et à condition de négliger les mouvements propres des deux compteurs:

$$C_i(\delta, \tau) = 2N_\beta' N_\gamma' \tau \left(1 - \frac{\varepsilon_\beta + \varepsilon_\gamma}{2} + \frac{\varepsilon_\beta - \varepsilon_\gamma}{2} \frac{\delta}{\tau}\right).$$

Or nous avons vu que lorsque $\delta > \tau$ ou $\delta < -\tau$, la fréquence moyenne des coïncidences instrumentales reste constante sur un certain intervalle de variation de $\delta$ et possède alors la valeur qu'elle avait pour $\delta = \tau$ ou $\delta = -\tau$ selon le cas. On a donc

$$C_i(\delta < -\tau, \tau) = 2N_\beta' N_\gamma' \tau (1 - \varepsilon_\beta)$$
$$C_i(\delta > \tau, \tau) = 2N_\beta' N_\gamma' \tau (1 - \varepsilon_\gamma).$$

Ce n'est que lorsque $\delta$ devient très grand en valeur absolue que l'on peut retrouver la valeur que l'on obtiendrait si les deux séries d'impulsions $\mathcal{N}_\beta'$ et $\mathcal{N}_\gamma'$ étaient indépendantes; à savoir

$$C_i(\tau) = 2N_\beta' N_\gamma' \tau.$$

Ceci nous montre que l'on ne doit pas essayer de déterminer le temps de résolution d'une installation à coïncidences $4\pi\beta - \gamma$ en comptant les coïncidences instrumentales qui se produisent lorsqu'on introduit un délai supérieur à $\tau$ dans l'une des voies.

Tout au plus, peut-on obtenir une évaluation de ce temps de résolution lorsque le délai est introduit dans la voie $\beta$, si l'efficacité $\varepsilon_\gamma$ est faible.

*Remerciements*—La partie expérimentale de cette étude a été effectuée dans le laboratoire de l'Agence Internationale de l'Energie Atomique à Vienne (Autriche) avec le concours technique de Mlle. M. Chino et de Mr. M. Miguel.

L'installation de mesure utilisée avait été réalisée par Mrs. E. Keroe et H. Figdor.

## REFERENCES

1. Campion P. J. *Int. J. appl. Rad. Isotopes* **4**, 232 (1959).
2. Evans R. D. *The Atomic Nucleus* p. 787. McGraw-Hill (1955).
3. Gandy A. et Barra J. R. Unpublished data.
4. Waugh J. B. S. *Transistorized Pulse Amplifiers –III. A Transistor Amplifier for Use with Methane Proportional Counters*. CREL–828. Atomic Energy of Canada Ltd. Report No. 886 (1959).

* Nous remercions J. J. Engelmann (C. E. N. Saclay) d'avoir attiré notre attention sur cette forme de l'équation (11) et sur les conséquences qui en découlent.

International Journal of Applied Radiation and Isotopes, 1961, Vol. 11, pp. 92–100. Pergamon Press Ltd. Printed in Northern Ireland

# Méthode Rapide d'Identification des Emetteurs-β et de Dosage d'Impuretés Radioactives-β

Y. LE GALLIC, J. LEGRAND et B. GRINBERG
Centre d'Etudes Nucléaires de Saclay, Gif-sur-Yvette (S. et O.), France

(*Received* 15 *February* 1961)

VOL
11
196

Description d'une méthode simple d'analyse radioactive, permettant de déterminer avec précision l'énergie maximum des émetteurs-$\beta$, ainsi que de déceler et de doser les impuretés radioactives dans un radionuclide.

La technique décrite utilise un scintillateur plastique. On exploite le fait que la courbe du nombre d'impulsions mesurées, en fonction du seuil de discrimination est une droite, pour un émetteur-$\beta$ pur. Une relation simple entre les caractéristiques de cette droite et l'énergie maximum du spectre-$\beta$ du radionuclide, correspondant, a été établie.

## RAPID METHOD OF IDENTIFICATION OF $\beta$-RAY EMITTERS AND OF $\beta$-RADIOACTIVE IMPURITY DOSAGE

We describe a simple method of radioactive analysis, which allows an accurate determination of maximal energies of $\beta$-emitters, and detection and titration of radioactive impurities in radionuclides as well.

The method described, which uses a plastic scintillator, is based on the fact that the curve obtained by plotting the number of pulses measured against the threshold is a straight line, in the case of pure $\beta$-emitters.

We then derive a simple relation between the datas of this straight line and the maximal energy of the $\beta$-spectrum of the radionuclide under consideration.

## МЕТОД БЫСТРОЙ ИДЕНТИФИКАЦИИ $\beta$-ИЗЛУЧАТЕЛЕЙ И РАДИОАКТИВНЫХ $\beta$-ЗАГРЯЗНЕНИЙ

Описан простой метод радиационного анализа, позволяющий точно определять максимальную энергию $\beta$-излучателей, а также обнаруживать и титровать радиоактивные примеси.

Описанный метод, использующий пластмассовой сцинтилляционный счетчик, основан на том факте, что, в случае чистых $\beta$-излучателей, зависимость числа импульсов от порога дискриминации является линейной.

Найдено простое соотношение между параметрами этой прямой и максимальной энергией $\beta$-спектра.

## EINE SCHNELLE METHODE ZUR IDENTIFIZIERUNG VON $\beta$-STRAHLEN UND ZUR DOSIERUNG VON $\beta$-AKTIVEN VERUNREINIGUNGEN

Wir beschreiben hier eine einfache radioanalytische Methode, welche eine genaue Bestimmung der Maximalenergie von $\beta$-Strahlen und die Auffindung und Titration von radioaktiven Verunreinigungen gestattet.

Die beschriebene Methode, bei welcher Plastikszintillatoren verwendet werden, beruht auf der Tatsache, dass die Kurve die man erhält, wenn man die Zahl der über einem Schwellenwert gemessenen Impulse aufträgt, eine Gerade ist, wenn es sich um reine $\beta$-Strahler handelt.

Eine einfache Beziehung zwischen den charakteristischen Werten dieser Geraden und der Maximalenergie des betrachteten Spektrums wurde abgeleitet.

L'IDENTIFICATION des radionuclides a une grande importance pour l'analyse, la mesure et la recherche d'impuretés radioactives. Plusieurs méthodes sont actuellement utilisées que l'on peut diviser en deux catégories: (a) méthodes basées sur la détermination de la période de l'élément radioactif, (b) méthodes basées sur la détermination de l'énergie du rayonnement émis.

(a) *Mesure des périodes*

Si l'on dispose d'un matériel courant (compteur Geiger–Müller associé à une échelle de comptage.), on ne peut étudier de trop longues périodes ($T > 10$ jours), d'autre part on ne peut séparer deux périodes voisines. Avec un dispositif à chambres différentielles, on peut déterminer des périodes plus longues, mais il faut utiliser des sources très actives et en cas de mélange, on ne peut pas séparer deux périodes voisines.

(b) *Identification des radioéléments par l'énergie des rayonnements émis*

Si le radioélément émet un rayonnement-$\gamma$, il est facile de déterminer l'énergie du rayonnement, donc de l'identifier, à l'aide d'un spectromètre-$\gamma$ (effet photoélectrique dans un cristal d'iodure de sodium).

Si le radioélément est un émetteur-$\beta$ pur, on peut déterminer l'énergie maximum à l'aide d'un spectromètre-$\beta$ à lentille magnétique, mais l'appareillage nécessaire est très onéreux, la technique est délicate, elle nécessite des sources de forte activité; d'autre part en cas de mélange les résultats sont difficilement analysables.

Une méthode plus couramment utilisée, consiste à étudier l'absorption du rayonnement dans la matière: la courbe log Activité en fonction de l'épaisseur de l'absorbant permet de déterminer le parcours $R$ dans la substance écran. Ce parcours est l'épaisseur d'absorbant correspondant au point à tangente verticale de la courbe d'absorption de ce corps (Fig. 1). La principale difficulté de la méthode consiste à déterminer la tangente verticale. En effet, l'expérience montre que même avec des écrans réduisant la fraction transmise à $10^{-4}$ de l'intensité initiale, la tangente verticale est impossible à déterminer avec précision. Plusieurs auteurs ont proposé des solution pour lever l'indétermination qui en résulte.

FEATHER[1] a proposé de calculer le parcours $R$ par comparaison entre la courbe d'absorption étudiée et celle du RaE pris comme étalon. Cette méthode, plus précise que la simple courbe d'absorption est très longue car elle nécessite de poursuivre les

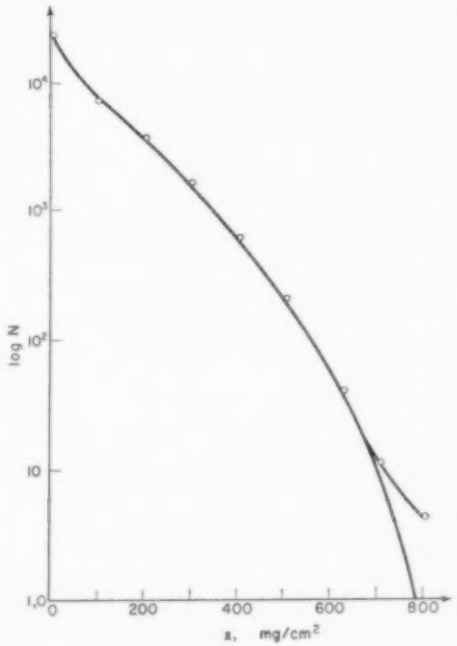


FIG. 1.

mesures jusqu'à de grandes épaisseurs d'absorbant pour éliminer les erreurs dues aux différentes formes de courbes d'absorption.

BLEULER et ZUNTI[2] ont établi par calcul les différentes formes théoriques des courbes d'absorption, en tenant compte de différents paramètres (Energie maximum, charge $Z$ du noyau, spectres interdits). Les réseaux de courbes ainsi obtenus permettent d'apporter les corrections nécessaires aux courbes expérimentales.

HARLEY et HALLDEN[3] ont mis au point expérimentalement une méthode sensiblement plus rapide qui consiste en utilisant

un système de coordonnées logarithmiques à exprimer la fraction transmise d'un rayonnement donné en fonction de la fraction transmise du rayonnement d'un corps pris comme étalon (ex: $P^{32}$) et ceci pour différentes épaisseurs d'absorbant. La courbe, pour un radionuclide pur est une droite dont le pente est caractéristique de son énergie maximum.

Ces divers procédés ont permis à leurs auteurs d'établir des relations entre les parcours dans l'aluminium et l'énergie maximum.

FEATHER: $R = 0{,}543\ E_{\beta_{max}} - 0{,}160$ pour $E_{\beta_{max}} > 0{,}8$ MeV

Glendenin
$$\begin{cases} R = 0{,}542\ E_{\beta_{max}} - 0{,}133 \text{ pour } E_{\beta_{max}} > 0{,}8 \text{ MeV} \\ R = 0{,}407\ E_{\beta_{max}}^{1{,}38} \text{ pour } 0{,}15 \text{ MeV} < E_{max} < 0{,}8 \text{ MeV} \end{cases}$$

Flammersfeld: $R = 0{,}11\ (\sqrt{1 + 22{,}4E_{\beta_{max}}^2} - 1$

BLEULER et ZUNTI: $R = 0{,}571\ E_{\beta_{max}} - 0{,}161$ pour $E_{\beta_{max}} > 1$ MeV.

Dans ces expressions, $R$ est exprimé en g/cm² et $E$ en MeV.

Ces relations appellent quelques remarques

En appliquant ces relations au $P^{32}$ d'énergie maximum 1,7 MeV, on trouve pour le parcours $R$ les valeurs suivantes, sensiblement divergentes:

782 mg/cm², Flammersfeld
766 mg/cm², FEATHER
793 mg/cm², Glendenin
810 mg/cm², BLEULER.

Parmi les différentes méthodes étudiées, celle de BLEULER et ZUNTI qui semble être la plus précise est très longue et en fait pratiquement inutilisable de façon courante.

Aussi nous sommes-nous demandé s'il n'était pas possible de trouver une grandeur, fonction simple de l'énergie maximum du spectre-$\beta$ et de détermination aisée. Si une telle grandeur existe, elle permettrait l' identification rapide des radioéléments émetteurs-$\beta$.

Si l'on considère le spectre théorique du $P^{32}$ (Fig. 2) et que l'on trace la courbe intégrale (Fig. 3), on constate que la courbe obtenue est une droite entre 0,4 et 0,9 MeV; en extrapolant cette droite jusqu'à son intersection avec l'axe des énergies, nous trouvons une énergie $E_e = 1225$ kV.

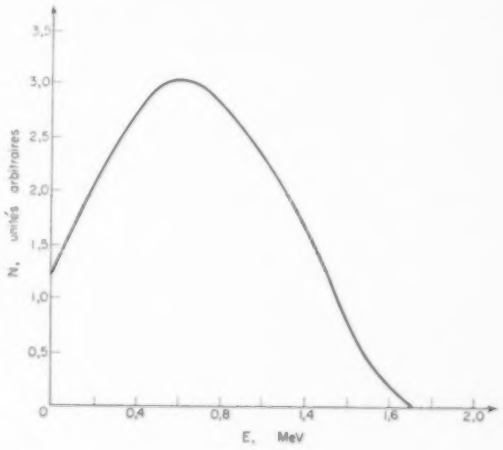


FIG. 2.

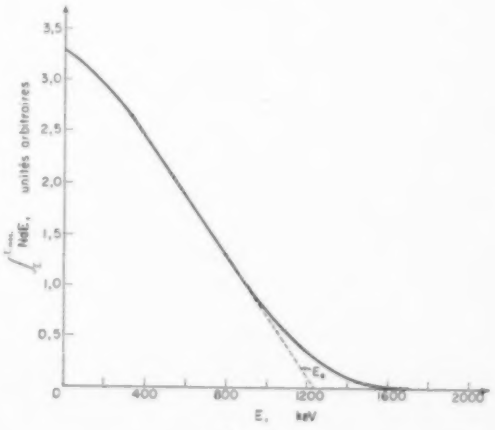


FIG. 3.

Nous avons procédé de même pour de nombreux radioéléments ($P^{32}$, $Y^{90}$, $Pr^{143}$, $Sr^{90}$, $Ca^{45}$, $Pm^{147}$, $S^{35}$) et nous avons déterminé $E_e$ dans chaque cas, les résultats sont résumés dans Tableau 1.

Pour chaque isotope, la partie rectiligne de la courbe 3, est très facile à déterminer. Nous avons ensuite examiné s'il était possible

TABLEAU 1

| Isotopes | Energies maximum (MeV) | $E_e$ (MeV) |
|---|---|---|
| $Y^{90}$ | 2,275 | 1,760 |
| $P^{32}$ | 1,7 | 1,225 |
| $Pr^{143}$ | 0,929 | 0,568 |
| $Sr^{90}$ | 0,545 | 0,316 |
| $Ca^{45}$ | 0,252 | 0,127 |
| $Pm^{147}$ | 0,227 | 0,103 |
| $S^{35}$ | 0,165 | 0,083 |

d'établir une relation entre la valeur $E_e$ trouvée et l'énergie maximum.

La courbe $E_e = f(E_{\beta_{max}})$ (Fig. 4) comporte une partie rigoureusement linéaire pour les énergies supérieures à 0,9 MeV dont l'équation est $E_e = 0{,}88$, $E_{\beta_{max}} - 0{,}27$ ($E$ est exprimé en MeV). Ceci évidemment peut paraitre surprenant compte tenu de la diversité des spectres étudiés (ex: $P^{32}$ et $S^{35}$, Fig. 2 et 5).

Au dessous de 0,9 MeV la courbe n'est plus rectiligne.

Ceci nous a conduit à nous demander s'il était possible d'obtenir également une relation linéaire à partir de spectres plus ou moins déformés tels que ceux obtenus à partir de méthodes spectrométriques courantes.

Nous avons utilisé un compteur à scintillations équipé d'un scintillateur d'anthracéne de 5 mm d'épaisseur et de 44 mm de diamètre protégé de la lumière par une fenêtre en aluminium de 2,5/100 mm.

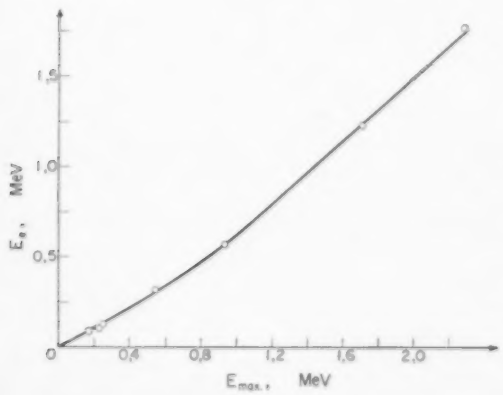


FIG. 4.

Le scintillateur est associé à un tube E.M.I 62.60; les impulsions sont envoyées sur un amplificateur à gain variable (constante d'intégration $10^{-7}$ sec, constante de différenciation: $3.10^{-6}$ sec) puis dans un discriminateur S.A.O. La haute tension appliquée sur le P.M. est 1600 V et le temps mort est de $5.10^{-6}$ sec ce qui nous permet de négliger les pertes de comptage même pour des taux de comptage élevés.

En traçant la courbe de discrimination de $P^{32}$, nous avons constaté que sur une grande partie, cette courbe était une droite, et en

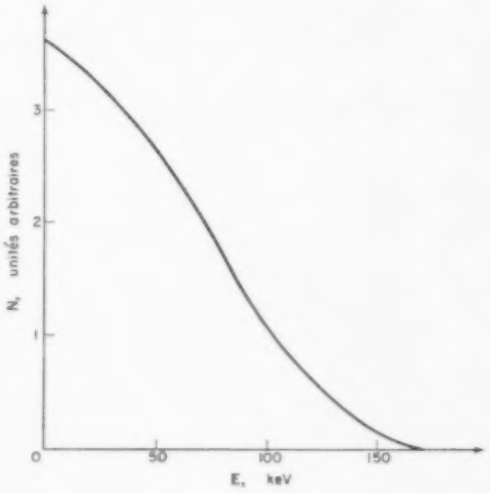


FIG. 5.

faisant varier le gain de l'ampli nous avons obtenu une famille de droites (Fig. 8).

Nous avons choisi le gain maximum ($G = 10.000$) pour pouvoir tracer les courbes de discrimination de rayonnements de faible énergie.

La droite trouvée coupe l'axe des abscisses (seuil) en un point $V$ qui semble caractéristique de l'énergie du rayonnement.

Afin de déterminer l'influence d'un certain nombre de facteurs (réflexion, absorption, distance) sur la position du point $V$ nous avons effectué les expériences suivantes.

(1) *Influence de la retrodiffusion.* Nous avons disposé sous les sources étudiées ($P^{32}$, $S^{35}$) un reflecteur de Pb de 2 mm d'épaisseur et nous avons constaté que la partie droite de

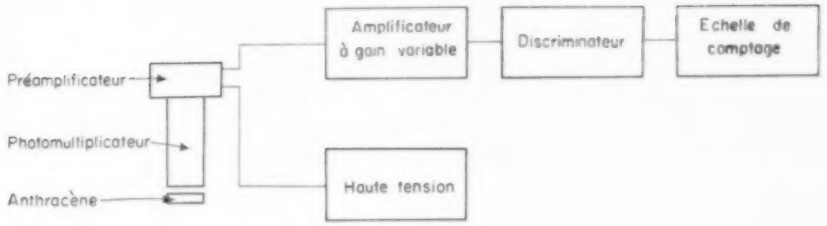


FIG. 6.

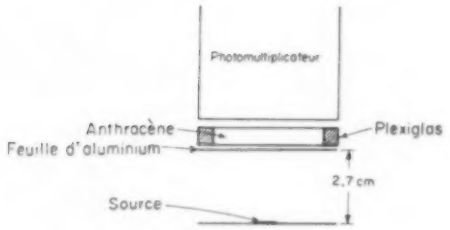


FIG. 7.

la courbe de discrimination passe toujours par le même point $V$ (Fig. 9).

(2) *Influence de l'absorption.* Entre la source de $P^{32}$ et le détecteur on a interposé un écran de 100 mg/cm² ce qui correspond environ à l'absorption moitié ($\times\frac{1}{2}$) d'un rayonnement-$\beta$ de 1,7 MeV d'énergie maximum; on constate alors que l'abscisse $V$ se trouve diminuée de 2 V ($\Delta V/V = 6\%$) (Fig. 7).

(3) *Influence de la distance source-détecteur.* (Angle solide, diffusion, reflexions etc. . . .). La courbe no. 10 montre que l'abscisse du point $V$ diminue régulièrement lorsqu'on fait croître la distance source-détecteur.

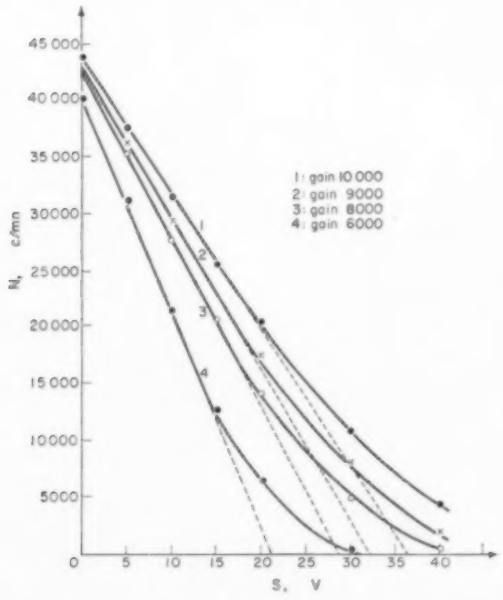


FIG. 8.

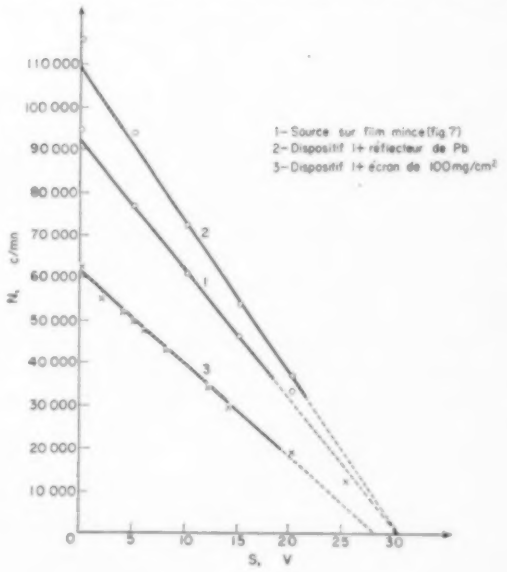


FIG. 9.

Cette variation étant en moyenne de 6% alors que la variation correspondante de l'activité mesurée était environ de 30%.

Cette partie de l'étude expérimentale montre que les phénomènes d'absorption, de réflexion, de rétrodiffusion etc. . . n'ont qu'une faible influence sur la détermination de la valeur $V$.

Afin de déterminer la correspondance entre la partie droite de la courbe de discrimination et de "spectre", nous avons

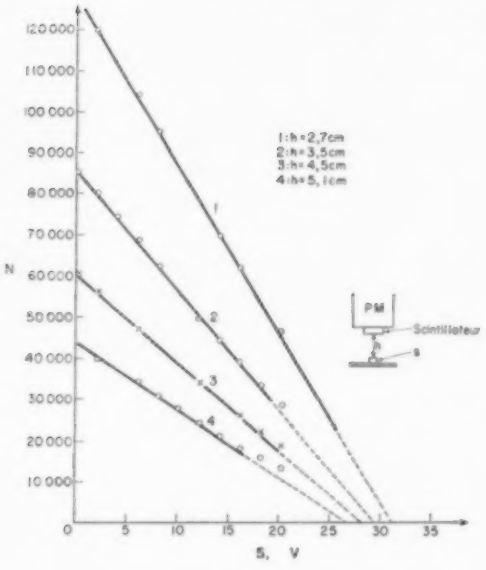


FIG. 10.

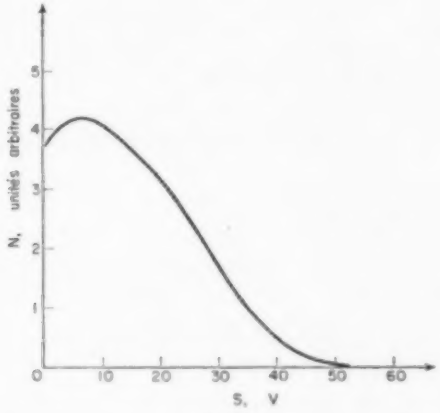


FIG. 11.

tracé le "spectre" du $P^{32}$ à l'aide d'un sélecteur à un canal, d'une largeur de bande de 1 V (Fig. 11). En intégrant la courbe obtenue, on obtient une droite qui coupe l'axe des abscisses au même point $V$.

## RESULTATS EXPERIMENTAUX

A partir de ces constatations, nous avons tracé systématiquement les courbes de discrimination d'un certain nombre de radioéléments et déterminé le point $V$ dans les conditions expérimentale décrites plus haut.

Les valeurs figurant dans le Tableau 2

TABLEAU 2

| Isotopes | Energie maximum (MeV) | $V$ (V) |
|---|---|---|
| $P^{32}$ | 1,71 | 35,6 |
| $Cs^{134}$ | 1,17 | 24,5 |
| $Cs^{137}$ | 0,514 | 12,25 |
| $Pm^{147}$ | 0,223 | 6,2 |
| $Tl^{204}$ | 0,764 | 16 |
| $Cl^{36}$ | 0,714 | 15,6 |
| $Ca^{45}$ | 0,25 | 5,5 |
| $S^{35}$ | 0,165 | 4,9 |

permettent de tracer la courbe $V = f(E_{\beta_{max}})$ (Fig. 12). Cette courbe dans le domaine étudié (0,165–1,7 MeV) est une droite dont l'équation est $V = 20\ E_{\beta_{max}} + 1{,}4$ ($E$ exprimé en MeV et $V$ en volts.)

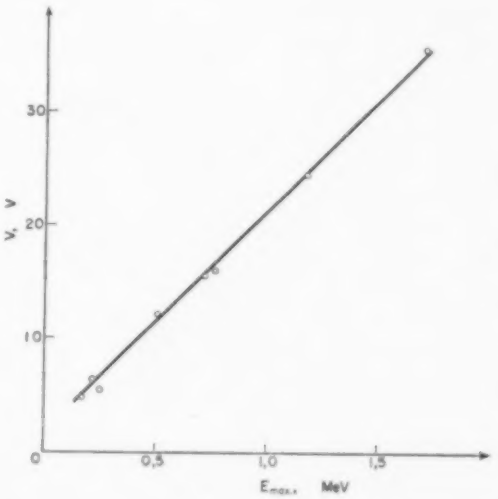


FIG. 12.

Ces résultats nous semblent intéressants puisque nous trouvons une droite dans un domaine d'énergie plus étendu que dans le cas précédent (Figs. 4 et 12).

Cette méthode permet de déterminer l'énergie d'un émetteur avec une précision de 2% pour une énergie 0,3 MeV et 5% pour une énergie inférieure à 0,3 MeV. Elle permet également de déterminer qualitativement les énergies d'un mélange.

## APPLICATION A L'IDENTIFICATION DES IMPURETES RADIOACTIVES

(1) *Analyse qualitative*

Au lieu d'utiliser des sources sèches ponctuelles déposées sur un film de mylar ou de polystyrène, il nous a paru plus pratique et plus rapide d'utiliser des sources liquides en couche épaisse: géométrie reproductible, autoabsorption invariable pour une énergie donnée, pesées évitées.

La solution (1 $cm^3$) est disposée dans une coupelle de plexiglass dont les parois ont été prealablement enduites d'un mouillant (Tween 20) de façon à n'avoir qu'un ménisque inappréciable.

La surface du liquide se trouve à 3 cm de la fenêtre du détecteur.

Nous avons tracé pour un certain nombre de radioéléments, les courbes de discrimination, et comme pour les sources solides, nous avons constaté que pour un émetteur-$\beta$ pur, cette courbe est une droite jusqu'à un certain seuil de discrimination. Si l'on extrapole cette droite jusqu'à son intersection avec l'axe des "Volts" on trouve une valeur $V$.

TABLEAU 3

| Isotopes | Energie maximum (MeV) | $V$ (V) |
|---|---|---|
| $Y^{90}$ | 2,225 | 38 |
| $P^{32}$ | 1,701 | 30 |
| $Sr^{89}$ | 1,5 | 26,8 |
| $Cs^{137}$ | 1,15 | 21,3 |
| $Tl^{204}$ | 0,768 | 15 |
| $Cl^{36}$ | 0,714 | 13,5 |
| $Cs^{134}$ | 0,658 | 13,7 |
| $Cs^{137}$ | 0,51 | 10,5 |
| $Ca^{45}$ | 0,45 | 5,5 |
| $Pm^{147}$ | 0,227 | |
| $Hg^{203}$ | 0,208 | 4,65 |

En traçant la courbe $V = f(E_{\beta_{max}})$ on trouve une droite pour les énergies supérieures à 0,5 MeV (Fig. 13) dont l'équation est:

$$V = 16E_{\beta_{max}} + 2,6$$

($V$ exprimé en volts, et $E$ en MeV).

Pour des énergies <0,5 MeV, la courbe est mal définie. Donc, comme pour une source solide, il est possible par cette méthode de déterminer l'énergie d'un rayonnement.

En résumé: pour des sources solides, il est possible de déterminer une énergie-$\beta$ entre 0,2 et 2,2 MeV en utilisant l'équation $V = 20\,E_{\beta_{max}} + 1,4$.

Pour une source liquide $V = 16\,E_{\beta_{max}} + 2,6$, et $0,5 < E_{\beta_{max}} < 2,2$ MeV.

(2) *Analyse quantitative*

Les sources et solutions utilisées ont été mesurées au compteur $4\pi$ avec une précision allant de 1 à 3 %. Ceci nous a permis d'étalonner en valeur absolue notre dispositif. A titre d'exemple le Tableau 4

TABLEAU 4

| Isotopes | Energie maximum (MeV) | Nombre de coups/minute pour 1 $\mu c$ |
|---|---|---|
| $Y^{90}$ | 2,225 | 100,000 |
| $P^{32}$ | 1,701 | 59,000 |
| $Sr^{89}$ | 1,5 | 27,000 |
| $Tl^{204}$ | 0,768 | 15,800 |
| $Cl^{36}$ | 0,714 | 14,400 |
| $Ca^{45}$ | 0,252 | 1,220 |
| $Pm^{147}$ | 0,223 | 43,5 |
| $S^{35}$ | 0,165 | 10 |

donne les résultats obtenus avec des sources liquides pour une discrimination de 2 V. Nous avons tracé la courbe du nombre de coups/minute pour 1 $\mu c/cm^3$ en fonction de l'énergie (Fig. 14), ce qui nous permet d'une part de déterminer l'activité d'une solution radioactive et d'autre part de déterminer les proportions d'impuretés décelables.

Par exemple dosage du $P^{32}$ dans $S^{35}$, du $P^{32}$ dans $Cl^{36}$ ou analyse d'autres mélanges où l'impureté radioactive est l'émetteur le plus énergique.

D'autre part on peut étudier certaines filiations par exemple $Ru^{106} + Rh^{106}$.

VOL
11
196

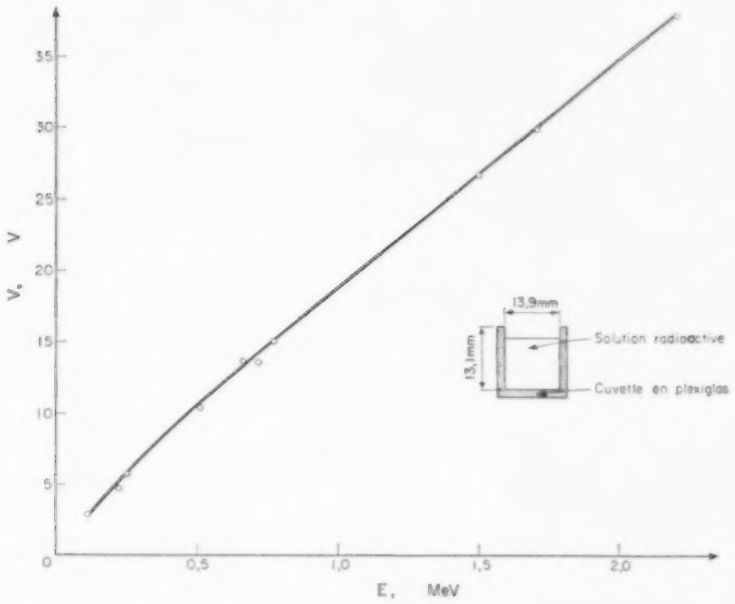


FIG. 13.

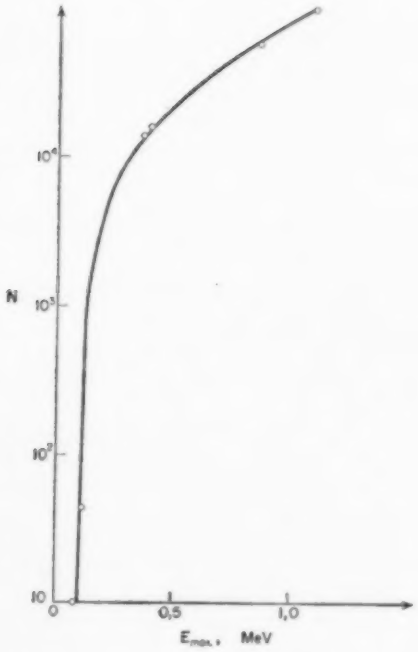


FIG. 14.

Dans le cas d'un mélange de deux émetteurs-$\beta$, la courbe $N$ en fonction du seuil de discrimination est d'abord curviligne; elle devient rectiligne, lorsque le rayonnement de l'émetteur le moins énergique est éliminé, c'est à dire dans sa partie terminale. En extrapolant à l'origine cette partie rectiligne, on obtient, si le dispositif a, au préalable, été étalonné pour le radioélément considéré, l'activité correspondante. En soustrayant la partie rectiligne extrapolée de la courbe totale, on obtient une courbe rectiligne correspondant au deuxième émetteur seul. La valeur à l'origine de $N$, permet de déduire l'activité de ce corps. Les Figs. 15 et 16, montrent les courbes obtenues dans le cas des mélanges $Sr^{90} + Y^{90}$ et $P^{32} + S^{35}$.

La méthode est donc utilisable aussi bien pour l'analyse qualitative de mélanges, que pour le dosage quantitatif des composantes. Ses possibilités, du point de vue, en particulier du dosage quantitatif, dépendent des valeurs respectives, d'une part des énergies maximales des composants, d'autre part, des activités.

Cette méthode comporte certaines limitations. En effet, pour tracer les courbes $V = f(E_{\beta_{max}})$, nous avons utilisé des émetteurs-$\beta$ et des émetteurs-$\beta$–$\gamma$ comme le $Cs^{137}$; cela a été possible dans ce dernier cas parce

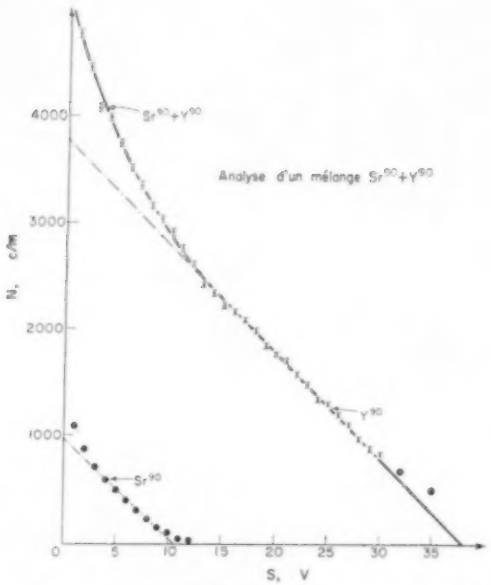


FIG. 15.

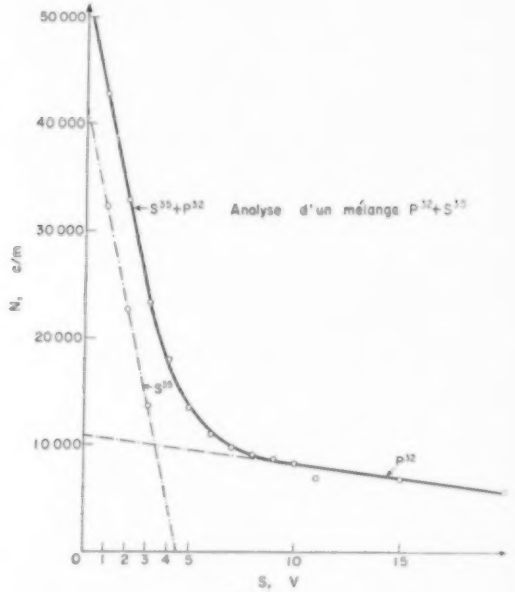


FIG. 16.

que le rayonnement-$\gamma$ du $Cs^{137}$ (0,661 MeV) ne provoque dans l'anthracène qu'un effet Compton peu important. Par contre l'analyse de l'émission-$\beta$ du $Co^{60}$ n'a pas permis de retrouver la droite caractéristique de $E_{\beta_{max}} = 0{,}306$ MeV en raison de l'énergie des $\gamma$ du $Co^{60}$ ($E_\gamma$ 1,17 et 1,33 MeV).

## CONCLUSION

La méthode qui vient d'être exposée, nous semble présenter par rapport aux méthodes habituelles un certain nombre d'avantages: (a) rapidité—une solution radioactive peut être analysée en 30 min; (b) très bonne reproductibilité permettant de s'affranchir de conditions expérimentales bien définies; (c) l'utilisation du dispositif décrit a entre autres avantages celui de permettre la mesure direte de solutions radioactives sans avoir à préparer des sources solides; (d) enfin le précision obtenue dans la détermination de l'énergie maximum de rayonnements-$\beta$ est plus grande que par les autres méthodes.

Pour $E_{\beta max} = 1{,}7$ MeV
- Méthode décrite $\dfrac{\Delta E}{E} = 2\%$
- Par absorption $\dfrac{\Delta E}{E} = 5\%$

Pour $E_{\beta max} = 0{,}3$ MeV
- Méthode décrite $\dfrac{\Delta E}{E} = 5\%$
- Par absorption $\dfrac{\Delta E}{E} = 7\%$.

## REFERENCES

1. FEATHER N. *Proc. Camb. phil. Soc.* **34,** 599 (1938).
2. BLEULER E. et ZUNTI N. *Helv. phys. acta* **19,** 375 (1946).
3. HARLEY J. H. et HALLDEN N. *Nucleonics* **13,** No. 1, 32 (1955).

International Journal of Applied Radiation and Isotopes, 1961, Vol. 11, pp. 101–107. Pergamon Press Ltd. Printed in Northern Ireland

# The Determination of Low Radon and Radium Concentrations in Liquids and Slurries

J. D. GREIG
Transvaal and Orange Free State Chamber of Mines Research Laboratories, Johannesburg, South Africa

(*First received* 21 *November and in revised form* 14 *March* 1961)

A rapid and simple procedure for the determination of low radon and radium concentrations in liquids and slurries is described. The method uses equipment available from air sampling as carried out in the United States of America and South Africa. No other specialized equipment is required.

Activated carbon is used to concentrate the radon without the necessity of extreme temperature conditions, and the method is applicable over the range $10^{-12}$–$10^{-6}$ c radon/l.

It is believed that this technique may be useful in other applications involving the concentration of volatile radioactive material, either alone or in the presence of non-volatile active material.

Applications to mining are discussed.

## LA DETERMINATION DES CONCENTRATIONS LEGERE DU RADON ET RADIUM DANS LIQUIDE ET SUSPENSIONS

Une méthode rapide pour le dosage des petites quantités de radon et de radium dans les liquides et des suspentions est décrite.

L'équipement utilisé couramment aux Etats Unis et en Afrique du Sud pour l'examen de l'air est suffisant et on n'a pas besoin de l'équipement spécial.

Le radon est concentré sur le carbon active, utilisant les températures moderées. La méthode est applicable aux quantités de $10^{-12}$–$10^{-6}$ c radon/l.

On croit que cette méthode pourait étre utilisée pour le dosage des autres substances radioactives volatiles, en absence ou en présence des substantes actives non-volatiles.

L'application de la méthode aux problèmes minières est discutée.

## ОПРЕДЕЛЕНИЕ НИЗКИХ КОНЦЕНТРАЦИЙ РАДОНА И РАДИЯ В ЖИДКОСТЯХ И ШЛАММАХ

Описан быстрый и простой способ определения низких концентраций радона и радия в жидкостяс и шламмах. Метод использует аппаратуру для отбора воздуха, применяемую в США и Южной Африке. Никакого другого специализированного оборудования не требуется.

Концентрирование радона осуществляется с помощью активированного углй и не требует создания особых температурных условий. Метод пригоден в области $10^{-12}$ — $10^{-6}$ кюри радон/литр.

Авторы считают, что данный метод пригоден и для других случаев, связанных с определением концентраций летучих радиоактивных веществ как в чистом виде, так и в присутствии летучего неактивного материала.

Рассмотрены возможности применения данного метода в шахтах.

DIE BESTIMMUNG NIEDRIGER RADON UND RADIUM KONZENTRATIONEN IN FLÜSSICKEITEN UND WÄSSERIGEN SCHLAMM

Ein einfaches und schnelles Verfahren zur Bestimmung von niedrigen Konzentrationen von Radon und Radium in Flüssigkeiten und wässerigen schlamm ist beschrieben.

Die gebräuchlichen Messinstrumente zur Bestimmung der Luftqualität, wie in Amerika und Süd-Afrika verwended, Können benützt werden. Keine Spezialgeräte sind erforderlich.

Aktivierte Kohle ist benützt um das Radon zu Konzentrieren ohne die Notwendigkeit einer extrem honen Temperatur. Die Methode kann verwended werden für den Bereich von $10^{-12}$ bis $10^{-6}$ c radon/l.

Es wird angenommen, dass die Methode nützlich sein wird für weitere Anwendungen im Zusammenhang mit der Bestimmung von flüchtigem radioaktiven Material allein oder in der Gegenwart von nicht-flüchtigem aktiven Material.

Anwendugen für die Minenindustrie sind diskutiert.

## INTRODUCTION

In the mining of uranium-bearing ore, radon gas is liberated resulting in micro-microcurie concentrations in the ventilating air. A survey of the concentrations of radon and its short-lived daughter products present in the ventilating air in South African mines is at present being carried out, using the methods developed in the United States of America and Canada.[1,2]

As indicated by the work of GILETTI and KULP[3], a possible mechanism for this radon release is by diffusion through micro-fissures in reef and country rock. Another possible additional mechanism of radon release is suggested. During the stoping of uranium reef bodies, large volumes of water are used in the various mining operations such as drilling, lashing, blasting, etc. After use, the water contains a large percentage of finely divided particulate material originating from the reef and surrounding ore body. This slurry material is drained away. During drainage, settling of the heavier mineral particles could cause a build-up of sludge rich in uranium and radium. The latter then would produce radon by radio-active decay and this could be released into the air through the overburden of water. The presence of rich uranium residues in underground dams is proven and this material is periodically worked for its uranium content. This method was therefore developed in order to examine the possible contribution from underground water and slurries to radon concentrations present in the air.

FRESCO *et al.*[4], KURODA and YOKOYAMA[5] and others have described methods for the determination of the short-lived daughters in water samples, from which the radon can be indirectly evaluated. These methods are not suitable for work on slurries.

EVANS[6] describes a comprehensive de-emanation technique for micromicrocurie amounts of radium, radon and thoron in solids, liquids and gases STOCKMANN[7], DANCER and MICHAELIS[8] and others have described similar de-emanation systems, all of which employ a large ionization chamber as the $\alpha$-detecting unit. These chambers are expensive, have to be custom made, and necessitate careful operation, so that the use of a scintillation counting system was preferred.

Activated carbon has been used (in air sampling) for the partial adsorption of radon concentrations of the order of $10^{-8}/m^3$ by CADUDAL[9], and by HURSH[10] to adsorb low radon concentrations in breath. STEHNEY *et al.*[11] adsorb radon quantitatively on activated charcoal cooled to $-80°C$, and LUCAS[12] uses this method, together with a low background scintillation counter, for estimating low radon concentrations. The work of GUBELI and STORI[13] on the adsorption isotherm of radon on activated carbon at partial pressures of radon of $10^{-12}$–$10^{-15}$ atm in various carrier gases, indicated that the technique would be suitable without the use of extreme cooling and heating conditions at these concentrations. It remained to be seen whether adsorption would still be quantitative at lower partial pressures.

## OUTLINE OF METHOD

The method consists essentially in desorbing the radon from solution by an air purge and concentrating the radon contained in this air stream by adsorption on activated charcoal at −10°C. The radon is then desorbed from the charcoal at 200°C into a counting flask and estimated after allowing 3 hr for the daughter products to come to equilibrium. Radium is subsequently estimated from measurement of the radon build up over a period of from 4 to 7 days by the same procedure. The concentrations at the sampling time are then calculated by using standard radioactive decay and growth formulae.

## DESCRIPTION OF APPARATUS

Note: The counting flask and scintillation counting equipment are those normally used for radon in mine air estimations.

(a) *Counting flask*

The counting flasks used were of approximately 200 ml capacity, pear-shaped (similar to a normal short-necked standard flask) fitted with a BI9 ground-glass joint and oblique bore stopcock. The technique of phosphoring the flask is described by HARRIS *et al.*[14]

Separate counting flasks must be used for high-level and low-level work since appreciable "plating out" of radon daughters onto the phosphor powder takes place, and this results in a gradual build-up of background count. The background count of individual flasks should be frequently checked.

(b) *Scintillation counting equipment*

A simple scintillation counter was used capable of housing the counting flasks in a light-proof mild-steel housing containing a 2 in. diameter photomultiplier* operated at 2000 V and followed by a normal pre-amplifier with a cathode-follower output. The overall gain of the pre-amplifier was 100. The counter unit was coupled with a commercial scaler.† The resolution of the whole system was approximately 5 $\mu$sec and the background count of the system with an evacuated flask was less than 1 c.p.m. No lead shielding was employed. A count rate of 5–5·5 counts/min $\mu\mu$c of radon is obtained.

(c) *Liquid or sludge container*

A 300 ml capacity gas-scrubbing bottle of the Dreschel type, similar to that described by STOCKMANN[7], was used. The sludge or water sample was introduced directly into this bottle at the sampling site, and then kept sealed until analysed.

(d) *Adsorber*

The rectangular adsorber consisted of a box with overall dimensions of $3\frac{5}{8} \times \frac{7}{8} \times 4\frac{1}{2}$ in. and was fitted with five baffle plates to ensure even flow distribution throughout the the whole of the interior volume. For good heat conductivity and strength, the adsorber was made from $\frac{1}{8}$ in. brass plate throughout. All baffle plates were recessed and held in position by countersunk screws. Silver solder was used in the assembly.

Fifty grammes (approximately 90 ml) of $\frac{1}{16}$–$\frac{1}{8}$ in. activated carbon was introduced through the filler holes and well packed, after which the filler plugs were firmly screwed home. The adsorber was then flushed with oxygen-free nitrogen and the end filler plugs and all countersunk screws silver soldered to make the adsorber air tight.

(e) *Heating and cooling baths*

The cooling bath made use of an ordinary domestic refrigerator unit and the hot bath was used at a temperature of approximately 200°C. Dow Corning Silicone fluid No. 550 was used as a heat exchange fluid in the hot bath.

For the cold bath, the ice cube compartment of a normal domestic refrigerator was replaced with a sump of capacity approximately 3 gal, filled with 35 % ethylene

* E.M.I. Type 6262.

† Isotope Developments Limited, Type 1700.

glycol in water. This coolant, cooled to approximately −15°C, was then pumped to the cold bath and overflowed back to the sump. A large capacity sump is desirable to prevent undue increase in temperature. All copper piping was well lagged with asbestos and taped over with non-porous masking tape. The flexible connexions to the bath itself were of tygon tubing. Under these conditions a stable temperature of from −8 to −10°C was obtained in the cold bath.

The hot bath was heated by a 500 W built-in immersion heater controlled off a "Variac" transformer to maintain the temperature at 200 ± 10°C.

Both baths were mounted on a rack which could be raised and lowered and moved along its axis. In this way the adsorber could be transferred quickly and easily from the hot to the cold bath and vice versa without disturbing the rest of the train.

(f) *Complete apparatus*

The fully assembled apparatus is shown in Fig. 1. One millimetre capillary glass tubing was used for connexion between bubbler and adsorber to keep the dead space to a minimum, and contact of radon with rubber tubing and stopcock grease was kept to an absolute minimum.

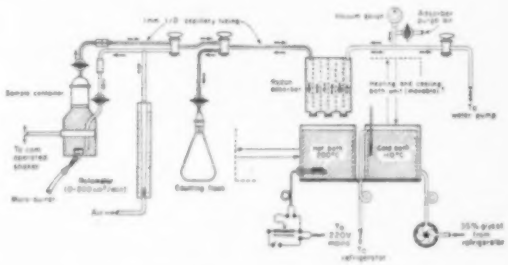

FIG. 1. Radon de-emanation and adsorption apparatus.

## PROCEDURE

The following procedure has been found to give accurate and consistent results.

(1) Heat the adsorber to 200°C and draw air through the system at approximately 200 ml/min for 2 min, by applying suction from a water pump.

(2) Evacuate the adsorber by means of an efficient water pump, and maintain for 4 min. Continue pumping until step (4).

(3) Transfer the adsorber to the cold bath (at approximately −10°C) and allow 10 min for temperature equilibrium to be established.

(4) Seal off the system from the pump, and connect the evacuated adsorber train to the water container.

(5) Heat the walls of the water container gently with a micro burner at the site of any adhering gas bubbles, sufficient to cause local boiling. If solids are present, heat the bottom of the flask enough to cause local boiling.

(6) Swirl and tilt the container gently and tap the glass walls to dislodge all gas bubbles adhering to the walls.

(7) Repeat steps (5–6). The overall temperature of the flask contents should now not exceed 40°C.

(8) Slowly open the tap on the fritted disk side of the water container and allow air to flow through the liquid at a rate of 20–30 ml/min. Direct the air flow onto the glass surfaces to dislodge any adhering gas bubbles still remaining.

(9) When the pressure in the adsorber returns to atmospheric, purge the system at the same rate (20–30 ml/min) for a further 5 min by gentle suction from the water pump, controlling the flow with the inlet tap on the sludge container.

(10) Stop the air flow by shutting the air inlet tap to the sludge container, slowly reduce the pressure in the adsorber to 15 in. of mercury, then seal off the adsorber and remove from the cold bath.

(11) Connect an evacuated counting flask to the adsorber and then insert the latter into the hot bath at about 200°C.

(12) When the vacuum gauge indicates a slight positive pressure, seal off and remove the counting flask, and connect a second flask. In this case the pressure as indicated by the gauge does not return to atmospheric. When steady conditions are indicated, air is purged through the adsorber into the counting flask utilising the remaining vacuum in the flask. The counting flask and the adsorber are now closed off and the counting flask removed.

(13) Allow 3 hr for radon to come to equilibrium with its short-lived daughter products before counting the two flasks in the scintillation counting equipment. (Note: Counting flasks are previously calibrated against a known concentration of radon gas developed in a radium solution bubbler as described by HOLADAY *et al.*[1])

(14) Allow the liquid or slurry in the container to stand for 4 or 5 days, then repeat the whole procedure to determine radon growth from any radium present so that the latter can be estimated.

## RESULTS

The following results were obtained in testing the apparatus, using a standard radium chloride solution obtained from Harwell, England.

A maximum count time of 30 min was adopted for this type of work as a compromise between accuracy and expediency.

| 1–10 $\mu\mu$c | | 10–100 $\mu\mu$c | | 100–1000 $\mu\mu$c | |
|---|---|---|---|---|---|
| Standard | Experimental | Standard | Experimental | Standard | Experimental |
| 0·9 | 1·4 | 18·2 | 22·1 | 180 | 180 |
| | | | | 186 | 196 |
| 1·8 | 2·4 | 18·3 | 17·6 | 193 | 181 |
| | | | | 199 | 228 |
| 3·2 | 3·9 | 32·8 | 36·0 | 310 | 297 |
| | | | | 416 | 399 |
| 5·7 | 6·0 | 33·9 | 33·2 | 488 | 453 |
| | | | | 896 | 896 |
| 7·5 | 8·3 | 93·2 | 89·5 | 1020 | 1001 |
| 9·6 | 13·1 | | | | |

Estimation of the precision of the method was made in terms of the coefficient of variation (c.v.) and standard deviation (s.d.), using the transformation $z = x^{\frac{1}{2}}$, where $x$ is the concentration and $z$ has the constant variance $\delta^2$. Applying this transformation, $\delta^2$ was found to be 0·00457.

As $\mathrm{var}(z) = \delta^2$ and $z = x^{\frac{1}{2}}$, c.v. $(x)$ and s.d.$(x)$ are given by

$$\text{c.v.}(x) = \frac{4\delta}{x^{\frac{1}{2}}} \times 100 \text{ per cent}$$

$$\text{s.d.}(x) = 4\delta x^{\frac{1}{2}}.$$

| Radon ($\mu\mu$c) | c.v.$(x)$ (%) | s.d.$(x)$ |
|---|---|---|
| 1 | 27·0 | 0·27 |
| 2 | 22·7 | 0·45 |
| 10 | 15·2 | 1·5 |
| 50 | 10·2 | 5·1 |
| 100 | 8·6 | 8·6 |
| 500 | 5·7 | 28 |
| 1000 | 4·8 | 48 |
| 10,000 | 2·7 | 270 |
| 10,000–300,000 | 2·4 | — |

The following are indicative of results obtained on mine water sludge samples analysed to date.

(The uranium results were obtained by standard fluorimetric methods using nitric acid–hydrofluoric acid digestion followed by "dilution" and "spiking" techniques.)

The high radium and uranium values observed in three of the samples were associated with relatively high solids content. As yet no tests have been made to distinguish between radon and radium associated with liquid or solid phases.

## DISCUSSION

Using this apparatus and technique, adsorption of radon is quantitative up to $3 \times 10^{-7}$ c (or $1 \times 10^{-6}$ c/l. assuming a 300 ml sample). Quantities of radon greater than $3 \times 10^{-7}$ c may be analysed by using a lower temperature of adsorption, or by taking a smaller sample to bring the final concentration within the range of the apparatus. The lower limit is determined by the counting apparatus. For accurate work at concentrations below $5 \times 10^{-12}$ c/l., a low-level counter as described by LUCAS[12] should be used and the purging gas pre-treated to remove trace radon concentrations.

Some uncertainty exists as to the best conditions for quantitative de-emanation of a gas in these sub-micro amounts. (The amount of radon gas involved is of the order of 1 $\mu$ml.) From preliminary experiments carried out at atmospheric pressure, it appears that about 75 per cent of the radon activity in radium solutions occurs in the air space above the liquid while the remainder is still present in the liquid itself. The radon present in the liquid is believed to be dissolved and can be removed by boiling.

Boiling the sample, as a means of liberating radon from the liquid, results in a large amount of water vapour which interferes with the adsorption and counting. Removal of this vapour by condensation or other means would introduce a possible loss of

TABLE 1

| Type of water or sludge | | Rn concentration ($\mu\mu$c/l.) | Ra concentration ($\mu\mu$c/l.) | U concentration (p.p.m.) |
|---|---|---|---|---|
| Fissure water | (clear) | 1540 | 28 | 0·005 |
| Drain water (containing sludge) from drive | | 110 | 738 | 9·1 |
| Drain water (containing sludge) from working stopes | | 696 | 3,220 | 57 |
| Machine water | (cloudy) | 35 | 240 | 2·0 |
| Surface water drainage | (cloudy) | 19 | 29 | <0·005 |
| Tap water | (clear) | <1 | <1 | <0·005 |

radon by solution. The vacuum system outlined in the procedure overcomes these difficulties. Decreasing the pressure above the liquid in the bubbler causes microscopic gas bubbles to expand and rise to the surface. This is facilitated by swirling and tapping the container while under vacuum, and by local heating with a micro burner. Bubbles still remaining on the glass surfaces are swept off by directing the flow of purging air onto the walls of the container where they are situated. By this means removal of all the radon from the air space above the liquid, the liquid itself and any adsorbed on the walls is effectively achieved.

With the design of the small volume de-emanating bubbler of HOLADAY *et al.*[1], the purging air effectively sweeps the walls and the total volume of liquid enclosed. It was not practical to scale up their design to accommodate the larger sample required for sensitivity at the low radon concentrations involved.

Decreasing the pressure in the system to 15 in. of mercury does not cause any significant desorption of radon from the activated carbon.

In the case of slurries or suspensions, this method is liable to underestimate radon and radium trapped in the interior of larger particles. It will estimate, however, the total amount of radon which could possibly be released from the slurry. For estimating the emanation of radon from mine water and slurries into the ventilating air, this was the desired objective.

To estimate radium only, the first de-emanation may be omitted. The sample is boiled vigorously with aeration for 10 min to remove radon. If the radium content is high (above 1 $\mu$c/l.), a 10 ml aliquot is introduced into the small volume bubbler of HOLADAY *et al.*[1], sealed, allowed to stand for 2–3 days and then the radon evolved determined by de-emanation into a single counting flask. If the radium content is below 1 $\mu$c/l., then the radon evolved from the radium in a 300 ml aliquot is determined as described above.

With suitable training, this method is suitable for operation by semi-skilled personnel. In an eighth of our working day, one operator can complete eight de-emanations and all the attendant counting. This method has been in use for several months in these laboratories on mine water samples with satisfactory results.

## APPLICATION TO OTHER GASES

The method described is suitable for the determination of an $\alpha$-active gaseous material. Where strong $\beta$- or $\gamma$-activity is desired to be determined, the adsorber itself could be designed for direct evaluation within a suitable detector. Due to the relatively high background found with $\beta$- or $\gamma$-counting equipment and other factors, the sensitivity of the method would, however, be reduced.

For volatile components the system of DHONT and WEURMAN[15] could be adapted.

*Acknowledgments*—My thanks are due to the Transvaal and Orange Free State Chamber of Mines for permission to publish this paper, to my colleagues in the, Research Laboratories for their valuable assistance and to MR. S. R. RABSON for his encouragement and advice.

## REFERENCES


1. *Control of Radon and Daughters in Uranium Mines and Calculations on Biological Effects.* U.S. Public Health Service, Publication No. 494 (1957).
2. Simpson S. D., Steward C. G., Yourt G. R. and Blov H. *Proceedings of the Second International Conference of the Peaceful Uses of Atomic Energy, Geneva*, P/219, Vol. 23, 195. United Nations, New York (1958).
3. Giletti B. J. and Kulp J. L. *Amer. Min.* **40,** 481 (1955).
4. Fresco J., Hardy E. and Harley J. United States Atomic Energy Commission. Report NYO-4664 (1955).
5. Kuroda P. K. and Yokoyama Y. *Analyt. Chem.* **26,** 1509 (1954).
6. Evans R. D. *Rev. sci. Instrum.* **6,** 99 (1935).
7. Stockmann L. L. *Radium Assay of Ores and Sludges by the Radon Method.* U.S. National Bureau of Standards, Internal Report. (December 1954).
8. Dancer G. H. C. and Michaelis M. *Radio-Chemical Centre*, U.K. Atomic Energy Authority: Report RCC/M-10 (June 1951).
9. Cadudal M. *J. Phys. Radium* **16,** 479 (1955).
10. Hursh J. B. *Nucleonics* **12,** 62 (1954).
11. Stehney A. F., Norris W. P., Lucas H. F. and Johnstone W. H. *Amer. J. Roentgenol.* **73,** 774 (1955).
12. Lucas H. F. *Rev. sci. Instrum.* **28,** 9 (1957).
13. Gubeli O. and Stori M. *Helv. chim. acta* **37,** 2224 (1954).
14. Harris W. B., LeVine H. D. and Watnick S. I. *Arch. industr. Hlth.* **16,** 493 (1957).
15. Dhont J. H. and Weurman C. *Analyst* **85,** 419 (1960).


VOL.
11
1961

International Journal of Applied Radiation and Isotopes, 1961, Vol. 11, pp. 108–113. Pergamon Press Ltd. Printed in Northern Ireland

# Measurements in a Total-Body Irradiation Facility*

A. C. MORRIS, JR.
Oak Ridge Institute of Nuclear Studies, Oak Ridge, Tennessee, U.S.A.

(*Received* 20 *April* 1961)

A total-body irradiation facility for human patients has been in clinical operation at the Oak Ridge Institute of Nuclear Studies, Medical Division, since May 1960. Before that date measurements were made to determine the radiation parameters. Investigations were made concerning room backgrounds, radiation leakage from nearby teletherapy rooms, uniformity of the exposure field, exposure rates available for treatment purposes and spectral changes at different exposure rates. Rate measurements were made with an ionization probe; spectral data were obtained with a scintillation crystal. Exposure rates are adjustable from 286 r/hr to 1·8 r/hr in thirty-two steps.

## DES MESURES DANS UNE FACILITE POUR L'IRRADIATION DU CORPS ENTIER

Une facilité pour l'irradiation du corps entier des malades humains est en fonctionnement clinique à l'Institut des Etudes Nucléaires, Division de Médecine, à Oak Ridge, depuis mai, 1960. Antérieurement à cette date on y fit des mesures pour obtenir les paramètres du rayonnement. On pour suivit des enquêtes en rapport des valeurs du bruit de fond dans la chambre, des fuites de rayonnement venant des chambres à téléthérapie voisinantes, de l'uniformité du champ d'exposition, des taux d'exposition dont on disposait pour le traitement et des variations spectrales pour les différents taux d'exposition. Les mesures de taux se firent au moyen d'une sonde à ionization; un cristal à scintillation rendit les données spectrales. Les taux d'exposition peuvent s'ajuster en trente deux gradins de 286 r/hr à 1,8 r/hr.

## АППАРАТУРА ДЛЯ ИЗМЕРЕНИЙ ПРИ ОБЩЕМ ОБЛУЧЕНИИ

Общее облучение пациентов в клинических условиях производится в Медицинском Отделе Института Ядерных Исследований в Оукридже, начиная с мая 1960 г. Предварительными измерениями были установлены параметры излучения. Был исследован фон комнат, возможное проникание излучения из близлежащих кабинетов телетерапии, равномерность поля облучения, имеющиеся мощности для лечебного облучения и изменения спектров при различных экспозициях. Определение мощностей производилось ионизационным детектором, а спектральные данные были получены при помощи кристаллического сцинтиллятора. Регулировка предусматривает 32 варианта мощностей облучения в пределах от 286 до 1,8 р/час.

## MESSUNGEN AN EINER GANZKÖRPER-BESTRAHLUNGSANLAGE

Eine Ganzkörper-Bestrahlungsanlage für menschliche Patienten ist seit Mai 1960 im Oak Ridge Institute of Nuclear Studies, Medical Division in klinischer Verwendung. Vor Inbetriebnahme dieser Anlage wurden Messungen zur Bestimmung der Strahlungsparameter durchgeführt. Die folgenden Untersuchungen wurden unternommen: Prüfung der Hintergrundstrahlung im Raum, Eindringen von Strahlung aus benachbarten Therapie-Räumen, Gleichmässigkeit des Bestrahlungsfeldes, die für Behandlungszwecke zur Verfügung stehende

* From the Medical Division, Oak Ridge Institute of Nuclear Studies, Oak Ridge, Tennessee, under contract with the United States Atomic Energy Commission.



VOL
11
196

Bestrahlungsrate und die spektrale Veränderung bei verschiedenen Bestrahlungsraten. Messungen der Bestrahlungsrate wurden mit einem Ionisierungsmessgerät, die spektralen Untersuchungen wurden mittels Szintillationskristall durchgeführt. Die Bestrahlungsraten sind zwischen 286 r/hr und 1,8 r/hr in 32 Stufen variabel.

## DESCRIPTION OF THE FACILITY

THE $Cs^{137}$ total-body irradiation facility of the Oak Ridge Institute of Nuclear Studies, Medical Division, has been in operation since May 1960. The purpose of this irradiator is to allow a study of the treatment of leukemia and other diseases with doses of total-body irradiation. The facility consists of a cubical room of 8 ft dimensions, with a centrally suspended bed. Eight $Cs^{137}$ sources, of 500 c each, are in the side walls of this room and are controlled by a pneumatic panel from another maze-connected room. Each source is beamed at the treatment bed from a different angle and is aimed so as to irradiate the whole length of the bed.

A means of varying the exposure rate from each source consists of a set of metal filter slides of varying thickness, which may be positioned in front of each source port. A total of thirty-two different filter thicknesses (and exposure rates) is possible for each source.

A more detailed description may be found in another publication.[1]

## OBJECTIVES OF THE MEASUREMENT PROGRAM

A large number of measurable parameters exist in such a facility. Of those quantities selected for examination, certain ones had to be evaluated before others. Therefore the measurements were divided into three separate groups: (a) those required before the loading of any therapy sources; (b) those to be performed during and after loading the sources but before the facility was released for clinical operation, and (c) those that could be made after release of the facility for treatment purposes.

It was imperative that the initial phase of this program be concluded as soon as possible, and the objectives within groups (a) and (b) were expedited and are the major concern of this report.

The basic questions to be answered from these initial studies were as follows.

(1) What are the spectral characteristics of the natural radiation in the total-body irradiation room?
(2) Is there any radiation leakage into this room from nearby teletherapy rooms?
(3) Is the exposure rate uniform throughout the patient-occupied volume just above the treatment bed? If it is not, can it be made more uniform?
(4) What changes in radiation spectrum result from changes in attenuating filter thickness?
(5) What is the actual exposure rate for each of the thirty-two possible filter combinations?

## METHODS AND CONDITIONS OF MEASUREMENTS

The measuring instruments were required to give two distinct types of information: (1) those having to do with the *rate* or quantity of exposure, and (2) those relating the *spectral shape* (or quality) of the radiation.

For rate measurements, a Victoreen ratemeter with a model 605 probe was used as a detector. The readings from this probe were corrected by comparison with a National Bureau of Standards calibrated probe, and also for ambient temperature and barometric pressure.

The problem of spectral analysis was not easy. A usual method of evaluating the various energy components of a radiation field is to use a physical detector to convert the energy of each incident ray into an electrical pulse height that is proportional to this

energy. One typical and common detector for such use is a scintillation crystal coupled to a photomultiplier tube. These detectors perform well in moderate or low-intensity radiation fields, but with the more intense therapeutic fields the pulses may become numerous enough to jam the analyzing mechanism. Spectrometry had to be done at lower levels of radiation intensity. One means was to use a set of mock therapy sources giving the same spectrum shape as the larger ones. To follow this approach a set of eight 2 mc sources was used.

For spectral detection, a 2 × 2 in. NaI(Tl) crystal was used. Although the efficiency of this crystal drops off above 500 keV, it gives adequate information about the relative changes in spectral energy above this level.

A trolley was mounted on steel rails near the ceiling of the room directly over the bed. By means of accurate linear scales, the ionization chamber and crystal detector could be reproducibly positioned above any portion of the bed. Figure 1 shows these two detector units in position.

## RESULTS

The following is a résumé of results obtained from this initial series of measurements, in the order of questions posed.

### "*Pure*" *natural background radiation*

The question of whether the natural radioactivity in the concrete and other building materials was of sufficient magnitude to be detrimental to further experimentation was explored first. The 2 × 2 in. crystal was positioned just above the bed center and the upper spectrum shown in Fig. 2 was recorded. The graph starts from 60 keV and runs up to 2000 keV. The energy window is plus and minus 20 keV for this recording. A small hint of a peak may be noticed around 1400 keV, probably caused by the potassium-40 in the concrete walls. Below this peak the plot continues almost level down to about 600 keV where a broad rise starts, reaching a peak in the region of 120 keV. This broad peak is probably the conglomerate result of primary and scattered radiation from thorium, uranium, potassium, radium and other constituents in the building materials. The sharp fall-off below 120 keV may signify the passing of a critical region of self-absorption of radiation in the building materials.

Counting rates observed from this curve were so low that corrections for natural background were considered unnecessary in the later measurements.

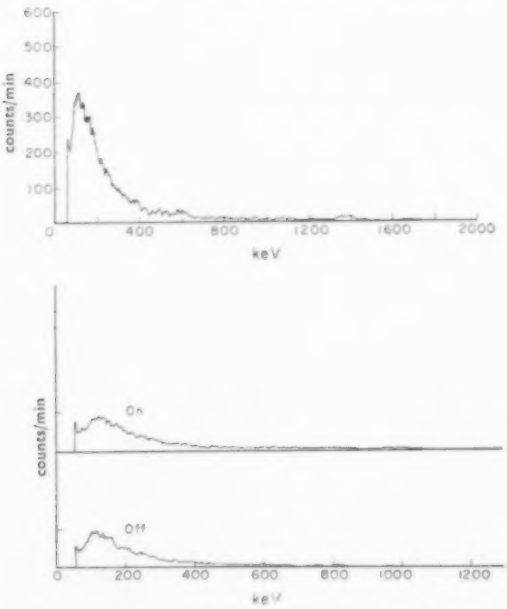


FIG. 2. Natural background spectrum (upper curve); and radiation leakage spectra (lower curves).

### *Leakage from teletherapy sources*

Another experiment (performed before loading any sources) investigated the possibility of radiation leakage from teletherapy sources located in nearby treatment rooms. The two lower curves of Fig. 2 show a comparison of background spectra with three $Co^{60}$ teletherapy units turned "on", pointed in the direction of the treatment room and also with these sources turned "off". No significant difference in the curves could be noted, indicating virtually no leakage into the irradiation room.

VOL
11
196

VOL.
11
1961

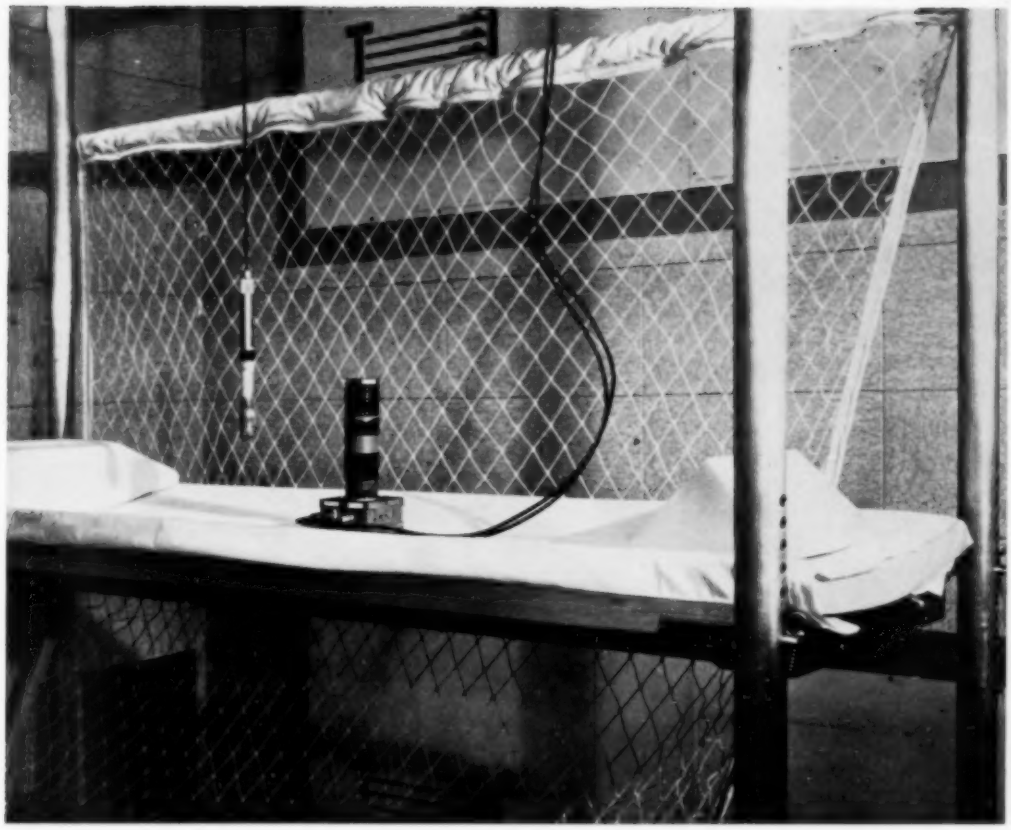

FIG. 1. Detectors used in total-body irradiation measurements.

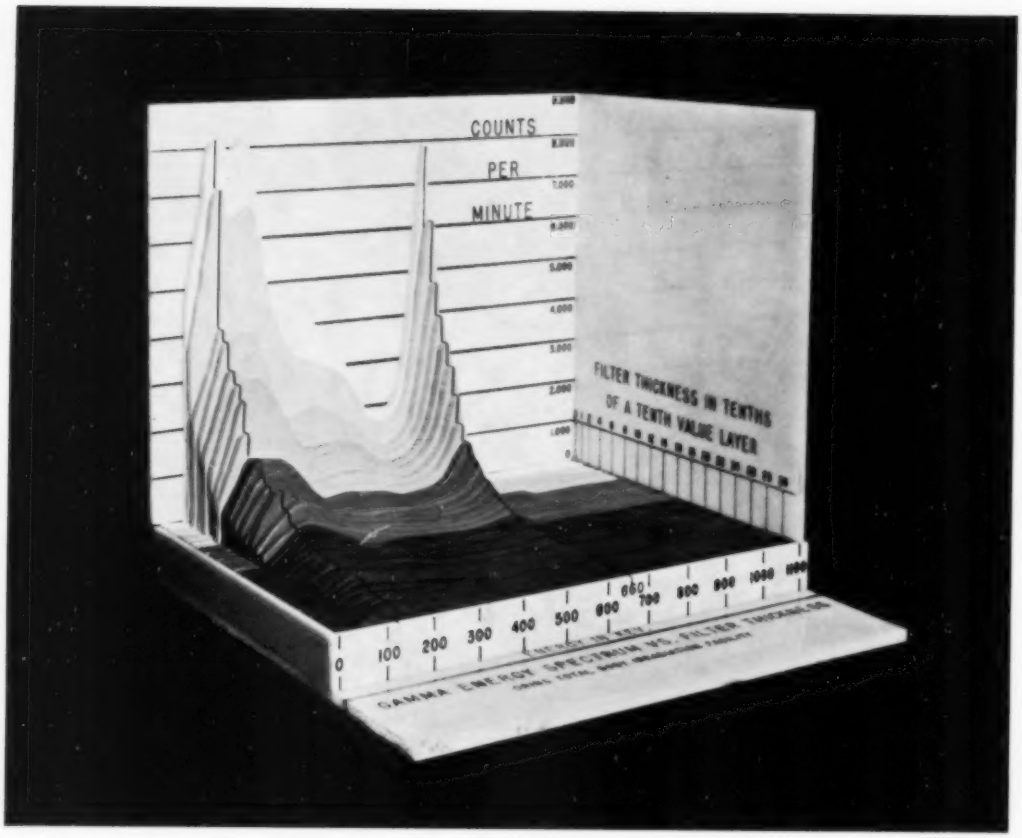


FIG. 4. Gamma-energy spectrum vs. filter thickness. Increasing shades of darkness shows the introduction of a thicker filter series.

*Uniformity of radiation exposure*

The initial background experiments were concluded, and the eight 500 c $Cs^{137}$ sources were loaded into the shields. One of the design features of this installation was to try for as uniform an exposure field to the patient as possible. Therefore, the eight sources were aimed to irradiate the subject from many different angles, each ported to expose the entire bed length. It was realized that scatter off the room walls and other variable factors might alter the desired uniformity, and a series of measurements was undertaken to investigate this possibility. The ion chamber was suspended at a point 12 cm above the bed center and was moved toward each end in 10 cm steps. The readings obtained are reproduced as the upper curve of Fig. 3. It indicates a smooth decrease in intensity toward each end of the bed. The maximum rate of 7·4 r/min at the bed center would allow an exposure of 444 r/hr—a good deal more than the 250 r/hr originally thought possible.

With an excess of exposure rate available, the suggestion was made to attempt to even the exposure field. For this purpose stacks of metal strips were made and installed to give an attenuated portion in the center of each beam. A pyramidal stack for each source with the thickest portion in the beam center gave the lower curve in Fig. 3. As illustrated, this curve is more uniform throughout its length and gives an exposure rate of about 300 r/hr.

Studies were also made in the lateral and vertical directions in the volume immediately above the bed. The variations of the field in these positions were not found to be large enough to require further compensation.

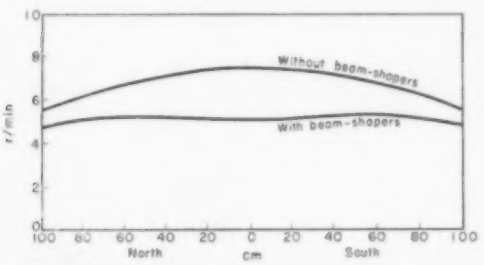


FIG. 3. Effect of beam-shaping filters.

*Changes in spectral form due to various filter settings*

Attenuating the rate of exposure to the patient by using increasing filter thicknesses[1] proved to be an excellent means of making these adjustments. Nevertheless, the question of spectral changes resulting from the introduction of these filters was an important one to examine because of possible changes in the depth–dose relationships in the patient.

The variations in spectrum with exposure rate were investigated using weak (2 mc) mock sources, in order to keep the intensity down to a reasonable level. The background for such measurements, however, is not the "natural" background investigated earlier, but rather that existing when the 500 c sources are present but are turned to the "off" position. The count rates for these backgrounds (and later for the gross counts) were found to be very low, to such an extent that recording of the count with a meter system was impractical. Therefore, seventeen spectral points of interest were selected and cumulative counts were made at each point for each filter setting. Some of these counts took as much as 10–20 min to complete, and a rather lengthy procedure resulted from the checking of thirty-two filter positions for seventeen spectral points. (Some of the counts were omitted where the radiation characteristics were changing slowly.) This process was repeated again for the gross counts and the background counts were subtracted.

After computation of the net counts, a series of curves was drawn representing the spectrum for each filter position. These curves were transferred to and cut out of wooden sheets of uniform thickness. Incorporating the thirty-two resulting curves into a solid model gave the three-dimensional representation of Fig. 4. The three axes in this model represent energy ($X$), count rate ($Y$) and filter thickness ($Z$). The two black lines running down the face of the curves denote the primary $Cs^{137}$ peak at 660 keV and the 120 keV scatter peak. The 660 keV primary radiation falls off in the smooth exponential fashion expected from increasing incremental filter thicknesses. The scatter components do not follow this smooth fall-off so well. The

scatter starts off as a double-peaked function, which drops rapidly in the first few filtrations to become a single-peaked curve at lower intensities. The initial rapid fall-off in the scatter component later becomes slow, whereas the attenuation of the primary peak continues unabated. This causes the scatter to persist even at the weakest intensities, where the primary peak is no longer visible. This

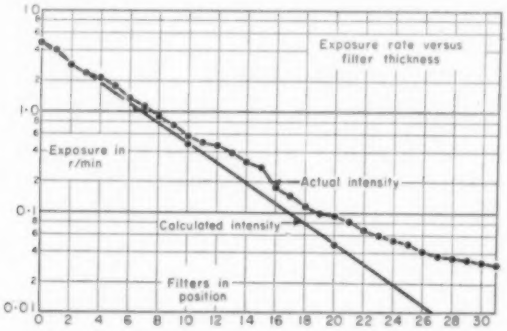


FIG. 5. Exposure attenuation curve.

residual scatter present may be the result of leakage around the edges of the filter, which is not tight against the source shield; or it may represent the degraded components of the primary radiation that finally trickles through the filters.

Generally speaking, the relative shape of these curves is reasonably constant except when the heaviest filter sections are in position. Unless treatments are to be given at very low dose rates, no corrections for spectral change are anticipated.

*Treatment exposure rates*

The last series of measurements made before release of the facility for clinical use was to determine the exposure rates available for treatment. The ionization chamber was positioned 12 cm above the center of the bed and successive readings were taken for each filter thickness. Figure 5 illustrates the result of this investigation by plotting exposure rate against increasing filter thickness. The actual curve deviates substantially from the calculated attenuation line at heavier filtrations. Probably this results from the leakage of radiation around the sides of the filter and, moreover, from the scattered component, which is not considered in calculating the theoretical attenuation line, that leaks through the filter.

The attenuating filters provide an intensity range of about 160 : 1, which is more than adequate for clinical studies. Currently, the maximum exposure rate is 286 r/hr and the minimum 1.8. For the convenience of the operators, a chart has been prepared[1]; it shows the treatment times required to deliver various total exposures (left-hand column) with any desired filter thickness. If a slow rate of treatment is desired, more filtration is added and the time lengthened, as shown. This relieves the technician of the responsibility of making a separate time calculation for each treatment, and thus minimizes the chance of error. Since the sources decay, losing 1 per cent every 5 months or so, the Table will need revision about once a year.

## CONCLUSIONS

The measurements outlined in this report were completed on 1 May, 1960, and the facility was released for clinical use. Other radiation parameters are being examined currently at times when the facility is not otherwise in use, and are the subjects of other investigations.

(1) A small peak at 1400 keV (potassium-40?) and a broad peak about 120 keV (low-energy gamma and Compton scatter?) were the notable constituents of the natural background in the total-body irradiation room.

(2) No radiation leakage could be detected from teletherapy sources operated in adjacent rooms.

(3) The radiation field with the eight 500 c sources turned on was found to have a maximum over the center of the bed. Beam-shaping filters reduced the variation within the patient-occupied volume to within $\pm 5$ per cent of the center intensity.

(4) The primary radiation component declined exponentially with increasing filter thickness and was not detectable at the

higher attenuations. Compton scatter regions decreased rapidly in the first few filtrations, but later became the only recognizable exposure component at the highest filtrations.

(5) The thirty-two filter combinations make it possible to vary the exposure rate, at the center of the bed, from 286 to 1.8 r/hr, in thirty-two steps. Each rate is about 80 per cent of the one above it.

(6) A program of evaluation in this type of facility is possible only if it is carefully planned to proceed without missing data links—such as the required room backgrounds. The actual measurements will take a long time and require many monotonous repetitive readings.

(7) The low-energy regions of the *natural* room background and the *scatter* portions of the irradiation beam are strikingly similar. Both rise to a broad peak at about 120 keV and both fall off sharply below 100 keV. This similarity is probably due to wall absorption in the concrete room.

(8) Theoretical formulas, used in calculating the thickness of attenuation filters for a radiation beam, may be in error if leakage and scatter components are not considered.

(9) The total exposure beam from these therapeutic sources was found to consist of two main components: (a) the primary 660 keV $\gamma$-radiation from $Cs^{137}$, and (b) a rather broad region of Compton scatter with maximum intensity occurring at about 120 keV. These two components, surprisingly, were of nearly equal magnitude in these measurements.

## REFERENCE

1. Brucer M. *Int. J. appl. Rad. Isotopes* **10,** 99 (1961).

VOL. 11 1961

International Journal of Applied Radiation and Isotopes, 1961, Vol. 11, pp. 114–122. Pergamon Press Ltd. Printed in Northern Ireland

# A Thin Plastic Radiation Dosimeter*

K. K. HARRIS and W. E. PRICE
Lockheed Missiles and Space Division, Palo Alto, California, U.S.A.

(*Received* 7 *February* 1961)

Because of their very short range, radiation doses of low-energy particles and X-rays are difficult to measure by the usual methods. To perfect a dosimeter to measure low-energy radiation doses, the change in optical transmission of thin plastic films was studied as a function of dose. A survey of twenty types of film placed in $\gamma$-radiation fields up to $10^7$ r was made. Saran No. 7 was found to have the most suitable characteristics. Optical densities of Saran at 2600 Å vs. exposure dose was found to be a straight line on a log–log plot from $5 \times 10^4$ r to $10^7$ r when irradiated by $\gamma$-radiation. A dose of $10^4$ r was detectable and the range may extend above $10^7$ r. The change in absorption of Saran caused by radiation is only slightly reduced when irradiated in vacuum and measured in an inert atmosphere.

## UN DOSIMETRE DU RAYONNEMENT EN PLASTIQUE MINCE

Vu leur très petite portée, il est difficile de mesurer par les méthodes habituelles les doses de rayonnement des particules et des rayons X de petite énergie. Afin de perfectionner un dosimètre pour mesurer les doses de rayonnement de petite énergie, on étudia la variation dans la transmission optique des pellicules minces de certaines matières plastiques, en fonction de la dose. On étudia vingt espèces de pellicule situées dans des champs de rayonnement gamma montant à $10^7$ r. Le Saran No. 7 se montra avoir les caractéristiques les plus appropriées. On trouva que la densité optique du Saran à 2.600 Å contre la dose d'exposition donnait une ligne droite sur une graphique log-log, à partir de $5 \times 10^4$ jusqu'à $10^7$ r lors de son exposition au rayonnement $\gamma$. On peut observer une dose de $10^4$ r, et la gamme peut s'étendre au delà de $10^7$r. La variation d'absorption produite dans le Saran par le rayonnement ne se baisse que légèrement lorsqu'il est irradié dans le vide et la mesure faite dans un atmosphère inerte.

## ТОНКИЙ ПЛАСТМАССОВЫЙ ДОЗИМЕТР ИЗЛУЧЕНИЙ

Дозы излучения частиц малой энергии и рентгеновских лучей трудно измерять обычными методами вследствие малой длины пробега этих частиц. С целью приспособить дозиметр к измерению доз малой энергии, была исследована зависимость изменения оптической плотности тонких пластмассовых пленок от дозы. Было испытано 20 типов пленок, подвергнутых $\gamma$-облучению в пределах до $10^7$ рентген. Наилучшие результаты были получены с пленкой Саран № 7. Логарифмический график зависимости плотностей Сарана при 2600 Å от дозы показывает, что при $\gamma$-облучении в пределах от $5.10^4$ до $10^7$ рентген эта зависимость является прямолинейной. Можно было определить дозу в $10^4$ рентген и, повидимому, превысить предел в $10^7$ рентген. Облучение в вакууме и измерения в инертной атмосфере вызывали лишь небольшое уменьшение поглощающей пособности Сарана под действием радиации.

## EIN STRAHLENDOSIMETER AUS DÜNNEM KUNSTSTOFF

Die Messung der Strahlendosis energiearmer Teilchen oder von Röntgenstrahlung mit den üblichen Methoden ist schwierig, infolge deren sehr kurzer Reichweite. Zur Herstellung eines

* This work was supported in part by the United States Air Force.



VOL
11
196

Dosimeters für niederenergetische Strahlung wurde die Veränderung der optischen Durchlässigkeit dünner Kunststoffolien als Funktion der Dosis untersucht. 20 verschiedene Folienarten wurden nach Bestrahlung im $\gamma$-Feld bis zu $10^7$ r geprüft. Saran N7 zeigte dabei die besten Eigenschaften. Die optische Dichte von Saran bei 2600 Å als Funktion der Expositionsdosis ergab in doppelt logarithmischer Darstellung eine gerade Linie im Bereich von $10^4$ bis $10^7$ r. Eine Dosis von $10^4$ r war noch nachweisbar, ausserdem konnte der Bereich über $10^7$ r hinaus verlängert werden. Die Veränderung der durch Strahlung hervorgerufenen Lichtabsorption des Saran wird nur geringfügig herabgesetzt, wenn die Bestrahlung im Vakuum und die Messung in inerter Atmosphäre durchgeführt werden.

VOL. 11 1961

POLYVINYL vinylidene (Saran) has been found to be effective for measuring doses of ionizing radiation in the range of $10^4$–$10^7$ r. Radiation-induced changes in the ultraviolet transmission through one-mil sheet stock were measured with a spectrophotometer.

A good dosimeter must possess a number of attributes in order to be useful. These attributes are listed below and are not in any special order of importance, since the order is necessarily dependent on the use of the dosimeter:

wide useful dose range
monotonic response to dose
nondependence on dose rate
nondependence on energy
simplicity in handling
simplicity in measurement
availability and low cost
small size
reproducibility
accuracy
stability before radiation and after radiation
nondependence on ambient conditions (temperature, humidity, ambient gas).

No single dosimeter can, at present, meet all these qualifications completely. For special applications there are other qualifications which might be added to the list and probably some which could be deleted. A frequent requirement is a dosimeter that will not affect the field of radiation in the vicinity of the dosimeter. Except for extremely low-energy radiation, a 0.001 in. thick Saran film will meet this qualification. Although there are other plastic dosimeters which utilize optical transmission changes,[1–9] the Saran dosimeter combines a number of qualifications which are not duplicated in other dosimeters reported in the current literature.[10–14]

This research effort was directed toward finding a solid-type dosimeter with the capability of measuring integrated doses of low-energy radiation in the range from $10^3$–$10^8$ r in a vacuum environment. Low-energy radiations can penetrate only short distances into most materials and since penetration is inversely proportional to the atomic number of a material, low $Z$ materials were required. Extremely thin material had to be used in order to avoid saturation of the radiation-induced change in a surface layer of material. These requirements suggested a plastic dosimeter.

## MATERIAL SELECTION

Twenty chemically different plastics of the order of 0.001 in. thickness were selected to be investigated to determine their response to $\gamma$-radiation from a $Co^{60}$ source. The method selected to determine the response was to measure any changes in optical density with a Beckman DU spectrophotometer. Thus, for the twenty samples, optical-density spectra were run on each sample in the visible and the ultraviolet regions. The wavelength region covered was from 1.5 $\mu$ to 2200 Å, approximately. These same samples were then given an exposure dose of $8 \times 10^6$ r. Optical density spectra were again run on the irradiated samples, and the changes from the unirradiated spectra were noted.

Of the twenty materials surveyed only four were found to have sufficient response to be used as a dosimeter. These four materials

and the wavelength region in which the response to $\gamma$-radiation was measurable were:

Saran (polyvinyl vinylidene): 2300–2700Å
polyvinyl chloride: 2250–2450 Å, and 2700–2800 Å
polyethylene: 2200–2300 Å
N-2 Pliofilm: 2450–2600 Å.

Although Saran showed the largest response, Saran, polyethylene and Pliofilm were unstable, showing an increase in optical density with time when left in a dry-air atmosphere. Polyvinyl chloride, though stable, had a threshold at $10^6$ r.

It was found that unirradiated Saran film, when subjected to vacuum for several hours, increased slightly in optical density but, when moved after evacuation to a dry-air atmosphere, became much more stable. It appears that one or more of the plasticizers or stabilizers added to the basic polymer are themselves unstable with respect to optical density, and by placing the sample in a vacuum the additive was either "pulled out" or its reaction increased to saturation. With this undesirable characteristic of Saran eliminated, Saran Type No. 7 was selected for more extensive investigation.

## EXPERIMENTAL TECHNIQUES

A kilocurie $Co^{60}$ source used for the irradiation of the plastic samples was calibrated by the Frick method. Since the radiation field near the source was accurately mapped, the effects of the dose rate, as well as the effect due to the integrated dose, could be readily determined.

Sample holders were made of 3/32 in. stock aluminum, in which two 1/2 in. diameter holes were drilled with a separation such as to fit in the sample position for a Beckman DU spectrophotometer. Samples of Saran were cut from a single sheet, 0.001 in. thick, into squares about 3/4 in. on a side. Saran samples were then mounted evenly over one of the holes in each of the sample holders and were then placed in a chamber evacuated to about 20 $\mu$ of Hg. It was determined that, at this pressure, about 24 hr were required to insure reproducible stability of the Saran samples. The optical density of the vacuum-treated Saran samples was then measured, using air as a standard, at a wavelength of 2600 Å and a slit width of 0.2 mm.

The Saran samples were divided into groups of five samples per group. Each group was given a different integrated exposure dose in the range from $10^4$ r to $5 \times 10^7$ r. In each group, four of the five samples were simultaneously irradiated to the specified dose, while the fifth sample was used as a control and placed in the same environmental conditions, but shielded from the radiation. Integrated doses up to and including $10^6$ r were obtained in a period of 1 hr. The higher doses up to $5 \times 10^7$ r were irradiated at a dose rate of $10^6$ r/hr, and hence their irradiation times were correspondingly longer. Though dose rates up to $2 \times 10^6$ r/hr were available, the radiation field was not uniform over the entire specimen above $10^6$ r/hr. Dose-rate independence of the dosimeters could be determined by comparing the responses to the different rates chosen.

Upon completion of the irradiation, the optical density of each irradiated sample and the corresponding control was measured and recorded at specified time intervals. The samples were stored in a desiccator and kept at room temperature which varied no more than 5°F throughout the experiment.

## SPECIAL HANDLING EFFECTS

In spectroscopic analysis there are many laboratory conditions that may affect the results of any particular measurement. Some of the more obvious effects have been investigated and attempts have been made to eliminate them. These investigations were carried out on unirradiated Saran in an attempt to determine the cause of the spontaneous darkening. The effects considered most important were: (1) humidity, (2)

temperature, (3) stress in film, (4) ultraviolet light while being measured, (5) surface conditions of film, (6) ambient oxygen conditions, and (7) vacuum environment. The effect on the unirradiated films due to the above-mentioned conditions are briefly discussed below.

*Humidity.* The films were prepared on the aluminum specimen holders in the manner described. The samples were then placed in water and left for a period of 3 hr. The increase in optical density after the 3 hr exposure to water was approximately 10 per cent. After measurement, the samples were again placed in water for approximately 70 hr, and when removed showed a total density increase of approximately 40 per cent after drying for 1 hr. With several hours of continued drying, the optical density was found to have decreased less than 4 per cent. These measurements indicate that the optical density of Saran increases with the amount of absorbed water. For this reason all samples were thereafter kept in a desiccator.

*Temperature.* Samples were placed in an environment with a temperature of 152°F. After approximately 5 hr the samples were removed and an increase in optical density of approximately 13 per cent was observed. Samples were also placed in an oven at 120°F. These samples had been evacuated as described above. Very little change in optical density was observed during the first 23 hr of heating. However, after 36 hr a small increase in optical density was noted. The optical density continued to change, and after 165 hr the increase was 32 per cent. The heating measurements were carried no further, and all samples were thereafter kept at room temperature.

*Stress.* It was suspected that applying tension in varying amounts, when preparing specimens on the aluminum holders, might have had a noticeable effect on the optical density, and that perhaps under irradiation this tension might be reduced or increased in some manner. Therefore, samples were measured at what was considered a normal amount of stress in their preparation, then measured with considerably greater stress (about 10 times), and finally measured again with the specimen completely relaxed. In these prescribed measurements there was no apparent variation in the optical density.

*Ultraviolet light.* It is known that in some plastics ultraviolet light causes an increase in the absorption in the infrared region.[15–18] The absolute intensity of the ultraviolet light, impinging upon the sample while being measured, was not determined. The average measurement time per sample was about $\frac{1}{2}$ min. Thus, to measure the effect of ultraviolet absorption by the samples while being measured, each sample was left in the beam of the spectrophotometer for over 10 hr. No noticeable increase in optical density was observed.

*Surface conditions.* Although dust particles collected on the film, only a small increase in optical density was observed. This may have been due to the fact that only a small number of the particles were in the measuring beam. This problem was eliminated by storing the samples in the relatively dust-free desiccator. Finger prints on the film also showed very little effect on the optical density.

The surface of a sample was rubbed briskly with a Kimwipe several times, leaving small scratch marks over the surface of the film. This increased the optical density about 7 per cent.

*Oxygen atmosphere.* Samples were placed in a pure oxygen atmosphere and remained there for 20 hr. No appreciable difference was noted in the optical density at 2600 Å or in the infrared spectrum of samples exposed to pure oxygen as compared with those in room atmosphere.

*Vacuum environment.* As has been mentioned above, vacuum had a marked effect on the Saran samples. It was found that, when placed in a vacuum chamber for about 20 hr at a pressure of 20 $\mu$ Hg, the optical density of the samples increased at an average of about 7 per cent. But when transferred to the dessicator the samples showed no increase in optical density with time and subsequent evacuation for another 50 hr also showed no further increase in optical density. By treating the samples of Saran with this vacuum process, it was therefore possible to obtain stable controls.

VOL. 11 1961

## RESULTS

When exposed to the $\gamma$-ray source, it was found that the Saran samples increased in optical density, with the lower detectable limit of the exposure dose being in the neighborhood of $10^4$ r. Although the upper limit of the exposure dose has not yet been determined, exposure doses of the order of $5 \times 10^7$ r have been measured.

Like many other plastics, Saran continues to increase in optical density following exposure to irradiation to a sufficient dosage. In the experiments described here, this density increase continued, eventually reaching saturation after 100 hr from the completion of irradiation, as can be seen from Fig. 1. On a linear plot, it may be determined from the data of Fig. 1 that the curves representing the lower exposure doses become essentially flat considerably sooner than those representing the higher exposure doses. This is to be expected, since an increase in exposure dose results in increased damage to the plastic. This probably affects the absorption mechanism such that it takes a longer time to reach saturation.

Attempts to decrease the time required for saturation of the absorption mechanism for Saran, such as suggested by ARTANDI and STONEHILL[2] in their work on polyvinyl chloride (keeping the samples in an oven at 120°F), have so far been unsuccessful. As pointed out in the paragraph on temperature, heating of the Saran samples has some detrimental effects.

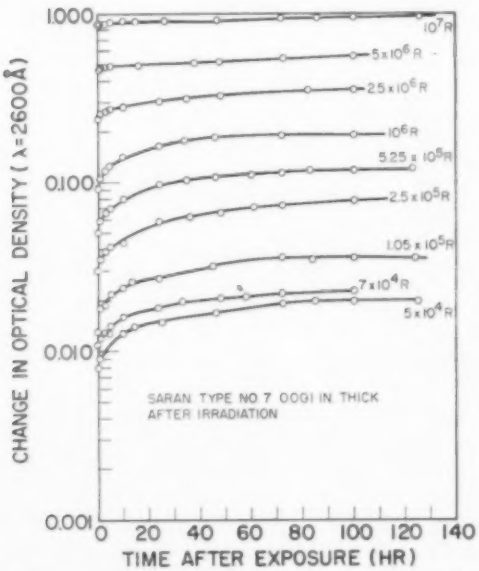


FIG. 1. Post-irradiation density increase (2600 Å) in Saran for various dosages.

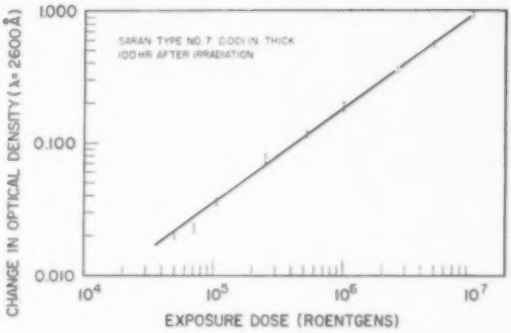


FIG. 2. Optical response (2600 Å) of Saran to gamma radiation.

The usefulness of Saran as a dosimeter is shown in Fig. 2. After saturation occurred, the change in optical density was plotted against exposure dose on log–log graph paper. Each point on Fig. 2 is an average of four, and in some cases eight, different samples exposed to the same dose. This procedure was necessary since the optical density of each sample varies somewhat randomly. The standard deviation of each group of four or more samples is represented on each point. It is seen that the change in optical density vs. dose is a straight line on a log–log plot over the range from $5 \times 10^4$ r to $10^7$ r. The following equation expresses the dose over this region.

$$\text{Dose} = 1{\cdot}1 \times 10^7 \, \Delta^{4/3}$$

where $\Delta$ is the change in optical density.

An exposure dose of $5 \times 10^7$ r was made on a group of four samples. The measured optical density was found to be slightly greater than 3·0; but at this optical density the resolution of the spectrophotometer is poor, and considerable error is always present in measurements in this region. However, an extrapolation of the curve of Fig. 2

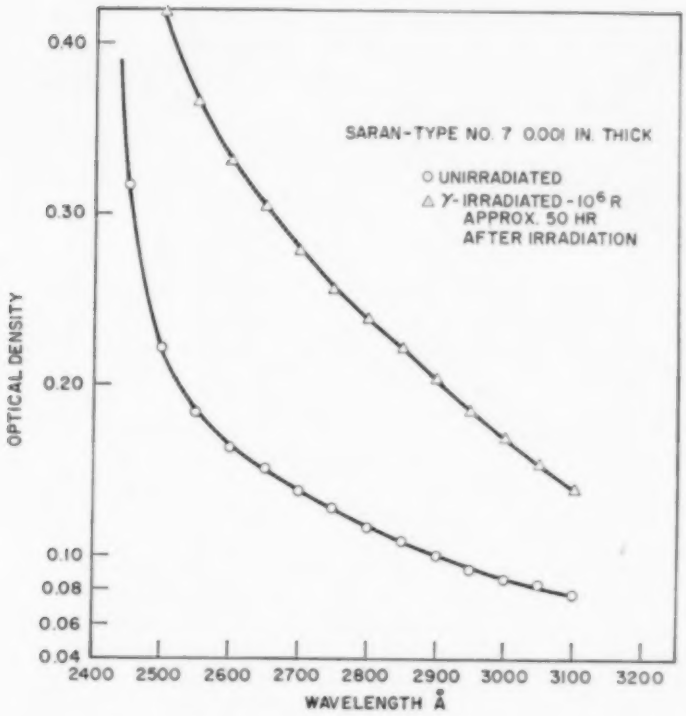


FIG. 3. Effect of radiation on the ultraviolet spectrum of Saran.

to an exposure dose of $5 \times 10^7$ r indicates an optical density change of 3.11, and thus, even though the measurement was approximate, it is very near the extrapolated value. This indicates that even at this high exposure dose the absorption mechanism has not become saturated with respect to exposure dose. To measure doses of the order of $5 \times 10^7$ r and greater, requires samples with an optical density of less than about 2.0. This may be achieved in two ways: (1) use of thinner samples because optical density is directly proportional to thickness (samples thinner than 0.001 in. would be needed for measurements at 2600 Å), and (2) use of longer wavelength measurements. From Fig. 3 it is noted that, although the sensitivity to radiation decreases as the wavelength increases, the optical density also decreases as the wavelength increases, thus, to measure doses greater than $10^7$ r with 0.001 in. thick Saran, the wavelength of the transmission light must be longer than 2600 Å.

Measurements at a wavelength of 3000 Å, after saturation was considered complete, were made on samples of 0.001 in. thick Saran which were exposed to doses ranging from $7 \times 10^4$ r to $5 \times 10^7$ r. The curve of the change in optical density vs. dose was a straight line on a log–log plot up to doses of about $5 \times 10^6$ r. The points for the $10^7$ r and $5 \times 10^7$ r doses were considerably above the extrapolated straight line. At present no reason can be offered for this behavior.

## DISCUSSION

*Accuracy*

In making dose determinations by using Saran as a dosimeter, it has been pointed out that there is some random error associated with one single sample measurement. Thus it requires several samples to get reasonably

good statistical results. The standard deviations for the various doses are indicated in Fig. 3. In the region from $5 \times 10^4$ r to $10^7$ r the largest percentage standard deviation in optical density is ~8 per cent. The mean percentage standard deviation in optical density for all doses is ~5 per cent. Upon drawing the best straight line through the points, it is found that the largest deviation in dose of any one of the points is 26 per cent. This is believed to be due to an experimental error. The mean percentage deviation of the points from the straight-line fit was found to be ~8 per cent.

*Mechanisms*

The mechanisms of the radiation-induced optical darkening in the ultraviolet spectrum in Saran are difficult to determine. The reasons for this are that (1) the additives of the plastic are unknown because of their proprietary nature, (2) there are a number of possible radiation interactions, and (3) there are a multitude of possible resultant chemical reactions. Nevertheless, it is interesting to note that irradiation almost always causes some optical darkening in transparent plastics.

The ultraviolet region shows no fine absorption spectra, but broad absorption peaks have been found for methyl methacrylate at 2920 Å[5], cellulose acetate at 2750 Å, cellulose triacetate at 2625 Å. Polystyrene shows a peak at 3300–3400 Å which disappears at higher doses due to the creep of the absorption edge.[1,5]

Another interesting point is that plastics containing chlorine apparently are very sensitive to optical darkening. For example, methyl methacrylate darkens with radiation, but methyl α-chloroacrylate darkens more readily, and the darkening in the latter increases with post-exposure time where the former decreases with post-exposure time.[16] It has been shown that oxygen plays a part in the fading of methacrylate.[7]

In irradiated plastics, the behavior of optical density with post-exposure time is probably linked with the radiation-induced chemical reactions. The most important of these is bond breakage which leads to gas formation, oxidation, crosslinking, polymerization, free-radical formation, double-bond formation, etc. Which of these causes the ultraviolet absorption under discussion is not clear. It is clear, however, that the disruption of bonds causes a continuing chemical reaction which takes place over long periods of time following irradiation.

The post-irradiation changes in optical density are both positive and negative, depending on the chemical type. Plastics that change negatively (fade) are methyl methacrylate, polystyrene and Mylar.[1,5] Plastics that darken are polyvinyl chloride, polyvinyl vinylidene, Pliofilm (chlorinated natural rubber) and Epoxy (Epon 828). Most plastics that darken following irradiation contain chlorine. An exception is polyethylene which also darkens in the ultraviolet region.

Infrared measurements on Saran before and after irradiation show a slight increase in the carbonyl absorption band. Since these experiments were carried out in air, this would be expected. It has been suggested that the ultraviolet absorption below 2600 Å may be due to C=O bonds or to C=C bonds.[17] HCl formation may also have some affect on the absorption.

*Energy dependence*

Experiments conducted on plastics indicate that the measured dose is nearly independent of the incident energy over a wide range.[1,3] This is to be expected on theoretical grounds, since absorbed energy is a function of the atomic number of the dosimeter material. Therefore, Saran may be expected to be reasonably energy independent except at very low energies.

*Oxygen effect*

The possibility of carbonyl bonds being a major contribution to the increased absorption in the dosimeter, prompted an experiment to be made on the effect of oxygen on the dosimeter. This was accomplished by constructing a special air-tight chamber with two transparent ports through which the optical density could be measured. The unirradiated samples were measured in the

VOL
11
196

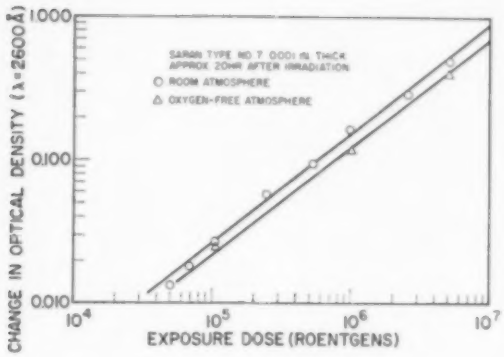


FIG. 4. Oxygen effect on irradiated Saran.

air-tight chamber and then placed in a small vacuum chamber and irradiated, at a pressure of about 20 $\mu$ Hg, to a specified dose. The samples were then removed from the vacuum chamber, placed in the air-tight chamber in an argon atmosphere, and the change in optical density determined.

Due to the complexity of the experiment, time limited the number of samples and the number of different dosages measured. Dose measurements were made at $10^5$, $10^6$ and $5 \times 10^6$ r, with only one sample at each dose. The samples were measured approximately 20 hr after irradiation.

The results of the experiment are indicated in Fig. 4, in which curves of change in optical density vs. exposure dose at approximately 20 hr are plotted for room atmosphere and for oxygen-free atmosphere. It is noted that the oxygen-free curve is a straight line which closely parallels the curve for room atmosphere. The oxygen-free atmosphere curve, however, is reduced by approximately 15 per cent. Thus, it appears that oxygen has a small effect which is no greater than 15 per cent of the total effect. Also, it is indicated by this experiment that the dosimeter is applicable for measuring radiation in vacuum environments. In order to calibrate the Saran dosimeter, however, it would be necessary to carry out more experiments of this kind with greater precision.

## CONCLUSION

Saran No. 7, 0.001 in. thick, can be used as a dosimeter to measure doses in the range from $5 \times 10^4$ r to $10^7$ r. The accuracy of a dose determination in this range is approximately 8 per cent. Exposure dose vs. change in optical density is a straight line from $5 \times 10^4$ r to $10^7$ r. Smaller doses down to $10^4$ r can be detected. Reproducibility of results is good, with a standard deviation in optical density of less than 8 per cent for all groups measured. It appears that the dosimeter is dose-rate independent in a range from $5 \times 10^4$ r/hr to $10^6$ r/hr which was the dose-rate range used for this study.

There exists in Saran a post-irradiation effect that cause the samples to continue to darken. The time required for this process to reach saturation was of the order of 100 hr for doses of $10^7$ r, and correspondingly less for smaller doses. At present no method has been found whereby this saturation time may be reduced.

The major absorption mechanism in Saran is not known. It does not appear to be due to oxygen bonding in the formation of the carbonyl group. Irradiation of Saran in a vacuum indicates that it is useful as a dosimeter in a vacuum environment.

The Saran dosimeter will not affect the field of radiation in its vicinity. In addition, it meets the requirements of simplicity in handling—small size, ready availability at low cost, and both ease and rapidity in making response measurements.

*Acknowledgments*—The authors would like to express their thanks to DR. MARION RINEHART for his suggestions, and to the Dow Chemical Company for supplying specimens used in these experiments.

## REFERENCES

1. FOWLER J. F. and DAY M. J. *Nucleonics* **13,** No. 12, p. 52 (1955).
2. ARTANDI C. and STONEHILL A. A. *Nucleonics* **16,** No. 5, 118 (1958).

3. Birnbaum M., Schulman J. H. and Seren L. *Rev. sci. Instrum.* **26,** No. 5, 457 (1955).
4. Johnson D. R. *Radiation Induced Ultra-Violet Absorption in Methyl Methacrylate as a Method of Dosimetry.* Wright Air Development Center. Technical Note 59-167 (June 1959).
5. Boag J. W., Dolphin G. W. and Rotblat J. *Radiat. Res.* **9,** 589 (1958).
6. Tillotson Lt. J. H. and Srp N. E., *Gamma Dosimetry Properties of Linear Polyethylene by Infrared Analysis.* Wright Air Development Center. Technical Note 56-196 (May 1956).
7. Day M. J. and Stein G. *Nature, Lond.* **168,** 644 (1951).
8. Henley E. J. and Miller A. *Nucleonics.* **9,** No 6, 62 (1951).
9. Henley E. J. *Nucleonics* **12,** No. 9, 62 (1954).
10. Measuring Large Radiation Doses, *Nucleonics* **17,** No. 10, 57 (1959).
11. Schulman J. H., *Proceedings of the Second International Conference on the Peaceful Uses of Atomic Energy, Geneva,* 1958, A/Conf. 15/P/1859, Vol. 21, p. 220. United Nations, N.Y. (1958).
12. Oestmann M. J., Kircher J. F. and Schall P. Jr. *A Survey of Current Research and Developments in the Field of Dosimetry.* Radio Effects Information Center Report No. 6, 31 May (1958); Radio Effects Information Center Report No. 6, Addendum (March 1959).
13. Taimuty S. I. *Recent Developments in Gamma Dosimetry.* American Soc. for Testing Materials, Special Techn. Pub. No. 276, June 1960.
14. Taimuty S. I. *Obtaining a System of Dosimetry,* Quartermaster Food and Container Institute for the Armed Forces. (28 September 1956–31 March 1959).
15. Alexander A. L., Cowling J. E. and Noonan F. M. *The Degradation of Polymers by Ultraviolet Irradiation*—I. United States Naval Research Laboratory Report No. 5257 (February 1959).
16. Schmidt D. L. *Effects of Gamma Radiation on Aircraft Transparent Materials,* Wright Air Development Center. Technical Note 56-557, Part II, (May 1958).
17. Dole M. Private communication (May 1960).
18. Reiney M. J., Tryon M. T. and Achhammer B. G. *J. Res. Nat. bur. Stand.* **51,** 155 (1953).

VOL
11
196

International Journal of Applied Radiation and Isotopes, 1961, Vol. 11, pp. 123–130. Pergamon Press Ltd. Printed in Northern Ireland

# Effect of Gamma Irradiation on the Catalytic Activity of Zinc Oxide and Chromic Oxide for the Decomposition of Methanol

A. J. TELLER, F. L. POSKA and H. A. DAVIES
Chemical Engineering Department, University of Florida, Fla., U.S.A.

VOL.
11
1961

(*First received* 13 *May* 1960 *and in revised form* 2 *December* 1960)

The effect of gamma radiation on the catalytic activity of an *n*- and a *p*-type semi-conductor catalyst was determined. The reaction studied was the vapor-phase decomposition of methanol under continuous flow conditions. Under dose rates ranging from 80,000 to 450,000 r/hr an increase in the catalytic activity of the *n*-type zinc oxide catalysts and a decrease in activity of the *p*-type chromic oxide catalysts were observed. The degree of change was related to the inherent activity of the catalyst (when not subjected to irradiation).

A "saturation" effect of irradiation appeared to exist. Low inherent activity *n*-type catalysts approached the activity of a high inherent activity *n*-type catalyst when subjected to $\gamma$-radiation. All *p*-type catalysts approached the same level of activity when exposed to $\gamma$-radiation.

## L'EFFET DU RAYONNEMENT GAMMA SUR L'ACTIVITE CATALYTIQUE DE L'OXYDE DE ZINC ET DE L'OXYDE CHROMIQUE POUR LA DECOMPOSITION DU METHANOL

L'effet du rayonnement gamma sur l'activité catalytique des catalyseurs mi-conductifs type *n* et type *p* a été mesuré. La réaction mise à l'étude fut la décomposition du méthanol en phase vapeur sous des conditions d'écoulement continu. Pour des taux de dose rangeant de 80.000 à 450.000 r/h on observa un renforcement de l'activité catalytique des catalyseurs d'oxyde de zinc type *n* et un affaiblissement de l'activité des catalyseurs d'oxyde chromique type *p*. L'étentue du changement avait un rapport à l'activité fondamentale du catalyseur (sans avoir subi le rayonnement).

Il sembla y avoir un effet de "saturation" quant à l'irradiation. Les catalyseurs type *n* de petite activité fondamentale approchaient l'activité d'un catalyseur type *n* de grande activité fondamentale après avoir subi le rayonnement $\gamma$. Tous les catalyseurs type *p* approchaient le même niveau d'activité lors de leur exposition au rayonnement $\gamma$.

## ДЕЙСТВИЕ ГАММА-ИЗЛУЧЕНИЯ НА КАТАЛИТИЧЕСКУЮ АКТИВНОСТЬ ОКИСИ ЦИНКА И ОКИСИ ХРОМА ПРИ РАЗЛОЖЕНИИ МЕТАНОЛА

Определялось действие гамма-излучения на каталитическую активность полупроводниковых катализаторов типа *n* и *p*. Исследуемой реакцией было парофазное разложение метанола в струе. При дозах в пределах от 80.000 до 450.000 *p*/час наблюдалось увеличение каталитической активности окиси цинка, катализатора типа *n*, уменьшение каталитической активность окиси хрома, катализатора типа 0. Степень изменения зависела от присущей катализатору активности (в отсутствии облучения).

Наблюдался эффект ''насыщения'' при действии излучения. Гамма-облучение катализаторов типа *n* низкой активности триближает их к катализаторам высокой активности того же типа. Все $\gamma$-облученные катализаторы типа *p* приближаются к одному и тому же уровню активности.

## DER EINFLUSS VON GAMMABESTRAHLUNG AUF DIE KATALYTISCHE WIRKUNG VON ZINKOXYD UND CHROMOXYD BEI DER ZERSETZUNG VON METHANOL

Der Einfluss von $\gamma$-Strahlung auf die katalytische Wirkung von *n*- und *p*-Halbleiterkatalysatoren wurde bestimmt. Die untersuchte Reaktion war der Abbau von Methanol in der Dampfphase bei kontinuierlichen Durchflussbedingungen. Im Dosisbereich von 80.000 bis 450.000 r/Stunde wurde eine Zunahme der katalytischen Wirkung des *n*-Type Zinkoxydkatalysators und eine Abnahme der Wirkung des *p*-Type Chromoxydkatalysators beobachtet. Der Grad der Änderung wurde in Beziehung gesetzt zu der jeweiligen Katalysatorwirkung (bei Nichtbestrahlung).

Anscheinend existiert ein "Sättigungseffekt" der Bestrahlung. *n*-Type Katalysatoren von geringer Wirksamkeit verwandeln sich in hochwirksame *n*-Type Katalysatoren unter dem Einfluss von $\gamma$-Strahlung. Alle *p*-Type Katalysatoren erreichen den gleichen Grad der Wirksamkeit wenn sie $\gamma$-Bestrahlung ausgesetzt werden.

VOL
11
196

CONCOMITANT with the greater availability of nuclear radiation sources, there has been an increasing activity in studies of the effect of radiation on the activity of catalysts.

The results of these studies have not indicated any consistent pattern of the effect of these radiations on catalytic activity. TAYLOR and WETHINGTON[1] found that exposure of zinc oxide to $\gamma$-irradiation decreased its effectiveness as a catalyst for the hydrogenation of ethylene. WEISZ and SWEGLER[2] found that, subsequent to exposure to neutron irradiation, the effectiveness of a silica catalyst increased for the double-bond isomerization of 1-hexene but that no change in activity was noted for the cracking of isoprophyl benzene. TAYLOR and KOHN[3] observed an increase in activity for aluminum oxide for the hydrogen–deuterium exchange, after the catalyst was exposed to $\gamma$-irradiation. CLARKE and GIBSON[4] studied the effect of $\gamma$-radiation on the activity of cobalt and iron catalysts in the Fisher–Tropsch reaction. The activity of the cobalt catalyst was unaffected, whereas the iron catalyst activity increased by 10–40 per cent.

It was felt that some of the inconsistencies may have been related to the fact that part of these studies were concerned only with the transient effects of radiation since the catalysts were subjected to radiation prior to the evaluation.

This study was concerned with the steady-state irradiation effect on catalyst activity while the reaction was on-stream. The reaction evaluated was the decomposition of methanol over zinc oxide and chromic oxide catalysts. These two catalysts were selected since it was anticipated that the effect of radiation would be more pronounced on semi-conductors, of which these represent two classes, than on metal or insulator-type catalysts.

It is firmly established that radiation has marked effects on the conductivity of semiconductors, and there is indication[5,6] that

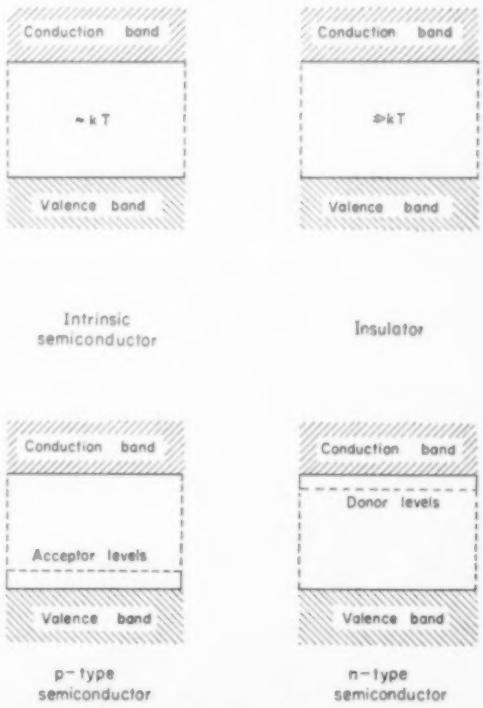


FIG. 1. Typical band structures.

a relationship may exist between the conductivity and the catalytic activity of semiconductors.

In the zinc oxide *n*-type semi-conductor, the localized energy levels lie below the conduction band but in proximity to it. Thus a moderate amount of ionization energy should raise the electrons in these energy levels into the conduction band, creating additional labile electrons (Fig. 1).

In the chromic oxide *p*-type semi-conductor, the localized energy levels lie above the valence band but in proximity to it. This energy band is due to the presence of acceptor atoms. Upon excitation, the valence electrons may reach the acceptor levels, leaving "holes" in the valence band, producing electron transfer via hole conduction (Fig. 1).

An ionization effect was anticipated from the interaction of the $\gamma$-rays and the catalyst. With gammas emitted from a cobalt-60 source having energies of 1.17 and 1.33 MeV, it was expected that the interaction would occur via the photoelectric and Compton effects.[8,9] Both of these effects cause the ejection of electrons from the parent atoms and molecules, such that the resultant effect of $\gamma$-irradiation should be internal electron bombardment, or ionization. In addition, the Compton electrons and photoelectrons whose energies are greater than the threshold value for atom displacement, can provide coulomb interaction with the nucleus. This would cause uniform defect distribution throughout the catalyst crystal.[9]

The ionization and defect production will alter the conductivity of the semiconductor. If the number of labile electrons are related to the catalytic activity, then a change in catalyst activity should be observed.

## APPARATUS AND PROCEDURE

The reaction, the decomposition of methanol to carbon monoxide and hydrogen, was operated at atmospheric pressure and at temperatures within the range 300–450°C. The continuous-flow reactor was placed in two positions in a 750 c cobalt source so that the reaction could be exposed to gamma flux densities of $0.81 \times 10^5$ r/hr and $4.5 \times 10^5$ r/hr.

The apparatus used in the present study consisted of a methanol feeding system, a vaporizing unit, a reactor, a methanol recovery system and a gas measuring device (Fig. 2).

The methanol feed system consisted of a syringe driving unit followed by a vaporizor.

The feed and discharge lines were constructed of $\frac{1}{4}$ in. copper tubing wrapped with insulated heating tape to prevent condensation. The catalytic unit and lead lines were encased in a $1\frac{1}{2}$ in. aluminum tube 12 ft long, for immersion in the $Co^{60}$ source.

The catalytic unit was constructed from 9 mm o.d. glass tubing and was wound with nichrome wire for heating (Fig. 3). The catalyst was placed in the annular space between the thermocouple well and the reactor wall, and was supported by glass

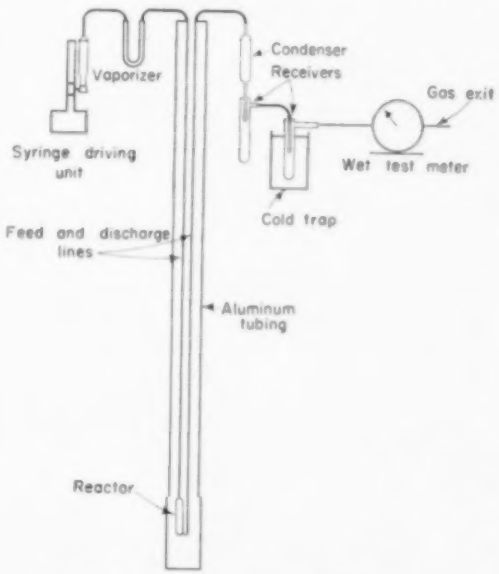


FIG. 2. Schematic diagram of apparatus.

wool. The catalyst capacity was approximately 1 g.

A water condenser (32°F) and a dry-ice acetone trap (−40°F) in series was used to condense the liquid products, and the volume of the gaseous products was measured with a wet test meter.

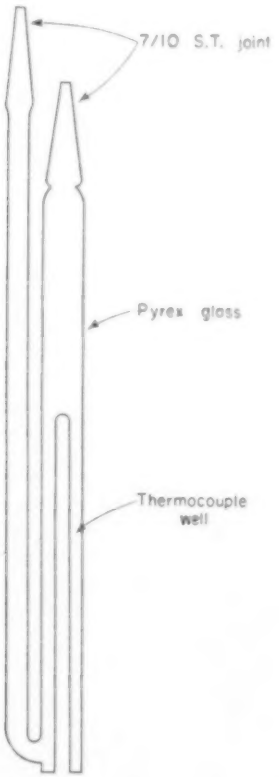


FIG. 3. Catalytic reactor.

The temperature was measured and recorded by a chromel–alumel thermocouple placed in the reactor thermocouple well.

Control of the reactor temperature was maintained by adjusting the voltage applied to the reactor heating coil.

Catalysts were prepared by precipitation as the hydroxide from a solution of the nitrates using ammonium hydroxide as the precipitating agent. The catalyst batches were digested under different conditions in order to yield varying particle and crystal sizes and therefore different inherent activities. The precipitate was then washed, filtered and dried. The dry hydroxide was then ground, compressed and sized.

The reactor was loaded with 1.118 g (1.3 ml) of the 28–35 mesh hydroxide, and the catalyst was activated by first feeding nitrogen at a rate of 1 $ft^3$/hr for a period of 2 hr at a temperature of 220°C and then feeding methanol vapor at a rate of 0.12 ml/min (measured as liquid at room temperature) for an additional 2 hr at 220°C.

When activation of the catalyst was complete, the reactor was brought to—and maintained at—the desired testing temperature until sufficient data were obtained at that temperature. The temperature was then adjusted to another value where additional data were obtained.

The data were taken every 10 minutes and consisted of feed rate, time, temperature, amount of methanol recovered and cubic feet of gas ($CO + 2H_2$) evolved. From these data the percentage conversion at various temperatures was calculated and curves of percentage conversion vs. temperature were constructed.

Runs were made with and without irradiation on the same batch of catalyst under identical conditions to ascertain the effect of irradiation.

Blank runs were also made in which the catalyst was replaced by glass wool. This was done in order to determine whether the $\gamma$-irradiation had any effect on the dissociation rate of methanol in the absence of a catalyst.

Before each run the reactor was loaded with fresh catalyst and each run in a given series was made in the same manner in order to eliminate any factors which might result from the previous history of the catalyst.

Feed and product analyses were made with the use of a vapor-phase chromatograph, that was precalibrated with pure hydrogen, carbon dioxide, carbon monoxide, methanol, dimethyl ether, formaldehyde and methyl formate.

VOL 11 196

## DISCUSSION

The activity of a zinc oxide catalyst under zero irradiation is a function of the reduction time to which the catalyst is exposed prior to use. This phenomenon results from a conversion of zinc hydroxide to the oxide and then partially to zinc. The zinc–zinc oxide complex structure developed during this reduction period is believed to be the catalytically active form of the zinc oxide.

The effect of reduction time (or the degree of conversion to the zinc–zinc oxide structure) on the catalytic activity is indicated in Fig. 4.

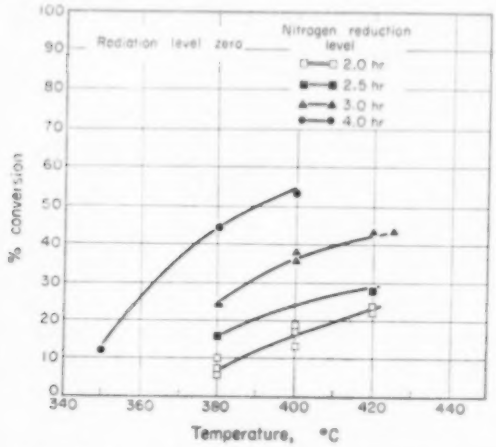


FIG. 4. Per cent conversion vs. temperature for catalyst B-1.

Additional activation occurs at the time of the methanol decomposition. This effect was not studied separately; however, the time cycle for decomposition was kept constant to eliminate any behavior variation resulting from any possible added activation by this means.

It was also noted that the activity diminished after exposure to reaction at 400°C for an extended period of time. This was attributed to carbonization taking place and thus poisoning the catalyst. The effect was minimized by using fresh catalyst for each run and keeping the time cycle short at the higher temperatures.

In view of the above activation phenomena, all runs evaluating the effect of irradiation on catalytic activity were made at a constant reduction period of 2 hr of nitrogen purging at 220°C followed by the given time cycle for methanol decomposition.

No measurable amount of methanol was decomposed during the blank run (in which the reactor, filled with glass wool, was subjected to $\gamma$-radiation in the absence of catalyst) up to 420°C, indicating that any increase in conversion was due to enhancement of the catalytic activity of the zinc oxide and not to decomposition of methanol by $\gamma$-rays.

The three zinc oxide catalysts of different inherent activities, as a result of variation in conditions of hydroxide precipitation (Fig. 5), were evaluated. The catalyst, having

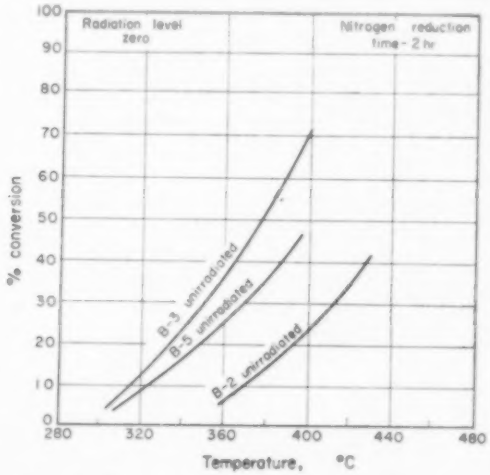


FIG. 5. Per cent conversion vs. temperature for catalysts B-2, B-3 and B-5 unirradiated.

the highest activity (B-3) at a zero irradiation level, was unaffected by exposure to radiation while on-stream (Fig. 6). Both the other catalysts (B-2 and B-5) exhibited significant increases in activity upon being subjected to radiation (Figs. 7 and 8). It should be noted, however, that the activities of both B-2 and B-5 at the highest irradiation level ($4.5 \times 10^5$ r/hr) approached that of the activity of the high-activity catalyst (B-3) in the unirradiated state (Fig. 9). Furthermore, the effect of radiation on

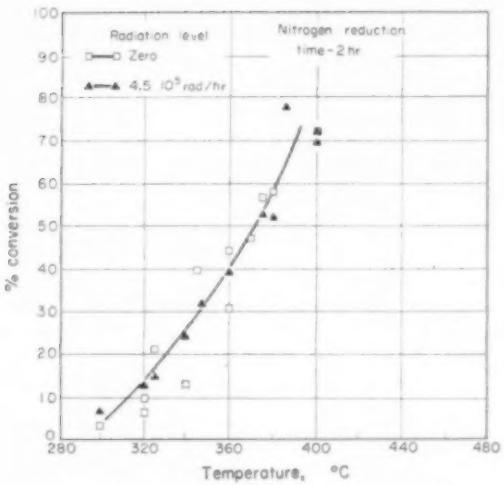


FIG. 6. Per cent conversion vs. temperature for catalyst B-3.

catalyst B-5 was significantly lower than on the inherently less active catalyst (B-2).

The products obtained in all tests with the zinc oxide catalyst were carbon monoxide and hydrogen, in addition to the unreacted methanol. The formaldehyde found in the product stream was equal to that of the impurity quantity in the feed stream (approximately 1 per cent).

In the reaction over chromic oxide catalysts, small quantities of dimethyl ether and methyl formate were found in the product stream. Since these materials constituted less than 1 per cent of the product stream, the conversion values were based on the carbon monoxide and hydrogen formed in the reaction. The formation of the by-products in the reaction over chromic oxide catalysts had previously been reported in studies of this system.[10,11]

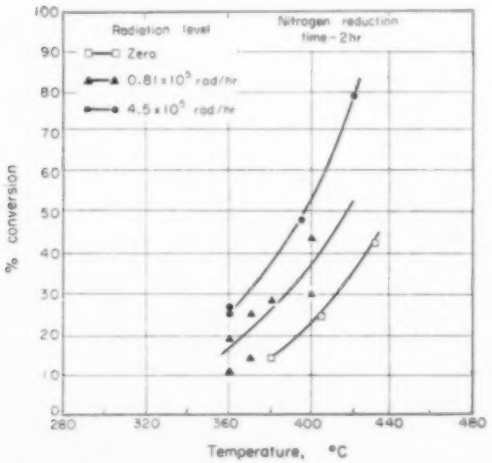


FIG. 7. Per cent conversion vs. temperature for catalyst B-2.

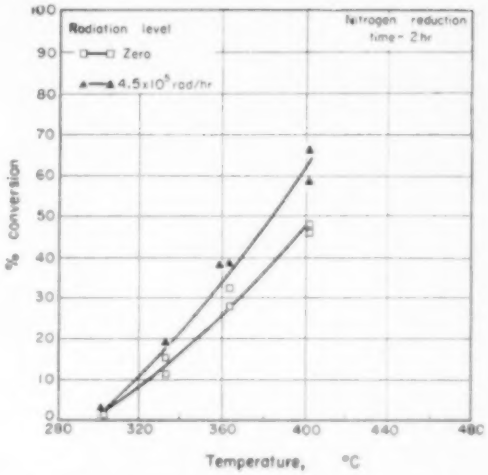


FIG. 8. Per cent conversion vs. temperature for catalyst B-5.

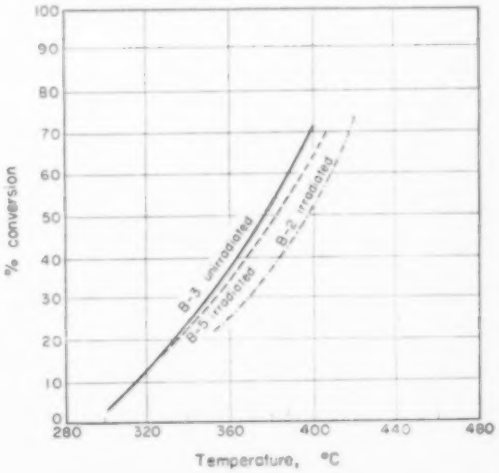


FIG. 9. Per cent conversion vs. temperature for catalyst B-3 unirradiated, and catalysts B-2 and B-5 irradiated at $4.5 \times 10^5$ rad/hr.

VOL. 11 1961

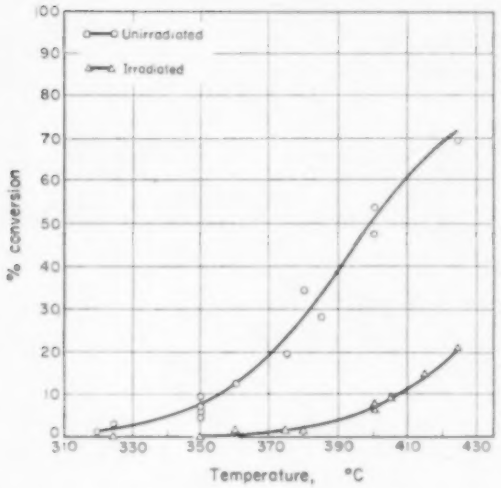


FIG. 10. Per cent conversion vs. temperature for catalyst C-1.

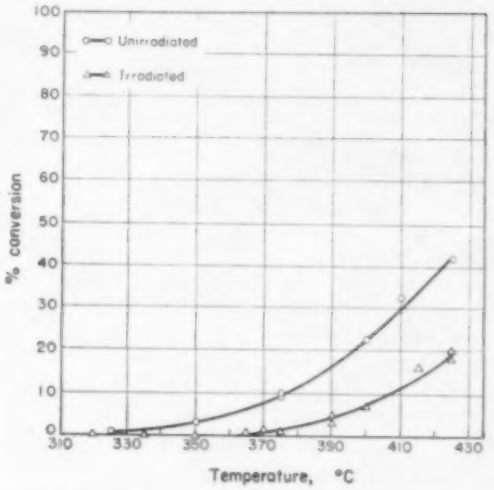


FIG. 12. Per cent conversion vs. temperature for catalyst C-3.

Exposure to $\gamma$-irradiation resulted in a decrease in the activity of the three chromic oxide catalysts having different initial activities when not exposed to irradiation (Figs. 10, 11, 12). Significantly, at close rates of $0.81 \times 10^5$ r/hr and $4.5 \times 10^5$ r/hr, the three catalysts exhibited the same activity as indicated by the conversion of methanol (Fig. 13).

A "saturation effect" of the radiation appears to have been reached, since the activities remained constant at the two significantly different radiation levels.

Since all of the catalysts exhibited the same activity while being subjected to $\gamma$-radiation, a greater relative decrease in conversion under irradiation compared to that obtained with a catalyst not subjected

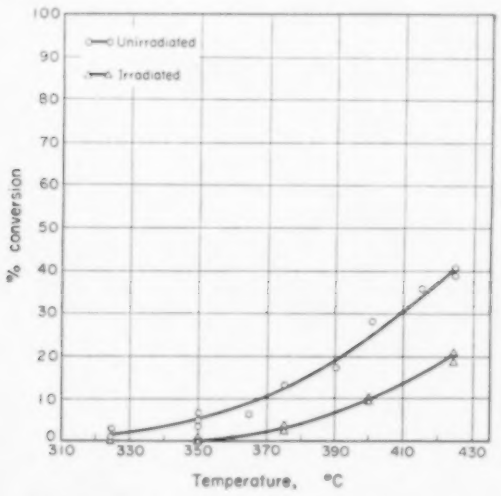


FIG. 11. Per cent conversion vs. temperature for catalyst C-2.

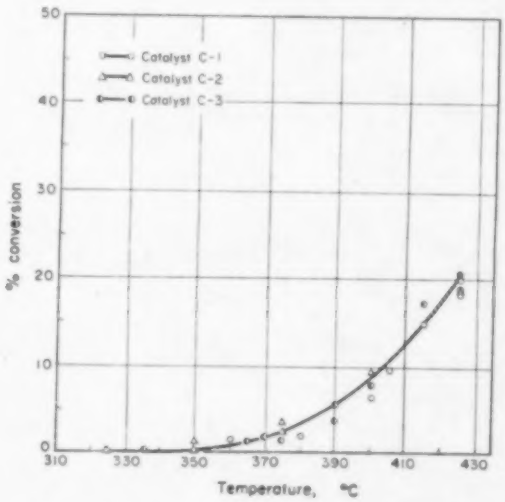


FIG. 13. Per cent conversion vs. temperature under irradiation for catalysts C-1, C-2 and C-3.

to radiation was found for the initial high-activity catalyst C-1 than with the catalysts C-2 or C-3.

The dependence of irradiation effects on the initial activity of catalysts has been noted previously. TAYLOR and KOHN[3], in their work with aluminum oxide, observed that irradiation increased the activity of a relatively inactive catalyst several thousand fold while the activity of an active catalyst was increased only seven fold. GIBSON *et al.*[12] also reported that, although the activity of mill-scale iron oxide catalysts are increased by $Co^{60}$ irradiation, the activity of iron oxide precipitated from iron salts in solution was unaffected by irradiation. This latter form exhibits a much higher catalytic activity than the mill-scale iron oxide.

Both of these studies confirm the fact that the effect of irradiation on catalytic activity is dependent on the initial activity of the catalyst. However, no mention was made concerning final activities of the catalysts under irradiation conditions. The present studies indicate that there is a limit to radiation effects.

At the temperatures involved, the major effect is believed to be transient in nature, that is, the phenomena which are responsible for the increased activity anneal out quite rapidly when removed from the radiation beam. Thus the parameter reported is intensity rather than total dose.

The alteration of catalytic activity due to irradiation is attributed to an increase in defects in oxides. From earlier studies[5,6] it is indicated that the activity of a semi-conductor catalyst is related to the number of electrons in the conduction band.

It is postulated that irradiation of zinc oxide by $\gamma$-rays induces donor levels in the lattice, thus lowering the activation energy for excitation of an electron to the conduction band and therefore increasing the number of quasi free electrons and metallic zinc atoms at any given temperature.

Previous work has shown that the conductivity of a *p*-type semi-conductor decreases with $\gamma$-radiation; this decrease is supposedly due to the increase in defects produced by the radiation. The radiation will introduce more electron acceptors, and also more hole traps will now be found. The acceptors will trap the excited electrons from the valence band and there will be fewer electrons in the conduction band than in an unirradiated *p*-type semi-conductor. Also, the hole traps will decrease the number of holes for valence-band conduction.

On the basis of assumption of the electron theory of catalysis, the decrease in catalytic activity of the chromic oxide as a result of $\gamma$-irradiation may be attributed to the decrease in number of conduction-band electrons via development of acceptor levels, and the increase in catalytic activity of the zinc oxide under irradiation, as a result of the increase in number of conduction-band electrons.

## REFERENCES


1. TAYLOR E. H. and WETHINGTON J. A. *J. Amer. chem. Soc.* **176,** 971 (1953).
2. WEISZ P. B. and SWEGLER E. W. *J. chem. Phys.* **23,** 1567 (1955).
3. TAYLOR E. H. and KOHN H. W. *J. Amer. chem. Soc.* **79,** 252 (1957).
4. CLARK R. W. and GIBSON E. J. *Nature, Lond.* **180,** 140 (1957).
5. HECKELSBERG L. F., CLARK A. and BAILEY G. C. *J. phys. Chem.* **60,** 559 (1956).
6. PARRAVANO G. and BOUDART M. *Advances in Catalysis and Related Subjects* Vol. 7, p. 50. Academic Press, New York (1955).
7. KITTEL C. *Introduction to Solid State Physics* p. 273. Wiley, New York. (1953).
8. DIENES G. J. and VINEYARD G. A. *Radiation Effects in Solids* p. 47. Interscience, New York (1957).
9. CLELAND J. W., CRAWFORD J. H. JR. and HOLMES D. K. *Phys. Rev.* **102,** 722 (1956).
10. HUFFMAN. J. R. and DODGE B. F. *Industr. Engng. Chem. (Anal.)* **21,** 1056 (1929).
11. HUTTIG V. G. F. and STRIAL K. *Z. Elektrochem.* **39,** 368 (1933).
12. GIBSON E. J., CLARK R. W., DORLING T. A. and POPE T. J. *Proceedings of the Second International Conference on the Peaceful Uses of Atomic Energy, Geneva,* (1958), A/Conf. 15/P/62. United Nations, New York, (1958).


VOL 11 196

International Journal of Applied Radiation and Isotopes, 1961, Vol. 11, pp. 131–138. Pergamon Press Ltd. Printed in Northern Ireland

# Dekorporation von Radionukliden durch veresterte Polyaminopolycarbonsäuren

A. CATSCH
Institut für Strahlenbiologie am Kernforschungszentrum, Karlsruhe, Deutschland

(*Received* 9 *November* 1960)

Von bestimmten Vorstellungen über den Wirkungsmechanismus von Chelatbildnern ausgehend, wurde der Einfluss der Ester bzw. Lactone der Hydroxyäthyläthylendiamintriessigsäure und der Bis(2-hydrocyclohexyl)äthylendiamindiessigsäure auf das Verhalten von Radiocer und Radioyttrium im Organismus der Ratte untersucht. Während die Calziumchelate der Polyaminosäuren wirkungslos sind, bewirken die Ester, auch bei peroraler Verabfolgung, eine stärkere Reduktion des Gehalts der Leber an Radionukliden, wobei die erhöhte Ausscheidung bevorzugt mit den Faeces erfolgt. Die Effektivität der Ester ist in starkem Masse vom Zeitpunkt der Verabfolgung abhängig. Die sich aus den Befunden ergebenden Fragen werden diskutiert.

## REMOVAL OF INTERNALLY DEPOSITED RADIONUCLIDES BY THE USE OF ESTERIFIED POLYAMINOPOLYCARBONIC ACIDS

Based on certain assumptions concerning the mode of action of chelating agents, the effect of the ester resp. lactone of the hydroxyethylethylenediaminetriacetic acid and bis(2-hydroxycyclohexyl)ethylenediaminediacetic acid on the behaviour of radio-cerium and radio-yttrium in the organism of the rat was studied. Whereas the calcium chelates of the polyamino acids are ineffective, the esters, even given orally, induce a pronounced reduction of the radionuclide content of the liver. The radionuclides in this case are preferentially excreted with the faeces. The effectiveness of the esters depend largely on the time of the administration. The implications of the experimental findings are discussed.

## DECORPORATION DES RADIONUCLIDES PAR LES ESTERS DES ACIDES POLYAMINOPOLYCARBONIQUES

Partant de conceptions déterminées relatives au mécanisme d'action des agents chélateurs, on a étudié l'influence des esters respectivement des lactones de l'hydroxy-éthyle-éthylènediamine-triacide acétique et de la bis(2-hydrocyclohexyle)éthylène-diamine-diacide acétique sur la tenue du radiocérium et du radioyttrium dans l'organisme du rat. Tandis que les chélates de calcium des polyaminoacides sont inefficaces, les esters effectuent—même si l'on donne aux rats des doses perorales—une réduction plus prononcée de la teneur en radioéléments dans le foie, l'excrétion plus élevée se réalisant de préférence avec les fèces. L'efficacité de l'ester dépend largement du temps de l'administration. Les questions qui surgissent à partir des résultats sont discutées.

## УДАЛЕНИЕ РАДИОАКТИВНЫХ АТОМОВ ПРИ ПОМОЩИ ЭТЕРИФИЦИРОВАННЫХ ПОЛИАМИНОКАРБОНОВЫХ КИСЛОТ

На основе некоторых предположений относительно действия агентов, вызывающих образование хелатных комплексов, было исследовано влияние сложного эфира лактона гидроксиэтилэтилендиаминтриуксусной кислоты и бис(2-гидроксициклогексил) этилендиаминдиуксусной кислоты на поведение радиоактивных церия и иттрия в организме крысы. Тогда как хелаты кальция полиаминокислот неэффективны, эфиры, вводимые per os вызывают уменьшение содержания радиоактивных атомов в печени. В этом случае радиоактивные атомы выделяются в основном с испражнениями. Эффективность эфира в значительной степени зависит от времени его введения. Обсуждаются полученные экспериментальные данные.

Bestimmte Polyaminopolycarbonsäuren wie die Äthylendiamintetraessigsäure (ÄDTA) und Diäthylentriaminpentaessigsäure (DTPA) werden neuerdings in stärkerem Masse verwendet, um die Ausscheidung inkorporierter radioaktiver oder stabiler Metallionen zu intensivieren. Die Polyaminosäuren liegen im Organismus praktisch zu fast 100% in Form ihrer Calziumchelate vor, die zumindest zweifach negativ geladene wasserlösliche Ionen darstellen. Dieser Umstand dürfte die Ursache für das nachgewiesene Unvermögen der Polyaminosäuren, Zellmembranen zu permeieren,[1] sowie auch für ihre geringe Wirksamkeit bei später Verabfolgung darstellen. Allerdings machen einige in neuerer Zeit erhobene Befunde die Annahme wahrscheinlich, dass eine zwar kleine, aber immer noch effektive Menge der DTPA sich im Zellinneren, zumindest in der Leber, anreichert (ausführliche Diskussion bei Catsch[2]). Die Möglichkeit wäre damit nicht ausgeschlossen, dass eine Änderung des Permeabilitätsvermögens der Chelatbildner, beispielsweise durch *Veresterung*, zu einer über längere Zeit erhöhten Konzentration innerhalb der Zelle und damit auch zu einer Verbesserung ihrer Wirksamkeit führen könnte. Durch die Veresterung der $COO^-$-Gruppen geht zwar der Chelatbildner seiner Donorgruppen verlustig, jedoch könnten diese durch Hydrolyse in der Zelle wieder freigesetzt und damit die angestrebte Erhöhung der Chelatbildnerkonzentration in der Zelle erreicht werden.

Die Chelatbildner, mit deren Einfluss auf das biologische Verhalten von Radiocer ($Ce^*$) und Radioyttrium ($Y^*$) sich vorliegende Untersuchungen befassen, sind:

(1) Die *N'-(2-hydroxyäthyl)äthylendiamin-NN'N'-triessigsäure* (HÄDTA)

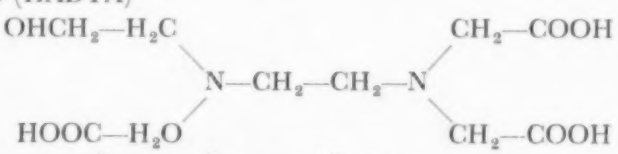

Der von uns verwendete *Äthylester* (ÄE) der HÄDTA

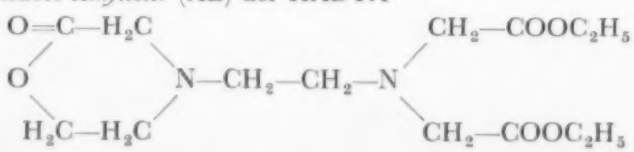

weist einen Lactonring, einen sog. inneren Ester auf; er ist bei pH 7 gut wasserlöslich und kann somit intravenös injiziert werden. Die HÄDTA selbst stellt nach unseren früheren Untersuchungen [3] bei später Verabfolgung einen nur sehr schwach wirksamen Chelatbildner dar.

(2) Das *Dilacton* (DOC-L)

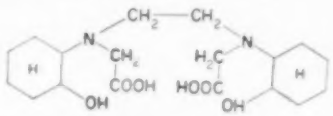

der *NN'-bis(2-hydroxycyclohexyl)äthylendiamin-NN'-diessigsäure* (DOC).

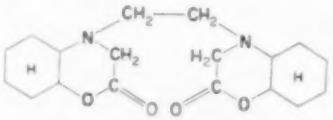

Das $CaNa_2$-Chalat der DOC wurde durch Hydrolyse der DOC-L bei pH 10 und 50°C erhalten.

Entsprechend der eingangs umrissenen Zielsetzung der Untersuchungen wurden alle Substanzen erst dann injiziert, wenn die Ablagerung des überwiegenden Teils der Radionuklide in den Organen bereits erfolgt war; bei intravenöser Inkorporation des $Ce^*$ ist dies nach etwa 2–3 Stunden der Fall.[4]

Als Versuchstiere dienten junge Ratten des Heiligenberg-Inzuchtstammes, denen ca. 1 Mikrocurie trägerfreies $Ce^{144}$–$Pr^{144}$ oder $Y^{91}$ als Chloride (pH 3) intravenös injiziert wurde. Bezüglich methodischer Einzelheiten verweisen wir auf unsere frühere Mitteilung.[3] Die in den Organen und Ausscheidungen festgestellte Aktivität wurde in

% der verabfolgten Gesamtaktivität ausgedrückt. Um die bei Versuchen dieser Art in der Regel ausgeprägte Varianzheterogenität auszuschalten, wurden die Versuchswerte bei der statistischen Analyse logarithmisch transformiert. Einzelne Versuchsgruppen waren mit Tieren von relativ unterschiedlichem Gewicht besetzt. Da eine deutliche Abhängigkeit des Verteilungsmusters des Ce* vom Gewicht vorliegt, und zwar im Sinne einer Zunahme des Lebergehalts und Abnahme des Skelettgehalts mit wachsendem Gewicht,[4,5] wurde diesem Umstand bei der statistischen Analyse durch eine Covarianzanalyse und entsprechende Korrekturen Rechnung getragen.

Der Zusammenstellung in Tabelle 1 ist zu entnehmen, dass die Verabfolgung von $CaNa_2$-HÄDTA nach 24 Stunden zu einer nur geringfügigen und statistisch nicht gesicherten Reduktion des Ce*-Gehalts der Leber führt, während die Verabreichung einer äquimolaren Menge von ÄE eine deutliche und reproduzierbare Abnahme ergibt (Versuch Nr. 1–4). Bei den bezüglich der ÄE-Dosis (100 $\mu$M) und Zeitpunkt der Verabfolgung (24 Std.) vergleichbaren Versuchsgruppen (Tabelle 1 und 2) errechnet sich für den Ce*-Gehalt der Leber ein (unter Berücksichtigung der unterschiedlichen Standardfehler und Zahl der Freiheitsgruppen) gewichteter Mutungsbereich ($P = 0{,}05$) von 73 bis 79% des Kontrollwerts. Die entsprechenden Werte für Nieren und Skelett betragen 88–101 bzw. 97–107%, die Effektivität des ÄE scheint sich somit auf die Leber zu beschränken. Die Ausscheidung des Ce* mit dem Urin, vor allem aber mit den Faeces ist, wie Abb. 1 zu entnehmen, im Laufe der zwei der Verabfolgung von ÄE folgenden Tage gegenüber der Kontrolle deutlich erhöht; insgesamt wurden rund 7% der Ce*-Dosis mehr als in der Kontrollgruppe zur Auscheidung gebracht, eine Menge, die mit den der Tabelle 1 zu entnehmenden Differenzen der Leberwerte in befriedigender Übereinstimmung steht.

Die Verweilzeit des nach Verabreichung von ÄE in der Leber noch verbleibenden Ce* ist gegenüber der Kontrolle unverändert (Versuch Nr. 7 in Tabelle 1) und kann durch

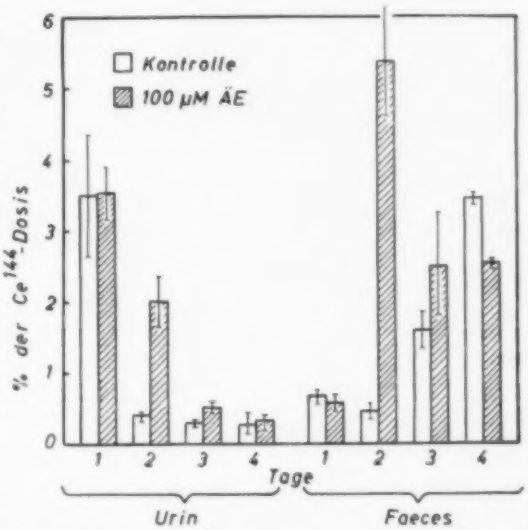


Abb. 1. Einfluss von ÄE, nach 24 Std. i.v. verabfolgt, auf die Ausscheidung von $Ce^{144}$. Je 6 ♂ (232–407g). Einfache Standardfehler.

eine einfache Exponentialfunktion mit einer HWZ von etwa 10 Tagen wiedergegeben werden. Die Effektivität des ÄE zeigt eine deutliche Äbhängigkeit von der Dosis (Versuch Nr. 8 der Tabelle 1), jedoch ist auch bei der kleinsten untersuchten Dosis von 25 $\mu$M ein noch gesicherter Effekt nachzuweisen. Weit stärker fällt demgegenüber die Abhängigkeit der Effektivität vom Zeitpunkt der Verabfolgung ins Gewicht: Bei Verabreichung nach 124 Stunden (Versuch Nr. 10, 11 der Tabelle 1) ist der ÄE praktisch wirkungslos, bei Verabreichung nach 96 Stunden (Versuch Nr. 9, 11 der Tabelle 1) die Reduktion des Ce*-Gehalts in der Leber mit $t_{(19)} = 2{,}31$ ($P = 0{,}05$–$0{,}02$) zwar noch gesichert, jedoch eindeutig schwächer als bei frühzeitigerer Applikation, insbesondere nach 6 Stunden. Im Gegensatz hierzu ist die Effektivität der nicht veresterten, allerdings im Vergleich zu HÄDTA auch wesentlich wirksameren *Diäthylentriamin-NNN′N′N″-pentaessigsäure* (DTPA) weitgehend unabhängig vom Zeitpunkt der Verabreichung (Versuch Nr. 9 der Tabelle 1). Die Wirksamkeit des ÄE bleibt auch bei intraperitonealer Verabreichung (Versuch Nr. 4 der Tabelle 1) in vollem Umfang erhalten, so dass eine stärker ins Gewicht fallende Verseifung des

TABELLE 1. $Ce^{144}$-Gehalt der Organe (in % der Dosis); in Klammern ist der durch den Standardfehler gegebene Bereich angeführt. Die Verabfolgung der Chelatbildner erfolgte, wenn nicht anders angegeben, intravenös. $N$ = Zahl der Tiere; $g$ = mittleres Gewicht

| Nr. | Chelatbildner | µM/Tier | Zeitpunkt (in Std.) der Injektion | Zeitpunkt (in Std.) der Sektion | $N$ | $g$ | Leber | Nieren | Skelett |
|---|---|---|---|---|---|---|---|---|---|
| 1 | — | — | — | 72 | 5 ♂ | 164 | 41,9 (40,1–43,7) | 1,49 (1,43–1,54) | 34,7 (33,0–36,5) |
| | HÄDTA | 100 | 30 | 72 | 5 ♂ | 172 | 38,4 (36,8–40,0) | 1,54 (1,47–1,62) | 32,1 (31,0–33,1) |
| | ÄE | 100 | 30 | 72 | 5 ♂ | 168 | 22,0 (18,7–25,8) | 1,57 (1,51–1,63) | 38,8 (36,4–42,2) |
| 2 | — | — | — | 96 | 6 ♂ | 191 | 38,2 (37,2–39,2) | 1,59 (1,39–1,82) | 27,5 (26,2–29,2) |
| | HÄDTA | 100 | 24 | 96 | 6 ♂ | 179 | 37,0 (35,9–38,1) | 1,54 (1,48–1,60) | 27,9 (27,7–28,2) |
| | ÄE | 100 | 24 | 96 | 6 ♂ | 194 | 28,9 (27,8–30,2) | 1,38 (1,30–1,48) | 28,2 (26,8–29,7) |
| 3* | — | — | — | 48 | 6 | 177 | 31,4 (30,8–32,0) | 1,13 (1,10–1,17) | 31,9 (31,0–33,0) |
| | HÄDTA | 100 | 26 | 48 | 6 | 171 | 31,0 (30,5–31,6) | 0,96 (0,93–0,98) | 31,3 (30,2–32,4) |
| | ÄE | 100 | 26 | 48 | 6 | 179 | 23,4 (22,9–23,8) | 0,96 (0,91–1,00) | 32,6 (31,5–33,7) |
| 4 | — | — | — | 48 | 5 ♂ | 205 | 40,7 (40,3–41,2) | 1,63 (1,55–1,71) | 26,0 (24,8–27,1) |
| | ÄE | 100 | 24 | 48 | 5 ♂ | 211 | 32,4 (31,3–33,5) | 1,63 (1,53–1,73) | 26,2 (25,0–27,4) |
| | ÄE i.p. | 100 | 24 | 48 | 5 ♂ | 202 | 30,6 (30,4–30,8) | 1,62 (1,51–1,75) | 26,0 (25,5–26,4) |
| 5† | — | — | — | 96 | 6 ♂ | 177 | 33,2 (32,4–34,0) | 1,60 (1,51–1,69) | 31,7 (30,5–33,0) |
| | ÄE p.o. | 100 | 24 | 96 | 6 ♂ | 163 | 26,3 (25,5–27,1) | 1,90 (1,79–2,01) | 35,0 (33,4–36,6) |
| 6† | — | — | — | 96 | 5 ♂ | 122 | 28,5 (27,3–29,8) | 1,92 (1,80–2,05) | 37,2 (36,0–38,2) |
| | ÄE p.o. | 200 | 24 | 96 | 5 ♂ | 134 | 22,7 (21,8–23,6) | 1,99 (1,86–2,12) | 38,7 (37,6–39,9) |
| | DTPA p.o. | 200 | 24 | 96 | 4 ♂ | 140 | 21,0 (20,1–21,9) | 1,70 (1,58–1,82) | 28,7 (27,9–29,6) |
| 7 | — | — | — | 48 | 5 ♀ | 137 | 49,0 (47,8–50,1) | 1,31 (1,19–1,45) | 25,6 (24,4–26,9) |
| | ÄE | 100 | 24 | 48 | 5 ♀ | 132 | 35,8 (34,5–37,1) | 1,16 (1,03–1,31) | 23,6 (21,4–26,1) |
| | — | — | — | 192 | 5 ♀ | 135 | 33,1 (31,0–35,3) | 0,75 (0,61–0,92) | 24,7 (23,2–26,3) |
| | ÄE | 100 | 24 | 192 | 5 ♀ | 136 | 25,2 (23,8–26,6) | 0,54 (0,49–0,60) | 25,7 (24,7–26,7) |
| | — | — | — | 768 | 5 ♀ | 133 | 4,98 (3,76–6,58) | 0,37 (0,29–0,46) | 24,9 (24,4–25,4) |
| | ÄE | 100 | 24 | 768 | 5 ♀ | 130 | 3,78 (3,02–4,72) | 0,38 (0,31–0,45) | 26,2 (25,4–26,9) |
| 8 | — | — | — | 48 | 5 ♂ | 169 | 44,2 (43,3–46,2) | 2,08 (2,02–2,15) | 34,1 (33,0–35,2) |
| | ÄE | 200 | 24 | 48 | 5 ♂ | 171 | 31,8 (30,4–33,4) | 1,84 (1,77–1,91) | 35,6 (33,9–37,3) |
| | ÄE | 100 | 24 | 48 | 5 ♂ | 164 | 35,7 (34,0–37,6) | 1,91 (1,66–2,18) | 32,7 (32,0–33,5) |
| | ÄE | 50 | 24 | 48 | 5 ♂ | 173 | 34,4 (33,1–35,6) | 1,96 (1,86–2,06) | 35,5 (32,9–38,3) |
| | ÄE | 25 | 24 | 48 | 5 ♂ | 176 | 38,6 (36,8–40,5) | 1,98 (1,89–2,07) | 33,6 (31,4–35,9) |
| 9 | — | — | — | 144 | 6 ♂ | 200 | 32,0 (30,0–34,1) | 1,61 (1,48–1,75) | 31,5 (30,7–32,3) |
| | ÄE | 100 | 96 | 144 | 6 ♂ | 212 | 29,0 (27,8–30,2) | 1,98 (1,89–2,07) | 33,6 (31,4–35,9) |
| | DTPA | 100 | 96 | 144 | 6 ♂ | 212 | 14,2 (13,0–15,4) | 1,07 (0,98–1,16) | 25,2 (24,5–26,0) |
| 10 | — | — | — | 192 | 8 ♀ | 167 | 30,6 (29,0–32,2) | 0,69 (0,63–0,76) | 27,2 (26,1–28,4) |
| | ÄE | 100 | 124 | 192 | 8 ♀ | 171 | 33,8 (32,8–34,8) | 0,63 (0,58–0,68) | 25,9 (24,9–26,9) |
| | HÄDTA | 100 | 124 | 192 | 8 ♀ | 170 | 31,7 (30,8–32,6) | 0,69 (0,62–0,76) | 27,2 (26,1–28,4) |
| 11 | — | — | — | 168 | 6 ♀ | 158 | 43,2 (41,9–44,5) | 0,60 (0,59–0,61) | 22,8 (21,4–24,1) |
| | ÄE | 100 | 6 | 168 | 6 ♀ | 181 | 25,3 (23,6–27,2) | 0,59 (0,54–0,63) | 23,0 (22,4–23,5) |
| | ÄE | 100 | 24 | 168 | 6 ♀ | 161 | 34,1 (33,1–35,2) | 0,63 (0,59–0,67) | 24,4 (23,9–25,0) |
| | ÄE | 100 | 96 | 168 | 6 ♀ | 162 | 39,6 (38,4–40,7) | 0,54 (0,51–0,57) | 23,6 (22,5–24,8) |

* Da in diesem Versuch ♂ und ♀ verwendet wurden und eine Geschlechtsabhängigkeit des Verteilungsmusters vorliegt, erfolgte bei der Berechnung der Mittelwerte eine entsprechende Korrektur mit Hilfe der Covarianzanalyse.

† Die p.o. Applikation erfolgte mit Hilfe einer Schlundsonde. Die Tiere erhielten 12 Stunden vorher kein Futter.

ÄE in der Bauchhöhle ausgeschlossen werden kann. Auch bei peroraler Verabfolgung (Versuch Nr. 5, 6 der Tabelle 1) wird der Ce*-Gehalt der Leber auf rund 80% des Kontrollwerts gesenkt; es liegt somit ein nur unwesentlicher Effektivitätsverlust im Vergleich zu der intravenösen Applikation vor. Demgegenüber ist die peroral verabreichte DTPA in Übereinstimmung mit früheren Untersuchungen[4] erheblich weniger wirksam als bei intravenöser oder intraperitonealen Injektion (Versuch Nr. 9 der Tabelle 1 und Nr. 12, 14 der Tabelle 2).

Im Hinblick auf den evtl. unterschiedlichen Wirkungsmechanismus des ÄE einerseits und des $CaNa_3$-Chelats der DTPA andererseits prüften wir, ob beide Substanzen sich bezüglich ihrer Effektivitäten additiv verhalten (Tabelle 2): ÄE wurde nach 23 Stunden, DTPA in Versuch Nr. 12 vorher, in Versuch Nr. 14 nachträglich injiziert. Der Versuchsstruktur nach handelt es sich um sog. $2 \times 2$-Faktor-Versuche; ergibt die Varianzanalyse eine nicht signifikante Wechselwirkung beider Faktoren, so bedeutet dies, dass eine volle Additivität der Einzelwirkungen vorliegt. Dies ist bei vorheriger Verabfolgung des ÄE der Fall, nicht aber, wenn zuerst DTPA injiziert wird; hierbei wird anstelle eines bei Annahme voller Additivität zu erwartenden Ce*-Gehalts der Leber von 3,3% ein Wert von nur 5%, wie auch bei alleiniger Verabfolgung von DTPA, beobachtet. Eine vorherige Verabreichung der an sich unwirksamen *Äthylendiamin-NNN'N'-tetraessigsäure* (ÄDTA) dagegen beeinflusst die Effektivität des ÄE nicht (Versuch Nr. 13). Da der Ce*-Gehalt der Nieren und des Skeletts auch in diesen Versuchen durch ÄE unbeeinflusst blieb, wurde auf eine Anführung dieser Daten in Tabelle 2 verzichtet.

Die wesentlicheren der in den vorangehenden Abschnitten angeführten Versuchsergebnisse konnten auch für Y* bestätigt werden (Tabelle 3): Vorausgesetzt, dass ÄE frühzeitig verabreicht wird, ist er wirksamer als HÄDTA, aber unwirksamer als DTPA. Die Wirkung ist wiederum auf die Leber beschränkt und bleibt bei intraperitonealer Verabfolgung erhalten.

Es sei hier kurz, ohne auf die möglichen Ursachen einzugehen, auf einen Nebenbefund hingewiesen, und zwar die unseres Wissens bisher noch nicht beschriebene Geschlechtsabhängigkeit des Verteilungsmusters der seltenen Erden. In Versuch Nr. 3 (Tabelle 1) zeigte der Ce*-Gehalt der Leber bei ♂♂ niedrigere Werte als bei ♀♀, während der Gehalt in den Nieren und im Skelett erhöht ist. Die ♂♂ zeigten auch in den Y*-Versuchen Nr. 2 und 3 (Tabelle 3) höhere Werte in den Nieren und niedrigere in der Leber. Die Unterschiede waren in allen Fällen statistisch signifikant.

Die Versuchsergebnisse mit DOC sind in Tabelle 4 zusammengestellt. Auch in diesem Fall führt das Dilacton zu einer stärkeren Reduktion des Ce*-Gehalts der Leber als das entsprechende $CaNa_2$-Chelat. Im Gegensatz zu den bei der HÄDTA und ÄE vorliegenden Verhältnissen erfahren das DOC-L und auch das DOC bei Verabreichung nach 4 Tagen (Versuch Nr. 16, 17) keine stärkeren Effektivitätsverluste. Hervorzuheben ist die hohe Lebereffektivität der DOC-L bei frühzeitiger Verabfolgung, d.h. 2 min nach Injektion von Ce* (Versuch Nr. 15). Der Lebergehalt ist auf rund 10% des Kontrollwerts gesenkt. Andere von uns untersuchte Chelatbildner, in Form der Ca-Chelate verabreicht, die eine ähnlich starke Lebereffektivität aufweisen, reduzieren den Ce*-Gehalt des Skeletts auf etwa 30–50%.[2,6] Dass dies im Falle der DOC-L *nicht* der Fall ist, spricht wiederum zugunsten unserer Annahme, dass die Chelierung des Ce* nicht bzw. in nur untergeordnetem Masse im extrazellulären Raum stattfindet.

Die im Vergleich zu den entsprechenden Ca-Chelaten höhere Wirksamkeit des Esters bzw. Lactons scheint die Richtigkeit der eingangs dargelegten Überlegungen zu bestätigen. In die gleiche Richtung weist auch die bevorzugte Intensivierung der faecalen Ausscheidung nach Verabfolgung des ÄE; HÄDTA selbst führt zu einer erhöhten Ausscheidung nur mit dem Urin.[3] Die Tatsache, dass die Verweilzeit des Ce* nach Verabreichung des ÄE gegenüber der Kontrolle unverändert bleibt, zeigt, dass der überwiegende Teil des in der Leber gebildeten

Tabelle 2. $Ce^{144}$-Gehalt der Leber. Varianzanalyse der Ergebnisse. Dosen: 100 $\mu$M ÄE i.v., 250 $\mu$M DTPA bzw. ÄDTA i.p

| Nr. | Injektion nach Stunden | | | Tag der Sektion | $N$ | $g$ | % der Dosis | Art der Varianz | $t$ | $P$ |
|---|---|---|---|---|---|---|---|---|---|---|
| | 5 | 23 | 47 | | | | | | | |
| 12 | — | — | — | 2 | 5 ♀ | 121 | 48,6 | DTPA | 22,8 | <0,001 |
| | DTPA | — | — | 2 | 5 ♀ | 122 | 5,04 | ÄE | 2,3 | 0,05–0,02 |
| | — | ÄE | — | 2 | 5 ♀ | 122 | 32,2 | Wechselwirkung | 2,3 | 0,05–0,02 |
| | DTPA | ÄE | — | 2 | 5 ♀ | 128 | 5,04 | | | |
| 13 | — | — | — | 2 | 5 ♂ | 195 | 44,0 | ÄDTA | Subnormal | |
| | ÄDTA | — | — | 2 | 5 ♂ | 191 | 42,1 | ÄE | 6,1 | <0,001 |
| | — | ÄE | — | 2 | 5 ♂ | 206 | 32,4 | Wechselwirkung | Subnormal | |
| | ÄDTA | ÄE | — | 2 | 5 ♂ | 185 | 32,6 | | | |
| 14 | — | — | — | 3 | 5 ♂ | 168 | 39,1 | DTPA | 10,3 | <0,001 |
| | — | — | DTPA | 3 | 5 ♂ | 156 | 19,3 | ÄE | 4,7 | <0,001 |
| | — | ÄE | — | 3 | 5 ♂ | 167 | 28,4 | Wechselwirkung | Subnormal | |
| | — | ÄE | DTPA | 3 | 5 ♂ | 163 | 13,9 | | | |

Tabelle 3. $Y^{91}$-Gehalt der Organe (in % der Dosis). Erklärungen s. Tabelle 1

| Nr. | Chelatbildner | $\mu$M/Tier | Zeitpunkt (in Std.) der | | $N$ | $g$ | Leber | Nieren | Skelett |
|---|---|---|---|---|---|---|---|---|---|
| | | | Injektion | Sektion | | | | | |
| 1 | — | — | — | 48 | 6 ♂ | 207 | 4,10 (3,68–4,57) | 1,95 (1,76–2,16) | 62,4 (60,5–64,2) |
| | HÄDTA | 100 | 24 | 48 | 6 ♂ | 201 | 3,32 (3,07–3,59) | 2,00 (1,86–2,16) | 53,8 (52,5–55,2) |
| | ÄE | 100 | 24 | 48 | 6 ♂ | 190 | 2,70 (2,58–2,82) | 2,47 (2,24–2,68) | 58,5 (57,0–60,1) |
| 2* | — | — | — | 48 | 5 | 134 | 3,19 (3,00–3,39) | 1,17 (1,01–1,34) | 71,5 (69,7–73,1) |
| | HÄDTA | 100 | 24 | 48 | 5 | 134 | 3,18 (2,98–3,38) | 1,01 (0,88–1,16) | 65,9 (64,4–67,4) |
| | ÄE | 100 | 24 | 48 | 5 | 141 | 2,17 (2,03–2,30) | 1,10 (0,95–1,26) | 69,4 (67,8–71,0) |
| | ÄE i.p. | 100 | 24 | 48 | 5 | 117 | 2,27 (2,13–2,41) | 1,02 (0,88–1,17) | 66,4 (64,9–68,2) |
| | DTPA | 100 | 24 | 48 | 3 | 148 | 1,81 (1,69–1,94) | 1,04 (0,93–1,16) | 57,6 (56,0–59,2) |
| 3* | — | — | — | 144 | 7 | 154 | 1,39 (1,28–1,51) | 0,85 (0,72–1,00) | 67,2 (65,5–68,8) |
| | HÄDTA | 100 | 72 | 144 | 7 | 151 | 1,02 (0,93–1,11) | 0,77 (0,65–0,90) | 64,7 (63,0–66,4) |
| | ÄE | 100 | 72 | 144 | 7 | 150 | 1,02 (0,92–1,12) | 0,91 (0,77–1,07) | 65,6 (64,0–67,4) |
| | DTPA | 100 | 72 | 144 | 6 | 141 | 0,68 (0,62–0,74) | 0,78 (0,66–0,92) | 52,5 (51,0–54,0) |
| 4 | — | — | — | 120 | 5 ♀ | 129 | 1,88 (1,67–2,12) | 2,79 (2,17–3,51) | 67,3 (66,6–68,0) |
| | HÄDTA | 100 | 72 | 120 | 5 ♀ | 137 | 1,58 (1,47–1,69) | 2,17 (1,81–2,60) | 61,1 (59,1–64,5) |
| | ÄE | 100 | 72 | 120 | 5 ♀ | 135 | 1,43 (1,31–1,57) | 2,23 (2,00–2,49) | 66,4 (63,4–69,6) |

* Da in diesem Versuch ♂ und ♀ verwendet wurden und eine Geschlechtsabhängigkeit des Verteilungsmusters vorliegt, erfolgte bei der Berechnung der Mittelwerte eine entsprechende Korrektur mit Hilfe der Covarianzanalyse.

VOL 11 196

Tabelle 4. $Ce^{144}$-Gehalt der Organe (in % der Dosis); Erklärungen s. Tabelle 1. Die Chelatbildner wurden in einer Dosis von 250 $\mu$M/Tier intraperitoneal injiziert

| Nr. | Chelatbildner | Zeitpunkt (in Std.) der | | N | g | Leber | Nieren | Skelett |
|---|---|---|---|---|---|---|---|---|
| | | Injektion | Sektion | | | | | |
| 15 | — | 24 | 96 | 5 ♂ | 180 | 34,3 (32,1–35,8) | 1,84 (1,64–2,05) | 37,0 (35,2–38,8) |
| | DOC | 24 | 96 | 5 ♂ | 179 | 29,7 (28,6–31,0) | 1,89 (1,73–2,11) | 36,2 (34,3–38,0) |
| | DOC-L | 24 | 96 | 5 ♂ | 185 | 23,4 (22,4–24,6) | 1,65 (1,48–1,85) | 34,2 (32,6–35,9) |
| | DOC-L | 2 min | 96 | 5 ♂ | 181 | 3,39 (3,24–3,54) | 1,06 (0,95–1,18) | 36,7 (34,9–38,5) |
| 16 | — | 96 | 192 | 5 ♀ | 159 | 29,8 (28,0–31,7) | 0,74 (0,68–0,79) | 24,5 (23,4–25,5) |
| | DOC | 96 | 192 | 5 ♀ | 142 | 24,1 (22,6–25,7) | 0,77 (0,71–0,82) | 28,2 (27,0–29,5) |
| 17 | — | 96 | 192 | 5 ♂ | 148 | 21,2 (19,7–22,8) | 1,08 (1,02–1,14) | 41,0 (39,6–42,4) |
| | DOC-L | 96 | 192 | 5 ♂ | 140 | 14,7 (13,7–15,9) | 1,12 (1,06–1,19) | 44,7 (43,2–46,2) |

Ce*-Chelats ausgeschieden und nicht zurückgehalten wird. Die Effektivität der Ester scheint sich nur auf die Leber zu beschränken; dies darf nicht ohne weiteres dahingehend gedeutet werden, dass sie sich selektiv nur im Leberparenchym anreichern bzw. dass nur in den Leberzellen die Bedingungen für ihre ausreichende Verseifung gegeben sind. Die fehlende Wirksamkeit in anderen Organen wie der Niere könnte nämlich auch ohne weiteres dadurch bedingt sein, dass in diesem Fall die Chelatbildungskonstanten und/oder Konzentrationen nicht ausreichend gross sind, um sich gegenüber der Konkurrenz biologischer Reaktionspartner durchzusetzen.

Was die ausgeprägte Abhängigkeit der ÄE-Effektivität vom Zeitpunkt der Verabfolgung betrifft, so ist sie ein allgemein gültiges Phänomen und die Folgeerscheinung davon, dass Metallionen mit zunehmender Zeit in den Geweben in eine fester gebundene und damit für Chelatbildner weniger zugängliche Form überführt werden.[5,6] Die im Vergleich zum ÄE grössere Wirksamkeit der DTPA ist nicht überraschend, wenn man den für die Wirksamkeit relevanten [6] Quotienten der Chelatstabilitätskonstanten $K^{Ce}_{CeZ}/K^{Ca}_{CaZ}$ berücksichtigt; er beträgt für die DTPA[7] $10^{9,3}$, für die HÄDTA[8] dagegen nur $10^6$.

Bei kombinierter Verabreichung von ÄE und DTPA war aufgrund obiger Überlegungen eine Additivität der Wirkungen bei *vorheriger* Verabreichung des ÄE zu erwarten und konnte experimentell auch verifiziert werden. Bei *nachträglicher* Verabfolgung des ÄE sollte jedoch das relativ leicht mobilisierbare Ce* bereits durch DTPA entfernt und der ÄE somit ineffektiv sein; auch dies bestätigte sich experimentell. Geht der Zuführung des ÄE die Verabfolgung eines schwächer wirksamen Chelatbildners wie der ÄDTA voraus, so kann die Effektivität des ÄE sich wieder voll manifestieren.

Da die DTPA in ihrer Wirksamkeit dem ÄE und DOC-L erheblich überlegen ist, ergeben sich aus unseren Ergebnissen zunächst noch keine unmittelbaren praktischen Folgerungen für die Frage der therapeutischen Verwendbarkeit. Der Nachweis der Effektivitätssteigerung von Polyaminopolycarbonsäuren durch Veresterung und der offenbar hohen Resorption der veresterten Chelatbildner aus dem Digestionstrakt dürfte jedoch insofern von grundsätzlicher Bedeutung sein, als er einen neuen Ansatzpunkt für die Bemühungen um eine Verbesserung der therapeutischen Effektivität von Chelatbildnern aufzeigt. Es ist beabsichtigt, die Untersuchungen mit Estern anderer Substanzen fortzusetzen.

*Anerkennung*—Für die Darstellung und Überlassung der Chelate sind wir der J. R. Geigy AG, Basel, insbesondere Herrn Dr. P. Moser und Herrn H. W. Schläpper zu Dank verpflichtet. Für gewissenhafte technische Assistenz danken wir Frl. L. Braun und Frl. B. Storck.

## LITERATUR

1. Foreman H., Vier M. und Magee M. *J. biol. Chem.* **203,** 1045 (1953).
2. Catsch A. *Fed. Proc.* (1961) Im Druck.
3. Catsch A. und Lê D. Kh. *Strahlentherapie* **104,** 494 (1957).
4. Catsch A. Lê D. Kh. und Melchinger H. *Strahlentherapie* **106,** 606 (1958).
5. Catsch A. *Strahlentherapie,* (1961) **114,** Nr. 4.
6. Heller H. J. und Catsch A. *Strahlentherapie* **109,** 464 (1959).
7. Anderegg G., Nägeli P., Müller F. und Schwarzenbach G. *Helv. chim. acta* **42,** 827 (1959).
8. Spedding F. H., Powell J. E. und Wheelwright E. J. *J. Amer. chem. Soc.* **78,** 34 (1956).

International Journal of Applied Radiation and Isotopes, 1961, Vol. 11, pp. 139–144. Pergamon Press Ltd. Printed in Northern Ireland

# The Mechanism of the Radiation Chemical Degradation of Amino Acids—I

## The Degradation of α-Aminobutyric Acid

J. KOPOLDOVÁ, J. LIEBSTER and A. BABICKÝ
Biological Institute of the Czechoslovak Academy of Sciences, Prague

(*First received* 17 *November* 1960 *and in final form* 20 *February* 1961)

The mechanism of the radiolysis of α-aminobutyric acid under the influence of γ-irradiation was investigated. A reaction pattern is suggested. An explanation of the degradation mechanism is attempted on the bases of calculations of the 100 eV yields. The main path of radiolysis was elucidated.

LE MECANISME DE LA DEGRADATION CHIMIQUE PRODUITE PAR LE RAYONNEMENT DANS LES AMINO-ACIDES

On a recherché le mécanisme de la radiolyse de l'acide α-aminobutyrique sous l'influence du rayonnement γ. On propose un modèle de la réaction. On essaye de faire une explication du mécanisme de la dégradation sur le base des calculs des rendements à 100 eV. On a élucidé le chemin général de la radiolyse.

МЕХАНИЗМ РАДИАЦИОННО-ХИМИЧЕСКОГО РАЗЛОЖЕНИЯ АМИНОКИСЛОТ—I

Разложение α-аминомасляной кислоты

Был исследован механизм радиолиза α-аминомасляной кислоты под действием γ-излучения. Предложена схема реакции. Объяснение механизма распада исходит из расчета выходов на 100 эв. Выяснен основной путь протекания радиолиза.

MECHANISMUS DES RADIOCHEMISCHEN ABBAUS VON AMINOSÄUREN—I ABBAU DER α-AMINO-BUTTERSÄURE

Der Nachweis der Radiolyse von α-Amino-Buttersäure unter Einwirkung von α-Strahlung wurde untersucht. Ein Modell für den Reaktionsverlauf wird vorgeschlagen. Eine Erklärung des Abbau-Nachweises wird versucht auf Berechnungsbasis von 100 eV Ausbeuten. Der Hauptweg der Radiolyse wird klargelegt.

THE radiation chemical degradation of α-aminobutyric acid was studied in continuance of our previous investigations[1] of the effects of radiation on methionine-$S^{35}$, where α-aminobutyric acid proved to be one of the main degradation products[2]. This paper simultaneously represents the first part of a wider study on the radiation effects on amino acids, e.g. valine, norvaline, leucine, isoleucine, norleucine etc., where the relation between the structure of the amino acids and the mechanism of the radiation degradation is investigated.

A similar study was undertaken by WEEKS and GARRISON[3] who presented a detailed mechanism of the radiolysis of glycine. Glycine however is a much simpler amino acid yielding only a small number of products upon irradiation. A much more complicated situation was encountered with the higher amino acids we attempted to study.

## EXPERIMENTAL

α-Aminobutyric acid and α-aminobutyric acid-1-$C^{14}$ were irradiated in 0·05 M aqueous solution saturated with oxygen. The solution, 8–10 ml, was irradiated in glass ampullae. A $Co^{60}$ source was used. Doses of 0·25, 0·50, 0·75, 1·00 and 1·25 × $10^{20}$ eV/ml were employed. The dose was measured with the Fricke dosimeter according to Weiss *et al*[4]. The dose rate was 1·74 × $10^{16}$ eV/ml per min.

## ANALYTICAL METHODS

Ammonia was determined by Conway's method; $CO_2$ was determined by titration. The ninhydrin-positive substances were separated by paper chromatography and quantitatively determined colorimetrically after elution. The radioactive products of the radiolysis of α-aminobutyric acid-1-$C^{14}$ were identified by autoradiography of the chromatograms and the determination of the radioactivity of the separated products. The identification was carried out by two-dimensional chromatography and comparison with standard compounds.

Keto-acids and aldehydes were determined as the 2:4-dinitrophenylhydrazones and compared with standard compounds.

The volatile acids were titrated after steam distillation and identified chromatographically.

Gaseous products were determined for the highest dose by gas chromatography.

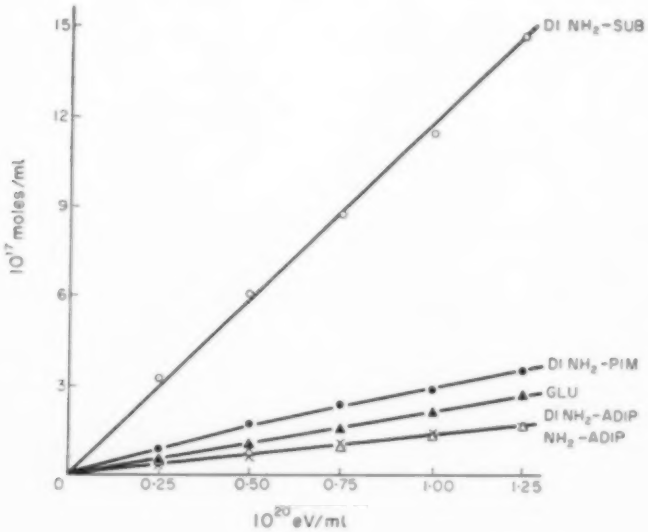


Fig. 1. Formation of ninhydrin-positive recombination products.
*x*-axis—radiation dose in $10^{20}$ eV/ml
*y*-axis—$10^{17}$ molecules/ml formed
○—diaminosuberic acid
●—diaminopimelic acid
△—diaminoadipic acid
▲—glutamic acid
×—aminoadipic acid.

## RESULTS AND DISCUSSION

The radiolysis of α-aminobutyric acid led to the formation of these compounds:

*Amino acids:* α,η-diaminosuberic acid, homoserine, aspartic acid, threonine, glutamic acid, alanine, α-aminoadipic acid, α,ε-diaminopimelic acid.

*Keto acids:* α-ketobutyric acid, pyruvic acid; oxaloacetic acid (traces).

*Acids:* acetic acid, propionic acid; oxalic acid, succinic acid and formic acid in traces.

*Aldehydes:* acetaldehyde, propionaldehyde; formaldehyde (traces).

*Gases:* $CO_2$, $NH_3$ and traces of ethane, methane, ethylene and CO.

The concentrations and amounts of the main products of radiolysis were determined

in dependence on the radiation dose and plotted in Figs. 1–4, the points on the curves representing average values from at least three experiments.

Based on the type of curves obtained for the products of radiolysis, a degradation pattern for α-aminobutyric acid is suggested (Table 2).

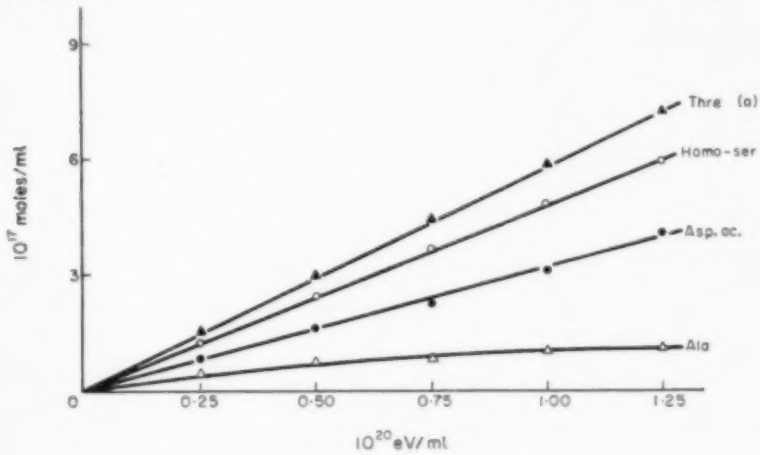


FIG. 2. Formation of ninhydrin-positive oxidation products.
*x*-axis—radiation dose in $10^{20}$ eV/ml
*y*-axis—$10^{17}$ molecules/ml formed
○—homoserine
●—aspartic acid
△—alanine
▲—threonine

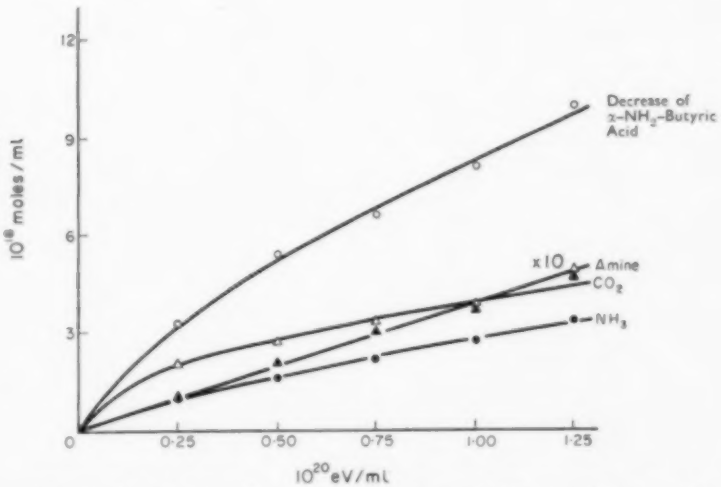


FIG. 3. Decrease of α-aminobutyric acid, formation of ammonia, amines and $CO_2$.
*x*-axis—radiation dose in $10^{20}$ eV/ml
*y*-axis—$10^{18}$ molecules/ml formed
○—decrease of α-aminobutyric acid
●—formation of ammonia
△—formation of amines
▲—formation of $CO_2$.

To support this reaction pattern the *G*-values of the products of radiolysis for the maximum dose of $1{\cdot}25 \times 10^{20}$ eV/ml were calculated and are given in Table 1.

When the *G*-values of all the products formed with the exception of $CO_2$ and $NH_3$ are added up, the values for the products formed by recombination being doubled, a yield of 7·6 is obtained, the experimentally determined value for the degradation of α-aminobutyric acid being 7·8. It is further necessary to add the sum of the values of *G* of the products formed in traces or not determined quantitatively (aldols) to the calculated value; this additional *G* was estimated at approximately 0·2.

For $G_{NH_3}$ a value of 2·6 was found, this value should be equal to the sum of the values of *G* for all compounds not containing an $NH_2$-group (except $CO_2$) plus the yields (*G*) of the compounds supposed to originate from the recombination of such a component (e.g. α-aminoadipic acid). For this calculated sum a value of 2·1 was found. This

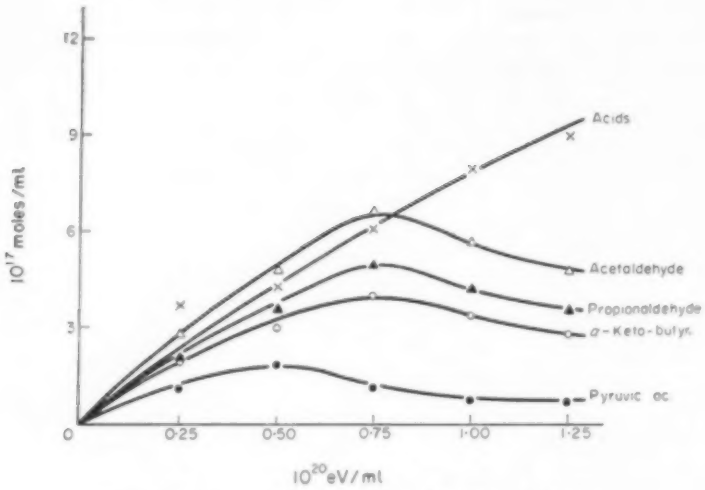


FIG. 4. Formation of keto-acids, aldehydes and acids.
*x*-axis—radiation dose in $10^{20}$ eV/ml *y*-axis—$10^{17}$ molecules/ml formed
○—α-ketobutyric acid ●—pyruvic acid
△—acetaldehydes ×—total acids ▲—propionaldehyde.

TABLE 1. *G*-values of the products of radiolysis for a dose of $1{\cdot}25 \times 10^{20}$ eV/ml

| Compound | *G* |
|---|---|
| Decrease of α-amino-butyric acid | 7·8 |
| $NH_3$ | 2·6 |
| Amines | 0·4 |
| $CO_2$ | 3·7 |
| Diaminosuberic acid | 1·2 |
| Diaminopimelic acid | 0·3 |
| Glutamic acid | 0·2 |
| Diaminoadipic acid | 0·1 |
| Aminoadipic acid | 0·1 |
| Threonine | 0·6 |
| Homoserine | 0·5 |
| Aspartic acid | 0·3 |
| Alanine | 0·1 |
| Acetic acid | 0·5 |
| Acetaldehyde | 0·4 |
| Propionic acid | 0·3 |
| Propionaldehyde | 0·3 |
| α-Ketobutyric acid | 0·2 |
| Pyruvic acid | 0·1 |

value again is somewhat lower than the value found for $G_{NH_3}$ as it does not include the values of *G* for several compounds, as in the previous instance, whose yield can be estimated as about 0·2.

Finally, the value of 3·7 found for $G_{CO_2}$ should be equal to the sum of the *G*-values of all the products formed by decarboxylation, the value for acetaldehyde and acetic acid being doubled as they are presumed to be formed by two decarboxylation reactions. Thus a value of 3·8 is obtained. Again it is necessary to add to this value the estimated yield of 0·4 for the products, whose *G* could not be determined. The higher value has to be employed here as the formation of most of these products, e.g. the aldols, is presumed to require two decarboxylations.

Good agreement was found between the calculated values and the yields obtained. Only in the instance of the sum of the *G*-values for the decarboxylated products was the value somewhat too high. This could be considered to support the opinion that glutamic acid could arise also by a different mechanism (e.g. the reaction of a $C_4$ and a $C_1$ compound or radical respectively, which was experimentally proved by the irradiation of α-aminobutyric acid and $C^{14}O_2$ yielding radioactive glutamic acid).* In this case the sum would be decreased by 0·3 as, according to the pattern, the formation of one molecule of glutamic acid requires three decarboxylations. It would be necessary to decrease simultaneously the sum of the *G*-values of all products by 0·1, the resulting sum amounting to about 7·6 after correction.

Comparison of the yields of the different products shows the main path of radiolysis to be the formation of the radical at $C_4$ of aminobutyric acid, with subsequent dimerization and oxidation of the radical. These reactions are participating in about 75 per cent in the total degradation of α-aminobutyric acid. The deamination reaction of α-aminobutyric acid leading to α-ketobutyric acid participates in 11 per cent, about one third of the ammonia formed arises in this reaction. Oxidation at $C_3$ leading to threonine participates with 9 per cent. The decarboxylation reactions, giving rise to the

* The results of these experiments will be published in a further paper.

TABLE 2. The suggested reaction pattern of the radiolysis of α-aminobutyric acid

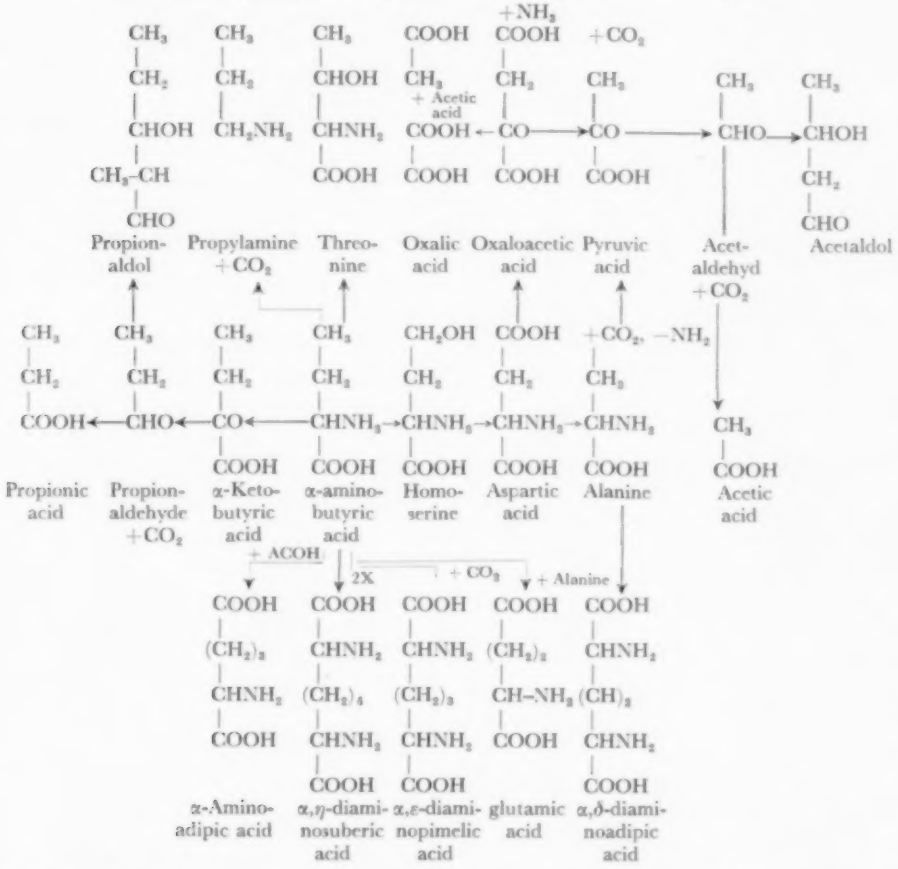


formation of amines, amount to less than 5 per cent. The comparatively small scale of the primary deamination was somewhat unexpected, However, it is proved by the finding that the pyruvic acid formed from α-aminobutyric acid-1-$C^{14}$ is radioactive. We therefore consider the main path of acetaldehyde formation to occur through pyruvic acid.

We then attempted to explain the mechanism of the radiolysis of α-aminobutyric acid.

According to DEWHURST and BURTON[5] the basic chemical reaction induced by the absorption of radiation in water is

$$H_2O \rightsquigarrow H, OH, H_2, H_2O_2. \quad (1)$$

In solutions saturated with oxygen the following reactions can be assumed to occur

$$H + O_2 \longrightarrow HO_2 \quad (2)$$

$$2HO_2 \longrightarrow H_2O_2 + O_2. \quad (3)$$

Considering that it is not possible to differentiate in this system between OH; $HO_2$ and $H_2O_2$, radicals and $H_2O_2$ were denoted by the common symbol X and the second product radicals formed in a given reaction by Y. As the system under consideration is a rather complicated one, only the reactions leading to the primary or the main products respectively are given here. The basic reaction leading to the most important part of the products is the formation of the radical of α-aminobutyric acid:

$$HOOC\,CH\,(NH_2)\,CH_2\,CH_2\,CH_3 + X \longrightarrow HOOC\,CH\,(NH_2)\,CH_2\,CH_2 + Y. \quad (4)$$

As evidence for the formation of the α-aminobutyric acid radical, the formation of the dimerization product, i.e. diaminosuberic acid, may be considered:

$$2HOOC\ CH\ (NH_2)\ CH_2\ CH_2 \longrightarrow [HOOC\ CH\ (NH_2)\ CH_2\ CH_2]_2. \quad (5)$$

As other authors (GARRISON *et al.*[9] and BAKH[8] were able to prove that free organic radicals easily react with molecular oxygen, the mechanism of the formation of some of the oxidation products of α-aminobutyric acid, e.g. aspartic acid and homoserine, could be explained by these reactions:

$$HOOC\ CH\ (NH_2)\ CH_2\ CH_2 + O_2 \longrightarrow HOOC\ CH\ (NH_2)\ CH_2\ CH_2\ O_2. \quad (6)$$

Hydrolysis of the peroxide should lead to the formation of homoserine.

From this peroxide, homoserine could be formed by a hydrolytic or other mechanism. The intermediate formation of a peroxide is acceptable as no formation of homoserine occurs in oxygen-free solutions, which was proved experimentally.*

The formation of threonine can be explained by analogous reactions.

Another important reaction in the radiolysis of α-aminobutyric acid is the deamination leading to the formation of α-ketobutyric acid and propionaldehyde, respectively, $CO_2$ and $NH_3$:

$$HOOC\ CH\ (NH_2)\ CH_2\ CH_3 + X \longrightarrow HOOC\ CO\ CH_2\ CH_3 + NH_3 + Y. \quad (7)$$

$$HOOC\ CH\ (NH_2)\ CH_2\ CH_3 + X \longrightarrow OHC\ CH_2CH_3 + NH_3 + CO_2 + Y. \quad (8)$$

The formation of pyruvic acid or acetaldehyde could be explained by analogous deamination reactions of alanine.

Further experiments for the elucidation of some of these reactions are under way.

*Acknowledgments*—The authors wish to express their gratitude to DR. HAVRÁNEK for the synthesis of α-aminobutyric acid-1-$C^{14}$ and to DR. VEREŠ, DR. TEPLÝ and DR. BEDNÁŘ for valuable suggestions and discussions.

## REFERENCES

1. KOPOLDOVÁ J., KOLOUŠEK J., BABICKÝ A. and LIEBSTER J. *Nature, Lond.* **182,** 1074 (1958).
2. KOPOLDOVÁ J., KOLOUŠEK J., LIEBSTER J. and BABICKÝ A. *Proceedings of the Second International Conference on the Peaceful Uses of Atomic Energy, Geneva,* 1958, P/2117, Vol. 22, p. 492. United Nations, New York (1958).
3. WEEKS B. M. and GARRISON W. M. *Radiat. Res.* **9,** 291 (1958).
4. WEISS J., ALLEN A. O. and SCHWARZ H. A. *Proceedings of the First International Conference on the Peaceful Uses of Atomic Energy, Geneva,* 1955, Vol. 14, p/155, pp. 179–181. United Nations, New York (1956).
5. DEWHURST H. A. and BURTON M. *J. Amer. chem. Soc.* **77,** 5781 (1955).
6. HART E. J. *J. Amer. chem. Soc.* **76,** 4312 (1954).
7. MACKUSICK W. E., MOCHEL W. E. and STACEY F. W. *J. Amer. chem. Soc.* **82,** 723 (1960).
8. BAKH N. A. *Proceedings of the Second International Conference on the Peaceful Uses of Atomic Energy, Geneva,* 1958, P/2293, Vol. 29, p. 128. United Nations, New York (1958).
9. GARRISON W. M., HAYMOND H. R., BENNET W. and COLE S. *Radiat. Res.* **10,** 273 (1959).

* The results of these experiments will be published in a further paper.

International Journal of Applied Radiation and Isotopes, 1961, Vol. 11, pp. 145–151. Pergamon Press Ltd. Printed in Northern Ireland

# Résistance aux Radiations Ionisantes de Quelques Souches de *Lactobacillus**

P. DUPUY et O. TREMEAU
Institut National de la Recherche Agronomique, Station de Technologie Végétale, Versailles, France

(*Received* 14 *February* 1961)

VOL. 11 1961

On a étudié la résistance aux rayons $\gamma$ de 21 souches de *Lactobacillus* culturées dans un milieu acide. Toutes les courbes de survie avaient un aspet sigmoïde. Les doses léthales 99 pour cent sont entre 22,8 et 38,2 krad. Ainsi ces bactéries ne semblant avoir aucune résistance particulière à la radiation, et leur comportement ressemble celui d'*E. Coli*. On ne trouva pas de différence entre la radio-sensibilité des souches homo-fermentatives et hetéro-fermentatives.

RESISTANCE OF CERTAIN STRAINS OF *LACTOBACILLUS* TO IONIZING RADIATIONS

The resistance to $\gamma$-rays of 21 strains of *Lactobacillus* grown in an acid medium was studied. All the inactivation curves which were obtained had a sigmoïd aspect. The lethal doses 99 per cent are between 22·8 and 38·2 krad. Thus these bacteria do not appear to have any special resistance to radiation, and their behaviour is similar to *E. coli*. No difference was found between the radio sensibility of homo- and hetero-fermentative strains.

ИССЛЕДОВАНИЕ РЕЗИСТЕНТНОСТИ НЕКОТОРЫХ ШТАММОВ *LACTOBACILLUS* К ИОНИЗИРУЮЩЕМУ ИЗЛУЧЕНИЮ

Была исследована резистентность к $\gamma$-излучению двадцати одного штамма *Lactobacillus* выращенного в кислой среде. Все полученные кривые инактивации были S-образной формы. Летальная доза (смертность 99%) находилась в диапазоне 22,8–38,2 килорад. Таким образом эти бактерии, повидимому, не обладают особой резистентностью к излучению и их поведение подобно поведению *E. Coli*. Разницы в по ведении гомо-и гетеро-ферментативных штаммов не наблюдалось.

WIDERSTANDSFÄHIGKEIT EINIGER *LACTOBACILLUS*-STÄMME GEGEN IONISIERENDE STRAHLUNG

Die Widerstandsfähigkeit gegenüber $\gamma$-Strahlung von 21 *Lactobacillus*-Stämmen, gezüchtet in saurem Medium, wurde untersucht. Die erhaltenen Inaktivierungskurven zeigen sigmoïden Charakter. Die 99% Lethaldosen liegen zwischen 22,8 und 38,2 krad. Diese Bakterien scheinen daher keine spezielle Strahlenresistenz zu besitzen und ihr Verhalten ist ähnlich wie bei *E. coli*. Zwischen der Strahlenempfindlichkeit der homo- und der heterofermentativen Stämme wurde kein Unterschied gefunden.

## A. INTRODUCTION

On peut déjà prévoir que l'utilisation des radiations ionisantes pour la "pasteurisation" des aliments se trouvera limitée par des substitutions de flores. Ceci provient du fait que les diverses espèces n'ont pas la même sensibilité aux rayonnements. Ce phénomène a

* Ce travail a été réalisé grâce au contrat de recherche No. 29 établi entre l'Agence Internationale de l'Energie Atomique et l'Institut National de la Recherche Agronomique.

été décrit par DRAKE *et al.*[1] lors de l'irradiation de saucisses de Francfort et par INGRAM et THORNLEY[2] dans le cas des carcasses de poulets. Pour arriver à un résultat convenable, il paraît nécessaire, non seulement de diminuer fortement le nombre de germes totaux, mais encore d'avoir parmi les survivants une proportion aussi forte que possible de microorganismes favorables à la conservation des aliments.

A ce point de vue, les *Lactobacillus* sont sûrement les bactéries les plus avantageuses aussi bien pour les produits animaux que pour les produits végétaux. A cause de leurs propriétés acidifiantes on les utilise déjà dans de nombreuses préparations alimentaires: fromages, charcuterie, choucroute . . .

Lorsqu'on se réfère à la liste de résistance dressée par NIVEN[3], on voit que ces microorganismes présentent justement une résistance assez élevée aux radiations. Nous avons donc pensé qu'il était utile de contrôler ces résultats en utilisant un milieu de culture différent et d'étendre les observations à de nouvelles souches, en vue de rechercher celles qui seraient les plus résistantes. Si de telles souches existaient, on pourrait ensuite essayer de les ensemencer dans les produits destinés à être pasteurisés par irradiation.

## B. TECHNIQUES UTILISEES

(1) *Souches*

Parmi les souches utilisées certaines proviennent des collections N.C.D.O., A.T.C.C. (National Collection of Dairy Organisms, American Type Culture Collection) elles présentent donc toutes les garanties désirables au point de vue de leur identification.

Les autres ont été isolées par nous-mêmes ou par d'autres chercheurs au cours d'études antérieures; elles proviennent de vin, de viande, de sucrerie, et de pulpes de betterave ensilées.

(2) *Milieu de culture*

Le même milieu a été utilisé pour les cultures et pour les numérations des bactéries irradiées.

Sa composition est la suivante:

| | |
|---|---|
| Extrait de levure Difco | 10 g |
| Extrait de viande de boeuf Difco | 3 g |
| Bacto tryptone Difco | 5 g |
| Acétate de Na cristallisé | 5 g |
| Phosphate disodique | 1 g |
| Glucose | 10 g |
| Acide d'l-malique | 7 g |
| Solution de sels minéraux de Wright et Skeggs | 5 ml |
| Jus de tomate | 70 ml |
| Tween 80 | 0,5 g |
| Biotine | 10 $\gamma$ |

pour 1 l. d'eau désionisée pH ajusté à 6,6 avec NaOH, stérilisation 15 min à 118°C.

Ce milieu, tel quel ou dilué, a été utilisé au cours de travaux antérieurs sur les *Lactobacillus.*[4,5] Il est dérivé de celui proposé par OCHOA[6] et contient en plus du jus de tomate qui apporte des facteurs favorables au développement de certaines souches.

Les bactéries destinées à l'irradiation proviennent de cultures obtenues à 25 ou 30°C sur milieu liquide en 20–30 hr et ayant atteint leur phase stationnaire.

La récolte des bactéries se fait par centrifugation suivie d'un lavage dans du tampon phosphaté 0,02 M, pH = 6,6 et de 5 min d'agitation avec des billes de verre pour disperser les amas. La suspension est reprise dans le tampon et diluée pour obtenir 100,000 cellules/ml. L'absence d'amas est contrôlée par un examen microscopique après coloration.

(3) *Irradiation*

La suspension est ensuite répartie dans des tubes à essais et irradiée dans une source de $Co^{60}$ donnant 450 rad/min. L'homogénéité de la dose reçue par les divers échantillons placés à l'intérieur de l'irradiateur a été mesurée avec des dosimètres au sulfate ferreux d'après SUTTON[7]. Dans les conditions d'emploi les résultats des dosimètres ne diffèrent pas de $\pm 1{,}6\%$. Il a été tenu compte de la décroissance de radioactivité du cobalt.

Les suspensions placées dans des tubes à

essais bouchés au coton ont été irradiées à la température ambiante, environ 4 hr après le début de la récolte. Sauf pendant l'irradiation, les bactéries ont été conservées à la température de 0°C. Après irradiation, la numération des survivants a été faite en plaçant dans une boite de Petri 1 ml d'une dilution appropriée, et en y coulant 15 ml du milieu indiqué contenant 18 g/l. de gélose et maintenu à 42°C. Après 4 jours à 25°C ou à 30°C pour certaines souches, le nombre de colonies visibles n'augmente plus et on procède à la numération. On fait dans les mêmes conditions des numérations sur la suspension non irradiée, au début et à la fin de l'expérience.

(4) *Caractère homo ou hétérofermentatif des souches*

Afin de déterminer les divers produits de fermentation du glucose obtenus avec les souches étudiées, on a utilisé le milieu précédent ne contenant ni acétate de Na, ni acide malique, ni jus de tomate. On introduit stérilement 50 ml de ce milieu dans un tube d'Eldredge[8] et on ensemence avec 0,1 ml d'une culture jeune. Dans l'autre branche, on place 25 ml de $Ba(OH)_2$, 0,2 N. On ensemence en même temps un tube d'Eldredge témoin avec le même milieu dépourvu de glucose. Après 10 jours d'incubation à 25°C on détermine le $CO_2$ fixé sur la baryte avec l'acide sulfurique 0,2 N. Sur le milieu de culture centrifugé on dose le glucose restant par la méthode de Bertrand, l'éthanol formé par l'oxydation chromique (Cordebard), l'acidité volatile par entrainement à la vapeur d'eau (Jaulmes), l'acidité totale par titrage en présence de phénolphthaléine.[9]

Les différences entre les valeurs trouvées dans le milieu glucosé et dans le milieu témoin permettent de calculer les produits de la fermentation du glucose. L'acidité volatile est exprimée en acide acétique et la différence, acidité totale moins acidité volatile, est exprimée en acide lactique. L'approximation de ces résultats sera discutée par la suite.

## C. RESULTATS

(1) *Courbes de survie*

Pour 21 souches de *Lactobacillus*, nous avons déterminé les courbes de survie avec des doses s'échelonnant de 0–50 krad (Fig. 1). Dans les conditions expérimentales que nous avons adoptées, ces courbes ne sont jamais exponentielles; il n'a donc pas été possible d'appliquer à nos résultats le calcul statistique qui nous aurait permis de déterminer la courbe la plus probable. De plus la forme de la courbe ne peut être expliquée par l'hypothèse de l'existence d'une seule cible. Les extrapolations graphiques laissent prévoir qu'il y aurait dans chaque bactérie un nombre important de cibles.

On peut rapprocher la forme sigmoïde de ces courbes du fait que les bactéries ont été cultivées dans un milieu qui, bien que tamponné, tendait à s'acidifier. Au moment du prélèvement, le pH était généralement compris entre 4 et 5. *E. coli*, cultivé sur le même milieu, ayant au moment de la récolte un pH de 5,65, présente aussi une courbe de destruction sigmoïde alors que d'après Marcovich[10] la même souche donne une courbe exponentielle lorsqu'elle est cultivée sur bouillon de viande, donc à un pH voisin de la neutralité.

Un résultat analogue a déjà été mis en évidence par Stapleton et Engel[11] qui l'ont attribué à une diminution de pH dans le milieu de culture.

(2) *Sensibilite des diverses souches*

Les cellules irradiées proviennent de la phase stationnaire de la culture, car on a constaté qu'à ce stade de la croissance la sensibilité aux radiations varie peu. De plus, elles ont été cultivées dans un milieu acide, riche en azote, contenant du glucose et des acides organiques, c'est-à-dire dans des conditions qui se rapprochent assez de celles rencontrées dans certaines substances alimentaires d'origine végétale. Il est certain que ce milieu ne représente pas le milieu optimum pour chacune des souches, mais il

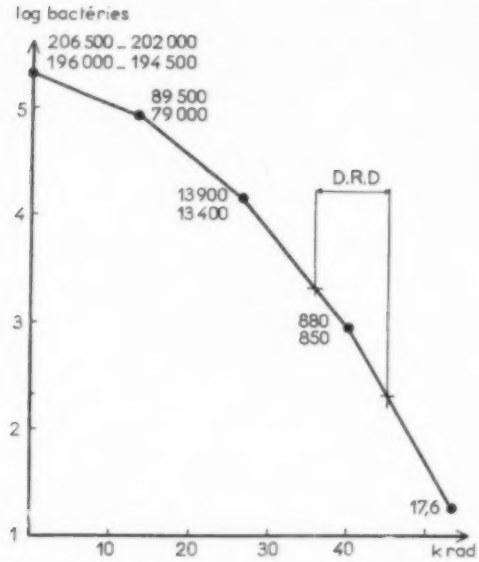


FIG. 1. Courbe de survie de la souche *L. arabinosus* 1. Chaque valeur indiquée correspond à une série de dilutions et à la moyenne de quatre boites de Pétri. Pour l'échantillon non irradié, la numération a été refaite après 120 min de conservation dans des conditions identiques à celles des échantillons irradies D.R.D. = dose de réduction décimale.

convient à la croissance de toutes. Il nous a paru indispensable de conserver le même milieu afin de pouvoir comparer les sensibilités respectives des diverses souches. La méthode de numération utilisée est moins précise que l'étalement à la surface de la gélose, mais elle nous est imposée par certaines souches, par exemple celles isolées du vin, dont la croissance est très lente. Le développement en surface est gêné par l'excès d'oxygène et par la dessiccation progressive de la gélose.

L'irradiation a été faite en présence d'air. On sait que la respiration des bactéries lactiques est faible, les déterminations réalisées dans des conditions optimales à 38°C en présence de glucose donnent avec des bactéries non proliférantes un $Q_{02}$ de 5,5 $\mu$ 1/mg/hr.[4] Les 100.000 bactéries de la suspension irradiée représentent 0,1 $\gamma$ de matière sèche et leur consommation au cours de 2 hr d'irradiation ne peut représenter que 1,1 $10^{-3}$ $\mu$ 1/ml. Comme 1 ml de tampon peut dissoudre environ 6 $\mu$ 1 d'$O_2$ il n'y a pas lieu de craindre une diminution de la tension de l'oxygène dissous.

Afin de pouvoir comparer plus facilement les diverses souches, on a déterminé graphiquement à partir des courbes d'inactivation les paramètres suivants:

DL 99—la dose exprimée en kilorads nécessaire pour inactiver le développement de 99% de la population.

DL 99,9—la dose pour inactiver 99,9%.

La différence des deux valeurs donne la dose de réduction décimale entre 1 pour 100 et 0,1 pour 100 de survie, c'est-à-dire, à un moment où la courbe se rapproche d'une exponentielle. Cette grandeur paraît particulièrement intéressante pour comparer entre elles les différentes souches, mais du fait des erreurs commises sur DL 99 et DL 99,9; sa précision reste faible.

A titre d'exemple nous indiquons dans le Tableau 1 les résultats obtenus dans six expériences réalisées à des époques différentes avec la même souche.

Les résultats obtenus avec les 21 souches de *Lactobacillus* étudiées sont rassemblés dans le Tableau 2. On remarque que les différences d'une souche à l'autre ne sont pas considérables. La souche la plus sensible paraît être *L. casei* et la plus résistante *L. fermenti*. Les valeurs de la DL 99 que nous avons trouvées ne concordent pas avec celles déjà publiées par DRAKE *et al.*[1] qui allaient de 43 à 74 krad pour les souches hétérofermentatives et de 172 à 209 pour les homofermentatives. En effet, on peut voir sur le Tableau 2 que la DL 99 des souches étudiées est comprise

TABLEAU 1. Dose létale en kilorads obtenue avec *L. arabinosus* 1 dans six répétitions de la même expérience

| Expériences | DL 99 | DL 99,9 | Dose réd. décimale (DL 99,9–DL 99) |
|---|---|---|---|
| 1 | 35,8 | 46 | 10,2 |
| 2 | 37,4 | 48,6 | 11,2 |
| 3 | 39,6 | 48,7 | 9,1 |
| 4 | 33,5 | 42,5 | 9 |
| 5 | 27,5 | 36,5 | 9 |
| 6 | 39,8 | 50,5 | 10,7 |
| Moyennes | 33,9 | 45,5 | 9,9 |

TABLEAU 2. Doses létales exprimées en kilorads pour diverses souches de *Lactobacillus*

| No. | Souches | DL 99 | DL 99,9 | D.R.D.* | pH de la culture |
|---|---|---|---|---|---|
| 1 | *L. brevis* NCDO 110 | 34 | 46 | 12 | 5,15 |
| 2 | *L. bulgaricus* NCDO 87 | 25,7 | 33,4 | 7,7 | 4,78 |
| 3 | *L. casei* NCDO 151 | 28 | 32,5 | 4,5 | 4,2 |
| 4 | *L. fermenti* NCDO 215 | 28,3 | 52,3 | 14 | 5,05 |
| 5 | *L. helveticus* NCDO 30 | 35,3 | 42,5 | 7,2 | 5,57 |
| 6 | *L. lactis* NCDO 280 | 28,6 | 34,6 | 6 | 4,92 |
| 7 | *L. plantarum* NCDO 343 | 39,8 | 48,4 | 8,6 | 4,28 |
| 8 | *L. arabinosus* 17/5 N.T.C.C. | 26 | 33,2 | 7,2 | — |
| 9 | *L. arabinosus* 1 | 35,8 | 46 | 10,2 | — |
| 10 | P 3 (Ensilages) | 27,3 | 37,6 | 10,3 | 4,82 |
| 11 | P 6 (Ensilages) | 31,5 | 44,3 | 12,8 | 4,76 |
| 12 | P 41 (Ensilages) | 22,8 | 31,3 | 8,5 | 5,05 |
| 13 | S 76 (Sucrerie) | 29,5 | 37,2 | 7,7 | 5,45 |
| 14 | S 269 (Sucrerie) | 34 | 41,7 | 7,7 | 5,30 |
| 15 | S 277 (Sucrerie) | 35 | 44,8 | 9,8 | 4,6 |
| 16 | S 302 (Sucrerie) | 28,7 | 35,3 | 6,6 | 5,1 |
| 17 | CB 7 (Viande) | 24 | 34,7 | 10,7 | 4,37 |
| 18 | CB 6 D (Viande) | 31,5 | 39,8 | 8,3 | 4,30 |
| 19 | WB 10 A (Viande) | 30,2 | 36,9 | 6,7 | 4,31 |
| 20 | 2 C 10 (Viande) | 23 | 28,1 | 5,1 | 4,87 |
| 21 | V 5 Vin | 23 | 31,5 | 8,5 | — |
| 22 | *Escherichia coli* K 12 | 39,3 | 49 | 9,7 | 5,65 |

Les souches Nos. 17, 18, 19 nous ont été fournies par NIVEN, la souche No. 20 par le Dr. Raibaud et la souche No. 22 par MARCOVICH.

* D.R.D. = dose de reduction décimale DL 99,9–DL 99.

entre 22,8 et 38,3 krad. Cette différence n'est pas imputable aux souches utilisées puisqu'elle a été retrouvée sur les trois souches homofermentatives CB 7, CB 6 D et WB 10 A, ayant déjà servi aux travaux des auteurs américains. Nous pensons plutôt qu'elle peut provenir des compositions du milieu de culture utilisé[12] et du milieu dans lequel se fait l'irradiation.[1] De nouvelles expériences sont entreprises pour préciser ce point.

Les valeurs trouvées pour les doses létales ont été contrôlées en irradiant dans les mêmes conditions une souche d'*E. coli* K 12 dont la résistance est bien connue. La dose de réduction décimale que nous avons déterminée avec la souche K 12 entre 1% et 0,1% de survie est 9,7 krad, valeur en accord avec les résultats de MARCOVICH[10]. Comme cette bactérie a été récoltée dans un milieu acide (pH = 5,65), la courbe de survie devient sigmoïde. Les doses DL 90 ont été trouvées dans deux expériences égales à 25 et 28 krad alors que les valeurs données par STAPLETON et ENGEL[11] sont 18 krad pour la souche *E. coli* B et 20 krad pour la souche H7. Il semble donc que la méthode de travail utilisée soit convenable puisque dans le cas d'*E. coli* elle nous a permis de retrouver des résultats du même ordre de grandeur que ceux publiés dans la littérature.

### (3) *Comportement des homo et hétérofermentatifs*

Les expériences de DRAKE *et al.*[1], qui ont porté sur sept souches, laissent apparaître une résistance plus importante chez les *Lactobacillus* homofermentatifs. Cette constatation n'est pas confirmée par nos résultats.

Le Tableau 3 indique les produits de la fermentation du glucose formés par les souches étudiées. Un bon classement entre homo et hétérofermentatifs est obtenu en calculant le rapport des poids: $\frac{CO_2}{\text{acide lactique}}$. Il se situe autour de 50% pour les hétérofermentatifs et tend vers zéro pour les homofermentatifs. Les valeurs trouvées sont bien groupées autour de l'un ou l'autre de ces

TABLEAU 3. Bilan des produits de fermentation du glucose pour diverses souches de *Lactobacillus*

| No. | Souches | | Glucose introduit | $CO_2$ | Acide lactique | Acide acétique | Ethanol | Glucose restant | Total | Différence | % de $CO_2$ en milligramme par rapport à l'acide lactique |
|---|---|---|---|---|---|---|---|---|---|---|---|
| 1 | *L. brevis* NCDO 110 | | 452 | 87,5 | 127,5 | 25,6 | 71,1 | 0 | 311,7 | −140,3 | 69 |
| 2 | *L. bulgaricus* NCDO 87 | | 470 | 2,5 | 234 | 7 | 0 | 180 | 423,5 | −46,5 | 1,1 |
| 3 | *L. casei* NCDO 151 | | 470 | 4,7 | 428 | 13,2 | 0 | 0 | 445,9 | −24,1 | 1,1 |
| 4 | *L. fermenti* NCDO 215 | | 452 | 78,2 | 158 | 9 | 80 | 0 | 335,2 | −116,8 | 49 |
| 5 | *L. helveticus* NCDO 30 | | 470 | 9,5 | 392 | 7 | 0 | 56 | 464,5 | −5,5 | 2,4 |
| 6 | *L. lactis* NCDO 280 | | 517 | 0 | 236 | 6,9 | 9,1 | 287 | 539 | +22* | 0 |
| 7 | *L. plantarum* NCDO 343 | | 517 | 1,5 | 478 | 7,8 | 0 | 0 | 487,3 | −29,7 | 0,31 |
| 8 | *L. arabinosus* 17/5 | | 455 | 3 | 301,5 | 5,4 | 0 | 0 | 309,9 | −145,1 | 1 |
| 9 | *L. arabinosus* 1 | | 498 | 7 | 432 | 11,7 | 1,1 | 0 | 451,8 | −46,2 | 1,6 |
| 10 | P 3 | Ensilages | 467 | 6,1 | 389 | 4,5 | 1,1 | 0 | 400,7 | −66,3 | 1,6 |
| 11 | P 6 | Ensilages | 467 | 4,9 | 385 | 6 | 1,7 | 0 | 397,6 | −69,4 | 1,3 |
| 12 | P 41 | Ensilages | 467 | 6,4 | 389 | 9 | 2,85 | 0 | 407,2 | −59,8 | 1,6 |
| 13 | S 76 | Sucrerie | 470 | 101,8 | 195 | 15,5 | 112,1 | 0 | 424,4 | −45,6 | 52 |
| 14 | S 269 | Sucrerie | 470 | 110 | 188 | 16,2 | 115,9 | 0 | 430,1 | −39,9 | 59 |
| 15 | S 277 | Sucrerie | 470 | 101 | 187,5 | 31 | 101,1 | 0 | 420,6 | −49,4 | 54 |
| 16 | S 302 | Sucrerie | 470 | 83,5 | 160 | 3,5 | 83 | 0 | 330 | −140 | 52 |
| 17 | CB 7 | Viande | 470 | 2,5 | 437 | 6,4 | 0 | 0 | 445 | −25 | 0,5 |
| 18 | CB 6 D | Viande | 470 | 1,25 | 208 | 4,6 | 2,3 | 205 | 422 | −48 | 0,5 |
| 19 | WB 10 A | Viande | 470 | 1,8 | 420 | 6,4 | 0 | 0 | 428,2 | −41,8 | 0,4 |
| 20 | 2 C 10 | Viande | 463 | 1,3 | 76,6 | 1,4 | 3,4 | 367 | 449,7 | −13,3 | 1,7 |
| 21 | V 5 | Vin | 517 | 41 | 83 | 26,9 | 23,3 | 279 | 453,2 | −63,8 | 50 |

* Le résultat a été confirmé par une deuxième expérience.

deux points. On peut se demander pourquoi la valeur zéro est rarement rencontrée. Il faut considérer que dans les conditions où les déterminations ont été réalisées, une partie du $CO_2$ peut provenir de la décarboxylation des acides aminés. Le dosage fait sur un témoin sans glucose ne permet pas d'éliminer entièrement cette cause d'erreur car la croissance est toujours plus forte sur le milieu contenant du glucose et la décarboxylation est favorisée par l'abaissement du pH dû à la formation d'acide lactique.

Sur la Fig. 2, on a fait correspondre, pour chacune des souches étudiées, la dose de réduction décimale à la valeur du rapport: $\frac{CO_2}{\text{acide lactique}}$. On voit que pour les deux groupes de souches les valeurs moyennes de la dose de réduction décimale sont très proches. Lorsqu'on envisage la DL 99 les moyennes trouvées dans nos expériences sont de 29,4 krad pour les homofermentatifs et 31,8 krad pour les hétérofermentatifs. Elles sont donc très différentes des valeurs déjà publiées: 172–209 krad pour les homofermentatifs et 43–74 krad pour les hétérofermentatifs. Avec la méthode employée, il n'a donc pas été possible de confirmer la différence de sensibilité observée par les auteurs déjà cités entre les deux grands groupes de *Lactobacillus*.

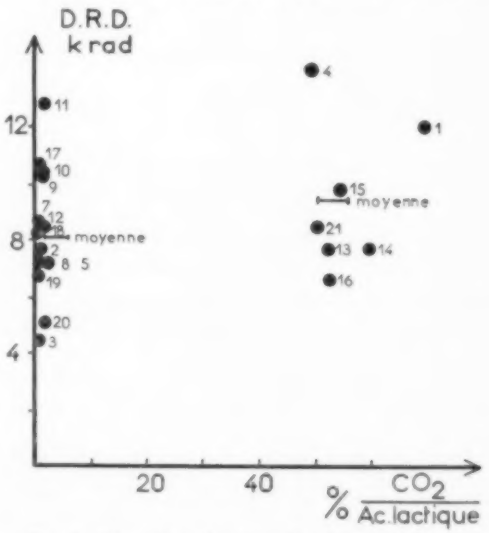


FIG. 2. Répartition des doses de réduction décimale (D.R.D.) en fonction du rapport $\frac{CO_2}{\text{Acide lactique}}$. Les numéros des souches correspondent à ceux du Tableau 2.

## D. CONCLUSION

D'après nos expériences, le genre *Lactobacillus* forme un groupe bien homogène du point de vue de la résistance aux radiations ionisantes. La distribution observée pour DL 99 et aussi pour la dose de réduction décimale est compatible avec une distribution de Gauss.

Lorsqu'on cherche à préciser la sensibilité

aux radiations ionisantes des *Lactobacillus*, il semble que les conditions de l'expérimentation ont une importance considérable puisque les mêmes souches étudiées dans deux laboratoires différents donnent pour DL 99 des valeurs allant de 1 à 7. Les conclusions que l'on peut tirer de l'inactivation de cultures pures en vue d'applications pratiques, par exemple la pasteurisation des aliments par radiation, seront donc très fragiles, tant que l'influence du milieu de culture ne sera pas mieux connue.

*Remerciements*—Nous tenons à remercier ici le Dr. Marcovich (Laboratoire Pasteur de l'Institut du Radium, Paris), le Dr. Niven (Meat Institute Foundation, Chicago) et le Dr. Raibaud (Institut National de la Recherche Agronomique, Jouy-en-Josas), qui nous ont procuré certaines des souches utilisées. Les irradiations ont été réalisées au Laboratoire des Isotopes de l'Institut Pasteur, grâce à l'hospitalité des Dr. Aubert et Milhaud.

## REFERENCES

1. Drake S. D., Evans J. B. et Niven C. F. *Food Res.* **23,** 291 (1958).
2. Ingram M. et Thornley M. J. *Int. J. appl. Rad. Isotopes* **6,** 122 (1959).
3. Niven C. F. *Ann. Rev. Microbiol.* **12,** 5 (1958).
4. Rosset R. et Dupuy P. *Ann. Tech. agricol.* **7,** 441 (1958).
5. Dupuy P. et Melamed N. 84 *ème Congrès des Sociétés Savantes*, p. 263 (1959).
6. Ochoa S. *The Enzymes* Vol. II, Part 2, p. 1023. Academic Press, N.Y. (1952).
7. Sutton H. C. *Phil. Med. Biol.* **1,** 153 (1956).
8. Society of American Bacteriologists *Manual of Methods for Pure Culture Study of Bacteria*, Leaflet VI, p. 10 (1942).
9. Jaulmes P. *Analyse des Vins*. Librairie Poulain, Montpellier (1951).
10. Marcovich H. *Etude Radiobiologique du Système Lysogène d'*E. coli K 12. Thèse, Paris (1957).
11. Stapleton G. E. et Engel M. S. *J. Bact.* **80,** 544 (1960).
12. Wolin E. F., Evans J. B. et Niven C. F. *Food Res.* **22,** 682 (1957).

VOL. 11 1961

# technical notes

## Cellulose as a Radiation Dosimeter*

(*First received* 7 *September* 1960 *and in final form* 23 *January* 1961)

DURING an investigation performed to study the feasibility of the radiation pulping of wood[1], it was found that cellulose, when irradiated with $\gamma$-rays to exposure doses in the range $10^{6\cdot25}$–$10^{8\cdot0}$ rads and then treated with aqueous sodium hydroxide, yielded an appreciable yellow colour reaction, the intensity of which was directly proportional to the dose.

The experimental results reported in this paper indicate that this system has a potential value in chemical dosimetry. Firstly, when sheets of purified cellulose (chromatography paper) are irradiated, the technique yields a visual spot-test dosimeter which is simple, cheap, rapid and accurate to $10^{0\cdot25}$. Secondly, quantitative data can be obtained to within 2 per cent using a spectrophotometric procedure.

Many solid state dosimeters have been reported in the literature to cover sections of the dose range $10^3$–$10^9$ rads. SCHULMAN[2] has recently reviewed the most important advances in this field. Most of the dosimeters reported depend upon changes in optical properties, especially absorption and luminescence. Systems mentioned in this review include the darkening of polyvinyl chloride film[3]; the evolution from P.V.C. of HCl, measured as such[4] or by the incorporation of a pH sensitive dye[5]; the darkening of silver phosphate glass[6]; the use of blue cellophane[7] and photographic print-out paper[8]. Each of these dosimeters is subject to certain limitations in use. Blue cellophane necessitates pre-irradiation treatment and the colour change is not visible. Silver phosphate glass is subject to fading and non-linear response, whilst the photographic print-out paper has a visual accuracy of only 30 per cent. For simplicity and ease of measurement, these dosimeters are limited to $10^7$ rads for practical purposes. The luminescent measurement of an anthracene/phenyl quinol system recently reported[9] covers the range $10^{5\cdot7}$–$10^{9\cdot7}$ rads with 10 per cent accuracy, but this method requires somewhat specialized equipment.

Perspex and other plastics have also been proposed for the range $10^5$–$2 \times 10^8$ rads[10]. Accuracy is good, but reproducibility was dependent on heat treatment, film thickness, contaminants such as monomers and various "post-irradiation" effects.

As a valuable addition to the simple solid-state dosimeters, cellulose is proposed for the range $10^{6\cdot25}$–$10^{8\cdot00}$ rads.

### Experimental

Strips (1 × 20 in.) of Whatman No. 41 chromatographic paper, a high purity cellulose, were uniformly irradiated in a 500 c cobalt-60 source at dose rates of up to $9 \times 10^4$ rads/hr. Twelve samples were exposed for the spot-test and spectrophotometric procedures, giving a range of dosages from $10^{4\cdot25}$–$10^{8\cdot00}$ rads. All doses were estimated by the conventional ferrous sulphate technique[11] and also by measurement with a Roentgen Rate-Meter (Victoreen Instrument Co., Model 510; probe 607; rated accuracy ±5 per cent; probe volume 0·175–0·190 ml).

In the spot-test procedure, one drop (0·05 ml) of 0·10 N NaOH from a calibrated micro-pipette was placed on each of the irradiated papers and the colour allowed to develop for 1 min. For the spectrophotometric method, samples (0·06–0·12 g) of irradiated paper were refluxed for 1 hr with 1·00% NaOH (80 ml), the solutions filtered through a Gooch crucible, washed with the 1% NaOH until the residue was colourless and the combined filtrates diluted with the same solvent to a known concentration. The optical density of these solutions was measured at a broad absorption peak (2880 Å) by means of a Cary recording spectrophotometer using a 1% NaOH blank.

### Results

(a) *Spot test*

In this technique samples with dosages of less than $10^{6\cdot25}$ rads exhibited very little colour reaction, whilst samples above $10^{8\cdot25}$ rads disintegrated upon contact with the alkaline solution. Between these two dose limits, a discreet variation in colour was observed from a pale greenish yellow for the $10^{6\cdot25}$ rads material to intense amber for the $10^{8\cdot00}$ sample.

(b) *Spectrophotometric procedure*

In this series of experiments, the results of the optical density measurements are shown in Figure 1.

* Presented in part at the Australian Atomic Energy Commission Conference on the Technological Uses of Radiation, University of New South Wales, 23–25 May, 1960.



VOL 11 196

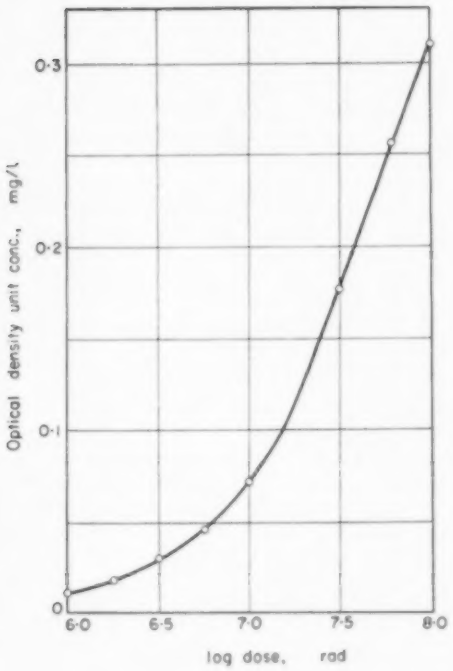


FIG. 1.

The relationship between optical density per unit concentration and log dose is shown to be linear over the range $10^{7\cdot25}$–$10^{8\cdot0}$ rads.

### Accuracy

In the spot tests, $10^{0\cdot25}$ rad differences were readily distinguished when colour standards were used as a basis for comparison.

In the spectrophotometric procedure, the error of estimate in log dose from optical density (expressed for unit concentration in milligrams per litre) was found from the regression equation to be $\pm 0\cdot02$ within 90 per cent confidence limits[12] (standard error of estimate 0·008, quadruplicate samples at each dose, doses at $10^{0\cdot25}$ rads increments).

Multiple exposures gave results agreeing within these limits. Samples of different chromatography paper (Munktells and 598) showed similar trends.

### Dosimeter stability

Although cellulose has been shown to be free from post-irradiation effects if stored in an inert atmosphere[13], reproducible results were obtained in these experiments under normal atmospheric conditions without special storage precaution if tests were performed at any time during the 2 days following irradiation.

### Range

From the accompanying graph, it is apparent that linearity for the relationship is only valid over the range $10^{7\cdot25}$–$10^{8\cdot00}$ rads. However, use of a calibration curve allows the range to be extended (although with diminishing accuracy) to approximately $10^{6\cdot25}$ rads.

### Mechanism of reaction

BLOUIN and ARTHUR[14] have recently reviewed the effects of radiation on cellulose and its derivatives. They report that the irradiation of purified cellulose with high-energy $\gamma$-rays with doses in excess of $10^{6\cdot25}$ rads results in carbonyl group formation, carboxyl formation and chain cleavage in the approximate ratio 20:1:1. These authors observed changes in other chemical properties including an increase in solubility in water and dilute alkali such that at $10^8$ rad, cellulose is 70–75 per cent soluble in 1% NaOH solution. At present there does not appear to be any evidence to show why radiolytic fission alone of bonds in the glucopyranose unit should result in the formation of functional groups in the ratio observed by BLOUIN and ARTHUR. The effect of other secondary processes must also be considered. The increase in copper number resulting from irradiation of de-waxed yarns and the irradiation of yarns on dry ice, recently observed by HUO-PING PAN *et al.*[15] suggests that products (such as peroxides), which are formed from the degradation of water present in the original cellulose, may contribute to the oxidation process. It is noteworthy that the linear relationship between molecular properties and dose, derived on the assumption of direct radiolytic fission by ARTHUR[16], is similarly obtained by the postulate that aqueous radiolytic degradation occurs as a rate-determining intermediate step. It is obvious that degradation occurs by both the primary and secondary processes, but the extent to which each of these mechanisms contributes to the overall fundamental result is at present being investigated in these laboratories.

### Colour reaction

Our data, as indicated in the graph and in analogous experiments reported elsewhere[1], follow similar trends to the reported chemical properties of irradiated cellulose[14]. The deep yellow colour of the alkaline solutions of cellulose samples irradiated to dose levels higher than $10^{7\cdot0}$ rads is attributed to enolization of the carbonyl groups under the alkaline conditions yielding a system which absorbs strongly in the u.v.

*Acknowledgments*—The authors wish to thank MR. C. SAMWAYS for assistance with the irradiations, also MESSRS. ALGAR and WERTHEIM and DR. MELLER of

the Research Laboratory, Australian Paper Manufacturers Ltd., for the benefit of many valuable discussions.

R. C. L. Bosworth
I. Ernst
*Department of Physical Chemistry* J. L. Garnett
*The University of New South Wales*
*Sydney, Australia*

### References

1. Garnett J. L. and Merewether J. W. T. *Chem. Ind.* 1215 (1959).
2. Schulman J. H. *Proceedings of the Second International Conference on the Peaceful Uses of Atomic Energy, Geneva*, 1958, P/1859, Vol. 21, p. 220. United Nations, New York (1958).
3. Artandi C. and Stonehill A. A. *Nucleonics* **16,** No. 5, 118 (1958).
4. Byrne J., Costekyan T. W., Hanford C. B., Johnson D. L. and Mann W. L. *Industr. Engng. Chem. (Anal.)* **45,** 2549 (1953).
5. Henley E. J. and Miller A. *Nucleonics* **9,** No. 6, 62 (1951).
6. Davison S., Goldblith S. A. and Proctor B. E. *Nucleonics* **14,** No. 1, 34 (1956).
7. Henley E. J. *Nucleonics* **12,** No. 9, 62 (1954).
8. Nitka H. F. and Jones D. P. *Nucleonics* **15,** No. 10, 128 (1957).
9. Attix F. H. *Nucleonics* **17,** No. 4, 142 (1959).
10. Boag J. W., Dolphin G. W. and Rotblat J. *Radiat. Res.* **9,** 589 (1958).
11. Rosinger S. *Proceedings of the Second International Conference on the Peaceful Uses of Atomic Energy, Geneva*, 1958, P/970, Vol. 21. United Nations, New York (1958).
12. Lark P. D. *Analyt. Chem.* **26,** 1712 (1954).
13. Glegg R. F. *Radiat. Res.* **6,** 469 (1957).
14. Blouin F. A. and Arthur Jr. J. C. *Text. Res. J.* **28,** 198 (1958).
15. Huo-Ping Pan, Proctor B. E., Goldblith S. A., Morgan H. M. and Naar R. Z. *Text. Res. J.* **29,** 415 (1959).
16. Arthur J. C. Jr. *Text. Res. J.* **28,** 202 (1958).

---

## On the Assay of Tritium as Tritio-Butane

(*First received* 8 *August* 1960 *and in final form* 4 *April* 1961)

### Introduction

The technique described by Glascock[1] for counting tritium as tritio-butane has been in use in this laboratory for several years. This method was first used here to assay relatively large amounts (0·1 ml) of tritiated water (TOH), and under these conditions satisfactory reproducibility (±2 per cent) was attained. However, the method gave unreliable and inaccurate results when applied to the much smaller amounts of water (10 μl or less) from semi-micro combustions of tritiated compounds. Poor results were still obtained when samples of TOH of the order of 10 μl were used directly. In general the smaller the volume of TOH of a given specific activity the lower was the specific activity of the butane produced. Different batches of the Grignard reagent sometimes gave different results.

The most likely explanation was that the samples of Grignard reagent were reacting with varying amounts of ordinary water during their preparation to produce non-radioactive butane and Mg(OH)Br. Little or no error could be caused by this butane since it was always removed by distillation *in vacuo* before the Grignard reagent was allowed to react with the TOH to be assayed. However, an exchange between the hydrogen atoms of Mg(OH)Br and TOH during the generation of the labelled butane could produce low and variable specific activities. This possibility has been examined in the experiments described here.

### Material and Methods

n-Butyl magnesium bromide was prepared and dispensed as described by Glascock[1]. Unless otherwise stated, the apparatus and reagents were thoroughly dried and immediately transferred to a glove-box containing several trays of calcium chloride and soda lime. The apparatus in which the Grignard reagent was prepared was also protected with drying tubes containing phosphorus pentoxide. The reagent was dispensed in the glove-box, thus preventing any access of moisture from the atmosphere. The preparation of the reaction tubes, the reaction with water and the counting of butane were carried out exactly as described by Glascock[1].

Volumes of water larger than 10 μl were dispensed from micro-pipettes. It was calculated that, depending on the humidity, up to 0·25 mg of water could be contained by the air in the section of the vacuum line used to introduce the sample. Errors of up to 2·5 per cent could thus have been introduced into 10 μl samples. The errors would have been proportionately larger for smaller volumes dispensed by pipette. Quantities of the standard tritiated water of less than 10 μl in volume were therefore dispensed in the vapour state, using a glass bulb of known volume attached through a stopcock to the vacuum manifold and through another stopcock to a reservoir of 10 ml of TOH.

A stock solution of TOH with a specific activity of about 1·0 μc/ml was used throughout.

VOL
11
196

## Experimental and Results

The results in Tables 1 and 2 show clearly that the exchange between Mg(OH)Br and the reacting TOH is fast enough to cause a lowering of the specific activity of the butane produced. The theoretical values were calculated on the assumption that the pre-treatment with ordinary water was quantitative, that is that half the hydrogen was lost as butane, and that the subsequent exchange between TOH and Mg(OH)Br was complete. The differences between the observed and calculated results in Table 2 were possibly due to different exchange and reaction rates depending on the physical form of the dry Grignard reagent.

TABLE 1. Demonstration of exchange of H between Mg(OH)Br and TOH.
Samples of n-BuMgBr were pre-treated with various amounts of distilled water and the butane generated in the usual way (GLASCOCK[1]). The reaction tubes were then evacuated, treated with 10 $\mu$l samples of the standard TOH and the specific activity of the tritiated butane measured

| $H_2O$ used for pre-treatment ($\mu$l) | Specific activity of butane (counts/sec per ml at NTP) | Specific activity (%) | |
|---|---|---|---|
| | | Observed | Theoretical |
| 0 | 10·1 | 100 | 100 |
| 3 | 8·9 | 88 | 87 |
| 5 | 7·9 | 78 | 80 |
| 10 | 6·3 | 63 | 67 |

To test the effect of exposing the Grignard reagent to the atmosphere, several samples were dispensed in the usual way, removed from the glove-box and exposed to the air for various times without being shaken or swirled. The stopcock adapter was then replaced, the tube connected to the vacuum manifold and processed in the usual way using 3 $\mu$l volumes of the standard TOH.

The results in Fig. 1 show that exposure for even a few seconds is sufficient to produce significant errors in the specific activity of butane generated from small volumes of water. These results also show that the absorption of moisture was approximately proportional to the exposure time up to 30 sec, and confirm that the exchange of H between TOH and solid Mg(OH)Br approaches completion.

The ratio of the specific activities of the 10 $\mu$l samples of TOH dispensed as vapour and as liquid allow an estimate to be made of the relative vapour pressures of TOH and HOH. The results (Table 3) show that this ratio was 0·91 $\pm$ 0·02 at 25 $\pm$ 4°C.

## Discussion

The results show clearly that the specific activity of samples of tritiated water can only be measured accurately by the butane method if stringent precautions are taken to exclude moisture during the preparation and handling of the n-butyl magnesium bromide. If such precautions are not taken, a rapid exchange occurs between the hydrogen atoms of Mg(OH)Br and of the TOH, thus lowering the specific activity of the butane formed. The resultant errors are only serious with samples of water smaller

TABLE 2. Demonstration of exchange of H between Mg(OT)Br and $H_2O$.
Samples of n-BuMgBr were pre-treated with TOH, the butane generated and its specific activity measured in the usual way. The reaction tubes were then evacuated, treated with 10 $\mu$l of $H_2O$ and the specific activity of the second portion of butane measured

| TOH used for pre-treatment ($\mu$l) | Specific activity of butane (counts/sec per ml at NTP) | | Specific activity (%) | |
|---|---|---|---|---|
| | From TOH | From $H_2O$ | Observed | Theoretical |
| 2 | 9·3 | 0·8 | 8·5 | 9·1 |
| 2·5 | 9·3 | 0·6 | 6·4 | 11·1 |
| 5 | 9·3 | 1·2 | 13 | 20 |
| 8 | 9·3 | 1·4 | 15 | 29 |

TABLE 3. The specific activity of various 10 $\mu$l samples of TOH dispensed as liquid and as vapour

| Specific activity of butane (counts/sec per ml at NTP) | | | |
|---|---|---|---|
| Dispensed as liquid | | Dispensed as vapour | |
| 10·5 | 10·2 $\pm$ 0·2 | 9·32 | 9·24 $\pm$ 0·08 |
| 10·4 | | 9·24 | |
| 10·1 | | 9·26 | |
| 10·0 | | 9·22 | |
| 10·2 | | 9·20 | |
| 10·0 | | 9·30 | |
| 10·3 | | 9·12 | |
| 10·1 | | | |
| 10·3 | | | |
| 9·7 | | | |

than about 10 $\mu$l. However, samples of this size are common in combustions of tritiated compounds. If adequate precautions to exclude moisture are not taken, then even a rigorously standardized procedure for the preparation and dispensing of the Grignard reagent would not produce results with the correct relative values unless water samples of exactly the same size were used.

exchange. It may well be that the error due to the exchange reaction only becomes apparent when the solid Grignard reagent, which reacts much more slowly with water, is used.

It was realized that the specific activity of the water dispensed as vapour would be lower than that of the liquid phase by an amount determined by the relative vapour pressures of HOH and TOH at the

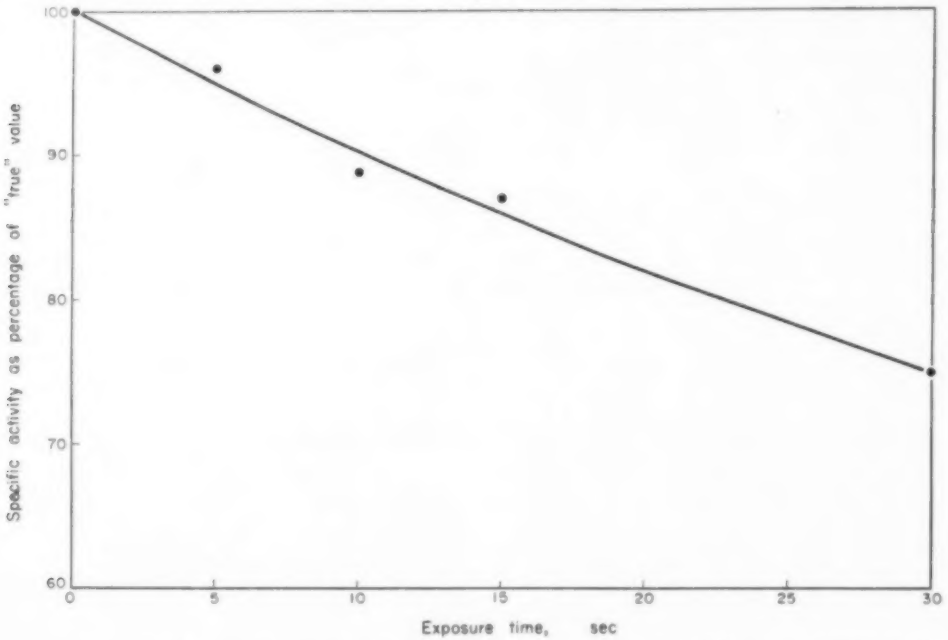


FIG. 1. Relative specific activities of butane obtained from the reaction of the standard TOH (3 $\mu$l) with n-butyl magnesium bromide samples (1·5 ml, 2 N) which had been exposed to the atmosphere for various times. The curve shown was calculated on the assumption that the values at 0 and 30 sec were correct, that the uptake of water was proportional to the exposure time, and that there was complete exchange between the TOH and the hydrogen in the Mg(OH)Br.

ASSARSSON[2] showed that small amounts of moisture entered solutions of n-butyl magnesium bromide in di-n-butyl ether. The resultant butane, unless removed by distillation of a portion of the solvent, lowered the specific activity of tritiated butane samples prepared subsequently by reaction with methanol. ASSARSSON did not discuss the possibility of a further error due to exchange of hydrogen between the Mg(OH)Br and the tritiated methanol which he used. However, since he used at least an eight-fold excess of methanol, the error would have been difficult to detect, especially if the reaction in solution of methanol with the Grignard reagent, producing butane, was fast compared to the rate of temperature concerned. However, the total amount of water dispensed (150 $\mu$l) was such a small fraction of the reservoir that isotopic enrichment of the residual water was negligible. This was confirmed later by measuring the specific activity of the residual water.

Our experiments show that the ratio of the vapour pressures of TOH and HOH was 0·91 $\pm$ 0·02 at 25°C (Table 3). This value could be up to 2·5 per cent high due to the uncertainty of the dilution of the 10 $\mu$l liquid samples with atmospheric water. After allowing for this, our ratio is still much higher than the value (0·77 at 25·70°C) published by PRICE[3]. Recently SIMPSON and GREENING[4] and AVINUR and NIR[5] also found that the fractionation of the hydrogen

isotopes during the distillation of TOH was much lower than expected from PRICE's results.

*C.S.I.R.O. Division of Animal Physiology, Ian Clunies Ross Animal Research Lab., Parramatta, N.S.W. Australia*

A. M. DOWNES
A. R. TILL

### References

1. GLASCOCK R. F. *Isotopic Gas Analysis for Biochemists*, Academic Press, New York (1954).
2. ASSARSSON L. O. *Acta chem. scand.* **12,** 1547 (1958).
3. PRICE A. H. *Nature, Lond.* **181,** 262 (1958).
4. SIMPSON J. D. and GREENING J. R. *Nature, Lond.* **186,** 467 (1960).
5. AVINUR P. and NIR A. *Nature, Lond.* **188,** 652 (1960).

## An Inexpensive Disposable Sample Container for Single Phototube Liquid Scintillation Counting

(*Received* 9 *February* 1961 *and in final form* 5 *April* 1961)

THE economical use of a single-tube liquid scintillation counter without automatic sample-changing mechanism necessitates a sample preparation which takes place independently from counting procedure. This requires a large amount of sample containers to prepare a reserve for uninterrupted counting. Apart from this a great number of containers has to be cleaned and to be checked thereafter from remaining contamination during the working hours of the counter. Depending on the size of the experiment from 50 up to several hundred containers may be necessary.

The high cost and the need of contamination control of the special glass containers required have encouraged us to test the applicability of inexpensive plastic containers for this purpose. The preferential use of toluene and xylene as solvents excluded the known transparent plastics, e.g., lucite, which are destroyed by these solvents within a few minutes. From a large number of other plastics tested a milky white semi-transparent high-density polyethylene*, which exhibits a weight increase of only 6·4 per cent when stored in toluene for 30 days, proved to be suitable as material for thin-walled cups with a tight closing lid.

All experiments were performed with an EKCO liquid scintillation counter N 612, which uses a Pyrex glass container of about 50 ml resembling a weighing bottle, furnished with the counter by the manufacturer (N 625). The technical instruction manual does not specify if a special, non fluorescent, low $K^{40}$ content glass is used. The optical coupling was accomplished in all experiments by silicone fluid MS 200, 20 centistokes. We replaced this container by the polyethylene cup with the same dimensions and a wall thickness of less than 1 mm. The count rates obtained with both types of containers filled with a standard $C^{14}$ and $S^{35}$ scintillator mixture and a blank scintillator solution (4 g 1,4-diphenylbenzene, 50 mg POPOP in 1000 ml toluene) are demonstrated below:

Relative yield and background values of standard samples of $H^3$, $C^{14}$ and $S^{35}$ in polyethylene containers compared with those in glass containers (100%)

| | |
|---|---|
| Background | 50% |
| $H^3$ | 220% |
| $C^{14}$, $S^{35}$ | 125% |

To examine the polyethylene containers for changes in optical density of the bottom due to the influence of toluene, 4 cups containing 10 ml scintillator mixture each were stored for 4 days at room temperature. Daily measurements did not show any significant deviation from count rate in brand new cups. As an average the background of a Pyrex glass container not previously stored in the dark is about twice as high as that of a polyethylene cup. Since most glasses are known to be second-rate material in containers for liquid scintillators because of $K^{40}$ content (background) and/or ultraviolet absorption, we suppose this to be the reason for the difference. The yield for $C^{14}$ and $S^{35}$ in our example is increased for 25 per cent and the yield for $H^3$ for 120 per cent. Besides the background reduction and increased counting efficiency the sharply reduced costs and the disposability, which eliminates the testing of the containers for contamination seems to be a distinct advantage.

### Summary

The use of a semi-transparent polyethylene container for single phototube liquid scintillation counting is recommended because of a reduction of background, unbreakability, low costs and disposability.

K. H. KIMBEL
J. WILLENBRINK

*Research Laboratories Schering AG, Berlin Germany*

* Lupolen R 6001H, Badische Anilin und Sodafabriken, Ludwigshafen, Germany.

# letters to the editors

## Assay of Tritium as Tritio-Butane

(*Received* 27 *April* 1961)

SINCE the publication of this method[1,2] we have re-examined it and have carried out experiments similar to those described by DOWNES and TILL[3]. Although we have not published our results we are in full agreement with their findings where we have done the same work. In particular we agree with their conclusion that specific activity can be measured accurately . . . "only if stringent precautions are taken to exclude moisture during the preparation and handling of the n-butyl magnesium bromide". The use of a glove box for this purpose is therefore standard in our laboratory. We find that many determinations of the specific activity of a large sample of tritiated water dispensed as vapour agree to within $\pm$ 1·5%.

We have not compared the specific activity of water samples dispensed as liquid and vapour and are therefore unable to confirm the observations of DOWNES and TILL on the vapour pressure of TOH. One factor which they do not mention, however, is the effect of overheating during the removal of ether from the n-butyl magnesium bromide. If exposed to temperatures greater than about 120° not only is the yield of butane much reduced but reproducibility may be no better than $\pm$5 per cent. We have not discovered why this is so.

We are grateful to Messrs. Downes and Till for their painstaking work and for the opportunity their paper affords us of making these comments.

R. F. GLASCOCK
R. W. SMITH

*National Institute for Research in Dairying (Univ. of Reading) Shinfield, Reading, Berks.*

### References

1. GLASCOCK R. F. *Nucleonics* **9,** No. 5, 28 (1951).
2. GLASCOCK R. F. *Isotopic Gas Analysis for Biochemists,* Academic Press Inc., N.Y. (1954).
3. DOWNES A. M. and TILL A. R. This issue, p. 154.

## Reply to GLASCOCK and SMITH's letter*

(*Received* 20 *May* 1961)

Dear Sir,

WE should like to thank Drs. Glascock and Smith for their comments.

In the early stages of our work we confirmed Dr. Glascock's original observation that samples of n-butyl magnesium bromide heated *in vacuo* at 110–120°C for 2 hr still liberated about 100 $\mu$l of gas on heating for a further hr. However, we found that the longer the time of heating the poorer the yield of butane obtained in the reaction with water. This possibly indicates that some ether has to be present for the reaction to occur and that the ether-Grignard co-ordination compound may be the reacting entity. In all subsequent assays we heated the n-butyl magnesium bromide at 110–120°C for 2 hr and usually obtained yields in the order of 95–100 per cent with occasional values as low as 70 per cent.

We have never heated the n-butyl magnesium bromide at temperatures above 120°C and have not studied the reproducibility of the specific activity determinations under conditions which produced poor yields of butane.

A. M. DOWNES
A. R. TILL

*C.S.I.R.O. Division of Animal Physiology, Ian Clunies Ross Animal Research Lab., Parramatta, N.S.W. Australia*

* See previous contribution.

# international news

### Conference on the Use of Radioisotopes in Animal Biology and the Medical Sciences, Mexico City, 21 November–1 December 1961

THE International Atomic Energy Agency (IAEA), the Food and Agriculture Organization of the United Nations (FAO) and the World Health Organization (WHO) are jointly organizing a *Conference on the Use of Radioisotopes in Animal Biology and the Medical Sciences* in Mexico City from 21 November–1 December 1961.

Its purpose is to bring together from all over the world specialists in the fields of animal biology and the medical sciences who are interested in the use of radioisotopes. It will also serve the purpose of making medical scientists more fully aware of the potentialities of radioisotope techniques in studies on general physiology and biochemistry, and also acquaint non-medical biologists with problems relating to the physiology of disease and with clinical uses of radioisotopes.

The programme of the Conference covers the following topics:

(i) Advances in radioisotope technique and methodology as applied in the biological sciences and medicine.
(ii) General physiology, biochemistry and metabolism, including: structure, function and biosynthesis of biologically important compounds; intermediary metabolism, biochemistry as related to genetics.
(iii) Mineral metabolism, including: digestion, absorption and transport; biochemical and physiological function of minerals; trace elements.
(iv) Skeletal physiology, including; calcium and phosphorus deposition in bone; strontium deposition in bone, remodelling; skeletal physiology and disease.
(v) Physiology of reproduction, including; duration of spermato-genesis and cogenesis; artificial insemination.
(vi) Physiology and biochemistry of the ruminant animal, including: digestion and synthesis, rumen microflora; rumen fluids; cobalt, copper and other minerals.
(vii) The physiology and biochemistry of lactation, including: synthesis and transport of milk precursors; synthesis in the mammary gland and secretion of milk; the intermediary metabolism of sugar, fat, amino acids and proteins.
(viii) Glandular function, endocrinology, including: the biochemistry of hormone production; transport and metabolism of regulators; correlation of glandular activities.
(ix) Poultry: physiology, nutrition and pathology.
(x) Microbiology and immunology.
(xi) Haematology including animal and comparative haematology.
(xii) Dentistry.
(xiii) Clinical research, including: body composition and electrolytes; metabolic studies; absorption studies; circulation studies; localization studies.

### International Conference on the Physics of Semiconductors, Exeter, 16 July–20 July 1962

THE Institute and Society on behalf of the International Union of Pure and Applied Physics, and the British National Committee for Physics is arranging an *International Conference on The Physics of Semiconductors*, which will be held at the University of Exeter from 16–20 July, 1962. The Conference is planned to follow the previous sequence of Conferences on the physics of semiconductors, which were held in Reading in 1950, Amsterdam in 1954, Garmisch in 1956, Rochester in 1958 and Prague in 1960.

Accommodation will be provided in Halls of Residence at the University. Further information regarding the Conference may be obtained from the *Administration Assistant, The Institute of Physics and The Physical Society, 47 Belgrave Square, London, S.W.1.*

VOL
11
196

International Journal of Applied Radiation and Isotopes, 1961, Vol. 11, pp. 161–173. Pergamon Press Ltd. Printed in Northern Ireland

# Untersuchungen zur Oberflächenpasteurisierung von verpackten, im Innern keimreichen Fisch- und Fleischproben mit weichen Röntgenstrahlen

W. SCHMIDT-LORENZ und A. BERGER
Mitteilung aus der Bundesforschungsanstalt für Lebensmittelfrischhaltung, Karlsruhe, Deutschland

(*Received* 5 *December* 1960)

Zur Prüfung der Wirksamkeit der Oberflächenbestrahlung wurde bei verpackten, im Innern keimreichen Seefisch- und Rindfleischproben die Zusammensetzung der Mikroflora und die Verteilung der vermehrungsfähigen Mikroorganismen zwischen Oberflächenschicht und Innerem der Probe vor und nach Bestrahlung mit 60 kV Röntgenstrahlen und einer Oberflächendosis von 3 Mr bestimmt.

Kurzzeitiges Gefrieren (−24°C, 12h) nach der Bestrahlung, wie es zur Abtrennung der Oberflächenschichten notwendig war, hatte keinen Einfluss auf das Ergebnis der Keimzählungen. In der Oberflächenschicht der Fisch- und Fleischproben war trotz hoher Oberflächendosis die durch die Bestrahlung bewirkte Keimzahlreduktion verhältnismässig gering (90–98%). Auch die Artenzusammensetzung der Mikroflora war nur wenig verändert.

Im Innern der Probe war nur bei sehr keimreichem Material eine etwas geringere, aber noch deutliche Keimzahlreduktion (70–80%) durch die Bestrahlung zu erreichen. Bei keimärmerem Material waren die Bakterienzahlen im Innern der Proben nach der Bestrahlung nicht verringert, sondern deutlich erhöht. Hierfür waren vor allem *Pseudomonas*- und *Achromobacter*-Arten verantwortlich.

Diese unerwarteten Befunde lassen sich nur mit einer Reinfektion der bestrahlten Oberflächen innerhalb der Verpackung sowie einem sekundären Keimtransport innerhalb des Gewebes durch den bei rohem Fisch und Fleisch immer vorhandenen und unter der Bestrahlungseinwirkung verstärkt austretenden Gewebssaft erklären. Eine wirksame Oberflächenbestrahlung von verpacktem, rohem Fleisch oder Fisch scheint daher nur bei einer von unten nach oben immer nur auf die Unterseite der verpackten Proben gerichteten Bestrahlung möglich.

## INVESTIGATION OF THE SURFACE PASTEURIZATION, BY MEANS OF SOFT X-RAYS, OF PACKED SAMPLES OF FISH AND MEAT CONTAINING INNER BACTERIA

The effect of surface irradiation on the composition of the microflora, and the distribution of the viable counts between surface layers and the inside of the samples was examined before and after irradiation with 60 kV X-rays at a surface dose of 3 Mr. Prepacked seafish and beef samples not sterile inside have been irradiated from above, and moved round to ensure uniform surface dosage.

Short freezing (−24°C, 12 hr) after irradiation, necessary for the separation of the surface layers, did not affect the results of the bacterial counts.

In the surface layers of the fish and beef samples the reduction of the viable counts through irradiation was low (90–98%) in spite of the high surface dose. Even composition of the microflora was not much affected.

Only a low reduction of viable counts (70–80%) has been attained in the inside through irradiation of more infected samples. The viable counts were not reduced but clearly increased after irradiation in the inside of less-infected samples. For this increase different types of *Pseudomonas* and *Achromobacter* were mainly involved.

These unexpected results could be explained only through a re-infection of the irradiated surfaces with the packaged samples and through a secondary distribution of the bacteria inside the tissue through the drip, which is produced by irradiation. An effective surface irradiation of packaged raw fish and beef seems only to be possible through irradiation directed from the bottom to the surface, e.g. only on the underside of the samples.

## RECHERCHE SUR LA PASTEURISATION SUPERFICIELLE, AU MOYEN DES RAYONS X DOUX, D'ECHANTILLONS DE POISSON ET DE VIANDE ENVELOPPES ET CONTENANT DANS L'INTERIEUR DES BACTERIES

On examina l'effet de l'irradiation superficielle sur la composition de la microflore et sur la distribution des comptes viables entre les couches superficielles et l'intérieur des échantillons, avant et après l'exposition aux rayons X de 60 kV à une dose superficielle de 3 Mr. Des échantillons enveloppés de poisson de mer et de boeuf, non stériles à l'intérieur, ont subi l'irradiation d'en dessus, étant tournés afin d'obtenir une dose superficielle uniforme.

Une brève période de gel (−24°C, 12 hr) après l'irradiation, nécessaire à la séparation des couches superficielles, n'affecta pas les résultats des comptes bactériens.

Dans les couches superficielles des échantillons de poisson et de boeuf la diminution des comptes viables à cause de l'irradiation fut petite (90–98%) malgré la forte dose superficielle. Même la composition de la microflore ne fut pas beaucoup changée.

On a atteint seulement une petite diminution des comptes viables (70–80%) dans l'intérieur à la suite de l'irradiation des échantillons les plus fortement infectés. Les comptes viables ne furent pas diminués, mais évidemment augmentés suivant l'irradiation, dans l'intérieur des échantillons moins fortement infectés. Cette augmentation provenait pour la plupart de différents types de *Pseudomonas* et d'*Achromobactère*.

Ces résultats inattendus pouvaient s'expliquer seulement par une ré-infection des surfaces irradiées des échantillons enveloppés et par une distribution secondaire des bactéries dans le tissu à cause du coulage que produit l'irradiation. L'irradiation effective de la surface du poisson ou boeuf cru enveloppé ne semble possible qu'en dirigeant le rayonnement du bas en haut, c'est-à-dire seulement sur la face inférieure des échantillons.

## ИССЛЕДОВАНИЕ ПОВЕРХНОСТНОЙ ПАСТЕРИЗАЦИИ МЯГКИМ РЕНТГЕНОВСКИМ ИЗЛУЧЕНИЕМ УПАКОВАННЫХ ОБРАЗЦОВ РЫБЫ И МЯСА

Исследовалось действие рентгеновского излучения в 60 кв, при поверхностной дозе в 3 миллирентгена, на состав микрофлоры и на распределение способных к размножению микроорганизмов по поверхности и в массе проб морской рыбы и мяса.

Кратковременное замораживание (−24°C, 12 часов) после облучения, необходимое для отделения поверхностных слоев, не оказывало заметного влияния на общее число бактерий. Даже при большой дозе облучения уменьшение бактерий в поверхностных слоях рыбы и мяса было сравнительно невелико (90-98%). Видовой состав микрофлоры также мало изменялся.

Немного меньшее, но все же заметное уменьшение бактерий (70-80%) в результате облучения было установлено только в случае богатых микрофлорой проб. Для проб же, бедных микрофлорой, количество бактерий в массе образца после облучения не уменьшалось, а заметно увеличивалось, что происходило прежде всего за счет видов *Pseudomonas* и ахроматических бактерий.

Эти неожиданные наблюдения можно объяснить только повторным зараженнем облученной таани, а также вторичным внутритканевым переносом бактерий тканевой

жидкостью, которая всегда имеется в сырой рыбе и сыром мясе и выделение которой усиливается при облучении. Эффективное поверхностное облучение упакованной сырой рыбы или мяса представляется поэтому возможным только при воздействии на пробу снизу или при одновременном воздействии на нижнюю и верхнюю поверхности пробы.

VOL. 11 1961

Der durch Mikroorganismen verursachte, rasche Verderb von frischem Fleisch und Fisch geht fast immer von der Oberfläche aus. Im Innern ist die Muskulatur gesunder, frischgeschlachteter Tiere meist keimarm, wenn nicht sogar lokal steril. Die Oberflächen werden dagegen während der Schlachtung und weiteren Verarbeitung immer erheblich von aussen her infiziert. Es wurde bereits des öfteren vorgeschlagen[1,2], diese Oberflächenflora durch eine auf die äusseren Schichten begrenzte Bestrahlung mit ionisierenden Strahlen abzutöten bzw. in ihrer Keimzahl stark zu reduzieren. Vor allem bei frischgeschlachtetem Fleisch oder Fisch müsste sich damit—insbesondere in Verbindung mit einer Kaltlagerung—eine erhebliche Haltbarkeitsverlängerung erreichen lassen.

Gegenüber der Bestrahlung der Lebensmittel mit ionisierenden Strahlen in der ganzen Schichtdicke könnte die bisher noch wenig untersuchte[3–6] Oberflächenbestrahlung erhebliche Vorteile bieten. Bei Begrenzung der Strahlenwirkung auf die Oberflächenschichten dürften die unerwünschten Strahlenveränderungen der Lebensmittel erheblich verringert werden. Gleichzeitig würden die Bestrahlungskosten, insbesondere die Investitionskosten der Bestrahlungsanlagen wesentlich niedriger liegen.

Eine wirksame Haltbarkeitsverlängerung ist allerdings nur bei solchen Lebensmitteln zu erwarten, bei denen die bakterielle Infektion tatsächlich nur auf die Oberflächenschichten begrenzt ist. Voraussetzung des Verfahrens ist offenbar eine weitgehende Keimfreiheit im Innern des zu bestrahlenden Materials. Die Erfüllung dieser Bedingung scheint eine der Hauptschwierigkeiten bei der praktischen Anwendung der Oberflächenbestrahlung zu sein. Auch bei sorgfältigster, hygienischer Schlachtung und Verarbeitung wird sich aber nie mit Sicherheit eine Keimfreiheit in allen Teilen der Muskulatur garantieren lassen. Unkontrollierbar können immer einzelne Muskelpartien vor allem über das Lymph- und Blutgefässsystem auch im Innern stärker mit Bakterien infiziert sein.[7–8] Noch weniger dürfte es sich bei der üblichen Praxis der Schlachtung und Fleischverarbeitung vermeiden lassen, dass einzelne Stücke im Innern stärker infiziert sind. Auch beim Seefisch, der meist erst nach mehrtägigem Transport nach dem Fang angelandet werden kann, ist normalerweise kaum noch mit einer Keimfreiheit im Innern der Muskulatur zu rechnen.

Die Oberflächenbestrahlung wird daher auch als wenig erfolgversprechend, höchst unzuverlässig und—im Hinblick auf das mögliche Überleben pathogener Bakterien—sogar als gefährlich abgelehnt[9]. Die gesundheitliche Gefährdung durch pathogene Bakterien dürfte allerdings kaum grösser sein als bei anderen pasteurisierenden Bestrahlungsverfahren. Durch eine konsequent durchgeführte Kaltlagerung nach der Bestrahlung ist die Entwicklung überlebender Pathogener mit genügender Sicherheit auszuschliessen. Schwerwiegender ist das Argument der Unzuverlässigkeit. Bevor man aber deswegen das ganze Verfahren von vornherein völlig verwirft, erscheint eine kritische experimentelle Prüfung insbesondere folgender Fragen notwendig: (1) Welche Wirkung hat die Oberflächenbestrahlung bei im Innern keimreichen Material? (2) Wie hoch darf bei den einzelnen Lebensmitteln der Keimgehalt im Innern sein, um noch eine wirksame Haltbarkeits-Verlängerung durch die Oberflächenbestrahlung zu gewährleisten?

In eigenen, unter diesen Gesichtspunkten durchgeführten Modellversuchen wurde zunächst die Wirkung einer Oberflächenpasteurisation durch weiche Röntgenstrahlen von geringer Halbwertsschicht auf die Verteilung und Zusammensetzung der überlebenden psychrophilen Mikroflora in verpackten, im Innern keimreichen Fisch- und Fleischproben untersucht. Hierüber soll im Folgenden berichtet werden.

## METHODIK

(1) *Material*

Aus grösseren Kabeljau- bzw. Schellfisch-Stücken wurden in gefrorenem Zustand quadratische 40 × 40 × 16 mm grosse Scheiben geschnitten, unter Vakuum in thermisch versiegelte Hostaphan-Polyäthylen-Siegelrand-Beutel* (12,5/50 $\mu$) verpackt und bis zur Bestrahlung bei −24°C gelagert. Zur Bestrahlung bei Zimmertemperatur wurden die Proben über Nacht im Kühlschrank langsam aufgetaut.

Die Rindfleischproben aus bindegewebs- und fettarmer Muskulatur des Oberschenkels—handelsüblich nach 9 Tage langer Kühlraum-Lagerung nach dem Schlachten bezogen—wurden ebenfalls in 40 × 40 × 16 mm grossen Scheiben in Folienbeuteln unter Vakuum verpackt und sofort ohne zwischenzeitliche Gefrierbehandlung bestrahlt.

(2) *Bestrahlung*

Als Strahlungsquelle diente eine mit 60 kV und 20 mA betriebene Weichstrahl-Röntgenröhre (Fa. Machlett) mit einem 1 mm starken Berylliumfenster. Die Verwendung des Be-Fensters bedingt den Austritt fast des gesamten weichen Anteils der erzeugten Röntgenstrahlung. Damit war eine Strahlung hoher Dosisleistung, aber auch sehr inhomogener spektraler Verteilung gegeben. Der Hauptanteil lag im Gebiet von 1,2 bis 4,2 A, der kurzwellige Anteil war nur geringfügig vertreten.

Die in Folienbeuteln verpackten Fisch- bzw. Fleischstücke wurden in 5,5 cm Abstand vom Brennfleck der Röhre (Strahlenaustrittswinkel = 48°) im zentralen Teil des Bestrahlungsfeldes zunächst einzeln auf jeder Breitseite, dann zu je zwei Stück zusammengestellt nacheinander auf den 4 Schmalseiten bestrahlt.

Die Dosismessung erfolgte mit einer Ionisationskammer wie an anderer Stelle ausführlich beschrieben[10]. Die Dosisleistung an der Oberfläche der Proben betrug 100 kr/min. Für jede Seite der Stücke kam bei einer Bestrahlungszeit von 30 min eine Oberflächendosis von 3 Mr zur Anwendung. Der durch die Folien und deren Schweissnähte absorbierte Anteil der Strahlung betrug etwa 2–5% der insgesamt angewandten Dosis und wurde vernachlässigt.

Zur Bestimmung der Dosisverteilung im bestrahlten Gewebe wurden Fleischscheiben unterschiedlicher Schichtdicke auf einer Folie über das Fenster der Ionisationskammer gelegt und durchstrahlt (10 kr/min). Aus der bei verschiedenen Schichtdicken gemessenen Röntgenstrahlen-Absorption wurden die Halbwertsschichten der angewandten Bestrahlung im biologischen Gewebe berechnet.

(3) *Bakteriologische Untersuchungen*

(a) *Probennahme.* Sofort nach der Bestrahlung wurden die bestrahlten Proben und die unbestrahlten, sonst aber gleich behandelten Parallelproben bei −24°C eingefroren. Nach 12- stundiger Gefrierlagerung wurden aus der gefrorenen Packung unter sterilen Kautelen auf der Breitseite mit einem Korkbohrer von 1 cm $\phi$ 4–5 Zylinder gefrorenen Materials herausgestanzt. Von Ober- und Unterseite jeder dieser 16 mm starken Zylinder wurde je eine 1,5 mm dicke Schicht abgeschnitten und getrennt vom Innenzylinder in sterile Behälter eingewogen. Nach Zusatz von Verdünnungslösung (0,1% Pepton + 0,85% NaCl)[11] wurde das aufgetaute Material im Homogenisator zerkleinert. Vom Homogenisat wurden nach entsprechender Verdünnung Zählplatten angelegt.

(b) *Zählung.* Die Zählung der vermehrungsfähigen Mikroorganismen im Plattengussverfahren erfolgte nach 4 Tage langer Bebrütung bei 20°C. Die angegebenen Keimzahlen sind immer auf 1 g Material berechnet und stellen Durchschnittswerte von jeweils 5 Parallelplatten je Verdünnungsstufe dar. Als Kulturmedium fand die sowohl für Fisch als auch für Fleisch gleich gut geeignete Nährlösung folgender Zusammensetzung Verwendung[12]: Bacto-Pepton

* Wir danken der Firma Kalle und Co., Wiesbaden, für die freundliche Überlassung der Folienbeutel.

0,2%; Bacto-Yeast-Extract 0,2%; Bacto-Beef-Extract 0,2% (alles Difco-Präparate); Glukose 0,1%, NaCl 0,85%, $K_2HPO_4$ 0,1% und 1,5% Agar; pH 7,0.

(c) *Zusammensetzung der Bakterienflora.* Von Zählplatten mit hoher Koloniedichte, aber noch deutlich voneinander getrennten Kolonien, wurden ca. 75–100 Einzelkolonien je Platte in oben angegebene Nährlösung abgeimpft. Hiervon wurden Reinkulturen angelegt, deren Gattungszugehörigkeit bestimmt und der prozentuale Anteil der einzelnen Gattungen an der Gesamtflora ermittelt. Zur vereinfachten Gattungsbestimmung wurden insbesondere folgende Merkmale geprüft: Morphologie, Beweglichkeit, Gramfärbung, Gelatine-Verflüssigung, Reaktion in Lackmusmilch, Antibiotika-Empfindlichkeit[13] und Glukose-Fermentation[14]. Soweit notwendig, wurden auch noch andere biochemische Reaktionen geprüft.

## ERGEBNISSE

(1) *Einfluss des Gefrierens auf das Ergebnis der Keimzählungen*

Eine befriedigende Trennung der 1,5 mm dicken Oberflächenschichten vom Innern der Proben war nur durch Schneiden im gefrorenen Zustand möglich. Ungefroren wird die Muskulatur beim Schneiden immer stark gequetscht. Unter dem Schneiddruck werden die Mikroorganismen im Gewebe in andere Gewebsschichten verdrängt und mit der austretenden Gewebsflüssigkeit örtlich ausgeschwemmt. Ausserdem werden die Schnitte dabei sehr unregelmässig. Dieselbe Gefahr besteht auch beim Schneiden und Wiederzusammensetzen dünner Schichten bereits vor der Bestrahlung nach der sogenannten Sandwich-Methode. Nur durch schnelles Gefrieren sofort nach der Bestrahlung lassen sich die Mikroorganismen im Gewebe örtlich fixieren.

Allerdings ist dabei zu berücksichtigen, dass auch nur kurzfristiges Gefrieren Schädigungen der Bakterien zur Folge haben kann. Damit besteht die Möglichkeit einer weiteren Keimzahl-Reduktion der überlebenden, möglicherweise subletal strahlengeschädigten Bakterien in bestrahltem Gewebe. Es musste daher zunächst überprüft werden, ob und inwieweit die Keimzählungen durch das zusätzliche Gefrieren beeinträchtigt werden.

Aus einzelnen grösseren Fisch- oder Fleischstücken wurden bis zu 10 nebeneinander liegende Probestücke geschnitten und sogleich verpackt. Abwechselnd blieb je ein Stück unbestrahlt, jedes zweite Stück wurde bestrahlt. Nach der Bestrahlung wurde jedes Stück halbiert. In der einen Hälfte wurden sofort im ungefrorenen Zustand, in der anderen Hälfte erst nach 12 Stunden langem Gefrieren bei −24°C und langsamem Auftauen Keimzählungen durchgeführt (Tab. 1, Vers. II).

In weiteren Versuchen wurde nur die 1,5 mm dicke Oberflächenschicht allein nach der Bestrahlung noch ungefroren vorsichtig abgetrennt. Nach Halbieren wurde der Keimgehalt ebenfalls vor und nach dem Gefrieren ermittelt (Tab. 1, Vers. IV).

Zum Vergleich wurde ausserdem noch der Keimgehalt im bestrahlten und unbestrahlten Fisch-Pressaft vor und nach dem Gefrieren bestimmt. Die Bestrahlung erfolgte unter Rühren in einer 3–4 mm hohen Schicht in einer offenen Kunststoffschale ebenfalls mit 60 kV-Röntgenstrahlen und einer Oberflächendosis von 0,5 Mr (Tab. 1, Vers. IX).

Aus den Ergebnissen dieser Versuche sind in Tab. 1 jeweils die Werte nur einer Versuchsreihe aufgeführt. Obwohl die Probestücke jeder Reihe immer nebeneinander aus einem einheitlichen Stück geschnitten waren, ergaben sich erhebliche Keimzahlschwankungen von Probe zu Probe. Geringere Unterschiede waren regelmässig bei den dünnen Oberflächenschichten zu beobachten. Der Gesamtkeimgehalt der Probestücke wird also hauptsächlich durch den lokal sehr unterschiedlichen Keimgehalt im Innern der Muskulatur bestimmt.

Eine nennenswerte Beeinflussung der durch Plattenzählung erfassbaren Anzahl

TABELLE 1. Einfluss des Gefrierens (12 Std. bei −24°C) auf die Keimzählung im unbestrahlten und bestrahlten Fisch bzw. Fisch-Pressaft

| Versuch | Material | Probe No. | Bakterien/g Fisch bzw. ml Pressaft* | | | |
|---|---|---|---|---|---|---|
| | | | Unbestrahlt | | Bestrahlt† | |
| | | | Ungefroren | Gefroren | Ungefroren | Gefroren |
| II | Kabeljau (Gesamte Probe) | 1 + 2 | 23,900 | 25,100 | 1,370 | 1,950 |
| | | 3 + 4 | 17,100 | 21,400 | 5,400 | 4,810 |
| | | 5 + 6 | 15,500 | 18,100 | 4,250 | 4,720 |
| | | 7 + 8 | 60,400 | 54,700 | 2,340 | 1,700 |
| | | 9 + 10 | 51,700 | 39,500 | 5,100 | 3,910 |
| | | 11 + 12 | 31,500 | 28,700 | 1,950 | 2,340 |
| | | — | 33,350 | 31,250** | 3,400 | 3,240** |
| IV | Kabeljau (nur Oberflächenschicht) | 1 + 2 | 11,700 | 9,800 | 1,210 | 1,470 |
| | | 3 + 4 | 19,300 | 16,100 | 1,740 | 1,910 |
| | | 5 + 6 | 20,700 | 23,600 | 2,910 | 2,420 |
| | | 7 + 8 | 27,700 | 24,100 | 3,610 | 3,180 |
| | | 9 + 10 | 18,400 | 21,300 | 2,780 | 2,560 |
| | | 11 + 12 | 10,100 | 9,700 | 1,180 | 1,480 |
| | | — | 18,000 | 17,400** | 2,240 | 2,170** |
| IX | Kabeljau (Pressaft) | 1 | 730,100 | 415,000 | 2,850 | 240 |
| | | 3 | 1,020,000 | 705,000 | 7,500 | 620 |
| | | 4 | 532,000 | 317,000 | 2,200 | 180 |
| | | 5 | 67,000 | 39,500 | 890 | 100 |
| | | 7 | 685,000 | 397,000 | 5,300 | 780 |
| | | 9 | 503,000 | 245,000 | 4,100 | 310 |
| | | 10 | 817,000 | 617,000 | 1,700 | 200 |
| | | 11 | 915,000 | 704,000 | 6,800 | 610 |
| | | — | 658,600 | 429,900†† (−35%)‡ | 3,920 | 380†† (−90%)‡ |

* Mittelwerte aus Plattenzählungen mit je 5 Parallelen/Verdünnung.
† Bestrahlungsanordnung und Dosis s. Text.
‡ Prozentuale Keimzahlreduktion nach dem Gefrieren.
** Unterschied statistisch nicht gesichert.
†† Unterschied statistisch gesichert ($P < 0{,}01$).

vermehrungsfähiger Mikroorganismen durch das Gefrieren und kurzfristiges Lagern war weder im unbestrahlten noch im bestrahlten Gewebe nachzuweisen. Die vergleichsweise geringen Unterschiede zwischen den beiden gefrorenen und ungefrorenen Hälften eines Stückes dürften in erster Linie auf den örtlich unterschiedlichen Ausgangskeimgehalt in beiden Hälften zurückzuführen sein. Ein eindeutiger, statistisch gesicherter Gefriereffekt war nur beim Fischpressaft nachzuweisen. Im unbestrahlten Pressaft bewirkte das Gefrieren eine durchschnittlich 35% ige Keimzahl reduktion. Im bestrahlten Pressaft war die Empfindlichkeit der überlebenden Bakterien gegenüber dem Gefrieren mit einer über 90%igen Keimzahlreduktion wesentlich höher. Da dieser nur im Pressaft nachweisbare Gefriereffekt in keinem Falle auch nur andeutungsweise im Fisch oder Fleisch zu beobachten war, ist also mit einer erheblichen protektiven Wirkung des Gewebes gegenüber den bestrahlten Bakterien zu rechnen. Ohne Bedenken konnten somit die Proben nach der Bestrahlung für kurze Zeit gefroren werden.

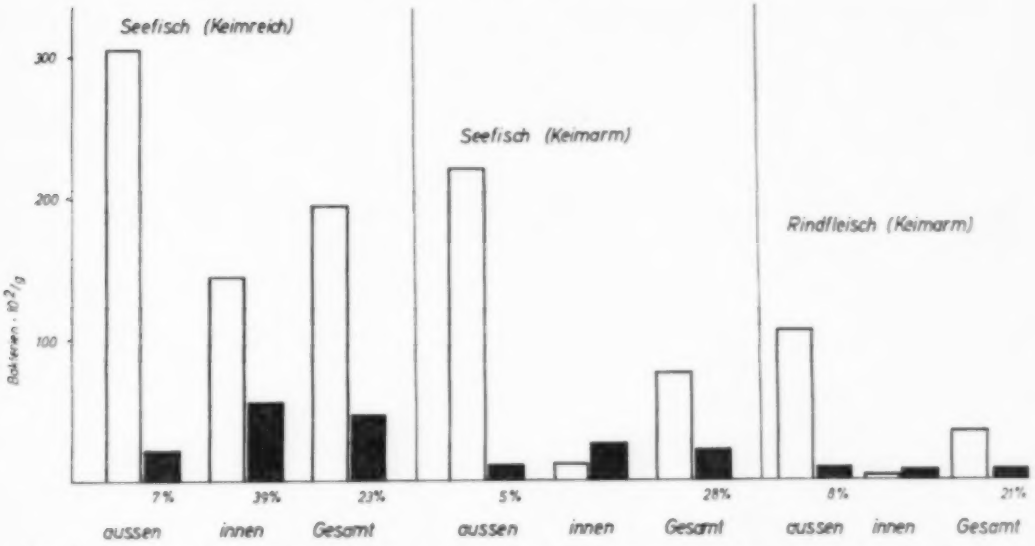


ABB. 1. Verteilung der vermehrungsfähigen, psychrophilen Mikroorganismen in Seefisch- und Rindfleischproben vor □ und nach ■ Oberflächenbestrahlung mit weichen 60 kV Röntgenstrahlen (Oberflächendosis 3 Mr, 1.HWS 0,8 mm).

Mittelwerte aus Versuchen mit 12 bzw. 15 verschiedenen Seefisch- und 9 Rindfleischproben. Bakterien/g in der 1,5 mm dicken Aussenschicht, im Innern und in der 40 × 40 × 16 mm grossen Gesamtprobe.

(2) *Mikroorganismen-Verteilung in oberflächlich bestrahltem Fisch und Fleisch*

Zur Bestimmung der Mikroorganismen-Verteilung wurden aus verschiedenen Seefisch- und Rindfleisch stücken jeweils nebeneinander 4 Probestücke geschnitten. Davon wurden immer Probe 1 und 3 bestrahlt; Probe 2 und 4 blieben unbestrahlt. Um grössere örtliche Schwankungen im Keimgehalt zwischen den Einzelproben auszugleichen, wurden die im gefrorenen Zustand abgetrennten Oberflächen und Innenproben der beiden bestrahlten bzw. unbestrahlten Probestücke zur Zählung jeweils vereinigt. In Anbetracht der unvermeidlichen Fehlerquellen bei der Probenahme, Keimzählung und beim Zuschneiden der Stücke sowie der ungleichmässigen Keimverteilung im Substrat sind die angegebenen Keimzahlen nur als angenäherte, für Vergleichszwecke aber genügende Durchschnittswerte anzusehen.

Die in Abb. 1 zusammengefassten Ergebnisse sind Mittelwerte von Zählungen bei (i) 12 verschiedenen, im Innern sehr keimreichen Fischen, (ii) 15 verschiedenen, im Innern keimärmeren Seefischen und (iii) bei 9 verschiedenen Rindfleischstücken.

Aus jeder dieser 3 Gruppen sind in Tab. 2 einige charakteristische Einzelergebnisse aufgeführt.

Die 1,5 mm dicken Oberflächenschichten waren nach der Bestrahlung keineswegs völlig steril, wie nach der hohen Oberflächendosis von 3 Mr zunächst zu erwarten war. Übereinstimmend war in allen Proben die durch Plattenzählung erfassbare Anzahl vermehrungsfähiger Bakterien gegenüber den Kontrollen lediglich um 90–98% verringert.

In der nicht weiter aufgeteilten, 12 mm dicken Innenschicht war nur bei sehr keimreichem Material eine eindeutige Keimzahlreduktion durch die Bestrahlung nachzuweisen.

Bei den keimärmeren Proben war lediglich in der Oberflächenschicht, in keinem Falle aber innen eine Keimzahlreduktion zu beobachten. Innen waren im Gegenteil die Bakterienzahlen nach der Bestrahlung gegenüber den Kontrollen stets um das 2–4 fache erhöht. Bei im Innern noch keimärmerem Material war der gleiche Effekt mit

TABELLE 2. Verteilung der vermehrungsfähigen, psychrophilen Mikroorganismen in verpackten Seefisch- und Rindfleischproben vor und nach Oberflächenbestrahlung mit weichen 60 kV Röntgenstrahlen

| Material | | Bakterien/g† | | |
|---|---|---|---|---|
| | | Aussenschicht (1,5 mm) | Innen | Gesamte* Probe |
| *Seefisch (innen keimreich)* | | | | |
| Kabeljau 3 | Unbestrahlt | 45,200‡ | 16,400 | 25,200 |
| | Bestrahlt | 3,450 (8%)‡ | 5,270 (32%) | 4,690 (19%) |
| Kabeljau 7 | Unbestrahlt | 18,500 | 13,000 | 14,700 |
| | Bestrahlt | 1,200 (7%) | 3,240 (25%) | 2,620 (18%) |
| *Seefisch (innen keimärmer)* | | | | |
| Kabeljau 10 | Unbestrahlt | 17,000 | 1,010 | 5,890 |
| | Bestrahlt | 980 (6%) | 3,520 | 2,750 (47%) |
| Schellfisch 3 | Unbestrahlt | 32,100 | 570 | 10,200 |
| | Bestrahlt | 770 (2%) | 2,070 | 1,670 (16%) |
| *Rindfleisch* | | | | |
| Rindfleisch 2 | Unbestrahlt | 10,400 | 280 | 3,780 |
| | Bestrahlt | 870 (8%) | 630 | 700 (19%) |
| Rindfleisch 4 | Unbestrahlt | 8,400 | 175 | 3,870 |
| | Bestrahlt | 570 (7%) | 520 | 530 (14%) |

* Berechnet aus den Keimzahlen für Aussenschicht (ca. 30% der Gesamtprobe) und Innen (ca. 70% der Gesamtprobe).
† Mittelwerte aus Plattenzählungen mit je 5 Parallelen/Verdünnung.
‡ Prozentuale Überlebensrate nach der Bestrahlung.

einer bis zu 10 fachen Keimzahlerhöhung nachzuweisen. In weiteren Versuchen mit ganz frischem, im Innern extrem keimarmem Material konnte nach der Bestrahlung eine noch grössere Keimanreicherung wahrscheinlich gemacht werden. Letztere Ergebnisse waren allerdings nicht eindeutig reproduzierbar, da hier die Grenzen der Zählmethode erreicht werden.

Die Bakterienzahlen für das ganze Probestück wurden unter Annahme konstanter Abmessungen der Stücke aus den experimentell gefundenen Werten für die Oberflächenschicht (= 30% der Gesamtprobe) und restliche Innenschicht (= ca. 70% der Gesamtprobe) berechnet (Tab. 2, Spalte 4). Zur Vereinfachung blieb die durch die allseitige Bestrahlung bedingte Verdoppelung der Dosis an den Kanten der Proben unberücksichtigt. Bei alleiniger Betrachtung dieser Gesamtkeimzahlen für das ganze Probestück gleichen sich Keimzahlreduktion aussen und innen im keimreichen Material einerseits und Keimzahlreduktion aussen—Anreicherung innen—beim keimärmeren Material andererseits weitgehend aus. Unabhängig vom inneren Keimgehalt war daher die prozentuale gesamte Keimzahlreduktion in allen Stücken mit nur 70–80% nahezu gleich gross. Lediglich bei im Innern extrem keimarmem Material war sie mit 90–95% etwas grösser.

### (3) *Zusammensetzung der Mikroflora vor und nach Oberflächenbestrahlung*

Die qualitative Analyse der Mikroflora neben der Keimzahlbestimmung wurde nur bei Proben von 4 verschiedenen, im Innern keimärmeren Fischen (Kabeljau, 75 bis 100 Isolierungen jeweils für unbestrahlt und bestrahlt, innen und aussen) durchgeführt. Zwischen den vier untersuchten Fischen—es handelte sich um beeisten Kutterfisch—bestanden keine signifikanten Unterschiede in der prozentualen Zusammensetzung der Flora, wie sie in Tab. 3 als Beispiel für einen dieser Fische dargestellt ist.

Die psychrophile Mikroflora des Ausgangsmaterials hatte insgesamt eine ziemlich heterogene Zusammensetzung mit annähernd

TABELLE 3. Die Wirkung der Oberflächenbestrahlung mit weichen 60 kV Röntgenstrahlen und einer Oberflächendosis von 3 Mr auf die prozentuale Zusammensetzung der Mikroflora beim Kabeljau

| | Prozent Kolonien von 20°C Zählplatten für | | | | | |
|---|---|---|---|---|---|---|
| | Aussenschicht (1,5 mm) | | Innen | | Gesamte Probe* | |
| | Kontrolle | Bestrahlt | Kontrolle | Bestrahlt | Kontrolle | Bestrahlt |
| *Pseudomonas* | 9 | 8 | 33 | 47 | 12 | 40 |
| *Achromobacter* | 18 | 16 | 29 | 29 | 20 | 27 |
| *Flavobacterium* | 14 | 3 | 13 | 12 | 14 | 10 |
| *Corynebacterium* | 17 | 6 | 17 | 5 | 17 | 5 |
| *Micrococcus* | 40 | 60 | 6 | 4 | 35 | 15 |
| Hefen | — | 7 | — | 3 | — | 3 |
| Verschied. | 2 | — | 2 | — | 2 | — |
| Anzahl d. isoliert. Stämme Mikroorganismen/g | 78 | 73 | 94 | 102 | 172 | 175 |
| | 28,000 | 1,350 | 2,120 | 2,460 | 10,100 | 2,120 |

* Berechnet aus den getrennt für Aussenschicht (ca. 30% der Gesamtprobe) und Innen (ca. 70% der Gesamtprobe) ermittelten Werten.

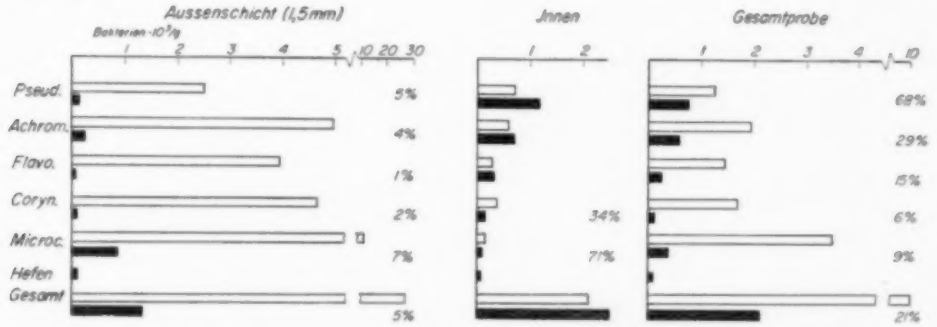


ABB. 2. Der Anteil der in den Oberflächenschichten, im Innern und in den gesamten Kabeljauproben vorhandenen Bakteriengattungen an der Gesamtkeimzahl vor □ und nach ■ Oberflächenbestrahlung mit weichen 60 kV-Röntgenstrahlen und einer Oberflächendosis von 3 Mr.

gleichen Anteilen von *Achromobacter-*, *Flavobacterium-*, *Corynebacterium-* und *Pseudomonas*-Arten; lediglich die *Micrococcus*-Arten traten etwas stärker hervor* (Tab. 3). Eine unterschiedliche Verteilung zwischen Oberflächenschicht und Innen lag nur bei den *Micrococcus-* und *Pseudomonas*-Arten vor. Das Vorkommen der Mikrokokken war hauptsächlich auf die Oberfläche beschränkt, während umgekehrt die *Pseudomonas*arten stärker im Innern und geringer in den Oberflächenschichten vertreten waren. Obligat anaerobe Bakterien waren in keinem der untersuchten Fische nachzuweisen; Sporenbildner kamen nur ganz vereinzelt vor.

Die Wirkung der Bestrahlung auf die Mikroflora wird besonders deutlich aus der in Abb. 2 gegebenen—aus prozentualer Artenzusammensetzung und Keimzahl berechneten—Gegenüberstellung des Anteils der einzelnen Gattungen an der jeweils für aussen und innen bestimmten Keimzahl. Wie die

* Nach Untersuchungen englischer Autoren besteht die Mikroflora von frischgefangenem Nordsee-Kabeljau primär überwiegend aus *Pseudomonas-* und *Achromobacter*-Arten, während der Anteil von *Flavobakterien*, *Corynebakterien* und Mikrokokken zusammen höchstens 10–20% der Gesamtflora ausmacht[15,16]. Während der Eislagerung nach dem Fang bis zur Anlandung und Verkauf kann sich aber die Zusammensetzung mehrfach ändern. Insbesondere nach der Anlandung konnte, ähnlich wie bei unserem relativ alten Fisch, eine stärkere Beteiligung der *Corynebacterium-* und *Micrococcus*-Arten beobachtet werden[17–19].

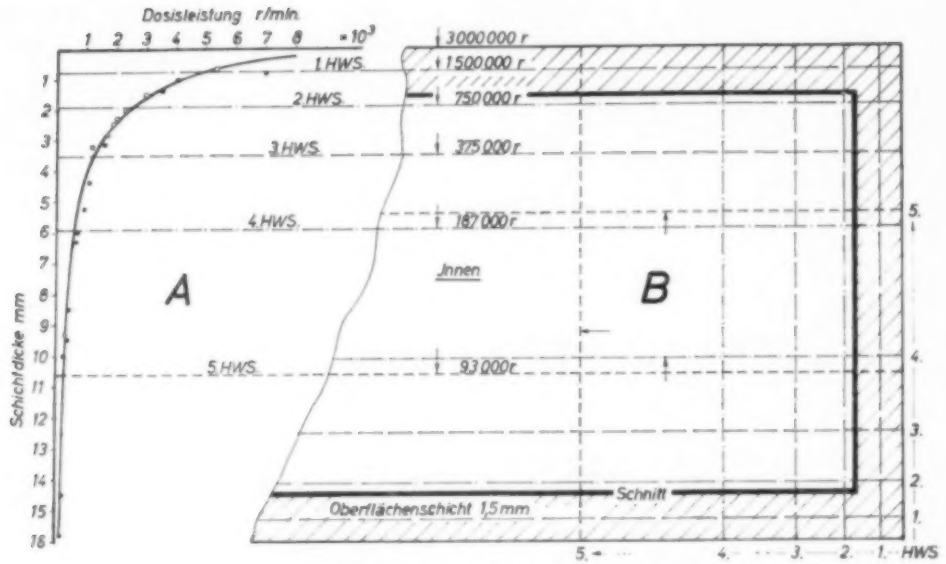


Abb. 3. Die Dosisverteilung in oberflächlich mit weichen 60 kV Röntgenstrahlen bestrahlten Rindfleischproben.
A. Gemessene Röntgenstrahlenschwächung bei verschiedenen Schichtdicken in Rindfleisch (10 kr/min).
B. Schema der Dosisverteilung im Querschnitt von 40 × 40 × 16 mm grossen Rindfleischproben bei einer Oberflächendosis von 3,000,000 r und bei Bestrahlung von 3 verschiedenen Seiten.

weiterhin daraus berechneten, in Abb. 2 angegebenen prozentualen Überlebensraten für die einzelnen Arten zeigen, war die Bestrahlung in der Oberflächenschicht nur wenig selektiv. Die *Flavobacterium-* und *Corynebacterium*-Arten wurden etwas stärker als die *Pseudomonas-* und *Achromobacter*-Arten reduziert; etwas resistenter waren nur die Mikrokokken.

Im Innern waren lediglich die grampositiven *Corynebacterium-* und *Micrococcus*-Arten von der Bestrahlung betroffen. Keinerlei Keimzahlreduktion, sondern im Gegenteil eine Anreicherung erfuhren innen die gramnegativen *Pseudomonas-*, *Achromobacter-* und *Flavobacterium*-Arten. Nur diese waren damit für die bei der Keimzählung beobachteten Bakterienanreicherung im Innern nach der Bestrahlung verantwortlich.

Insgesamt resultiert daraus eine veränderte prozentuale Artenzusammensetzung in der Gesamtprobe, die vor allem durch eine Verminderung der grampositiven Arten und eine entsprechende Erhöhung der *Pseudomonas*-Arten gekennzeichnet ist (Tab. 3).

## BESPRECHUNG DER ERGEBNISSE

Der Dosisabfall der angewandten, weichen 60 kV Röntgenstrahlen in Abhängigkeit von der Schichtdicke war verhältnismässig stark. Beim Rindfleisch lag die erste Dosishalbwertsschicht in einer Tiefe von ungefähr 0,7–0,8 mm, die zweite und dritte Halbwertsschicht bei 1,9 bzw. 3,5 mm (Abb. 3A). Die Genauigkeit der Messungen war allerdings begrenzt, da beim rohen Fleisch und noch mehr beim Fisch die Herstellung gleichmässiger Schichtdicken Schwierigkeiten macht. Für die Fischmuskulatur ist annähernd derselbe Dosisverlauf der Strahlen anzunehmen. Wie aus der in Abb. 3 B schematisch dargestellten Dosisverteilung in den bestrahlten Probestücken ersichtlich ist, war trotz geringer Strahlenhärte bei der hohen Oberflächendosis von 3 Mr in der Mitte der Stücke immer noch mit einer Dosis von über 100 kr zu rechnen. Bedingt

VOL.
11
1961

Abb. 4. Intensitätsverlauf weicher 60 kV Röntgenstrahlen in einem Modellblock aus 2% Agargel mit 0,05% 2,3,5-Triphenyl-Tetrazoliumchlorid bei Bestrahlung von 3 verschiedenen Seiten und einer Oberflächendosis von 1,5 Mr.

VOL
11
196

durch die allseitige Bestrahlung erfolgte zusätzlich noch an den Kanten sowie Ecken und auch im Innern der Stücke eine zum Teil mehrfache Überlagerung der Dosis. Mit Modellstücken aus Agargel, das mit dem Farbstoff TTC* versetzt worden war, liessen sich die begrenzte Strahleneindringtiefe und die relative Dosisverteilung auch direkt sichtbar machen (Abb. 4); auch die Dosisverdoppelung an den Kanten war dabei durch stärkere Anfärbung gut erkennbar.

In Anbetracht der verhältnismässig geringen Strahlenresistenz vegetativer Bakterien wären bei dieser Dosisverteilung—sofern keine extrem resistenten Bakterien vorhanden sind—eine vollständige Sterilität der Oberflächenschicht und eine deutliche Keimzahlreduktion im Innern zu erwarten.

In ergänzenden Untersuchungen[20] wurde die Bestrahlungsresistenz einiger typischer Stämme aus sämtlichen der in Tab. 3 aufgeführten Gattungen aus der Fisch-Mikroflora ermittelt. Nach Bestrahlung von $10^6$ Bakterien/ml Suspensionslösung (0,1% Pepton + 0,85% NaCl) mit 60 kV Röntgenstrahlen wurden für die *Pseudomonas*- und *Flavobacterium*-Arten D-Werte ($= LD_{90}$) von 3 bis 6 kr, für die *Achromobacter*- und *Corynebacterium*-Arten von 8–19 kr bestimmt. Resistenter waren lediglich die Mikrokokken und Hefen mit D-Werten von 23 bis 74 bzw. 40 bis 55 kr.

Auch bei Annahme einer möglicherweise 2–3 fachen Steigerung dieser Strahlenresistenz im natürlichen Substrat, wie sie z.B. bei *Pseudomonas* im Fleisch gegenüber Puffer- und anderen einfachen Suspensionslösungen beobachtet werden konnte[21], wäre bei einer Dosis von über 900 kr in 1,5 mm Tiefe, für eine Dosis von 700–450 kr in 2–3 mm Tiefe, eine vollständige Abtötung zumindest aller gramnegativen Arten zu erwarten. Auch unter Berücksichtigung grösserer Abweichungen von der 1,5 mm Schnittdicke dürften also in den Aussenschichten nach der Bestrahlung allenfalls geringe Mengen der strahlenresistenteren Mikrokokken, keinesfalls aber gramnegative Arten vorhanden sein. Ebenso wäre auch im Innern bei einer Dosis von über 100 kr mit einer weitgehenden Reduktion wenigstens der sehr strahlenempfindlichen *Pseudomonas*-Arten zu rechnen.

Als Ursache für die im Gegensatz dazu beobachtete, wenig selektive und höchstens 98%ige Keimzahlreduktion in den Oberflächenschichten kann nur eine Sekundärinfektion in Frage kommen. Bei der zur Verhütung von Reinfektionen notwendigen Verpackung in Folienbeuteln treten bei rohem Fleisch oder Fisch immer merkliche Mengen Gewebesaft aus. Weitere Gewebeflüssigkeit sammelt sich während der Bestrahlung an, da unter der Einwirkung der Bestrahlung das Wasserhaltevermögen der Muskulatur abnimmt. Dieser Gewebesaft umgibt das ganze Fleisch auch bei eng anliegender Vakuumverpackung und bildet eine Flüssigkeitsschicht zwischen Fleisch und Folie bzw. grössere Flüssigkeitssäcke besonders an den Schmalseiten der Proben. Bei von oben gerichteter Bestrahlung sammelt sich dieser Gewebesaft auf der Unterseite der Beutel an. Nach Umdrehen der Packung fliesst der nicht von der Bestrahlung getroffene Gewebesaft wieder nach unten und reinfiziert damit die vorher durch Bestrahlung keimfrei gemachte Unterseite. Damit findet auch die wenig veränderte Artenzusammensetzung der Flora, insbesondere die stärkere Beteiligung empfindlicher *Pseudomonas*-Arten auch nach der Bestrahlung eine Erklärung. Durch Anfärbung der Fleischoberfläche und des Gewebesaftes mit zur Dosismessung geeigneten Farbstoffen, wie z.B. Methylenblau, liess sich auch experimentell zeigen, dass bei allseitiger Bestrahlung der Proben ein erheblicher Anteil des frei beweglichen Gewebesaftes von der Bestrahlung nicht getroffen wird.

Die beobachtete Keimanreicherung im Innern nach der Bestrahlung dürfte ebenfalls

* TTC = 3,4,5-Triphenyl-Tetrazolium-Chlorid, das in der Biologie häufig zur Sichtbarmachung von Reduktionsorten benutzt wird, scheint nach unseren bisherigen Erfahrungen besonders gut zur Sichtbarmachung des Strahlenverlaufs bzw. des Strahlungsfeldes geeignet. Der besondere Vorteil der Tetrazolium-Farbstoffe besteht darin, dass umgekehrt wie bei den meisten zur Dosimetrie benutzten Farbstoffe die oxydative Stufe farblos und die unter Einfluss der Bestrahlung irreversibel daraus gebildete Reduktionsstufe (Formazan) farbig ist. Damit lässt sich die Bestrahlungseinwirkung z.B. beim TTC am Orte der Reaktion durch eine rote Färbung direkt sichtbar machen.

auf einen rein mechanischen Keimtransport zurückzuführen sein. Sobald unter der Einwirkung der Bestrahlung aus der Muskulatur Gewebesaft freigesetzt wird, wird dieser durch das Gewebe ebenfalls nach unten abfliessen. Dabei besteht die Möglichkeit, dass Bakterien mitgeführt und aus den oberen Schichten in die unteren, nicht mehr so stark von der Bestrahlung getroffenen Schichten herausgeschwemmt werden. Bei allseitiger Bestrahlung und mehrfachem Umdrehen der Proben kann es so nach und nach zu einer Keimanreicherung im Innern kommen. Der experimentelle Beweis wurde zwar ebenfalls mit Farbstoffen versucht, war aber nicht eindeutig zu bringen. Da es sich bei den für die Keimanreicherung allein verantwortlichen *Pseudomonas*- und *Achromobacter*-Arten überwiegend um stark bewegliche Formen handelt, ist u. U. mit einer zusätzlichen aktiven Eigenbewegung der Bakterien zumindest über kleine Wegstrecken zu rechnen.

Die Keimanreicherung im Innern wird in vorliegenden Untersuchungen wahrscheinlich besonders deutlich, weil eine allseitige Bestrahlung durch von oben auf die Probe auftreffende Strahlung und Drehen der Probe erfolgte und zur Erreichung der notwendigen Oberflächendosis von 3 Mr relativ lange Bestrahlungszeiten für jede Seite erforderlich waren. Bei kürzerer Bestrahlungszeit dürfte dieser Effekt eine geringere Rolle spielen. Auch bei grösserer Strahlenhärte wird dieser sekundäre Keimtransport ins Innere weniger in Erscheinung treten. Je geringer die Strahlenhärte ist, um so eher besteht die Möglichkeit, dass noch nicht abgetötete Bakterien aus der besonders keimreichen Oberfläche nach innen ausgeschwemmt werden. Bei grösserer Strahleneindringtiefe wird dagegen der grösste Teil der oberflächlich lokalisierten Bakterien von der Bestrahlung erfasst, so dass nur noch ein geringer Teil überlebt und nach innen ausgeschwemmt werden kann. Vielleicht lässt sich mit einer derartigen sekundären Keimverschleppung auch der von Nickerson[22] beobachtete zunächst nicht erklärbare Effekt deuten, wonach bei der Bestrahlung von Fisch bei gleicher Dosis mit 3 MeV Elektronenstrahlen eine bessere Haltbarkeitsverlängerung als mit 2 MeV Elektronenstrahlen geringerer Eindringtiefe festgestellt werden konnte.

Zusammenfassend lässt sich also auf Grund vorliegender Modellversuche folgendes zur Oberflächenbestrahlung von verpacktem, rohen Fleisch oder Fisch feststellen:

(1) Die bei Röntgen- oder Elektronenstrahlengeneratoren übliche Bestrahlungsanordnung mit einseitigem Strahlenaustritt —d.h. eine von oben nach unten auf waagerecht liegende Proben bzw. seitlich auf senkrecht stehende Proben gerichtete Strahlung —ist zur Oberflächenbestrahlung von verpacktem, rohem Fleisch oder Fisch ungeeignet, da bei diesen Produkten beim Bestrahlen Saft austritt. Bei jedem Umdrehen der Proben, wie es zur vollständigen Bestrahlung aller Seiten notwendig ist, erfolgt eine Reinfektion der bereits bestrahlten Oberflächen durch den auf der Unterseite der Proben sich ansammelnden und von der Bestrahlung nicht direkt getroffenen Gewebesaft. Die oberflächlich sterilisierende Wirkung der Bestrahlung wird durch diese nachträgliche Reinfektion innerhalb der Verpackung weitgehend wieder aufgehoben.

(2) Bei der üblichen Bestrahlungsanordnung wird sich diese Reinfektion innerhalb der Verpackung nur durch Bestrahlen des Materials im gefrorenen Zustand vermeiden lassen. Die zusätzliche Gefrierbehandlung erscheint allerdings bei einem Pasteurisierungsverfahren, bei dem der Rohcharakter der Produkte weitgehend erhalten bleiben sollte, nicht zweckmässig. Zur Oberflächenbestrahlung in der üblichen Bestrahlungsanordnung mit dem Strahlenflux von oben nach unten dürften daher nur wenig wasserabgebende Lebensmittel, wie z.B. vorgekochtes Fleisch oder ähnliche Fleischwaren, geeignet sein.

(3) Eine wirksame Oberflächenbestrahlung von verpacktem, rohem Fleisch oder Fisch kann durch Bestrahlung von unten, d.h. nur auf der Unterseite der Proben oder durch gleichzeitiges Bestrahlen von unten und oben erzielt werden. Damit würde bei Bestrahlung jeder Seite gleichzeitig auch der grösste Teil des in der Packung sich ansammelnden Gewebesaftes erfasst und pasteurisiert werden können. Die Reinfektionsgefahr

innerhalb der Packung würde damit stark verringert.

Bei Röntgenanlagen mit beweglicher Röntgenröhre dürfte diese Bestrahlungsanordnung verhältnismässig leicht zu verwirklichen sein. Bei Elektronengeneratoren der üblichen Bauart mit senkrecht nach unten oder waagerecht gerichtetem Elektronenstrahl wäre allerdings eine weit aufwendigere, magnetische Umlenkung des Elektronenstrahls notwendig.

*Anerkennung*—Wir danken dem Bundesministerium für Atomkernenergie und Wasserwirtschaft für die Unterstützung bei der Durchführung dieser Arbeit.

## LITERATUR


1. Hannan R. S. *Food Invest.* **61,** 140 (1955).
2. Kuprianoff J. *Z. Lebensm.-Untersuch. Forsch.* **100,** 275 (1955); *Kältetechnik* **9,** 90 (1957).
3. Rogers Th. *Radiology* **48,** 6 (1947).
4. Robinson R. F. und McMaster R. C. *Cathode Press* **10,** Nr. 3 (1953).
5. Radouco-Thomas C. *Int. J. appl. Rad. Isotopes* **6,** 129 (1959).
6. Zender R., Lataste-Doselle C., Collet R. A., Rowinski P., Radouco-Thomas C., Busset R. und Mouton R. F. *Proceedings of the Second International Conference on the Peaceful Uses of Atomic Energy, Geneva,* 1958, Vol. 27, p. 384. United Nations, N.Y. (1958).
7. Lepovetsky B. C., Weiser H. H. und Deatherage F. *Appl. Microbiol.* **1,** 57 (1953).
8. Nottingham P. M. *J. Sci. Food Agric.* **11,** 436 (1960).
9. Ingram M. *Int. J. appl. Rad. Isotopes* **6,** 147 (1959).
10. Berger A. *Atompraxis* **8,** 301 (1960).
11. Schmidt-Lorenz W. *Arch. Lebensm.-Hyg.* **11,** 60 (1960).
12. Dyer W. J., Dyer F. E. und Snow M. *J. Fish. Res. Board Canada* **6,** 403 (1946).
13. Shewan J. M., Hodgkiss W. und Liston J. *Nature, Lond.* **173,** 208 (1954).
14. Hugh R. und Leifson E. *J. Bact.* **66,** 24 (1953).
15. Georgalla D. L. *J. gen. Microbiol.* **18,** 84 (1958).
16. Shewan J. M. und Stewart J. *Bull. Inst. Int. Froid,* Annex 1958-2, S. 549 (1958).
17. Shewan J. M. und Georgalla D. L. *Proc. Nutr. Soc.* **16,** 161 (1957).
18. Shewan J. M. und Liston J. *Bull. Int. Inst. Refrig.* Suppl. Annex 1, S. 137 (1956).
19. Spencer R. *J. appl. Bacteriol.* **22,** 73 (1959).
20. Schmidt-Lorenz W. und Farkas *Z. Arch. Mikrobiol.* **39,** 1 (1961).
21. Wolin E. F., Evans J. B. und Niven Jr. C. F. *Food Res.* **22,** 682 (1957).
22. Nickerson J. T. R., Lockhardt E. E., Proctor B. E. und Licciardelle J. J. *Food Technol.* **8,** 32 (1954).

International Journal of Applied Radiation and Isotopes, 1961, Vol. 11, pp. 174–183. Pergamon Press Ltd. Printed in Northern Ireland

# Olfactory and Chemical Changes in Irradiated Essential Oils

H. FAZAKERLEY,* P. G. GARRATT,† P. R. HILLS and R. ROBERTS
Isotope Research Division, Wantage Research Laboratory (A.E.R.E.), Wantage, Berks.

(*Received* 10 *May* 1961)

It has been found that the olfactory properties of a range of essential oils and isolates may be improved by small doses of radiation. At the dose most favourable to the process, no changes in the physical or chemical properties of the irradiated oils can be detected. In the case of Brazilian peppermint oil very high doses of electron or $\gamma$-radiation result in the destruction of camphene. Similar effects are noted with ultraviolet irradiation, but the disappearance of camphene is accompanied by the appearance of a new product. This product has been tentatively identified on chromatographic evidence as tricyclene, an intermediate previously encountered in the hydration and dehydration reactions involving camphene.

## DES VARIATIONS OLFACTIVES ET CHIMIQUES DANS LES HUILES ESSENTIELLES SUIVANT L'IRRADIATION

On a trouvé que les propriétés olfactives d'une gamme d'huiles essentielles et de matières isolées peuvent s'améleorer à cause de petites doses de rayonnement. A la dose la plus favorable au procédé on ne peut observer aucune variation des propriétés physiques ou chimiques des huiles irradiées. Dans le cas de l'huile de menthe poivrée brésilienne, de très fortes doses de rayonnement, soit par électrons soit par rayons $\gamma$, détruisent le camphène. On remarque des effets semblables avec le rayonnement ultra-violet, mais la disparition du camphène s'accompagne de l'apparition d'un nouveau produit. Au moyen de la chromatographie on fait l'identification tentative de ce produit comme le tricyclène, produit intermédiaire préalablement retrouvé dans les réactions d'hydration et de déshydration où prend part le camphène.

## АРОМАТИЧЕСКИЕ И ХИМИЧЕСКИЕ ИЗМЕНЕНИЯ ЛЕТУЧИХ МАСЕЛ ПОСЛЕ ОБЛУЧЕНИЯ

Было найдено, что свойства ароматичности ряда масел и вытяжек из них можно улучшить облучением небольшими дозами. При наиболее благоприятных для этого процесса дозах никаких изменений в физических или химических свойствах облученных масел не наблюдалось. В случае Бразильского мятного масла высокие дозы облучения электронами или гамма-лучами приводили к исчезновению камфена. То же наблюдалось при воздействии ультрафиолетом, но исчезновение камфена сопровождалось появлением нового продукта. Этот продукт был идентифицирован ориентировочно как трициклен, встречавшийся уже ранее в виде промежуточного продукта реакций гидратации и дегидратации с участием камфена.

## VERÄNDERUNG DER CHEMISCHEN-UND DUFT-EIGENSCHAFTEN VON BESTRAHLTEN, LEICHT FLÜCHTIGEN ÖLEN

Es wurde gefunden, dass die Dufteigenschaften einer Reihe von leicht flüchtigen Ölen und Raffinaten durch kleine Bestrahlungsdosen verbessert werden können. Bei der für den Prozess günstigen Dosis wurden keine Veränderungen der übrigen physikalischen und chemischen Eigenschaften der bestrahlten Öle aufgefunden. Im Falle des Brasilianischen Pfefferminzöles bewirkt sehr hohe Elektronen- oder $\gamma$-Bestrahlung einen Abbau des Camphens. Ähnliche

* Present address: Glaxo Laboratories Ltd., Sefton Park, Stoke Poges, Bucks.
† Present address: Royal Military College of Science, Shrivenham, Wilts.



VOL
11
196

Effekte werden bei UV-Bestrahlung bemerkt, jedoch ist das Verschwinden des Camphens begleitet von dem Auftauchen eines neuen Produktes. Dieses Produkt wurde versuchsweise auf chromatographischem Wege als Tricyclen identifiziert, ein Zwischenprodukt, welches bei Hydrierungs-und Dehydrierungsprozessen des Camphens gefunden wurde.

## INTRODUCTION

THE development of unpleasant flavours and odours in irradiated natural products is not uncommon, and often occurs when foodstuffs are treated with large doses of radiation. Many of these changes can be related to radiolytic changes involving nitrogen or sulphur containing materials. It has been found that the irradiation of many essential oils and isolates, which are substantially compounds containing only carbon, hydrogen and oxygen, induces changes in flavour and odour which are beneficial. The effect of ultraviolet light, $\beta$- and $\gamma$-irradiation on the olfactory properties of a variety of fragrant extracts has been examined, and attempts have been made to correlate the changes in flavour and odour with the chemical changes which occur in irradiated Brazilian peppermint oil.

VOL. 11 1961

## EXPERIMENTAL

### *Radiation conditions*

Gamma irradiations (dose rate, $0{\cdot}175 \times 10^6$ rad/hr) were carried out in a cobalt-60 source, and electrons (dose rate, $3{\cdot}96 \times 10^7$ rad/hr) were obtained from a 4 MeV linear accelerator. To counteract the heating effect that accompanied electron bombardment, cooling was applied by means of a blast of air. In this way the sample was kept within a few degrees of ambient temperature. For the olfactory test, samples were irradiated in cork-stoppered tubes. To make allowance for any variation on the final assessment of the oils that arose due to exposure to heat or light during transit of the samples, two controls were prepared. One was retained at the point of dispatch and the other accompanied the samples sent for irradiation. The samples were evaluated in the customary manner by their olfactory properties when examined on strips of absorbent paper. For the chemical examination, samples of Brazilian peppermint oil (2 ml) were irradiated in sealed 5 ml ampoules. Screw-cap tubes were used for the samples treated under nitrogen or oxygen. The appropriate gas was allowed to pass through the sample for 15 min before sealing.

### *Analysis of oil*

The Brazilian peppermint oil had the following physical properties: $\eta_D^{23{\cdot}5}$, 1·485; $(a)_D$, $-27°44' \pm 7'$; $\lambda_{max}^{EtOH}$, 228–229 m$\mu$ ($E_{1cm}^{1\%}$, 51); and $\nu_{max}^{liq}$ 3390 (hydroxyl), 1724 (shoulder, ester), 1701 (ketone), 1601 ($\alpha\beta$-unsaturated ketone), 1044, 1022, 917, 886, 846 cm$^{-1}$. Menthol, menthone and menthyl acetate were analysed by standard techniques[2].

### *Separation of ketonic materials*

Substituted hydrazones of the ketonic constituents of the oil were prepared by refluxing oil (2 parts) and trimethyl-ammonium acetohydrazide chloride—Girard T reagent[3]—(1 part) in 10:1 ethanol-acetic acid (40 parts) for 1¼ hr. After ether extraction of the cooled solution to remove unchanged oil, the aqueous solution of the ketonic derivative had $\lambda_{max}$, 237–238 m$\mu$, characteristic of a saturated ketone[4]. Acidification afforded a material with an infra-red spectrum identical to that of menthone: $\nu_{max}$, 1701 cm$^{-1}$. This material provided a 2:4-*dinitrophenylhydrazone*, yellow needles: m.p., 144–145°C; $\lambda_{max}^{CHCl_3}$, 369 m$\mu$ ($\varepsilon$, 23,700). Authentic menthone 2:4-dinitrophenylhydrazone had a m.p. of 145–146°C, $\lambda_{max}^{CHCl_3}$, 369 m$\mu$ ($\varepsilon$, 23,300). Treatment of the ether soluble oil with 2:4-dinitrophenylhydrazine resulted in the slow precipitation of a minute amount of a 2:4-*dinitrophenylhydrazone:* m.p.,

108°C; $\lambda_{max}^{EtOH}$, 373–374 m$\mu$ ($\varepsilon$, 24,500). Piperitone 2:4-dinitrophenylhydrazone: m.p., 117–118°C; $\lambda_{max}^{EtOH}$, 373–374 m$\mu$ ($\varepsilon$, 25,100)[5].

*Determination of peroxides*

Peroxides were determined by a modification of the ferrous thiocyanate method[6]. Solutions of peppermint oil (0·15 per cent) in methanol were prepared. Aliquots (5 ml) were treated with 2 ml of freshly prepared ferrous thiocyanate reagent made up as follows: equal amounts (5 ml) of 20 % ferrous sulphate and 20 % ammonium thiocyanate were mixed and allowed to stand for 5 min. Aliquots of this solution (2 ml) and 2 ml of water diluted to 50 ml with methanol gave a solution which was 0·014 M in ferrous ion. The light absorption of the mixed solutions (7 ml) was measured at 438 m$\mu$ in 2 cm cells. Maximum extinction was reached 20 min after mixing.

A calibration curve for peroxide was constructed using standard solutions of hydrogen peroxide in methanol ($1 \times 10^{-5}$ to $7 \times 10^{-5}$ M). Maximum extinction at 438 m$\mu$ was attained 15 min after mixing. The molarities of ferrous and thiocyanate ions (0·004 M) in the solution for spectrophotometric measurements were in at least sixty-fold excess of the molarity of the peroxide present. The methanolic solutions of hydrogen peroxide were standardized spectrophotometrically, after dilution with water, by the titanium sulphate method[7] at 410 m$\mu$.

*Gas-liquid chromatography*

This was carried out using a Perkin–Elmer model-116 instrument. Preliminary experiments were conducted using a 20 per cent wt./wt. Apiezon "L"-celite column under the following conditions: column, 2 m long, 6 mm bore; carrier gas, helium; column temperature, 132°C; sample size, 10 or 50 $\mu$l. Greater resolution was obtained by using two of the above columns in tandem.

Calibration curves were constructed for the terpene hydrocarbons using standard solutions (100–1000 $\mu$g/50 $\mu$l) of the hydrocarbons. The amount injected was normally 50 $\mu$l when the sensing system was operated at one-quarter of maximum sensitivity. The $\alpha$-pinene and limonene used were 99 per cent pure. The camphene was 84 per cent pure and contained $\alpha$-pinene (16 per cent). The $\beta$-pinene was 87·5 per cent pure and contained $\alpha$-pinene (5·3 per cent), camphene (1·9 per cent) and limonene (5·3 per cent). The detector gave essentially the same response for the four terpene hydrocarbons. At maximum sensitivity, full-scale deflection was produced with approximately 300 $\mu$g of hydrocarbon. The minimum detectable amount of hydrocarbon was 2 $\mu$g.

*Synthetic peppermint oil*

This was made up using the best quality materials available, and contained $\alpha$-pinene (1·00 per cent), camphene (1·6 per cent), $\beta$-pinene (1·1 per cent), limonene (2·4 per cent), menthone (37·0 per cent), menthol 42·1 per cent), piperitone (3·1 per cent) and menthyl acetate (11·7 per cent), by weight. The terpene hydrocarbon percentages were corrected for impurities by gas chromatography.

## RESULTS AND DISCUSSION

(a) *The olfactory effects of radiation*

During the course of the investigations, fifty-six essential oils or isolates were irradiated. The changes observed were limited to variation in odour. No significant differences were noted in the density or specific rotation of any of the oils listed in Table 1, and in the case of peppermint oil, spectral characteristics both in the ultra-violet and infra-red were unchanged by $\beta$- or $\gamma$-radiation. Gas liquid chromatograms were identical. Only in two cases were visual changes noted. Jasmine oil became less turbid and the colour of rose oil faded slightly.

Olfactory changes for a number of materials exposed to a dose of $10^7$ rad of $Co^{60}$ $\gamma$-radiation are reported in Table 1. These oils were assessed by a number of experienced

perfumers using the conventional technique, in which a strip of absorbent paper is impregnated with the oil to be evaluated. This is allowed to volatilize slowly by exposure to the atmosphere, and the odour is compared with that of a similarly treated control over an extended period. During the volatilization, a skilled assessor can discriminate a variety of "notes" or "tones" which comprise the overall bouquet of the complete oil. The changes in odour observed were mild. They were most apparent on freshly impregnated paper strips, and after 2 hr evaporation could hardly be detected.

For floral oils, radiation enhances the fidelity to the flower. While the intensity of the odour is sometimes reduced, it is also more balanced and persistent. From a survey it appears that the degree of change is related to the content of alcohols, terpenes and other hydrocarbons in the oil. In the case of the citrus oils, however, the most outstanding effect was one of preservation. In the irradiated samples, the resinification that had occurred in the controls was absent.

Further experiments were designed to establish the behaviour of typical constituents of essential oils, as well as the optimum type and dose of radiation (Table 2). On olfactory evidence, the order of resistance to radiation was aldehyde > alcohol > ester > hydrocarbon > phenol. Since the materials tested were of terpenic origin, it was not to be expected that the order of stability would be identical to that encountered with simpler alkyl- and alkyl-substituted constituents. Nevertheless, the marked stability of the aldehydes was surprising, but was consonant with experiments in which several oils were exposed in tubes open to the atmosphere. While oxidative degradation was pronounced, the persistence of the aldehydes was well marked. Of the various treatments applied, electron irradiation generally afforded a superior product to that obtained with $\gamma$-radiation. High doses brought about a gross deterioration in the oil, and improved characteristics were most prevalent at the lowest dose, $10^6$ rad. Peppermint and citrus oils in general responded best to the treatment. Peppermint is improved in odour and flavour, and citrus oils are preserved against decomposition.

Further experiments were restricted to a Brazilian peppermint oil. The range of doses was extended downwards to $0{\cdot}3 \times 10^6$ rad, at which level no change in odour could be detected. With independent assessors, the superiority of the electron-treated material at higher doses was confirmed. Gamma irradiations of de-aerated peppermint oil produced an improved oil which was comparable to the previously superior electron-irradiated material.

This effect may be related to the rate at which the electron and $\gamma$-radiation were applied (respectively, 39·6 and $0{\cdot}175 \times 10^6$ rad/hr). At the higher electron dose rate, the oxygen may react so rapidly that its concentration cannot be maintained by diffusion from the air space in the sample tube. In these circumstances the conditions would become almost anaerobic. At the lower $\gamma$-dose, reaction would not be so fast, and the oxygen concentration can easily be maintained by diffusion. It is not surprising, therefore, that the de-aerated sample was at least as good as the normal electron-irradiated oil. Alternatively, the difference in olfactory properties might be due to the dose-rate dependence of the oxidation process. For oxidation reactions in general, the rate of reaction is frequently proportional to the square root of the radiation intensity. If such conditions were to apply to the oxidation of peppermint oil, it would be expected that relatively less chemical change would occur at the highest dose rate.

(b) *The chemical changes in irradiated peppermint oil*

(i) *The constitution of Brazilian peppermint oil.* About forty different components have been identified in the various peppermint oils of commerce. The principal constituents common to all oils are menthol, menthone and menthyl esters, accompanied by a range of terpenes. Many of the compounds are present in minute amounts. The Brazilian peppermint oil was subjected to gas–liquid chromatography and the compounds isolated are listed in Table 3. Compound "A" is

TABLE 1. Olfactory properties of some irradiated essential oils

| Material | Observations |
|---|---|
| *Oils* | |
| Ambrette | More persistent |
| Angelica Root | Angelica note enhanced |
| Balm | Citron note less pronounced |
| Basil | Sweeter and more persistent; terpene notes reduced |
| Bitter almonds | Sweeter, less acid |
| Carrot seed | Persistence increased, more balanced odour |
| Celery seed | Controls resinified, irradiated sample unchanged, rounder odour |
| Chamomile | Chamomile character very slightly accentuated |
| Citron | Citral note accentuated, accompanied by "green" notes |
| Clove | Eugenol less apparent; woody notes appear |
| Coriander | Finer odour reduced in intensity |
| Cypress | Cypress character lost; terebinth notes emphasized |
| Genet | Sweeter and more faithful to the flower |
| Geranium (Algeria) | Heavy "green" notes emphasized; geraniol less apparent |
| Geranium Palmorosa | Sweeter and lighter; geranyl acetate accentuated |
| Jasmin | Floral character enhanced |
| Jasmin "Pommade" | Greasy notes reduced; more faithful to the flower |
| Lavender | Less linaloöl; odour more sustained |
| Mandarin | Methyl anthranylate note reduced; rounder odour |
| Nutmeg | Finer odour and more body; terpenes reduced |
| Orange (bitter) | Controls resinified but not irradiated oil; rounder and more agreeable |
| Oak Moss | Unchanged |
| Peppermint glacial | Mentholic character improved; finer material flavour more pronounced |
| Petitgrain | More bitter, some loss of floral tone |
| Pimento | Some character lost; eugenol odour appears |
| Sandalwood | More woody; the feeble sandalwood note remaining is finer and more sustained |
| Savory | Predominant note of Thyme; more rounded odour |
| Styrax | Hardly changed; slightly more phenylpropyl alcohol |
| Tree Moss | Unchanged |
| Verbena | Less freshness, finer rounder odour |
| Vetyver | Stronger, less earthy |
| Ylang-ylang | Heady notes reduced; finer and more mellow |
| *Absolutes* | |
| Rose | Less rose-like and less powerful |
| Tuberose | Floral notes accentuated |
| Violet | Almost unchanged |
| *Concretes* | |
| Carnation | Floral notes emphasized |
| Cassia | Slightly more floral |
| Iris | Less powerful but of finer odour; myristic acid note less pronounced |
| Mimosa | Warmer toned |
| Narcissus | Sweeter, less strong; methyl-*p*-cresol less pronounced |
| Orange | Finer, sweetish odour |
| *Resinoids* | |
| Castoreum | Slightly weaker, no pronounced difference |
| Civet | Little different |
| Costus | Animal notes suppressed |
| Feve Tonka | Coumarin note reduced |
| Myrrh | Unchanged |
| Labdanum | Unchanged |

TABLE 2. The effect of radiation on some essential oil constituents

| Compound | Oil | Observation |
|---|---|---|
| *Alcohols* | | |
| Geraniol | Palmorosa | Geraniol unchanged; terpenes broken down; A(1)* superior to control |
| Linaloöl | Rosewood | Linaoöl stable except at highest dose; A(1) superior to control |
| Vetiverol | Vetyver | Vetiverol stable; earthy note lost in A(2); fruity note appears |
| Menthol | Peppermint | Menthol affected at high doses; A(1), A(2), B(1), B(2) samples better than controls; A treatment superior to B |
| *Esters* | | |
| Linalyl acetate | Bergamot | Unstable at higher doses |
| Linalyl acetate | Petitgrain | Unstable; A(1) improved |
| Linalyl acetate | Lavender<br>Lavendin hybrid | A(1) unaffected; A(2), B(2) more matured; B treatment superior |
| Linalyl acetate | Lavendin | A(1), B(1) unaffected; A(2), B(2) marginal improvement; B(2) better than A(2); camphor character remains predominant |
| Linalyl acetate | Lavendin abrialis | No change |
| *Aldehydes* | | |
| Citral | Lemon grass | Citral stable; terpenes break down |
| Citral | Pure | Unchanged |
| $C^7$ aldehyde | Pure | Unchanged |
| *Hydrocarbons* | | |
| Limonene | Pure | Unstable; varnish odour appears |
| Limonene | Orange | A(1), B(1) treatments result in loss of fatty aldehyde note; higher doses decompose; B(1) improved keeping properties of oil |
| Limonene | Lemon | A(1) unaffected; higher doses decompose |
| *Phenols* | | |
| Eugenol | Clove bud<br>Clove deterp. | Eugenol breaks down and woody notes appear |
| *Miscellaneous* | | |
| | Ylang-Ylang | Unstable; acid notes develop |

* *Key to radiation treatment*
A—electrons; B—$\gamma$-radiation.
Doses: (1) $10^6$ rad, (2) $3 \times 10^6$ rad, (3) $10^7$ rad, (4) $3 \times 10^7$ rad.

relatively volatile and is eluted between carbon tetrachloride and benzene on chromatography at 34°C. It is probably a solvent contaminant introduced during the processing. Compound "E" is probably piperitone (approximately 3 per cent wt./wt.), or a similar $\alpha\beta$-unsaturated ketone. Its presence was inferred by the ultra-violet absorption at 228–229 m$\mu$ of the original oil. Additionally the residual oil, after the removal of the substituted hydrazones formed by reaction with Girard-T reagent, formed a 2:4-dinitrophenylhydrazone which had similar spectroscopic properties, in the ultra-violet, to the authentic piperitone derivative.

Using a modified chromatographic technique, greater resolution of the oil was obtained (Fig. 1). Under these conditions two new peaks appeared, one between the $\alpha$-pinene and the camphene peaks (compound "B"), and the other immediately following the menthol (compound "D"). Additionally, the camphene peak appeared as a partially resolved doublet comprising a main peak,

TABLE 3. The constituents of peppermint oil as detected by gas–liquid chromatography

| Constituent | Percentage, wt./wt. |
|---|---|
| Water | 0·4 |
| Compound "A" | 0·4 |
| α-Pinene | 0·9 |
| Camphene | 1·5 |
| β-Pinene | 1·0 |
| Limonene | 4·7 |
| Menthone* | 35·2 ± 0·3† |
| Menthol* | 40·0 ± 4·0 |
| Compound "E" | — |
| Menthyl acetate | 11·5 ± 0·4‡ |

* Analysed chemically.
† Carbonyl content expressed as menthone.
‡ Ester content expressed as menthyl acetate.

camphene, with a relatively high shoulder (compound "C") on the curve of the peak. The imperfect resolution of the three new compounds did not allow their quantitative evaluation. Other workers[8] have observed the presence of an unidentified peak between α-pinene and camphene on a chromatogram of German turpentine oil obtained using two silicone oil columns in tandem at 100°C. It is interesting to note that neither isomenthol nor isomenthone, which are frequently found in peppermint oil chromatograms, were detected.

(ii) *The irradiation of peppermint oil with electrons and γ-radiation.* The physical properties of the oil were unchanged by irradiation. A dose of $10^6$ rad produced no change in the density, refractive index, specific rotation or ultra-violet and infra-red spectra. The formation of hydroperoxides from the terpenes contained in essential oils is known to occur on storage[9]. It was shown that the natural peroxide content of the peppermint oil was doubled by a dose of $10^6$ rad. The peroxide concentrations of treated and untreated oils were respectively, 5·5 and 2·75 × $10^{-5}$ moles/g. If it is assumed that the

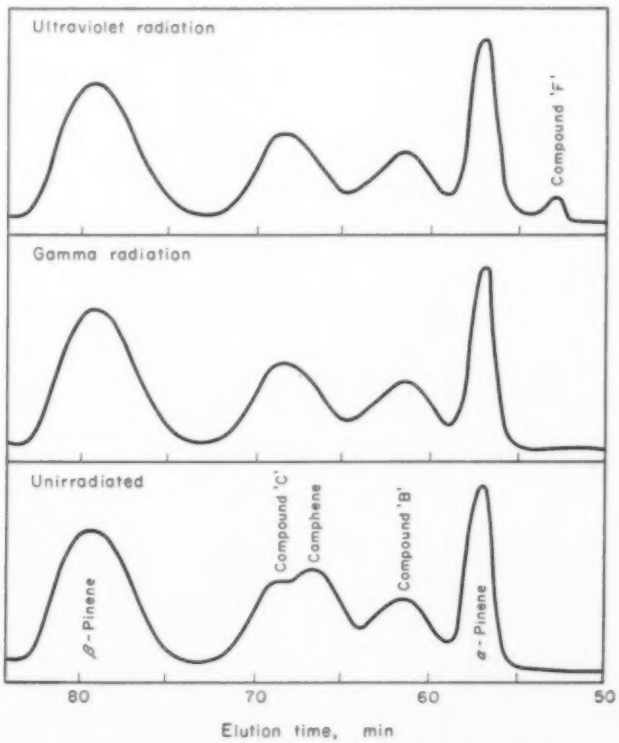


FIG. 1. Gas–liquid chromatograms of the terpene fraction of Brazilian peppermint oil.

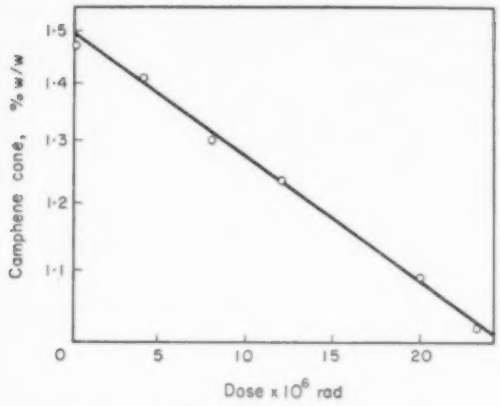


FIG. 2. The radiation-induced formation of peroxides in Brazilian peppermint oil.

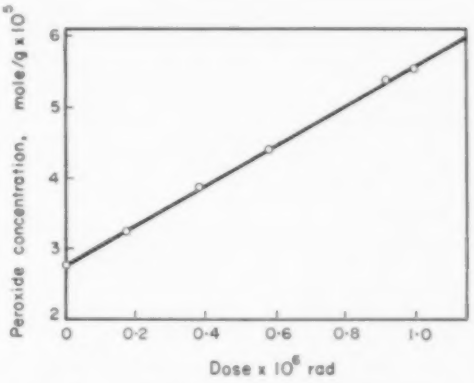


FIG. 3. The radiation-induced decomposition of camphene in Brazilian peppermint oil.

hydroperoxide is formed from a monoterpene, the peroxide concentration would be 0·46 and 0·92 per cent (wt./wt.), respectively. The formation of peroxides was linear with respect to dose up to at least $10^6$ rad (Fig. 2). From the slope of the line the *G*-value (the number of molecules of product formed for an energy absorption of 100 eV) was 26.

Upon chromatography no reaction products were observed in either the electron or $\gamma$-irradiated material up to doses of $2{\cdot}5 \times 10^7$ rad. In both cases, however, the camphene concentration was reduced. Qualitative results were obtained by calibration with standard solutions of camphene in benzene. The authentic camphene employed contained a significant quantity of $\alpha$-pinene, but the resolution was such that a correction could be employed chromatographically. The disappearance of camphene vs. dose is shown graphically in Fig. 3. A log–linear plot yielded a linear relationship indicating that the reaction of camphene is first-order with respect to the camphene concentration. After a dose of approximately $10^7$ rad, the camphene concentration was reduced by nearly 20 per cent. Significant points could not be obtained below $4 \times 10^6$ rad, due to the limit of precision of the analytical method. The *G*-value for disappearance of camphene was 1·5. No detectable changes were observed in the concentration of the other terpene constituents of the oil up to $2{\cdot}5 \times 10^7$ rad. Other workers[10] have shown that de-aerated $\alpha$-pinene gives on $\gamma$-irradiation, a *G*-value of 3·7 for total isomerized product formation after a dose of $7 \times 10^7$ rad.

The specific susceptibility of camphene to radiation is surprising in view of the fact that camphene is chemically one of the more stable terpenes. After doses of $6 \times 10^7$ rad in air, pure camphene exhibited no chromatographic changes or reaction products; neither were any changes observed in irradiated benzene solutions after a dose of $1{\cdot}1 \times 10^7$ rad. Since benzene might exert a preferential protective effect[11] for the camphene, limonene was also used as a solvent. Again, no changes were observed. A synthetic oil containing camphene was compounded using the purest samples available of the major constituents of Brazilian peppermint oil. Upon irradiation, the camphene disappeared at a rate similar to that encountered for the natural oil. The olfactory properties of the synthetic oil were also improved. It would therefore appear that the reaction of camphene must be dependent on the participation effect of other constituents.

The rate of disappearance of camphene is similar for both electron and $\gamma$-radiation. Since the dose rates employed in each case differ widely, it would seem that the process is not dose-rate dependent. The reaction rate is not affected by de-aeration with a

TABLE 4. Boiling-point data for the monoterpenes

| Compound* | B.p. (°C) | Compound† | B.p. (°C) |
|---|---|---|---|
| Compound "F"‡ | — | Bornylene | 146 (750 mm) |
| α-Pinene | 155 | β-Thujene | 147 (739 mm) |
| Compound "B" | — | β-Fenchene | 150·5–153·5 |
| Camphene | 160 | Tricyclene | 153 |
| Compound "C"** | — | α-Fenchene | 155–156 |
| β-Pinene | 164–166 | Camphane | 156–157 |
| Limonene | 177–178 | Thujane | 157 |

* In order of chromatographic elution.
† Terpene hydrocarbons described in literature (2a) with boiling points in the range 140–170°C.
‡ Detected only in the u.v. irradiated oil.
** Present in the oil and in "authentic" camphene.

stream of nitrogen before irradiation, but is increased by a factor of about 40 per cent when the oil is saturated with oxygen. Considering these circumstances and the $G$-values for formation of peroxide ($G = 26$) and the corresponding value for the disappearance of camphene ($G = 1{\cdot}5$), it appears that the changes that take place cannot be explained solely in terms of a camphene–oxygen reaction. Further evidence would require a detailed analysis on the chromatography column of the eventual products formed by the thermal decomposition of the peroxides. In view of the low concentrations involved and the complexity of the parent oil, it is not surprising that such products have proved to be beyond the limits of analysis.

(iii) *The effects of ultra-violet irradiation*
Chromatograms of ultra-violet and γ-irradiated oils show a general similarity. In both cases the camphene concentration was reduced. However, the ultra-violet-irradiated oil exhibited a new peak (compound "F") with a retention time slightly less than that of α-pinene. The yield of compound "F" increased as the amount of camphene remaining decreased, on prolonged irradiation. Since no significant changes in the amounts of the other constituents were observed, it seems likely that compound "F" is formed from camphene. In Table 4 are listed the identified and unidentified terpene hydrocarbons found in Brazilian peppermint oil, together with other terpene hydrocarbons in the same boiling-point range. On non-polar chromatographic columns the retention time normally increases with the boiling point, as observed with the known hydrocarbon constituents of the oil. It would appear that compound "F" corresponds most nearly to bornylene, β-thujene, β-fenchene or tricyclene. On the basis of the chromatographic results, the best agreement obtains for tricyclene.

A chemical relationship between camphene (I) and tricyclene (II) is shown in several reactions. Both compounds give, on hydration, the stereoisomeric borneols (III).[12,13] Depending on the reaction conditions, the borneols can be dehydrated to give either camphene[14] or bornylene (IV). When bornylene is produced, it is always accompanied by some tricyclene[15]. On reduction over a nickel catalyst, tricyclene is reduced to isocamphene, but it has been shown that under the conditions of the experiment, tricyclene isomerizes to camphene prior to reduction[16]. Hydrogen chloride reacts with tricyclene to give

I II III IV

camphene hydrochloride[13], and similarly tricyclene affords α-nitrocamphene upon nitration[17].

It is generally believed[18] that the absorption of radiant energy by an olefine results in the rupture of one of the ethylenic bonds. For camphene, the radiation-induced rupture of the double bond could be followed by rearrangement to tricyclene with little modification of the spatial relationships of the carbon atoms comprising the camphene skeleton. The tentative identification of compound "F" as tricyclene is therefore quite plausible.

*Acknowledgments*—The authors are indebted to Mr. P. T. Petley, who suggested the olfactory examination of irradiated essential oils, and to Messrs. Camilli, Albert and Laloue of Grasse, to Dr. R. Favre and Dr. G. Davies of Unilever Ltd., and to Fritsche Brothers of New York, for the olfactory assessments.

## REFERENCES

1. Hills P. R., Petley P. T. and Roberts R. *Perfumery and Essential Oil Record.* In press.
2. Guenther E. *The Essential Oils* Vol. I, pp. 265, 272, 286. Van Nostrand, New York (1948); *ibid.* Vol. II.
3. Girard A. and Sandulesco G. *Helv. chim. Acta* **19,** 1095 (1936).
4. Hoyer G. *Scand. J. clin. Lab. Invest.* **3,** 303 (1951).
5. Dupont G., Dulou R. and Crabbe P. *Bull. Soc. chim. France* 621 (1955).
6. Egerton E. G., Minkoff G. J., Everett A. J. and Rudrakanchana S. *Analyt. chim. acta* **10,** 422 (1954).
7. Eisenberg G. *Industr. Engng. Chem. (Anal.)* **15,** 327 (1943).
8. Liberti A. and Cartoni G. P. *Proceedings of the Second Symposium of the Gas Chromatography Discussion Group, Amsterdam* p. 321. (1958).
9. Lang S. and Hock H. *Chem. Ber.* **75,** 300 (1942).
10. Bates T. H. and Williams T. F. *Nature, Lond.* **187,** 665 (1960).
11. Burton M. and Lipsky S. *J. phys. Chem.* **61,** 1461 (1957).
12. Kachler J. and Spitzer F. V. *Annalen* **200,** 354 (1880).
13. Simonson J. *The Terpenes* Vol. II, p. 339. Cambridge University Press (1957).
14. Wallach O. *Annalen* **230,** 237 (1885).
15. Bradt J. and Sandkuhl H. *Annalen* **366,** 1 (1909).
16. Meerwein H. and Van Emster K. *Chem. Ber.* **53,** 1915 (1920).
17. Nametkin S. and Zabradina A. S. *Annalen* **441,** 121 (1925).
18. Ellis C. and Wells A. A. *The Chemical Action of Ultraviolet Rays* p. 406. Reinhold, New York (1941).

# technical notes

## Radioisotope Technique for Determination of Cerebral Circulation Time

(*Received* 27 *January* 1961)

ALTHOUGH KETY and SCHMIDT[1] as well as NYLIN *et al.*[2] have described relatively precise methods for the estimation of cerebral blood flow, there has been no rapid simplified method for the estimation of cerebral arterio-venous transit time. TÖNNIS[3] has made an attempt to correlate angiographic findings with various pathological states and has noted relationships of intracranial processes to acceleration or delay in cerebral vascular transit times. During the past year we obtained measurements with a radioactive technique and have compared this data with that obtained by angiography. Although we were unable to give precise volume of flow data, we have devised a method which can give rapid accurate measurements of cerebral vascular transit times. The resolving time of the system is in the order of 100 $\mu$sec. The data which is obtained is useful in evaluating various dynamic vascular flow patterns and can be correlated or substantiated with the findings obtained by routine cerebral angiography.

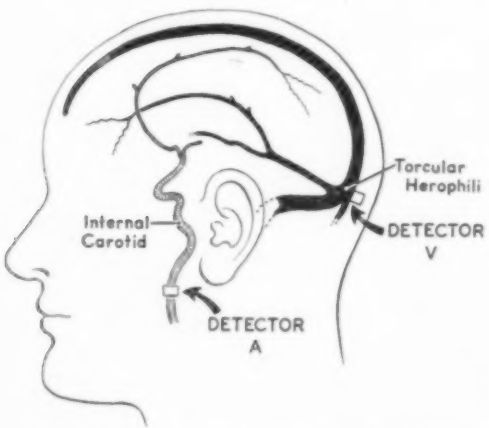


FIG. 1. A schematic diagram to show the position of detector *A* over the internal carotid artery, and detector *V* over the confluence of the venous sinuses.

### Instrument

Prior to this time there has been a severe limitation in the measurement of transit times of the arterial—venous channels of the brain. The systems have been limited by: (1) the finite number of measurements available with angiographic techniques, usually 12 sec; (2) the usage of nitrous-oxide techniques which are limited by the overall general condition of the patient, and (3) inability to observe dynamic measurements without direct arterial or venous sampling.

These objections have been partially eliminated by the use of a radioactive slug which can be measured with suitable detectors. These detectors are placed (Fig. 1): (1) over the major arterial input of the neck which is over the internal carotid artery, and (2) the output counter is placed over the site which is opposite the confluence of the venous sinuses. In the past the scintillation probes have been limited in their application because of unusual size and lack of proper resolution. This problem has been solved by the availability of the Nuclear-Chicago probe DS 8-1 which has a small physical size, high sensitivity and excellent resolution. The limitation of finite time of observation has been overcome by the coupling of the probes to an independent set of rate meters, the output of which is presented to a dual-track tape recorder. The data is presented to two rate meters which feed in turn to two independent recording channels (Fig. 2 (a)). The tape recorder–rate meter circuit allows enhancement in the display of data. Thus, the data is never lost, but may be enhanced and the recording time is unlimited.

### Procedure

Following the termination of angiography, the intra-carotid needle is left *in situ*. The scintillation probes (Fig. 2 (b)) are placed (1) over the internal carotid artery just above the point of arterial puncture and (2) over the external occipital protuberance. This placement allows information to be obtained from two



VOL
11
196

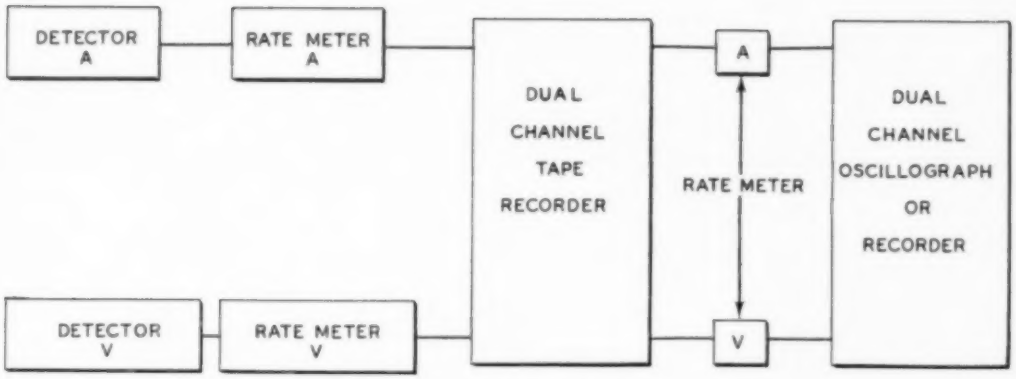


FIG. 2(a). Block diagram of circuit.

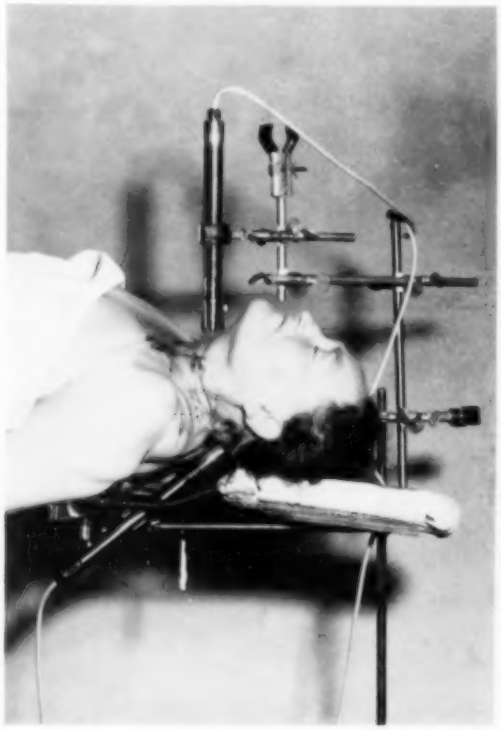

FIG. 2(b). Physical arrangement of the probes. Detector *A* is anterior and detector *V* is posterior. Resolution may be improved with extra shielding, or the use of another isotope such as $Hg^{203}$ neohydrin.

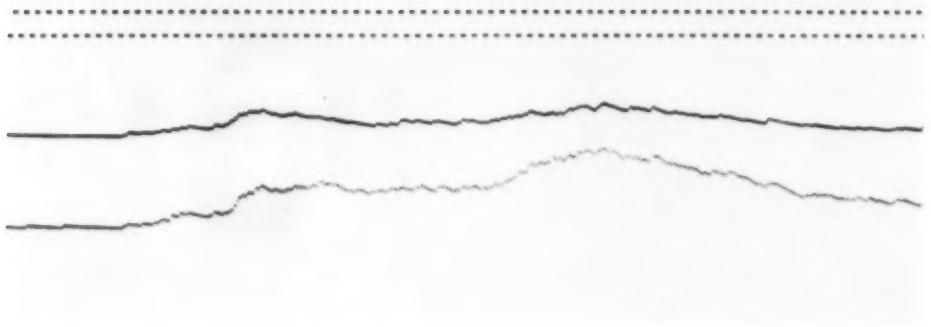

FIG. 4. Effect of poor angulation of the venous output recording head in top tracing. Note the double peak in the lower arterial tracing. Effect limited by shielding and proper placement. Artery—bottom; venous—top.

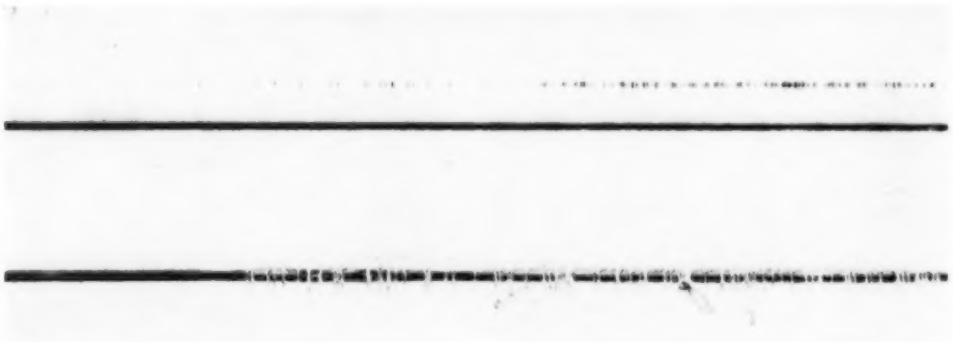

FIG. 7. A tracing obtained with another technique on the taped output. Top recording is venous which was processed through a limiter circuit. Bottom recording is of raw pulses from the tape recorder.

VOL
11
196

widely separated points which correspond to the arterial input and venous output of the brain. After the probes are placed, the stylette of the needle is withdrawn and 100 $\mu c$ of radioactivity in the form of RISA or neohydrin ($Hg^{203}$) is injected intra-arterially. The recorders are activated just before injection takes place and are permitted to run at least 5 min or longer.

This particular record was obtained in a child and was measured at a time of 4.5 sec. Children have for the most part a very fast arterio-venous transit time when there is no intra-cranial lesion.

In the presence of increased intra-cranial pressure or involvement of the cerebral circulation, there are marked changes in the record of the activity and the

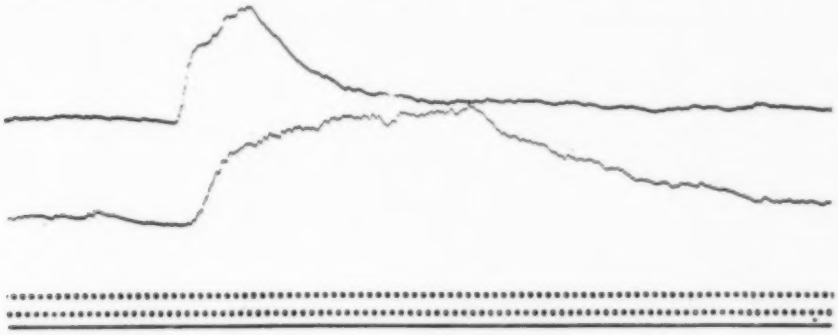

FIG. 3. A normal circulation pattern. Artery recording is above the venous recording. The time marker is 0.3 sec in all recordings.

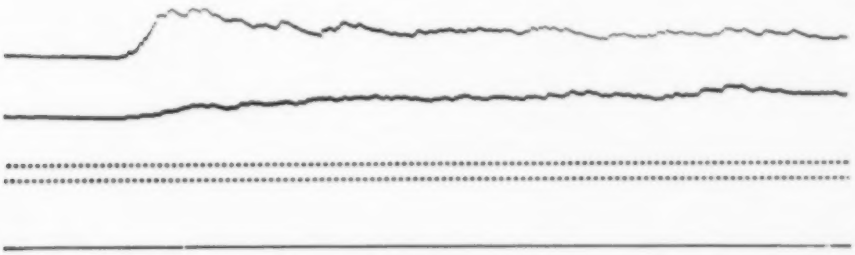

FIG. 5. Tracing of patient harboring a right temporal lobe hematoma. Note steady slow rise of the lower venous tracing.

The recorded data are then played back through rate meters to the recording oscillograph.

## Results

Approximately twenty-five patients have been studied with this technique. Our results have been correlated with observations obtained from angiography. In general there has been agreement in the measurement of transit times between the internal carotid artery and the confluence of the major venous sinuses.

The record (Fig. 3) shows a transit time of 7.2 sec and was considered to be in a normal patient. If by chance the arterial probe is centered at an unusual angle over the carotid-jugular bulb, as in Fig. 4, there is a double maximum corresponding first to the arterial input and then to the venous jugular output.

arterio-venous transit times. Figure 5 is a tracing of activity obtained from a patient harboring a large right temporal lobe hematoma. There is a prompt rise in arterial activity, but an extremely slow rise in the venous activity. The angiogram failed to show adequate flow even after 12 sec of observation. The radioactive measurement indicated that the venous maximum was in excess of 13 sec and the activity persisted in excess of 20 sec. In this patient there was extremely poor visualization of arterial-venous networks as demonstrated by angiography.

A record obtained from a patient having increased intra-cranial pressure associated with subarachnoidal bleeding is shown in Fig. 6. Contrary to expectation, this patient showed a transit time of 5.4 sec, and a return to venous base line after another 11.4 sec. This finding was substantiated by angiography.

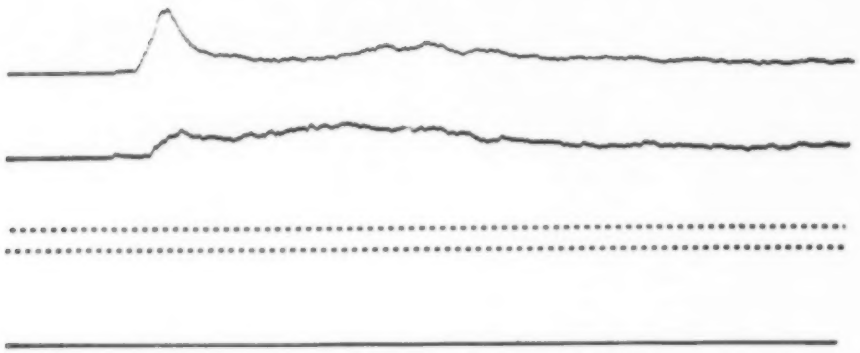

FIG. 6. Obtained from patient with subarachnoidal bleeding.

Finally, there is a variant in recording technique. The arterial recording may be fed from the tape recorder directly to the oscillograph whereas the venous tracing may be fed through a monostable trigger circuit in order to lengthen and limit the pulses (Fig. 7). This transit time was measured at 6.25 sec and was found to be normal.

### Conclusion

An accurate measurement of cerebral arterio-venous transit times can be made by the use of intra-arterial RISA or neohydrin $Hg^{203}$ and suitable measuring circuits. This data can be substantiated by correlating with arterial angiography. A more precise appreciation of the data can be obtained only after considerable use of the system.

*Department of Neurosurgery* R. L. BELL
*State University of New York*
*Downstate Medical Center, and the*
*Neurosurgical Service of*
*Kings County Hospital*
*Brooklyn, New York, U.S.A.**

*Physics Department of the* G. J. HERTSCH
*City of New York*
*Department of Hospitals*
*Delafield Hospital, New York, U.S.A.*

### References

1. KETY S. S. and SCHMIDT C. F. *J. clin. Invest.* **27,** 476 (1948).
2. NYLIN G., SILFVERSKIÖLD B. P., LÖFSTEDT S., REGNSTRÖM O. and HEDLUND S. *Brain* **83,** 293 (1960).
3. SCHIEFER W., TÖNNIS W. and UDVARHELYI G. *Acta Neurochir.* **4,** 76 (1954).

* Present address: Sec. Neurosurgery U.S. Veterans' Administration Hospital, Wadsworth Division, Wadsworth, Kansas, U.S.A.

## The Effects of γ-Radiation on the Protein Content of Apples and Pears

(*First received* 14 *April* 1961 *and in final form* 15 *May* 1961)

THE physiological and biochemical effects of ionizing radiations have been investigated for many years, but it was not until the last decade that work commenced with fruit tissue. This recent interest has been stimulated by the possible application of ionizing radiation in the food industry to extend the shelf life of perishable commodities.

Previous investigations showed that the percentage of rots in apples due to *Gloesporium spp.* could be markedly reduced by doses between $1 \times 10^5$ and $2 \times 10^5$ rad[1]. This improvement in storage properties was associated with an increase in the rate of breakdown of the apples[3], the symptoms of which were similar to those of "core flush"[2]. SMOCK and SPARROW[4], and MIKAELSON[5] have suggested that the response of apples to ionizing radiation depends upon the stage of maturity of the apple and they emphasized the position of the climacteric in relation to the time of irradiation. During the climacteric, there is a period of protein synthesis,[6–8] and this investigation was made to determine whether radiation affected this synthesis in a way which could account for the increased percentage of internal breakdown in apples.

Evidence obtained previously[9] indicated that the rate of ripening of pears could be retarded by treatment with ionizing radiation, and it is possible that this inhibition is also correlated with a disturbed protein metabolism[10].

The conditions during irradiation, the sampling procedures and the methods used in the preparation of the tissue for analysis, will be reported in detail elsewhere[11]. Apples and pears, which had received $1 \times 10^5$ rad and $2 \times 10^5$ rad in air at 20°C, were

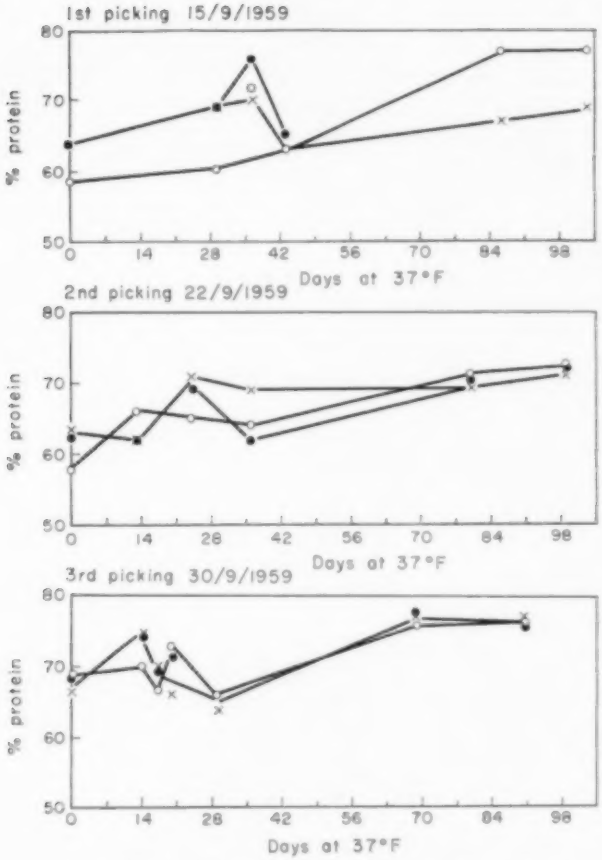


FIG. 1. The effect of γ-radiation on the protein content* of apples (Cox's Orange Pippin). ○—○ Control; ×—× $1 \times 10^5$ rad; ●—● $2 \times 10^5$ rad.

* Alcohol-insoluble $N_2$ calculated as percentage of total $N_2$.

stored with untreated fruit in air at 37 and 32°F, respectively. Each sample consisted of twenty fruits selected at random. After the fruits had been halved and the core and pips removed, the pulp and peel were frozen in liquid nitrogen. Samples were stored in Polythene bottles at −20°C until required for analysis. The frozen material was ground and mixed, and duplicates of 100 g were taken for each determination. The alcohol-insoluble nitrogen content, regarded as primarily protein, was determined in the residues, remaining after extraction with 80% alcohol, by GUNNING's[12] method which was adapted to semi-micro analysis. After digestion, the contents were made up to volume and an aliquot was taken for nitrogen determination according to the method of YUEN and POLLARD[13]. The nitrogen content of the fraction soluble in 80% alcohol was determined by the same method. Total experimental error was within +3 per cent.

In general, the results obtained with apple tissue (Fig. 1) indicated that protein synthesis was unaffected by the treatment. Only in the first picking, where the highest incidence of internal breakdown was noted[1], was there an indication that the protein content of the irradiated fruit was less than the untreated fruit at the end of the storage period. In the early stages of the experiment, the protein content of the irradiated fruit was higher than the untreated fruit and it suggests the possibility that protein synthesis had been stimulated prematurely. If this

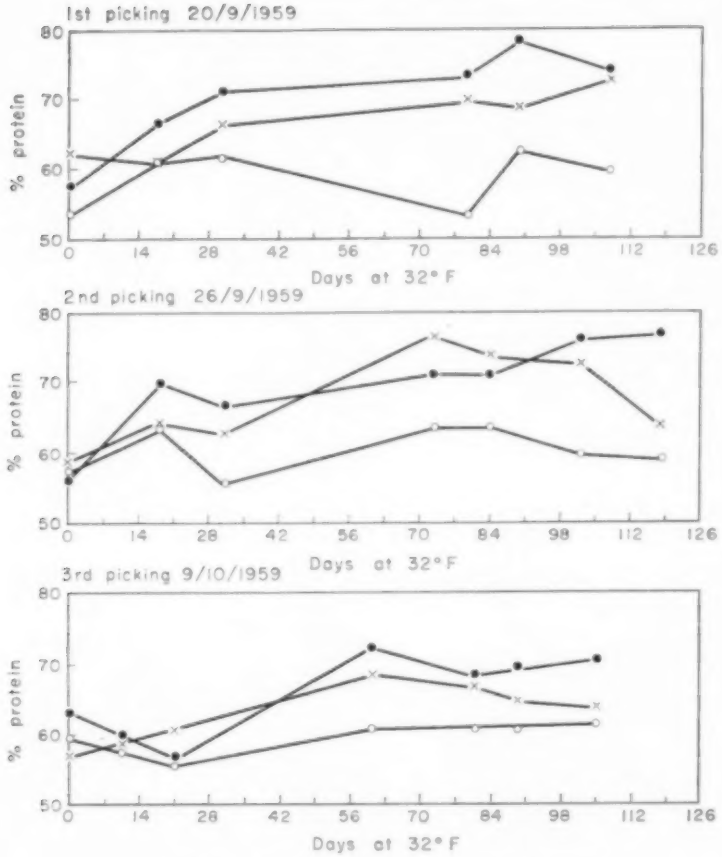


FIG. 2. The effects of $\gamma$-radiation on the protein content* of pears (Doyenne du Commice).
○—○ Control; ×—× $1 \times 10^5$ rad; ●—● $2 \times 10^5$ rad.

was so, then the accelerated rate of breakdown may be due to a rapid onset of senescence as well as radiation injury induced by the treatment.

The results obtained with pear tissue clearly indicate that the treatment induced protein synthesis during the storage period, whilst the levels of protein nitrogen in the untreated fruit remained at a fairly steady level (Fig. 2). Initially, there were no clearly defined increases in protein nitrogen in the treated fruits. There was also a slight indication that the earlier the fruit was picked the greater the stimulation in protein synthesis induced by the treatment. Unfortunately, the differences are small and further work is required to establish a definite relationship between these two variables. No evidence is available concerning the nature of this protein or other alcohol-insoluble compounds, and whether or not it is identical with the protein which is synthesized normally during the climacteric is unknown. If this induced protein synthesis is symptomatic of an accelerated normal protein synthesis, then it is difficult to consider how this process may be involved in the retardation of ripening noted previously.

I. D. CLARKE
S. J. G. FERNANDES*

*Wantage Research Laboratory*
*Wantage, Berks.*

## References

1. CLARKE I. D. Unpublished data (1959–60).
2. SMOCK F. M. and NEUBERT A. M. *Apples and Apple Products*. Interscience, New York (1950).

* Present address: Laboratorio Quimico Agricola Rebelo Da Silva Tapada De Ajuda, Lisbon, Portugal.

VOL
11
196

3. Clarke I. D. *Proceedings of the Ninth International Congress of Botany, Montreal* 1959. University of Toronto Press, Toronto. In press.
4. Smock F. M. and Sparrow A. H. *Proc. amer. Horti. Soc.* **70,** 71 (1957).
5. Mikaelson K., Brennan H. K. and Landfall R. *Proceedings of the Second International Conference on the Peaceful Uses of Atomic Energy, Geneva,* 1958, P/401, Vol. 27. United Nations, N.Y. (1958).
6. Hulme A. C. *Rept. Fd. Invest. Board, London,* No. 1936, 128 (1937).
7. Robertson R. N. and Turner J. F. *Aust. J. sci. Res., Ser. B.* **4,** 92 (1951).
8. Hulme A. C. *Advanc. Food Res.* **8,** 297 (1958).
9. Clarke I. D. *Int. J. appl. Rad. Isotopes* **6,** 175 (1959).
10. Ulrich R. *Bull. Soc. Botan. France* **98,** 133 (1951).
11. Fernandes S. J. G. and Clarke I. D. In preparation.
12. *Official Methods of Analysis of the Association of Official Agricultural Chemists* (7th Ed.) p. 13 (1950).
13. Yuen S. H. and Pollard A. G. *J. sci. Food Agric.* **3,** 441 (1952).

VOL.
11
1961

International Journal of Applied Radiation and Isotopes, 1961, Vol. 11, pp. 190–229. Pergamon Press Ltd. Printed in Northern Ireland

# Research with the Stable Isotopes of Oxygen ($O^{17}$ and $O^{18}$) during 1958–1960

D. SAMUEL and F. STECKEL
Isotope Department, The Weizmann Institute of Science, Rehovoth, Israel

VOL.
11
196

THE following supplement to *Bibliography of the Stable Isotopes of Oxygen* ($O^{17}$ *and* $O^{18}$) by D. SAMUEL and F. STECKEL, Pergamon Press, London (1959), lists all papers published on this subject during the years 1958–1960. The supplement consists of a *Subject Index* and an *Author Index*.

Work on nuclear reactions of oxygen-18 and oxygen-17 has been included only when this appears to have analytical applications. A few papers published before 1958, but not listed in the original bibliography, have also been added. By using both Subject and Author Indexes a comprehensive review of research with the stable isotopes of oxygen during the past three years can be obtained.

The *Subject Index* lists both subjects and individual compounds. Each entry is followed by the letter–number symbols referring to the relevant papers in the Author Index. The nomenclature adopted by *Chemical Abstracts* is used, but a few variations have been made in order to keep similar compounds in a group. Esters and salts are listed under the acid radical or anion in alphabetical order, e.g. "Sulphate, diethyl", "Sulphate, sodium". The words "Isotope" or "Oxygen-18" are not used when the meaning is clear, thus "Abundance" means abundance of oxygen-18, "Exchange" refers to isotopic exchange of oxygen-18, "Hydrolysis" to hydrolysis using oxygen-18 as tracer. The infra-red and microwave spectra refer to oxygen-18 labelled compounds and the chemical shifts refer to oxygen-17. Papers dealing with oxygen-17 are listed under this heading. The symbol $O^{18}$ after the full name of a compound indicates uniform labelling of all oxygen atoms. When a specific oxygen atom is labelled, this is indicated as follows:

Benzoate, methyl-$O^{18}$
Benzoate, methyl-*alkoxy*-$O^{18}$
Benzoate, methyl-*carbonyl*-$O^{18}$.

"Exchange" includes cases where exchange was shown not to occur and no distinction has been made between results of a single experiment and extensive kinetic surveys. No listing has been made under "Water" since research involving water may be found under "Abundance", "Analysis", "Exchange", "Hydrolysis" or "Separation".

The *Author Index* is arranged alphabetically according to the name of the author, or the first author of a group of authors. The papers of each author, or group of co-authors, are arranged in chronological order. Wherever possible the *Chemical Abstracts* reference is given after the main reference. Each reference is identified by a letter–number symbol used in the Subject Index.

VOL.
11
1961